

Georgia State University

ScholarWorks @ Georgia State University

Physics and Astronomy Dissertations

Department of Physics and Astronomy

8-10-2021

Young Stars amid External Radiation and Colliding Associations

Alexandra Yep

Follow this and additional works at: https://scholarworks.gsu.edu/phy_astr_diss

Recommended Citation

Yep, Alexandra, "Young Stars amid External Radiation and Colliding Associations." Dissertation, Georgia State University, 2021.

doi: <https://doi.org/10.57709/23991663>

This Dissertation is brought to you for free and open access by the Department of Physics and Astronomy at ScholarWorks @ Georgia State University. It has been accepted for inclusion in Physics and Astronomy Dissertations by an authorized administrator of ScholarWorks @ Georgia State University. For more information, please contact scholarworks@gsu.edu.

Young Stars amid External Radiation and Colliding Associations

by

ALEXANDRA C. YEP

Under the Direction of Russel J. White, PhD

ABSTRACT

We explore star-star and cluster-cluster interactions in the Gum Nebula. The hot stars ζ Pup and γ^2 Vel powering the Gum Nebula photoevaporate dense cloud cores into cometlike shapes, called cometary globules. According to our analysis of HIRES spectra from the Keck I telescope, the stellar association near cometary globule CG 30 (FUV flux ratio $G_0 = 6.6^{+3.2}_{-2.7}$) has an accretion disk fraction of only $29\% \pm 14\%$, low for the association's young age of $0.5 - 2$ Myr. This low accretor fraction serves as evidence for hot-star erosion of young stars' protoplanetary disks.

We find another seven associations in the Gum Nebula, three of which are new (Yep 1, 2, and 3), for a total sample of 8. We identify a total of 1873 stellar members of these associations and obtain high dispersion CHIRON spectra of 284 stars. We also obtain high-quality spectra of 81 spectral standard stars with high SNR $\gtrsim 100$. This catalogue is made available to all CHIRON users. The 8 associations are aged $2 - 650$ Myr and have $G_0 = 2.1 - 17.0$. The five youngest associations ($\lesssim 10$ Myr) exhibit low accretion fractions for their ages (1.6 – 29%).

We serendipitously discover that the associations UPK 535 and Yep 3 collided with each other 0.84 ± 0.03 Myr ago. According to our Monte Carlo simulation, a mean of 54 ± 7 pairs of stars come within 1 pc of each other. The tightest star-star interaction is on average 0.13 ± 0.06 pc, or $27,000 \pm 12,000$ AU, less than the radial extent of the Sun's Oort cloud ($\sim 50,000$ AU). The strongest impulse on a star's Oort cloud comets (if present) is on average $2.7^{+3.1}_{-1.1} M_{\odot}$ pc $^{-2}$ km $^{-1}$ s, large enough to throw 410^{+560}_{-190} of every million comets' inward and potentially cause heavy bombardment events. Other associations in the vicinity have also recently interacted, suggesting cluster interactions may play a larger role in star, cluster, and exoplanet evolution than previously considered, at least in the Gum Nebula straddling the Galactic plane.

INDEX WORDS: Young Stars— Cometary Globules— Associations

Young Stars amid External Radiation and Colliding Associations

by

ALEXANDRA C. YEP

A Dissertation Submitted in Partial Fulfillment of the Requirements of

Doctor of Philosophy

in the College of Arts and Sciences

Georgia State University

2021

Copyright by
Alexandra C. Yep
2021

Young Stars amid External Radiation and Colliding Associations

by

ALEXANDRA C. YEP

Committee Chair:	Russel J. White
Committee:	Todd Henry
	Wei-Chun Jao
	Sebastien Lepine
	Tom Megeath

Electronic Version Approved:

Office of Graduate Studies

College of Arts and Sciences

Georgia State University

August 2021

ACKNOWLEDGEMENTS

A. C. Yep thanks her dissertation committee Dr. R. J. White, Dr. W.-C. Jao, Dr. T. Henry, Dr. S. Lepine, and Dr. T. Megeath for their time, expertise, and helpful advice. A. C. Yep and R. J. White thank L. A. Hillenbrand for her help in initiating this work. NSF AAG grant 1517762 provided support. We thank A. Nisak for providing initial Python codes for measuring radial velocity, rotational velocity, and elemental abundances. We thank A. Nisak, H. James, L. Paredes, and W.-C. Jao for scheduling our targets on CHIRON and reducing our spectra, and T. Henry for granting internal telescope time. We thank Keck Observatory for use of its cutting-edge facilities, and the indigenous people of Hawaii for the opportunity to observe the stars from the peak of Mauna Kea. This paper was made possible through queued observations on the CHIRON spectrograph on the CTIO/SMARTS telescope on Cerro Tololo and the fine people who operate the facility. This publication makes use of data products from the Two Micron All Sky Survey, which is a joint project of the University of Massachusetts and the Infrared Processing and Analysis Center/California Institute of Technology, funded by the National Aeronautics and Space Administration and the National Science Foundation. This work has made use of data from the European Space Agency (ESA) mission *Gaia* (<https://www.cosmos.esa.int/gaia>), processed by the *Gaia* Data Processing and Analysis Consortium (DPAC, <https://www.cosmos.esa.int/web/gaia/dpac/consortium>). This research has made use of the VizieR catalogue access tool, CDS, Strasbourg, France (DOI: 10.26093/cds/vizier), with original description published in A&AS 143, 23. Funding for the DPAC has been provided by national institutions, in particular the institutions participating in the *Gaia* Multilateral Agreement. Thank you to W. Fischer, L. A. Hillenbrand, and the

referee for providing such thorough, helpful feedback on A. C. Yep's first paper. Thank you to Dr. Jao, Dr. Henry, and Dr. Lepine for their early feedback on the discovery of the colliding stellar associations. The authors also thank Dr. Karnath, Dr. Matthieu, Dr. Stauffer, Dr. Megeath, and Dr. Mamajek for their help contextualizing the colliding associations, information on association energies, and knowledge of stellar associations in general. A special thanks to A. C. Yep's advisor R. J. White for working many an evening, night, and weekend to assist with this research and answer all A. C. Yep's questions, big and small. She thanks everyone in the GSU astronomy department for providing the friendliest, most supportive learning environment she has ever experienced. She also thanks her parents, her parents-in-law, her sister, and her extended family and friends for attending her several public talks on her research. Finally, A. C. Yep thanks her devoted partner R. C. Marks for lighting up her life and always walking with her in her journey amidst the stars, and for helping her assemble her bibliography.

TABLE OF CONTENTS

LIST OF TABLES.....	
LIST OF FIGURES	
1 INTRODUCTION	1
1.1 Clusters and Associations	2
1.2 The Moderate Radiation Environment of the Gum Nebula	4
1.3 Colliding Associations: Laboratories for Studying Close Stellar Encounters .	5
1.4 Overview of the Chapters in This Dissertation	6
2 A CASE STUDY: YOUNG STARS NEAR COMETARY GLOBULE CG 30 IN THE GUM NEBULA	8
2.1 Introduction	8
2.2 Observations	10
2.2.1 Keck I HIRES Spectra	10
2.2.2 Reduction and Extraction	11
2.3 Spectroscopic Analysis	12
2.3.1 Li I λ 6708 Å Equivalent Width	12
2.3.2 H α 10%-Widths and Equivalent Widths	14
2.3.3 Radial Velocity	15
2.3.4 Rotational Velocity	17
2.3.5 Veiling and Spectral Types	18

2.4	Stellar Properties	21
2.4.1	Photometry	22
2.4.2	Veiling Correction	22
2.4.3	Extinction Correction	23
2.4.4	Bolometric Correction	24
2.4.5	Near Infrared Excess	25
2.4.6	Distances from <i>Gaia</i> DR2 Parallaxes and Apparent Associations . . .	25
2.4.7	Bolometric Luminosity	26
2.4.8	Effective Temperature	27
2.4.9	Masses and Ages from an HR Diagram	28
2.5	Discussion	30
2.5.1	Kinematics	30
2.5.2	Far-Ultraviolet Radiation	34
2.5.3	Star Formation in Cometary Globules	37
2.5.4	Young Star Evolution in a Moderate Radiation Environment	39
2.6	Summary	41

3	FINDING OTHER YOUNG ASSOCIATIONS IN THE GUM NEBULA	43
3.1	Introduction	43
3.2	Finding Clusters near Cometary Globules	43
3.3	Association Candidates	46
3.3.1	CG 4 Association	47
3.3.2	CG 22 Association	47
3.3.3	CG 30 Association	49
3.3.4	Yep 1 Association near CG 3	49
3.3.5	Yep 2 Association near CG 14	49
3.3.6	Yep 3 Association near CG 17	50
3.3.7	UPK 535 Association near GDC 1	50

3.3.8	Alessi 3 Association near CG 1	51
3.3.9	Association Ages	51
3.4	High Dispersion Optical Spectra	51
3.4.1	Association Observations and Data Reduction	53
3.4.2	Spectral Types, Extinctions, Masses, and Infrared Excesses	53
3.4.3	Radial Velocities	56
3.4.4	Projected Rotational Velocities	59
3.4.5	Li Equivalent Widths	61
3.4.6	H α Widths	63
3.4.7	Near-Infrared Excess	64
3.4.8	Exceptions	67
3.5	Association Properties	68
3.5.1	Association Verification	68
3.5.2	Total Stellar Masses	68
3.6	Summary	70
4	PROPERTIES AND ASSOCIATIONS	72
4.1	Introduction	72
4.2	Star Formation Associated with Cometary Globules	72
4.2.1	CG 4 Association and CG 4	73
4.2.2	CG 22 Association and CG 22	73
4.2.3	CG 30 Association and CG 30	73
4.2.4	Alessi 3 and CG 1	75
4.3	Gum Nebula Radiation Environment	76
4.4	Photoevaporated Protoplanetary Disks	76
4.5	High Rotational Velocities for Age	77
4.6	Characteristics of Cometary Globule Associations	78
4.7	Summary	79

5 COLLIDING ASSOCIATIONS	81
5.1 Introduction	81
5.2 Stellar and Association Properties of UPK 535 and Yep 3	83
5.3 Ellipsoid Fits	86
5.4 Discussion	88
5.4.1 Colliding Associations	88
5.4.2 Impulse	93
5.4.3 Other Colliding Associations	96
5.4.4 Kinetic Energy vs. Gravitational Potential Energy	97
5.5 Conclusions	100
6 SUMMARY	102
BIBLIOGRAPHY	105
A CHIRON SPECTRAL STANDARDS	118
B ASSOCIATION MEMBER KINEMATICS AND PROPERTIES	127
C STELLAR PROPERTIES OF SPECTROSCOPICALLY OBSERVED STARS	233

LIST OF TABLES

2.1	Basic Properties of Stars Observed with Keck HIRES	11
2.2	Equivalent Widths	16
2.3	Radial and Rotational Velocities	19
2.4	PH α 41 A and B Velocities Across 3 Epochs	19
2.5	Veiling and Spectral Types	21
2.6	HR Diagram Parameters	27
2.7	Proper Motions and Radial Velocities	31
2.8	Hot Star Parameters	36
2.9	Accretor Fractions of Star-Forming Regions	40
3.1	Search Parameters and Cuts	45
3.2	Sample of Each Association’s Member Kinematics and Properties	58
3.3	Sample of Stellar Properties of Spectroscopically Observed Stars	66
3.4	Association Properties	69
5.1	Position and motion cuts for isolating the associations UPK 535 and Yep 3 from <i>Gaia</i> DR2 data. We also impose error cuts < 0.1 mas in parallax and < 0.16 mas yr ⁻¹ in proper motion.	83
5.2	UPK 535 and Yep 3 Association Properties	85
5.3	Energies and energy ratios of Gum Nebula clusters.	98
A.1	CHIRON Standards	121

B.1	CG 4 Assn. Member Kinematics and Properties	128
B.2	CG 22 Assn. Member Kinematics and Properties	130
B.3	CG 30 Assn. Member Kinematics and Properties	136
B.4	Yep 1 Member Kinematics and Properties	138
B.5	Yep 2 Member Kinematics and Properties	167
B.6	Yep 3 Member Kinematics and Properties	191
B.7	UPK 535 Member Kinematics and Properties	208
B.8	Alessi 3 Member Kinematics and Properties	218
C.1	Sample of Stellar Properties of Spectroscopically Observed Stars	234

LIST OF FIGURES

1.1	Hot stars ζ Pup (wolf) and γ^2 Vel (binary unicorns) spur the formation of stars in cometary globules throughout the Gum Nebula. Oracle, AZ, 2018, ink on paper.	1
2.1	The top panel displays the main ionizers of the Gum Nebula (white circles), namely the O-type stars ζ Pup and γ^2 Vel, OB association Vela OB2, and supernova remnant Vela XYZ. The target young stars (cyan star symbols from Pettersson (1987), orange diamonds from Kim et al. (2005), and magenta square from Neckel & Staude (1995)) lie at the Gum Nebula's northern edge (blue box). This region is enlarged in the bottom panel. Four PH α young stars, CG 30 IRS 4, and 10 KWW stars from Kim et al. (2005) trace dust near cometary globule CG 30 of the CG 30/31/38 cometary globule complex. Five PH α stars and 1 star from Neckel & Staude (1995) trace dust spatially near H II region RCW 19. The background images have been generated in Aladin using DSS2 (red, blue, infrared), and star locations have been plotted in PyPlot.	9

2.2	Five spectral regions of interest are displayed for the 9 PH α stars. Spectral features are labeled at the top of the figure. The first and last columns show Ca, Fe, and Ti, typically strong in K-type stars (e.g. PH α 44). The middle column shows TiO molecular bands, wide and deep for M-type stars (e.g. PH α 14). The second column shows lithium absorption, associated with young stars. The fourth column tracks surface-gravity with K I λ 7700 Å, which is relatively weak for young stars still in the process of gravitationally settling. All the stars in our sample exhibit a shallowing of spectral lines and bands, called veiling.	13
2.3	We compare the same 5 spectral regions of interest as in Figure 2 for the embedded star CG 30 IRS 4 (blue, smoothed) and the veiled T Tauri star Haro 6-13 (fuchsia) of the same spectral type, M0 (White & Hillenbrand 2004). The infrared source inside the cometary globule has a well defined photosphere.	15
2.4	We measure H α widths at 10% up the peak (green lines). Red dashed lines mark zero-velocity 6562.8 Å. Blueshifted dips within the emission peaks are likely absorption lines from cool winds.	17
2.5	M3.5 V standard spectrum (a., fuchsia) is manipulated (gray) with v_r shift (b.), rotational broadening (c.), and veiling (d.) until it matches the young star spectrum of PH α 14 (e., blue).	18

2.6 We plot luminosity vs. temperature for the 14 CG 30 Association stars and candidates (blue star symbols), the 5 stars near PH α 41 (orange diamonds), and the 3 other stars (magenta squares). The 6 defining members of the CG 30 Association are outlined in purple. *Gaia* DR2 distances are incorporated where available and are represented with large symbols. Stars assigned distances for possible relation to the CG 30 Association or PH α 41 (see text and Table 2.6) are represented with small symbols. Mass tracks and isochrones are from Baraffe et al. (2015) (dotted and dashed, gray, mass $\leq 1.4 M_{\odot}$) and supplemented with MESA (dot-dashed, paler pinker gray, mass $> 1.4 M_{\odot}$; Dotter 2016; Choi et al. 2016; Paxton et al. 2011, 2013, 2015). The Baraffe et al. (2015) 0.5 Myr isochrone (blue dotted) passing through the CG 30 Association stars is used to calculate isochrone distances (see Table 2.6). Eight stars of interest are labeled.

28

2.7 We plot the *RA* and *Dec* of 21 stars, with the color bar showing v_r and arrows indicating proper motion in mas yr $^{-1}$, scaled up by a factor of 10 in the figure (see proper motion scale in black in the lower left corner). Star symbols mark CG 30 Association stars and candidates, with the 6 CG 30 Association members outlined in purple. Diamonds mark the 4 stars near PH α 41. Other stars are represented by squares. The v_r color legend extends over the range of interest from 20.0 – 33.69 km s $^{-1}$. Stars with v_r outside this range have no color. The star KWW 1302 with no v_r bears an *X*. At least 13 of the stars spatially near CG 30 may be dynamically related. The relation of the stars near PH α 41 is weakly suggested.

34

3.1 Shown is a majority of the Gum Nebula, grayscaled from Aladin’s DSS2 image (combined blue, red, and infrared), and plotted in PyPlot. Radiation sources ζ Pup, γ^2 Vel, and Vel XYZ are plotted in orange. CGs and their cometlike tails are plotted and labeled, although at this scale only the longest tails are visible. Spatial scale at distance = 360 pc is displayed in the bottom right corner. The 8 associations found using Cluster Finder are marked with rings and labeled with slightly enlarged font. The color bar shows radial velocities for cometary globules, where available, and our radial velocities for our 8 associations. Arrows indicate proper motions. Proper motion scale is displayed in the bottom left corner. Other previously known associations and clusters in the region are marked with black diamonds. The dashed dark gray line marks the Galactic plane.	44
3.2 Cluster Finder process, demonstrated on Yep 1. We start with <i>Gaia</i> DR2 data with parallax limited to within the Gum Nebula (leftmost panel). We then make proper motion cuts (middle left panel) and refine the distance cuts (middle right panel). Finally, we make error cuts to keep only stars with high-quality astrometry (rightmost panel).	45
3.3 <i>RA</i> vs. <i>Dec</i> of 8 young associations in the Gum Nebula. Cometary globules and dark clouds are marked with black triangles and labeled. The CG 4, 22, and 30 Associations are sparse and may be associated with their nearby cometary globules.	48
3.4 Associations Yep 1 (orange triangles) and Yep 2 (azure circles). We empirically split the two associations using an empirical quadratic (gray line) in μ_α vs. <i>Dec</i> space (left panel). The two associations spatially overlap but are distinct (right panel).	50

3.5 Color-magnitude diagrams. <i>Gaia</i> colors are corrected for redenning, and absolute G magnitudes are calculated using distances from (Bailer-Jones et al. 2018) and corrected for extinction. Isochrones are from MESA: dotted gray is 1 Myr, dashed gray is 10 Myr, and solid gray is 100 Myr. Spectroscopically observed stars are plotted as gold stars. Unobserved stars are azure circles. Solid blue isochrones display our age fits, while lilac-shaded regions mark asymmetric age uncertainties. Seven of the 8 associations are fit best by supersolar metallicities, and all are younger than 1 Gyr. Five are $\lesssim 10$ Myr.	52
3.6 Sample of normalized CHIRON spectra. Order 1 (left panels) is rich in atomic lines and useful for spectral classification and velocity measurements. Order 41 (right panels) contains Li I $\lambda 6708$, present in young stars.	55
3.7 Example of cross-correlation procedure, for order 11 of K2V-type star TYC8137-2850-1. Left panel: The location of the peak of the cross-correlation function between the spectra of the standard star 41 Ara and the star TYC8137-2850-1 gives the applied Doppler shift, from which we calculate relative radial velocity and barycentric radial velocity v_r . Right panel: We auto-correlate the target star's cross-correlation-peak width with its applied broadening v_b to derive an empirical relation between $v_{rot} \sin(i)$ and applied rotational broadening. Pink dot matches measured cross-correlation-peak width with amount of applied rotational broadening, which is then combined with the standard's measured rotational broadening (3.2).	57
3.8 Projected rotational velocities $v_{rot} \sin(i)$ vs. ages. We have measured $v_{rot} \sin(i)$ for 271 association members based on CHIRON data and 5 members based on Keck I HIRES data (see Chapter 2). Five of the 8 associations contain stars with $v_{rot} \sin(i) > 40$ km s $^{-1}$. Circles are single-star association members. Diamonds are confirmed binaries (fat) or potential binaries (skinny). Twenty-seven cool stars later than type F5 are fast rotators.	61

3.9 Li EW vs. T_{eff} . Light colored dots are from Gutiérrez Albarrán et al. (2020) and represent ages 1 – 3 Myr (cyan), 10 – 20 Myr (light blue), 34 – 41 Myr (lavender), 248 – 450 Myr (light pink), and 763 – 977 Myr (hot pink). Younger stars have stronger Li absorption, as do lower-mass stars. The associations in the Gum Nebula (dark blue stars) are fairly young, with ages 2 – 650 Myr. Their positions in Li EW vs. T_{eff} space are generally consistent with our isochrone age estimates.	62
3.10 Sample of H α profiles with emission or mixed emission and absorption, in normalized flux vs. gas velocity. Equivalent width is calculated over the magenta portion. Lime green marks the H α 10% width for emitters. Pink vertical lines up through the 10% width indicate a gas motion spread of 270 km s $^{-1}$, our empirical boundary between accreting and nonaccreting stars. . .	65
3.11 Infrared excess in $J - K$ vs. age. The dust in young stars' accretion disks or a debris disks tend to cause infrared excess. We calculate infrared excess by comparing stars' apparent $J - K$ colors with their intrinsic colors according to their spectral types and the dwarf colors of (Pecaut & Mamajek 2013). . .	67
4.1 Association accretor fraction vs. association age. Quiescent-region associations (orange circles) tend to have higher accretor fractions per age than external-radiation-region associations (steel blue circles). Gum Nebula associations' accretor fractions (azure stars) appear more consistent with the external-radiation-region trend.	78

5.1	The sky positions of five associations in the Gum Nebula. Associations UPK 535 (blue squares) at 318.08 ± 0.29 pc and Yep 3 (red diamonds) at 339.54 ± 0.25 pc have elongated shapes and spatially overlap. Their centers of mass are marked by a dark blue $+$ and a dark red x , respectively. Center-of-mass motions over 1 Myr are marked by dark blue and dark red arrows. UPK 535 and Yep 3 are near other associations UPK 545 at 326.80 ± 0.24 pc (dark grey circles, south), UPK 533 at 344.08 ± 0.46 pc (grey circles, west), and Pozzo 1 at 346.75 ± 0.23 pc (light grey circles, northwest).	82
5.2	75%-stars ellipsoid fits to UPK 535 (blue) and Yep 3(red) today (top panel) and 0.84 Myr ago (bottom panel). The associations have significant volume overlap, shown in magenta.	87
5.3	Distributions of distances and kinematics for UPK 535 (blue) and Yep 3 (red). The spatially overlapping associations share distances and proper motions in right ascension (purple overlap), but their proper motions in declination and radial velocities are divergent, indicating they did not form together. Rather, they recently encountered each other.	89
5.4	Projected positions of UPK 535 (squares) and Yep 3 (diamonds) at three points in time: 3.0 Myr ago (bottom panel), 0.84 Myr ago (middle panel), and 1.5 Myr from now (top panel). <i>RA</i> corresponds roughly with y , <i>Dec</i> with z , and distance with x , all in pc. The coordinates are zeroed on UPK 535. Dark outlines mark stars with spectroscopically measured v_r . Yep 3 moves north and away into UPK 535, reaching closest approach 0.84 ± 0.03 Myr ago and receding thereafter. The apparent expansion back in time results from a combination of proper motion uncertainties ~ 0.13 mas yr $^{-1}$ and linear extrapolation.	90

A.1	Sample of normalized CHIRON spectra. Order 1 (left panels) is rich in atomic lines and useful for spectral classification and velocity measurements. Order 41 (right panels) contains Li I λ 6708, present in young stars.	118
A.2	CHIRON standards parameter space for temperatures and metallicities of dwarfs (azure circles), giants (orange diamonds), and a supergiant (pink square). Points are scaled by $v_{\text{rot}} \sin(i)$ values, with range 1.6 – 49.0 km s ⁻¹ .	120

CHAPTER 1

INTRODUCTION



Figure 1.1: Hot stars ζ Pup (wolf) and γ^2 Vel (binary unicorns) spur the formation of stars in cometary globules throughout the Gum Nebula. Oracle, AZ, 2018, ink on paper.

Stars are not born in isolation. Rather, they are born in groups from massive, extensive clouds of molecular gas that collapse and fragment into hundreds or thousands of stars (Shu et al. 1987; Lada & Lada 2003; Krumholz et al. 2019). These stellar clusters or associations are not necessarily alone either and, especially in the Galactic plane, may exist near other

clusters. One may well ask, are stars affected by neighboring stars? Are clusters affected by neighboring clusters? The answer to both questions is *yes*. My thesis specifically explores whether hot stars' radiation disrupts the disks and planet formation abilities of young stars within even a hundred light years, and how stellar association collisions dynamically affect constituent stars and their solar system architectures.

1.1 Clusters and Associations

Groups of stars are typically classified into four categories: globular clusters, open clusters, associations, and moving groups. Exact definitions vary and can overlap, but the most distinguishing factors are stellar density, age, and metallicity, or stars' relative abundance of elements heavier than hydrogen. Globular clusters formed billions of years ago and are the densest ($\gtrsim 100$ stars pc $^{-3}$; Moraux 2016) and most massive ($> 10,000$ M $_{\odot}$; Krumholz et al. 2019) stellar groups. They have relatively low metallicities and often contain multiple stellar generations (Bastian & Lardo 2018). They are strongly gravitationally bound and have maintained their cohesion for several Gyr. Open clusters, on the other hand, formed more recently, have densities $\sim 1 - 100$ stars pc $^{-3}$ (Moraux 2016), and tend to have higher, Sun-like metallicities (Friel 1995). Open clusters are loosely gravitationally bound and can last 100 Myr – a few Gyr (Moraux 2016; Krumholz et al. 2019). Associations are like sparse open clusters; they contain 10s or 1000s of stars and are much more spread out than open clusters, with densities < 1 pc $^{-3}$ (Mamajek et al. 2013; Moraux 2016). They are gravitationally unbound and tend to dissolve in < 100 Myr. Clusters or associations that have dissolved but whose stars are still moving through space together are called moving groups (Zuckerman & Song 2004; Faherty et al. 2018). Groups of young stars still embedded in their natal gas are difficult to classify as clusters or associations because gas helps gravitationally bind the stars when present but tends to disperse within 10 Myr, after which point the young stars may or may not remain gravitationally bound to each other (Moraux 2016; Krumholz et al. 2019).

Since 2018, the *Gaia* DR2 catalogue of 1.7 billion stars has brought precise astrometry, proper motions, and unprecedented opportunity for finding and studying nearby clusters and associations (Gaia Collaboration et al. 2016, 2018). Increasingly expansive catalogues of clusters and associations are being assembled using supervised and unsupervised machine learning by Kounkel & Covey (2019), Cantat-Gaudin et al. (2018), Castro-Ginard et al. (2020), and others. Two to three thousand open clusters and associations are now known, and the census is far from complete (Moraux 2016; Castro-Ginard et al. 2020).

Studying clusters and associations of stars is worthwhile for several reasons. A cluster or association provides a sample of stars with a range of stellar masses, but with similar ages, metallicities, and environmental factors, such as surrounding stellar densities and radiation from nearby hot stars. Each star in the group thus serves as a massed case study for a set age, composition, and environment. Additionally, several stellar properties, particularly age, are easier to measure in ensemble. Isochrone fits to a whole cluster or association's color-magnitude diagram can provide age estimates (e.g. Bressan et al. 2012; Choi et al. 2016; Monteiro & Dias 2019) more expediently than individual signatures of youth like lithium absorption or hydrogen emission, which can themselves be usefully studied in ensemble (e.g. Mamajek & Hillenbrand 2008). Exoplanets orbiting members of clusters and associations with known ages provide constraints on exoplanet formation and migration theories (e.g. Quinn et al. 2016; Mann et al. 2017; Gaidos et al. 2017; Ragusa et al. 2018; Winter et al. 2020; Longmore et al. 2021).

We focus on eight stellar associations in this dissertation. One of them, the CG 30 Association, has been studied for star formation in its namesake cometary globule CG 30 (Reipurth 1983; Bertoldi 1989; Sridharan 1992; Bhatt 1993; Pettersson 1987; Kim et al. 2005). We independently find another seven associations using an empirical, visualized search on *Gaia* DR2 data (Gaia Collaboration et al. 2016, 2018). Four of these associations have been studied before, but we present the first spectroscopic results. The other three associations are essentially new. Associations in the Gum Nebula are of particular interest because they are

(1.) bathed in the Gum Nebula’s moderate radiation environment and (2.) in the cluster-busy Galactic plane.

1.2 The Moderate Radiation Environment of the Gum Nebula

The Gum Nebula is a diffuse, extensive H II region in the constellations of Vela and Puppis in the Southern sky (Gum 1952; Reipurth 1983; Pettersson 2007; Choudhury & Bhatt 2009). The nebula is powered by the hot O-type stars ζ Pup, γ^2 Vel, and, until its recent catastrophic demise, the progenitor of the supernova remnant Vela XYZ (Pettersson 2007; Choudhury & Bhatt 2009). The ultraviolet light from these stars is strong enough to have photoevaporated dense cloud cores into cometlike shapes (Sridharan 1992; Kim et al. 2005). These so-called cometary globules may be precursors to Bok globules (Reipurth 1983; Bertoldi 1989; Sridharan 1992; Kim et al. 2005; Pettersson 2007; Maheswar & Bhatt 2008; Nakatani & Yoshida 2019). Cometary globules have been identified near OB associations (e.g. Orion Nebula, Rosette Nebula, Tr 37; Herbig 1974, Sicilia-Aguilar et al. 2013) but are particularly large, distinct, and numerous in the Gum Nebula, where at least 32 encircle the triangle formed by ζ Pup, γ^2 Vel, and Vela XYZ (Sridharan 1992; Kim et al. 2005; Choudhury & Bhatt 2009). The cometary globules are a testament to the Gum Nebula’s moderate levels of far-ultraviolet radiation. Stars are born into and possibly by means of this radiation, which may spur cometary globules to condense and form associations (Bhatt 1993; Maheswar & Bhatt 2008; Elmegreen 2011). These associations are generally sparse and consist of low-mass stars (Bhatt 1993; Kim et al. 2005; Maheswar & Bhatt 2008; Elmegreen 2011; Walch et al. 2013). Our Sun, lacking known siblings, may have been born into an association of this type (Kim et al. 2005).

The ionizing radiation that shapes the cometary globules can be characterized by G_0 , a region’s far-ultraviolet (FUV) flux relative to the average ISM value, $G_{0,ISM} = 1.6 \times 10^3$ ergs s $^{-1}$ cm $^{-2}$ (Habing 1968; Winter et al. 2018). G_0 from a known hot (OB-type, $>10,000$ K) stellar population can be calculated for a given location by integrating hot stellar models’

FUV fluxes over $912 - 2400 \text{ \AA}$ and scaling for a given location’s distance from each of the hot stars. G_0 values in the Gum Nebula range from 2.1 to 11.2. Such radiation from the 3 ionizing sources is vastly weaker than in the dense Orion Nebula Cluster ($G_0 \sim 30,000$, Winter et al. 2018) or in NGC 1977 in the Orion A cloud ($G_0 \sim 3,000$, Kim et al. 2016a), but it is stronger than in the more quiescent Tau-Aur star-forming region ($G_0 \sim 1$; Cohen & Kuhi 1979) and may be powerful enough to enhance star formation rates and then photoevaporate protoplanetary disks of the Gum Nebula’s young stars (Bhatt 1993; Kim et al. 2005; Concha-Ramírez et al. 2019; Yep & White 2020). Such irradiation could limit young stars’ accretion and planet formation timescales and could damage or destroy ingredients necessary to planet formation (Walter et al. 1988; Hillenbrand 1997; Kim et al. 2005; Eisner et al. 2008; Sabbi et al. 2020).

1.3 Colliding Associations: Laboratories for Studying Close Stellar Encounters

In regions where many clusters and associations form, like the Gum Nebula, clusters and associations may dynamically interact and possibly collide. Cluster and association collisions have not been widely considered in astronomy. However, any discovered colliding associations or clusters could serve as ideal laboratories for studying close stellar encounters and their potential effects on solar systems. Short of collisions, spatially overlapping clusters and associations have been detected. Galadi-Enriquez et al. (1998) studied NGC 1750 and NGC 1758, spatially overlapping but too distant to measure well. Several clusters consist of two or more overlapping, slightly kinematically distinct components, including σ Ori (Jeffries et al. 2006), R136 (Sabbi et al. 2012), and γ Vel OB2 (Jeffries et al. 2014). Using *Gaia* DR2 data, Wright & Parker (2019) found two mass-separated components of NGC 6530, where the motions of high-mass stars differ from those of low-mass stars.

Approaching this topic from another angle, astronomers have searched for and identified stars that have or will pass close to the Sun. These have the potential to perturb Oort cloud comets into inner orbits, potentially resulting in heavy-bombardment or mass-extinction

events (Weissman 2006; Yeomans & Chamberlin 2012; Feng & Bailer-Jones 2015; Bailer-Jones 2015). Stellar density within clusters, meanwhile, may be a cause of hot jupiters (Winter et al. 2020; Longmore et al. 2021), although this has yet to be disentangled from other factors such as cluster age (Adibekyan et al. 2021). In short, despite the vast emptiness of space, clusters and associations can and do pass near each other, and stars in close proximity to other stars can affect each other’s planets.

1.4 Overview of the Chapters in This Dissertation

In Chapter 2 we present a case study of photoevaporation of protoplanetary disks in the young CG 30 Association. We find that the fraction of accreting vs. nonaccreting young stars is low for the clusters’ age, when compared to similar-age quiescent regions like Tau Aur and ρ Oph. The low accretor fraction suggests that neighboring hot stars can disturb young stars’ protoplanetary disks. This work has been published in (Yep & White 2020).

In Chapter 3, we develop a technique to find clusters and associations in the Gum Nebula using *Gaia* DR2. We obtain spectra, confirm membership, and determine stellar and association properties. We also present a catalogue of CHIRON spectral standards.

In Chapter 4, we consider the 8 associations in the context of the Gum Nebula. The associations exhibit low accretor fractions for their ages, consistent with hot stars’ disruption of nearby young stars’ disks. We also explore which clusters may be associated with their nearby cometary globules and assign association distances to those globules. This work in Chapters 3 and 4 is in preparation for publication.

In Chapter 5 we present the first-ever analysis of a recent collision of two associations, UPK 535 and Yep 3 in the Gum Nebula. We utilize a Monte Carlo simulation to statistically grasp how this collision may affect stars and planets in the two associations. The positions and kinematics of other nearby associations imply they too are interacting; therefore, such interactions may happen more often than astronomers have taken into account. This work

has been submitted to the *Monthly Notices of the Royal Astronomical Society* and is under revision for publication.

Chapter 6 summarizes our findings on how stars and stellar associations affect each other.

The appendices provide full data tables for our catalogue of CHIRON spectral standards, positions and kinematics of all association members, and spectroscopic properties of spectroscopically observed association members.

CHAPTER 2

A CASE STUDY: YOUNG STARS NEAR COMETARY GLOBULE CG 30 IN THE GUM NEBULA

2.1 Introduction

Once a star emerges from its formative gas and dust, external radiation from any nearby OB stars can act on the young star's protoplanetary disk. Disks in the fiery heart of the Orion Nebula Cluster, the proplyds, are visibly elongated (e.g. O'Dell et al. 1993). Even from tens of parsecs away, the light from OB stars may disperse a young star's protoplanetary disk faster than normal and disrupt accretion and planet formation (Walter et al. 1988; Kim et al. 2005; Hillenbrand 2005; Eisner et al. 2008).

The moderate radiation environment of the Gum Nebula is home to at least 32 distinct cometary globules (Zealey et al. 1983), including the cometary globule CG 30 at its northern edge. CG 30 is 34^{+10}_{-7} pc from the O4fI-type star ζ Pup and 70^{+12}_{-1} pc from the WC8 + O7.5III-type binary star γ^2 Vel. Young stars in close proximity to CG 30 serve as our pilot study on the effects of radiation on protoplanetary disks.

The young stars in this chapter have been examined before. In 1988, Pettersson spectroscopically observed 9 stars near CG 30 as part of an H α prism survey (see Table 2.1). Four stars (including PH α 12 = KWW 1892, PH α 14 = KWW 975, and PH α 15 = 1043 in Kim et al. 2005) trace a dusty cloud near CG 30, and 5 trace a cloud near the background H II region RCW 19 (Rodgers et al. 1960; Pettersson 1987; see Figure 2.1). East of RCW 19 is another young star IRAS 08159-3543, which appears abnormally luminous (Neckel & Staude 1995).

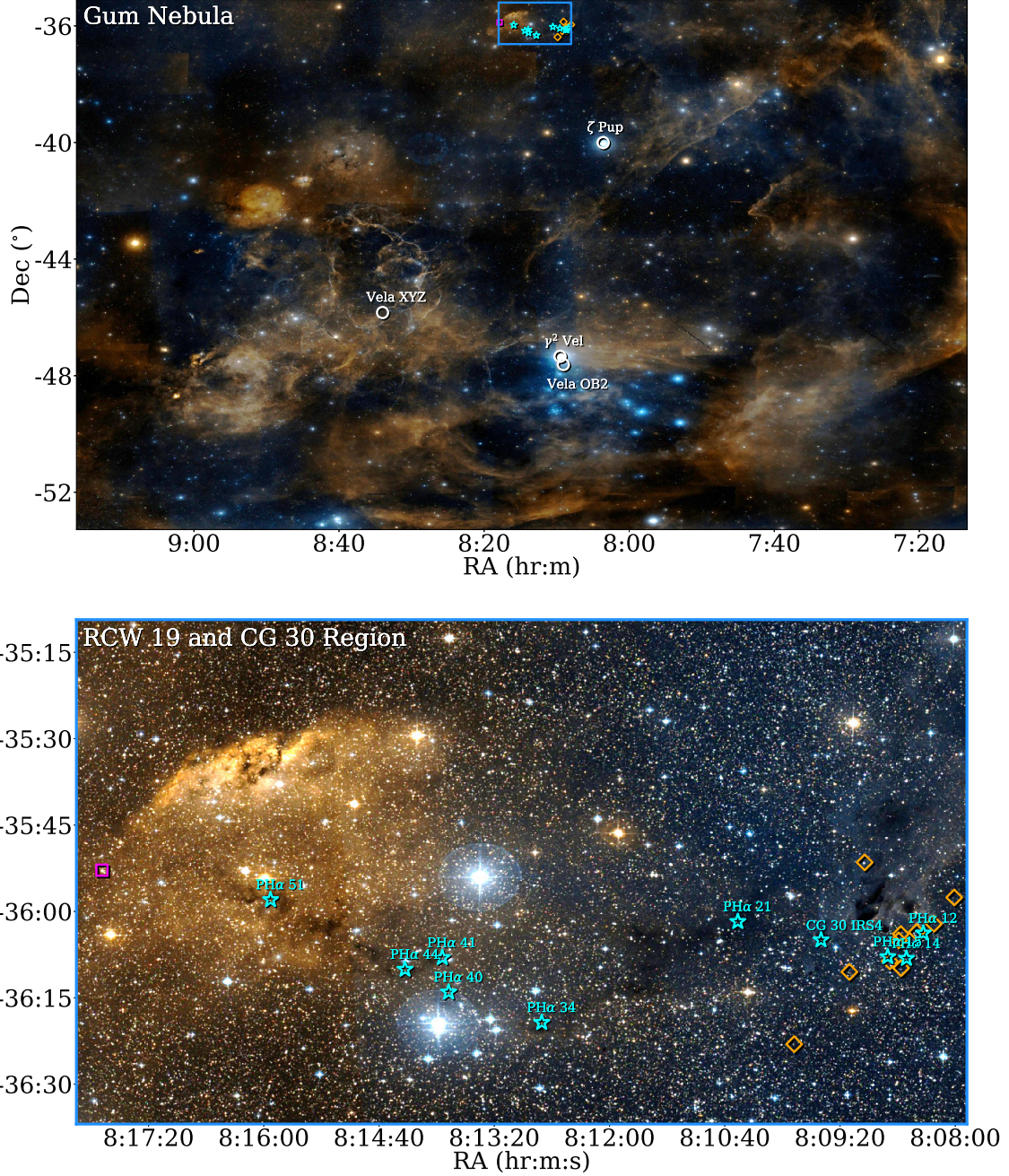


Figure 2.1: The top panel displays the main ionizers of the Gum Nebula (white circles), namely the O-type stars ζ Pup and γ^2 Vel, OB association Vela OB2, and supernova remnant Vela XYZ. The target young stars (cyan star symbols from Pettersson (1987), orange diamonds from Kim et al. (2005), and magenta square from Neckel & Staude (1995)) lie at the Gum Nebula's northern edge (blue box). This region is enlarged in the bottom panel. Four PH α young stars, CG 30 IRS 4, and 10 KWW stars from Kim et al. (2005) trace dust near cometary globule CG 30 of the CG 30/31/38 cometary globule complex. Five PH α stars and 1 star from Neckel & Staude (1995) trace dust spatially near H II region RCW 19. The background images have been generated in Aladin using DSS2 (red, blue, infrared), and star locations have been plotted in PyPlot.

All these stars show $H\alpha$ emission width in excess of 10 Å (Pettersson 1987; Kim et al. 2005). Kim et al. (2005) studied 10 additional stars near CG 30 as part of an x-ray survey, 9 of which show $H\alpha$ emission, strong Li absorption, or both. Kim et al. (2005) suggest 11 young stars (including 3 from Pettersson 1987) are related to each other and CG 30. CG 30 itself contains five known infrared sources, 2 of which (IRS 3 and IRS 4) are near a Herbig-Haro object HH120 (Persi et al. 1994; Pettersson 2007; Kajdič et. al 2010). A wide protobinary system powers the Herbig Haro object (Reipurth 1983; Chen et al. 2008; Kajdič et. al 2010).

To understand this population more completely, we obtained high-dispersion optical spectra of the 9 young stars from Pettersson (1987) and of CG 30 IRS 4 to measure their rotational and radial velocities, Li absorption, and accretion properties. We also gather 2MASS photometry and *Gaia* DR2 data for these 10 stars, plus 10 additional stars from Kim et al. (2005) and 1 luminous star from (Neckel & Staude 1995). In all, we examine the stellar properties, accretion properties, kinematics, and possible associations of 21 young stars near CG 30 and RCW 19.

In §2.2 we discuss observations taken with the Keck I telescope’s high-resolution spectrometer. In §2.3 we plot our spectra and present Li and $H\alpha$ equivalent widths, radial velocities, rotational velocities, spectral types, and veiling, which is a filling-in of spectral lines caused by accretion (Hartigan et al. 1989). We correct photometry for veiling and reddening in §2.4 to calculate extinctions and luminosities and plot an HR diagram. We discuss kinematics, far-ultraviolet radiation, and accretor fractions in §2.5 and summarize in §2.6.

2.2 Observations

2.2.1 Keck I HIRES Spectra

We observed the 10 young stars using the High-Resolution Echelle Spectrometer (HIRES) (Vogt et al. 1994) on the W. M. Keck I telescope on 2003 February 17, 2003 February 18, and 2004 April 4. We obtained 1 epoch for PH α 12, 14, 15, 21, 40, 44, and 51, 2 epochs for PH α 34, and 3 epochs for PH α 41 and CG 30 IRS 4. All observations were obtained

Table 2.1: Basic Properties of Stars Observed with Keck HIRES

Star Name	<i>RA</i> 2000 ^b (h:m:s)	<i>Dec</i> 2000 ^b (°:':")	Spectral Type ^a	<i>V</i> ^a (mag)	<i>K</i> ^a (mag)
PH α 12	08 08 22.15	-36 03 47.07	M1.5	15.206 \pm 0.029	10.323 \pm 0.021
PH α 14	08 08 33.87	-36 08 10.00	M2	15.85 \pm 0.22	10.299 \pm 0.023
PH α 15	08 08 46.82	-36 07 52.69	M3	15.61 \pm 0.84	10.628 \pm 0.024
PH α 21	08 10 30.91	-36 01 46.39	M4	16.42 \pm 0.13	11.058 \pm 0.023
PH α 34	08 12 47.05	-36 19 17.90	K3	15.16 \pm 0.29	11.031 \pm 0.023
PH α 40	08 13 51.69	-36 14 01.32	M0.5	16.547 \pm 0.080	11.326 \pm 0.021
PH α 41	08 13 56.08	-36 08 01.96	cont.	14.3 \pm 1.1	8.914 \pm 0.024
PH α 44	08 14 21.96	-36 10 03.38	K7 – M0	16.004 \pm 0.045	11.713 \pm 0.019
PH α 51	08 15 55.31	-35 57 58.19	K7 – M0	16.17 \pm 0.37	11.090 \pm 0.023
CG 30 IRS 4	08 09 33.16	-36 04 57.81	12.077 \pm 0.044

REFS. — (a) Pettersson 1987; (b) 2MASS

prior to the HIRES CCD upgrade in 2004, so light was recorded on the former Tektronix 2048 CCD. We used the red collimator and the RG-610 filter. Light was projected through the D1 decker ($1'' \cdot 15 \cdot 14'' \cdot 00$), slit width 4 pixels, yielding a resolving power \sim 34,000. The cross-disperser and echelle angles were set at approximately $1^\circ 41$ and $-0^\circ 28$, respectively, to achieve a wavelength coverage of $6300 - 8750 \text{ \AA}$, spanning 16 orders with $20 - 80 \text{ \AA}$ gaps between the orders. Each night we obtained an internal quartz lamp for flat-fielding and a ThAr lamp for wavelength calibration.

We note our setup is identical to that used in the spectroscopic study of young stars in Taurus-Auriga (White & Hillenbrand 2004). From this previous study, we have a wide range of K- and M-type standards and several young stars observed in an identical fashion for reliable comparisons.

2.2.2 Reduction and Extraction

The HIRES data were reduced using the facility *makee* reduction script written by T. Barlow. The reductions included bias subtraction, flat-fielding, spectral extraction, sky subtraction, and wavelength calibration. The spectra were interpolated onto a log-linear scale for cross-correlation purposes. With the exception of CG 30 IRS 4, the projected spectra have spatial profiles with full widths at half-maximum of $\sim 2''$, set by the seeing at the elevation of

these southern-declination targets (Dec $-36^{\circ}20'$ to $-35^{\circ}57'$). CG 30 IRS 4 is slightly spatially extended; some of the visible light is likely scattered off the nebula. For all stars, we calibrate the wavelength solution using the telluric A-band at $7600 - 7630$ Å, which should remain stable down to 0.015 km s $^{-1}$ (Cochran 1988).

2.3 Spectroscopic Analysis

Five spectral regions of interest are displayed in Figures 2.2 and 2.3, including temperature-sensitive Ca, Fe, and TiO, and gravity-sensitive K I. All 10 stars show Li I $\lambda 6708$ Å absorption (Figure 2.2, 2nd column) and H α emission (Figure 2.4). Stars PH α 34 and 41 show particularly strong H α emission and a myriad of other emission lines, including Ca I $\lambda 6455$ Å, Fe II $\lambda 6456$ Å, K I $\lambda 7700$ Å, and O I $\lambda 8446$ Å. Observations of PH α 41 on two consecutive nights reveal that it is a double-lined spectroscopic binary with a period $\lesssim 2$ days; the components swap redward and blueward position and are well separated in velocity.

2.3.1 Li I $\lambda 6708$ Å Equivalent Width

Lithium equivalent width (Li EW) is a signature of youth and provides a rough stellar age estimate independent from isochrone fits on a color-magnitude diagram. Lithium is destroyed via proton-helium reactions within a star's interior when temperatures reach $\sim 3 \cdot 10^6$ K (Bodenheimer 1965). Surface lithium is depleted in cool stars with outer convective zones over the course of 10 – 100 Myr.

Because of deep convection, significant depletion of atmospheric lithium takes 10 – 20 Myr for mid-M-type stars and ~ 100 Myr for early K-type stars (Jeffries et al. 2014). As a first assessment of youth, we measure Li I $\lambda 6708$ Å equivalent widths (Li EW) using IRAF's Gaussian-fitting *splot* package. Uncertainties stem from ambiguity in the local continuum, with a minimum uncertainty of 0.01 Å imposed to account for systematics.

We report Li equivalent widths from all epochs and include the 2 data in Kim et al. (2005) for reference (see Table 2.2). The majority of the stars show lithium equivalent widths 0.5

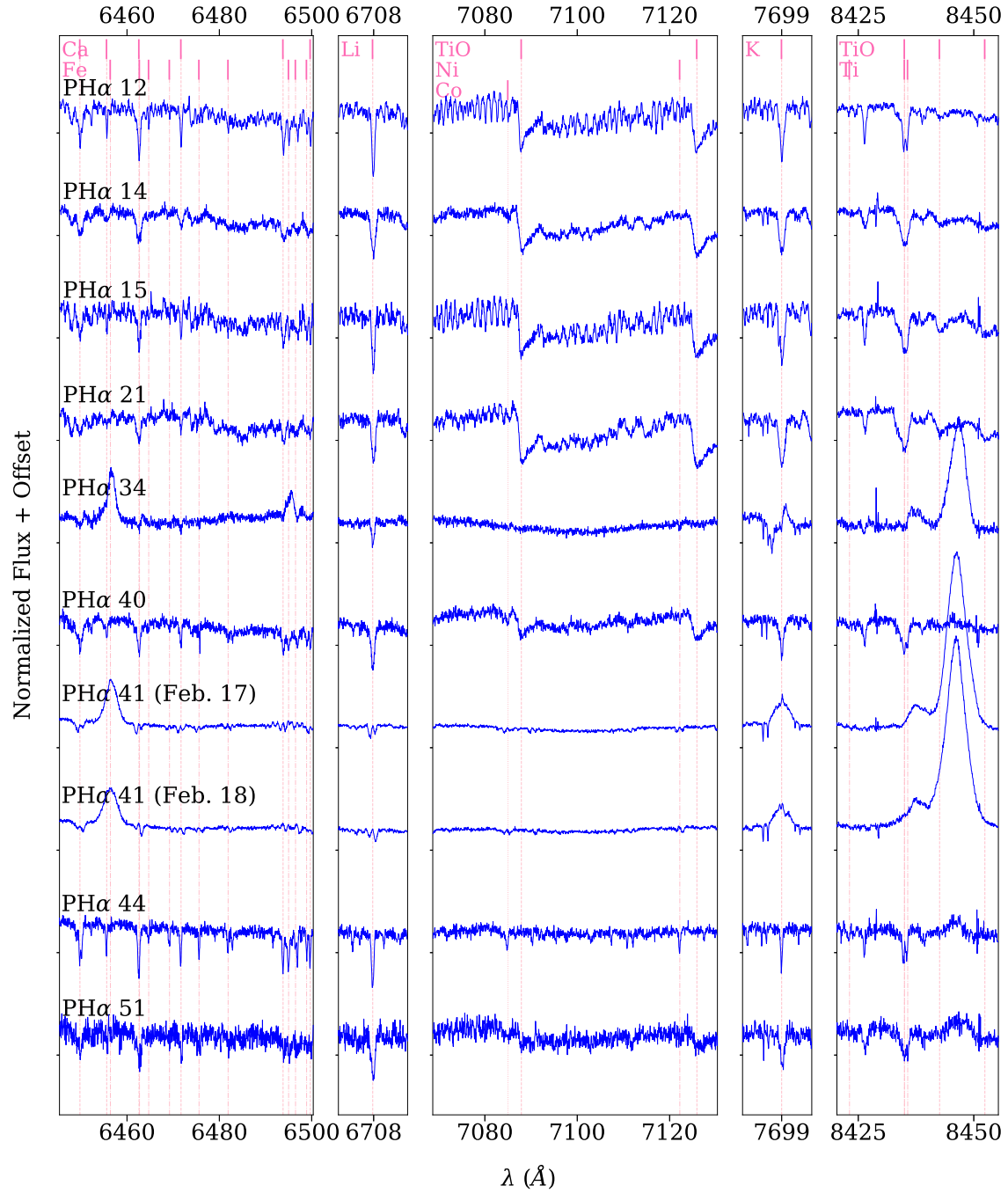


Figure 2.2: Five spectral regions of interest are displayed for the 9 PH α stars. Spectral features are labeled at the top of the figure. The first and last columns show Ca, Fe, and Ti, typically strong in K-type stars (e.g. PH α 44). The middle column shows TiO molecular bands, wide and deep for M-type stars (e.g. PH α 14). The second column shows lithium absorption, associated with young stars. The fourth column tracks surface-gravity with K i λ 7700 Å, which is relatively weak for young stars still in the process of gravitationally settling. All the stars in our sample exhibit a shallowing of spectral lines and bands, called veiling.

– 0.6 Å, similar to stars with no lithium depletion in Taurus-Auriga (e.g. Basri et al. 1991; Magazzú et al. 1992; Martín et al. 1994) or Orion (e.g. Palla et al. 2005, 2007) at ages of 1 – 3 Myr. The 2 stars with much smaller equivalent widths are substantially veiled ($\text{PH}\alpha$ 34; see §2.3.5 on veiling) or veiled and have a spectroscopic companion ($\text{PH}\alpha$ 41). CG 30 IRS 4 shows the highest lithium equivalent width. However, due to noise, the continuum level of CG 30 IRS 4 is more difficult to determine than other stars’.

2.3.2 $H\alpha$ 10%-Widths and Equivalent Widths

White & Basri (2003) demonstrate that the width of the $H\alpha$ emission profile at 10% peak height above the continuum ($H\alpha$ 10% W) more reliably distinguishes classical T Tauri stars (accreting) from weak-line T Tauri stars (non-accreting) than $H\alpha$ equivalent width ($H\alpha$ EW). Using Python, we measure $H\alpha$ 10% W values for the ten stars, ranging from 225 to 621 km s⁻¹ (see Table 2.2). Based on the accretion criterion $W_{10}(H\alpha) > 270$ km s⁻¹ (White & Basri 2003), 8 of our targets are classical T Tauri stars, while $\text{PH}\alpha$ 12 is a weak-line T Tauri star ($H\alpha$ 10% W = 226 km s⁻¹), although only slightly below the classical T Tauri limit. Surprisingly, embedded CG 30 IRS 4 ($H\alpha$ 10% W = 225 km s⁻¹) also falls below the classical T Tauri star limit. However, as noted previously, the continuum level of CG 30 IRS 4 is ambiguous. This star also has jets and outflow (Chen et al. 2008) that might absorb some of its $H\alpha$ emission. Because $\text{PH}\alpha$ 41 exhibits blue-shifted absorption that drops below the continuum, its 10%-widths are lower limits for the whole binary.

We also measure $H\alpha$ EW using IRAF as described for Li I $\lambda 6708$ Å (§2.3.1). The revealed young stars’ $H\alpha$ EW values range from -83 to -11.5 Å, similar to those of accreting T Tauri stars. Embedded CG 30 IRS 4 has the weakest emission, with range -6.6 – -0.5 Å. Our values for $H\alpha$ EW differ from previous values by up to a factor of 2. This is fairly typical of young stellar objects, which tend to vary over short timescales (Pettersson 1987; Kim et al. 2005).

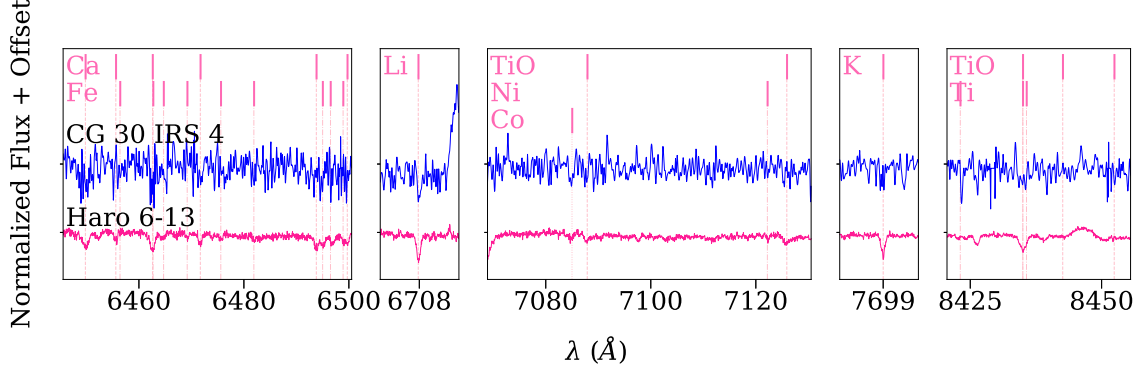


Figure 2.3: We compare the same 5 spectral regions of interest as in Figure 2 for the embedded star CG 30 IRS 4 (blue, smoothed) and the veiled T Tauri star Haro 6-13 (fuchsia) of the same spectral type, M0 (White & Hillenbrand 2004). The infrared source inside the cometary globule has a well defined photosphere.

2.3.3 Radial Velocity

Radial velocities are obtained relative to a catalogue of G-, K-, and M-type dwarf standards (see §2.2.1) with radial velocities accurate to $0.3 - 0.4 \text{ km s}^{-1}$ (Nidever et al. 2002; Valenti & Fischer 2005), slow rotation $\leq 3 \text{ km s}^{-1}$ (Delfosse et al. 1998; Valenti & Fischer 2005), no disks, and no veiling. Through cross-correlation analysis of the Doppler shifts for between 7 and 11 spectral regions (see Figure 2.2), we measure velocities relative to between 5 and 7 standards of similar spectral type to each young star (see Figure ??). We also measure the Doppler shift of the Li I $\lambda 6708 \text{ \AA}$ absorption feature using the T Tauri stars DN Tau and V 836 Tau, with known radial velocities (White & Hillenbrand 2004). Star spots on DN Tau and V 836 Tau may introduce velocity oscillations of 1 km s^{-1} or less (Prato et al. 2008). For some of our young stars, including CG 30 IRS 4, Li I $\lambda 6708 \text{ \AA}$ is the most prominent absorption feature.

Using the uncertainty-weighted mean of the median relative velocities from all spectral regions, we calculate radial velocities v_r relative to the center of mass of the Solar System. Stars within 20 arcminutes of CG 30 have $v_r = 21.99 - 26.77 \text{ km s}^{-1}$, whereas stars within 30 arcminutes of PH α 41 have $v_r = 30.29 - 33.69 \text{ km s}^{-1}$ (see Table 2.3). We estimate uncertainties of $0.15 - 0.89 \text{ km s}^{-1}$.

Table 2.2: Equivalent Widths

Star Name	Date Obs.	Lit. ^a ^b H α EW (Å)	Our H α EW (Å)	$W_{10}(\text{H}\alpha)$ (Å)	Lit. ^b Li EW (Å)	Our Li EW (Å)
PH α 12	2004-04-04	-16.1, -26.6	-11.5 \pm 0.6	-4.94	226	0.54 \pm 0.04
PH α 14	2004-04-04	-22.0, -8.43	-12.9 \pm 0.3	-9.33	427	0.50 \pm 0.06
PH α 15	2004-04-04	-130.5	-45.4 \pm 2.9	-6.46	295	...
PH α 21	2004-04-04	-48.1	-28.9 \pm 1.0	-8.68	397	...
PH α 34	2003-02-17	-60.5	-61.8 \pm 3.2	-13.58	621	...
	2004-04-04		-71.8 \pm 3.8	-12.65	579	0.30 \pm 0.01
PH α 40	2004-04-04	-18.7	-33.0 \pm 0.8	-7.43	340.	...
PH α 41 A	2003-02-17	-98.6	-78.5 \pm 9.3 ^c	<-10.44 ^c	>478 ^c	...
	2003-02-18		-83 \pm 10. ^c	<-10.07 ^c	>461 ^c	0.07 \pm 0.01
	2004-04-04		-80.4 \pm 5.7 ^c	<-11.73 ^c	>537 ^c	0.05 \pm 0.01
PH α 41 B	2003-02-17	-98.6	-78.5 \pm 9.3 ^c	<-10.44 ^c	>478 ^c	...
	2003-02-18		-83 \pm 10. ^c	<-10.07 ^c	>461 ^c	0.11 \pm 0.01
	2004-04-04		-80.4 \pm 5.7 ^c	<-11.73 ^c	>537 ^c	0.08 \pm 0.01
PH α 44	2004-04-04	-50.7	-27.8 \pm 0.9	-8.26	378	...
PH α 51	2003-02-18	-70.1	-54.7 \pm 2.1	-10.25	469	...
CG 30 IRS 4	2003-02-17	...	-0.5 \pm 1.4	-5.26	241	...
	2003-02-17		-3.5 \pm 1.2	-4.98	228	0.60 \pm 0.38
	2003-02-18		-6.6 \pm 1.8	-4.93	225	0.67 \pm 0.11

REFS. — (a) Pettersson 1987; (b) Kim et al. 2005

(c) Because the two H α emission components cannot be resolved, we give H α emission values for the whole binary (see text).

PH α 41 and CG 30 IRS 4 require special handling. For PH α 41, since the components are well separated in velocity, we isolate and independently measure one member of the binary at a time. An overabundance of emission lines forces us to use just 2 – 4 spectral regions to measure the relative velocities of each star. The v_r uncertainties across all 3 epochs are 0.19 – 0.44 km s $^{-1}$ for A and 1.3 – 1.5 km s $^{-1}$ for B (see Table 2.4).

To calculate the binary’s systemic v_r , we determine the two stars’ masses based on the stars’ spectral types and the main-sequence dwarf grid of Pecaut & Mamajek (2013) (see §2.4.1), 0.72 M $_{\odot}$ for the K5 primary and 0.70 M $_{\odot}$ for the K6 secondary. The center-of-mass velocity is then

$$v_{r,cm} = \frac{m_A}{m_A + m_B} v_{r,A} + \frac{m_B}{m_A + m_B} v_{r,B}. \quad (2.1)$$

The v_r errors of the two stars are added in quadrature. We take the error-weighted mean of the three nights’ results for a final systemic $v_r = 29.69 \pm 0.41$ km s $^{-1}$.

To combat CG 30 IRS 4’s low signal-to-noise ratio (4 – 12), we have smoothed the spectra across each 1 Å using IRAF’s *dispcor* routine before performing cross-correlation. Stellar

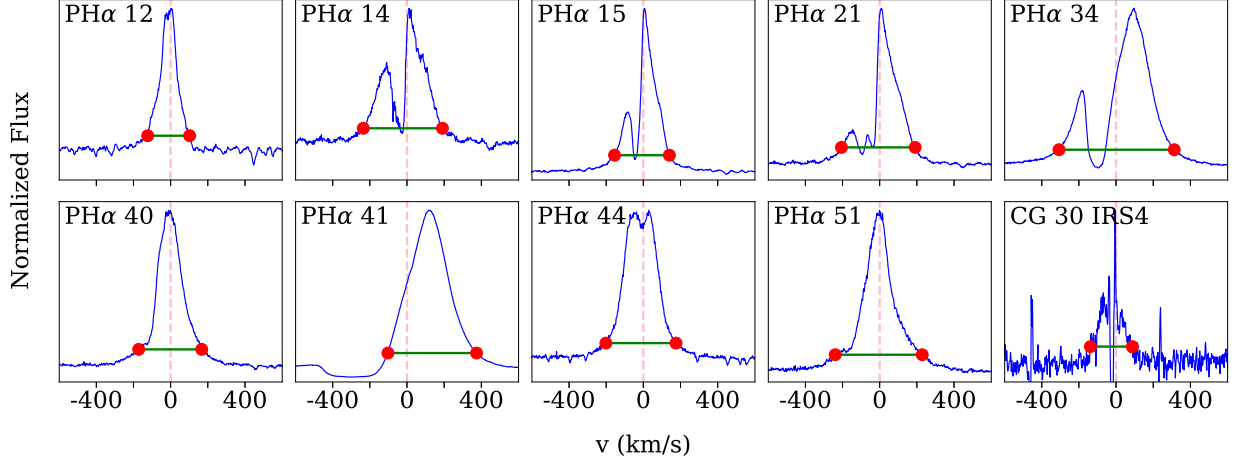


Figure 2.4: We measure H α widths at 10% up the peak (green lines). Red dashed lines mark zero-velocity 6562.8 Å. Blueshifted dips within the emission peaks are likely absorption lines from cool winds.

features are visible in all 3 epochs, including strong lithium absorption and several Ca and Fe lines (Figure 2.3). We obtain $v_r = 22.5 \pm 2.0 \text{ km s}^{-1}$.

2.3.4 Rotational Velocity

We derive stars' projected rotational velocities $v_{rot} \sin(i)$ from the widths of the cross-correlation functions described in the previous section. We artificially broaden the standard spectra following Gray (1992), assuming a limb darkening coefficient $\epsilon = 0.6$, until the width of the standard's auto-correlation peak matches the width of the standard's cross-correlation peak with the young star. As with v_r , we take the error-weighted mean of the 5 – 7 standards' rotational velocity medians of the 7 – 11 spectral regions. We estimate uncertainty from the standard deviation of the median values. Because the velocity resolution and rotation uncertainties add in quadrature, we assume a minimum measurement limit of $\sim 8.8/\sqrt{2} = 6.2 \text{ km s}^{-1}$. Measured values $\leq 6.2 \text{ km s}^{-1}$ are set to 6.2 km s^{-1} . All median values are larger than this number, so specifying this resolution limit does not affect final $v_{rot} \sin(i)$; it serves chiefly to constrain final uncertainties.

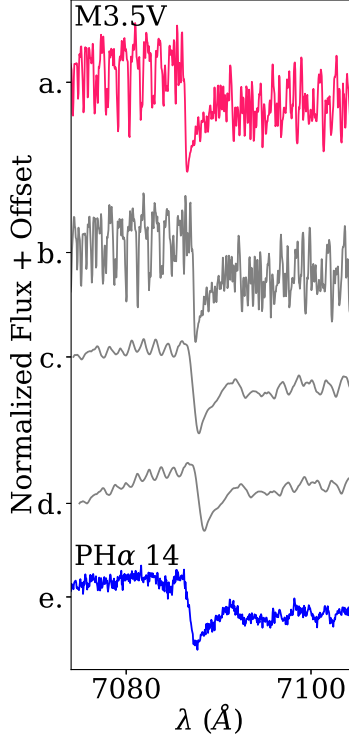


Figure 2.5: M3.5 V standard spectrum (a., fuchsia) is manipulated (gray) with v_r shift (b.), rotational broadening (c.), and veiling (d.) until it matches the young star spectrum of PH α 14 (e., blue).

We obtain $v_{rot} \sin(i) = 6.3 - 27.8 \text{ km s}^{-1}$ (see Table 2.3). CG 30 IRS 4's is the lowest. Uncertainties are $0.2 - 2.7 \text{ km s}^{-1}$. We measure $v_{rot} \sin(i)$ of PH α 41's two components separately, as detailed above for v_r .

2.3.5 Veiling and Spectral Types

The hot spots (up to 10^6 K; Gullbring et al. 2000) from accretion shocks of infalling circumstellar gas produce extra light at UV and optical wavelengths and diminish the depths of spectral lines, or veil them (Hartigan et al. 1989; Hartmann et al. 2016; Rei, Petrov, & Gameiro 2018). We measure this veiling as the ratio of continuum excess to photospheric continuum, $r = F_{ex}/F_{phot}$ (Hartigan et al. 1989). Veiling is wavelength-dependent and tends to be stronger at bluer wavelengths (Hartigan et al. 1991). We measure average veiling r_{6500}

Table 2.3: Radial and Rotational Velocities

Star Name	v_r (km s $^{-1}$)	$v_{rot} \sin(i)$ (km s $^{-1}$)
PH α 12	23.07 ± 0.15	8.0 ± 0.6
PH α 14	26.77 ± 0.89	27.8 ± 2.7
PH α 15	21.99 ± 0.20	11.2 ± 0.5
PH α 21	24.12 ± 0.21	20.4 ± 1.1
PH α 34	31.65 ± 0.29	12.7 ± 0.5
PH α 40	32.16 ± 0.29	13.2 ± 0.8
PH α 41 A	29.69 ± 0.41^a	14.4 ± 0.7
PH α 41 B	29.69 ± 0.41^a	10.7 ± 1.2
PH α 44	30.29 ± 0.15	8.3 ± 0.6
PH α 51	33.69 ± 0.44	10.6 ± 1.1
CG 30 IRS 4	22.5 ± 2.0	6.3 ± 0.2

REFS. (a) reported v_r for PH α 41 A and B is the systemic velocity of the pair (see text).

 Table 2.4: PH α 41 A and B Velocities Across 3 Epochs

MJD	v_r (km s $^{-1}$)		$v_{rot} \sin(i)$ (km s $^{-1}$)	
	A	B	A	B
52687.47	4.27 ± 0.19	51.7 ± 1.3	16.4 ± 1.1	12.6 ± 3.1
52688.48	58.49 ± 0.44	1.1 ± 1.5	14.4 ± 1.4	9.0 ± 1.4
53099.35	63.73 ± 0.32	-0.7 ± 1.5	11.8 ± 1.2	17.2 ± 3.0

in 4 spectral regions near 6500 Å to trace continuum excess in the R band, and r_{8400} in 3 regions near 8400 Å for the I band.

Measuring veiling involves adding a flat, featureless continuum to a standard star’s spectrum and renormalizing the spectrum until its lines are shallow enough to match the young star spectrum. Doing so requires properly accounting for v_r and $v_{rot} \sin(i)$. Figure 2.5 illustrates the process for M3.5V-type standard GL 669 A and young star PH α 14. In our sample, R -band veiling r_{6500} ranges from 0.16 to 7.49, and I -band veiling ranges from 0.00 to 7.54.

Measurement of veiling is sensitive to absorption strength and thus to assigned spectral type. While minimum root-mean-square values from the cross-correlation procedure rec-

ommend likely spectral types, all spectral types are confirmed through visual inspection of line strengths, line ratios, and TiO band depths. We find spectral types M4.5 to K5, with uncertainties of 0.5 spectral class for M-type stars and 1 spectral class for K-type stars (see Table 2.5). The spectral types we assign differ somewhat from those given in Pettersson (1987) but are based on higher resolution spectra and account for veiling.

Veiling uncertainties are derived from the sample standard deviation to veiling values from spectral types 0.5 – 1 classes above and below the assigned spectral type. We impose a veiling uncertainty lower limit of 0.10 to account for continuum uncertainty and systematics.

$\text{PH}\alpha$ 41 A and B (spectral types K5 and K6) are once again handled specially. Light from the companion contaminates each star's measured continuum excess, causing the above procedure to overestimate the veiling. What we measure for $\text{PH}\alpha$ 41 A and B are $r_A = (F_{ex} + F_B)/F_A$ and $r_B = (F_{ex} + F_A)/F_B$, where F_{ex} is the combined continuum excesses of both stars: $F_{ex} = F_{ex,A} + F_{ex,B}$; there is no way to determine the relative contribution of each to the total excess with this analysis. We define combined veiling for each star as follows:

$$r'_A = \frac{F_{ex}}{F_A} = r_A - \frac{F_B}{F_A} \quad (2.2)$$

$$r'_B = \frac{F_{ex}}{F_B} = r_B - \frac{F_A}{F_B}, \quad (2.3)$$

where we know the flux ratios of the two photospheres from their spectral types K5 and K6: $F_A/F_B = 1.629$ (Pecaut & Mamajek 2013). It is these combined veiling values r'_A and r'_B that we report for $\text{PH}\alpha$ 41 A and B, respectively.

Veiling values range from 0.16 to 0.94 near 6500 Å and from 0.0 to 1.36 near 8400 Å for most of the 10 young stars (see Table 2.5). The values soar to 3.1 – 7.54 for $\text{PH}\alpha$ 34, 41 A, and 41 B, the stars with abundant emission lines. The presence of numerous emission lines is associated with strong accretion and possibly a second source of veiling: In addition to continuum veiling from accretion-fed hot spots on the star, line-dependent veiling can

result from abnormal chromospheric structures heated by particularly powerful accretion (Rei, Petrov, & Gameiro 2018). CG 30 IRS 4 (spectral type M0) shows moderate veiling, 0.86 ± 0.10 near 6500 Å and 0.15 ± 0.20 near 8400 Å.

Table 2.5: Veiling and Spectral Types

Star Name	Spectral Type	r_{6500}	r_{8400}
PH α 12	M3 \pm 0.5	0.16 ± 0.13	0.02 ± 0.10
PH α 14	M3.5 \pm 0.5	0.21 ± 0.18	0.00 ± 0.10
PH α 15	M4 \pm 0.5	0.20 ± 0.15	0.00 ± 0.20
PH α 21	M4.5 \pm 0.5	0.29 ± 0.10	0.31 ± 0.37
PH α 34	K7 \pm 1.0	6.04 ± 0.63	3.1 ± 1.7
PH α 40	M0.5 \pm 0.5	0.67 ± 0.11	0.45 ± 0.10
PH α 41 A	K5 \pm 1.0	5.24 ± 0.22	3.62 ± 0.33
PH α 41 B	K6 \pm 1.0	7.49 ± 0.10	7.54 ± 0.10
PH α 44	K5 \pm 1.0	0.21 ± 0.10	0.15 ± 0.14
PH α 51	M0.5 \pm 0.5	0.94 ± 0.15	1.36 ± 0.51
CG 30 IRS 4	M0 \pm 1.0	0.86 ± 0.10	0.15 ± 0.20

2.4 Stellar Properties

The determined spectroscopic properties of the 9 PH α stars and CG 30 IRS 4 are used in combination with photometry and parallax measurements to estimate their stellar luminosities and temperatures for comparison with stellar evolutionary models. We add 10 pre-main sequence G-, K-, and M-type stars identified by Kim et al. (2005) to our analysis, for which Kim et al. (2005) provide spectroscopic and photometric results. KWW 975, 1043, and 1892 are already included in our analysis as PH α 14, 15, and 12. Eleven of the 13 young stars studied by Kim et al. (2005) are believed to be dynamically related to CG 30. We also look at the star IRAS 08159-3543 near RCW 19 (see Figure 2.1), known to power a bipolar wind and ascribed an incredible luminosity of $24,000 L_\odot$ (Neckel & Staude 1995; Bronfman et al. 1996). In all, we photometrically examine 21 young stars.

2.4.1 Photometry

We flux-average Johnson-Cousins $UBVRI$ photometry from Pettersson (1987) and Kim et al. (2005) (see Table 2.1 for V magnitudes). We propagate fluxes' sample standard deviations into magnitude uncertainties. $\text{PH}\alpha\ 15$ and $\text{PH}\alpha\ 41$ vary by more than 1.5 mag, so their magnitude uncertainties are large, 0.84 mag and 1.1 mag, respectively.

For all 21 stars from Pettersson (1987), Neckel & Staude (1995), and Kim et al. (2005), we gather J , H , and K magnitudes from 2MASS (Skrutskie et al. 2006). Stars CG 30 IRS 4, KWW XRS 9, and IRAS 08159-3543 have only infrared photometry. 2MASS lacks J and H uncertainties for CG 30 IRS 4, indicating these values are likely brightness upper limits.

For the unresolved binary $\text{PH}\alpha\ 41$, we divide the flux in each band between $\text{PH}\alpha\ 41\ A$ and B based on the absolute-magnitude-derived K5/K6 flux ratio of Pecaut & Mamajek (2013). This assumes any excess optical or infrared light scales similarly for the 2 components.

Intrinsic colors and effective temperatures are assigned based on spectral types and the main-sequence dwarf grid of Pecaut & Mamajek (2013). Though Pecaut & Mamajek (2013) offer a grid specifically for young stars, we opt for their dwarf grid for its inclusion of $R - I$ colors, currently unavailable in the young star grid. The mismatch in evolutionary stages of the dwarf color grid and young targets may introduce small systematic errors, discussed where encountered.

For each of the following steps, we propagate magnitude uncertainties in the flux regime, where errors are assumed to be Gaussian. Magnitude uncertainties from the empirical data of Pecaut & Mamajek (2013) are roughly 0.001 – 0.01 mag, from Rieke & Lebofsky (1985), 0.03 mag; both are neglected.

2.4.2 Veiling Correction

To measure the brightness of the young stars' photospheres and determine their luminosities, we must unveil and deredden the stars. Using veiling values r_{6500} for R and r_{8400} for I ,

we remove excess continuum as follows:

$$R_u = R + 2.5 \log(1 + r_{6500}) \quad (2.4)$$

$$I_u = I + 2.5 \log(1 + r_{8400}), \quad (2.5)$$

where R_u and I_u are the unveiled magnitudes. We apply this procedure to the 9 PH α stars, for which we have spectroscopically determined veiling and optical photometry. CG 30 IRS 4 has measured veiling values but no optical photometry.

Kim et al. (2005) did not measure veiling values. All 10 KWW stars are reportedly weak-line T Tauri stars (Kim et al. 2005), associated with weak or no accretion and weak or no veiling. We therefore set the veiling for these stars to zero, but we include a veiling uncertainty of 0.2 in r_{6500} and 0.1 in r_{8400} in case the stars resemble PH α 12, a weak-line T Tauri star with slight veiling. IRAS 08159-3543, reportedly a deeply embedded F0 – G0 star with broad H α emission (Neckel & Staude 1995), lacks veiling measurements and optical photometry.

2.4.3 Extinction Correction

Intervening dust in the ISM and a star’s own disk dims and reddens the star’s light, so we quantify light lost through how reddened its color is compared to an unreddened standard’s. Because the R and I bands dodge the brunt of blue veiling and infrared excess, $R - I$ is considered the most reliable color for determining the visual extinction of young stars (Meyer et al. 1997). For the 9 PH α stars and 9 KWW stars with optical photometry, we quantify extinction A_V by comparing unveiled $R_u - I_u$ to intrinsic $(R - I)_{int}$ of Pecaut & Mamajek (2013) and utilizing the extinction relations of Rieke & Lebofsky (1985). The A_V values from this $R - I$ approach range from 0.00 to 2.3 mag. Comparison of Pecaut & Mamajek (2013) $V - I$ main-sequence colors to young star colors suggests that the $(R - I)_{int}$ we assign will tend to be systematically slightly blue and therefore slightly overestimate extinctions.

For the 3 stars CG 30 IRS 4, KWW XRS 9, and IRAS 08159-3543 without optical photometry, we derive extinctions using the classical T Tauri star locus of Meyer et al. (1997) in $JH-HK$ color-color space. We solve the locus for extinction A_V :

$$A_V = \frac{0.58(H - K) - (J - H) + 0.52}{1.58A_H/A_V - 0.58A_K/A_V - A_J/A_V}, \quad (2.6)$$

where $A_J/A_V = 0.282$, $A_H/A_V = 0.175$, and $A_K/A_V = 0.112$ (Rieke & Lebofsky 1985). Resulting A_V values range from 0.0 to 0.99 magnitudes.

This $JH-HK$ method does not account for veiling or infrared excess directly and is based predominantly on spectral type M0, with correspondingly red $J - K$ color (Meyer et al. 1997). The extinction of IRAS 08159-3543, with a spectral type between F0 and G0, is likely underestimated. The extinction of CG 30 IRS 4 may also be underestimated, as its J and H magnitudes are only upper limits.

2.4.4 Bolometric Correction

We estimate each star's apparent bolometric magnitude by adding a spectral-type-determined bolometric correction BC_V and intrinsic color $(V - M_\lambda)_{int}$ from Pecaut & Mamajek (2013) to each star's unveiled and dereddened R_{ud} and I_{ud} and dereddened J_d magnitudes. Specifically, for the 18 stars with optical photometry, we define final apparent bolometric magnitude m_{bol} as the flux-weighted average of the two bolometric magnitudes calculated from R_{ud} and I_{ud} . These two bolometric magnitudes are within 0.4 of each other for all 18 stars and identical for 13. For the 3 stars without optical photometry, we set m_{bol} equal to bolometric magnitude calculated from J_d . Final apparent bolometric magnitudes for the 21 stars range from 10.90 to 16 mag.

Bolometric magnitude uncertainties range from 0.23 to 2.1 mag. In most cases, the young stars' fundamental photometric variability is the largest source of uncertainty.

2.4.5 Near Infrared Excess

We quantify young stars' near-infrared excesses as $\Delta K = (J - K)_{obs} - (J - K)_{int}$, from observed $J - K$ color versus intrinsic Pecaut & Mamajek (2013) main-sequence $J - K$ color. Near infrared excesses here range from -0.19 to 1.3 mag (see Table 2.6). Uncertainties are flux-propagated from the uncertainties in photometry. These excess values appear somewhat correlated with veiling values, and most stars with low veiling have no infrared excess. Our results for the 10 KWW stars corroborate those of Kim et al. (2005), who found only KWW 873 exhibits an infrared excess. In total, 7 of the 21 stars show an infrared excess $\gtrsim 0.1$ mag, including CG 30 IRS 4. Because CG 30 IRS 4's J magnitude is an upper limit only, its near infrared excess may be underestimated.

2.4.6 Distances from *Gaia* DR2 Parallaxes and Apparent Associations

Gaia DR2 parallaxes are available for 16 of the 21 stars. We adopt the probabilistically inferred distances d of Bailer-Jones et al. (2018) (see Table 2.6). Eleven *Gaia* DR2 stars within 20.1 arcminutes of CG 30, excepting PH α 21, which has a negative parallax (see Bailer-Jones et al. 2018), appear fairly clustered at a distance of ~ 360 pc, especially the 6 stars PH α 14 and 15 and KWW 464, 598, 1863, and 2205, with distances 354.1 – 370 pc. Based on these 6 stars, we define the CG 30 Association and assign it the six stars' error-weighted-mean distance of 358.1 ± 2.2 pc. This value is similar to distances to ζ Pup and γ^2 Vel at the heart of the Gum Nebula (Apellániz et al. 2008). In the vicinity of the CG 30 Association are 8 candidate members, 3 with positive *Gaia* DR2 parallaxes, 1 with a negative parallax, and 4 with none. The 4 with positive parallaxes are 121 – 420 pc ahead of or behind the CG 30 Association distance. For purposes of calculating luminosity, we assign the 4 candidate stars without parallaxes the adopted CG 30 Association distance, including CG 30 IRS 4, assumed to be inside cometary globule CG 30. We thus suggest 358.1 ± 2.2 pc is the distance to the entire CG 30/31/38 cometary globule complex. The globules are then 34^{+10}_{-7} pc from ζ Pup and 70^{+12}_{-1} pc from γ^2 Vel.

KWW XRS 9’s distance of 223.3 ± 2.4 pc is inconsistent with the CG 30 Association. Its kinematics are also inconsistent with the association’s (see §2.5.1.2). We also exclude the star from candidacy.

$\text{PH}\alpha$ 41 lies farther away at 985^{+32}_{-30} pc, which places it beyond the Gum Nebula. Negative parallaxes could place $\text{PH}\alpha$ 40 and 44 even farther away; however, parallaxes for faint objects at distances $\gtrsim 1$ kpc are highly uncertain (Lindegren et al. 2018; Bailer-Jones et al. 2018). $\text{PH}\alpha$ 40, 41, 44, and 51, and possibly $\text{PH}\alpha$ 34, visually trace a dust lane (Pettersson 1987), and their v_r agree reasonably well, $29.69 - 33.69 \text{ km s}^{-1}$. Under the assumption that the young stars tracing the dust lane near $\text{PH}\alpha$ 41 are related to $\text{PH}\alpha$ 41 (see §2.5.1.2), we group $\text{PH}\alpha$ 40, 41, 44, and 51 and assign $\text{PH}\alpha$ 51 the distance to $\text{PH}\alpha$ 41.

At 153^{+17}_{-14} pc, $\text{PH}\alpha$ 34 is apparently a foreground star. IRAS 08159-3543 has a small and very uncertain parallax, yielding a distance of 2500 pc. It is probably beyond the Gum Nebula.

2.4.7 Bolometric Luminosity

From m_{bol} and d , we calculate bolometric luminosity L in Solar units based on Solar bolometric magnitude $M_{bol,\odot} = 4.7554 \pm 0.0004$ mag (Pecaut & Mamajek 2013). Results range from 0.02 to 76 L_\odot , with median $L = 0.60 L_\odot$ (see Table 2.6). Flux-propagated bolometric magnitude uncertainties and distance uncertainties are converted to asymmetric luminosity errors. Stars with the largest night-to-night variations in magnitude ($\text{PH}\alpha$ 15 and 41) and stars with unmeasured distances ($\text{PH}\alpha$ 21, 40, and 44) have the largest luminosity uncertainties. Because our comparisons to a main-sequence color grid causes a slight systematic overestimation of extinction (see §2.4.3), young star luminosities may be systematically high, 5.6% on average, 26% at most, based on flux-propagation of extinction errors.

Table 2.6: HR Diagram Parameters

Star Name	A_V (mag)	ΔK (mag)	m_{bol} (mag)	Parallax (mas)	d (pc)	T_{eff} (K)	L (L_\odot)	d_{soc} (pc)
CG 30 Association								
PH α 14	1.0 ± 1.2	-0.04 ± 0.10	13.07 ± 0.53	2.83 ± 0.50	370^{+100}_{-67}	3250^{+160}_{-50}	$0.65^{+0.48}_{-0.39}$	265
PH α 15	1.1 ± 4.3	0.09 ± 0.11	12.6 ± 1.9	2.794 ± 0.036	$354.4^{+4.7}_{-4.5}$	3200^{+50}_{-100}	0.9 ± 1.6	191
KWW 464	0.00 ± 0.96	-0.19 ± 0.11	13.88 ± 0.39	2.746 ± 0.031	$360.5^{+4.1}_{-4.0}$	3410^{+90}_{-160}	0.29 ± 0.11	500
KWW 598	2.25 ± 0.94	0.04 ± 0.11	13.49 ± 0.38	2.798 ± 0.072	$354.1^{+9.3}_{-8.8}$	3550^{+100}_{-50}	0.40 ± 0.14	482
KWW 1863	0.52 ± 0.92	0.05 ± 0.13	12.60 ± 0.37	2.774 ± 0.031	$356.9^{+4.0}_{-3.9}$	3700^{+75}_{-50}	0.92 ± 0.32	360
KWW 2205	0.00 ± 0.93	-0.14 ± 0.10	13.74 ± 0.38	2.709 ± 0.053	$365.5^{+7.2}_{-7.0}$	3200^{+50}_{-100}	0.34 ± 0.12	327
CG 30 Association Candidates with Gaia DR2 Distances								
PH α 21	0.3 ± 1.3	-0.07 ± 0.10	13.77 ± 0.57	-0.01 ± 0.29	3800^{+2500*}_{-1500}	3100^{+100}_{-70}	36^{+51}_{-34}	280
KWW 873	0.55 ± 0.92	0.11 ± 0.10	12.34 ± 0.37	4.21 ± 0.22	237^{+14}_{-12}	4050^{+150}_{-200}	0.52 ± 0.19	424
KWW 1637	0.00 ± 0.92	0.05 ± 0.10	11.15 ± 0.37	1.42 ± 0.38	780^{+670}_{-250}	4200^{+250}_{-150}	17^{+29}_{-12}	282
KWW 1953	0.30 ± 0.93	-0.18 ± 0.10	13.26 ± 0.38	2.20 ± 0.23	456^{+55}_{-45}	3410^{+90}_{-160}	$0.83^{+0.35}_{-0.33}$	376
CG 30 Association Candidates Assigned CG 30 Association Distance								
PH α 12	0.35 ± 0.67	-0.01 ± 0.10	13.15 ± 0.29	...	$[358.1 \pm 2.2]$	3410^{+90}_{-160}	0.56 ± 0.15	358
KWW 1055	0.97 ± 0.92	0.06 ± 0.11	13.33 ± 0.37	...	$[358.1 \pm 2.2]$	5530^{+240}_{-250}	0.48 ± 0.16	2776
KWW 1302	0.00 ± 0.92	-0.05 ± 0.14	13.34 ± 0.37	...	$[358.1 \pm 2.2]$	3200^{+50}_{-100}	0.47 ± 0.16	271
CG 30 IRS 4	0.99	0.61	16	...	$[358.1 \pm 2.2]$	3850^{+200}_{-75}	0.04	1882
Stars near PH α 41 Outside the Gum Nebula								
PH α 40	1.55 ± 0.53	0.05 ± 0.10	14.40 ± 0.23	-0.21 ± 0.27	4400^{+2500*}_{-1600}	3775 ± 75	27^{+31}_{-20}	876
PH α 41 A	2.0 ± 5.0	0.52 ± 0.10	14.6 ± 2.1	0.988 ± 0.032	985^{+32}_{-30}	4450^{+170}_{-250}	1.1 ± 2.2	1762
PH α 41 B	0.7 ± 5.0	0.52 ± 0.10	16.3 ± 2.1	0.988 ± 0.032	985^{+32}_{-30}	4200^{+250}_{-150}	0.23 ± 0.45	3034
PH α 44	1.46 ± 0.65	0.18 ± 0.12	14.29 ± 0.28	-0.66 ± 0.18	7000^{+2800*}_{-2000}	4450^{+170}_{-250}	76^{+64}_{-48}	1526
PH α 51	0.0 ± 1.3	0.29 ± 0.11	15.95 ± 0.55	...	$[985^{+32}_{-30}]$	3775 ± 75	0.32 ± 0.17	1789
Other Stars Outside the Gum Nebula								
PH α 34	2.3 ± 1.9	0.34 ± 0.12	14.74 ± 0.85	6.53 ± 0.64	155^{+18}_{-15}	4050^{+150}_{-200}	0.02 ± 0.02	1283
KWW XRS 9	0.0 ± 1.1	-0.00 ± 0.10	10.90 ± 0.31	4.451 ± 0.048	223.3 ± 2.4	5660^{+20}_{-70}	1.73 ± 0.50	1073
IRAS 08159-3543	0.0	1.3	14	0.38 ± 0.52	2500^{+2200}_{-1200}	6510^{+690}_{-590}	13	9536

NOTE — Distances and temperatures in brackets [] are assigned according to possible physical association with another star or stars (see text). Distances followed by asterisks * are derived from negative parallaxes (see Bailer-Jones et al. 2018). The top 14 stars are considered part of the CG 30 Association in the Gum Nebula. The other 7 stars are not and lie outside the Gum Nebula.

2.4.8 Effective Temperature

We assign young stars' effective temperatures T_{eff} based on their spectral types and the main-sequence grid of Pecaut & Mamajek (2013). Temperatures range from 3100 K to 6510 K (see Table 2.6). For most stars, we take uncertainties as the difference in temperature between best spectral type and the types 0.5 – 1 above and below, according to spectral type uncertainty (see §2.3.5). KWW 1055, with spectral type range G2 to K0 (Kim et al. 2005), is assigned an intermediate spectral type of G7 with temperature 5530^{+240}_{-250} K. IRAS 08159-3543 is assigned a range of spectral types from F0 to G0 and has a corresponding range in temperature (Neckel & Staude 1995).

Though Pecaut & Mamajek (2013) provide pre-main-sequence temperatures, we use their main-sequence temperatures to maintain consistence with our use of their main-sequence

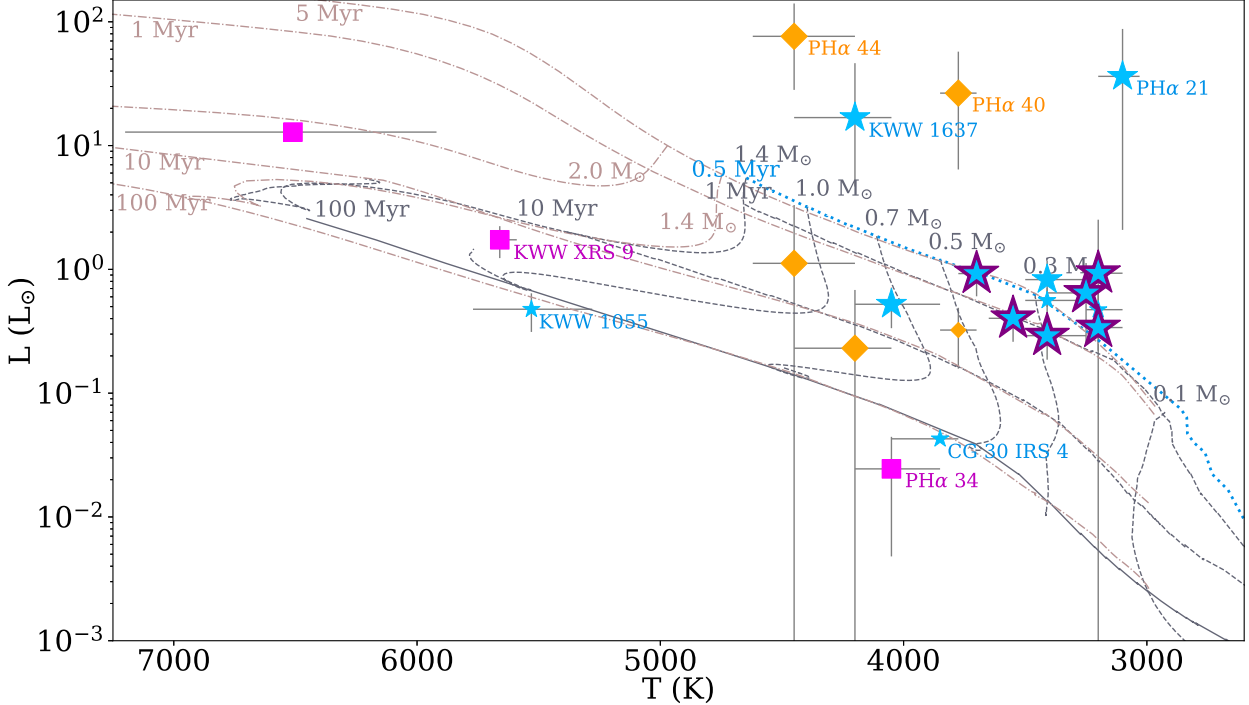


Figure 2.6: We plot luminosity vs. temperature for the 14 CG 30 Association stars and candidates (blue star symbols), the 5 stars near PH α 41 (orange diamonds), and the 3 other stars (magenta squares). The 6 defining members of the CG 30 Association are outlined in purple. *Gaia* DR2 distances are incorporated where available and are represented with large symbols. Stars assigned distances for possible relation to the CG 30 Association or PH α 41 (see text and Table 2.6) are represented with small symbols. Mass tracks and isochrones are from Baraffe et al. (2015) (dotted and dashed, gray, mass $\leq 1.4 M_\odot$) and supplemented with MESA (dot-dashed, paler pinker gray, mass $> 1.4 M_\odot$; Dotter 2016; Choi et al. 2016; Paxton et al. 2011, 2013, 2015). The Baraffe et al. (2015) 0.5 Myr isochrone (blue dotted) passing through the CG 30 Association stars is used to calculate isochrone distances (see Table 2.6). Eight stars of interest are labeled.

$R - I$ colors. Consequent systematic differences in temperature range from -130 to +310 K for G-, K-, and M-type stars. These differences are comparable to uncertainties from determining spectral type and on average may overestimate temperature by 100 K.

2.4.9 Masses and Ages from an HR Diagram

We plot the 21 stars' L vs. T on an HR diagram, along with the mass tracks and isochrones of Baraffe et al. (2015) for comparison (Figure 2.6). All temperatures, photometric properties, and distances are listed in Table 2.6, grouped by possible associations.

Most of the stars apparently have masses $< 1.0 M_{\odot}$, as expected of K- and M-type young stars. Of the 14 CG 30 Association stars and candidates, 12 map to an age of near or less than 1 Myr. Isochrones from Baraffe et al. (2015) and MESA (Figure 2.6) and from Baraffe et al. (1998) suggest an age of ~ 0.5 Myr, while isochrones from Siess et al. (2000) and Feiden (2016) suggest an age of ~ 1 Myr. In all scenarios, the majority of stars near CG 30 appear to belong to a very young, coeval population aged $\lesssim 1$ Myr. The G-type star KWW 1055, as well as kinematically disqualified KWW XRS 9, might be older, perhaps 50-100-Myr-old field stars as Kim et al. (2005) suggests.

The remaining CG 30 Association star, CG 30 IRS 4 itself, appears very underluminous compared to other CG 30 Association members and candidates. Its position near the zero-age main sequence is inconsistent with its embedded state, strong lithium absorption, and signatures of accretion. We suspect this stems from the scattering of the star's light, consistent with its spatially extended appearance (see §2.2.1), and the underestimation of its extinction ($A_V = 0.99$). Photospheres revealed through scattered light (e.g. HL Tau, HV Tau C; White & Ghez 2001) are artificially blue, causing the extinction to be underestimated. The star's J and H magnitudes are also only upper limits.

$\text{PH}\alpha$ 34 also sits below the zero-age main sequence on the HR diagram. This star exhibits heavy veiling, which can be associated with underestimated luminosity (White & Ghez 2001).

The stars $\text{PH}\alpha$ 21, 40, and 44 and KWW 1637 appear markedly overluminous, 12 – 230 times brighter than the 1 Myr isochrone at their temperatures. The distance 780^{+670}_{-250} pc to KWW 1637 is relatively uncertain and may be overestimated. The negative-parallax distances to $\text{PH}\alpha$ 21, 40, and 44 may especially be overestimated, feasibly by a factor of 4 – 10 considering *Gaia* DR2's drop in reliability past 1 kpc values (Lindegren et al. 2018; Bailer-Jones et al. 2018).

The broad $\text{H}\alpha$ emissions, Li absorptions, veiling values, and positions on the HR diagram confirm that most of the stars studied here are young. Many of the CG 30 Association stars and candidates sit at or above the 1 Myr isochrone. If we assume an age of 0.5 Myr, we can

use the 0.5 Myr isochrone to determine an isochrone distance d_{isoc} for given T_{eff} and m_{bol} . This allows us to estimate distances without *Gaia* DR2 data, and to test results where *Gaia* DR2 data are available.

Isochrone distances vary from 191 to 9536 pc (see Table 2.6). Values for the 14 CG 30 Association members and candidates hover around a median of 360. pc, suggesting the 14 stars are indeed very young, inside the Gum Nebula, and possibly related to each other. Isochrone distances for stars spatially near PH α 41 are 109 – 804 pc off from PH α 41’s distance, much shorter than the Bailer-Jones et al. (2018) estimates. The isochrone distance to PH α 34 (1283 pc) is also more similar to PH α 41’s *Gaia* DR2 distance (985^{+32}_{-30} pc) than to PH α 34’s *Gaia* DR2 distance (155^{+18}_{-15} pc). Isochrone distances for PH α 41 itself, KWW XRS 9, and IRAS 08159-3543 are vast overestimates. The stars near PH α 41 and other stars are not likely related to CG 30.

2.5 Discussion

We have assembled stellar properties of 21 stars at the northern edge of the Gum Nebula. The youth and proximity of 14 of these stars, specifically the CG 30 Association stars and candidates studied by Pettersson (1987) and Kim et al. (2005), strongly suggest they formed as one population $\lesssim 1$ Myr ago.

2.5.1 Kinematics

Radial velocities coupled with *Gaia* DR2 proper motions allow us to investigate the 3-D motions of stars in this region (see Figure 2.7). We assemble v_r for the 9 PH α stars and CG 30 IRS 4 from our own spectroscopic analysis. For the 10 KWW stars and IRAS 08159-3543, we convert the local standard of rest velocities of Kim et al. (2005) and Bronfman et al. (1996) to v_r by adding 17.3 km s $^{-1}$ to each. *Gaia* DR2 and Choudhury & Bhatt (2009) provide proper motions for 18 of the 21 stars studied here (see Table 2.7).

Table 2.7: Proper Motions and Radial Velocities

Star Name	v_r (km s $^{-1}$)	μ_α (mas yr $^{-1}$)	μ_δ (mas yr $^{-1}$)
CG 30 Association			
PH α 14	26.77 \pm 0.89	-7.32 \pm 0.90	11.72 \pm 0.90
PH α 15	21.99 \pm 0.20	-7.579 \pm 0.068	11.451 \pm 0.067
KWW 464	24.0 \pm 3.0 ^a	-7.510 \pm 0.051	11.603 \pm 0.051
KWW 598	21.5 \pm 3.0 ^a	-7.89 \pm 0.13	10.98 \pm 0.13
KWW 1863	26.2 \pm 3.0 ^a	-7.400 \pm 0.056	12.025 \pm 0.056
KWW 2205	25.3 \pm 3.0 ^a	-7.728 \pm 0.093	11.675 \pm 0.087
CG 30 Association Candidates with Gaia DR2 Distances			
PH α 21	24.12 \pm 0.21	-6.26 \pm 0.48	6.62 \pm 0.57
KWW 873	22.3 \pm 3.0 ^a	-4.19 \pm 0.38	9.15 \pm 0.39
KWW 1637	22.8 \pm 3.0 ^a	-4.55 \pm 0.77	7.81 \pm 0.78
KWW 1953	24.5 \pm 3.0 ^a	-6.14 \pm 0.39	12.79 \pm 0.40
CG 30 Association Candidates Assigned CG 30 Group Distance			
PH α 12	23.07 \pm 0.15	-6.5 \pm 4.8 ^b	7.7 \pm 4.7 ^b
KWW 1055	20.0 \pm 3.0 ^a
KWW 1302
CG 30 IRS 4	22.5 \pm 2.0
Stars near PH α 41 Outside the Gum Nebula			
PH α 40	32.16 \pm 0.29	-1.95 \pm 0.43	4.76 \pm 0.51
PH α 41	29.69 \pm 0.41 ^c	-4.738 \pm 0.050	4.791 \pm 0.051
PH α 44	30.29 \pm 0.15	-3.27 \pm 0.29	7.23 \pm 0.31
PH α 51	33.69 \pm 0.44	-6.4 \pm 4.8 ^b	0.5 \pm 4.6 ^b
Other Stars Outside the Gum Nebula			
PH α 34	31.65 \pm 0.29	-9.0 \pm 1.1	6.4 \pm 1.1
KWW XRS 9	-74.1 \pm 3.0 ^a	-22.948 \pm 0.072	21.203 \pm 0.077
IRAS 08159-3543	49.2	-4.03 \pm 0.91	1.67 \pm 0.88

REFS. — (a) Kim et al. 2005; (b) Choudhury & Bhatt 2009

NOTE — (c) reported v_r for PH α 41 is the systemic v_r of the binary (see text).

2.5.1.1 CG 30 Association

Radial velocities, available for 13 of the 14 CG 30 Association stars and candidates, support the proposition of Kim et al. (2005) that several stars near CG 30 are dynamically related. A dispersion of $\leq 5 \text{ km s}^{-1}$ is typical of open clusters (Soubiran et al. 2018), while $1 - 2 \text{ km s}^{-1}$ is typical of young open clusters. The 6 defining members of the CG 30 Association recede at $v_r = 21.5 - 26.77 \text{ km s}^{-1}$, with error-weighted mean 22.3 km s^{-1} and sample standard deviation 2.0 km s^{-1} . Including all candidates barely increases the v_r range to $20.0 - 26.77 \text{ km s}^{-1}$, with error-weighted mean 23.1 km s^{-1} and sample standard deviation 1.9 km s^{-1} . Thus v_r data support the grouping of 13 of the CG 30 Association members and candidates, including KWW 1055, which if part of the CG 30 Association may be younger than it appears on the HR diagram (Figure 2.4.9). Though KWW 1055 lies below the main sequence, it shows undepleted Li I $\lambda 6708 \text{ \AA}$ (Kim et al. 2005).

The gas of cometary globule CG 30 has $v_r = 22.8 \text{ km s}^{-1}$ (Zealey et al. 1983; De Vries et al. 1984), well within the range of the CG 30 Association stars, as expected (Kim et al. 2005). This further supports ascribing the CG 30 Association distance to the cometary globule itself.

Gaia DR2 and Choudhury & Bhatt (2009) provide proper motions μ_α in right ascension and μ_δ in declination for 11 of the 14 CG 30 Association and candidate stars. The 6 tight CG 30 Association members' proper motions agree well, with $\mu_\alpha = -7.89 - -7.32 \text{ mas yr}^{-1}$ and $\mu_\delta = 10.98 - 12.025 \text{ mas yr}^{-1}$. This yields error-weighted means and sample standard deviations $\mu_\alpha = -7.53 \pm 0.19 \text{ mas yr}^{-1}$ ($-12.79 \pm 0.32 \text{ km s}^{-1}$ at distance 358.1 pc) and $\mu_\delta = 11.67 \pm 0.32 \text{ mas yr}^{-1}$ ($19.82 \pm 0.54 \text{ km s}^{-1}$). Including all candidates results in similar averages $\mu_\alpha = -7.5 \pm 1.2 \text{ mas yr}^{-1}$ ($-12.7 \pm 2.0 \text{ km s}^{-1}$) and $\mu_\delta = 11.6 \pm 2.0 \text{ mas yr}^{-1}$ ($19.7 \pm 3.4 \text{ km s}^{-1}$), supporting the grouping of 11 of the CG 30 Association members and candidates.

When the range of velocities in each direction (radial, right ascension, and declination) is small, as here, the coordinate system can be assumed roughly Cartesian (Kuhn et al. 2019). Following the example of Kuhn et al. (2019), we define a 1-dimensional velocity dispersion

σ_{1D} from the mean variance of the 3 orthogonal dispersions:

$$\sigma_{1D}^2 = \frac{\sigma_{v_r}^2 + \sigma_{\mu_\alpha}^2 + \sigma_{\mu_\delta}^2}{3}, \quad (2.7)$$

where σ_{v_r} , σ_{μ_α} , and σ_{μ_δ} are the sample standard deviations of v_r , μ_α , and μ_δ , respectively, all in km s⁻¹. The 28 clusters examined by Kuhn et al. (2019) have $\sigma_{1D} = 0.8 - 2.8$ km s⁻¹ and tend to expand over time. The tight CG 30 Association members have $\sigma_{1D} = 1.2$ km s⁻¹, the association plus candidates, 2.5 km s⁻¹. Both values fall within the range of Kuhn et al. (2019).

We conclude that PH α 12, 14, 15, and 21, KWW 464, 598, 873, 1055, 1302, 1637, 1863, 1953, and 2205, and CG 30 IRS 4 all constitute the CG 30 Association near cometary globule complex CG 30/31/38 at distance 358.1 ± 2.2 pc. Our findings confirm Kim et al. (2005) and recommend adding PH α 21, KWW 1055, and CG 30 IRS 4 to the association.

2.5.1.2 Stars Outside the Gum Nebula

KWW XRS 9, though possibly inside the Gum Nebula at 223.3 ± 2.4 pc, has velocities inconsistent with the CG 30 Association ($v_r = -74.1 \pm 3.0$ km s⁻¹, $\mu_\alpha = -22.948 \pm 0.072$ mas yr⁻¹, and $\mu_\delta = 21.203 \pm 0.077$ mas yr⁻¹) and may be a young foreground star.

The v_r of the 4 stars near PH α 41, as well as PH α 34, appear to match, 29.69 – 33.69 km s⁻¹. The proper motions of PH α 34, 40, 41, 44, and 51 are also somewhat similar; however, their σ_{1D} is high at 8.0 km s⁻¹. Age, position, and kinematics weakly suggest the stars near PH α 41 may be related.

IRAS 08159-3543 appears not to be kinematically associated with any other stars in our sample (see Table 2.7). The star was ascribed an aberrantly high luminosity of $24,000 L_\odot$ by Neckel & Staude (1995), versus our much more modest estimate of $13 L_\odot$. We use a smaller distance (2,500 pc) than the Neckel & Staude (1995) estimate of 4,300 pc, smaller even than their lower limit of 3,400 pc assumed for RCW 19, although the parallax of IRAS

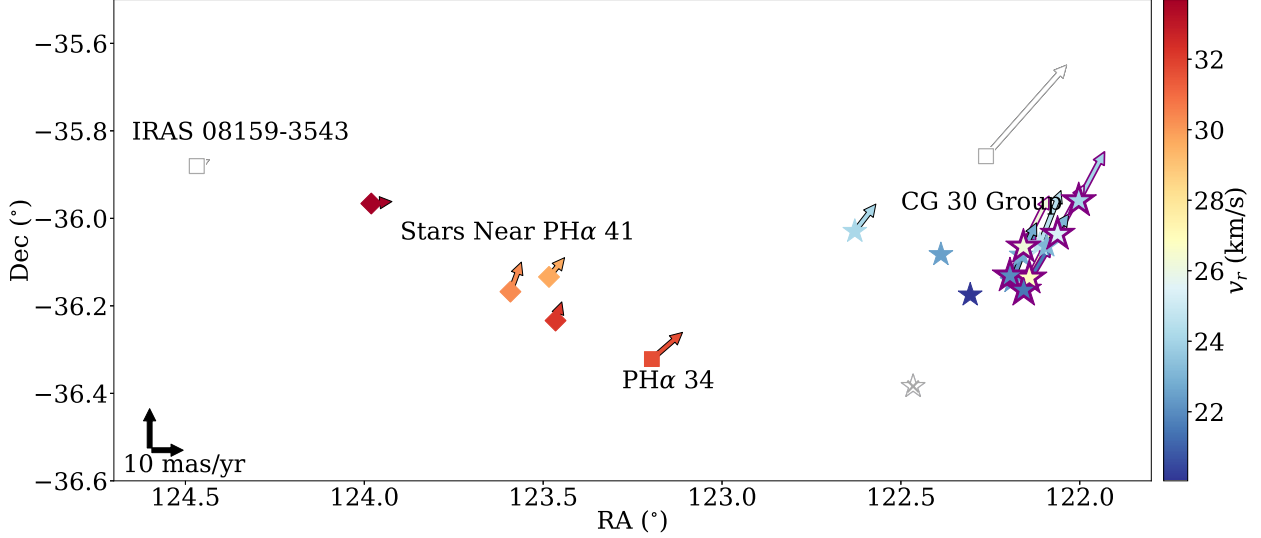


Figure 2.7: We plot the *RA* and *Dec* of 21 stars, with the color bar showing v_r and arrows indicating proper motion in mas yr^{-1} , scaled up by a factor of 10 in the figure (see proper motion scale in black in the lower left corner). Star symbols mark CG 30 Association stars and candidates, with the 6 CG 30 Association members outlined in purple. Diamonds mark the 4 stars near $\text{PH}\alpha$ 41. Other stars are represented by squares. The v_r color legend extends over the range of interest from $20.0 - 33.69 \text{ km s}^{-1}$. Stars with v_r outside this range have no color. The star KWW 1302 with no v_r bears an X . At least 13 of the stars spatially near CG 30 may be dynamically related. The relation of the stars near $\text{PH}\alpha$ 41 is weakly suggested.

08159-3543 is quite uncertain. The high luminosity estimate of Neckel & Staude (1995) stems chiefly from their large assigned extinction of $A_V = 43$ that is difficult to reconcile with IRAS 08159-3543's optical spectrum. The star nevertheless appears to be young and of intermediate mass, with a strong near infrared excess and a wind (Neckel & Staude 1995).

2.5.2 Far-Ultraviolet Radiation

We consider the Gum Nebula an irradiated environment, with O-type stars, an OB association, and cometary globules, as opposed to a quiescent environment relatively free of hot stars. The FUV radiation shaping CG 30 and other cometary globules in the Gum Nebula can be quantified with factor G_0 , the ratio of a region's FUV flux and the average ISM FUV flux $G_{0,ISM} = 1.6 \times 10^3 \text{ ergs s}^{-1} \text{ cm}^{-2}$ (Habing 1968; Winter et al. 2018). To calculate G_0 , we model ζ Pup, γ^2 Vel, and the Vela XYZ progenitor using Castelli & Kurucz (2004) model

atmospheres of O-type dwarfs with Solar metallicity. Taking the stars' distances from Earth into account, we scale the model fluxes to match the stars' observed UBV magnitudes (see Table 2.8). This calibrates each star's absolute brightness. We then scale the flux again based on each star's distance from CG 30. We integrate each stars' scaled flux over the wavelength range $912 - 2400 \text{ \AA}$ for individual G_0 . Finally, we sum the 3 stars' G_0 values and incorporate a relatively small contribution from B stars in Vela OB2. Uncertainties in G_0 stem chiefly from uncertainties in distances to ζ Pup, γ^2 Vel, and Vela XYZ. Within the stars' distance uncertainties, we calculate a maximum G_0 closest to CG 30 and a minimum G_0 farthest from CG 30. Total $G_0 = 6.6^{+3.2}_{-2.7}$.

The Wolf-Rayet star of binary γ^2 Vel is approximated as an O-type dwarf with $T_{eff} = 50,000 \text{ K}$, the hottest model available from Castelli & Kurucz (2004). De Marco & Schmutz (1999) and De Marco et al. (2000) find a primary-to-total-flux ratio at 4700 \AA $f(O)_{4700}/f(O + WR)_{4700} = 0.795$. From this we derive UBV flux ratios of 0.786, 0.795, and 0.801, respectively, and divide dereddened UBV magnitudes between the primary and secondary accordingly. We scale each component model to its set of UBV magnitudes and sum the results for γ^2 Vel's G_0 of $2.0^{+0.1}_{-0.8}$.

Vela XYZ likely resulted from a Type 1a or 1b supernova, entailing a massive progenitor (Reipurth 1983). We crudely substitute a star like ζ Pup at the location of Vela XYZ, which, having exploded just 11,000 yr ago (Reipurth 1983), presumably shone on the CG 30 stars during most of their existence.

To quantify the B-type star contribution to G_0 , we first derive a G_0 vs. *Gaia* color $BP - RP$ relation, second find a $BP - RP$ limit for B-type stars, and third tally B-type stars in Vela OB2 using our $BP - RP$ limit and the catalogue of Cantant-Gaudin et al. (2019). From 15 field B-type stars with *Gaia* DR2 data and known temperatures from Soubiran et al. (2016), placed at the location of γ^2 Vel, we calculate their G_0 and fit a 2nd-degree polynomial to $\log(G_0)$ vs. $BP - RP$. From a broader sample of 200 field B-type stars with *Gaia* DR2 data and known spectral types, we ascertain that the latest B-type stars have flux-mean

Table 2.8: Hot Star Parameters

Star Name	T_{eff} (K)	U (mag)	B (mag)	V (mag)	A_V (mag)	d (pc)	r (R_\odot)	v_r (km s $^{-1}$)	μ_α (mas yr $^{-1}$)	μ_δ (mas yr $^{-1}$)	G_0
ζ Pup	39000 ⁱ	0.89 ⁱ	1.98 ⁱ	2.25 ⁱ	0.13 ^d	335 ^{+12e} ₋₁₁	16 ^f	-23.90 \pm 2.9 ^g	-29.71 \pm 0.08 ^h	16.68 \pm 0.09 ^h	3.7 ^{+2.7} _{-1.6}
γ^2 Vel	35000, 57000 ^a	0.64 ^c	1.58 ^c	1.83 ^c	0.51 ^d	349 ^{+44e} ₋₃₅	18.7 ^{+2.3} _{-1.9} , 3.2 ^a	15.0 \pm 3.1 ^g	-6.07 \pm 0.30 ^h	10.43 \pm 0.32 ^h	2.0 ^{+0.1} _{-0.8}
Vela XYZ	294 ^{+76b} ₋₅₀	0.5 ^{+0.4} _{-0.3}

REFS. — (a) De Marco & Schmutz 1999; De Marco et al. 2000; (b) Caraveo et al. 2001; (c) Ducati 2002; (d) Schröder et al. 2004; (e) Apellániz et al. 2008; (f) Pasinetti Fracassini et al. 2001; (g) Gontcharov 2006; (h) Van Leeuwen 2007; (i) Soubiran et al. 2016

$BP - RP = -0.003$ mag. We find 64 stars in Vela OB2 that have $BP - RP < -0.003$ mag. Using our $\log(G_0)$ vs. $BP - RP$ relation, we calculate a Vela OB2 B-type star G_0 contribution of 0.3. A finer calculation is possible with available *Gaia* DR2 data but would be nontrivial, as Vela OB2 has multiple components (Cantant-Gaudin et al. 2019).

We calculate G_0 only from the local O stars and the B stars of Vela OB2. Contribution from a late B star in Vela OB2 is already small, $G_0 \sim 0.002$. Contribution from the G star KWW 1055 within the CG 30 cluster is negligible, $G_0 < 10^{-5}$.

We extrapolate from current G_0 and the O-type stars' radial velocities and proper motions to estimate G_0 at CG 30 1 Myr ago. Runaway ζ Pup had a larger separation from CG 30 (79_{-16}^{+17} pc vs. 34_{-7}^{+10} pc), whereas γ^2 Vel had a smaller separation (62_{-14}^{+6} pc vs. 70_{-1}^{+12} pc). Holding G_0 from Vela XYZ and Vela OB2 constant and neglecting stars' luminosity changes due to stellar evolution, we find that G_0 at CG 30 was $4.1_{-1.8}^{+1.7}$ 1 Myr ago, about two-thirds today's value.

2.5.3 Star Formation in Cometary Globules

The Gum Nebula hosts at least 32 cometary globules (Sridharan 1992; Kim et al. 2005), and at least 16 are associated with IRAS point sources (Bhatt 1993). Three (Bernes 135 = NX Pup A in CG 1, PH α 92 = Wray 220 in CG 22, and CG 30 IRS 4 in CG 30) are spectroscopically confirmed young stars associated with cometary globule heads. Acted on by external radiation, cometary globules are theorized to host an enhanced rate of star formation and possibly higher accretion rates (Bhatt 1993; Maheswar & Bhatt 2008). Bhatt (1993) found that cometary globules of the Gum Nebula contain a surface density of young-star-like IRAS sources 3 – 12 times higher than a control group of neighboring dark clouds, which combined with their compact size suggests a star formation efficiency of up to $\sim 30\%$ (Bhatt 1993). Globules may preferentially form low-mass, isolated stars like the Sun (Bhatt 1993; Kim et al. 2005; Walch et al. 2013). It is reasonable to assume that several young stars in

the Gum Nebula may have originated inside cometary globules, perhaps a few stars per head (Pettersson 1987; Bhatt 1993; Kim et al. 2005).

Of the few specimens observed, we see a range of spectral types and masses. Bernes 135 at the edge of CG 1 is thought to be an F1 – F2-type star 1 Myr of age and mass 2.5 – 3.0 M_{\odot} , with luminosity 27 – 30 L_{\odot} if at a Gum Nebula distance of 350 pc (Reipurth 1983). The star may have 2 companions: NX Pup B of type F5 – G8 with luminosity 5.4 – 11 L_{\odot} , and NX Pup C of type M0.5 – M1.5 with luminosity 0.27 – 0.51 L_{\odot} (Pettersson 2007). Optically revealed PH α 92 in front of CG 22 is a T Tauri star of type K2 – K3 with luminosity 8.9 L_{\odot} (Sahu & Sahu 1992). Outside the Gum Nebula, globule IC 1396A hosts a T Tauri star of type M2 and a protostar (Sicilia-Aguilar et al. 2013).

The infrared source CG 30 IRS 4 has been shown to power the Herbig-Haro object HH 120 (Persi et al. 1994; Pettersson 2007; Kajdič et. al 2010; Chen et al. 2008) and overlaps the sub-millimeter source CG 30 SMM-N associated with large bipolar jet HH 950 (Kajdič et. al 2010). The complexity of the Herbig-Haro objects may signify that the star is part of a wide binary system (Pettersson 2007; Kajdič et. al 2010; Chen et al. 2008). Our high-dispersion spectroscopy shows CG 30 IRS 4 is a low-mass star of type M0 with moderate veiling of 0.86 near 6500 Å and 0.15 near 8400 Å. It is definitely young, with lithium equivalent width 0.47 – 0.67 Å. Kim et al. (2005) propose the object is as young as just 10^5 yr. Strong 1.3 mm emission and NH₃ observations suggest the star is embedded in a dense cloud core of size 0.14 pc (at distance 358.1 pc) and mass 8 M_{\odot} . Chen et al. (2008) suggest an outflow mass of 1.4 M_{\odot} . The star's luminosity may be as high as $13.6 \pm 0.8 L_{\odot}$ (Pettersson 2007; Chen et al. 2008).

CG 30 IRS 4 has the lowest $v_{rot} \sin(i)$ of our sample, 6.3 ± 0.2 km s⁻¹. Though embedded, the star seems already to have dissipated much of the angular momentum of its formation, suggesting this may happen during the embedded stage (White & Hillenbrand 2004). Rotation speed may then hold fairly constant until dissipation of the circumstellar disk (Gallet & Bouvier 2013). With its relatively slow $v_{rot} \sin(i)$, defined photosphere, strong lithium

absorption, weak but present H α emission, and moderate veiling, CG 30 IRS 4 resembles the optically revealed T Tauri stars of the CG 30 Association. CG 30 IRS 4 may essentially be an embedded T Tauri star. Perhaps stars develop T Tauri properties (e.g. photosphere, disk) before emerging from a cloud.

Considering the 14 CG 30 Association stars' proximity to actively star-forming cometary globules, it is possible that all formed inside cometary globules (Kim et al. 2005). The 14 T Tauri stars do not appear to differ from low-mass T Tauri stars formed by the traditional collapse of a large molecular cloud. While FUV radiation forms cometary globules that appear to host enhanced isolated-low-mass-star formation rates (Bhatt 1993; Walch et al. 2013), the radiation may not penetrate deep enough to affect the star formation process itself (Elmegreen 2011; Paron et al. 2015).

2.5.4 Young Star Evolution in a Moderate Radiation Environment

If the moderate radiation environment of the Gum Nebula is affecting young stars' disks, then we should see a smaller ratio of accretors to nonaccretors in the CG 30 Association than in more quiescent regions of similar age (e.g. Tau-Aur). Mohanty et al. (2005) calculate the accretor fraction as N_{acc}/N_{tot} , where N_{acc} is the number of classical T Tauri stars with $W_{10} > 200 \text{ km s}^{-1}$, and N_{tot} is the total number of T Tauri stars both weak and classical. The accretor fractions for various star-forming regions range from $59 \pm 16\%$ for 1 – 3-Myr-old Tau-Aur to $2 \pm 2\%$ for the 10-Myr-old NGC 7160 (see Table 2.9).

To the Mohanty et al. (2005) compilation, we add accretor fractions from Mortier et al. (2011), who distinguish accretors from nonaccretors using H α 10% W and the same prescription as Mohanty et al. (2005); from Sicilia-Aguilar et al. (2005a,b, 2013), Fang et al. (2013), Biazzo et al. (2014), and Briceño et al. (2019), who use H α 10% W and the prescription of White & Basri (2003); and from Hernández et al. (2007), who distinguish accretors from nonaccretors photometrically based on thick vs. thin disks. Assembling accretor fractions from multiple sources measured in different ways inevitably introduces bias. However, there

Table 2.9: Accretor Fractions of Star-Forming Regions

Region	Age (Myr)	N_{acc}/N_{tot}	%
Quiescent			
ρ Oph	<1 ^{a,c}	10/20 ^c	50 ± 16
Tau-Aur	1 – 3 ^{j,k}	42/71 ^c	59 ± 9
Lup	1 – 3 ^{j,k}	25/45 ^g	56 ± 11
IC 348	2 – 3 ^{j,k}	29/87 ^c	33 ± 6
Cha I	2 – 3 ^{j,k}	28/63 ^c	44 ± 8
TW Hyd	10 ^{a,c}	...	~15 ^c
Irradiated			
CG 30	≤1	4/14	29 ± 14
L1641	0.1 – 3 ^{f,h}	159/450 ^h	35 ± 3
ONC	0.8–3 ^l	136/237 ^d	57 ± 5
L1615/1616	1 – 3 ^{a,i}	15/54 ⁱ	28 ± 7
Tr 37	1 – 4 ^{b,d}	46/116 ^d	40 ± 5
NGC 1977/1980	2 – 4 ^{a,b,m}	63/222 ^m	28 ± 4
σ Ori	3 – 5 ^{j,k}	...	33.9 ± 3.1 ^e
Upper Sco	5 – 10 ^{j,k}	12/170 ^c	7 ± 2
NGC 7160	10 ^{b,d}	1/55 ^d	2 ± 2

REFS. — (a) Baraffe et al. 1998; (b) Siess et al. 2000; (c) Mohanty et al. 2005; (d) Sicilia-Aguilar et al. 2005a,b, 2013; (e) Hernández et al. 2007; (f) Dotter et al. 2008; (g) Mortier et al. 2011; (h) Fang et al. 2013; (i) Biazzo et al. 2014; (j) Baraffe et al. 2015; (k) Cazzoletti et al. 2019; (l) Winter et al. 2019; (m) Briceño et al. 2019

is no established way of measuring accretor fraction yet, and synthesizing results provides us with useful context (see also Table 2 in Fedele et al. 2010). In Table 2.9, we group clusters by environment: quiescent (no cometary globules or OB associations) vs. irradiated (present cometary globules or OB associations). The quiescent clusters ρ Oph, Tau-Aur, Lup, IC 348, Cha I, and TW Hyd tend to have higher accretor fractions (15 – 59%), whereas the clusters L1641, L1615/1616, Tr 37, NGC 1977/1980, σ Ori, Upper Sco, and NGC 7160 near cometary globules or OB associations tend to have lower accretor fractions (2 – 40%). Accretor fractions generally decline with age, which dominates after 5 Myr (Mohanty et al. 2005; Fedele et al. 2010).

The ONC, despite containing proplyds and several massive stars, has a relatively high accretor fraction inconsistent with other irradiated clusters of similar age ($57 \pm 5\%$ vs. $28 - 40\%$). This may be due to the region’s complex and recent star formation history (Winter et al. 2019).

Of the 14 CG 30 Association stars and candidates, 3 are classical T Tauri stars by our criterion of $W_{10}(\text{H}\alpha) > 270 \text{ km s}^{-1}$, and 11 are weak-line. CG 30 IRS 4, though classified among the weak-line, is embedded and veiled and likely still accreting. Thus we count 4 accretors in the 14-star CG 30 Association. The CG 30 Association then has an accretor fraction of $29 \pm 14\%$ (4/14). By the criterion of Mohanty et al. (2005), the accretor fraction would be $36 \pm 16\%$ (5/14). Either fraction is low for the CG 30 Association’s age of $\lesssim 1$ Myr, as Kim et al. (2005) have suggested. The similarly aged Tau-Aur and ρ Oph clusters have accretor fractions about twice as high. The CG 30 Association’s accretor fraction is more consistent with irradiated clusters than quiescent clusters.

The CG 30 Association measurement is subject to low number statistics, although the association itself appears sparse, with only 6 additional potential members since found via *Gaia* DR2 (Yep and White, in prep.). It is also worth considering selection biases. Young stars identified via broad H α emission (Pettersson 1987; Neckel & Staude 1995) tend to be classical T Tauri stars, whereas young stars identified via X-ray luminosity (Kim et al. 2005) tend to be weak-line T Tauri stars. Using a dual identification approach, as here, has provided the most comprehensive membership lists in comparison star-forming regions (e.g. Cohen & Kuhi 1979 and Neuhäuser et al. 1995 for Tau-Aur). The greater distance to CG 30 compared to these other regions may bias against finding X-ray-bright weak-line T Tauri stars, which, if present, would further reduce the accretor fraction.

2.6 Summary

We study 21 young stars near CG 30 and RCW 19 to investigate whether these stars are related to each other and how the Gum Nebula’s moderate radiation environment

$(G_0 = 6.6^{+3.2}_{-2.7})$ may be affecting them. We have observed 9 stars from Pettersson (1987) and CG 30 IRS 4 itself using high-dispersion ($R \sim 34,000$) spectroscopy and gathered photometry for all 21 young stars from the literature (2MASS; Pettersson 1987; Kim et al. 2005; Neckel & Staude 1995).

- Spectral types of the 9 Pettersson (1987) stars and CG 30 IRS 4 range from M4.5 to K5.
- The 9 Pettersson (1987) stars and CG 30 IRS 4 show undepleted Li $\lambda 6708 \text{ \AA}$, H α 10% widths $225 - 621 \text{ km s}^{-1}$, and veiling. Eight of the 10 are classical T Tauri stars. Three of the stars associated with CG 30 are classical T Tauri stars.
- Projected rotational velocities of the 10 young stars are $6.3 - 27.8 \text{ km s}^{-1}$. CG 30 IRS 4's is the lowest.
- The star CG 30 IRS 4 inside the cometary globule appears to be an embedded T Tauri star. Though its H α 10% width (225 km s^{-1}) falls below the classical T Tauri star limit, it is embedded, exhibits moderate veiling, and is probably still accreting.
- By youth ($\lesssim 1 \text{ Myr}$), distance ($358.1 \pm 2.2 \text{ pc}$), and kinematics (radial velocity $23.1 \pm 1.9 \text{ km s}^{-1}$, proper motions $-7.5 \pm 1.2 \text{ mas yr}^{-1}$ in right ascension and $11.6 \pm 2.0 \text{ mas yr}^{-1}$ in declination, and 1-D dispersion 2.5 km s^{-1}), 14 stars near CG 30 are likely related to each other and the CG 30/31/38 cometary globule complex. This is the CG 30 Association.
- The CG 30 Association has an accretor fraction of $29 \pm 14\%$, low compared to young quiescent clusters but consistent with young irradiated clusters.

CHAPTER 3

FINDING OTHER YOUNG ASSOCIATIONS IN THE GUM NEBULA

3.1 Introduction

The low accretor fraction of the irradiated CG 30 Association in the Gum Nebula (see Figure 3.1) suggests even a moderate FUV radiation environment ($G_0 = 6.6^{+3.2}_{-2.7}$) disrupts young protoplanetary disks. To confirm this result, we search for associations or clusters near other cometary globules in the Gum Nebula.

In §3.2 we describe our technique for identifying young stellar associations in the Gum Nebula. In §3.3 we expand association membership with reference to other catalogues. We analyze CHIRON spectra of 284 young stars in §3.4 and derive association properties in §3.5. Finally, we summarize our findings in §3.6. Information on our catalogue of spectral standards is presented in Appendix A.

3.2 Finding Clusters near Cometary Globules

As members of a cluster move through space together, a natural way to find a cluster is to look for a spatially compact group of stars with similar distances and space motions. We have developed a Python code called Cluster Finder to accomplish this search visually.¹

All our searches begin with a 2° -radius *Gaia* DR2 field centered on a cometary globule, with parallax $2.10 - 4.04$ mas to stay within the Gum Nebula (see Figure 3.2). We derive this $248 - 476$ pc depth by centering the Gum Nebula at 360 pc and approximating a 226-pc

¹https://github.com/alexandrayep/Cluster_Finder

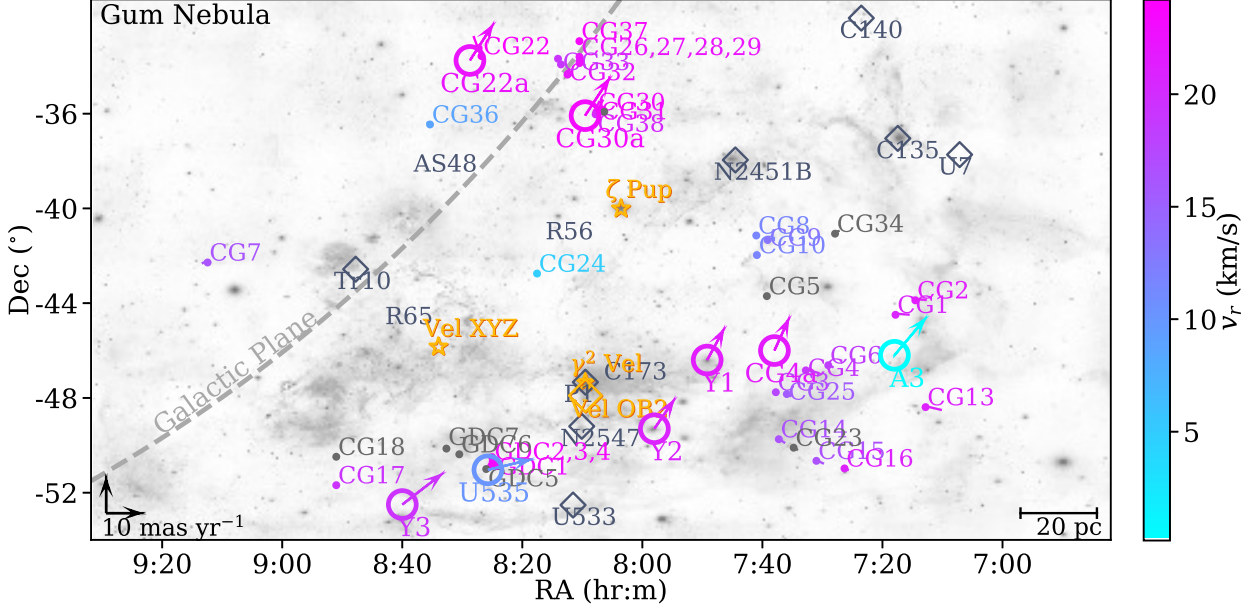


Figure 3.1: Shown is a majority of the Gum Nebula, grayscaled from Aladin’s DSS2 image (combined blue, red, and infrared), and plotted in PyPlot. Radiation sources ζ Pup, γ^2 Vel, and Vel XYZ are plotted in orange. CGs and their cometlike tails are plotted and labeled, although at this scale only the longest tails are visible. Spatial scale at distance = 360 pc is displayed in the bottom right corner. The 8 associations found using Cluster Finder are marked with rings and labeled with slightly enlarged font. The color bar shows radial velocities for cometary globules, where available, and our radial velocities for our 8 associations. Arrows indicate proper motions. Proper motion scale is displayed in the bottom left corner. Other previously known associations and clusters in the region are marked with black diamonds. The dashed dark gray line marks the Galactic plane.

diameter from its 36° width. Because we add members from other catalogues later, the fine details of our initial search have only a marginal effect on our final membership lists. Cometary globule coordinates and motions are from Reipurth (1983), Zealey et al. (1983), Sridharan (1992), and Choudhury & Bhatt (2009) and are charted in Figure 3.1. We impose parallax error < 0.1 mas and proper motion error < 0.16 mas yr^{-1} to eliminate sources with poor astrometry. We plot right ascension versus declination and toggle color-coding for distance $\approx \text{parallax}^{-1}$ and each proper motion. We apply distance- and proper motion cuts until a cluster visually emerges as more or less a single color. If candidate cluster members appear centered beyond the edge of our search, we recenter the field off the cometary globule. If candidates spill past all edges of the search radius, we expand our search radius in

Table 3.1: Search Parameters and Cuts

CG Name	Cone Search			Cuts				
	RA (°)	Dec (°)	Radius (°)	RA (°)	Dec (°)	Distance (pc)	μ_α (mas yr $^{-1}$)	μ_δ (mas yr $^{-1}$)
CG 1	109.5	-46.2	3	105.5 – 113	-48 – -44	247.0 – 320.0	-12 – -8	10.5 – 13
CG 3	117.3	-46.4	4	113.8 – 121.8	-50.5 – -44	360.0 – 420.0	-5.2 – -3.8	7.8 – 10
CG 4	114.5	-46.0	3	112 – 114	-48 – -45	405.0 – 450.0	-5 – -2.0	7 – 10
CG 14	119.5	-49.3	4	114.5 – 124.4	-51.0 – -45.5	400.0 – 430.0	-5.9 – -4.8	7.6 – 8.7
CG 17	130.0	-52.5	3	126.3 – 134	-55 – -49.5	320.0 – 370.0	-14.5 – -11.5	9 – 12
CG 22	127.2	-33.8	2	126.2 – 127.8	-35.6 – -33.5	320.0 – 390.0	-8.6 – -5.0	9.5 – 13.1
CG 30	122.4	-36.1	2	121.7 – 123.3	-36.9 – -35.75	340.0 – 390.0	-8.5 – -6.0	9.5 – 12.0
GDC1	126.4	-51.0	4	123 – 131	-55 – -47.5	290.0 – 350.0	-14.5 – -11.5	1.1 – 4.1

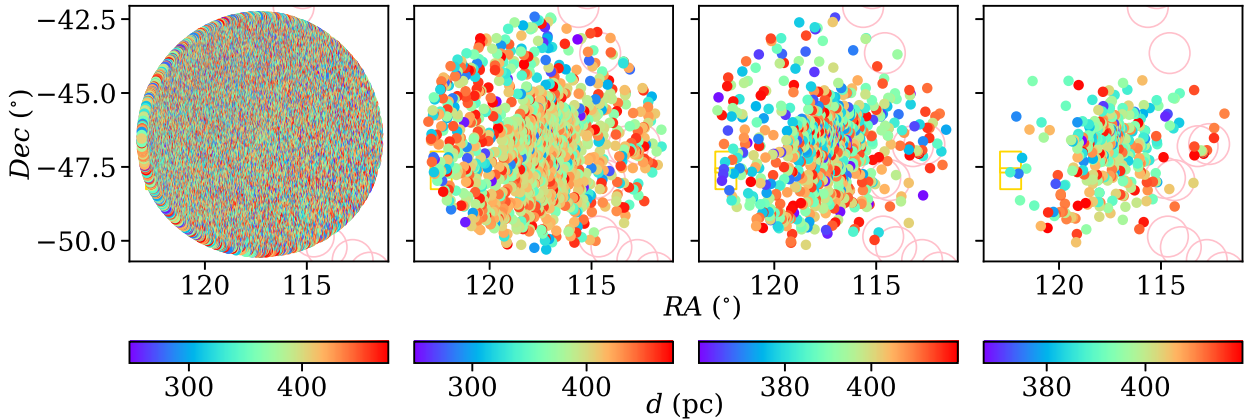


Figure 3.2: Cluster Finder process, demonstrated on Yep 1. We start with *Gaia* DR2 data with parallax limited to within the Gum Nebula (leftmost panel). We then make proper motion cuts (middle left panel) and refine the distance cuts (middle right panel). Finally, we make error cuts to keep only stars with high-quality astrometry (rightmost panel).

increments of 1° until the apparent overdensity of the cluster is contained within the field. We fine-tune cuts to favor membership probability over completeness, narrowing the cuts until the roughly uniform distribution of surrounding stars dwindles to near zero. Finally, we crop right ascension and declination to the cluster edges.

Using this method for all 39 CGs and globular dark clouds (GDCs) within 20° of the heart of the Gum Nebula at the projected center of ζ Pup (335^{+12}_{-11} pc; Apellániz et al. 2008), γ^2 Vel (349^{+44}_{-35} pc; Apellániz et al. 2008), and Vela XYZ (294^{+76}_{-50} pc; Caraveo et al. 2001), we have recovered the CG 30 Association and found 7 other associations, or sparse clusters, $7 – 87$ pc in diameter (see Figure 3.3). We include stars down to $V \sim 20$ mag, with V calculated from

Gaia DR2 magnitudes using the prescriptions of Evans et al. (2018) and Jao et al. (2018):

$$V = \begin{cases} G + 0.0176 + 0.00686(BP - RP) + 0.1732(BP - RP)^2, & \text{if } BP - RP < 1, \\ 0.97511 \times BP + 0.02489 \times RP - 0.20220, & \text{if } BP - RP \geq 1. \end{cases} \quad (3.1)$$

Cluster Finder’s strengths are its speed and ease of use for finding core members of a cluster or association. In favoring high membership probability over completeness, we likely exclude less-well-measured and less-bound members, such as runaway stars and some binaries. Our use of proper motions instead of calculated transverse motions may introduce a small degree of incompleteness and contamination. We do not use RUWE, so we may include a few close binary stars in our intended single-star sample. Associated stars further out from the dense center of a cluster or association may evade detection, although Cluster Finder is well suited to handle clusters and associations of all shapes and sizes. Two associations (near CG 4 and CG 30) are sparse and filamentary, and two others (near CG 17 and GDC 1) are significantly elongated along the plane of the Galaxy. We include each association’s search parameters and right-ascension-, declination-, distance-, and proper-motion cuts in Table 3.1.

3.3 Association Candidates

All of the associations we found using Cluster Finder have been previously identified, at least in part. Three appear in the catalogue of Cantat-Gaudin and Anders (2020), who found clusters and associations using an unsupervised member classification method based on *Gaia* DR2 and 3-D velocities (see Cantat-Gaudin et al. 2019), and four appear in the catalogue of Kounkel & Covey (2019), who found clusters and associations and so-called strings using unsupervised machine learning. These other catalogues’ search radii tend to be wider than ours. We incorporate these other catalogues’ candidates by applying our slightly expanded cuts (± 5 pc in *Gaia* DR2 parallax-derived distance and ± 0.1 mas yr $^{-1}$ in proper motions) to their membership lists. We then gather distances calculated in Bailer-Jones et al. (2018) for

all final association members. We discard candidates with Bailer-Jones et al. (2018) distances >500 pc and distance uncertainties >50 pc.

In naming the 8 associations, we keep the established names of two associations identified in Cantat-Gaudin and Anders (2020). Three associations previously studied alongside their nearby cometary globules inherit the names of those cometary globules. Three associations that appear only loosely in the large strings of Kounkel & Covey (2019) are given new names according to convention, with the lead author’s surname (Yep) and a number.

Here we summarize the identified members of each of the 8 associations, comprising a total of 1873 stars.

3.3.1 CG 4 Association

We identify 34 stars as members of the CG 4 Association near CG 4. Young stars within and around CG 4 have been studied by Reipurth & Pettersson (1993), Rebull et al. (2011), and Kim et al. (2006), most notably the star RP93 7 = CG-H α 7. We present our own membership list of 34 stars, including RP93 7. We have obtained spectra of 7 of the 34 stars in the CG 4 Association.

3.3.2 CG 22 Association

We identify 102 stars as members of the CG 22 Association near CG 22. Young stars within and around CG 22 have been studied by Reipurth & Pettersson (1993) and Sahu & Sahu (1992), most notably PH α 92 = Wray 220. The CG 22 Association also corresponds to Theia 31 in Kounkel & Covey (2019). We combine our membership list with that of Kounkel & Covey (2019). Our lists share 63 members. Kounkel & Covey (2019) add 11 members, and we add 27 plus PH α 92. We have obtained spectra of 11 of the 102 stars in the CG 22 Association.

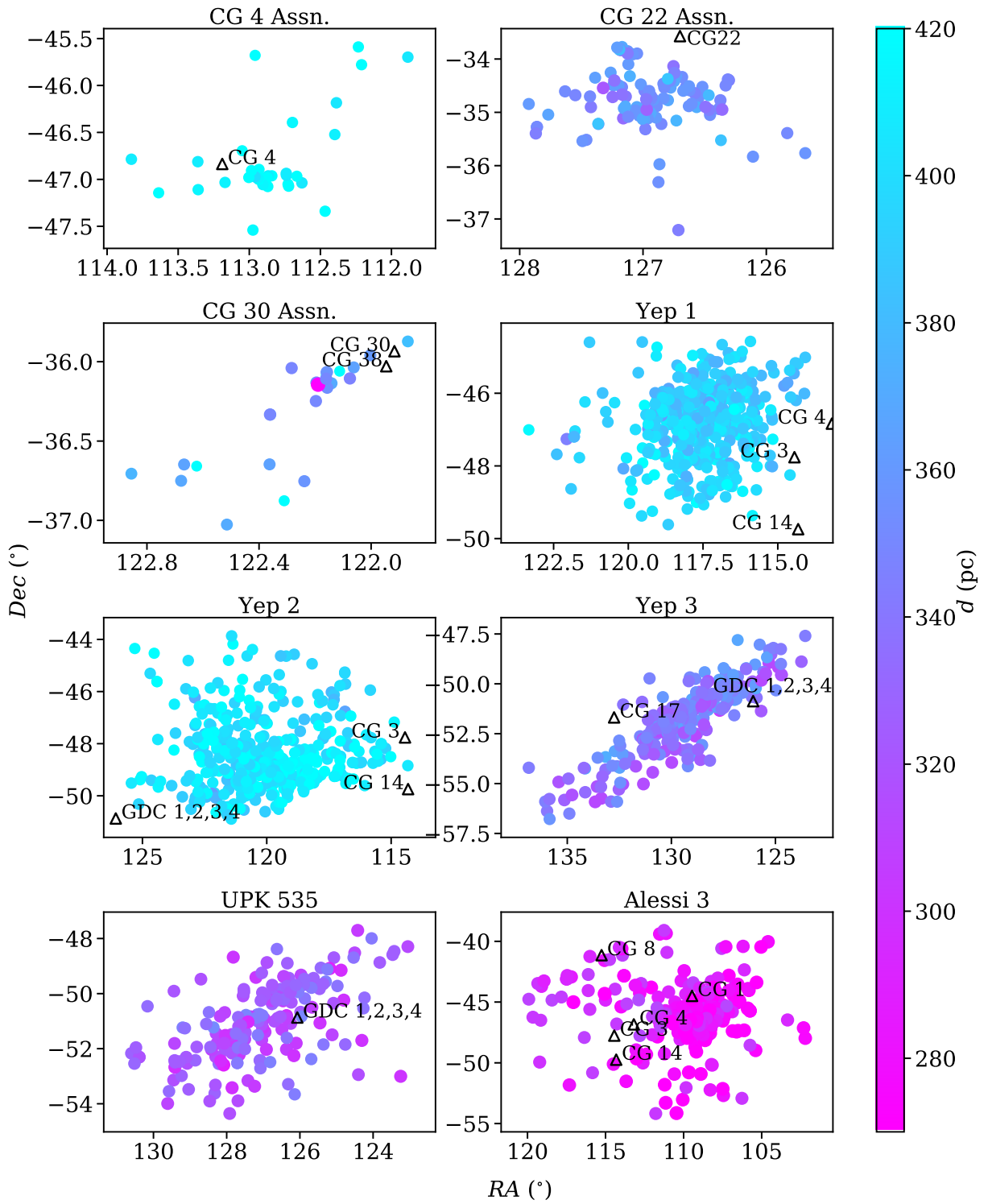


Figure 3.3: RA vs. Dec of 8 young associations in the Gum Nebula. Cometary globules and dark clouds are marked with black triangles and labeled. The CG 4, 22, and 30 Associations are sparse and may be associated with their nearby cometary globules.

3.3.3 CG 30 Association

We identify 29 stars as members of the CG 30 Association near CG 30. This association has been studied by Pettersson (1987), Kim et al. (2005), the authors in Chapter 2, and others for its distinct, star-forming cometary globule and several young stars, one of which (CG 30 IRS 4) is inside CG 30 itself. We present our membership list of 29 stars, which includes all 14 candidates from Chapter 2, 4 of which lack *Gaia* DR2 data. We have Keck I HIRES spectra of 5 stars in the CG 30 Association (see §2.2.1).

3.3.4 Yep 1 Association near CG 3

We identify 535 stars as members of the Yep 1 association near CG 3. The association appears loosely in the catalogue of (Kounkel & Covey 2019), constituting 12.4% of Theia 22. Theia 22 may be a conglomerate of several possibly unrelated associations (see also §3.3.5, so we rename this clustered portion Yep 1. Our membership lists for Yep 1 and Theia 22 share 360 stars. Our cuts keep an additional 104 stars from Theia 22. We contribute another 71 stars. We have obtained spectra of 56 of the 535 stars in Yep 1.

Yep 1 and Yep 2 are spatially close to each other, partially overlap in distance, and have similar space motions. It is possible they are two components of one association. We refine their memberships in the space they are most separate, μ_α vs. Dec , using an empirical quadratic to separate the two associations (see Figure 3.4).

3.3.5 Yep 2 Association near CG 14

We identify 443 stars as members of the Yep 2 association near CG 14. This association, like Yep 1, appears in the catalogue of Kounkel & Covey (2019) as another portion of Theia 22. Yep 2 contains 11.2% of the stars in Theia 22 and does not have any members in common with Yep 1. The membership lists of Yep 2 and Theia 22 share 219 stars, and our cuts take 198 additional stars from Theia 22. We contribute an additional 26 stars. We have obtained spectra of 46 of the 443 stars in Yep 2.

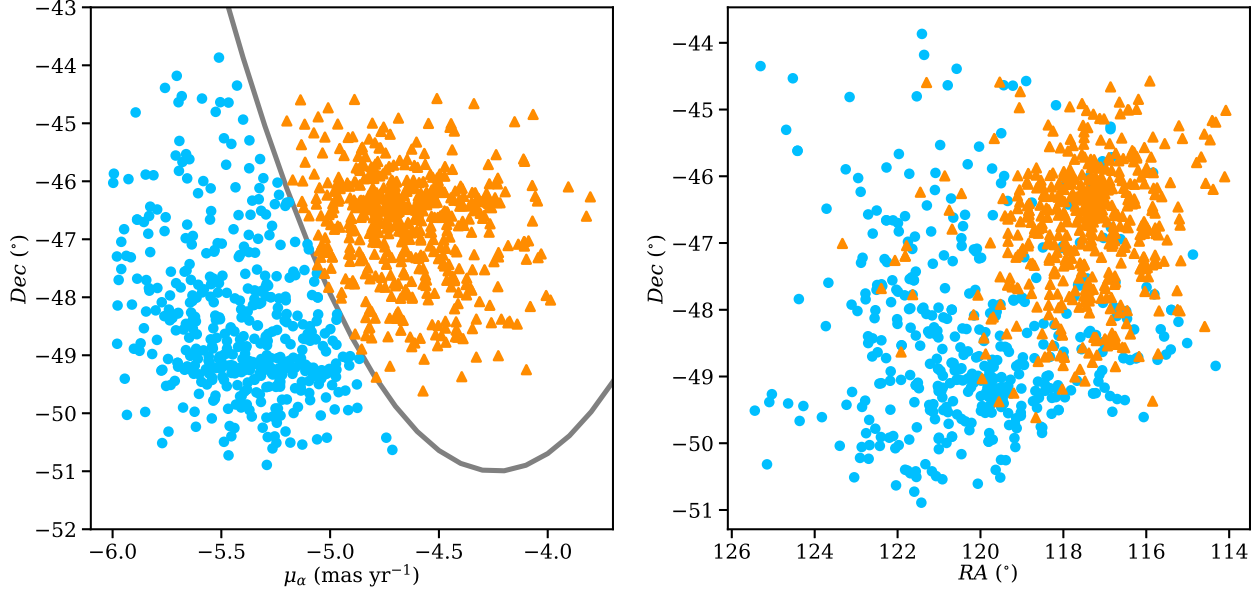


Figure 3.4: Associations Yep 1 (orange triangles) and Yep 2 (azure circles). We empirically split the two associations using an empirical quadratic (gray line) in μ_α vs. Dec space (left panel). The two associations spatially overlap but are distinct (right panel).

3.3.6 Yep 3 Association near CG 17

We identify 297 stars as members of the Yep 3 association near CG 17. This association appears very loosely in Kounkel & Covey (2019) as a westerly 16.2% of the spuriously large Theia 120. Our membership lists for Yep 3 and Theia 120 share 111 stars. Applying our cuts, we take an additional 153 stars from Theia 120 and contribute another 33 stars near the center of Yep 3. We have obtained spectra of 59 of the 297 stars in Yep 3.

3.3.7 UPK 535 Association near GDC 1

We identify 174 stars as members of the UPK 535 association near GDC 1. Sim et al. (2019) discovered the association via visual inspection of Gaia DR2 data. Cantat-Gaudin and Anders (2020) catalogue the association. Our lists share 86 members. Cantat-Gaudin and Anders (2020) contribute an additional 30 stars, and we contribute 58 stars. We have obtained spectra of 36 of the 174 stars in UPK 535.

3.3.8 Alessi 3 Association near CG 1

We identify 260 stars as members of the Alessi 3 association near CG 1. Alessi et al. (2003) discovered the association using the statistical method of Sanders (1971) on Tycho-2 data. Cantat-Gaudin and Anders (2020) refined and expanded Alessi 3 membership. Within our 3° search radius, our membership lists agree on 123 stars. Cantat-Gaudin and Anders (2020) contribute an additional 107 stars, and we add 30 stars. We have obtained spectra of 63 of the 260 stars in Alessi 3.

3.3.9 Association Ages

We estimate association ages by fitting MESA isochrones to the extinction-corrected (see §3.4.2) single-star main sequences in *Gaia* M_G vs. corrected $BP - RP$, as illustrated in Fig. 3.5 (Paxton et al. 2011, 2013, 2015; Choi et al. 2016; Dotter 2016). Association ages range from 2 to 650 Myr. The isochrones also provide us with a rough estimate for metallicity [Fe/H]. All associations' main sequences are best fit by Solar or supersolar isochrones of 0 – 0.2 dex. Age uncertainties stem from a discrepancy in fitting the main sequence turnoff vs. the bright-for-their-color cool stars. This is a common problem when fitting model isochrones, perhaps due to magnetism, star spots, or other difficult-to-quantify phenomena of cool stars (Herczeg & Hillenbrand 2015; Asensio-Torres et al. 2019), and perhaps due to blue stragglers (Beasor et al. 2019). Our isochrone-fit ages are supported by lithium measurements (see §2.3.1).

3.4 High Dispersion Optical Spectra

CHIRON is a very stable spectrograph on the SMARTS 1.5 m telescope on Cerro Tololo in Chile (Tokovinin et al. 2013). Its $4500 - 8500 \text{ \AA}$ wavelength range includes signatures of youth H α and Li I $\lambda 6708$. In fiber mode, its resolving power $R \approx 25,000$ yields a velocity resolution of 12 km s^{-1} .

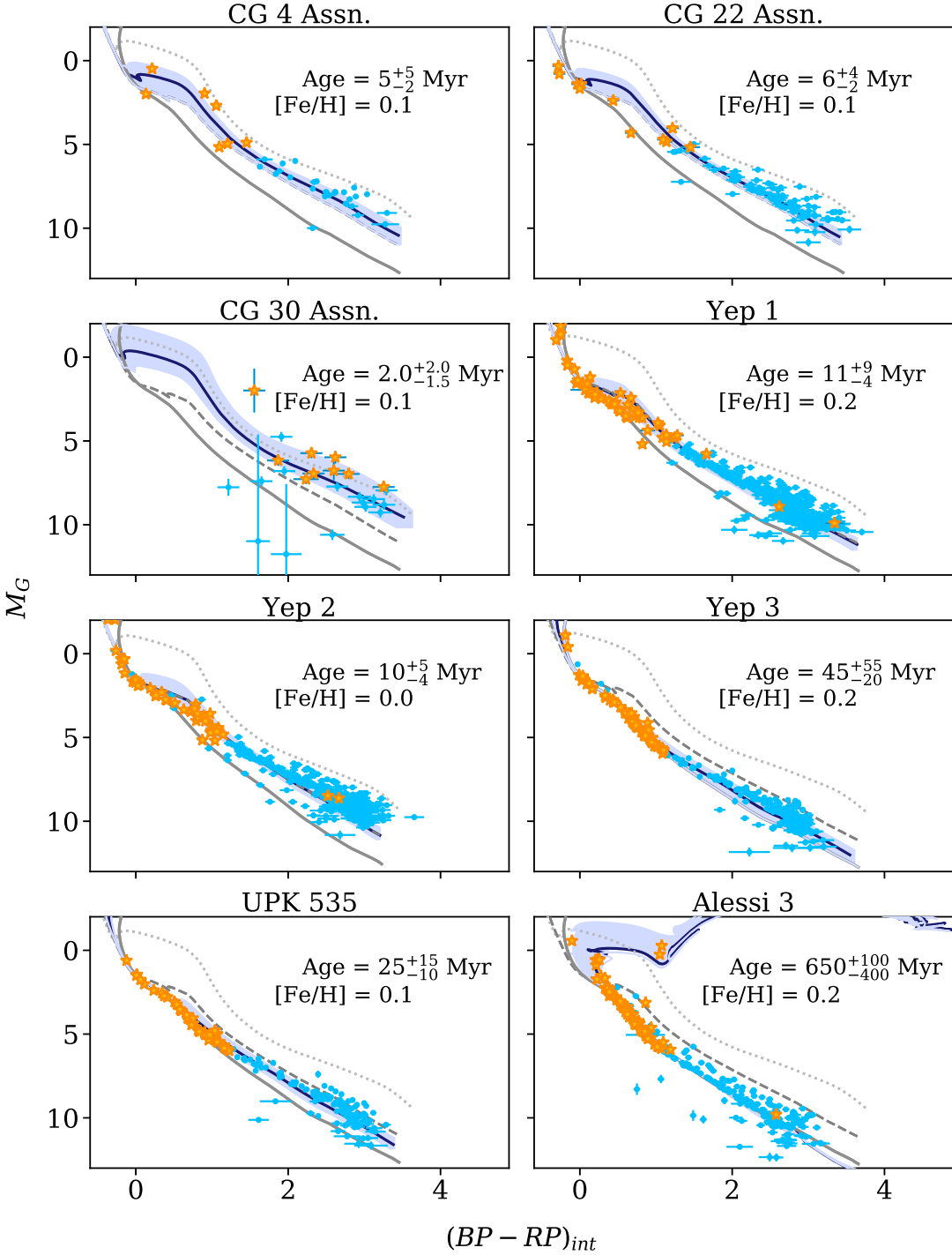


Figure 3.5: Color-magnitude diagrams. *Gaia* colors are corrected for redenning, and absolute G magnitudes are calculated using distances from (Bailer-Jones et al. 2018) and corrected for extinction. Isochrones are from MESA: dotted gray is 1 Myr, dashed gray is 10 Myr, and solid gray is 100 Myr. Spectroscopically observed stars are plotted as gold stars. Unobserved stars are azure circles. Solid blue isochrones display our age fits, while lilac-shaded regions mark asymmetric age uncertainties. Seven of the 8 associations are fit best by supersolar metallicities, and all are younger than 1 Gyr. Five are $\lesssim 10$ Myr.

3.4.1 Association Observations and Data Reduction

From 2018 Oct 22 to 2021 June, we observed 284 stars in Alessi 3, Yep 1, Yep 2, CG 4 Association, Yep 3, CG 22 Association, and UPK 535 for at least 1 epoch each with the CHIRON spectrograph in fiber mode. We also obtain high-quality ($\text{SNR} \gtrsim 100$) spectra of 81 spectral standard stars, publicly available to all CHIRON users (see Appendix A).² Association stars were selected along the apparent single-star main sequence of a *Gaia* $BP - RP$ color vs. BP magnitude diagram (see Fig. 3.5 for corrected color-magnitude diagrams). We imposed a general brightness cutoff of $V = 13.5$ mag. Twenty-seven dimmer stars with V down to 14.2 mag were also observed before the limit was imposed. We observed each star for up to 1200 s, achieving an SNR of 30 for $V < 9.3$ mag and SNR 30 – 10 for V 9.3 – 13.5 mag. Dimmer stars had SNR 5 – 10. Stars with the weakest spectra (particularly PH α 92) were reobserved to bring their SNR into the 10 – 30 range. This SNR of 10 – 30 is sufficient to determine each star’s spectral type, radial velocity, stellar rotational speed, continuum excess, H α emission, and Li I $\lambda 6708$ absorption.

CHIRON echelle spectra are reduced by the CHIRON instrumentation team using an IDL pipeline (Paredes et al. 2021). Spectra are normalized by dividing out the blaze function (see Appendix A). We focus on 30 well-behaved orders without telluric features and pressure-broadened lines (e.g. Na D), plus the order containing H α .

Stars in the CG 30 Association are too dim to achieve sufficient SNR within our set exposure time limits for CHIRON, so we incorporate CG 30 Association results presented in Chapter 2, derived from spectra from the High-Resolution Echelle Spectrometer (HIRES) on the Keck I telescope in Hawaii.

3.4.2 Spectral Types, Extinctions, Masses, and Infrared Excesses

Spectral types are determined via visual comparison to our catalogue of CHIRON spectral standards (see Figure 3.6 and Appendix A). We assign each star the spectral type of the

²https://github.com/alexandrayep/CHIRON_Standards

most similar standard star, and we assign spectral type uncertainties based on the spread of similar standard stars. Spectral types of $V \leq 13.5$ range from K5V to B2V across the 7 spectroscopically measured associations. Spectral types of dimmer stars reach as low as M1.5V, but these stars have $\text{SNR} < 5$ and are not well measured. Two stars in Alessi 3 are giants, types K0III and G9III.

The star CD-46 3194 in the CG 4 Association is a clear double-line spectroscopic binary. Both components are assigned spectral type A6V. The star 2MASS J08443526-5234117 in Yep 3 is a possible double-line or even triple-line spectroscopic binary, but its low $\text{SNR} \sim 5$ renders its binary classification less certain.

To quantify the reddening caused by extinction, we measure *Gaia* color excess $E(BP - RP)$ by comparing spectroscopically observed stars' apparent *Gaia* colors $BP - RP_{\text{obs}}$ with their spectral types' intrinsic colors $BP - RP_{\text{int,M}}$ according to the dwarf colors of Pecaut & Mamajek (2013).³ To avoid biasing results with anomalous red or blue outliers, possibly caused by a variation in local extinction, or skewed by stars with poor photometry or fast rotation that are more difficult to classify, we measure whole-association color excesses $E(BP - RP)_{\text{assn}}$ by taking the flux-error-weighted mean of the middle quartiles of $E(BP - RP)$ values. Stars' *Gaia* color excesses range from -0.661 to 2.378 mag, with median uncertainty 0.052 mag, and association means range from 0.036 to 0.349 mag, with a median uncertainty of 0.049 mag, derived from the flux standard deviations of the middle quartiles of each association's $E(BP - RP)$ values. We determine all stars' intrinsic colors $(BP - RP)_{\text{int}}$ by correcting for whole-association reddening: $(BP - RP)_{\text{int}} = (BP - RP)_{\text{obs}} - E(BP - RP)_{\text{assn}}$. Values for $(BP - RP)_{\text{int}}$ span -0.370 – 3.703 mag (see Table 3.2).

There is no one-to-one relation between *Gaia* color and extinction in BP or RP , but there is an approximate relation between extinction in *Gaia* magnitude G and $E(BP - RP)$ that follows from the PARSEC models: $A_G \approx 2 \cdot E(BP - RP)$ (Andrae et al. 2018). We adopt this approximation to calculate association extinction $A_G \approx 2 \cdot E(BP - RP)_{\text{assn}}$. Extinction

³http://www.pas.rochester.edu/~emamajek/EEM_dwarf_UBVIJHK_colors_Teff.txt, version 2021.03.02

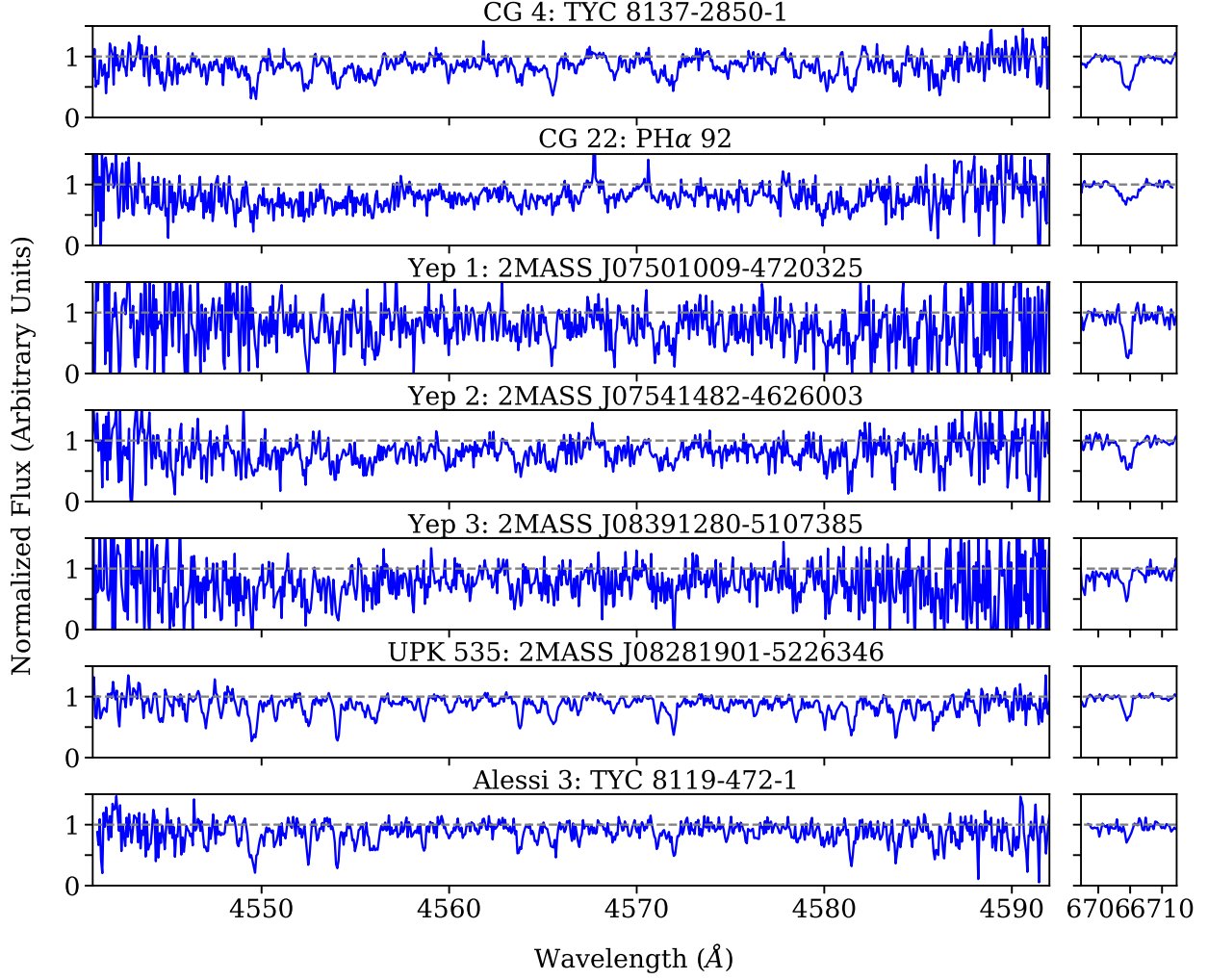


Figure 3.6: Sample of normalized CHIRON spectra. Order 1 (left panels) is rich in atomic lines and useful for spectral classification and velocity measurements. Order 41 (right panels) contains Li I λ 6708, present in young stars.

values range from 0.072 to 0.698 mag (see Table 3.4). From these extinctions and Bailer-Jones et al. (2018) distances, we calculate corrected absolute magnitude M_G for each star. Values for M_G span -2.50– 12.36 mag.

Masses can be interpolated from spectral type, $(BP - RP)_{\text{int}}$, or *Gaia* absolute magnitude M_G , using the dwarf spectral type or color or magnitude relations of Pecaut & Mamajek (2013), respectively. We use spectral-type-derived masses for all 284 spectroscopically observed stars, color-derived masses for 1515 stars, and absolute-magnitude-derived masses for the 33 stars lacking *BP* or *RP*. Spectral-type-derived-mass uncertainties are propagated from spectral

type uncertainties, with lower limit set to 5% of stellar mass to account for uncertainties in choice of stellar model. Spectral-type-derived masses and color-derived masses show an average absolute difference of $\sim 8\%$. Color-derived-mass uncertainties are propagated from color uncertainties, with lower limit set to 8% of stellar mass. Spectral-type-derived masses and absolute-magnitude-derived masses show an average absolute difference of $\sim 11\%$. Absolute-magnitude-derived-mass uncertainties are propagated from G - and distance uncertainties, with lower limit set to 11% of stellar mass. Stellar masses range from 0.12 to 7.30 M_{\odot} , with median mass 0.37 M_{\odot} and median uncertainty 8% of stellar mass (see Table 3.2). Two giant stars in Alessi 3 are assigned the mass of the highest-mass dwarf star in Alessi 3 (2.75 M_{\odot}).

Our stellar mass uncertainties are statistical. Systematic uncertainties, especially because the stars are pre-main sequence, are likely larger.

3.4.3 Radial Velocities

From the Doppler shift of spectral features, we measure stars' radial velocities. We derive relative velocities using cross-correlation analysis with PyAstronomy's *crosscorrRV* in Doppler mode, comparing each star to 1 – 11 standards within 2 spectral classes of the target star, across 30 spectral orders (see Figure 3.7 for example). Aberrant orders with velocities differing from the median by $> 3\sigma$ or > 10 km s^{-1} are discarded. Most stars with projected rotational velocity $v_{rot} \sin(i) < 100$ keep all 30 orders. For each good order, we compute the intrinsic Doppler uncertainty, lowest for orders with the most spectral features (Butler et al. 1996). We then compute the Doppler-uncertainty-weighted-mean relative velocity from all good orders for each standard. The uncertainty is the sample standard deviation of the good orders' relative velocities, added in quadrature with the uncertainty in the standard's radial velocity. Fifty-eight stars with rapid rotation > 100 km s^{-1} , few features, and low SNR < 10 have determined radial velocity uncertainties $\sigma_{v_r} > 10$ km s^{-1} and are considered unmeasured. We successfully measure 226 stars' radial velocities.

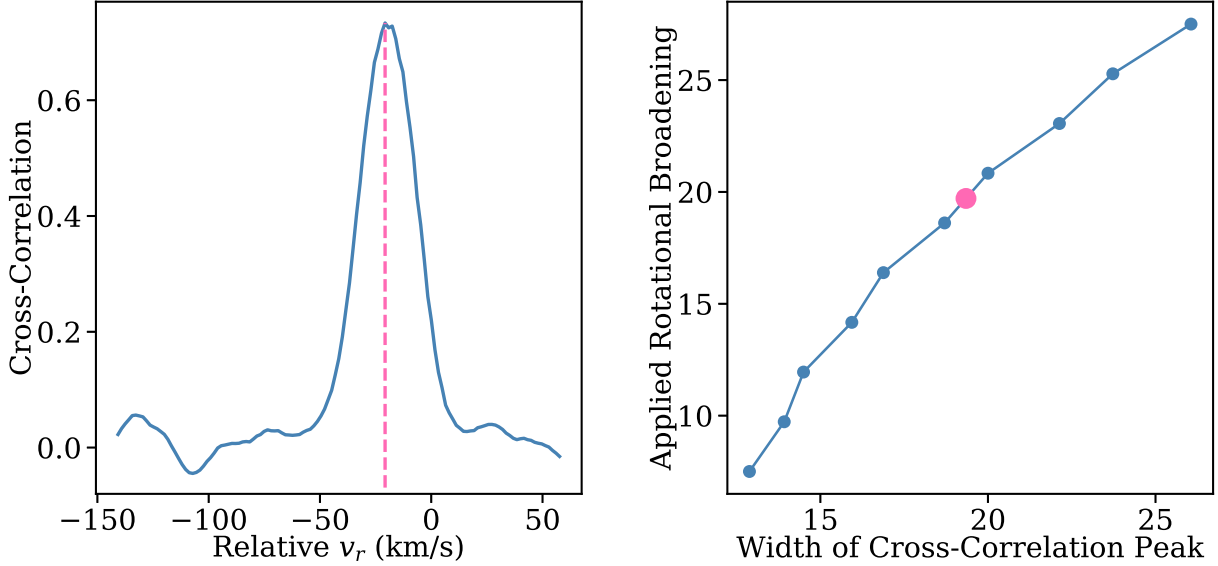


Figure 3.7: Example of cross-correlation procedure, for order 11 of K2V-type star TYC8137-2850-1. Left panel: The location of the peak of the cross-correlation function between the spectra of the standard star 41 Ara and the star TYC8137-2850-1 gives the applied Doppler shift, from which we calculate relative radial velocity and barycentric radial velocity v_r . Right panel: We auto-correlate the target star’s cross-correlation-peak width with its applied broadening v_b to derive an empirical relation between $v_{rot} \sin(i)$ and applied rotational broadening. Pink dot matches measured cross-correlation-peak width with amount of applied rotational broadening, which is then combined with the standard’s measured rotational broadening (3.2).

Relative velocity is converted to radial velocity relative to the center of the Solar System using each standard’s barycentric correction, calculated using the PyAstronomy function *helcorr* (Czesla et al. 2019).⁴ Final radial velocity v_r for each star is the error-weighted mean of the comparison standards’ results. Final uncertainty is the greater of the following: the error-weighted-mean error or, usually, the sample standard deviation of the comparison standards’ results. Including results for possible spectroscopic binaries, radial velocities range from -60.59 to 101.87 km s $^{-1}$ (see Table 3.2). Associations’ error-weighted-mean radial velocities range from 0.2 to 22.8 km s $^{-1}$ (see Table 3.4). The median radial velocity uncertainty is 0.52 km s $^{-1}$.

By the nature of our Cluster Finder search, all stars observed have positions, distances, and proper motions consistent with their associations. They also share Li I $\lambda 6708$ (see §2.3.1)

⁴<https://github.com/sczesla/PyAstronomy>

Table 3.2: Sample of Each Association’s Member Kinematics and Properties

Star Name	RA ($^{\circ}$)	D_{cc} (mas)	Parallax (mas)	μ_{α} (mas yr $^{-1}$)	μ_{δ} (mas yr $^{-1}$)	v_r (km s $^{-1}$)	G (mag)	BP (mag)	RP (mag)	d (pc)	Mass (M $_{\odot}$)
CG 4 Assn.											
...	112.2327 -45.5894	2.335 ± 0.076	-3.65 ± 0.15	9.50 ± 0.14	...	16.944 ± 0.001	18.848 ± 0.029	15.611 ± 0.005	424 $^{+14}_{-13}$	0.243 ± 0.019	
CD-46 3194	112.3984 -46.5226	2.403 ± 0.033	-4.036 ± 0.065	8.998 ± 0.074	7.1 ± 1.7	9.254 ± 0.001	9.483 ± 0.002	8.919 ± 0.003	411.4 $^{+5.7}_{-5.6}$	1.830 ± 0.092	
CG 22 Assn.											
...	126.8512 -35.2181	2.824 ± 0.035	-6.930 ± 0.056	10.482 ± 0.052	...	15.139 ± 0.004	16.325 ± 0.020	14.049 ± 0.011	350.6 $^{+4.4}_{-4.3}$	0.528 ± 0.042	
2MASS J08284752-3429298	127.1980 -34.4916	2.726 ± 0.030	-6.820 ± 0.045	11.273 ± 0.048	20.79 ± 0.43	12.277 ± 0.007	12.933 ± 0.025	11.493 ± 0.019	363.0 $^{+4.0}_{-3.9}$	0.860 ± 0.060	
CG 30 Assn.											
PHe 15	122.1950 -36.1313	2.794 ± 0.036	-7.579 ± 0.068	11.451 ± 0.067	21.99 ± 0.20	15.116 ± 0.013	16.259 ± 0.074	13.980 ± 0.033	354.4 $^{+4.5}_{-4.7}$	0.230 ± 0.043	
KWW 1863	122.1576 -36.0653	2.774 ± 0.031	-7.400 ± 0.056	12.025 ± 0.056	26.2 ± 3.0	13.584 ± 0.001	14.819 ± 0.004	12.469 ± 0.003	356.9 $^{+3.9}_{-4.0}$	0.500 ± 0.038	
Yep 1											
...	115.7942 -47.7632	2.474 ± 0.048	-4.910 ± 0.089	8.463 ± 0.093	...	16.086 ± 0.003	17.454 ± 0.025	14.890 ± 0.006	399.7 $^{+7.9}_{-7.6}$	0.389 ± 0.031	
...	118.3498 -48.0738	2.477 ± 0.049	-4.836 ± 0.090	8.76 ± 0.10	...	15.599 ± 0.002	16.952 ± 0.010	14.413 ± 0.004	399.3 $^{+8.0}_{-7.7}$	0.396 ± 0.032	
Yep 2											
...	121.9038 -48.5335	2.49 ± 0.12	-5.86 ± 0.24	8.31 ± 0.22	...	17.585 ± 0.002	19.350 ± 0.065	16.233 ± 0.008	398 $^{+20}_{-18}$	0.226 ± 0.019	
...	122.5352 -48.0071	2.36 ± 0.15	-5.61 ± 0.27	7.52 ± 0.27	...	18.279 ± 0.003	19.82 ± 0.12	16.845 ± 0.016	421 $^{+30}_{-26}$	0.260 ± 0.038	
Yep 3											
TYC 8163-2131-1	129.9593 -51.5401	2.876 ± 0.026	-12.625 ± 0.050	9.199 ± 0.053	-10.15 ± 0.95	11.888 ± 0.001	12.273 ± 0.004	11.346 ± 0.003	344.3 $^{+3.2}_{-3.1}$	1.25 ± 0.16	
TYC 8163-809-1	129.9754 -51.9476	2.814 ± 0.028	-12.101 ± 0.050	10.556 ± 0.053	12.06 ± 0.16	11.876 ± 0.000	12.163 ± 0.002	11.439 ± 0.001	351.8 $^{+3.5}_{-3.4}$	1.180 ± 0.059	
UPK 535											
...	126.3425 -48.8964	3.041 ± 0.062	-12.44 ± 0.10	2.77 ± 0.10	...	16.325 ± 0.002	17.575 ± 0.013	15.183 ± 0.004	326.0 $^{+6.8}_{-6.5}$	0.414 ± 0.033	
2MASS J08280595-4957545	127.0248 -49.9652	3.062 ± 0.016	-12.913 ± 0.031	2.989 ± 0.029	5.7 ± 1.7	13.334 ± 0.002	13.872 ± 0.008	12.651 ± 0.006	323.5 ± 1.7	0.798 ± 0.064	
Alessi 3											
...	126.3425 -48.8964	3.041 ± 0.062	-12.44 ± 0.10	2.77 ± 0.10	...	16.325 ± 0.002	17.575 ± 0.013	15.183 ± 0.004	326.0 $^{+6.8}_{-6.5}$	0.414 ± 0.033	
2MASS J07140743-4628549	108.5310 -46.4819	3.559 ± 0.014	-10.246 ± 0.025	12.073 ± 0.032	0.65 ± 0.79	13.165 ± 0.001	13.646 ± 0.003	12.540 ± 0.002	278.7 ± 1.1	0.730 ± 0.040	

NOTE— Full tables are available in Appendix B. “SBI1” marks two-epoch confirmed single-line spectroscopic binaries. “SBI?” marks suspected single-line spectroscopic binaries based on single-epoch radial velocities >5 km s $^{-1}$ discrepant from their association medians. “SB2?” marks visually clear double-line spectroscopic binaries, and “SB2,” possible double-line spectroscopic binaries.

and H α (see §3.4.6). Although we targeted stars along the apparent single-star main sequence, one star is clearly a double-line spectroscopic binary, one star is possibly a double-line spectroscopic binary, and 52 stars have radial velocities >5 km s $^{-1}$ discrepant from their association medians (see §3.5.1). Of these, five stars have serendipitous CHIRON followup observations with radial velocity shifts >5 km s $^{-1}$ confirming their binarity. The remaining 47 stars are treated as single-line spectroscopic binaries in this study.

3.4.4 Projected Rotational Velocities

We measure each star’s rotational broadening relative to the same comparison standards used in the cross-correlation analysis for determining radial velocities (see §3.4.3). For each spectral order, we artificially broaden each standard using PyAstronomy’s *rotBroad* based on Gray (1992), with limb-darkening coefficient $\epsilon = 0.6$, appropriate for optical wavelengths. We derive a relation between the amount of broadening applied to the standard and the Gaussian width of the peak of the standard’s autocorrelation function with its unbroadened self (see Figure 3.7). We then measure the width of the peak of the cross-correlation between the target star and the unbroadened standard and use the autocorrelation-derived width vs. broadening relation to determine applied broadening v_b . Each standard has a known or estimated projected rotational velocity v_i . The total measured projected rotational velocity of the target star is a combination of v_b and v_i :

$$r = \sqrt{v_b^2 + v_i^2} \quad (3.2)$$

$$\theta = \arctan\left(\frac{v_b}{v_i}\right) \quad (3.3)$$

$$v_0 = 0.044r \quad (3.4)$$

$$v_{rot} \sin(i) = \begin{cases} r + \frac{4v_0}{\pi}\theta, & \text{if } \theta \leq \frac{\pi}{4} \\ r - \frac{4v_0}{\pi}\theta + 2v_0, & \text{if } \theta > \frac{\pi}{4}, \end{cases} \quad (3.5)$$

where r is the standard rotational velocity and the applied broadening added in quadrature and v_0 is the empirically determined maximum deviation from addition in quadrature in polar coordinates. Orders for which the width falls below the derived broadening-width relation have their broadening interpolated on a quadratic fit to the relation. Orders that fail to interpolate a width are neglected. Most stars with rotation speed $< 100 \text{ km s}^{-1}$ utilize all 30 orders. The measured projected rotational velocity according to a given standard is the Doppler-uncertainty-weighted mean of the good orders' results. The uncertainty is the sample standard deviation of the good orders' results, added in quadrature with the standard's projected rotational velocity. Final projected rotational velocity $v_{rot} \sin(i)$ is the error weighted mean of the comparison standards' results. Final uncertainty is the greater of the error-weighted-mean error or, usually, the sample standard deviation of the comparison standards' results.

Testing this approach on our spectral standards with known projected rotational velocities, we find that we systematically overestimate the final $v_{rot} \sin(i)$ by $< 2 \text{ km s}^{-1}$ for $v_{rot} \sin(i) > 4 \text{ km s}^{-1}$, and our measurements are unreliable for $v_{rot} \sin(i) < 4 \text{ km s}^{-1}$ due to insufficient spectral resolution. All $v_{rot} \sin(i) < 4 \text{ km s}^{-1}$ are upper limits only. All $v_{rot} \sin(i) > 150 \text{ km s}^{-1}$ are lower limits only. Our method is most effective at measuring $v_{rot} \sin(i) > 2 \times$ the comparison standard's rotational velocity. Our catalogue of standards are amenably slow-rotating (see Appendix A).

We successfully measure $v_{rot} \sin(i)$ values for 271 stars in the Gum Nebula, 18 of which have upper limits of 4 km s^{-1} , 33 of which have lower limits of 150 km s^{-1} . 116 stars are fast rotators with $v_{rot} \sin(i) \geq 40 \text{ km s}^{-1}$ (see Figure 3.8). Median uncertainty is 2.3 km s^{-1} , lower for slow rotators (median uncertainty 1.64 km s^{-1} for $v_{rot} \sin(i) < 40 \text{ km s}^{-1}$) and higher for fast rotators (median uncertainty 6.32 km s^{-1} for $v_{rot} \sin(i) \geq 40 \text{ km s}^{-1}$).

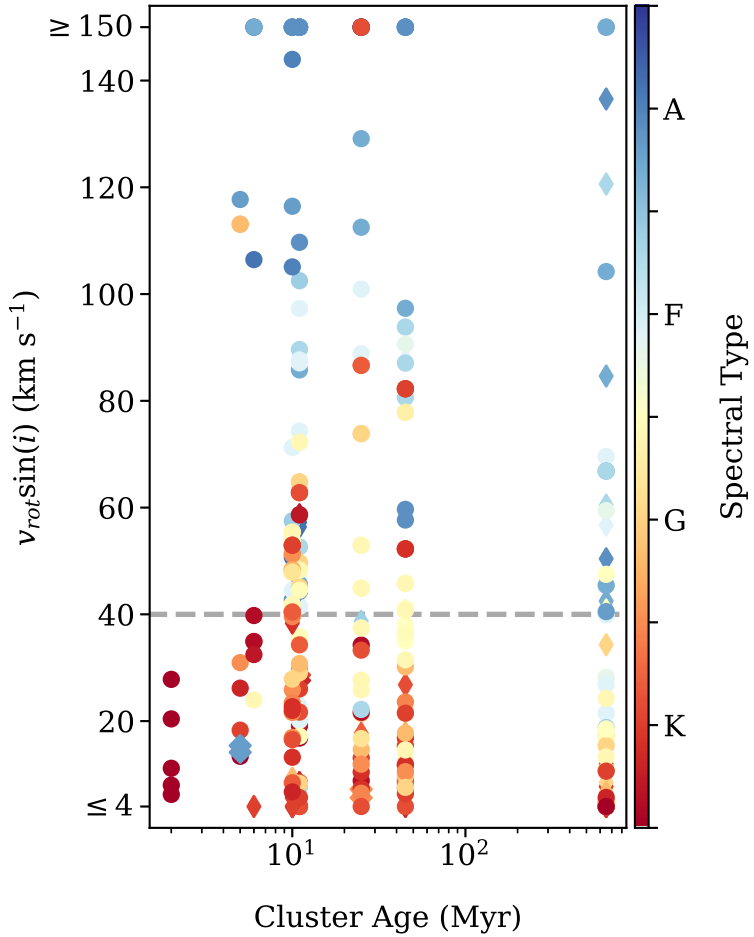


Figure 3.8: Projected rotational velocities $v_{rot} \sin(i)$ vs. ages. We have measured $v_{rot} \sin(i)$ for 271 association members based on CHIRON data and 5 members based on Keck I HIRES data (see Chapter 2). Five of the 8 associations contain stars with $v_{rot} \sin(i) > 40$ km s⁻¹. Circles are single-star association members. Diamonds are confirmed binaries (fat) or potential binaries (skinny). Twenty-seven cool stars later than type F5 are fast rotators.

3.4.5 Li Equivalent Widths

To assess associations' youth, we measure equivalent widths (EW) of Li I $\lambda 6708$ (see Figure 3.6). We fit three Gaussians to the 6706 – 6710 Å region to account for the two lines of the lithium doublet at 6707.7635 Å and 6707.9145 Å and the blended iron line at 6707.4308 Å (see Nisak et al. 2021). Equivalent width is calculated from the lithium components of the best-fit triple Gaussian. Uncertainties σ_{EW} are calculated as follows (Cayrel 1988; Deliyannis et al. 1993; Nisak et al. 2021):

$$\sigma_{EW} \approx \frac{\sqrt{fp}}{SNR}. \quad (3.6)$$

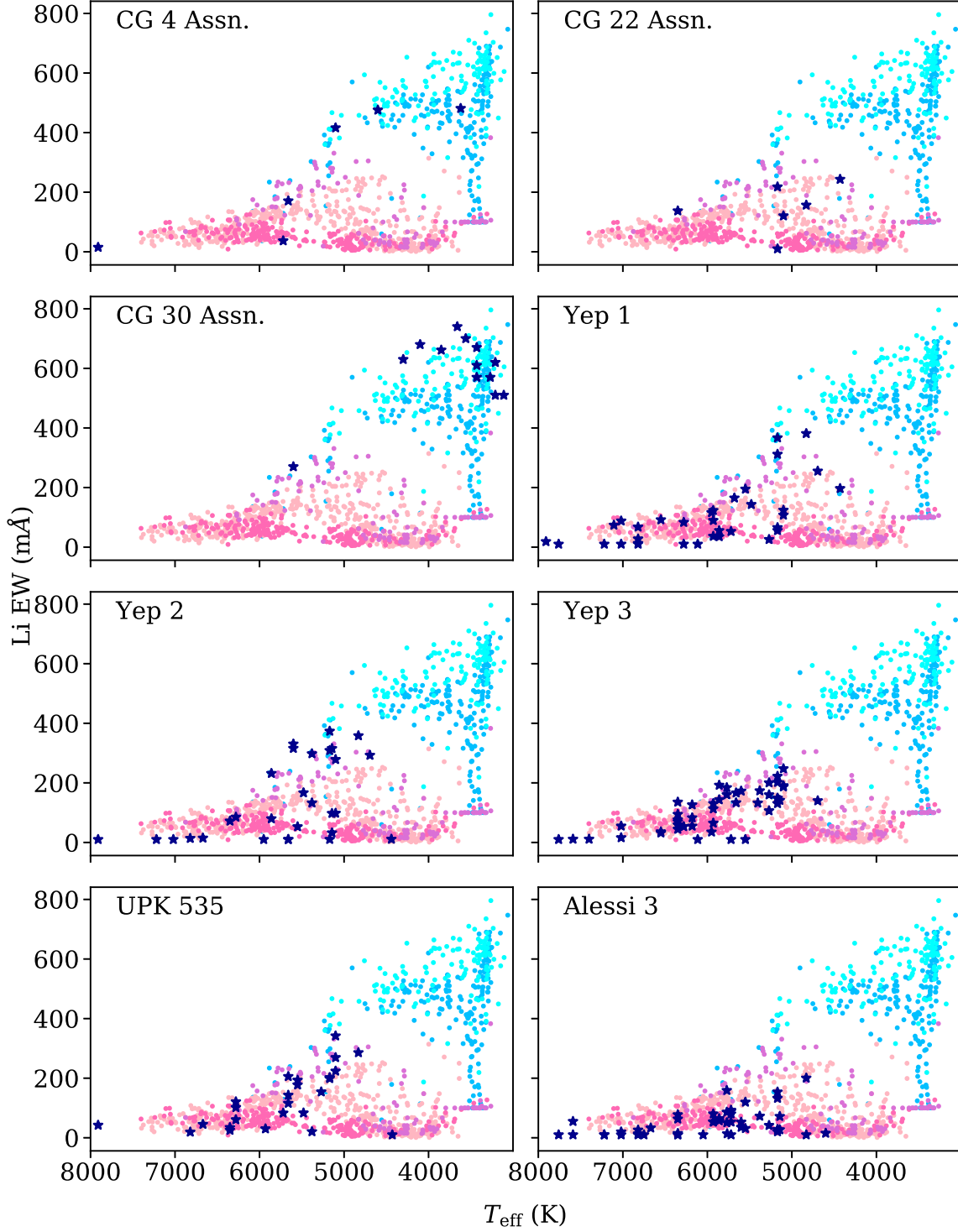


Figure 3.9: Li EW vs. T_{eff} . Light colored dots are from Gutiérrez Albarrán et al. (2020) and represent ages 1 – 3 Myr (cyan), 10 – 20 Myr (light blue), 34 – 41 Myr (lavender), 248 – 450 Myr (light pink), and 763 – 977 Myr (hot pink). Younger stars have stronger Li absorption, as do lower-mass stars. The associations in the Gum Nebula (dark blue stars) are fairly young, with ages 2 – 650 Myr. Their positions in Li EW vs. T_{eff} space are generally consistent with our isochrone age estimates.

Here f is the full width at half maximum of the spectral line, p is the wavelength per pixel scale = 0.100 Å at λ 6708 Å, and SNR is the signal-to-noise ratio per pixel in the spectral line. We measure values of Li EW from <0.01 to 0.48 Å, with median uncertainty 0.01 Å. Values <0.01 Å are set to 0.01 Å as an upper limit. We do not measure Li EW stars with $v_{rot} \sin(i) \geq 150$ km s⁻¹. We do not correct Li EW for veiling, the continuum excess emitted by hot spots during stellar accretion, so the Li EW of stars in the youngest (\lesssim 10 Myr) associations may be underestimated. Li EW for stars in the CG 30 Association are from Kim et al. (2005) and Yep & White (2020).

Lithium equivalent width (Li EW) provides a stellar age estimate independent from isochrone fits on a color-magnitude diagram. Because the rate of lithium depletion is spectral-type dependent (Randich et al. 1997; Jeffries et al. 2014; Gutiérrez Albarrán et al. 2020), we plot associations' Li EW vs. T_{eff} in Figure 3.9. Comparisons with the lithium measurements of Gutiérrez Albarrán et al. (2020) provide empirical age ranges spanning from 1 Myr to 1 Gyr. The CG 4 and CG 30 associations have positions consistent with ages between 1 and 10 Myr (see Figure 3.9). Yep 1 and Yep 2 appear <34 Myr. UPK 535 is in the 34 – 41 Myr range. CG 22 and Yep 3 appear between 41 and 248 Myr. Alessi 3 appears older than 248 Myr but younger than 763 Myr.

Our approximate age ranges from Li EW vs. T_{eff} space are consistent with our isochrone-fit age estimates (see §3.3.9), with the exception of CG 22, whose isochrone-estimated age of 6^{+4}_{-2} Myr is significantly younger than its Li EW vs. T_{eff} age. Part of the discrepancy may be due to unmeasured veiling. Because of this and the probable connection between the CG 22 Association and its nearby star-forming cometary globule CG 22 (see §4.2), we defer to the isochrone-determined age.

3.4.6 H α Widths

Broad H α emission is associated with gas infall during accretion from a young star's circumstellar disk (Muzerole et al. 1998). Narrow H α emission is associated with chromospheric

activity, and H α absorption is simply from a star's photosphere. To measure H α $\lambda 6562.81$ Å emission or absorption, we first fit a Gaussian to the 6538 – 6588 Å region. We then integrate the normalized spectrum across the width of the Gaussian for which Gaussian flux < 0.99 for absorption or > 1.01 for emission. We choose to integrate the normalized spectrum because several of the H α features are broadened, saturated, or oddly shaped due to mixed absorption and emission (see Figure 3.10). Uncertainties are calculated as in Equation 3.6 with p set to 0.097 Å at $\lambda 6562.81$ Å. Twenty-eight spectra with low signal or mixed emission and absorption are measured manually and include additional uncertainty from visual inspection, added in quadrature to the σ_{EW} above. Our sample includes 36 stars with H α emission, 25 stars with mixed H α emission and absorption, and 224 stars with H α absorption. H α equivalent widths (EW) range from 4.46 Å (absorption) to -32.29 Å (emission; see Table 3.2). The median H α EW is 1.94 Å (absorption), and the median uncertainty is 0.02 Å. H α emitters appear in all 8 associations, even the older Alessi 3, but are more numerous in the younger associations.

For the 36 stars with H α emission and one star with mixed H α emission and absorption, we measure H α width at 10%-peak above the continuum, in km s $^{-1}$. Fast gas motions are associated with ongoing stellar accretion, whereas lower gas speeds are associated with chromospheric activity (White & Basri 2003; see §4.1). H α 10% widths range from 4 to 684 km s $^{-1}$. H α EW for stars in the CG 30 Association are from Kim et al. (2005) and Chapter 2, and their 10% widths are from Chapter 2.

3.4.7 Near-Infrared Excess

Hot dust in a young star's inner disk causes a near-infrared excess above the photosphere. We utilize the dwarf colors of Pecaut & Mamajek (2013) to measure infrared excess in $J - K$ color. We cross-match our association membership lists with 2MASS using CDS X-Match (Skrutskie et al. 2006; Boch et al. 2012). We then compare all apparent $J - K$ colors with stars' intrinsic $J - K$ colors based on their spectral types. We only measure color excesses

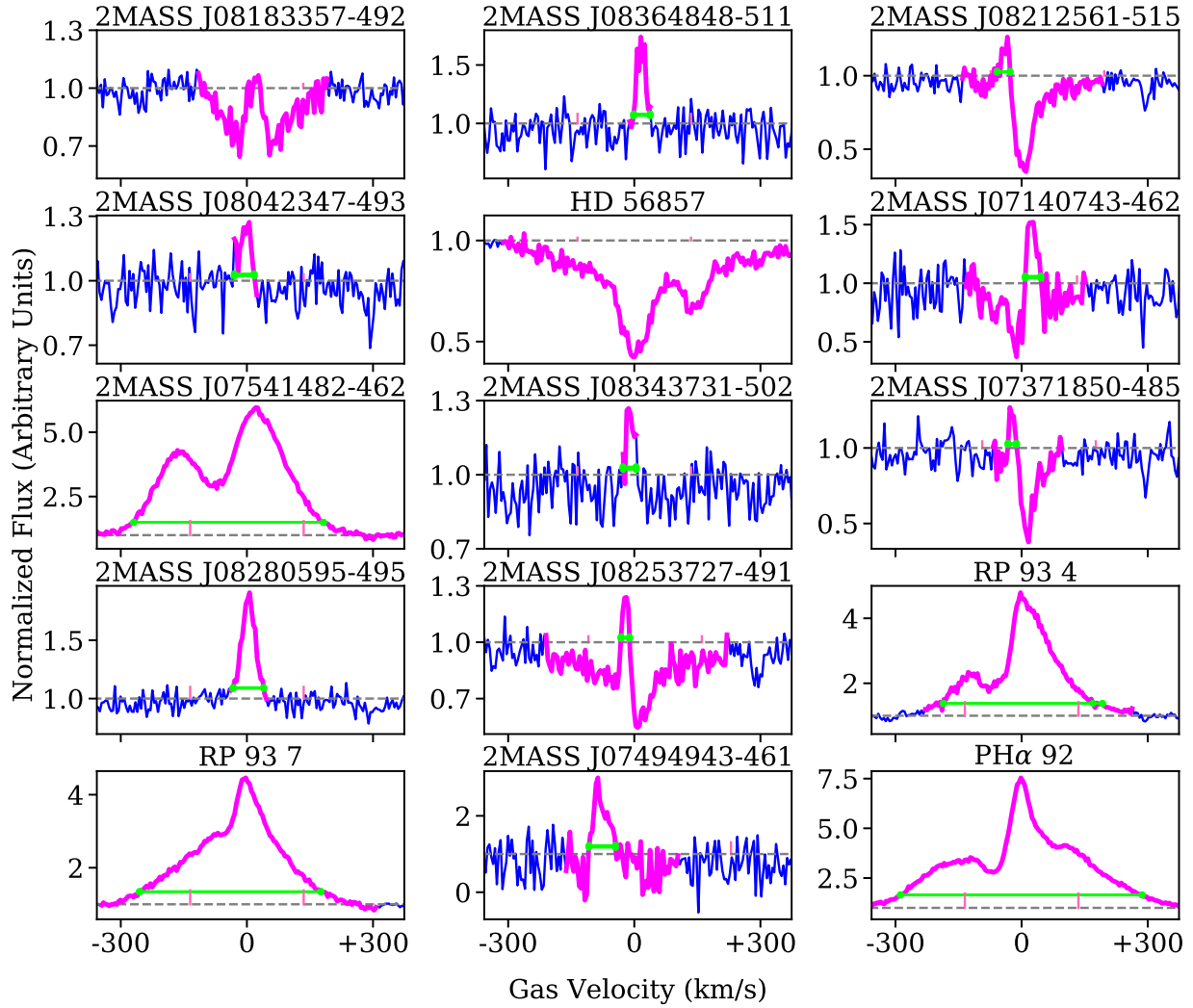


Figure 3.10: Sample of H α profiles with emission or mixed emission and absorption, in normalized flux vs. gas velocity. Equivalent width is calculated over the magenta portion. Lime green marks the H α 10% width for emitters. Pink vertical lines up through the 10% width indicate a gas motion spread of 270 km s $^{-1}$, our empirical boundary between accreting and nonaccreting stars.

Table 3.3: Sample of Stellar Properties of Spectroscopically Observed Stars

Star Name	Spectral Type	Class	v_r	$v_{\text{rot}} \sin(i)$	Binary Flag	$\text{H}\alpha$ EW (Å)	$\text{H}\alpha$ 10% W (km s $^{-1}$)	Li EW (Å)	Infrared Excess (mag)	Assn. Name
CD-463194	1 A6V	1.0	7.1 ± 1.7	...	SB2	2.8903 ± 0.0074	...	0.0151 ± 0.0074	0.197 ± 0.049	CG 4 Assn.
RP93 7	1 K4V	1.0	22.47 ± 0.42	26.2 ± 1.6		-14.6412 ± 0.017	431 ± 12	0.476 ± 0.026	0.477 ± 0.062	CG 4 Assn.
2MASSJ08264387-3420129	1 K3.5V	1.0	24.82 ± 0.96	39.8 ± 1.7		-0.219 ± 0.027	141 ± 12	0.243 ± 0.020	...	CG 22 Assn.
PH α 92	1 K3V	1.0	20.09 ± 0.92	32.5 ± 1.9		-32.293 ± 0.012	575 ± 12	0.157 ± 0.016	0.933 ± 0.075	CG 22 Assn.
2MASS J07541482-4626003	1 K2.5V	1.0	21.30 ± 0.40	19.11 ± 0.80		-26.482 ± 0.023	451 ± 12	0.255 ± 0.018	...	Yep 1
CD-483205	1 A2V	1.0	20.1 ± 3.5	44 ± 28		4.273 ± 0.018	...	0.0100 ± 0.0033	0.194 ± 0.042	Yep 1
TYC 8138-2794-1	1 A2V	1.0	...	150.		4.000 ± 0.030	0.128 ± 0.036	Yep 2
TYC 8143-2246-1	1 F4V	1.0	22.22 ± 0.98	54.0 ± 4.0		3.220 ± 0.014	...	0.0147 ± 0.0039	0.059 ± 0.039	Yep 2
HD 76901	1 A2V	2.0	...	60.		4.329 ± 0.014	-0.043 ± 0.052	Yep 3
HD 70977	1 A9V	2.0	19.3 ± 2.0	87.1 ± 3.1		3.825 ± 0.018	...	0.0112 ± 0.0044	0.022 ± 0.049	Yep 3
TYC 8162-73-1	1 A6V	1.0	4.2 ± 1.7	39 ± 15	SB1?	2.980 ± 0.015	...	0.0423 ± 0.0077	0.130 ± 0.033	UPK 535
HD 71969	1 B9V	1.0	...	150.		3.740 ± 0.026	0.039 ± 0.045	UPK 535
CD-46 3075	1 A7V	1.0	-10.1 ± 6.6	121 ± 15	SB1?	3.364 ± 0.014	...	0.0100 ± 0.0085	0.091 ± 0.035	Alessi 3
2MASS J07110162-4530379	1 G1V	1.0	0.66 ± 0.13	5		1.591 ± 0.015	...	0.0643 ± 0.0073	...	Alessi 3

NOTE—Full table is available in Appendix C.

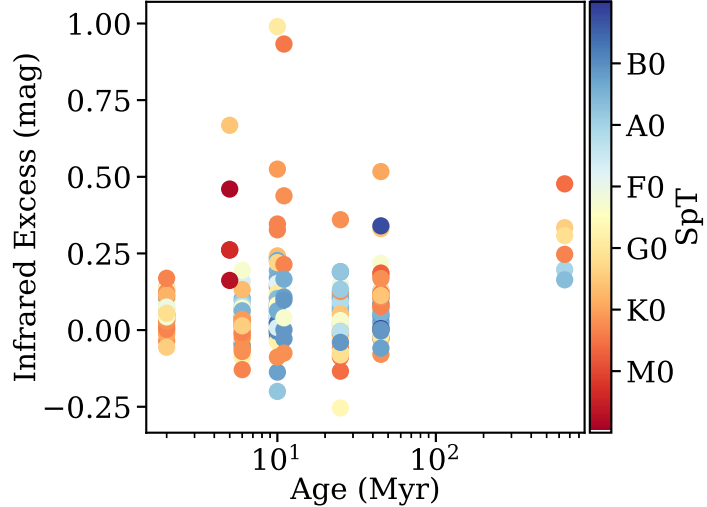


Figure 3.11: Infrared excess in $J - K$ vs. age. The dust in young stars' accretion disks or a debris disks tend to cause infrared excess. We calculate infrared excess by comparing stars' apparent $J - K$ colors with their intrinsic colors according to their spectral types and the dwarf colors of (Pecaut & Mamajek 2013).

for spectroscopically observed stars. Association-averaged results range from 0.024 to 0.311 mag and generally decrease with increasing association age (see Figure 3.11 and Table 3.3)).

Near-infrared excess is associated with a strong signal of accretion, spectral veiling (see §2.3.5), a filling-in of spectral lines and bluing of color (White & Ghez 2001). We see this effect in several spectra but have not measured it.

3.4.8 Exceptions

In measuring the radial velocity of the double-line spectroscopic binary star CD-46 3194, each of the two cross-correlation peaks are measured separately. We assume both stars have the same mass and therefore average their radial velocities to derive a systemic velocity of 7.1 ± 1.7 km s $^{-1}$. In measuring rotational velocity, each of the two cross-correlation peaks of the binary star CD-46 3194 are again measured separately. One component has $v_{\text{rot}} \sin(i) = 15.4 \pm 3.4$ km s $^{-1}$, and the component has $v_{\text{rot}} \sin(i) = 14.2 \pm 4.0$ km s $^{-1}$.

The spectrum of the candidate double-line spectroscopic binary 2MASS J08443526-5234117 does not manifest double cross-correlation peaks, perhaps because its SNR is too low or

because the star is not a spectroscopic binary (see §3.4.2). We treat 2MASS J08443526-5234117 like a single star when measuring its radial and rotational velocity.

The lithium feature CD-46 3194 cannot be resolved into two separate lines, so both components are measured together. Thus Li EW for CD-46 3194 is an upper limit. The H α feature of CD-46 3194 also could not be resolved into two separate lines, so both components are measured together. Thus H α EW for CD-46 3194 is also an upper limit.

3.5 Association Properties

We determine the ensemble association v_r , $E(BP - RP)_{\text{assn}}$, and A_G by taking the error-weighted mean of associations' member star measurements (see §3.4.2, and §3.4.3). We give our prescription for verifying association members and determine association age and total mass. Association properties are assembled in Table 3.4.

3.5.1 Association Verification

Our initial star selection process was relatively narrow (see 3.2), so chance of association membership is high. Nonetheless, we calculate each star's z-score (difference from association mean divided by association standard deviation) in RA , Dec , d , μ_α , μ_δ , and, where available, v_r and Li EW. Stars with a high z-score in a couple parameters (e.g. stars towards the edge of the association) may still be members, but stars with a high z-score in several parameters may not be. We therefore calculate an average absolute-value z-score and inspect any stars that score higher than 2. One star in Yep 1, two stars in Yep 2, and three stars in Theia 120 are deemed nonmembers and discarded. All six nonmembers are dimmer than $V = 13.5$ mag.

3.5.2 Total Stellar Masses

Total stellar mass of each association is calculated by summing individual stellar masses, the estimated mass of undiscovered cool stars according to an initial mass function (IMF),

Table 3.4: Association Properties

Association	No.	Age	$E(BP - RP)_{\text{assn}}$	A_G	Infrared	M_{tot}	v_r	Accretion	
Name	Stars	[Myr]	[Fe/H]	(mag)	Excess (mag)	(M_\odot)	(km s $^{-1}$)	Fraction (%)	G_0
69	CG 4 Assn.	34	5 $^{+5}_{-2}$	0.1	0.349 \pm 0.028	0.698 \pm 0.056	0.311 \pm 0.037	30.8 \pm 3.1	21.6 \pm 1.1
	CG 22 Assn.	102	6 $^{+4}_{-2}$	0.1	0.223 \pm 0.077	0.45 \pm 0.15	0.109 \pm 0.045	77.0 \pm 9.4	22.2 \pm 1.9
	CG 30 Assn.	29	2.0 $^{+2.0}_{-1.5}$	0.1	0.04 \pm 0.14	0.08 \pm 0.29	0.245 \pm 0.065	20.8 \pm 2.7	22.8 \pm 2.0
	Yep 1	534	11 $^{+9}_{-4}$	0.2	0.134 \pm 0.055	0.27 \pm 0.11	0.062 \pm 0.031	398 \pm 56	21.4 \pm 1.8
	Yep 2	443	10 $^{+5}_{-4}$	0.0	0.161 \pm 0.054	0.32 \pm 0.11	0.068 \pm 0.034	327 \pm 50.	20.8 \pm 1.4
	Yep 3	297	45 $^{+55}_{-20}$	0.2	0.036 \pm 0.027	0.072 \pm 0.053	0.024 \pm 0.022	252 \pm 27	19.4 \pm 1.6
	UPK 535	174	25 $^{+15}_{-10}$	0.1	0.059 \pm 0.022	0.120 \pm 0.043	0.053 \pm 0.016	145 \pm 13	10.1 \pm 1.6
	Alessi 3	260	650 $^{+100}_{-400}$	0.2	0.037 \pm 0.044	0.075 \pm 0.088	0.039 \pm 0.034	300. \pm 26	0.2 \pm 1.1
								0.0 \pm 0.0	3.4 $^{+2.7}_{-2.1}$

and estimated unresolved binary companion masses for a total binarity of 50%. Uncertainties are worst-case uncertainties, summed directly.

Our samples extend down to apparent $G \sim 20$ mag and are reasonably complete down to $\sim 0.2 M_{\odot}$, or spectral type \sim M4V. According to the IMF of Kroupa (2001), 48% of stars are M-type stars and contribute 28% of the total association mass, and 38% are brown dwarfs that contribute 4.3% of the total association mass. Counting all stars up to each association's largest stellar mass, we calculate that we are missing anywhere from 9 to 42% of the mass of each association, median 20%, with an assigned uncertainty of 20% of the missing amount to account for uncertainties in choice of IMF and the edge of our samples' spectral type completeness.

To account for binary companions when summing stellar masses, we double the mass of double-line binary stars, and we approximate each confirmed or suspected single-line binary star's companion mass as half the mass of the primary (see §3.4.3 for binary criteria). Known-companion mass adds 2 to 22% of the single-star mass to the total mass, median 9% of the total single-star mass. If the associations have 50% binarity and companion stars each possess half the mass of their primaries, randomly assigned unresolved binarity over 10,000 randomized trials adds mass equaling 20 – 24% of the total single-star mass, median 22%.

Summing all masses and uncertainties within each association, association total stellar masses M_{tot} span $21 - 398 M_{\odot}$ (see Table 3.4), with a median worst-case uncertainty (all component uncertainties summed directly) of 11% of total stellar mass. This is again statistical uncertainty, with systematic uncertainty likely higher.

3.6 Summary

The Gum Nebula in the plane of the Galaxy is crowded with young stellar associations.

- We develop an empirical method Cluster Finder for finding clusters and associations in *Gaia* DR2 data. Using this method, we find 8 young associations in the Gum Nebula.

- We present a catalogue of 81 high-quality spectral standards observed with CHIRON in fiber mode, spanning from spectral type O9.5V to M5.5V.
- We observe 284 stars in 7 of the 8 associations in the Gum Nebula.
- From spectra and *Gaia* DR2 data, we derive stellar and association properties.
- Five of the 8 associations we study in the Gum Nebula, including the CG 30 Association, are young (≤ 10 Myr), based on lithium abundances and isochrone fits.
- Stars exhibiting H α emission are present in all 8 associations. Stars with strong H α emission indicative of ongoing accretion are present in the five young associations.

We explore the implications of the 8 associations' properties in the following chapter.

CHAPTER 4

PROPERTIES AND ASSOCIATIONS

4.1 Introduction

We here examine the implications of stellar and association properties (determined in Chapter 3) of 8 associations in the Gum Nebula.

In §4.2 we ascertain which associations may be connected with their nearby cometary globules. In §4.3 we quantify far ultraviolet radiation in the Gum Nebula. In §4.4 we examine effects of the Gum Nebula’s moderate radiation environment on the 8 young associations, namely low accretor fractions. In §4.5 we look at possibly high projected rotational velocities. We interpret results in §4.6. We summarize in §4.7.

4.2 Star Formation Associated with Cometary Globules

As described in §3.2, the associations were first identified by searching for stellar associations in close proximity to cometary globules in the Gum Nebula. However, the identified associations may or may not be physically associated with these ongoing sites of isolated star formation. Here we examine all 8 associations for connections with their nearby cometary globules. We consider the cometary globules we invoked when searching for the found associations as well as six additional cometary globules and dark clouds that have measured radial velocities (see Figures 3.3 and 3.1).

A cometary globule’s connection with a stellar association gives us a way to estimate a first distance to that globule, a typically difficult quantity to measure for diffuse clouds.

4.2.1 CG 4 Association and CG 4

The CG 4 Association is sparse and young, 5^{+5}_{-2} Myr. Of all 7 new associations in this paper, the association by CG 4 most closely resembles the CG 30 Association in its sparseness and its core's proximity to a globule actively forming stars (Reipurth & Pettersson 1993; Pettersson 2007; Kim et al. 2005). CG 4 is spatially within the CG 4 Association, 0.24° from the center. CG 6 is also spatially very near the association (Reipurth & Pettersson 1993; Kim et al. 2006), about 0.63° from the center. CGs 4 and 6 have radial velocities 19.0 ± 1.2 km s $^{-1}$ and 18.2 ± 1.1 km s $^{-1}$, respectively (Sridharan 1992), and the association has a median velocity of 21.6 ± 1.1 km s $^{-1}$, so their connection with the CG 4 Association is plausible. We therefore estimate the distances to CG 4 and CG 6 are the association's error-weighted-mean distance of 415.8 ± 1.0 pc. This puts CG 4 and CG 6 about 1.8 pc and 4.6 pc from the center of the CG 4 Association, respectively.

4.2.2 CG 22 Association and CG 22

CG 22 is 1.18° from the center of the CG 22. Choudhury & Bhatt (2009) deduced CG 22's motion from the young star PH α 92 within it. Following Choudhury and Bhatt's example, we can infer that CG 22's v_r is 20.09 ± 0.92 km s $^{-1}$. The CG 22 Association's error-weighted-mean v_r is similar, 22.2 ± 1.9 km s $^{-1}$, and the association's proper motions match PH α 92's. Considering CG 22's young age (6^{+4}_{-2} Myr) and ongoing star formation in its bright-rimmed head, CG 22 is likely associated with the CG 22 Association. We therefore estimate the distance to CG 22 is the association's error-weighted-mean distance of 355.06 ± 0.54 pc. This puts CG 22 about 7.3 pc away from the center of the CG 22 Association.

4.2.3 CG 30 Association and CG 30

CG 30 is spatially within the CG 30 Association, 0.31° from the center. The CG 30 Association is very young ($2.0^{+2.0}_{-1.5}$ Myr) and moves at $v_r = 22.8 \pm 2.0$ km s $^{-1}$, consistent with the cometary globule's $v_r = 22.8$ km s $^{-1}$). Two other cometary globules in the vicinity, CG

31 and CG 38, have radial velocities $23.3 - 24.2 \text{ km s}^{-1}$ and $20.3 \pm 1.2 \text{ km s}^{-1}$, respectively, that are also consistent with the association's. The association and the CG 30-31-38 cometary globule are dynamically connected (Kim et al. 2005; Chapter 2). We therefore estimate the distance to the CG 30-31-38 cometary globule complex is the association's error-weighted-mean distance of $356.6 \pm 1.4 \text{ pc}$. This slightly revises our distance from Chapter 2 ($358.1 \pm 2.2 \text{ pc}$) and puts CG 30 about 1.9 pc from the center of the CG 30 Association.

4.2.3.1 *Yep 1 and CG 3*

Yep 1 is populous (535 stars), large, round, and fairly young, 11^{+9}_{-4} Myr . The radial velocity of CG 3 is $17.4 \pm 1.0 \text{ km s}^{-1}$ (Sridharan 1992), whereas the median radial velocity of the association is $21.4 \pm 1.8 \text{ km s}^{-1}$. With a 3.9 km s^{-1} discrepancy in radial velocity and a 2.32° separation between CG 3 and the association center (would be 15.9 pc at Yep 1's distance), connection with the globule is possible but unlikely.

4.2.3.2 *Yep 2 and CG 14*

The globule CG 14 is beyond the edge of the association, 3.91° from the association's core (would be 27.5 pc at Yep 2's distance). The radial velocity of CG 14 is $16.4 \pm 1.0 \text{ km s}^{-1}$ (Sridharan 1992), while the median radial velocity of Yep 2 is $20.9 \pm 1.5 \text{ km s}^{-1}$. Though the association is young, 10^{+5}_{-4} Myr , it may not be physically connected with the cometary globule CG 14.

4.2.3.3 *Yep 3 and CG 17*

The cometary globule CG 17 is 2.06° from the median center position of 45-Myr-old Yep 3 (would be 12.2 at Yep 3's distance) and moving at a radial velocity of $19.3 \pm 0.4 \text{ km s}^{-1}$. The association has a very similar median radial velocity of $19.4 \pm 1.6 \text{ km s}^{-1}$. Despite the similar kinematics, Yep 3's age of $45^{+55}_{-20} \text{ Myr}$ is well past when most clusters lose their molecular

cloud material (Krumholz et al. 2019; Karnath et al. 2019). Therefore we assume Yep 3 and CG 17 are not connected.

4.2.3.4 UPK 535 and GDC 1

GDC 1 is spatially within UPK 535 and moving at a radial velocity of $22.6 \pm 1.2 \text{ km s}^{-1}$. Its proper motions are unknown. UPK 535 is about 22 Myr old, has a median radial velocity of $10.1 \pm 1.6 \text{ km s}^{-1}$, and is not associated with GDC 1.

UPK 535 has a drawn-out shape much like Yep 3 and in fact partially overlaps it. As described in detail in Chapter 5, these two associations have recently collided.

4.2.4 Alessi 3 and CG 1

Though CG 1 is within our search radius for Alessi 3, it is unlikely they are associated. Alessi 3 is an older open association, 500 Myr according to Alessi et al. (2003) and 650^{+100}_{-400} Myr according to our own analysis (see §§3.4.5 & 3.5). An association of this age is unlikely to be associated with the new star formation at CG 1. Additionally, the proper motions and radial velocities of Alessi 3 and CG 1 differ ($\mu_\alpha = -9.81 \pm 0.16$ vs. $-4.2 \pm 2.0 \text{ mas yr}^{-1}$, $\mu_\delta = 11.85 \pm 0.17$ vs. $6.1 \pm 1.9 \text{ mas yr}^{-1}$, and $v_r = 0.2 \pm 1.1$ vs. $20.6 \pm 1.4 \text{ km s}^{-1}$, respectively (Sridharan 1992; Alessi et al. 2003; Choudhury & Bhatt 2009; see §3.4.3)).

Our categorization of irradiated vs. quiescent is preliminary. Detailed, consistent calculation of G_0 values for all our comparison clusters has never been done before, and local variations in G_0 due to occasional within-association B-type stars have not been taken into account. Additionally, methods for distinguishing accretors from nonaccretors vary across the several studies synthesized in Chapter 2, and external photoevaporation of disks may also depend on host star mass (Adams et al. 2004). Calculation of average and local G_0 and consistent designation of accretors vs. nonaccretors in all comparison clusters and associations would be worthwhile.

4.3 Gum Nebula Radiation Environment

We quantify ionizing radiation throughout the Gum Nebula with factor G_0 , the ratio of a region's FUV radiation compared to average interstellar $G_{0,ISM} = 1.6 \times 10^3 \text{ ergs s}^{-1} \text{ cm}^{-2}$ (Habing 1968; Winter et al. 2018). Following the prescription in Chapter 2, we calculate G_0 values at the position of each of the 8 associations. We find that G_0 ranges from 2.1 to 11.2, with median 4.8. These G_0 values and the presence of cometary globules and O-type stars lead us to designate the Gum Nebula a moderate radiation environment.

The presence of B-type stars within some associations may locally raise G_0 by 1 – 10 points, but we do not at present take this into account. Ideally we would include each association's B-type stars to map local G_0 . We could then check if disk loss is more due to local B-type stars or the O-type stars powering the Gum Nebula.

We gather comparison clusters and associations from Mohanty et al. (2005) and Table 2.9. We categorize these comparison clusters and associations as *irradiated* if cometary globules or OB associations are present and as *quiescent* if no cometary globules or OB associations are present. This categorization is preliminary. Ideally we would determine an averaged G_0 cutoff between irradiated and quiescent clusters, but G_0 has never been calculated for most of our comparison clusters and associations. Additionally, some of the youngest clusters are embedded, which may shield some of their young stars from radiation in complex ways. A detailed, consistent calculation of G_0 for all our target- and comparison clusters and associations is in order, but that is beyond the scope of this dissertation.

4.4 Photoevaporated Protoplanetary Disks

Young stars possess dusty, gaseous accretion disks for the first few million years of their lives, until stellar winds or the pressure of their own radiation dispels them. The fraction of stars in an association that are still accreting, N_{acc}/N_{tot} , thus decreases over time. In a quiescent star-forming region free of massive stars, such as Tau-Aur, $N_{acc}/N_{tot} = 30 – 50\%$ is

normal for age 1 – 5 Myr, and $N_{acc}/N_{tot} = 15 – 30\%$ is normal for age 5 – 10 Myr (Mohanty et al. 2005; Yep & White 2020). In an irradiated region that is inhabited by an O-type star or several B-type stars, $N_{acc}/N_{tot} = 10 – 30\%$ is normal for age 1 – 5 Myr, and $N_{acc}/N_{tot} = 1 – 10\%$ is normal for age 5 – 10 Myr (see Table 2.9).

White & Basri (2003) demonstrate that $W_{10}(\text{H}\alpha) > 270 \text{ km s}^{-1}$ is associated with accretion. This easy-to-measure indicator is less sensitive to stellar mass than H α EW and optical veiling (White & Basri 2003; Adams et al. 2004), and potentially affected only slightly by circumstellar disk inclination. Based on the number of accretors in each association divided by the number of stars in each association, we calculate each association’s accretor fraction N_{acc}/N_{tot} , the fraction of stars that still have their accretion disks.

None of the three older associations (>11 Myr) have any stars that are accreting. All five young associations (1 – 11 Myr) within the Gum Nebula exhibit low accretor fractions for their ages, 0 – 29% for ages 2 – 11 Myr. To illustrate this, we plot the accretor fractions vs. ages of quiescent and irradiated regions in Figure 4.1, using data from Mohanty et al. (2005) and Table 2.9. We then fit a power law to the quiescent regions and another power law to the irradiated regions. The accretor fractions of the five young clusters in the Gum Nebula appear more consistent with the irradiated environments than the quiescent environments. This finding, however, relies on our preliminary distinction between irradiated and quiescent environments, and on inhomogeneous methods for distinguishing accretors from nonaccretors across the several studies synthesized in Table 2.9. In addition to calculation of average and local G_0 , a consistent, improved designation of accretors vs. nonaccretors in all target- and comparison associations and clusters will yield more robust results.

4.5 High Rotational Velocities for Age

Fast rotation of cool (FGK-type) stars, along with Li abundance and chromospheric activity (itself correlated with fast rotation), is associated with youth (Cutispoto et al. 2002). Because a cool star’s interaction with its own protoplanetary disk could magnetically brake

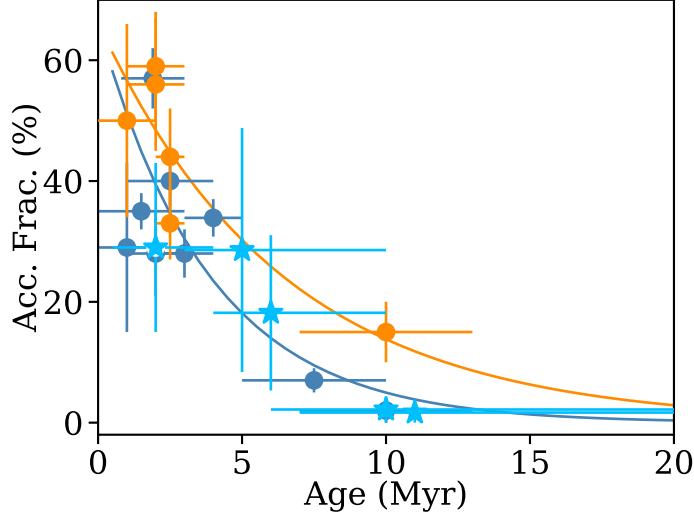


Figure 4.1: Association accretor fraction vs. association age. Quiescent-region associations (orange circles) tend to have higher accretor fractions per age than external-radiation-region associations (steel blue circles). Gum Nebula associations' accretor fractions (azure stars) appear more consistent with the external-radiation-region trend.

the star's rotation, cool-star fast rotation for age could be a sign of early disk dispersal. Across the eight associations, 27 cool stars earlier than type F5 have projected rotational velocity $v_{rot} \sin(i) > 40 \text{ km s}^{-1}$ (see Figure 3.8). Three cool stars (CD-46 3212, 2MASS J08292220-5050369, 2MASS J08351629-5156166) are extraordinarily fast, with $v_{rot} \sin(i) > 100 \text{ km s}^{-1}$. The fastest, K2V-type star 2MASS J08292220-5050369, is rotating at $>150 \pm 20 \text{ km s}^{-1}$.

To use projected rotation speeds to indirectly probe early disk dispersal, we require a comparison sample of $v_{rot} \sin(i)$ values in young quiescent regions. Barnes (2010) or de Freitas (2020) may provide theoretical comparisons.

4.6 Characteristics of Cometary Globule Associations

The three clusters most likely associated with their nearby cometary globules are the CG 4, CG 22, and CG 30 Associations (Kim et al. 2005; Pettersson 2007; Yep & White 2020). All three globules are actively forming stars (Reipurth & Pettersson 1993; Kim et al. 2006; Rebull et al. 2011; Yep & White 2020). All three are also fairly sparse, each association comprising $\lesssim 100$ stars, and the structures of the CG 4 and CG 30 Associations are filamentary. The

CG 4, CG 22, and CG 30 Associations' sparseness is consistent with the suggestion that cometary globules produce isolated, low-mass stars (Bhatt 1993; Kim et al. 2005; Walch et al. 2013), due to external radiation spurring relatively low-mass globules to form stars (Bhatt 1993; Maheswar & Bhatt 2008). The highest-mass stars in the CG 4, CG 22, and CG 30 Associations are 1.86, 2.75, and $0.97 M_{\odot}$, respectively. CG 4 and CG 30 have no stars $> 2 M_{\odot}$, while CG 22 has 5 such stars.

External radiation from the hot bright O-type stars at the Gum Nebula's heart may limit Gum Nebula young stars' ability to form planets. Far-ultraviolet radiation erodes protoplanetary disks early in even moderate-radiation environments ($G_0 = 2.1 - 7.8$ for the five young clusters; see Table 3.4 and Figure 4.1). Far-ultraviolet radiation may also damage or destroy the ingredients necessary to planet formation (Sabbi et al. 2020). These factors could result in a lower number of planets around stars in the Gum Nebula and other hot-star-irradiated regions.

4.7 Summary

The Gum Nebula is home to hot stars, cometary globules, and several young associations and is thus an ideal location to study effects of external radiation on star formation and young stars' planet-forming disks. From spectroscopic observations of 284 stars in seven of the eight young associations we here study throughout the Gum Nebula, combined with *Gaia* DR2 data, we conclude the following:

- All five young associations exhibit low accretor fractions (0 – 29%) for their ages (2 – 11 Myr), possibly due to the Gum Nebula's moderate radiation environment ($G_0 = 2.1 - 7.8$) eroding young stars' protoplanetary disks. Such external radiation may thus shorten Gum Nebula stars' timescales for forming planets, damage or destroy planet-forming ingredients, and reduce Gum Nebula stars' abilities to form planets.

- Three of the eight associations (CG 4, 22, and 30 Associations) are likely associated with their nearby cometary globules. These associations are relatively sparse, and two have filamentary structure.
- Based on cometary globules' connections with their nearby stellar associations, we estimate first distances to several cometary globules: CG 4 and CG 6 are 415.4 ± 1.0 pc away, CG 22 is 354.96 ± 0.53 pc away, and CG 30, CG 31, and CG 38 are 358.1 ± 2.2 pc away.

Young stars in the Gum Nebula exist in a moderate radiation environment and, due to external ionizing radiation from their massive neighbors, may lose their protoplanetary disks early.

CHAPTER 5

COLLIDING ASSOCIATIONS

We have just explored how hot stars' radiation can affect other stars and their planet-forming disks. Now we examine how stellar associations can dynamically affect stars in other associations. Specifically, we discuss the collision of two associations in our sample, UPK 535 and Yep 3.

5.1 Introduction

Interactions between clusters or associations could play a role in their evolution. Spatially overlapping clusters and associations have been detected, including NGC 1750 and NGC 1758 (Galadi-Enriquez et al. 1998), two components of σ Ori (Jeffries et al. 2006), two components of R136 (Sabbi et al. 2012), and two components of γ Vel OB2 (Jeffries et al. 2014). Since 2018, the precise astrometry and proper motions of *Gaia* DR2 have brought unprecedented opportunity for finding and studying interacting clusters and associations (Gaia Collaboration et al. 2016, 2018). Wright & Parker (2019) found two mass-separated components of NGC 6530 (Wright & Parker 2019).

This chapter presents the first-ever kinematic case study of two distinct stellar associations in the process of colliding (see Fig. 5.1). The associations are UPK 535 and Yep 3 in the Gum Nebula (Gum 1952; Sim et al. 2019; Cantat-Gaudin et al. 2019; Kounkel & Covey 2019). Whereas the overlapping populations of σ Ori, R136, γ Vel OB2, and NGC 6530 are each believed to be evolving components of a single cluster (Jeffries et al. 2006; Sabbi et al. 2012; Jeffries et al. 2014; Wright & Parker 2019), with distinguishable but similar space motions,

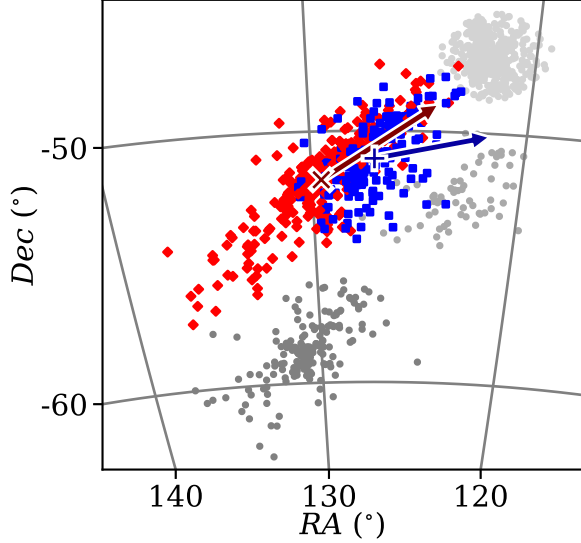


Figure 5.1: The sky positions of five associations in the Gum Nebula. Associations UPK 535 (blue squares) at 318.08 ± 0.29 pc and Yep 3 (red diamonds) at 339.54 ± 0.25 pc have elongated shapes and spatially overlap. Their centers of mass are marked by a dark blue + and a dark red x, respectively. Center-of-mass motions over 1 Myr are marked by dark blue and dark red arrows. UPK 535 and Yep 3 are near other associations UPK 545 at 326.80 ± 0.24 pc (dark grey circles, south), UPK 533 at 344.08 ± 0.46 pc (grey circles, west), and Pozzo 1 at 346.75 ± 0.23 pc (light grey circles, northwest).

UPK 535 and Yep 3 exhibit disparate space motions and spatially overlap as a result of a chance encounter. Their collision could shed light on how association interactions affect association structure, association dispersal, and even heavy bombardment of exoplanets.

We identified the stellar associations UPK 535 and Yep 3 as part of our study of stars associated with cometary globules in the Gum Nebula (see Chapter 3). These two associations are not likely connected with cometary globules (see §4.2), but they are connected with each other: Both associations are distinctly nonspherical and occupy the same general position in the sky (see Figure 5.1). Their distances overlap, but their motions are distinct (see Table 5.1). These two associations have recently collided.

In §5.2, we list spectral types, masses, radial velocities, and association properties of UPK 535 and Yep 3. In §5.3 we fit ellipsoids to both nonspherical associations to estimate volume and stellar density. In §5.4, we analyze kinematics, a linear-motion Monte Carlo simulation,

Table 5.1: Position and motion cuts for isolating the associations UPK 535 and Yep 3 from *Gaia* DR2 data. We also impose error cuts < 0.1 mas in parallax and < 0.16 mas yr $^{-1}$ in proper motion.

Assn. Name	<i>RA</i> ($^{\circ}$)	<i>Dec</i> ($^{\circ}$)	<i>d</i> (pc)	μ_{α} (mas yr $^{-1}$)	μ_{δ} (mas yr $^{-1}$)
UPK 535	123.0 – 131.0	-55.0 – -47.5	290 – 350	-14.5 – -11.5	1.1 – 4.1
Yep 3	126.3 – 134.0	-55.0 – -49.5	320 – 370	-14.5 – -11.5	9.0 – 12.0

other associations in the vicinity of UPK 535 and Yep 3, and association kinematic and potential energies. Finally, in §5.5, we summarize our results.

5.2 Stellar and Association Properties of UPK 535 and Yep 3

We observed 36 stars in UPK 535 and 59 stars in Yep 3 using the CHIRON spectrograph. Stellar properties are derived in Chapter 3, so here we provide a brief summary. Spectral types range from K3.5 to B9 in UPK 535 and from K2.5 to B3 in Yep 3 (see Tables B.7 and B.6). The averaged *Gaia* color excess $E(BP - RP)_{\text{assn}}$ are 0.059 ± 0.022 mag for UPK 535 and 0.036 ± 0.027 mag for Yep 3 (see Table 5.2). Since these stars are old enough (> 10 Myr) to have lost the majority of their circumstellar material (Haisch et al. 2001), we assume that $E(BP - RP)_{\text{assn}}$ represents reddening along line of sight. We calculate extinctions $A_G \approx 0.120 \pm 0.043$ mag for UPK 535 and 0.072 ± 0.053 for Yep 3 (see Table 5.2). Overlapping at similar distances from Earth, these associations can be expected to have the same level of extinction. Their values are within 1σ of each other. From these extinctions and Bailer-Jones et al. (2018) distances, we calculate corrected absolute magnitudes M_G as $0.612 - 11.657$ mag for UPK 535 and $-1.094 - 11.834$ mag for Yep 3. Individual stellar masses from spectral types, intrinsic colors, and absolute magnitudes range from 0.17 to $2.75 M_{\odot}$ in UPK 535 and from 0.18 to $5.40 M_{\odot}$ in Yep 3 (see Tables B.7 and B.6).

We successfully measure radial velocities for 89 of the 95 spectroscopically observed association stars and adopt *Gaia* DR2 radial velocities for three stars. Based on radial velocities, UPK 535 sample has five possible single-lined binaries, one of which is confirmed

based on multiple v_r measurements. Yep 3 has twelve stars that are identified as possible single-lined binaries, and one star is visually suspected to be a double-lined spectroscopic binary. From twenty-four single stars' radial velocities, UPK 535 has an error-weighted mean radial velocity of 10.14 ± 0.06 km s $^{-1}$ with a standard deviation of 1.6 km s $^{-1}$. From thirty-eight single stars' radial velocities, Yep 3 has an error-weighted mean radial velocity of 19.40 ± 0.04 km s $^{-1}$ with a standard deviation of 1.6 km s $^{-1}$. The median radial velocity uncertainty σ_{v_r} of the two-association sample is ~ 0.33 km s $^{-1}$.

By fitting MESA isochrones to the extinction-corrected (see §3.4.2) single-star main sequences, as illustrated in Fig. 3.5 in Chapter 3, we find that both associations are young, with UPK 535 (25^{+15}_{-10} Myr) younger than Yep 3 (45^{+55}_{-20} Myr) (see Table 5.2). We adopt supersolar metallicities of 0.1 dex for UPK 535 and 0.2 dex for Yep 3 because they yield more consistent ages for stars spanning from the main sequence turnoffs to the low-mass ends. The associations' positions in T_{eff} space are consistent with ages near 35 Myr (see Fig. 3.9), with UPK 535 appearing slightly younger than Yep 3.

Towards total stellar mass, the single stellar masses sum to 95.9 ± 7.2 M $_{\odot}$ for UPK 535 and 175 ± 19 M $_{\odot}$ for Yep 3. Based on the IMF of Kroupa (2001), we are missing about 20% of the single-star mass of UPK 535 and 12% of the single-star mass of Yep 3. Completing the IMF thus adds 19.6 ± 3.9 M $_{\odot}$ to UPK 535 and 20.3 ± 4.0 M $_{\odot}$ to Yep 3, with assigned uncertainties of 20% to account for uncertainties in choice of IMF and the edge of our samples' spectral type completeness. Accounting for potential spectroscopic binary stars adds 6.7 ± 0.4 M $_{\odot}$ to UPK 535 from five companion stars and 17.9 ± 1.4 M $_{\odot}$ to Yep 3 from thirteen companion stars. If the associations have 50% binarity, randomly assigned unresolved binarity over 10,000 trials adds 22.3 ± 1.5 M $_{\odot}$ to UPK 535 and 39.2 ± 2.2 M $_{\odot}$ to Yep 3. Finally, summing all masses and uncertainties, the association total stellar mass M_{tot} with worst-case uncertainty is 145 ± 13 M $_{\odot}$ for UPK 535 and 252 ± 27 M $_{\odot}$ for Yep 3 (see Table 5.2). Both associations are older than 5 Myr, so we assume their natal molecular gas has fully dispersed (Lada & Lada 2003). Thus the associations' total masses are assumed equal

Table 5.2: UPK 535 and Yep 3 Association Properties

Assn.	No.	Age	Adopted $E(BP - RP)$	A_G	Infrared	Total Stellar	v_r	ρ_h	t_{cr}
Name	Stars (Myr)	[Fe/H]	(mag)	(mag)	Excess (mag)	Mass (M_\odot)	(km s $^{-1}$)	(M_\odot pc $^{-3}$)	(Myr)
UPK 535	174	25^{+15}_{-10}	0.1	0.059 ± 0.022	0.120 ± 0.043	0.053 ± 0.016	145 ± 13	10.1 ± 1.6	0.008
Yep 3	297	45^{+55}_{-20}	0.2	0.036 ± 0.027	0.072 ± 0.053	0.024 ± 0.022	252 ± 27	19.4 ± 1.6	0.006

to their association stellar masses. Total stellar mass uncertainties are statistical; systematic uncertainties are likely higher.

5.3 Ellipsoid Fits

Both associations are distinctly nonspherical (see Fig. 5.1). They are elongated in the southeast-northwest direction, especially Yep 3. Because the elongation stretches roughly along the Galactic plane, tidal disruption could be at least partly responsible (Chen et al. 2004). To examine the spatial distribution of each association, we project association stars' 3-D positions and velocities into xyz space, with $RA \sim y$, $Dec \sim z$, and distance $\sim x$. We set the origin at the median position of UPK 535. Median distance uncertainties $\sigma_d \sim 7.6$ pc are significantly larger than median spatial uncertainties $\sigma_{RA} \approx \sigma_{Dec} \sim 0.01$ AU, and median radial velocity uncertainties (0.56 km s $^{-1}$) are 2.4 times larger than median proper motion uncertainties (0.22 km s $^{-1}$). This anisotropy in uncertainties artificially stretches the associations in the radial direction. The stretch is hidden when distance is projected into the depth direction x but is revealed in other projections.

Referencing stars' xyz positions and estimated stellar masses, including binary companion masses for identified potential binary stars (see §3.4.2), we determine each association's center of mass. As an approximation of association size, we take the median of stars' distances from each association's center of mass. These median radial extents are 14.6 pc for UPK 535 and 16.3 pc for Yep 3.

For volume, density, and stellar crossing time, we fit an ellipsoid to each association using the PYTHON code ELLIPSOID,¹ with fit tolerance set to 0.15. This captures the overall morphology of each association. The initial ellipsoid for UPK 535 contains 89.1% of stars, for Yep 3, 91.9%. We define a half-mass ellipsoid by dilating the initial ellipsoid until it contains half the measured mass of the association (i.e. accounting for identified possible binaries, but excluding unidentified binaries and IMF adjustments).

¹Dr. Imelfort, <https://github.com/minillinim/ellipsoid>

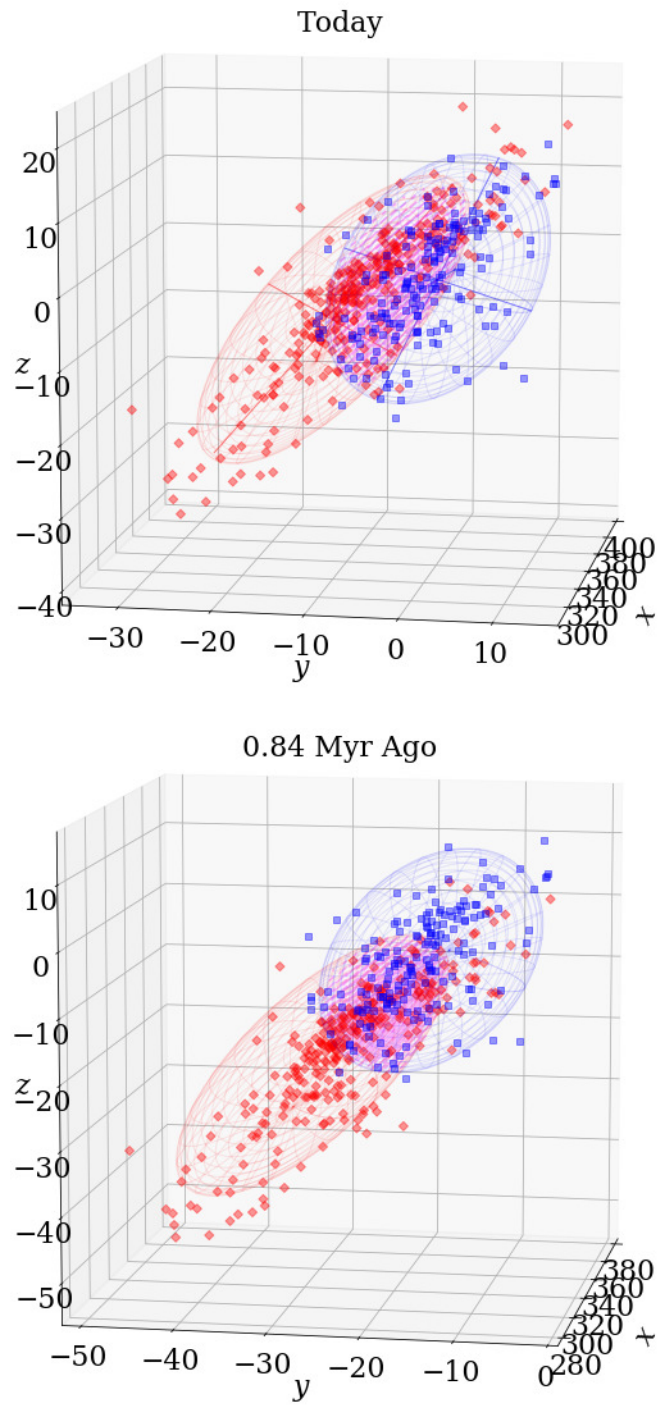


Figure 5.2: 75%-stars ellipsoid fits to UPK 535 (blue) and Yep 3(red) today (top panel) and 0.84 Myr ago (bottom panel). The associations have significant volume overlap, shown in magenta.

To adjust for anisotropically large uncertainties in distance, we subtract out the association’s projected median distance uncertainty in quadrature from the three ellipsoidal axes. We then compute the volume of the half-mass ellipsoid and calculate stellar density ρ_h , equal to $0.008 \text{ M}_\odot \text{ pc}^{-3}$ for UPK 535 and $0.006 \text{ M}_\odot \text{ pc}^{-3}$ for Yep 3. These densities are an order of magnitude lower than the local field star density of 0.09 pc^{-3} (Henry et al. 2018) but reasonable for stellar associations (Moraux 2016). The densities imply stellar crossing times $t_{\text{cr}} \approx 1/2 (G \rho_h)^{-1/2} \approx 82 \text{ Myr}$ for UPK 535 and 92 Myr for Yep 3. Adjusting volumes for the median distance uncertainty has raised densities and lowered crossing times by about $3 - 10\%$ each. Crossing times from how long it takes to cross the half-mass ellipsoid axes at the speed of the 1-dimensional velocity dispersions, $2r/\sigma_{v,1\text{D}}$ (Kuhn et al. 2019; see §??), where r is half-mass radial extent of each ellipsoidal association, are $44 - 100 \text{ Myr}$ for UPK 535 and $22 - 84 \text{ Myr}$ for Yep 3, a factor of a few smaller than the density-derived crossing times. This is reasonable for unbound associations. Furthermore, velocity-dispersion-derived crossing times being roughly equal to association ages imply the associations have expanded since their formation (Kuhn et al. 2019), perhaps partly due to shear forces from the Galactic plane (see Figure 5.1 and §3.5).

5.4 Discussion

5.4.1 Colliding Associations

The distributions of distances and kinematics for UPK 535 and Yep 3 are shown in Fig. 5.3. Their distance distributions overlap, and their proper motions in right ascension μ_α are indistinguishable (see Table 5.1). Their motions diverge, however, in proper motion in declination μ_δ and radial velocity v_r . The farther association is moving north and away faster than the nearer association at a relative space velocity of $16.2 \pm 1.4 \text{ km s}^{-1}$. Associations UPK 535 and Yep 3 have recently collided.

With median radial extents of 14.6 pc and 16.3 pc , the associations’ current center-of-mass separation of $22.7 \pm 3.8 \text{ pc}$ corresponds to 8.2 pc of median radial overlap. To estimate

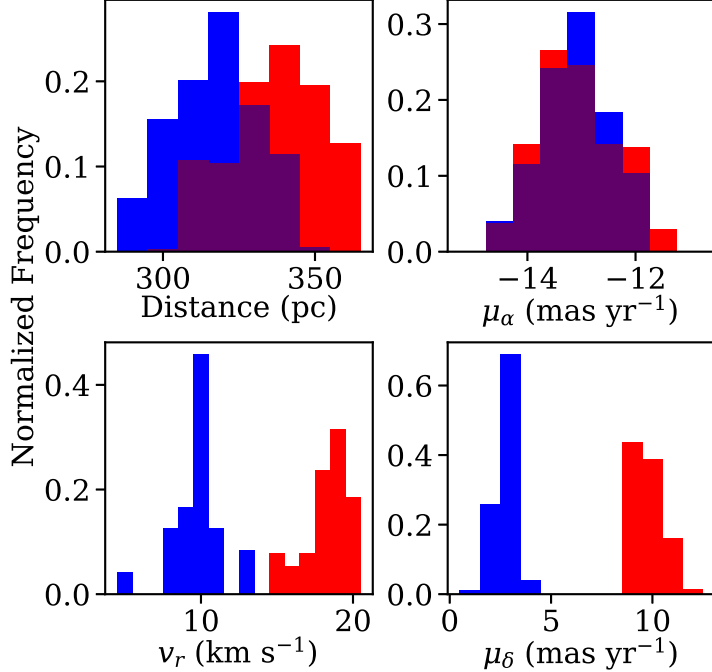


Figure 5.3: Distributions of distances and kinematics for UPK 535 (blue) and Yep 3 (red). The spatially overlapping associations share distances and proper motions in right ascension (purple overlap), but their proper motions in declination and radial velocities are divergent, indicating they did not form together. Rather, they recently encountered each other.

association volume overlap, we scale the associations' initial ellipsoids to contain 75% of each association's stars. By a cubic parsec grid calculation, the overlap region includes 26.1% of UPK 535's 75-per-cent-stars ellipsoid volume and 19.3% of Yep 3's. This association overlap is considerable, holding 50 UPK 535 stars and 43 Yep 3 stars (see Figure 5.2).

To explore the association collision, we run a 10,000-trial Monte Carlo simulation of the association stars' current xyz -transformed positions, motions, and uncertainties, linearly extrapolated forward and backward in time (see Fig. 5.4). We ignore stars' close-encounter path deflections (extremely unlikely; see Bailer-Jones 2015), accelerations in the gravitational potential of the two associations, and accelerations in the gravitational potential of the Galaxy (see below for effects). Potential binary stars and stars lacking v_r measurements are assigned their association's error weighted mean v_r , with uncertainty set to the standard deviation of association stars' v_r values (see §3.4 and Table 5.2). Based on the associations' center-of-mass relative velocity of $16.2 \pm 1.4 \text{ km s}^{-1}$ and time-step 0.01 Myr, the collision

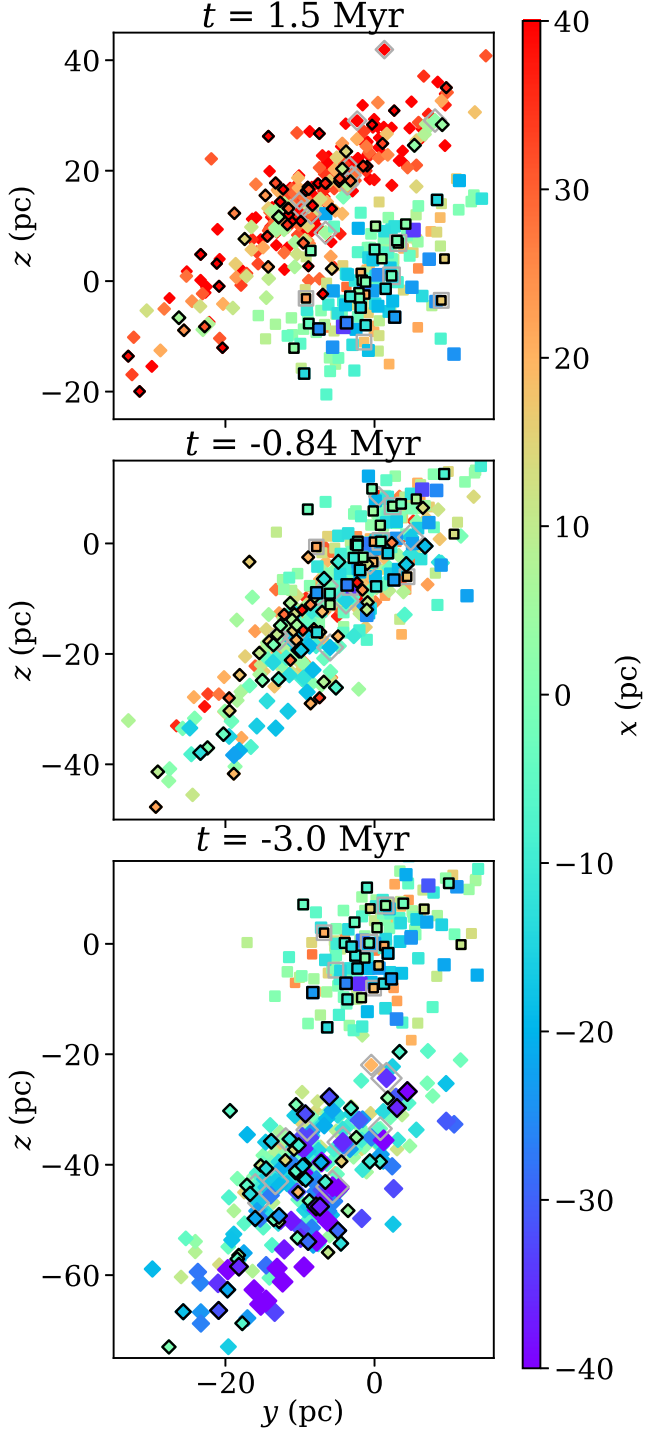


Figure 5.4: Projected positions of UPK 535 (squares) and Yep 3 (diamonds) at three points in time: 3.0 Myr ago (bottom panel), 0.84 Myr ago (middle panel), and 1.5 Myr from now (top panel). *RA* corresponds roughly with y , *Dec* with z , and distance with x , all in pc. The coordinates are zeroed on UPK 535. Dark outlines mark stars with spectroscopically measured v_r . Yep 3 moves north and away into UPK 535, reaching closest approach 0.84 ± 0.03 Myr ago and receding thereafter. The apparent expansion back in time results from a combination of proper motion uncertainties ~ 0.13 mas yr $^{-1}$ and linear extrapolation.

simulation's spatial resolution is essentially $\sim 0.166 \pm 0.014$ pc per time-step. We find that using a finer time-step does not significantly alter our results. Though we do not integrate through gravitational potentials, stellar masses do affect center-of-mass calculations, so we account for the masses of known potential binaries (see §3.5.2) and impose a stellar mass lower limit of $0.08 M_{\odot}$ on all stars.

In the simulation, the associations' centers of mass experience a mean closest approach of 18.89 ± 0.73 pc at time 0.84 ± 0.03 Myr ago (see Fig. 5.5 and the middle panel of Fig. 5.4). Holding the 75%-stars ellipsoids constant and shifting them by their center-of-mass velocities for 0.84 Myr into the past, we recalculate association volume overlap at time of closest centers-of-mass approach: 23.4% of the volume of UPK 535 and 17.3% of the volume of Yep 3 fall within the overlap region (see Figure 5.2). The overlap region at closest centers-of-mass approach encompasses 37 UPK 535 stars and 44 Yep 3 stars.

We track stellar close encounters < 1 pc within each trial. Measurement uncertainties in distances (~ 7.6 pc) and a limited number of radial velocities (21.5% of our sample) prevent us from predicting specific star-star encounters. However, we can track which stars are most likely to undergo a close encounter with any other-association star. In our Monte Carlo simulation, over the course of 3.15 ± 0.50 Myr $\ll t_{\text{cr}}$ from the first close stellar encounter to the last, a mode of 54 ± 7 close stellar encounters occur (see Fig. 5.5). The closest encounter of any two stars is on average 0.13 ± 0.06 pc $\approx 27,000 \pm 12,000$ AU, a distance well within the estimated extent of the Solar Oort cloud ($\sim 50,000$ AU).

A star's chance of close encounter is affected by its location within the association (see Fig. 5.6). Stars in UPK 535 have a median 16.9% chance of undergoing a close encounter with a star in Yep 3. The chance of close encounter is stronger for stars in the eastern half of UPK 535 than the western half. Stars in Yep 3 have a median 14.2% chance of close encounter with a star in UPK 535, with chance of close encounter higher in the western two thirds of the association. Two stars in UPK 535 and two in Yep 3 undergo a close encounter in $> 70\%$ of trials. These stars undergo multiple close encounters in $\sim 30\%$ of trials. 93.7%

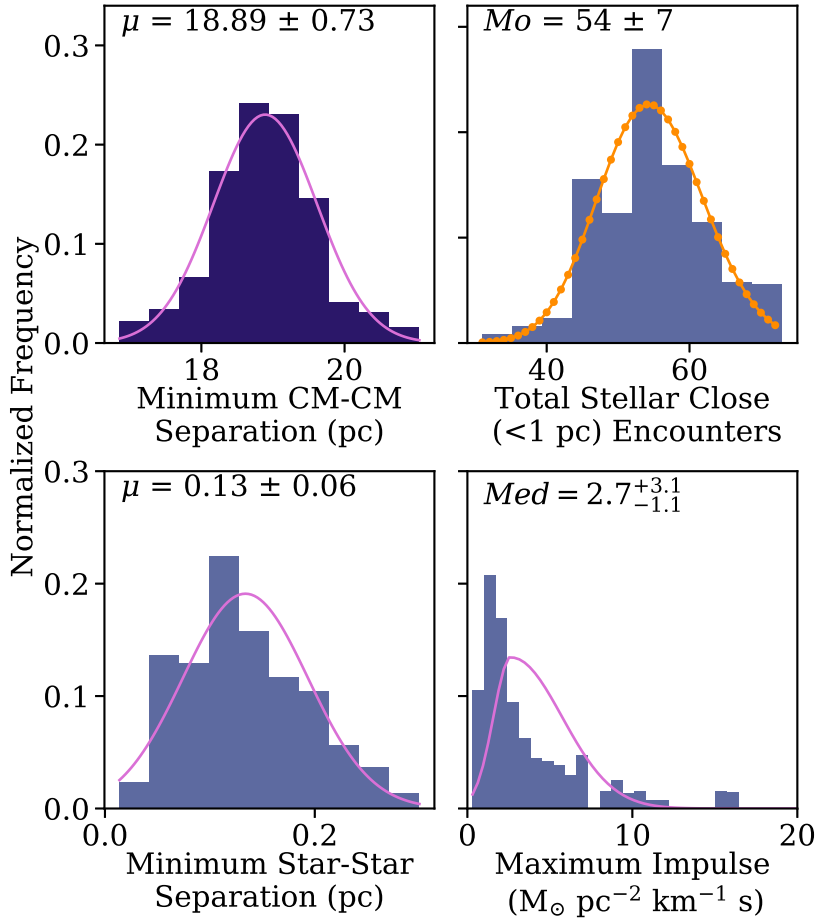


Figure 5.5: Distributions of four parameters across 10,000 trials in our Monte Carlo simulation. Each parameter is fitted with a Gaussian (lavender line) based on mean and standard deviation or a Poisson distribution (orange line) based on mode. The centers of mass of the two associations (top left) experience a closest approach of 18.89 ± 0.73 pc about 0.84 ± 0.03 Myr ago. During the collision, 54 ± 7 close (<1 pc) stellar encounters tend to occur (top right). The most likely closest approach of any two stars (bottom left) is 0.13 ± 0.06 pc, or $27,000 \pm 12,000$ AU, well within the estimated radial size of our Solar Oort cloud. So close an encounter could disrupt debris in a stars' Oort cloud with an impulse of $2.7^{+3.1}_{-1.1} M_\odot pc^{-2} km^{-1} s$ (bottom right) and initiate a heavy bombardment event for any exoplanets the stars may harbour.

of stars in UPK 535 and 84.2% of stars in Yep 3 experience a close encounter in at least one trial. Improved parallaxes with $\sigma_d \sim 1$ pc plus additional high-resolution spectroscopic observations with resolution $\sigma_{v_r} \sim 0.1$ km s $^{-1}$ could enable us to predict specific star-star close encounters within 1 – 2 pc and their effects on the stars’ theoretical solar systems.

Ideally we would integrate positions and motions through the gravitational potential of the Galaxy and, if strong enough, the gravitational potentials of the associations themselves. According to Bailer-Jones (2015), who ran both linear and integrated-through-gravitational-potential simulations, our simple linear-motion approach can introduce star-star distance errors ≥ 0.5 pc for up to 17% of stars, with underestimation about twice more frequent than overestimation (Bailer-Jones 2015). This systematic underestimation of star-star distances will systematically inflate the number of close stellar encounters.

5.4.2 *Impulse*

It has been theoretically demonstrated that a star passing close to our Sun could dislodge comets from the Oort cloud and send several into the inner Solar System (e.g. Weissman 2006; Yeomans & Chamberlin 2012; Feng & Bailer-Jones 2015; Bailer-Jones 2015). Long-period comets, because larger and faster-moving than common near-Earth asteroids, may be more likely to inflict extinction-level impacts (Weissman 2006; Yeomans & Chamberlin 2012). Heightened comet fluxes during a close stellar encounter would raise the probability of a catastrophic cometary impact.

Origins of the Sun’s Oort Cloud remain mysterious. The Oort Cloud may have evolved over 100 – 1000 Myr, shaped by planetary migrations, Galactic tidal forces, debris capture, and, in fact, close stellar encounters (Higuchi & Kokubo 2015; Portegies Zwart et al. 2021). The Oort Cloud as we know it could be a unique structure (Portegies Zwart et al. 2021), although the evolution of Oort-like structures around other stars is certainly possible, over timescales of 10 – 200 Myr (Portegies Zwart 2021; Portegies Zwart et al. 2021).

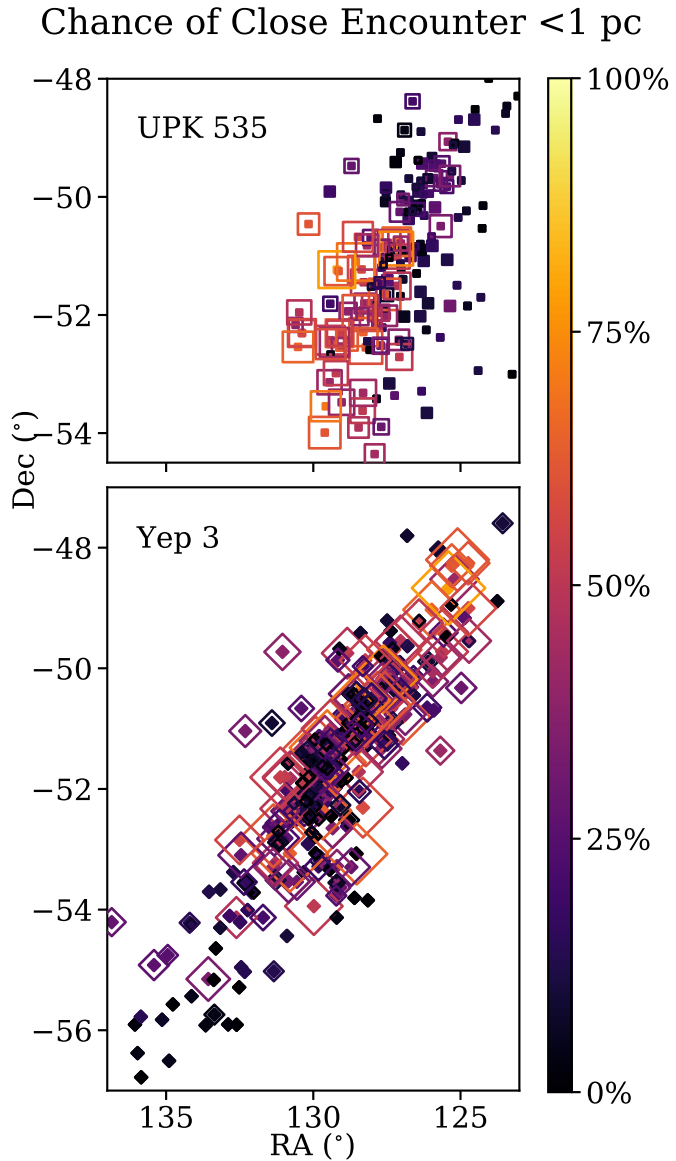


Figure 5.6: Symbols' colors represent each star's chance of undergoing a close (<1 pc) encounter, and symbols' outlines are scaled to chance of undergoing more than one close encounter. In UPK 535 (top panel, square symbols), each star's chance of close encounter is strongly dependent on location. Stars in the eastern half of UPK 535 are more likely to encounter Yep 3 stars than are stars in the western half of UPK 535. Chance of close encounter is more spread out in Yep 3 (bottom panel, diamond symbols).

If the stars in UPK 535 and Yep 3 possess \sim 50,000 AU Oort clouds similar to our Sun's, an encounter as close as $27,000 \pm 12,000$ AU could perturb Oort cloud objects significantly. We estimate stellar influence on cometary motions and induced comet flux through a simple impulse-tracing parameter $Md^{-2}v^{-1}$, where M is the mass of the encountering star, d is the star-star separation, and v is the stars' relative space velocity (Feng & Bailer-Jones 2015; Bailer-Jones 2015). In the close encounters of our Monte Carlo simulation, where the closest encounter induces the highest impulse parameter just over half of the time, the median maximum impulse parameter any star imparts to another star's Oort cloud comets is $2.7^{+3.1}_{-1.1}$ M_{\odot} pc $^{-2}$ km $^{-1}$ s. Uncertainties are from the first and third quartiles of the asymmetric impulse parameter distribution (see Fig. 5.5). Extrapolating from the Solar-System-based model of Feng & Bailer-Jones (2015), we find the impulse is strong enough to inject a median of 410^{+560}_{-190} of every 1 million Oort Cloud comets into a star's inner solar system. For reference, our own Solar System has an estimated $10^{11} - 10^{12}$ Oort Cloud comets, which would entail up to 400 million comets injected (Feng & Bailer-Jones 2015). Because travel from the Oort cloud into inner orbits takes time (Feng & Bailer-Jones 2015), comet showers may plague the close-encountering stars' exoplanets in a few million years.

A passing star's Oort cloud itself could also sweep through another star's solar system. Additionally, a passing star's tidal tails of asteroids could sweep through another star's solar system millions of years before or after the stars' closest approach (Portegies Zwart 2021).

If the stars in UPK 535 and Yep 3 do not possess Oort Clouds, it is possible the perturbations from close stellar encounters could spur their creation; a combination of within-cluster stellar interactions and a strong close stellar encounter may have shaped the Sun's Oort Cloud (Portegies Zwart et al. 2021). Perturbation of a Kuiper-belt-like structure or asteroids is also possible during close stellar encounters (Portegies Zwart 2021). Perturbation of planets is less likely.

We compare interassociation impulses to intra-association- and field-star-induced impulses. Because the associations are sparse and moving through space together, the separation

between stars within each cluster may not change drastically over the course of a few Myr and should hover around $(0.01\text{pc}^3)^{-1/3} \approx 5$ pc, which, squared, should dominate the effect of slower velocities and render intrassociation impulses overall weaker than the strongest interassociation impulses. However, the field star population (especially in the plane of the Galaxy) is likely denser than each association by at least an order of magnitude. The local field star density near our Sun, for example, is 0.09 stars pc^{-3} (Henry et al. 2018), for typical stellar separation ~ 2.2 pc. Based on the initial cone search of *Gaia* DR2 stars in the vicinity of UPK 535, the field stars' spread in relative space velocities $\sim 33 \text{ km s}^{-1}$ is larger than the relative space velocity $16.2 \pm 1.4 \text{ km s}^{-1}$ between UPK 535 and Theia 120, partly offsetting the higher field-star density. For close encounters $1.0 - 0.1$ pc and median mass $0.37 M_\odot$, the impulse parameter ranges from $0.01 - 1.1 M_\odot \text{ pc}^{-2} \text{ km}^{-1} \text{ s}$, comparable to the interassociation maximum impulse parameter value.

5.4.3 Other Colliding Associations

In the vicinity of UPK 535 and Yep 3 are three other associations, UPK 533, UPK 545, and Pozzo 1. When we simulate their *Gaia* DR2 positions and motions through time with the same linear approach described above, we find that these associations could also interact with UPK 535, Yep 3, and each other. The centers of mass of UPK 535 and UPK 533 on average reach a closest approach of 23.6 ± 4.3 pc about 0.94 ± 0.65 Myr, possibly constituting a triple collision for UPK 535 during that time. In the UPK 535-UPK 533 interaction, a mean of 5 ± 2 stellar close encounters occur. The centers of mass of Yep 3 and UPK 545 on average reach a closest approach of 9.8 ± 1.7 pc about 0.52 ± 0.07 Myr from now, during which time a mean of 9 ± 3 stellar close encounters occur. UPK 533 and Pozzo 1 have an encounter of similar significance to that of UPK 535 and Yep 3. The centers of mass of UPK 533 and Pozzo 1 reach an average closest approach of just 3.4 ± 2.1 pc about 0.03 ± 0.14 Myr from now, and a mean of 50 ± 7 close stellar encounters occur. Minimum stellar separation of any two of their stars is on average just 0.13 ± 0.05 pc $\approx 27,000 \pm 10,000$ AU.

These results for UPK 533, UPK 545, and Pozzo 1 are preliminary, with association radial velocities based only on a handful of available *Gaia* DR2 radial velocities. The stellar membership list of Pozzo 1 is also incomplete. Nonetheless, our tests imply that association interactions are commonplace, at least in the Gum Nebula, located in the plane of the Galaxy. Though star-star interactions have only a limited impact within associations (Winter et al. 2018), we may have to consider how increased close stellar encounters during association collisions affect association evolution, stellar and binary evolution, and planetary evolution through instigated episodes of heavy bombardment.

5.4.4 Kinetic Energy vs. Gravitational Potential Energy

An association's ratio of kinetic energy T to absolute value of gravitational energy $|U|$ describes how bound the association is and how quickly it may dissolve (Shu et al. 1987; Krumholz et al. 2019). Systems that are gravitationally bound are expected to obey the virial theorem, $T = -1/2 U$. A log energy ratio of $\log(T/|U|) = -0.3$ dex therefore represents a virial, bound, stable star cluster, whereas $\log(T/|U|) > -0.3$ dex represents a supervirial, unbound, expanding stellar association.

To assess the bound or unbound nature of UPK 535 and Yep 3, we compute $\log(T/|U|)$ for them and nine other associations throughout the Gum Nebula, including the other six associations from Chapters 3 and 4 and the three associations UPK 533, UPK 545, and Pozzo 1 in the vicinity of UPK 535 and Yep 3 (see Figure 5.1). The kinetic energy T of each association is calculated from stars' velocity dispersion from the association mean velocity:

$$T = \frac{3}{2} M_{\text{tot}} \sigma_{v,1D}^2. \quad (5.1)$$

Here, M is the sum of all measured stellar masses, including masses from binary companions and mass from completing the IMF (see §??). Because the aberrant radial velocities of single-epoch binary stars can skew kinetic energy towards high values (Mathieu 1985; Karnath

Table 5.3: Energies and energy ratios of Gum Nebula clusters.

Assn. Name	No. Stars	T (M_{\odot} km 2 s $^{-2}$)	U (M_{\odot} km 2 s $^{-2}$)	$\log(T/ U)$ (dex)
CG 4 Assn.	34	26 ± 31	-0.162 ± 0.062	2.21 ± 0.54
CG 22 Assn.	102	70 ± 130	-1.28 ± 0.20	1.74 ± 0.84
CG 30 Assn.	29	200 ± 2800	-0.0082 ± 0.0039	4.4 ± 6.3
Yep 1	534	300 ± 1100	-30.1 ± 2.3	1.0 ± 1.5
Yep 2	443	260 ± 890	-13.8 ± 1.0	1.3 ± 1.5
Yep 3	297	350 ± 730	-7.63 ± 0.32	1.66 ± 0.90
UPK 535	174	90 ± 140	-3.250 ± 0.099	1.43 ± 0.69
Alessi 3	260	560 ± 880	-11.57 ± 0.27	1.68 ± 0.69

et al. 2019), the radial velocities of all identified binaries are set to each association’s error-weighted mean. With binaries thus controlled, $\sigma_{v,1D}$ is the 1-dimensional velocity dispersion of the association, derived from the three orthogonal dispersions as $\sigma_{v,1D}^2 = (\sigma_{v_x}^2 + \sigma_{v_y}^2 + \sigma_{v_z}^2 - \sigma_{v_{r,med}}^2 - \sigma_{v_{\alpha,med}}^2 - \sigma_{v_{\delta,med}}^2)/3$. Here $\sigma_{v_{r,med}}$ is the smaller of the median radial velocity uncertainty of the association, or 0.56 km s $^{-1}$, the median radial velocity uncertainty of our whole sample of spectroscopically measured radial velocities in the Gum Nebula. $\sigma_{v_{\alpha,med}}$ and $\sigma_{v_{\delta,med}}$ are the median proper motion uncertainties in km s $^{-1}$. These three median uncertainties are subtracted in quadrature from the velocity dispersion to avoid artificially inflating T with scatter in motion measurements (see §5.2).

The gravitational potential energy U is the sum of each star’s potential gravitational energy derived from total stellar mass interior to that star:

$$U = -G \frac{\sum_i \sum_{j, r_j < r_i} m_i m_j}{r_i}. \quad (5.2)$$

Here, G is the gravitational constant. Quantities m_i and m_j are measured stellar masses, including companion mass of identified potential binaries, times M_{tot}/M_b , where M_b is the sum of all single-star masses and identified binary masses. Multiplying by this factor lets us include masses from unidentified binaries and IMF completion, without altering the identified mass distribution. The value r is a given star’s distance from the center of mass. From this

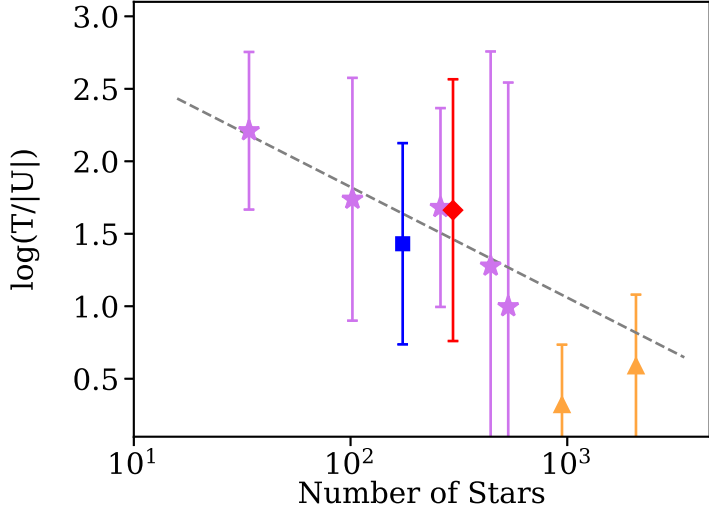


Figure 5.7: Log ratios of associations' kinetic to potential energies are plotted vs. the number of stars in each association. We have spectroscopically derived radial velocities for stars in UPK 535 (blue square), Yep 3 (red diamond), and five other associations (lavender stars) throughout the Gum Nebula. For comparison, we include the two subclusters of Cep OB3b from outside the Gum Nebula (orange triangles, Karnath et al. 2019). Association energy ratios in the Gum Nebula are consistent with the energy ratios of Cep OB3b. The grey correlation line is an error-weighted fit to the Gum Nebula data.

distance, we in quadrature subtract $\sigma_{d_{\text{med}}}$, the smaller of the association's median distance uncertainty or 8.5 pc, the median distance uncertainty of our whole sample of Gum Nebula stars.

The log energy ratio for UPK 535 is 1.43 ± 0.69 dex, and for Yep 3, 1.66 ± 0.90 dex. Both associations are unbound. Results for five of the nine other associations in the Gum Nebula range from 1.0 to 2.21 dex, also unbound. The remaining four associations (UPK 533, UPK 545, and Pozzo 1, which lack spectroscopic observations, and the CG 30 Association) have errors >3 dex, so we consider their $\log(T/|U|)$ unmeasured. When we calculate $\log(T/|U|)$ in two dimensions instead of three, omitting $x \sim d$, log energy ratios differ by -0.58 – -0.03 dex from the 3-D values. These are within uncertainties but always lower, suggesting artificial radial elongation and general radial uncertainty systematically elevate our 3-D log energy ratios.

All seven of our measured associations have fewer than 1000 members. The sparser associations tend to have lower $|U|$ than T , whereas the more populous associations tend to

have more balanced $|U|$ and T (see Table 5.3). An association's $\log(T/|U|)$ appears to be correlated with its star count (see Fig. 5.7).

We compare these results to the two populous subclusters of Cep OB3b from outside the Gum Nebula, studied by Karnath et al. (2019). The mean 50-per-cent-binaryity $\log(T/|U|)$ for Cep OB3b are 0.58 ± 0.49 dex for the west subcluster and 0.32 ± 0.41 dex for the east. Cep OB3b is overall unbound and expanding, but portions of the western subcluster may be bound (Karnath et al. 2019). The Gum Nebula associations' median $\log(T/|U|)$ is 1.66 dex, over 1 dex greater than Cep OB3b's values. However, the Gum Nebula associations' energy vs. star count trend remains consistent with Cep OB3b, within 2σ . Even UPK 535 and Yep 3, despite their recent collision, have energy ratios in line with the other associations and Cep OB3b's. Association collisions may not significantly affect association energies, perhaps due to their brevity or the low densities of the associations in our sample. More comparisons with *Gaia*-observed associations and clusters outside the Gum Nebula are needed to verify this result.

5.5 Conclusions

UPK 535 and Yep 3 in the Gum Nebula are the first observed colliding open associations close enough to Earth (318.08 ± 0.29 pc and 339.54 ± 0.25 pc, respectively) that their dynamical interaction can be investigated in detail. Our 10,000-trial Monte Carlo simulation reveals the following averaged results:

- The associations attain a closest centers-of-mass approach of 18.89 ± 0.73 pc about 0.84 ± 0.03 Myr ago.
- 54 ± 7 close encounters < 1 pc occur between stars of UPK 535 and Yep 3.
- The closest encounter is 0.13 ± 0.06 pc $\approx 27,000 \pm 12,000$ AU, close enough for stars to sweep through each other's Oort clouds, if the stars possess Oort clouds similar to our Sun's.

- Two stars in UPK 535 and two in Yep 3 undergo a close encounter in >70% of trials, and multiple close encounters in \sim 30% of trials.
- The maximum impulse parameter of $2.7_{-1.1}^{+3.1} M_{\odot}$ pc $^{-2}$ km $^{-1}$ s is strong enough to potentially inject 410_{-190}^{+560} of every 1 million Oort Cloud comets into inner orbits and cause heavy bombardment of any exoplanets there, if these relatively young stars possess Oort Clouds.
- Other Gum Nebula associations (UPK 533, UPK 545, and Pozzo 1) may also be interacting with UPK 535, Yep 3, and each other. Association collisions may be commonplace, at least in the Gum Nebula in the plane of the Galaxy.
- Gum Nebula association log-ratios of kinetic energy to gravitational potential energy (1.00 – 2.21 dex) vs. star count are consistent with Cep OB3b’s, suggesting association collisions may not significantly affect cluster energies. More robust comparisons with *Gaia*-observed associations are needed to verify this implication.

The relatively young, nearby associations UPK 535 and Yep 3 provide a case study for association-association interactions and their possible effects on the evolution of solar systems.

CHAPTER 6

SUMMARY

The Gum Nebula is home to hot stars, cometary globules, and several young associations and is thus an ideal location to study effects of external radiation on star formation and young stars' planet-forming disks, and the effects of associations on each other and the stars and planets within them. From spectroscopic observations of 284 stars in seven of the eight young associations we here study throughout the Gum Nebula, combined with *Gaia* DR2 data, we conclude the following:

- Based on high dispersion optical spectra from Keck I HIRES, the 9 Pettersson (1987) stars and CG 30 IRS 4 show undepleted Li $\lambda 6708 \text{ \AA}$, H α 10% widths $225 - 621 \text{ km s}^{-1}$, and veiling. Eight of the 10 are classical T Tauri stars. Three of the stars associated with CG 30 are classical T Tauri stars.
- Projected rotational velocities of the 10 young stars are $6.3 - 27.8 \text{ km s}^{-1}$. CG 30 IRS 4's is the lowest.
- The star CG 30 IRS 4 inside the cometary globule appears to be an embedded T Tauri star. Though its H α 10% width (225 km s^{-1}) falls below the classical T Tauri star limit, it is embedded, exhibits moderate veiling, and is probably still accreting.
- We develop an empirical method Cluster Finder for finding clusters and associations in *Gaia* DR2 data. Using this method, we find 8 young associations in the Gum Nebula.

- We present a catalogue of 81 high-quality spectral standards observed with CHIRON in fiber mode, spanning from spectral type O9.5V to M5.5V.
- We observe 284 stars in 7 of the 8 associations in the Gum Nebula.
- Five of the 8 associations we study in the Gum Nebula, including the CG 30 Association, are young (≤ 10 Myr), based on lithium abundances and isochrone fits.
- Stars exhibiting H α emission are present in all 8 associations. Stars with strong H α emission indicative of ongoing accretion are present in the five young associations.
- All five young associations exhibit low accretor fractions (0 – 29%) for their ages (2 – 11 Myr), possibly due to the Gum Nebula’s moderate radiation environment ($G_0 = 2.1 - 7.8$) eroding young stars’ protoplanetary disks. Such external radiation may thus shorten Gum Nebula stars’ timescales for forming planets, damage or destroy planet-forming ingredients, and reduce Gum Nebula stars’ abilities to form planets.
- Three of the eight associations (CG 4, 22, and 30 Associations) may be associated with their nearby cometary globules. These associations are relatively sparse, and two have filamentary structure.
- Based on cometary globules’ connections with their nearby stellar associations, we estimate first distances to several cometary globules: CG 4 and CG 6 are 415.4 ± 1.0 pc away, CG 22 is 354.96 ± 0.53 pc away, and CG 30, CG 31, and CG 38 are 358.1 ± 2.2 pc away.
- Two associations (Yep 3 and UPK 535) have recently collided. The associations attain a closest centers-of-mass approach of 18.89 ± 0.73 pc about 0.84 ± 0.03 Myr ago.
- Based on Monte Carlo simulations of the collision, we determine that on average 54 ± 7 close encounters < 1 pc occur between stars of UPK 535 and Yep 3.

- We also find that on average the closest encounter is 0.13 ± 0.06 pc $\approx 27,000 \pm 12,000$ au, close enough for stars to sweep through each other's Oort clouds, if the stars possess Oort clouds similar to our Sun's.
- The maximum impulse parameter of $2.7_{-1.1}^{+3.1}$ M_{\odot} pc $^{-2}$ km $^{-1}$ s is strong enough to potentially inject 410_{-190}^{+560} of every 1 million Oort Cloud comets into inner orbits and cause heavy bombardment of any exoplanets there.
- Other Gum Nebula associations (UPK 533, UPK 545, and Pozzo 1) may also be interacting with UPK 535, Yep 3, and each other. Association collisions may be commonplace, at least in the Gum Nebula in the plane of the Galaxy.

The Gum Nebula demonstrates that associations, stars, and planets exist together in a highly dynamic environment.

Bibliography

- Adams, F. C., Hollenbach, D., Laughlin, G., et al. 2004, ApJ, 611, 360
- Adibekyan, V., Santos, N. C., Demangeon, O. D. S., et al. 2021, A&A, 649, 111
- Aguilera-Gómez, C., Ramírez, I., & Chanamé, J. 2018, A&A, 614, A55
- Alessi, B. S., A. Moitinho, & W. S. Dias. 2003, A&A 410, 565
- Ammler-von Eiff, M., & A. Reiners. 2012, A&A, 542, 116
- Andrae, R., M. Fouesneau, O. Creevey, et al. 2018, A&A, 616, A8
- Apellániz, M., J., E. J. Alfaro, & A. Sota. 2008, arXiv, 0804.2553v1
- Asensio-Torres, R., Currie, T., Janson, M., et al. 2019, A&A, 622, A42
- Bailer-Jones, C. A. L. 2015, A&A, 575, A35
- Bailer-Jones, C. A. L., Rybizki, J., Fouesneau, M., Mantelet, G., & Andrae, R. 2018, AJ, 156, 58
- Baraffe, I., G. Chabrier, F. Allard, & P. H. Hauschildt. 1998, A&A, 337, 403
- Baraffe, I., D. Homeier, F. Allard, & G. Chabrier. 2015, A&A, 577, 42
- Barnes, J. R., Jenkins, J. S., Jones, H. R. A., et al. 2014, MNRAS, 439, 3094
- Basri, G., E. L. Martín, & C. Bertout. 1991, A&A, 252, 625
- Bastian, N. & Lardo, C. 2018, ARA&A, 56, 83

- Bate, M. R., I. A. Bonnell, & V. Bromm. 2003, MNRAS, 339, 577
- Barnes, S. A. 2010, ApJ, 722, 222. doi:10.1088/0004-637X/722/1/222
- Beasor, E. R., Davies, B., Smith, N., et al. 2019, MNRAS, 486, 266
- Bernacca, P. L. & Perinotto, M. 1970, Contributi dell’Osservatorio Astrofisica dell’Università di Padova in Asiago, 239, 1
- Bertoldi, F. 1989, ApJ, 346, 735
- Beuermann, C. P. 1973, Ap&SS, 20, 27
- Bhatt, H. C. 1993, MNRAS, 262, 812
- Bochanski, J. J., Faherty, J. K., Gagné, J., et al. 2018, AJ, 155, 149
- Bodenheimer, P. 1965, ApJ, 142, 451
- Boch, T., Pineau, F., & Derriere, S. 2012, Astronomical Data Analysis Software and Systems XXI, 461, 291
- Bouvier, J., Matt, S. P., Mohanty, S., et al. 2014, Protostars and Planets VI, 433
- Biazzo, K., J. M. Alcalá, A. Frasca, et al. 2014, A&A 572, 84
- Brandt, J. C., T. P. Stetzer, D. L. Crawford, & S. P. Maran. 1971, ApJ, 163, 99
- Bressan, A., Marigo, P., Girardi, L., et al. 2012, MNRAS, 427, 127
- Briceño, C., N. Calvet, J. Hernández, et al. 2019, AJ, 157, 85
- Bronfman, L., L. A. Nyman,& J. May. 1996, A&A, 115, 81
- Bronfman, L., L. A. Nyman,& J. May. 1992, A&A, 265, 577
- Butler, R. P., G. W. Marcy, E. Williams, et al. 1996, PASP, 108, 500

- Cantat-Gaudin, T., Jordi, C., Vallenari, A., et al. 2018, A&A, 618, A93
- Cantat-Gaudin, T., C. Jordi, N. J. Wright, et al. 2019, A&A, 626, 17
- Cantat-Gaudin, T., M. Mapelli, L. Balaguer-Núñez, et al. 2019, A&A, 621, 115
- Cantat-Gaudin, T., & F. Anders. 2020, A&A, 633, 99
- Caraveo, P.A., A. De Luca, R. P. Mignani, & G. F. Bignami. 2001, ApJ, 561, 930
- Castelli, F. & Kurucz, R. L. 2004, A&A, 419, 725
- Castro-Ginard, A., C. Jordi, X. Luri, et al. 2020, A&A., 635, 45
- Cayrel, R. 1988, IAUS, 132, 345
- Cazzoletti, P., C. F. Manara, H. Baobab Liu, et al. 2019, A&A, 626, 11
- Cha, A. N., K. R. Sembach, & A. C. Danks. 1999, ApJ, 515L, 25
- Chen, W. P., Chen, C. W., & Shu, C. G. 2004, AJ, 128, 2306. doi:10.1086/424855
- Chen, X., T. L. Bourke, R. Launhardt, & T. Henning. 2008, ApJ, 686, 107
- Choi, J., A. Dotter, C. Conroy, et al. 2016, ApJ, 823, 102
- Choudhury, R., & H. C. Bhatt. 2009, MNRAS, 393, 959
- Cochran, W. D. 1988, ApJ, 334, 349
- Cohen, M., & L. V. Kuhí. 1979, ApJS, 41, 743
- Concha-Ramírez, F., Wilhelm, M. J. C., Portegies Zwart, S., et al. 2019, MNRAS, 490, 5678
- Cutispoto, G., L. Pastori, L. Pasquini, et al. 2002, A&A 384, 491
- Czesla, S., S. Schröter S., C. P. Schneider, et al. 2019, PyA: Python astronomy-related packages (ascl:1906.010)

- de Freitas, D. B. 2020, arXiv:2003.01444
- Delfosse, X., T. Forveille, C. Perrier, & M. Mayor. 1998, A&A, 331, 581
- De Marco, O., & W. Schmutz. 1999, A&A, 345, 163
- De Marco, O., W. Schmutz, P. A. Crowther, et al. 2000, A&A, 358, 187
- De Medeiros, J. R., S. Alves, S. Udry, et al. 2014, A&A, 561, 126
- De Vries, C. P., J. Brand, F. P. Israel, et al. 1984, A&AS, 56, 333
- Deliyannis, C. P., Pinsonneault, M. H., & Duncan, D. K. 1993, ApJ, 414, 740
- Desidera, S., E. Covino, S. Messina, et al. 2015, A&A, 573, 126
- Dotter, A., B. Chaboyer, D. Jevremović, et al. 2008, ApJS, 178, 89
- Dotter, A. 2016, ApJS, 222, 8
- Dias, W. S., B. S. Alessi, A. Moitinho, & J. R. D. Lépine. 2002, A&A, 389, 871
- Díaz, C. G., J. F. González, H. Levato, & M. Grosso. 2011, A&A, 531, 143
- Ducati, J. R. 2002, yCat, 2237, 0
- Eisner, J. A., R. L. Plambeck, J. M. Carpenter, et al. 2008, ApJ, 683, 304
- Elmegreen, B. G. 2011, EAS Publications Series, 51, 45
- Erspamer, D. & North, P. 2003, A&A, 398, 1121
- Evans, D. W., M. Riella, F. De Angeli, et al. 2018, A&A 616, 4
- Faherty, J. K., Bochanski, J. J., Gagné, J., et al. 2018, ApJ, 863, 91
- Fang, M., J. S. Kim, R. Van Boekel, et al. 2013, ApJS, 207, 5

- Fedele, D., M. E. van den Ancker, T. Henning, R. Jayawardhana, & J. M. Oliveira. 2010, A&A 510, 72
- Feng, F., & C. A. L. Bailer-Jones. 2015, MNRAS, 454, 3267
- Feiden, G. A. 2016, A&A, 593, 99
- Franciosini, E., Sacco, G. G., Jeffries, R. D., et al. 2018, A&A, 616, L12
- Friel, E. D. 1995, ARA&A, 33, 381
- Gaia Collaboration, Prusti, T., de Bruijne, J. H. J., et al. 2016, A&A, 595, A1
- Gaia Collaboration, Brown, A. G. A., Vallenari, A., et al. 2018, A&A, 616, A1
- Gaidos, E. & Mann, A. W. 2014, ApJ, 791, 54
- Gaidos, E., Mann, A. W., Lépine, S., et al. 2014, MNRAS, 443, 2561
- Gaidos, E., Williams, J., & Kraus, A. 2017, Research Notes of the American Astronomical Society, 1, 13
- Galadi-Enriquez, D., C. Jordi, & E. Trullols. 1998, A&A, 337, 125
- Gallet, F., & J. Bouvier. 2013, A&A, 556, 36
- Gontcharov, G. A. 2006, AstL, 32, 759
- Gray, D. 1992, *The Observation and Analysis of Stellar Photospheres*, Cambridge: Cambridge Univ. Press
- Guillout, P., Klutsch, A., Frasca, A., et al. 2009, A&A, 504, 829
- Gullbring, E., N. Calvet, J. Muzerolle, & L. Hartmann. 2000, ApJ, 544, 927
- Gum, C. S. 1952, Observatory, 72, 151

- Gutiérrez Albarrán, M. L., D. Montes, M. Gómez Garrido, et al. 2020, A&A 643, 71
- Habing, H. J. 1968, BAN, 19, 421
- Haisch, K. E., Jr., E. A. Lada, & C. J. Lada. 2001, ApJ, 553, 153
- Hartigan, P., L. Hartmann, S. J. Kenyon, R. Hewett, & J. Stauffer. 1989, ApJS, 70, 899
- Hartigan, P., S. J. Kenyon, L. Hartmann, et al. 1991, ApJ, 382, 617
- Hartmann, L., G. Herczeg, & N. Calvet. 2016, ARA&A, 54, 135
- Hekker, S. & Meléndez, J. 2007, A&A, 475, 1003
- Herbig, G. H. 1974, PASP, 86, 604
- Herczeg, G. J. & Hillenbrand, L. A. 2015, ApJ, 808, 23
- Hernández, J., L. Hartmann, T. Megeath, et al. 2007, ApJ, 662, 1067
- Higuchi, A., & E. Kokubo. 2015, AJ, 150, 26
- Hillenbrand, L. A. 1997, AJ, 113, 1733
- Hillenbrand, L. A. 2005, astro-ph/0511083
- Hillenbrand, L. A., A. Bauermeister, & R. J. White. 2008, in ASP Conf. Ser., Cool
- Hojjatpanah, S., Figueira, P., Santos, N. C., et al. 2019, A&A, 629, A80
- Jao, W.-C., T. J. Henry, D. R. Gies, & N. C. Hambly. 2018, ApJ, 861, 11
- Jeffries, R. D., Maxted, P. F. L., Oliveira, J. M., et al. 2006, MNRAS, 371, L6
- Jeffries, R. D., R. J. Jackson, M. Cottaar, et al. 2014, A&A, 563, 94
- Jofré, E., Petrucci, R., Saffe, C., et al. 2015, A&A, 574, A50
- Kajdič, P., B. Reipurth, A. C. Raga, & J. Walawender. 2010, RMAA, 46, 67

Karnath, N., J. J. Prchlik , R. A. Gutermuth, et al. 2019, ApJ, 871, 46

Kharchenko, N. V., R.-D. Scholz, A. E. Piskunov, S. Röser, E. Schilbach. 2007, AN, 328, 889

Kim, J. S., F. M. Walter, & S. J. Wolk. 2005, ApJ, 129, 1564

Kim, J. S., Walter, F. M., Wolk, S. J., et al. 2006, American Astronomical Society Meeting Abstracts

Kim, J. S., C. J. Clarke, M. Fang, & S. Facchini. 2016, ApJ, 826, 15

Kim, K. H., D. M. Watson, P. Manoj, et al. 2016, ApJ, 226, 8

Kounkel, M. & Covey, K. 2019, AJ, 158, 122

Kroupa, P. 2001, MNRAS, 322, 231

Krumholz, M. R., McKee, C. F., & Bland-Hawthorn, J. 2019, ARA&A, 57, 227

Kuhn, M. A., Hillenbrand, L. A., Sills, A., et al. 2019, ApJ, 870, 32

Lada, J. C., & E. A. Lada. 2003, ARA&A, 41, 57

Leahy, D. A., J. Nousek, & G. Garmire. 1992, ApJ, 385, 561

Lemke, M. 1989, A&A, 225, 125

Lindgren, L., J. Hernández, A. Bombrun, et al. 2018, A&A, 616, 2

Longmore, S. N., Chevance, M., & Kruijssen, J. M. D. 2021, ApJ, 911, L16

Luck, R. E. & Heiter, U. 2006, AJ, 131, 3069

Luck, R. E. & Heiter, U. 2007, AJ, 133, 2464

Luck, R. E. 2014, AJ, 147, 137

Luck, R. E. 2017, AJ, 153, 21

- Luck, R. E. 2018, AJ, 155, 111.
- Magazzú, A., R. Rebolo, & Y. V. Pavlenko. 1992, ApJ, 392, 159
- Maldonado, J., R. M. Martínez-Arnáiz, C. Eiroa, D. Montes, & B. Montesinos. 2010, A&A, 521, 12
- Maldonado, J. & Villaver, E. 2016, A&A, 588, A98
- Mamajek, E. E. & Hillenbrand, L. A. 2008, ApJ, 687, 1264
- Mamajek, E. E., Pecaut, M. J., Nguyen, D. C., et al. 2013, Protostars and Planets VI Posters
- Mann, A. W., Dupuy, T., Muirhead, P. S., et al. 2017, AJ, 153, 267. doi:10.3847/1538-3881/aa7140
- Maheswar, G., & H. C. Bhatt. 2008, ASS, 315, 215
- Marsden, S. C., P. Petit, S. V. Jeffers, et al. 2014, MNRAS, 444, 3517
- Martín, E. L., R. Rebolo, A. Magazzú, & Y. V. Pavlenko. 1994, A&A, 282, 503
- Martínez-Arnáiz, R., Maldonado, J., Montes, D., et al. 2010, A&A, 520, A79
- Martínez-Arnáiz, C., J. Maldonado, D. Montes, C. Eiroa, & B. Montesinos. 2010, A&A, 520, 79
- Massarotti, A., D. W. Latham, R. P. Stefanik, & J. Fogel. 2008, AJ, 135, 209
- Mathieu, R. D. 1985, IAUS, 113, 427
- Meyer, M. R., N. Calvet, & L. A. Hillenbrand. 1997, AJ, 114, 288
- Mohanty, S., R. Jayawardhana, & G. Basri. 2005, ApJ, 626, 498
- Monteiro, H. & Dias, W. S. 2019, MNRAS, 487, 2385

Montes, D., R. González-Peinado, H. M. Tabernero, et al. 2018, MNRAS, 479, 1332

Moraux, E. 2016, EAS Publications Series, 80-81, 73

Mortier, A., I. Oliveira, & E. F. van Dishoeck. 2011, MNRAS, 418, 1194

Murray, N. 2011, ApJ, 729, 133

Muzerole, J., N. Calvet, & L. Hartmann. 1998, ApJ, 492, 743

Nakatani, R. & Yoshida, N. 2019, ApJ, 883, 127

Neckel, T., & H. J. Staude. 1995, ApJ, 448, 832

Neuhäuser, R., M. F. Sterzik, J. H. M. M. Schmitt, R. Wichmann, & J. Krautter. 1995, A&A, 297, 391

Nidever, D. L., G. W. Marcy, R. P. Butler, D. A. Fischer, & S. S. Vogt. 2002, ApJ, 141, 503

Nisak, A., R. J. White, W. C. Jao, et al. 2021, in prep.

O'Dell, C. R., Z. Wen, & X. Hu. 1993, ApJ, 410, 696

Palla, F., S. Randich, E. Flaccomio, & R. Pallavicini. 2005, ApJ, 626, 49

Palla, F., S. Randich, Y. V. Pavlenko, E. Flaccomio, & R. Pallavicini. 2007, ApJ, 659, 41

Paredes, L., T. Henry, W. C. Jao, et al. 2021, AAS.

Paron, S., M. E. Ortega, G. Dubner, et al. 2015, AJ, 149, 193

Pasinetti Fracassini, L. E., L. Pastori, S. Covino, & A. Pozzi. 2001, A&A 367, 521

Paxton, B., L. Bildsten, A. Dotter, et al. 2011 ApJS, 192, 3

Paxton, B., M. Cantiello, P. Arras, et al. 2013, ApJS, 208, 4

Paxton, B., P. Marchant, J. Schwab, et al. 2015, ApJS, 220, 15

Pecaut, M. J., & E. E. Mamajek. 2013, ApJ, 208, 9, Web version 2017.09.25

Persi, P., M. Ferrari-Toniolo, A. R. Marenzi, et al. 1994, A&A, 282, 233

Pettersson, B. 1987, A&A, 171, 101

Pettersson, B. B. Reipurth, ed. 2007, Astronomical Society of the Pacific, *Handbook of Star Forming Regions Vol. II*

Portegies Zwart, S. 2021, A&A, 647, A136

Portegies Zwart, S. F., S. Torres, M. X. Cai, & A. G. A. Brown. 2021, arXiv, 2105.12816v2

Prato, L., M. Huerta, C. M. Johns-Krull, et al. 2008, ApJ, 687, 103

Purcell, C. R., B. M. Gaensler, X. H. Sun, et al. 2015, ApJ, 804, 22

Quinn, S. N., White, R. J., Latham, D. W., et al. 2016, AAS

Ragusa, E., Rosotti, G., Teyssandier, J., et al. 2018, MNRAS, 474, 4460

Ramírez, I., C. Allende Prieto, & D. L. Lambert. 2007, A&A, 465, 271

Ramírez, I., Allende Prieto, C., & Lambert, D. L. 2013, ApJ, 764, 78

Randich, S., Aharpour, N., Pallavicini, R., et al. 1997, A&A, 323, 86

Rebull, L. M., C. H. Johnson , V. Hoette, et al. 2011, AJ, 142, 25

Rei, A. C. S., P. P. Petrov, & J. F. Gameiro. 2018, A&A, 610, 40

Reipurth, B. 1983, A&A, 117, 183

Reipurth, B., & B. Pettersson. 1993, A&A, 267, 439

Reynolds, R. J. 1976, ApJ, 206, 679

Rieke, G. H., & M. J. Lebofsky. 1985, ApJ, 288, 618

Rodgers, A. W., C. T. Campbell, & J. B. Whiteoak. 1960, MNRAS, 121, 103

Royer, F., J. Zorec, & A. E. Gómez. 2007, A&A, 463, 671

Royer, F., Gebran, M., Monier, R., et al. 2014, A&A, 562, A84

Sabbi, E., D. J. Lennon, M. Gieles, et al. 2012, ApJ, 754, 37

Sabbi, E., M. Gennaro, J. Anderson, et al. 2020, ApJ, 891, 2

Sahu, M., & K. C. Sahu. 1992, A&A, 259, 265

Sanders, W. L. 1971, A&A, 14, 226

Schilbach, E., & S. Röser. 2008, A&A, 489, 105

Schröder, S. E., L. Kaper, H. J. G. L. M. Lamers, & A. G. A. Brown. 2004, A&A 428, 149

Schröder, C., A. Reiners, & J. H. M. M. Schmitt. 2009, A&A, 493, 1099

Shu, F. H., F. C. Adams, & S. Lizano. 1987, ARA&A, 25, 23

Sicilia-Aguilar, A., L. W. Hartmann, A. H. Szentgyorgyi, et al. 2005, AJ, 129, 363

Sicilia-Aguilar, A., L. W. Hartmann, J. Hernández, C. Briceño, & N. Calvet. 2005, ApJ, 130, 188

Sicilia-Aguilar, A., J. S. Kim, A. Sobolev, et al. 2013, A&A, 559, 3

Siess, L., E. Dufour, & M. Forestini. 2000, A&A, 358, 593

Sim, G., S. H. Lee, H. B. Ann, & S. Kim. 2019, JKAS, 52, 145

Simón-Díaz, S. & Herrero, A. 2014, A&A, 562, A135

Skrutskie, M. F., R. M. Cutri, R. Stiening, et al. 2006, AJ, 131, 1163

Smith, K. C. & Dworetsky, M. M. 1993, A&A, 274, 335

- Soto, M. G., & J. S. Jenkins. 2018, A&A, 615, 76
- Soubiran, C., Bienaymé, O., Mishenina, T. V., et al. 2008, A&A, 480, 91
- Soubiran, C., J.-F. Le Campion, N. Brouillet, & L. Chemin. 2016, A&A, 591, 118
- Soubiran, C., T. Cantat-Gaudin, M. Romero-Gomez, et al. 2018, A&A, 619, 155
- Sridharan, T. K. 1992, A&A, 13, 217
- Takeda, Y., B. Sato, E. Kambe, et al. 2005, PASJ, 57, 13
- Henry, T. J., Jao, W.-C., Winters, J. G., et al. 2018, AJ, 155, 265. doi:10.3847/1538-3881/aac262
- Tokovinin, A., D. A. Fischer, M. Bonati, et al. 2013, PASP, 125, 1336
- Torres, C. A. O., G. R. Quast, L. da Silva, et al. 2006, A&A, 460, 695
- Valenti, J. A., & D. A. Fischer. 2005, ApJ, 159, 141
- Van den Bergh, S., & W. Herbst. 1975, AJ, 80, 208
- Van Leeuwen, F. 2007, A&A, 474, 653
- Vogt, S. S., S. L. Allen, B. C. Bigelow, et al. 1994, Proc. SPIE, 2198, 362
- Walch, S., A. P. Whitworth, T. G. Bisbas, R. Wünsch, & D. A. Hubber. 2013, MNRAS, 435, 917
- Walter, F. M., A. Brown, R. D. Mathieu, P. C. Myers, & F. J. Vrba. 1988, AJ, 96, 297
- Weissman, P. R. 2007, IAUS, 236 eds. G. B. Valsecchi, D. Vokrouhlický, & A. Milani, 441
- White, R. J., & A. M. Ghez. 2001, ApJ, 556, 265
- White, R. J., & G. Basri. 2003, ApJ, 582, 1109

- White, R. J., & L. A. Hillenbrand. 2004, ApJ, 616, 998
- White, R. J., Gabor, J. M., & Hillenbrand, L. A. 2007, AJ, 133, 2524
- Wilson, R. E. 1953, Carnegie Institute Washington D.C. Publication, 0
- Winter, A. J., C. J. Clarke, G. Rosotti, J. Ih, S. Facchini, & T. J. Haworth. 2018, MNRAS, 478, 2700
- Witner, A. J., C. J. Clarke, G. Rosotti, A. Hacar, & R. Alexander. 2019, arXiv, 1909.04093v1
- Winter, A. J., Kruijssen, J. M. D., Longmore, S. N., et al. 2020, Nature, 586, 528
- Woermann, B., M. J. Gaylard, & R. Otrupcek. 2001, MNRAS, 325, 1213
- Wright, N. J. & Parker, R. J. 2019, MNRAS, 489, 2694
- Yeomans, D. K., & A. B. Chamberlin. 2012, Acta Astron., 90, 3
- Yep, A. C., & R. J. White. 2020, ApJ, 889, 50
- Yep, A. C., & R. J. White. 2021, MNRAS, under review
- Zealey, W. J., Z. Ninkov, E. Rice, M. Hartley, & S. B. Tritton. 1983, ApL, 23, 119
- Zuckerman, B. & Song, I. 2004, ARA&A, 42, 685

Appendix A

CHIRON SPECTRAL STANDARDS

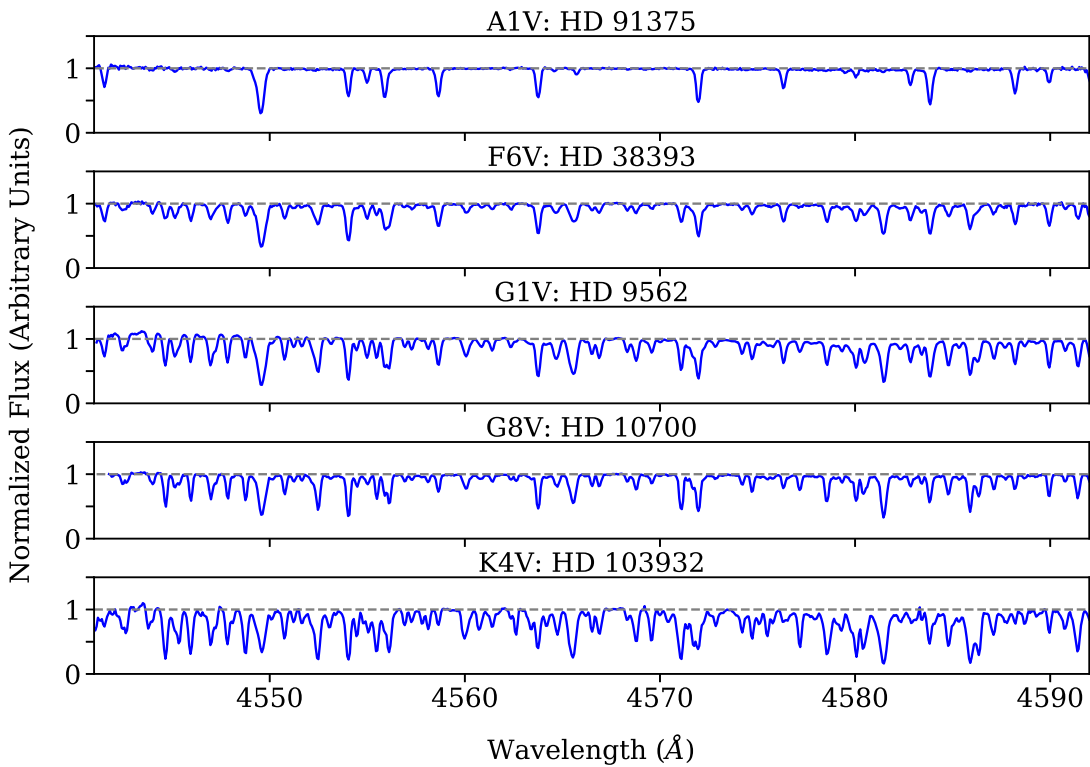


Figure A.1: Sample of normalized CHIRON spectra. Order 1 (left panels) is rich in atomic lines and useful for spectral classification and velocity measurements. Order 41 (right panels) contains Li I $\lambda 6708$, present in young stars.

We present a comprehensive, high-quality catalogue (see Figure A.1) of 81 spectral standard stars for the CHIRON spectrograph on the SMARTS 1.5 m telescope on Cerro Tololo in Chile (Tokovinin et al. 2013). Standards are selected from the radial velocity catalogue of Nidever et al. (2002) and the effective temperature catalogue of PASTEL (Soubiran et al. 2016) whenever possible. Spectral types include dwarfs M5.5V – O9.5V,

giants K5III – G5III, and one supergiant B9.5I (see Figure A.2). Standard star properties are provided in Table A.1. All standards’ properties and spectra are publicly available on GitHub.¹

The standards have been observed with the same fixed setup as the association stars, but with higher SNR $\gtrsim 100$. We aim for peak flux counts 10,000 – 200,000. Spectra of these standards have been likewise extracted, wavelength calibrated, and normalized in the same manner as the association stars. Because CHIRON is a very stable instrument, we are able to normalize spectra by dividing out a blaze function derived order by order from the fairly featureless, slow-rotating A3V-type star HD 11753 and the B9.5I supergiant HD 111613. This blaze function is also available on GitHub. Standards’ normalized spectra are available in beta.

Thirty-six of the 81 the standards have radial velocities from (Nidever et al. 2002), accurate to 0.1 km s⁻¹. For 13 stars that consistently miss the median radial velocity measurements given by similar stars by ≥ 0.5 km s⁻¹, we use the spectra of similar standards to determine the poorly measured standards’ radial velocities, accurate to 0.06 – 1.52 km s⁻¹. Stars measured by other sources have radial velocity uncertainties 0.1 – 1.9 km s⁻¹. All standards have no disks, no veiling, and relatively slow projected rotations: 3.7 – 19.5 km s⁻¹ for F-type stars, 0.73 – 17.5 km s⁻¹ for G-type, and 0.5 – 6.79 km s⁻¹ for K-type. Full $v_{\text{rot}} \sin(i)$ range is 1.6 – 49.0 km s⁻¹, median 4.35 km s⁻¹. Seventy-six of the 81 standards have well-measured effective temperatures T_{eff} from PASTEL (Soubiran et al. 2016). For standards with multiple T_{eff} values, we take the median and treat the sample standard deviation of the values as the uncertainty.

¹https://github.com/alexandrayep/CHIRON_Standards

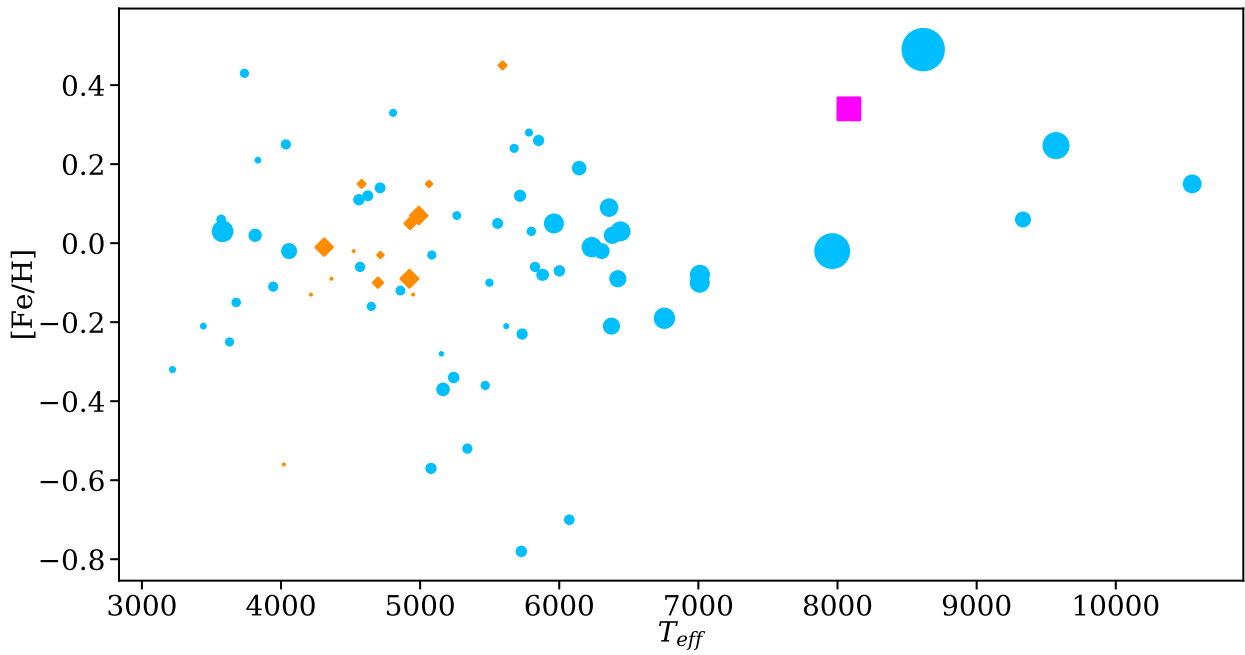


Figure A.2: CHIRON standards parameter space for temperatures and metallicities of dwarfs (azure circles), giants (orange diamonds), and a supergiant (pink square). Points are scaled by $v_{\text{rot}} \sin(i)$ values, with range 1.6 – 49.0 km s⁻¹.

Table A.1: CHIRON Standards

Standard	RA	Dec	V	Spectral	T_{eff}	v_r	$v_{rot} \sin(i)$	[Fe/H]	Refs. for
Name	(hh mm ss)	(°, ′, ″)	(mag)	Type	(K)	(km s ⁻¹)	(km s ⁻¹)	(dex)	$v_r, v_{rot} \sin(i), [\text{Fe}/\text{H}]$
ζ Oph	16 37 09.54	-10 34 01.5	2.56	O9.5V	29200 ± 2000	-9.0 ± 5.5	311.0 ± 8.0	...	15, 31, -
HD 4622	00 48 01.06	-21 43 21.0	5.57	B9V	10310 ± 450	21.5 ± 1.9	61	...	15, 17, -
E Cen	12 08 14.71	-48 41 32.9	5.34	A0V	9893.0 ± 7.0	7.20 ± 0.50	74	...	11, 17, -
HD 91375	10 30 20.13	-71 59 34.1	4.718	A1V	9333	7.50 ± 0.40	10.	0.06	11, 17, 5
HD 65900	08 01 13.89	+04 52 47.4	5.646	A1V	9570. ± 91	44.20 ± 0.10	33	0.25	11, 17, 30
HD 106819	12 17 03.33	-16 41 37.5	6.07	A2V	8770 ± 160	-11.7 ± 1.6	79.00 ± 0.60	...	11, 23, -
HIP 113673	23 01 23.04	-22 47 27.2	6.28	A2V	8299 ± 77	-10.40 ± 0.50	91.9 ± 1.3	...	11, 23, -
HD 138105	15 30 36.25	-20 43 42.8	6.205	A3V	8072 ± 75	-10.9 ± 1.5	29	...	11, 17, -
HD 96568	11 06 24.25	-64 50 23.9	6.381	A3V	8511 ± 79	-3.00 ± 0.40	13	...	11, 17, -
HD 216956	22 57 39.05	-29 37 20.1	1.16	A4V	8620 ± 340	6.50 ± 0.50	91.60 ± 0.50	0.49	11, 23, 8
HD 168525	18 21 12.41	-26 05 06.4	6.9	A6V	8020 ± 210	-9.40 ± 0.40	12	...	11, 17, -
73 Vir	13 32 02.81	-18 43 44.0	6.008	A7V	7962 ± 92	-17.50 ± 0.90	61	-0.02	15, 17, 37
β Oct	22 46 03.51	-81 22 53.8	4.141	A9V	7745 ± 54	31.8 ± 1.5	49	...	43, 17, -
α Crv	12 08 24.82	-24 43 44.0	4.0	F1V	7010 ± 150	2.80 ± 0.30	16.9 ± 1.5	-0.08	11, 24, 12
HD 40136	05 56 24.29	-14 10 03.7	3.72	F1V	7010 ± 130	-2.06 ± 0.42	17	-0.1	43, 22, 25
ξ Oph	17 21 00.38	-21 06 46.6	4.39	F2V	6760 ± 110	-8.93 ± 0.30	19.5 ± 1.0	-0.19	38, 24, 39

Table A.1—Continued

Standard Name	RA (hh mm ss)	Dec ($^{\circ}$, $'$, $''$)	V (mag)	Spectral Type	T_{eff} (K)	v_r (km s $^{-1}$)	$v_{rot} \sin(i)$ (km s $^{-1}$)	[Fe/H] (dex)	$v_{rot} \sin(i)$, [Fe/H]	Refs. for v_r
58 Oph	17 43 25.79	-21 40 59.5	4.873	F5V	6421 ± 89	10.16 ± 0.23	11.80 ± 0.60	-0.09	38, 24, 39	
53 Vir	13 12 03.54	-16 11 55.0	5.04	F5.5V	6380 ± 430	-12.55 ± 0.11	11.7 ± 1.0	-0.21	43, 24, 25	
τ PsA	22 10 08.78	-32 32 54.3	4.92	F6V	6358 ± 82	-16.26 ± 0.10	14.10 ± 0.70	0.09	7, 24, 10	
HD 30652	04 49 50.41	+06 57 40.6	3.19	F6V	6440 ± 160	24.32 ± 0.25	16.80 ± 0.40	0.03	43, 29, 10	
HD 38393	05 44 27.79	-22 26 54.2	3.6	F6V	6300 ± 250	-9.19 ± 0.19	10.	-0.02	40, 22, 39	
20 Oph	16 49 50.02	-10 46 58.8	4.646	F7V	6382 ± 87	1.56 ± 0.27	12	0.02	38, 9, 36	
122 HD 19994	03 12 46.44	-01 11 46.0	5.07	F8.5V	6143 ± 92	19.33 ± 0.10	7.95 ± 0.98	0.19	7, 41, 10	
171 Pup	07 45 35.02	-34 10 20.5	5.37	F9V	5730 ± 120	106.16 ± 0.10	4.40 ± 0.20	-0.78	7, 24, 39	
γ Pav	21 26 26.6	-65 21 58.3	4.22	F9V	6070 ± 140	-29.84 ± 0.19	3.70 ± 0.70	-0.7	38, 24, 39	
HD 152555	16 54 08.14	-04 20 24.7	7.82	G0V	5962 ± 98	-16.40 ± 0.19	16.80 ± 0.60	0.05	38, 20, 10	
HD 143809	16 02 22.42	+03 39 07.2	8.76	G0V	6234 ± 78	-9.393 ± 0.089	17.5 ± 1.5	-0.01	43, 20, 20	
HD 34721	05 18 50.47	-18 07 48.2	5.96	G0V	6001 ± 96	40.45 ± 0.10	4.40 ± 0.20	-0.07	7, 24, 10	
HD 9562	01 33 42.84	-07 01 31.2	5.76	G1V	5852 ± 63	-14.99 ± 0.10	4.20 ± 0.50	0.26	7, 29, 10	
18 Sco	16 15 37.27	-08 22 10.0	5.5	G2V	5800 ± 120	11.75 ± 0.10	2.60 ± 0.50	0.03	7, 29, 10	
HD 38858	05 48 34.94	-04 05 40.7	5.97	G2V	5730 ± 420	31.54 ± 0.10	4	-0.23	7, 21, 10	
HD 114613	13 12 03.19	-37 48 10.9	5.55	G3V	5676 ± 43	-12.85 ± 0.18	2.38 ± 0.23	0.24	38, 41, 10	

Table A.1—Continued

Standard Name	RA (hh mm ss)	Dec ($^{\circ}$, $'$, $''$)	V (mag)	Spectral Type	T_{eff} (K)	v_r (km s $^{-1}$)	$v_{rot} \sin(i)$ (km s $^{-1}$)	[Fe/H] (dex)	$v_{rot} \sin(i)$, [Fe/H]	Refs. for v_r ,
HD 59967	07 30 42.51	-37 20 21.7	6.635	G3V	5826 ± 54	9.37 ± 0.18	3	-0.06	38, 21, 39	
HD 4391	00 45 45.59	-47 33 07.1	5.8	G3V	5878 ± 64	-11.01 ± 0.21	5	-0.08	38, 21, 39	
HD 20630	03 19 21.7	+03 22 12.7	4.85	G5V	5718 ± 70.	19.02 ± 0.10	5.20 ± 0.40	0.12	7, 29, 10	
HD 111031	12 46 30.84	-11 48 44.8	6.87	G5V	5782 ± 45	-20.46 ± 0.10	1.73 ± 0.27	0.28	7, 41, 10	
HD 90156	10 23 55.27	-29 38 43.9	6.92	G5V	5619 ± 31	26.93 ± 0.10	0.73 ± 0.24	-0.21	7, 41, 10	
HD 21019	03 23 17.7	-07 47 38.8	6.2	G5.5V	5468 ± 78	41.63 ± 0.10	2.50 ± 0.42	-0.36	7, 41, 10	
HD 115617	13 18 24.31	-18 18 40.3	4.74	G6.5V	5557 ± 56	-7.85 ± 0.10	3.90 ± 0.90	0.05	7, 24, 10	
HD 10700	01 44 04.08	-15 56 14.9	3.5	G8V	5340 ± 100	-16.62 ± 0.10	3	-0.52	7, 22, 10	
ϵ For	03 01 37.64	-28 05 29.6	5.85	G9V	5080 ± 110	38.51 ± 0.10	4	-0.57	43, 21, 10	
HD 100623	11 34 29.49	-32 49 52.8	5.98	K0V	5164 ± 72	-21.96 ± 0.10	7	-0.37	7, 22, 10	
41 Ara	17 19 03.84	-46 38 10.4	5.48	K0V	5241 ± 60.	25.94 ± 0.10	4	-0.34	43, 21, 10	
HD 26965	04 15 16.32	-07 39 10.3	4.43	K0V	5150 ± 400	-42.33 ± 0.10	0.50 ± 0.30	-0.28	7, 29, 10	
12 Oph	16 36 21.45	-02 19 28.5	5.77	K1V	5264 ± 47	-12.86 ± 0.10	2.20 ± 0.40	0.07	7, 29, 10	
HD 22049	03 32 55.84	-09 27 29.7	3.73	K2V	5084 ± 71	16.33 ± 0.10	2.40 ± 0.40	-0.03	7, 29, 10	
HD 32147	05 00 49.0	-05 45 13.2	6.21	K3V	4806 ± 95	21.55 ± 0.10	1.70 ± 0.40	0.33	7, 29, 10	
HD 16160	02 36 04.89	+06 53 12.7	5.83	K3V	4858 ± 96	24.49 ± 0.10	2.90 ± 0.40	-0.12	43, 29, 10	

Table A.1—Continued

Standard Name	RA (hh mm ss)	Dec ($^{\circ}$, $'$, $''$)	V (mag)	Spectral Type	T_{eff} (K)	v_r (km s $^{-1}$)	$v_{rot} \sin(i)$ (km s $^{-1}$)	[Fe/H] (dex)	$v_{rot} \sin(i)$, [Fe/H]	Refs. for v_r ,
HD 50281	06 52 18.05	-05 10 25.4	6.57	K3.5V	4710 \pm 110	-7.08 \pm 0.10	4	0.14	7, 21, 10	
HD 103932	11 57 56.21	-27 42 25.4	6.964	K4V	4560 \pm 120	48.50 \pm 0.10	4	0.11	7, 21, 36	
HD 131977	14 57 28.0	-21 24 55.7	5.72	K4V	4624 \pm 76	26.96 \pm 0.10	4	0.12	7, 21, 10	
HD 36003	05 28 26.1	-03 29 58.4	7.642	K5V	4568 \pm 39	-55.035 \pm 0.068	3	-0.06	43, 22, 36	
ϵ Ind	22 03 21.66	-56 47 09.5	4.69	K5V	4650 \pm 110	-40.06 \pm 0.10	2.49 \pm 0.11	-0.16	43, 41, 36	
HD 157881	17 25 45.23	+02 06 41.1	7.56	K7V	4035 \pm 80.	-23.20 \pm 0.10	3	0.25	7, 22, 35	
HD 217357	23 00 16.12	-22 31 27.7	7.869	K7V	3940 \pm 200	16.42 \pm 0.18	3	-0.11	43, 22, 1	
HD 32450	05 02 28.42	-21 15 23.9	8.32	K7V	...	-15.88 \pm 0.24	5	-0.34	43, 21, 2	
HD 165222	18 05 07.58	-03 01 52.8	9.36	M0V	3630. \pm 30.	32.03 \pm 0.11	2.47 \pm 0.29	-0.25	43, 42, 2	
HD 111631	12 50 43.57	-00 46 05.3	8.47	M0V	3830 \pm 130	5.04 \pm 0.10	1	0.21	7, -, 2	
HD 191849	20 13 53.4	-45 09 50.5	7.966	M0V	3548 \pm 14	-33.46 \pm 0.52	1	...	38, 13, -	
HD 42581	06 10 34.62	-21 51 52.7	8.125	M1V	3814	4.72 \pm 0.10	6	0.02	7, 21, 2	
HD 36395	05 31 27.4	-03 40 38.0	7.968	M1.5V	3737 \pm 58	8.66 \pm 0.10	2.50 \pm 0.29	0.43	7, 42, 1	
HD 217987	23 05 52.04	-35 51 11.0	7.34	M2V	3678 \pm 41	8.17 \pm 0.14	2.70 \pm 0.50	-0.15	38, 32, 1	
GJ 628	16 30 18.06	-12 39 45.3	10.072	M3V	3570.	-21.22 \pm 0.10	2.89 \pm 0.23	0.06	7, 42, 2	
GJ 581	15 19 26.82	-07 43 20.2	10.61	M3V	3442 \pm 54	-9.40 \pm 0.10	1	-0.21	7, -, 2	

Table A.1—Continued

Standard Name	RA (hh mm ss)	Dec ($^{\circ}$, $'$, $''$)	V (mag)	Spectral Type	T_{eff} (K)	v_r (km s $^{-1}$)	$v_{rot} \sin(i)$ (km s $^{-1}$)	[Fe/H] (dex)	$v_{rot} \sin(i)$, [Fe/H]	Refs. for v_r ,
GJ 273	07 27 24.5	+05 13 32.8	9.872	M3.5V	...	18.22 ± 0.10	1	0.02		7, -, 2
GJ 83.1	02 00 12.96	+13 03 07.0	12.298	M4.5V	...	-28.57 ± 0.10	1	-0.1		7, -, 1
GJ 54.1	01 12 30.64	-16 59 56.4	12.074	M4.5V	...	28.09 ± 0.10	1	-0.26		7, -, 1
GJ 1061	03 35 59.7	-44 30 45.7	13.07	M5.5V	...	1.33 ± 0.27	5.0 ± 5.0	...		43, 26, -
HD 24160	03 49 27.25	-36 12 00.9	4.17	G7III	5064 ± 65	2.62 ± 0.23	1.0 ± 1.0	0.15		38, -, 28
HD 38529	05 46 34.91	+01 10 05.5	5.938	G8III	5590 ± 380	30.21 ± 0.10	1.63 ± 0.29	0.45		7, 33, 10
HD 9270	01 31 29.01	+15 20 45.0	3.62	G8III	4923 ± 25	13.78 ± 0.17	8.4 ± 7.0	-0.09		18, 18, 34
θ Cet	01 24 01.41	-08 10 59.7	3.59	K0III	4697 ± 89	15.969 ± 0.059	3	-0.1		43, 18, 16
HD 201381	21 09 35.65	-11 22 18.1	4.52	K0III	4990. ± 52	-11.26 ± 0.15	8	0.07		38, 4, 16
HD 25069	03 58 52.39	-05 28 11.8	5.843	K0.5III	4928 ± 72	38.48 ± 0.10	3.30 ± 0.50	0.05		7, 29, 35
HD 25723	04 04 22.72	-12 47 32.3	5.622	K1III	4714 ± 60.	26.75 ± 0.10	1	-0.03		7, -, 14
HD 26846	04 14 23.69	-10 15 22.6	4.86	K2III	4580 ± 620	6.033 ± 0.055	2	0.15		43, 18, 19
HD 217459	23 00 42.9	+03 00 42.5	5.852	K2.5III	4215 ± 45	18.63 ± 0.10	0.	-0.13		4, 7, 14
χ Sco	16 13 50.91	-11 50 15.9	5.252	K3III	4310. ± 87	-23.61 ± 0.10	8	-0.01		4, 7, 14
HD 223559	23 50 33.29	-14 24 05.4	5.711	K4.5III	4020. ± 70.	-62.84 ± 0.10	0.	-0.56		7, -, 14
N Vel	09 31 13.35	-57 02 03.8	3.158	K5III	4105	-14.39 ± 0.33	1	...		27, 27, -

Table A.1—Continued

Standard Name	RA (hh mm ss)	Dec (° ′ ″)	V (mag)	Spectral Type	T_{eff} (K)	v_r (km s ⁻¹)	$v_{r\text{rot}} \sin(i)$ (km s ⁻¹)	[Fe/H] (dex)	$v_{r\text{rot}} \sin(i)$, [Fe/H]	Refs. for v_r ,
HD 111613	12 51 17.98	-60 19 47.2	5.72	B9.5I	8100 ± 1100	-21.9 ± 1.4	27.3 ± 6.0	0.34	11, 24, 28	

REFS.—(1) Gaidos & Mann 2014; (2) Gaidos et al. 2014b; (3) Wilson 1953; (4) Bernacca & Perinotto 1970; (5) Lemke 1989; (6) Smith & Dworetsky 1993; (7) Nidever et al. 2002; (8) Espanier & North 2003; (9) Takeda et al. 2005; (10) Valenti & Fischer 2005; (11) Gontcharov 2006; (12) Luck & Heiter 2006; (13) Torres et al. 2006; (14) Hekker & Meléndez 2007; (15) Kharchenko et al. 2007; (16) Luck & Heiter 2007; (17) Royer et al. 2007; (18) Massarotti et al. 2008; (19) Soubiran et al. 2008; (20) Guillout et al. 2009; (21) Schröder et al. 2009; (22) Martínez-Arnáiz et al. 2010; (23) Díaz et al. 2011; (24) Ammler-von Eiff & Reiners 2012; (25) Ramírez et al. 2013; (26) Barnes et al. 2014; (27) De Medeiros et al. 2014; (28) Luck 2014; (29) Marsden et al. 2014; (30) Royer et al. 2014; (31) Simón-Díaz & Herrero 2014; (32) Desidera et al. 2015; (33) Jofré et al. 2015; (34) Maldonado & Villaver 2016; (35) Luck 2017; (36) Aguilera-Gómez et al. 2018; (37) Bochanski et al. 2018; (38) Gaia Collaboration et al. 2018; (39) Luck 2018; (40) Montes et al. 2018; (41) Soto & Jenkins 2018; (42) Hojjatpanah et al. 2019; (43) Yep et al., in prep.; (44) White et al. 2007

Appendix B

ASSOCIATION MEMBER KINEMATICS AND PROPERTIES

We have refined the membership of eight clusters in the Gum Nebula. Here are *Gaia* DR2 data and calculated masses for all members of each association. Names are included for sources we have spectroscopically observed. Data for KWW sources are from Kim et al. (2005).

Table B.1: CG 4 Assn. Member Kinematics and Properties

Star Name	<i>RA</i> ($^{\circ}$)	<i>Dec</i> ($^{\circ}$)	Parallax (mas)	μ_{α} (mas yr $^{-1}$)	μ_{δ} (mas yr $^{-1}$)	v_r (km s $^{-1}$)	G (mag)	BP (mag)	RP (mag)	<i>d</i> (pc)	Mass (M $_{\odot}$)
...	112.2102	-45.7789	2.345 \pm 0.074	-4.33 \pm 0.14	9.40 \pm 0.14	...	16.865 \pm 0.001	18.517 \pm 0.029	15.627 \pm 0.003	422 $^{+14}_{-13}$	0.359 \pm 0.029
...	112.2327	-45.5894	2.335 \pm 0.076	-3.65 \pm 0.15	9.50 \pm 0.14	...	16.944 \pm 0.001	18.848 \pm 0.029	15.611 \pm 0.005	424 $^{+14}_{-13}$	0.243 \pm 0.019
2MASS J07293289-4611036	112.3871	-46.1843	2.435 \pm 0.015	-4.141 \pm 0.027	9.274 \pm 0.034	19.88 \pm 0.93	13.894 \pm 0.003	14.556 \pm 0.008	13.112 \pm 0.006	405.9 $^{+2.5}_{-2.4}$	0.980 \pm 0.049
CD-46 3194	112.3984	-46.5226	2.403 \pm 0.033	-4.036 \pm 0.065	8.998 \pm 0.074	7.1 \pm 1.7	9.254 \pm 0.001	9.483 \pm 0.002	8.919 \pm 0.003	411.4 $^{+5.7}_{-5.6}$	1.830 \pm 0.092
...	112.4666	-47.3395	2.347 \pm 0.052	-4.122 \pm 0.091	8.24 \pm 0.13	...	16.023 \pm 0.001	17.525 \pm 0.009	14.801 \pm 0.003	421.2 $^{+9.4}_{-9.0}$	0.404 \pm 0.032
...	112.6964	-46.3940	2.379 \pm 0.039	-3.878 \pm 0.081	8.961 \pm 0.094	...	15.756 \pm 0.002	17.011 \pm 0.009	14.635 \pm 0.004	415.5 $^{+7.0}_{-6.7}$	0.521 \pm 0.042
...	112.7232	-47.0726	2.364 \pm 0.062	-4.54 \pm 0.12	8.96 \pm 0.13	...	15.388 \pm 0.002	418 \pm 11	0.725 \pm 0.080
...	112.7273	-47.0519	2.327 \pm 0.071	-4.09 \pm 0.13	8.82 \pm 0.13	...	16.421 \pm 0.002	18.281 \pm 0.022	15.065 \pm 0.010	425 $^{+13}_{-12}$	0.248 \pm 0.020
...	112.7387	-46.9558	2.428 \pm 0.037	-2.886 \pm 0.074	7.687 \pm 0.074	...	14.734 \pm 0.001	16.033 \pm 0.006	13.592 \pm 0.003	407.1 $^{+6.2}_{-6.0}$	0.498 \pm 0.040
...	112.7399	-46.9365	2.421 \pm 0.062	-4.48 \pm 0.12	8.64 \pm 0.13	...	16.584 \pm 0.004	18.194 \pm 0.024	15.228 \pm 0.012	409 $^{+11}_{-10}$	0.328 \pm 0.026
RP34	112.8411	-46.9622	2.330 \pm 0.015	-4.227 \pm 0.028	8.842 \pm 0.029	23.52 \pm 0.53	13.725 \pm 0.007	14.581 \pm 0.026	12.778 \pm 0.017	423.8 \pm 2.7	0.47 \pm 0.20
TYC 8137-2862-1	112.8672	-46.9629	2.420 \pm 0.027	-4.026 \pm 0.046	8.533 \pm 0.042	22.0 \pm 2.6	10.745 \pm 0.000	10.931 \pm 0.002	10.449 \pm 0.001	408.5 $^{+4.6}_{-4.5}$	1.860 \pm 0.093
...	112.8699	-47.0761	2.360 \pm 0.065	-3.96 \pm 0.12	8.56 \pm 0.12	...	16.786 \pm 0.001	18.800 \pm 0.017	15.415 \pm 0.004	419 $^{+12}_{-11}$	0.210 \pm 0.017
TYC 8137-2850-1	112.8735	-46.9802	2.347 \pm 0.020	-3.739 \pm 0.037	9.005 \pm 0.038	21.16 \pm 0.21	11.507 \pm 0.002	12.151 \pm 0.008	10.747 \pm 0.007	420.9 \pm 3.6	0.820 \pm 0.041
...	112.9028	-47.0037	2.300 \pm 0.029	-4.425 \pm 0.060	8.789 \pm 0.051	...	14.757 \pm 0.022	15.735 \pm 0.081	13.695 \pm 0.065	429.5 $^{+5.4}_{-5.3}$	0.646 \pm 0.052
...	112.9044	-47.0559	2.383 \pm 0.033	-3.996 \pm 0.061	8.885 \pm 0.057	...	15.558 \pm 0.002	16.682 \pm 0.010	14.496 \pm 0.005	414.7 $^{+5.8}_{-5.7}$	0.571 \pm 0.046
...	112.9316	-46.8941	2.320 \pm 0.072	-4.28 \pm 0.14	8.35 \pm 0.13	...	16.701 \pm 0.002	18.476 \pm 0.021	15.394 \pm 0.006	426 $^{+14}_{-13}$	0.282 \pm 0.023
...	112.9327	-46.9717	2.311 \pm 0.064	-4.05 \pm 0.13	9.03 \pm 0.11	...	16.757 \pm 0.003	18.401 \pm 0.034	15.440 \pm 0.008	428 $^{+12}_{-11}$	0.330 \pm 0.026

Table B.1: CG 4 Assn.—Continued

Star Name	RA ($^{\circ}$)	Dec ($^{\circ}$)	Parallax (mas)	μ_{α} (mas yr^{-1})	μ_{δ} (mas yr^{-1})	v_r (km s^{-1})	G (mag)	BP (mag)	RP (mag)	d (pc)	Mass (M_{\odot})
CD-46 3212	112.9338	-47.0003	2.335 \pm 0.021	-3.051 \pm 0.040	7.807 \pm 0.038	22.4 \pm 2.1	10.786 \pm 0.002	11.347 \pm 0.006	10.095 \pm 0.005	423.0 $^{+3.8}_{-3.7}$	0.990 \pm 0.090
...	112.9401	-46.9882	2.383 \pm 0.046	-4.198 \pm 0.089	9.057 \pm 0.084	...	16.031 \pm 0.009	17.509 \pm 0.035	14.819 \pm 0.028	414.8 $^{+8.2}_{-7.9}$	0.412 \pm 0.033
...	112.9604	-46.9724	2.467 \pm 0.056	-4.28 \pm 0.11	8.72 \pm 0.11	...	16.358 \pm 0.001	17.807 \pm 0.015	15.135 \pm 0.002	401.0 $^{+9.3}_{-8.9}$	0.417 \pm 0.033
...	112.9743	-47.5403	2.366 \pm 0.025	-4.483 \pm 0.050	9.092 \pm 0.049	...	14.939 \pm 0.002	16.118 \pm 0.010	13.842 \pm 0.006	417.5 $^{+4.5}_{-4.4}$	0.550 \pm 0.044
...	112.9848	-46.9063	2.294 \pm 0.036	-4.354 \pm 0.082	8.526 \pm 0.063	...	15.464 \pm 0.011	16.614 \pm 0.042	14.382 \pm 0.028	430.6 $^{+6.8}_{-6.6}$	0.560 \pm 0.045
...	113.0033	-46.9800	2.342 \pm 0.032	-4.244 \pm 0.058	8.643 \pm 0.048	...	15.159 \pm 0.003	16.140 \pm 0.016	14.162 \pm 0.007	421.8 $^{+5.8}_{-5.6}$	0.661 \pm 0.053
...	113.1704	-47.0329	2.396 \pm 0.056	-3.72 \pm 0.11	7.89 \pm 0.10	...	16.611 \pm 0.005	18.191 \pm 0.035	15.345 \pm 0.014	412.7 $^{+9.9}_{-9.4}$	0.374 \pm 0.030
...	113.3595	-47.1098	2.385 \pm 0.069	-3.82 \pm 0.14	8.96 \pm 0.13	...	16.885 \pm 0.002	18.468 \pm 0.013	15.635 \pm 0.005	415 \pm 12	0.374 \pm 0.030
...	113.3619	-46.8118	2.414 \pm 0.017	-4.208 \pm 0.030	9.109 \pm 0.034	22.47 \pm 0.42	13.719 \pm 0.003	14.431 \pm 0.011	12.877 \pm 0.007	409.3 $^{+2.9}_{-2.8}$	0.730 \pm 0.040
Rp337	112.6298	-47.0371	2.44 \pm 0.14	-3.68 \pm 0.28	9.09 \pm 0.30	...	17.836 \pm 0.012	19.90 \pm 0.13	16.249 \pm 0.016	407 $^{+26}_{-23}$	0.168 \pm 0.015
...	112.6654	-46.9667	2.31 \pm 0.19	-4.51 \pm 0.35	9.16 \pm 0.38	...	18.643 \pm 0.003	20.64 \pm 0.18	17.019 \pm 0.011	432 $^{+39}_{-33}$	0.171 \pm 0.024
...	112.9588	-45.6790	2.30 \pm 0.12	-4.81 \pm 0.23	9.17 \pm 0.26	...	18.098 \pm 0.012	19.999 \pm 0.074	16.734 \pm 0.007	431 $^{+25}_{-23}$	0.236 \pm 0.019
...	113.0499	-46.6948	2.24 \pm 0.10	-3.92 \pm 0.18	9.10 \pm 0.21	...	17.465 \pm 0.012	19.269 \pm 0.034	16.160 \pm 0.004	443 $^{+22}_{-20}$	0.275 \pm 0.022
...	113.6374	-47.1435	2.30 \pm 0.12	-4.16 \pm 0.23	8.95 \pm 0.23	...	17.561 \pm 0.015	19.357 \pm 0.074	16.170 \pm 0.006	430 $^{+25}_{-22}$	0.255 \pm 0.020
...	113.8293	-46.7858	2.43 \pm 0.17	-4.25 \pm 0.32	9.33 \pm 0.33	...	18.754 \pm 0.002	20.219 \pm 0.068	17.548 \pm 0.011	409 $^{+31}_{-27}$	0.417 \pm 0.033
...	111.8846	-45.6980	2.436 \pm 0.076	-3.93 \pm 0.14	9.66 \pm 0.14	...	17.012 \pm 0.005	18.813 \pm 0.030	15.656 \pm 0.009	406 $^{+13}_{-12}$	0.263 \pm 0.021

Table B.2: CG 22 Assn. Member Kinematics and Properties

Star Name	<i>RA</i> ($^{\circ}$)	<i>Dec</i> ($^{\circ}$)	Parallax (mas)	μ_{α} (mas yr $^{-1}$)	μ_{δ} (mas yr $^{-1}$)	v_r (km s $^{-1}$)	G (mag)	BP (mag)	RP (mag)	<i>d</i> (pc)	Mass (M $_{\odot}$)
...	126.7129	-37.2092	2.883 \pm 0.082	-7.35 \pm 0.13	10.52 \pm 0.13	...	16.701 \pm 0.002	18.286 \pm 0.016	15.462 \pm 0.006	344 $^{+10}_{-9.5}$	0.334 \pm 0.029
...	126.8746	-36.3103	2.790 \pm 0.076	-7.13 \pm 0.14	10.70 \pm 0.13	...	16.964 \pm 0.002	18.707 \pm 0.017	15.674 \pm 0.004	355.2 $^{+9.9}_{-9.4}$	0.263 \pm 0.021
...	127.8604	-35.2754	2.792 \pm 0.016	-6.906 \pm 0.025	10.582 \pm 0.026	...	13.585 \pm 0.002	14.354 \pm 0.006	12.720 \pm 0.005	354.5 \pm 2.1	0.706 \pm 0.057
...	125.8299	-35.3895	2.820 \pm 0.038	-7.275 \pm 0.063	11.008 \pm 0.065	...	15.292 \pm 0.003	16.434 \pm 0.013	14.214 \pm 0.007	351.0 $^{+4.7}_{-4.6}$	0.531 \pm 0.042
...	127.8605	-35.2743	2.821 \pm 0.060	-6.846 \pm 0.090	10.303 \pm 0.095	...	16.487 \pm 0.002	18.029 \pm 0.016	15.177 \pm 0.004	351.1 $^{+7.6}_{-7.3}$	0.324 \pm 0.030
...	127.9264	-34.8435	2.743 \pm 0.062	-6.788 \pm 0.091	10.650 \pm 0.089	...	15.808 \pm 0.002	17.417 \pm 0.012	14.555 \pm 0.005	361.1 $^{+8.4}_{-8.0}$	0.320 \pm 0.031
...	126.8666	-35.9739	2.75 \pm 0.10	-7.14 \pm 0.16	10.59 \pm 0.16	...	17.284 \pm 0.002	19.432 \pm 0.031	15.892 \pm 0.006	360.0 $^{+14}_{-13}$	0.166 \pm 0.013
...	127.8693	-35.3956	2.872 \pm 0.054	-6.921 \pm 0.078	10.561 \pm 0.078	...	16.096 \pm 0.008	17.192 \pm 0.046	14.965 \pm 0.021	344.9 $^{+6.6}_{-6.3}$	0.528 \pm 0.042
...	127.1600	-35.1109	2.97 \pm 0.11	-6.46 \pm 0.14	11.09 \pm 0.18	...	16.810 \pm 0.002	18.763 \pm 0.020	15.456 \pm 0.006	334 $^{+12}_{-11}$	0.200 \pm 0.017
...	126.1079	-35.8317	2.776 \pm 0.056	-7.014 \pm 0.089	10.87 \pm 0.10	...	15.525 \pm 0.002	17.022 \pm 0.009	14.324 \pm 0.003	356.8 $^{+7.4}_{-7.1}$	0.377 \pm 0.030
...	125.6838	-35.7657	2.774 \pm 0.088	-7.18 \pm 0.14	10.83 \pm 0.18	...	17.239 \pm 0.002	18.976 \pm 0.023	15.948 \pm 0.004	357 $^{+12}_{-11}$	0.264 \pm 0.021
HD 71269	126.3030	-34.3975	2.862 \pm 0.040	-7.006 \pm 0.060	10.736 \pm 0.058	19.2 \pm 7.5	8.931 \pm 0.000	8.923 \pm 0.001	8.969 \pm 0.001	346.1 $^{+4.8}_{-4.7}$	2.75 \pm 0.60
...	126.3115	-34.3829	2.840 \pm 0.054	-6.971 \pm 0.090	10.803 \pm 0.082	...	15.894 \pm 0.001	17.225 \pm 0.010	14.743 \pm 0.003	348.8 $^{+6.7}_{-6.4}$	0.431 \pm 0.034
...	126.3294	-34.4957	2.830 \pm 0.067	-6.993 \pm 0.097	10.71 \pm 0.10	...	16.486 \pm 0.001	18.056 \pm 0.012	15.265 \pm 0.003	350.1 $^{+8.5}_{-8.1}$	0.351 \pm 0.028
...	126.3859	-34.9361	2.825 \pm 0.076	-7.16 \pm 0.12	10.57 \pm 0.14	...	16.869 \pm 0.002	18.637 \pm 0.016	15.577 \pm 0.004	350.8 $^{+9.8}_{-9.3}$	0.256 \pm 0.020
...	126.4563	-35.0484	2.799 \pm 0.069	-7.141 \pm 0.096	10.91 \pm 0.14	...	16.317 \pm 0.001	17.852 \pm 0.009	15.089 \pm 0.003	354.0 $^{+8.5}_{-8.5}$	0.359 \pm 0.029
...	126.4640	-34.9519	2.872 \pm 0.055	-7.193 \pm 0.083	11.116 \pm 0.093	...	16.014 \pm 0.001	17.461 \pm 0.009	14.829 \pm 0.004	344.9 $^{+6.7}_{-6.5}$	0.395 \pm 0.032
2MASS J08260440-3431206	126.5184	-34.5224	2.772 \pm 0.018	-7.326 \pm 0.024	11.173 \pm 0.028	22.77 \pm 0.68	13.048 \pm 0.002	13.662 \pm 0.010	12.304 \pm 0.007	357.0 \pm 2.3	0.82 \pm 0.10

Table B.2: CG 22 Assn.—Continued

Star Name	RA ($^{\circ}$)	Dec ($^{\circ}$)	Parallax (mas)	μ_{α} (mas yr $^{-1}$)	μ_{δ} (mas yr $^{-1}$)	v_r (km s $^{-1}$)	G (mag)	BP (mag)	RP (mag)	d (pc)	Mass (M $_{\odot}$)
...	126.5240	-34.6362	2.769 \pm 0.047	-7.401 \pm 0.067	11.065 \pm 0.073	...	15.795 \pm 0.003	17.195 \pm 0.014	14.617 \pm 0.007	357 $^{+6.1}_{-5.9}$	0.409 \pm 0.033
...	126.5500	-34.7263	2.791 \pm 0.068	-6.955 \pm 0.097	10.86 \pm 0.11	...	16.378 \pm 0.001	17.950 \pm 0.011	15.146 \pm 0.002	354.9 $^{+8.9}_{-8.5}$	0.348 \pm 0.028
...	126.5648	-34.9027	2.660 \pm 0.077	-7.12 \pm 0.12	10.75 \pm 0.13	...	16.942 \pm 0.002	18.702 \pm 0.020	15.666 \pm 0.004	372 $^{+11}_{-10.}$	0.262 \pm 0.021
...	126.5805	-34.6408	2.854 \pm 0.019	-6.916 \pm 0.028	10.939 \pm 0.026	...	13.587 \pm 0.002	14.266 \pm 0.007	12.786 \pm 0.005	346.9 \pm 2.3	0.762 \pm 0.061
...	126.6226	-34.5856	2.787 \pm 0.031	-6.807 \pm 0.045	10.654 \pm 0.043	...	15.434 \pm 0.018	16.071 \pm 0.096	14.520 \pm 0.043	355.2 $^{+4.0}_{-3.9}$	0.734 \pm 0.059
...	126.6489	-34.5097	2.815 \pm 0.058	-7.381 \pm 0.090	10.98 \pm 0.11	...	16.151 \pm 0.001	17.658 \pm 0.010	14.937 \pm 0.004	351.9 $^{+7.3}_{-7.1}$	0.370 \pm 0.030
2MASS J08264387-3420129	126.6828	-34.3369	2.798 \pm 0.027	-7.387 \pm 0.043	10.947 \pm 0.040	24.82 \pm 0.96	12.903 \pm 0.010	12.184 \pm 0.007	353 $^{+3.5}_{-3.4}$	0.823 \pm 0.066	
...	126.7305	-34.3239	2.730 \pm 0.064	-7.068 \pm 0.097	11.044 \pm 0.097	...	15.892 \pm 0.003	17.298 \pm 0.016	14.702 \pm 0.006	362 $^{+8.7}_{-8.3}$	0.405 \pm 0.032
...	126.7473	-34.4167	2.683 \pm 0.045	-7.275 \pm 0.067	10.926 \pm 0.068	...	15.229 \pm 0.001	16.442 \pm 0.005	14.128 \pm 0.002	368.9 $^{+6.3}_{-6.1}$	0.499 \pm 0.040
...	126.7762	-34.5373	2.706 \pm 0.096	-7.05 \pm 0.14	10.94 \pm 0.14	...	17.062 \pm 0.001	18.806 \pm 0.029	15.767 \pm 0.004	366 \pm 13	0.261 \pm 0.021
...	126.7807	-34.4093	2.811 \pm 0.094	-7.37 \pm 0.14	10.84 \pm 0.13	...	16.958 \pm 0.001	18.613 \pm 0.023	15.695 \pm 0.003	353 $^{+12}_{-11}$	0.300 \pm 0.029
...	126.7971	-34.7731	2.690 \pm 0.090	-7.03 \pm 0.13	10.94 \pm 0.14	...	17.085 \pm 0.001	18.803 \pm 0.024	15.797 \pm 0.003	369 $^{+13}_{-12}$	0.269 \pm 0.025
...	126.8273	-34.5337	2.809 \pm 0.085	-7.27 \pm 0.12	10.80 \pm 0.12	...	16.436 \pm 0.001	18.321 \pm 0.018	15.119 \pm 0.002	353 $^{+11}_{-10.}$	0.222 \pm 0.018
...	126.8334	-34.7381	2.773 \pm 0.089	-6.74 \pm 0.13	10.86 \pm 0.15	...	17.186 \pm 0.001	18.954 \pm 0.026	15.883 \pm 0.005	357 $^{+12}_{-11}$	0.253 \pm 0.020
...	126.8343	-34.4638	2.801 \pm 0.020	-7.968 \pm 0.029	11.033 \pm 0.031	...	14.033 \pm 0.004	14.945 \pm 0.014	13.081 \pm 0.009	353 $^{+2.6}_{-2.5}$	0.679 \pm 0.054
...	126.8512	-35.2181	2.824 \pm 0.035	-6.930 \pm 0.056	10.482 \pm 0.052	...	15.139 \pm 0.004	16.325 \pm 0.020	14.049 \pm 0.011	350.6 $^{+4.4}_{-4.3}$	0.528 \pm 0.042
...	126.8893	-34.8830	2.794 \pm 0.064	-6.77 \pm 0.10	10.68 \pm 0.10	...	16.377 \pm 0.001	17.997 \pm 0.010	15.122 \pm 0.003	354.5 $^{+8.3}_{-7.9}$	0.316 \pm 0.034
...	126.8943	-35.0988	2.739 \pm 0.022	-6.852 \pm 0.033	10.672 \pm 0.038	...	14.757 \pm 0.002	15.752 \pm 0.008	13.760 \pm 0.006	361.3 $^{+2.9}_{-2.8}$	0.601 \pm 0.048
...	126.9122	-34.7610	2.744 \pm 0.062	-7.005 \pm 0.097	10.870 \pm 0.096	...	16.420 \pm 0.001	17.996 \pm 0.016	15.183 \pm 0.002	360.8 $^{+8.3}_{-7.9}$	0.337 \pm 0.029

Table B.2: CG 22 Assn.—Continued

Star Name	RA ($^{\circ}$)	Dec ($^{\circ}$)	Parallax (mas)	μ_{α} (mas yr^{-1})	μ_{δ} (mas yr^{-1})	v_r (km s^{-1})	G (mag)	BP (mag)	RP (mag)	d (pc)	Mass (M_{\odot})
...	126.9337	-34.7448	2.813 \pm 0.063	-7.176 \pm 0.098	...	16.224 \pm 0.001	17.809 \pm 0.010	14.990 \pm 0.003	352.2 $^{+8.0}_{-7.7}$	0.335 \pm 0.029	
...	126.9339	-34.6969	2.826 \pm 0.067	-7.068 \pm 0.097	10.82 \pm 0.10	...	16.449 \pm 0.001	17.991 \pm 0.012	15.211 \pm 0.002	350.6 $^{+8.5}_{-8.1}$	0.354 \pm 0.028
CD-344836	126.9380	-35.0148	2.677 \pm 0.038	-6.948 \pm 0.057	10.288 \pm 0.065	...	9.689 \pm 0.000	9.767 \pm 0.001	9.578 \pm 0.001	369.6 $^{+5.4}_{-5.2}$	2.18 \pm 0.35
...	126.9622	-35.1160	2.763 \pm 0.028	-6.947 \pm 0.043	10.775 \pm 0.048	...	15.062 \pm 0.003	16.191 \pm 0.013	13.970 \pm 0.007	358.2 $^{+3.7}_{-3.6}$	0.530 \pm 0.042
...	126.9678	-34.8456	2.793 \pm 0.058	-7.250 \pm 0.090	11.116 \pm 0.086	...	16.088 \pm 0.003	17.482 \pm 0.013	14.879 \pm 0.006	354.7 $^{+7.4}_{-7.1}$	0.403 \pm 0.032
...	126.9852	-34.9147	2.822 \pm 0.016	-7.129 \pm 0.027	11.137 \pm 0.027	...	13.622 \pm 0.006	14.270 \pm 0.026	12.817 \pm 0.014	350.8 \pm 2.0	0.772 \pm 0.062
...	126.9878	-34.5918	2.838 \pm 0.061	-7.163 \pm 0.086	10.94 \pm 0.11	...	16.306 \pm 0.001	17.806 \pm 0.014	15.079 \pm 0.004	349.0 $^{+7.7}_{-7.3}$	0.369 \pm 0.029
...	126.9914	-35.1361	2.673 \pm 0.074	-6.32 \pm 0.12	10.54 \pm 0.12	...	16.784 \pm 0.001	18.466 \pm 0.016	15.490 \pm 0.003	371.9 $^{+10.0}_{-9.9}$	0.277 \pm 0.025
...	127.0016	-35.1284	2.708 \pm 0.056	-7.202 \pm 0.084	10.817 \pm 0.091	...	16.123 \pm 0.001	17.534 \pm 0.014	14.916 \pm 0.004	365.6 $^{+7.7}_{-7.4}$	0.399 \pm 0.032
...	127.0176	-34.4756	2.743 \pm 0.056	-7.058 \pm 0.084	10.60 \pm 0.10	...	16.089 \pm 0.003	17.452 \pm 0.018	14.887 \pm 0.006	360.9 $^{+7.5}_{-7.2}$	0.412 \pm 0.033
...	127.0326	-35.0618	2.760 \pm 0.046	-6.983 \pm 0.075	10.584 \pm 0.080	...	15.620 \pm 0.004	16.939 \pm 0.016	14.474 \pm 0.012	358.7 $^{+6.1}_{-5.9}$	0.436 \pm 0.035
...	127.0480	-33.8968	2.791 \pm 0.046	-7.067 \pm 0.060	11.365 \pm 0.075	...	15.338 \pm 0.001	16.716 \pm 0.006	14.172 \pm 0.004	354.7 $^{+5.9}_{-5.7}$	0.417 \pm 0.033
...	127.0498	-34.9005	2.686 \pm 0.068	-7.08 \pm 0.11	10.62 \pm 0.12	...	16.331 \pm 0.004	17.950 \pm 0.020	15.066 \pm 0.013	368.7 $^{+9.5}_{-9.1}$	0.312 \pm 0.034
...	127.0609	-34.9671	2.762 \pm 0.023	-6.888 \pm 0.035	10.633 \pm 0.043	...	14.494 \pm 0.003	15.444 \pm 0.011	13.529 \pm 0.008	358.3 \pm 2.9	0.645 \pm 0.052
...	127.1188	-34.0972	2.745 \pm 0.070	-6.87 \pm 0.10	10.87 \pm 0.11	...	16.633 \pm 0.001	18.194 \pm 0.011	15.395 \pm 0.004	360.9 $^{+9.4}_{-8.9}$	0.349 \pm 0.028
...	127.1402	-34.7038	2.898 \pm 0.073	-7.08 \pm 0.10	10.97 \pm 0.14	...	16.832 \pm 0.001	18.442 \pm 0.042	15.569 \pm 0.003	342.0 $^{+8.8}_{-8.4}$	0.316 \pm 0.036
...	127.1555	-34.9247	2.699 \pm 0.067	-6.82 \pm 0.10	10.61 \pm 0.13	...	16.422 \pm 0.001	17.921 \pm 0.012	15.202 \pm 0.003	366.9 $^{+9.3}_{-8.9}$	0.371 \pm 0.030
...	127.1710	-34.5262	2.832 \pm 0.018	-6.868 \pm 0.028	10.856 \pm 0.029	...	13.543 \pm 0.002	14.255 \pm 0.007	12.721 \pm 0.005	349.5 \pm 2.2	0.741 \pm 0.059

Table B.2: CG 22 Assn.—Continued

Star Name	RA ($^{\circ}$)	Dec ($^{\circ}$)	Parallax (mas)	μ_{α} (mas yr $^{-1}$)	μ_{δ} (mas yr $^{-1}$)	v_r (km s $^{-1}$)	G (mag)	BP (mag)	RP (mag)	d (pc)	Mass (M $_{\odot}$)
2MASS J08284752-3429298	127.1980	-34.4916	2.726 ± 0.030	-6.820 ± 0.045	11.273 ± 0.048	20.79 ± 0.43	12.277 ± 0.007	12.933 ± 0.025	11.493 ± 0.019	363.0 $^{+4.0}_{-3.9}$	0.860 ± 0.060
TYC 7143-998-1	127.2413	-34.4935	2.725 ± 0.030	-6.481 ± 0.043	10.714 ± 0.051	...	9.645 ± 0.000	9.741 ± 0.001	9.502 ± 0.001	363.2 $^{+4.0}_{-3.9}$	2.05 ± 0.10
TYC 7143-191-1	127.2625	-34.2544	2.714 ± 0.031	-6.885 ± 0.040	11.056 ± 0.046	22.51 ± 0.21	10.643 ± 0.000	10.909 ± 0.001	10.248 ± 0.001	364.7 $^{+4.2}_{-4.1}$	1.250 ± 0.062
...	127.3616	-35.2188	2.736 ± 0.095	-6.67 ± 0.14	10.70 ± 0.15	...	17.276 ± 0.001	19.106 ± 0.005	15.968 ± 0.005	362. $^{+13}_{-12}$	0.236 ± 0.019
...	127.3882	-34.3502	2.722 ± 0.055	-6.888 ± 0.073	11.025 ± 0.082	...	15.779 ± 0.001	17.078 ± 0.007	14.635 ± 0.003	363.8 $^{+7.5}_{-7.2}$	0.443 ± 0.035
...	127.4225	-34.9011	2.889 ± 0.044	-6.894 ± 0.063	10.613 ± 0.071	...	15.839 ± 0.001	17.215 ± 0.008	14.671 ± 0.003	342.9 $^{+5.3}_{-5.1}$	0.417 ± 0.033
...	127.4593	-35.5163	2.799 ± 0.079	-6.29 ± 0.12	10.63 ± 0.12	...	16.321 ± 0.001	18.298 ± 0.021	14.973 ± 0.003	354. $^{+10.}_{-9.7}$	0.196 ± 0.016
HD 72138	127.4908	-35.5392	2.770 ± 0.045	-7.207 ± 0.074	10.834 ± 0.069	...	8.532 ± 0.000	8.519 ± 0.001	8.578 ± 0.002	357.4 $^{+5.9}_{-5.7}$	2.75 ± 0.60
...	127.6321	-34.6063	2.813 ± 0.062	-6.949 ± 0.096	10.587 ± 0.099	...	15.912 ± 0.001	17.501 ± 0.006	14.675 ± 0.002	352.2 $^{+8.0}_{-7.6}$	0.333 ± 0.029
...	126.3720	-34.7728	2.84 ± 0.10	-7.01 ± 0.17	11.12 ± 0.17	...	17.504 ± 0.001	19.350 ± 0.038	16.187 ± 0.003	350. $^{+13}_{-12}$	0.230 ± 0.020
...	126.4665	-34.6792	2.64 ± 0.22	-6.74 ± 0.29	10.03 ± 0.32	...	18.575 ± 0.000	20.34 ± 0.11	17.033 ± 0.013	379. $^{+35}_{-30.}$	0.200 ± 0.026
...	126.6281	-34.8838	2.774 ± 0.098	-7.10 ± 0.16	10.46 ± 0.17	...	17.240 ± 0.010	19.423 ± 0.039	15.844 ± 0.004	358. $^{+13}_{-12}$	0.161 ± 0.013
...	126.6733	-34.5957	2.76 ± 0.17	-7.19 ± 0.24	11.24 ± 0.26	...	18.007 ± 0.001	19.930 ± 0.059	16.608 ± 0.008	360. $^{+24}_{-22}$	0.196 ± 0.019
...	126.7294	-35.1547	2.63 ± 0.12	-6.94 ± 0.18	11.10 ± 0.20	...	17.696 ± 0.002	19.508 ± 0.030	16.361 ± 0.011	377. $^{+17}_{-16}$	0.234 ± 0.020
...	126.7528	-34.1352	2.94 ± 0.11	-6.73 ± 0.15	11.27 ± 0.17	...	17.632 ± 0.002	19.326 ± 0.058	16.294 ± 0.032	338. $^{+13}_{-12}$	0.263 ± 0.029
...	127.1061	-34.3209	2.66 ± 0.12	-7.08 ± 0.17	10.91 ± 0.20	...	17.826 ± 0.001	19.924 ± 0.074	16.444 ± 0.006	374. $^{+17}_{-16}$	0.173 ± 0.014
...	127.1437	-34.8891	2.674 ± 0.099	-6.95 ± 0.16	10.51 ± 0.19	...	17.272 ± 0.002	19.129 ± 0.046	15.900 ± 0.005	371. $^{+14}_{-13}$	0.216 ± 0.019
...	127.1694	-34.6665	2.938 ± 0.099	-6.99 ± 0.15	10.69 ± 0.19	...	16.746 ± 0.006	18.630 ± 0.017	15.407 ± 0.003	338. $^{+12}_{-11}$	0.218 ± 0.017
...	127.5488	-34.6778	2.846 ± 0.097	-6.34 ± 0.16	10.99 ± 0.17	...	17.205 ± 0.001	19.431 ± 0.035	15.794 ± 0.006	349. $^{+12}_{-11}$	0.155 ± 0.012

Table B.2: CG 22 Assn.—Continued

Star Name	RA ($^{\circ}$)	Dec ($^{\circ}$)	Parallax (mas)	μ_{α} (mas yr^{-1})	μ_{δ} (mas yr^{-1})	v_r (km s^{-1})	G (mag)	BP (mag)	RP (mag)	d (pc)	d (pc)	Mass (M_{\odot})
...	126.3677 -35.5241	2.572 \pm 0.042	-7.176 \pm 0.060	9.705 \pm 0.064	35	13.349 \pm 0.003	14.170 \pm 0.011	12.451 \pm 0.007	384.7 $^{+6.4}_{-6.2}$	0.693 \pm 0.055		
...	126.6267 -34.5104	2.752 \pm 0.057	-5.963 \pm 0.090	10.030 \pm 0.089	...	14.664 \pm 0.001	15.738 \pm 0.005	13.628 \pm 0.004	359.8 $^{+7.5}_{-7.2}$	0.559 \pm 0.045		
...	126.7445 -34.2405	2.860 \pm 0.043	-6.255 \pm 0.063	11.631 \pm 0.068	...	14.744 \pm 0.001	15.916 \pm 0.007	13.650 \pm 0.004	346.2 $^{+5.3}_{-5.2}$	0.516 \pm 0.041		
...	126.9495 -34.5996	2.790 \pm 0.046	-6.985 \pm 0.067	11.010 \pm 0.067	...	15.423 \pm 0.004	354.8 $^{+6.0}_{-5.8}$	0.671 \pm 0.074		
...	126.9808 -35.3161	2.850 \pm 0.049	-6.902 \pm 0.087	10.845 \pm 0.083	...	15.858 \pm 0.002	347.6 $^{+6.1}_{-5.9}$	0.624 \pm 0.069		
CD-344842B	127.0026 -35.1194	2.670 \pm 0.032	-7.116 \pm 0.048	11.379 \pm 0.055	...	9.953 \pm 0.000	10.040 \pm 0.001	9.819 \pm 0.001	370.7 $^{+4.5}_{-4.4}$	2.75 \pm 0.94		
...	127.0819 -33.9102	2.765 \pm 0.036	-7.047 \pm 0.052	11.428 \pm 0.061	...	14.996 \pm 0.003	16.143 \pm 0.020	13.905 \pm 0.005	358.8 $^{+4.7}_{-4.6}$	0.525 \pm 0.042		
...	127.1243 -33.8528	2.769 \pm 0.017	-6.815 \pm 0.025	11.616 \pm 0.026	...	13.538 \pm 0.004	357.4 \pm 2.2	0.901 \pm 0.099		
...	127.1303 -33.8741	2.762 \pm 0.054	-6.801 \pm 0.077	11.686 \pm 0.083	...	15.608 \pm 0.001	17.126 \pm 0.004	14.391 \pm 0.002	358.5 $^{+7.1}_{-6.8}$	0.367 \pm 0.029		
PHe 92	127.1696 -33.7729	2.678 \pm 0.053	-6.499 \pm 0.082	13.095 \pm 0.081	20.09 \pm 0.92	13.452 \pm 0.022	14.186 \pm 0.075	12.512 \pm 0.068	369.7 $^{+7.5}_{-7.2}$	0.780 \pm 0.045		
...	127.1821 -33.8328	2.899 \pm 0.040	-5.822 \pm 0.059	11.395 \pm 0.063	...	14.623 \pm 0.001	16.015 \pm 0.005	13.454 \pm 0.003	341.6 $^{+4.7}_{-4.6}$	0.413 \pm 0.033		
...	127.2325 -34.4027	2.932 \pm 0.061	-6.461 \pm 0.092	10.78 \pm 0.12	...	15.278 \pm 0.002	16.253 \pm 0.026	13.994 \pm 0.007	337.9 $^{+7.1}_{-6.9}$	0.518 \pm 0.041		
...	127.3229 -34.5424	3.085 \pm 0.090	-5.77 \pm 0.14	11.27 \pm 0.14	...	15.568 \pm 0.001	17.095 \pm 0.011	14.345 \pm 0.002	321.5 $^{+9.6}_{-9.1}$	0.362 \pm 0.029		
...	127.3633 -35.2132	2.569 \pm 0.073	-6.97 \pm 0.10	10.94 \pm 0.12	...	15.898 \pm 0.001	17.704 \pm 0.016	14.595 \pm 0.004	385 \pm 11	0.243 \pm 0.020		
...	127.4298 -34.7020	2.822 \pm 0.077	-6.41 \pm 0.11	11.42 \pm 0.13	...	16.526 \pm 0.002	18.194 \pm 0.024	15.151 \pm 0.007	351.1 $^{+9.8}_{-9.3}$	0.260 \pm 0.021		
2MASS J08310444-3502348	127.7685 -35.0430	2.698 \pm 0.036	-6.023 \pm 0.053	12.193 \pm 0.054	48.28 \pm 0.14	12.577 \pm 0.000	12.948 \pm 0.002	12.056 \pm 0.001	366.8 $^{+4.9}_{-4.8}$	0.860 \pm 0.043		
...	126.3578 -34.9481	2.975 \pm 0.098	-6.70 \pm 0.14	10.60 \pm 0.23	...	17.339 \pm 0.012	19.302 \pm 0.038	15.993 \pm 0.005	334 \pm 11	0.199 \pm 0.017		
...	126.4930 -34.8980	2.97 \pm 0.25	-7.80 \pm 0.39	10.78 \pm 0.47	...	18.936 \pm 0.002	20.73 \pm 0.14	17.506 \pm 0.019	338 $^{+32}_{-27}$	0.217 \pm 0.036		

Table B.2: CG 22 Assn.—Continued

Star Name	<i>RA</i> ($^{\circ}$)	<i>Dec</i> ($^{\circ}$)	Parallax (mas)	μ_{α} (mas yr^{-1})	μ_{δ} (mas yr^{-1})	v_r (km s^{-1})	G (mag)	BP (mag)	RP (mag)	<i>d</i> (pc)	Mass (M $_{\odot}$)
...	126.6048	-34.8386	2.78 \pm 0.10	-7.48 \pm 0.17	11.62 \pm 0.90	...	15.691 \pm 0.001	357 $^{+14}_{-13}$	0.650 \pm 0.072
...	126.7991	-34.3714	2.59 \pm 0.20	-6.87 \pm 0.32	11.26 \pm 0.29	...	18.460 \pm 0.002	20.80 \pm 0.13	17.034 \pm 0.009	386 $^{+34}_{-29}$	0.141 \pm 0.017
...	126.9700	-34.9495	3.02 \pm 0.11	-6.96 \pm 0.18	10.71 \pm 0.18	...	17.427 \pm 0.001	19.509 \pm 0.038	16.035 \pm 0.004	329 $^{+13}_{-12}$	0.173 \pm 0.014
...	126.9737	-34.7539	2.91 \pm 0.15	-6.98 \pm 0.23	10.43 \pm 0.24	...	17.327 \pm 0.001	19.240 \pm 0.032	15.937 \pm 0.004	342 $^{+20}_{-18}$	0.201 \pm 0.017
...	127.1200	-35.0830	2.816 \pm 0.090	-6.30 \pm 0.10	10.18 \pm 0.29	...	15.317 \pm 0.001	352 $^{+12}_{-11}$	0.684 \pm 0.075
...	127.1251	-33.8958	2.91 \pm 0.17	-6.80 \pm 0.24	11.63 \pm 0.23	...	18.245 \pm 0.004	19.74 \pm 0.11	16.662 \pm 0.084	343 $^{+22}_{-19}$	0.251 \pm 0.043
...	127.1888	-33.8060	2.77 \pm 0.12	-6.55 \pm 0.18	11.72 \pm 0.20	...	17.750 \pm 0.001	19.968 \pm 0.077	16.302 \pm 0.009	359 $^{+17}_{-15}$	0.152 \pm 0.012
...	127.1927	-33.8229	2.60 \pm 0.11	-6.20 \pm 0.16	11.45 \pm 0.19	...	17.578 \pm 0.001	19.447 \pm 0.052	16.235 \pm 0.010	381 $^{+18}_{-16}$	0.220 \pm 0.021
...	127.2097	-33.7342	2.73 \pm 0.13	-6.58 \pm 0.19	12.06 \pm 0.20	...	17.693 \pm 0.000	19.824 \pm 0.052	16.216 \pm 0.009	364 $^{+18}_{-16}$	0.158 \pm 0.013
...	127.2463	-34.7113	2.96 \pm 0.10	-6.82 \pm 0.15	10.46 \pm 0.16	...	17.319 \pm 0.004	19.149 \pm 0.032	15.992 \pm 0.005	336 \pm 12	0.231 \pm 0.019

Table B.3: CG 30 Assn. Member Kinematics and Properties

Star Name	RA ($^{\circ}$)	Dec ($^{\circ}$)	Parallax (mas)	μ_{α} (mas yr $^{-1}$)	μ_{δ} (mas yr $^{-1}$)	v_r (km s $^{-1}$)	G (mag)	BP (mag)	RP (mag)	d (pc)	Mass (M $_{\odot}$)
PH α 14	122.1411	-36.1359	2.84 ± 0.50	-7.32 ± 0.90	11.72 ± 0.90	26.77 ± 0.89	14.700 ± 0.007	15.988 ± 0.010	13.344 ± 0.012	370, $^{+67}_{-100}$	0.270 ± 0.070
PH α 15	122.1950	-36.1313	2.794 ± 0.036	-7.579 ± 0.068	11.451 ± 0.067	21.99 ± 0.20	15.116 ± 0.013	16.259 ± 0.074	13.980 ± 0.033	354.4, $^{+4.5}_{-4.7}$	0.230 ± 0.043
KWW 464	122.0027	-35.9592	2.746 ± 0.031	-7.510 ± 0.051	11.603 ± 0.051	24.0 ± 3.0	14.819 ± 0.002	16.080 ± 0.007	13.701 ± 0.004	360.5, $^{+4.0}_{-4.1}$	0.370 ± 0.038
KWW 598	122.1566	-36.1640	2.798 ± 0.072	-7.89 ± 0.13	10.98 ± 0.12	21.5 ± 3.0	15.578 ± 0.001	17.534 ± 0.009	14.235 ± 0.003	354.1, $^{+8.8}_{-9.3}$	0.440 ± 0.019
KWW 1863	122.1576	-36.0653	2.774 ± 0.031	-7.400 ± 0.056	12.025 ± 0.056	26.2 ± 3.0	13.584 ± 0.001	14.819 ± 0.004	12.469 ± 0.003	356.9, $^{+3.9}_{-4.0}$	0.500 ± 0.038
KWW 2205	122.0619	-36.0359	2.709 ± 0.053	-7.728 ± 0.093	11.675 ± 0.087	25.3 ± 3.0	14.873 ± 0.001	16.474 ± 0.005	13.635 ± 0.003	365.5, $^{+7.0}_{-7.2}$	0.230 ± 0.043
KWW 873	122.1891	-36.1444	4.21 ± 0.22	-4.19 ± 0.38	9.15 ± 0.39	22.2 ± 3.0	13.132 ± 0.005	14.074 ± 0.012	12.160 ± 0.014	237, $^{+12}_{-14}$	0.640 ± 0.049
KWW 1637	122.1636	-36.0837	1.42 ± 0.38	-4.55 ± 0.77	7.81 ± 0.78	22.8 ± 3.0	11.541 ± 0.003	12.302 ± 0.010	10.702 ± 0.007	780, $^{+250}_{-670}$	0.690 ± 0.055
KWW 1953	122.1121	-36.0598	2.20 ± 0.23	-6.14 ± 0.39	12.79 ± 0.40	24.5 ± 3.0	14.359 ± 0.001	15.822 ± 0.004	13.158 ± 0.005	456, $^{+45}_{-55}$	0.370 ± 0.051
...	122.0756	-36.1054	2.857 ± 0.054	-7.784 ± 0.097	11.172 ± 0.093	...	16.120 ± 0.011	17.795 ± 0.042	14.813 ± 0.030	346.7, $^{+6.4}_{-6.6}$	0.231 ± 0.035
...	122.1585	-36.0667	2.775 ± 0.069	-7.88 ± 0.12	11.42 ± 0.12	...	12.605 ± 0.004	13.577 ± 0.018	11.621 ± 0.011	357.1, $^{+8.6}_{-9.1}$	0.554 ± 0.044
...	122.1605	-36.1071	2.829 ± 0.047	-7.431 ± 0.082	11.22 ± 0.10	...	15.532 ± 0.001	17.018 ± 0.009	14.329 ± 0.003	350.0, $^{+5.7}_{-5.9}$	0.318 ± 0.051
...	122.1969	-36.2480	2.833 ± 0.067	-7.44 ± 0.12	11.24 ± 0.11	...	16.277 ± 0.002	18.114 ± 0.024	14.944 ± 0.005	349.7, $^{+8.1}_{-8.5}$	0.191 ± 0.025
...	122.2382	-36.7531	2.767 ± 0.028	-6.250 ± 0.046	10.292 ± 0.047	...	15.260 ± 0.000	16.076 ± 0.003	14.382 ± 0.001	357.7, $^{+3.5}_{-3.6}$	0.674 ± 0.054
...	122.2836	-36.0401	2.839 ± 0.063	-7.56 ± 0.12	11.44 ± 0.12	...	15.754 ± 0.001	17.739 ± 0.008	14.404 ± 0.002	349.0, $^{+7.5}_{-7.9}$	0.169 ± 0.017
...	122.3600	-36.3333	2.739 ± 0.087	-7.10 ± 0.14	10.41 ± 0.14	...	17.148 ± 0.002	18.986 ± 0.063	15.730 ± 0.015	362, $^{+11}_{-12}$	0.178 ± 0.023
...	122.3608	-36.3330	2.834 ± 0.061	-7.064 ± 0.098	10.88 ± 0.10	...	16.485 ± 0.001	18.167 ± 0.017	15.142 ± 0.008	349.5, $^{+7.4}_{-7.7}$	0.221 ± 0.032
...	122.3623	-36.6469	2.714 ± 0.076	-7.37 ± 0.13	10.60 ± 0.13	...	16.708 ± 0.004	18.629 ± 0.034	15.326 ± 0.009	365.0, $^{+9.9}_{-11}$	0.173 ± 0.019

Table B.3: CG 30 Assn.—Continued

Star Name	RA ($^{\circ}$)	Dec ($^{\circ}$)	Parallax (mas)	μ_{α} (mas yr $^{-1}$)	μ_{δ} (mas yr $^{-1}$)	v_r (km s $^{-1}$)	G (mag)	BP (mag)	RP (mag)	d (pc)	Mass (M $_{\odot}$)
...	122.6674	-36.6477	2.706 ± 0.027	-7.316 ± 0.045	10.505 ± 0.050	...	14.704 ± 0.004	15.668 ± 0.021	13.675 ± 0.008	365.7 $^{+3.6}_{-3.7}$	0.545 ± 0.044
...	122.8556	-36.7057	2.634 ± 0.079	-6.89 ± 0.13	10.79 ± 0.14	...	16.903 ± 0.002	18.658 ± 0.024	15.597 ± 0.005	376 $^{+11}_{-12}$	0.214 ± 0.032
...	121.8688	-35.8721	2.71 ± 0.43	-8.52 ± 0.75	10.32 ± 0.73	...	15.765 ± 0.012	16.255 ± 0.004	14.995 ± 0.002	382 $^{+59}_{-86}$	0.778 ± 0.062
...	122.3101	-36.8764	2.67 ± 0.78	-7.6 ± 1.1	11.4 ± 1.3	...	20.092 ± 0.009	20.58 ± 0.14	18.565 ± 0.020	450 $^{+190}_{-1500}$	0.538 ± 0.071
...	122.5146	-37.0264	2.68 ± 0.15	-6.62 ± 0.24	12.14 ± 0.27	...	18.533 ± 0.003	19.921 ± 0.070	17.297 ± 0.010	371 $^{+20}_{-23}$	0.348 ± 0.056
...	122.6225	-36.6582	2.78 ± 0.92	-6.9 ± 1.4	12.1 ± 1.7	...	19.406 ± 0.018	19.863 ± 0.054	18.214 ± 0.031	460 $^{+210}_{-2500}$	0.668 ± 0.053
...	122.6780	-36.7505	2.69 ± 0.10	-7.11 ± 0.15	10.16 ± 0.22	...	17.185 ± 0.001	369 $^{+13}_{-14}$	0.443 ± 0.049
PH α 12	122.0922	-36.0630	23.07 ± 0.15	14.166 ± 0.002	15.385 ± 0.007	13.034 ± 0.004	...
CG30	122.3882	-36.0827	22.5 ± 2.0	0.570 ± 0.045
KWW 1302	122.4657	-36.3840	14.725 ± 0.003	16.218 ± 0.013	13.477 ± 0.006	...	0.230 ± 0.050
KWW 1055	122.3061	-36.1748	20.0 ± 3.0	14.131 ± 0.001	14.696 ± 0.004	13.400 ± 0.004	...	0.970 ± 0.060

Table B.4: Yep 1 Member Kinematics and Properties

Star Name	RA ($^{\circ}$)	Dec ($^{\circ}$)	Parallax (mas)	μ_{α} (mas yr $^{-1}$)	μ_{δ} (mas yr $^{-1}$)	v_r (km s $^{-1}$)	G (mag)	BP (mag)	RP (mag)	d (pc)	Mass (M $_{\odot}$)
...	122.0624 -47.2605	2.43 \pm 0.13	-4.90 \pm 0.31	9.09 \pm 0.20	...	17.021 \pm 0.003	...	14.848 \pm 0.002	15.976 \pm 0.007	13.769 \pm 0.003	384.1 \pm 4.2
...	121.8154 -47.1961	2.621 \pm 0.040	-5.050 \pm 0.066	8.339 \pm 0.064	...	18.087 \pm 0.003	19.309 \pm 0.092	16.726 \pm 0.007	417 $^{+28}_{-25}$	384 \pm 0.031	0.462 \pm 0.051
...	123.3303 -47.0063	2.39 \pm 0.15	-4.86 \pm 0.27	8.06 \pm 0.26	...	18.962 \pm 0.028	20.09 \pm 0.11	17.51 \pm 0.10	400 $^{+17}_{-16}$	386 \pm 0.048	...
...	121.7828 -47.0390	2.53 \pm 0.26	-4.11 \pm 0.48	7.96 \pm 0.48	...	17.818 \pm 0.003	19.127 \pm 0.053	16.442 \pm 0.005	418 $^{+17}_{-16}$	356 \pm 0.029	...
...	117.3524 -46.3610	2.371 \pm 0.092	-4.51 \pm 0.19	8.73 \pm 0.17	...	17.902 \pm 0.003	...	17.854 \pm 0.003	19.705 \pm 0.076	16.546 \pm 0.008	414 $^{+24}_{-21}$
...	121.6366 -47.7735	2.54 \pm 0.20	-4.57 \pm 0.34	9.36 \pm 0.32	...	17.870 \pm 0.002	19.705 \pm 0.076	16.546 \pm 0.008	414 $^{+24}_{-21}$	212 \pm 0.020	0.403 \pm 0.044
...	117.4412 -45.0144	2.40 \pm 0.13	-5.12 \pm 0.21	8.86 \pm 0.22	...	17.854 \pm 0.003	19.593 \pm 0.054	16.557 \pm 0.005	410 $^{+19}_{-18}$	240 \pm 0.019	...
...	117.5257 -45.2368	2.42 \pm 0.11	-5.02 \pm 0.19	8.60 \pm 0.20	...	18.270 \pm 0.003	20.36 \pm 0.11	16.878 \pm 0.007	415 $^{+29}_{-25}$	82 \pm 0.12	...
2MASS J07510378-4532244	117.7657 -45.5401	2.40 \pm 0.15	-4.24 \pm 0.31	8.70 \pm 0.27	...	18.102 \pm 0.003	20.051 \pm 0.051	16.702 \pm 0.006	418 $^{+29}_{-25}$	178 \pm 0.014	...
...	117.5532 -45.6699	2.38 \pm 0.15	-5.12 \pm 0.28	8.78 \pm 0.29	...	18.403 \pm 0.003	20.120 \pm 0.095	17.050 \pm 0.012	388 $^{+26}_{-23}$	231 \pm 0.025	...
...	116.6548 -45.9304	2.57 \pm 0.16	-4.96 \pm 0.31	8.44 \pm 0.29	...	17.938 \pm 0.003	19.703 \pm 0.050	16.576 \pm 0.007	407 $^{+25}_{-22}$	219 \pm 0.018	...
...	116.2895 -46.3395	2.44 \pm 0.14	-4.05 \pm 0.25	9.09 \pm 0.21	...	17.020 \pm 0.003	19.020 \pm 0.038	15.676 \pm 0.006	355 $^{+16}_{-15}$	178 \pm 0.014	...
...	116.4423 -46.3502	2.79 \pm 0.12	-4.31 \pm 0.19	9.16 \pm 0.18	...	17.967 \pm 0.003	19.534 \pm 0.086	16.627 \pm 0.007	372 $^{+22}_{-20}$	272 \pm 0.031	...
...	117.0792 -46.1704	2.42 \pm 0.13	-4.97 \pm 0.24	9.54 \pm 0.24	...	17.783 \pm 0.003	19.638 \pm 0.078	16.390 \pm 0.008	410 $^{+23}_{-21}$	194 \pm 0.018	...
2MASS J07512365-4601262	117.8485 -46.0239	2.39 \pm 0.12	-5.01 \pm 0.20	9.22 \pm 0.20	...	17.709 \pm 0.002	19.650 \pm 0.056	16.368 \pm 0.006	416 $^{+22}_{-20}$	185 \pm 0.015	...
2MASS J07543619-4552285	118.6508 -45.8745	2.69 \pm 0.12	-5.07 \pm 0.19	8.97 \pm 0.21	...	17.712 \pm 0.006	19.368 \pm 0.069	16.408 \pm 0.014	369 $^{+17}_{-15}$	259 \pm 0.022	...
...	117.1560 -46.4606	2.76 \pm 0.11	-4.98 \pm 0.24	8.83 \pm 0.20	...	16.954 \pm 0.003	18.572 \pm 0.026	15.667 \pm 0.005	359 $^{+14}_{-13}$	272 \pm 0.022	...

Table B.4: Yep 1—Continued

Star Name	RA ($^{\circ}$)	Dec ($^{\circ}$)	Parallax (mas)	μ_{α} (mas yr $^{-1}$)	μ_{δ} (mas yr $^{-1}$)	v_r (km s $^{-1}$)	G (mag)	BP (mag)	RP (mag)	d (pc)	Mass (M $_{\odot}$)
...	117.0825 -46.5378	2.37 ± 0.10	-4.99 ± 0.19	9.11 ± 0.20	...	17.503 ± 0.003	18.89 ± 0.13	16.136 ± 0.011	417 $^{+19}_{-17}$	0.326 ± 0.050	
...	116.7581 -46.8551	2.530 ± 0.037	-4.900 ± 0.067	8.201 ± 0.083	...	15.223 ± 0.002	16.460 ± 0.009	14.086 ± 0.005	473 $^{+28}_{-25}$	0.437 ± 0.035	
...	117.7201 -47.7138	2.435 ± 0.097	-4.43 ± 0.20	8.11 ± 0.20	...	17.163 ± 0.002	19.168 ± 0.043	15.804 ± 0.006	407 $^{+17}_{-16}$	0.176 ± 0.014	
...	117.2325 -47.1165	2.397 ± 0.096	-4.11 ± 0.20	8.62 ± 0.17	...	17.177 ± 0.002	18.999 ± 0.021	15.841 ± 0.005	413 $^{+17}_{-16}$	0.212 ± 0.017	
HD 65445	119.1431 -47.2136	2.380 ± 0.028	-4.736 ± 0.053	8.483 ± 0.056	...	10.339 ± 0.002	10.444 ± 0.002	10.174 ± 0.002	415.2 $^{+5.0}_{-4.9}$	1.930 ± 0.096	
...	115.8245 -46.1795	2.416 ± 0.096	-4.20 ± 0.19	9.34 ± 0.22	...	17.526 ± 0.003	19.133 ± 0.029	16.231 ± 0.009	410. $^{+17}_{-16}$	0.273 ± 0.022	
...	116.6427 -46.0141	2.421 ± 0.089	-4.70 ± 0.17	9.49 ± 0.17	...	17.507 ± 0.002	19.294 ± 0.041	16.173 ± 0.006	409 $^{+16}_{-15}$	0.220 ± 0.018	
...	116.6642 -45.7684	2.807 ± 0.065	-4.88 ± 0.13	9.38 ± 0.13	...	16.218 ± 0.003	17.836 ± 0.012	14.960 ± 0.005	352.9 $^{+8.4}_{-8.0}$	0.280 ± 0.022	
...	121.8141 -47.1955	2.621 ± 0.040	-5.050 ± 0.066	8.339 ± 0.064	...	14.848 ± 0.002	15.976 ± 0.007	13.769 ± 0.003	377.5 $^{+5.8}_{-5.6}$	0.513 ± 0.041	
...	122.3937 -47.6813	2.579 ± 0.034	-4.929 ± 0.061	8.492 ± 0.058	...	14.393 ± 0.003	15.402 ± 0.013	13.383 ± 0.007	383.6 $^{+5.1}_{-5.0}$	0.560 ± 0.045	
...	120.6846 -46.7915	2.56 ± 0.18	-4.96 ± 0.31	8.55 ± 0.28	...	18.404 ± 0.003	20.240 ± 0.074	17.090 ± 0.009	390 $^{+31}_{-27}$	0.214 ± 0.020	
...	117.4964 -47.3169	2.416 ± 0.095	-4.04 ± 0.18	8.76 ± 0.17	...	17.725 ± 0.002	19.521 ± 0.045	16.382 ± 0.006	410. $^{+17}_{-15}$	0.216 ± 0.017	
...	117.3757 -47.7068	2.404 ± 0.086	-4.46 ± 0.16	8.89 ± 0.17	...	17.119 ± 0.002	18.656 ± 0.045	15.695 ± 0.012	412 $^{+15}_{-14}$	0.258 ± 0.021	
...	117.4837 -47.8772	2.565 ± 0.086	-4.35 ± 0.18	8.48 ± 0.17	...	17.297 ± 0.002	18.822 ± 0.035	16.024 ± 0.005	386 $^{+13}_{-12}$	0.312 ± 0.026	
...	117.0919 -47.8273	2.361 ± 0.065	-5.01 ± 0.12	8.38 ± 0.12	...	16.679 ± 0.003	18.399 ± 0.037	15.393 ± 0.006	419. $^{+12}_{-11}$	0.247 ± 0.020	
...	116.5186 -48.5686	2.369 ± 0.066	-4.42 ± 0.14	8.26 ± 0.15	...	16.744 ± 0.003	18.357 ± 0.012	15.490 ± 0.007	418 $^{+12}_{-11}$	0.282 ± 0.023	
HD 64759	118.3168 -47.6183	2.358 ± 0.040	-4.722 ± 0.072	8.762 ± 0.081	...	9.938 ± 0.002	10.011 ± 0.002	9.835 ± 0.002	419.1 $^{+7.3}_{-7.0}$	1.98 ± 0.44	
...	117.2648 -48.4122	2.438 ± 0.091	-4.18 ± 0.20	8.19 ± 0.20	...	16.728 ± 0.003	18.568 ± 0.017	15.391 ± 0.005	406 $^{+16}_{-15}$	0.209 ± 0.017	
...	118.1085 -46.1269	2.648 ± 0.080	-4.71 ± 0.12	8.60 ± 0.17	...	16.867 ± 0.002	18.513 ± 0.041	15.608 ± 0.004	374 $^{+12}_{-11}$	0.272 ± 0.022	

Table B.4: Yep 1—Continued

Star Name	RA ($^{\circ}$)	Dec ($^{\circ}$)	Parallax (mas)	μ_{α} (mas yr $^{-1}$)	μ_{δ} (mas yr $^{-1}$)	v_r (km s $^{-1}$)	G (mag)	BP (mag)	RP (mag)	d (pc)	Mass (M $_{\odot}$)
...	119.5537 -49.3772	2.50 ± 0.15	-4.79 ± 0.28	7.95 ± 0.28	...	18.421 ± 0.003	20.44 ± 0.12	16.993 ± 0.009	398 $^{+26}_{-23}$	0.166 ± 0.015	
...	117.7213 -49.0072	2.36 ± 0.12	-4.23 ± 0.23	7.76 ± 0.25	...	17.760 ± 0.003	19.771 ± 0.064	16.355 ± 0.008	420 $^{+24}_{-21}$	0.170 ± 0.014	
...	118.4446 -48.7071	2.51 ± 0.14	-4.59 ± 0.28	7.82 ± 0.31	...	17.914 ± 0.003	19.545 ± 0.056	16.608 ± 0.007	395 $^{+24}_{-21}$	0.264 ± 0.021	
...	119.5173 -47.9188	2.58 ± 0.17	-4.95 ± 0.34	8.14 ± 0.35	...	18.654 ± 0.003	20.458 ± 0.076	17.272 ± 0.010	425 $^{+13}_{-12}$	0.207 ± 0.020	
2MASS J07392987-4839424	119.8744 -48.6118	2.380 ± 0.030	-4.488 ± 0.057	8.570 ± 0.048	23.35 ± 0.10	11.445 ± 0.002	11.778 ± 0.002	10.963 ± 0.002	415.3 $^{+5.2}_{-5.1}$	0.990 ± 0.050	
...	121.9152 -48.6326	2.544 ± 0.052	-4.88 ± 0.11	8.380 ± 0.098	...	15.865 ± 0.002	17.429 ± 0.009	14.625 ± 0.004	389.0 $^{+8.1}_{-7.8}$	0.309 ± 0.025	
...	115.1671 -47.2654	2.390 ± 0.082	-4.34 ± 0.15	8.39 ± 0.17	...	17.236 ± 0.003	18.967 ± 0.047	15.912 ± 0.004	414 $^{+15}_{-14}$	0.235 ± 0.019	
...	116.3067 -45.7829	2.67 ± 0.12	-4.87 ± 0.24	9.72 ± 0.25	...	17.932 ± 0.003	19.604 ± 0.070	16.604 ± 0.011	372 $^{+18}_{-16}$	0.249 ± 0.022	
...	117.3390 -45.7453	2.46 ± 0.11	-4.47 ± 0.21	8.44 ± 0.25	...	17.262 ± 0.003	403 $^{+19}_{-18}$	0.472 ± 0.052	
...	117.2031 -45.8787	2.71 ± 0.10	-4.54 ± 0.20	9.30 ± 0.19	...	17.555 ± 0.003	19.367 ± 0.057	16.216 ± 0.007	367 $^{+15}_{-13}$	0.214 ± 0.017	
...	116.5849 -46.0640	2.53 ± 0.12	-4.86 ± 0.23	8.80 ± 0.24	...	17.879 ± 0.002	19.837 ± 0.052	16.533 ± 0.005	392 $^{+19}_{-18}$	0.183 ± 0.015	
...	117.3428 -46.0283	2.52 ± 0.14	-4.92 ± 0.27	8.89 ± 0.28	...	18.210 ± 0.003	20.085 ± 0.086	16.851 ± 0.011	394 $^{+24}_{-21}$	0.196 ± 0.019	
...	117.9177 -46.1219	2.71 ± 0.11	-4.64 ± 0.20	8.91 ± 0.23	...	17.427 ± 0.003	19.007 ± 0.059	16.116 ± 0.005	367 $^{+16}_{-15}$	0.276 ± 0.026	
...	118.2731 -46.2993	2.38 ± 0.14	-4.96 ± 0.26	8.76 ± 0.28	...	17.883 ± 0.002	19.70 ± 0.12	16.579 ± 0.008	417 $^{+27}_{-24}$	0.221 ± 0.029	
...	118.0838 -46.3694	2.40 ± 0.12	-4.52 ± 0.24	8.51 ± 0.28	...	18.089 ± 0.003	20.155 ± 0.068	16.738 ± 0.010	414 $^{+23}_{-21}$	0.170 ± 0.014	
...	117.0944 -46.2843	2.73 ± 0.11	-4.44 ± 0.22	9.28 ± 0.20	...	17.836 ± 0.002	19.438 ± 0.072	16.495 ± 0.006	364 $^{+15}_{-14}$	0.263 ± 0.026	
...	117.5156 -46.3068	2.37 ± 0.10	-4.76 ± 0.21	9.00 ± 0.20	...	17.804 ± 0.003	19.655 ± 0.039	16.435 ± 0.010	419 $^{+19}_{-17}$	0.200 ± 0.016	
...	117.3300 -46.3632	2.59 ± 0.12	-4.74 ± 0.23	8.99 ± 0.20	...	17.837 ± 0.003	18.778 ± 0.050	16.487 ± 0.009	383 $^{+18}_{-16}$	0.450 ± 0.036	

Table B.4: Yep 1—Continued

Star Name	RA ($^{\circ}$)	Dec ($^{\circ}$)	Parallax (mas)	μ_{α} (mas yr $^{-1}$)	μ_{δ} (mas yr $^{-1}$)	v_r (km s $^{-1}$)	G (mag)	BP (mag)	RP (mag)	d (pc)	Mass (M $_{\odot}$)
...	117.0006 -46.3401	2.73 \pm 0.12	-4.59 \pm 0.22	9.70 \pm 0.30	...	17.988 \pm 0.003	19.667 \pm 0.062	16.648 \pm 0.007	363 $^{+17}_{-15}$	0.244 \pm 0.021	
...	116.7708 -46.5890	2.42 \pm 0.10	-4.29 \pm 0.18	8.88 \pm 0.24	...	17.482 \pm 0.003	19.137 \pm 0.036	16.160 \pm 0.004	410 $^{+18}_{-17}$	0.254 \pm 0.020	
...	116.6327 -46.7472	2.68 \pm 0.15	-5.00 \pm 0.27	9.15 \pm 0.30	...	18.055 \pm 0.003	19.945 \pm 0.077	16.701 \pm 0.009	372 $^{+22}_{-20}$	0.195 \pm 0.018	
...	117.6598 -46.3364	2.39 \pm 0.16	-4.86 \pm 0.31	9.09 \pm 0.27	...	18.377 \pm 0.004	20.447 \pm 0.080	16.953 \pm 0.010	416 $^{+30}_{-26}$	0.161 \pm 0.013	
...	117.3459 -46.8275	2.55 \pm 0.14	-4.98 \pm 0.24	9.14 \pm 0.24	...	18.205 \pm 0.003	20.077 \pm 0.063	16.755 \pm 0.008	389 $^{+23}_{-21}$	0.181 \pm 0.014	
...	116.7567 -46.9657	2.48 \pm 0.13	-4.66 \pm 0.24	8.96 \pm 0.32	...	17.637 \pm 0.005	19.32 \pm 0.11	16.274 \pm 0.008	400 $^{+22}_{-20}$	0.236 \pm 0.028	
...	118.7016 -47.3337	2.42 \pm 0.11	-4.50 \pm 0.24	8.80 \pm 0.25	...	17.845 \pm 0.004	410 $^{+20}_{-18}$	0.417 \pm 0.046	
...	117.9616 -46.9805	2.51 \pm 0.11	-4.58 \pm 0.25	8.52 \pm 0.23	...	17.803 \pm 0.002	19.588 \pm 0.039	16.488 \pm 0.006	395 $^{+19}_{-17}$	0.223 \pm 0.018	
...	118.1953 -47.4322	2.46 \pm 0.11	-4.45 \pm 0.19	8.96 \pm 0.23	...	17.646 \pm 0.002	19.441 \pm 0.059	16.337 \pm 0.005	404 $^{+18}_{-17}$	0.224 \pm 0.018	
...	117.5600 -47.4312	2.45 \pm 0.11	-4.74 \pm 0.21	8.85 \pm 0.25	...	17.761 \pm 0.003	19.642 \pm 0.035	16.398 \pm 0.010	405 $^{+20}_{-18}$	0.195 \pm 0.016	
...	117.4711 -47.7040	2.44 \pm 0.11	-4.56 \pm 0.20	8.42 \pm 0.22	...	17.867 \pm 0.003	19.671 \pm 0.063	16.533 \pm 0.006	406 $^{+19}_{-18}$	0.217 \pm 0.018	
...	116.9566 -47.8202	2.44 \pm 0.11	-4.44 \pm 0.23	8.35 \pm 0.25	...	18.122 \pm 0.003	20.047 \pm 0.053	16.732 \pm 0.007	406 $^{+20}_{-18}$	0.182 \pm 0.015	
...	116.8418 -47.8169	2.38 \pm 0.13	-4.23 \pm 0.26	8.07 \pm 0.27	...	18.224 \pm 0.003	20.156 \pm 0.089	16.784 \pm 0.009	418 $^{+24}_{-22}$	0.175 \pm 0.014	
2MASS J07513612-4601216 117.9006 -46.0226 2.379 \pm 0.027 -4.591 \pm 0.042 9.055 \pm 0.052 20.2 \pm 1.0 14.029 \pm 0.002 14.861 \pm 0.025 13.066 \pm 0.013 394.7 $^{+3.9}_{-3.8}$ 0.820 \pm 0.041											
...	118.1266 -46.3138	2.566 \pm 0.088	-4.68 \pm 0.18	8.71 \pm 0.22	...	17.479 \pm 0.002	19.312 \pm 0.037	16.158 \pm 0.008	386 $^{+14}_{-13}$	0.213 \pm 0.017	
...	119.3667 -48.3609	2.46 \pm 0.12	-4.73 \pm 0.23	8.83 \pm 0.21	...	17.927 \pm 0.003	19.716 \pm 0.062	16.618 \pm 0.009	403 $^{+21}_{-19}$	0.224 \pm 0.019	
...	117.3003 -48.7573	2.58 \pm 0.10	-4.61 \pm 0.20	8.96 \pm 0.21	...	17.471 \pm 0.003	19.175 \pm 0.035	16.184 \pm 0.006	384 $^{+16}_{-14}$	0.251 \pm 0.020	
...	117.5339 -48.5683	2.50 \pm 0.15	-4.68 \pm 0.31	7.96 \pm 0.26	...	18.144 \pm 0.003	20.130 \pm 0.097	16.715 \pm 0.011	397 $^{+27}_{-23}$	0.170 \pm 0.014	
...	117.2064 -48.4616	2.50 \pm 0.11	-4.14 \pm 0.23	8.20 \pm 0.22	...	18.055 \pm 0.003	19.769 \pm 0.054	16.751 \pm 0.006	397 $^{+18}_{-17}$	0.244 \pm 0.020	

Table B.4: Yep 1—Continued

Star Name	RA ($^{\circ}$)	Dec ($^{\circ}$)	Parallax (mas)	μ_{α} (mas yr $^{-1}$)	μ_{δ} (mas yr $^{-1}$)	v_r (km s $^{-1}$)	G (mag)	BP (mag)	RP (mag)	d (pc)	Mass (M $_{\odot}$)
...	118.1856 -48.1983	2.41 ± 0.12	-4.43 ± 0.23	8.46 ± 0.29	...	17.734 ± 0.002	19.453 ± 0.037	16.413 ± 0.007	412 $^{+23}_{-20}$	0.238 ± 0.019	
...	116.1745 -48.7000	2.40 ± 0.10	-4.81 ± 0.20	8.21 ± 0.20	...	17.711 ± 0.002	19.458 ± 0.043	16.402 ± 0.006	414 $^{+19}_{-17}$	0.235 ± 0.019	
...	116.8265 -48.3498	2.55 ± 0.11	-4.84 ± 0.21	8.72 ± 0.22	...	16.848 ± 0.002	18.672 ± 0.023	15.516 ± 0.006	389 $^{+17}_{-15}$	0.213 ± 0.017	
...	116.6189 -47.9304	2.68 ± 0.11	-4.56 ± 0.22	9.16 ± 0.24	...	17.680 ± 0.002	19.440 ± 0.046	16.364 ± 0.007	371 $^{+16}_{-15}$	0.229 ± 0.018	
...	117.6208 -47.5248	2.55 ± 0.13	-4.29 ± 0.25	8.06 ± 0.25	...	18.061 ± 0.002	20.055 ± 0.067	16.698 ± 0.006	390 $^{+21}_{-19}$	0.177 ± 0.014	
...	119.2358 -47.6576	2.41 ± 0.18	-4.76 ± 0.34	8.57 ± 0.31	...	18.592 ± 0.003	20.417 ± 0.090	17.204 ± 0.007	414 $^{+34}_{-29}$	0.201 ± 0.021	
...	119.5274 -47.5060	2.41 ± 0.14	-4.41 ± 0.24	8.52 ± 0.26	...	17.812 ± 0.003	19.502 ± 0.035	16.493 ± 0.006	413 $^{+25}_{-23}$	0.246 ± 0.020	
...	118.7453 -47.3037	2.42 ± 0.11	-4.23 ± 0.24	8.61 ± 0.21	...	17.809 ± 0.002	19.471 ± 0.062	16.498 ± 0.006	409 $^{+20}_{-18}$	0.255 ± 0.021	
...	118.9824 -47.0841	2.44 ± 0.14	-4.14 ± 0.26	7.96 ± 0.23	...	18.166 ± 0.003	19.779 ± 0.067	16.860 ± 0.011	406 $^{+24}_{-22}$	0.269 ± 0.026	
...	119.3345 -46.9735	2.79 ± 0.12	-5.02 ± 0.20	9.28 ± 0.26	...	17.535 ± 0.003	19.401 ± 0.095	16.162 ± 0.007	356 $^{+17}_{-15}$	0.196 ± 0.020	
...	119.7612 -46.9975	2.48 ± 0.14	-4.64 ± 0.32	8.48 ± 0.20	...	17.131 ± 0.003	401 $^{+24}_{-22}$	0.495 ± 0.054	
...	118.2123 -47.0261	2.62 ± 0.13	-4.09 ± 0.23	9.23 ± 0.26	...	18.038 ± 0.003	19.921 ± 0.073	16.675 ± 0.006	378 $^{+19}_{-18}$	0.194 ± 0.017	
...	119.0575 -46.2031	2.39 ± 0.14	-4.72 ± 0.28	8.79 ± 0.28	...	18.309 ± 0.003	20.111 ± 0.060	16.971 ± 0.007	416 $^{+26}_{-23}$	0.216 ± 0.017	
...	117.6298 -46.6216	2.50 ± 0.11	-4.52 ± 0.20	7.97 ± 0.20	...	18.025 ± 0.002	19.101 ± 0.053	16.911 ± 0.007	397 $^{+18}_{-16}$	0.526 ± 0.042	
...	117.3777 -46.6509	2.74 ± 0.11	-4.36 ± 0.22	9.14 ± 0.21	...	18.058 ± 0.002	19.817 ± 0.058	16.723 ± 0.006	362 $^{+15}_{-14}$	0.225 ± 0.018	
...	117.1348 -46.1685	2.713 ± 0.093	-4.42 ± 0.18	9.02 ± 0.16	...	17.321 ± 0.002	18.990 ± 0.035	16.044 ± 0.005	365 $^{+13}_{-12}$	0.262 ± 0.021	
...	117.3386 -46.3303	2.558 ± 0.087	-4.41 ± 0.17	9.08 ± 0.16	...	17.625 ± 0.003	18.995 ± 0.092	16.267 ± 0.005	387 $^{+14}_{-13}$	0.336 ± 0.038	
...	117.3434 -46.3292	2.535 ± 0.090	-4.85 ± 0.18	9.14 ± 0.17	...	17.494 ± 0.016	18.912 ± 0.059	16.128 ± 0.047	391 $^{+14}_{-13}$	0.316 ± 0.038	

Table B.4: Yep 1—Continued

Star Name	RA ($^{\circ}$)	Dec ($^{\circ}$)	Parallax (mas)	μ_{α} (mas yr $^{-1}$)	μ_{δ} (mas yr $^{-1}$)	v_r (km s $^{-1}$)	G (mag)	BP (mag)	RP (mag)	d (pc)	Mass (M $_{\odot}$)
...	117.3887	-46.3813	2.590 \pm 0.098	-4.27 \pm 0.20	8.77 \pm 0.21	...	17.825 \pm 0.003	19.329 \pm 0.068	16.459 \pm 0.006	383 $^{+15}_{-14}$	0.281 \pm 0.029
...	117.7129	-46.4478	2.667 \pm 0.080	-4.27 \pm 0.15	9.26 \pm 0.16	...	17.236 \pm 0.002	18.871 \pm 0.024	15.972 \pm 0.004	371 \pm 11	0.274 \pm 0.022
...	116.2905	-47.1556	2.374 \pm 0.050	-4.467 \pm 0.097	8.751 \pm 0.090	...	15.983 \pm 0.002	17.535 \pm 0.010	14.749 \pm 0.004	416.5 $^{+8.9}_{-8.5}$	0.316 \pm 0.025
...	117.9877	-46.5423	2.357 \pm 0.099	-4.69 \pm 0.18	8.72 \pm 0.21	...	17.832 \pm 0.003	19.524 \pm 0.034	16.509 \pm 0.009	420 $^{+18}_{-17}$	0.245 \pm 0.020
HD 65167	118.8294	-46.5728	2.374 \pm 0.042	-5.005 \pm 0.074	8.452 \pm 0.072	...	9.922 \pm 0.002	9.963 \pm 0.002	9.874 \pm 0.002	416.4 $^{+7.4}_{-7.2}$	1.860 \pm 0.093
...	118.5546	-46.1273	2.408 \pm 0.081	-4.63 \pm 0.15	8.00 \pm 0.16	...	16.844 \pm 0.004	18.240 \pm 0.031	15.553 \pm 0.010	411 $^{+14}_{-13}$	0.356 \pm 0.028
...	119.4583	-46.3332	2.368 \pm 0.061	-4.73 \pm 0.10	8.64 \pm 0.11	...	16.411 \pm 0.002	17.851 \pm 0.017	15.228 \pm 0.005	418 $^{+11}_{-10}$	0.373 \pm 0.030
...	115.9499	-47.5057	2.361 \pm 0.038	-4.591 \pm 0.073	8.841 \pm 0.077	...	15.482 \pm 0.003	16.515 \pm 0.014	14.445 \pm 0.010	418.6 $^{+6.9}_{-6.7}$	0.548 \pm 0.044
...	115.7552	-47.3055	2.475 \pm 0.033	-4.990 \pm 0.056	8.901 \pm 0.061	...	15.044 \pm 0.005	16.033 \pm 0.019	14.031 \pm 0.013	424 $^{+18}_{-17}$	0.559 \pm 0.045
...	116.4964	-47.0014	2.393 \pm 0.099	-4.64 \pm 0.19	8.09 \pm 0.21	...	17.499 \pm 0.002	19.208 \pm 0.029	16.214 \pm 0.006	414 $^{+18}_{-16}$	0.250 \pm 0.020
HD 63254	116.4363	-46.7709	2.369 \pm 0.035	-4.965 \pm 0.070	7.936 \pm 0.066	...	9.942 \pm 0.002	10.012 \pm 0.002	9.835 \pm 0.002	417.1 $^{+6.3}_{-6.1}$	2.18 \pm 0.35
...	117.3229	-46.4599	2.671 \pm 0.078	-4.33 \pm 0.17	8.84 \pm 0.16	...	17.376 \pm 0.002	19.124 \pm 0.049	15.962 \pm 0.006	371 $^{+11}_{-10}$	0.212 \pm 0.017
...	117.0642	-46.6228	2.671 \pm 0.083	-4.50 \pm 0.14	8.75 \pm 0.19	...	17.004 \pm 0.002	18.652 \pm 0.022	15.733 \pm 0.004	371 $^{+12}_{-11}$	0.269 \pm 0.022
...	117.3023	-46.4262	2.788 \pm 0.095	-4.36 \pm 0.21	9.31 \pm 0.18	...	17.618 \pm 0.003	19.163 \pm 0.077	16.169 \pm 0.006	356 $^{+13}_{-12}$	0.250 \pm 0.024
...	117.5486	-45.9759	2.416 \pm 0.094	-5.17 \pm 0.17	8.48 \pm 0.19	...	16.501 \pm 0.002	18.107 \pm 0.012	15.259 \pm 0.003	410 $^{+17}_{-15}$	0.294 \pm 0.024
...	115.7663	-46.8593	2.396 \pm 0.077	-4.65 \pm 0.15	9.01 \pm 0.17	...	17.065 \pm 0.002	18.853 \pm 0.022	15.764 \pm 0.004	413 $^{+14}_{-13}$	0.226 \pm 0.018
...	114.7864	-45.7943	2.703 \pm 0.028	-4.438 \pm 0.052	9.892 \pm 0.050	...	14.939 \pm 0.002	15.905 \pm 0.024	13.861 \pm 0.013	366.1 $^{+3.8}_{-3.7}$	0.554 \pm 0.044
...	115.1841	-46.7322	2.568 \pm 0.076	-4.26 \pm 0.14	9.12 \pm 0.15	...	16.603 \pm 0.001	18.975 \pm 0.018	15.394 \pm 0.004	386 $^{+12}_{-11}$	0.357 \pm 0.029
TYC 8133-155-1	115.2017	-46.6386	2.584 \pm 0.037	-4.299 \pm 0.058	9.470 \pm 0.061	18.97 \pm 0.76	11.777 \pm 0.001	12.159 \pm 0.005	11.247 \pm 0.003	382.8 $^{+5.6}_{-5.4}$	1.060 \pm 0.053

Table B.4: Yep 1—Continued

Star Name	RA ($^{\circ}$)	Dec ($^{\circ}$)	Parallax (mas)	μ_{α} (mas yr $^{-1}$)	μ_{δ} (mas yr $^{-1}$)	v_r (km s $^{-1}$)	G (mag)	BP (mag)	RP (mag)	d (pc)	Mass (M $_{\odot}$)
...	115.2440	-47.9977	2.502 \pm 0.060	-4.62 \pm 0.12	9.22 \pm 0.14	...	16.936 \pm 0.002	18.521 \pm 0.025	15.687 \pm 0.006	395.4 $^{+9.7}_{-9.2}$	0.299 \pm 0.024
...	115.2576	-47.7140	2.547 \pm 0.018	-4.896 \pm 0.039	9.076 \pm 0.041	...	14.673 \pm 0.001	15.522 \pm 0.004	13.755 \pm 0.003	388.2 $^{+2.8}_{-2.7}$	0.685 \pm 0.055
TYC 8134-2159-1	115.5542	-45.5105	2.613 \pm 0.025	-5.035 \pm 0.044	9.344 \pm 0.058	23.1 \pm 2.0	11.221 \pm 0.001	11.466 \pm 0.002	10.834 \pm 0.001	378.5 $^{+3.7}_{-3.6}$	1.330 \pm 0.066
...	115.5730	-47.2730	2.589 \pm 0.056	-4.48 \pm 0.11	9.37 \pm 0.12	...	16.457 \pm 0.001	17.906 \pm 0.017	15.244 \pm 0.004	382.3 $^{+8.4}_{-8.0}$	0.362 \pm 0.029
...	115.6926	-48.0171	2.414 \pm 0.015	-4.676 \pm 0.027	8.381 \pm 0.033	...	13.877 \pm 0.002	14.564 \pm 0.008	13.067 \pm 0.005	409.4 \pm 2.5	0.723 \pm 0.058
...	115.7067	-46.8785	2.583 \pm 0.023	-4.350 \pm 0.047	9.314 \pm 0.044	...	15.319 \pm 0.001	16.390 \pm 0.007	14.288 \pm 0.003	382.9 $^{+3.4}_{-3.3}$	0.541 \pm 0.043
...	115.7543	-47.3043	2.475 \pm 0.033	-4.990 \pm 0.056	8.901 \pm 0.061	...	15.044 \pm 0.005	16.033 \pm 0.019	14.032 \pm 0.013	399.5 $^{+5.3}_{-5.2}$	0.559 \pm 0.045
TYC 8134-3161-1	115.7849	-46.2726	2.639 \pm 0.022	-4.535 \pm 0.042	9.759 \pm 0.039	18.8 \pm 2.7	11.358 \pm 0.000	11.616 \pm 0.001	10.960 \pm 0.001	374.9 $^{+3.2}_{-3.1}$	1.500 \pm 0.075
...	115.7850	-46.7745	2.508 \pm 0.068	-4.54 \pm 0.13	9.36 \pm 0.14	...	16.935 \pm 0.001	18.528 \pm 0.052	15.546 \pm 0.019	395 $^{+11}_{-10}$	0.253 \pm 0.020
...	115.7871	-46.2741	2.559 \pm 0.072	-4.57 \pm 0.14	9.55 \pm 0.15	...	16.953 \pm 0.001	18.265 \pm 0.046	15.708 \pm 0.005	387 \pm 11	0.391 \pm 0.031
...	115.7874	-47.1816	2.535 \pm 0.030	-4.652 \pm 0.052	8.435 \pm 0.064	...	15.051 \pm 0.003	15.934 \pm 0.020	13.873 \pm 0.034	390.1 $^{+4.6}_{-4.5}$	0.550 \pm 0.044
...	115.7875	-46.5519	2.650 \pm 0.044	-4.310 \pm 0.083	9.013 \pm 0.092	...	16.276 \pm 0.002	17.608 \pm 0.015	15.127 \pm 0.007	373.5 $^{+6.3}_{-6.1}$	0.411 \pm 0.033
...	115.7942	-47.7632	2.474 \pm 0.048	-4.910 \pm 0.089	8.463 \pm 0.093	...	16.086 \pm 0.003	17.454 \pm 0.025	14.890 \pm 0.006	399.7 $^{+7.9}_{-7.6}$	0.389 \pm 0.031
...	115.8465	-47.3280	2.561 \pm 0.071	-4.59 \pm 0.13	9.08 \pm 0.13	...	16.706 \pm 0.003	18.215 \pm 0.013	15.492 \pm 0.008	387 $^{+11}_{-10}$	0.338 \pm 0.027
...	115.8577	-46.5072	2.584 \pm 0.066	-4.34 \pm 0.12	9.05 \pm 0.15	...	16.905 \pm 0.001	18.674 \pm 0.021	15.611 \pm 0.004	383 $^{+10}_{-9.6}$	0.233 \pm 0.019
...	115.8847	-45.7128	2.629 \pm 0.068	-4.66 \pm 0.12	9.48 \pm 0.14	...	16.424 \pm 0.006	17.826 \pm 0.031	15.210 \pm 0.015	376.7 $^{+9.9}_{-9.4}$	0.375 \pm 0.030
...	115.9401	-46.8091	2.572 \pm 0.044	-4.794 \pm 0.082	9.022 \pm 0.083	...	16.039 \pm 0.001	17.411 \pm 0.008	14.879 \pm 0.003	384.7 $^{+6.7}_{-6.5}$	0.398 \pm 0.032
...	115.9752	-47.3683	2.466 \pm 0.050	-4.863 \pm 0.096	8.547 \pm 0.093	...	16.214 \pm 0.003	17.552 \pm 0.012	15.068 \pm 0.007	401.0 $^{+8.2}_{-7.9}$	0.410 \pm 0.033

Table B.4: Yep 1—Continued

Star Name	RA ($^{\circ}$)	Dec ($^{\circ}$)	Parallax (mas)	μ_{α} (mas yr^{-1})	μ_{δ} (mas yr^{-1})	v_r (km s^{-1})	G (mag)	BP (mag)	RP (mag)	d (pc)	Mass (M_{\odot})
...	115.9947 -45.8733	2.582 \pm 0.037	-4.496 \pm 0.067	9.122 \pm 0.082	...	15.921 \pm 0.002	17.104 \pm 0.013	14.823 \pm 0.007	383.1 $^{+5.6}_{-5.4}$	0.457 \pm 0.037	
...	116.0123 -47.3810	2.440 \pm 0.016	-4.909 \pm 0.031	8.934 \pm 0.030	...	13.626 \pm 0.002	14.265 \pm 0.008	12.866 \pm 0.005	405.0 \pm 2.7	759 \pm 0.061	
...	116.0183 -46.7945	2.512 \pm 0.018	-4.906 \pm 0.031	9.108 \pm 0.033	...	14.560 \pm 0.003	15.475 \pm 0.011	13.616 \pm 0.008	393.6 $^{+2.8}_{-2.7}$	0.623 \pm 0.050	
...	116.0342 -47.7260	2.463 \pm 0.027	-4.626 \pm 0.054	8.497 \pm 0.057	...	15.021 \pm 0.001	16.031 \pm 0.006	14.015 \pm 0.003	401.4 $^{+4.5}_{-4.4}$	0.560 \pm 0.045	
...	116.0437 -46.1129	2.487 \pm 0.051	-4.754 \pm 0.099	9.31 \pm 0.11	...	16.372 \pm 0.012	17.290 \pm 0.054	15.306 \pm 0.029	397.8 $^{+8.3}_{-8.0}$	0.566 \pm 0.045	
...	116.0547 -46.6799	2.507 \pm 0.054	-4.580 \pm 0.097	9.239 \pm 0.096	...	16.175 \pm 0.001	17.557 \pm 0.011	15.006 \pm 0.002	394.7 $^{+8.6}_{-8.3}$	0.393 \pm 0.031	
...	116.0555 -47.2089	2.483 \pm 0.035	-5.020 \pm 0.062	9.029 \pm 0.066	...	15.197 \pm 0.003	16.298 \pm 0.011	14.140 \pm 0.006	398.2 $^{+5.7}_{-5.6}$	0.522 \pm 0.042	
...	116.0660 -47.2110	2.455 \pm 0.037	-4.524 \pm 0.066	8.727 \pm 0.071	...	15.575 \pm 0.001	16.700 \pm 0.006	14.511 \pm 0.003	402.7 $^{+6.1}_{-5.9}$	0.526 \pm 0.042	
...	116.1068 -46.7374	2.478 \pm 0.026	-4.730 \pm 0.047	9.077 \pm 0.046	...	15.147 \pm 0.001	16.199 \pm 0.010	14.119 \pm 0.004	398.9 $^{+4.2}_{-4.1}$	0.546 \pm 0.044	
...	116.1171 -47.4997	2.521 \pm 0.047	-4.996 \pm 0.092	8.530 \pm 0.085	...	15.783 \pm 0.001	16.991 \pm 0.006	14.683 \pm 0.002	392.4 $^{+7.4}_{-7.1}$	0.457 \pm 0.037	
...	116.1209 -46.0115	2.383 \pm 0.059	-4.88 \pm 0.11	9.22 \pm 0.13	...	16.619 \pm 0.001	18.125 \pm 0.015	15.408 \pm 0.003	415 $^{+10}_{-9.9}$	0.347 \pm 0.028	
TYC 8138-168-1	116.1473 -47.3850	2.568 \pm 0.032	-4.673 \pm 0.057	8.811 \pm 0.057	20.1 \pm 2.6	10.335 \pm 0.001	10.434 \pm 0.001	10.188 \pm 0.001	385.1 $^{+4.8}_{-4.7}$	1.880 \pm 0.094	
...	116.1492 -46.8743	2.436 \pm 0.058	-4.66 \pm 0.12	8.61 \pm 0.11	...	16.613 \pm 0.002	18.175 \pm 0.016	15.373 \pm 0.005	406.0 $^{+9.9}_{-9.5}$	0.310 \pm 0.025	
...	116.2298 -45.7040	2.573 \pm 0.016	-4.792 \pm 0.030	9.312 \pm 0.030	...	14.078 \pm 0.002	14.865 \pm 0.007	13.216 \pm 0.004	384.3 \pm 2.4	0.692 \pm 0.055	
...	116.2805 -46.1201	2.536 \pm 0.022	-4.393 \pm 0.040	8.980 \pm 0.043	...	14.589 \pm 0.002	15.423 \pm 0.008	13.699 \pm 0.005	389.9 $^{+3.5}_{-3.4}$	0.672 \pm 0.054	
...	116.2963 -45.6385	2.661 \pm 0.052	-4.68 \pm 0.11	9.41 \pm 0.10	...	16.843 \pm 0.001	18.395 \pm 0.018	15.616 \pm 0.004	372.0 $^{+7.4}_{-7.1}$	0.318 \pm 0.025	
...	116.3422 -45.7081	2.534 \pm 0.035	-4.563 \pm 0.076	9.247 \pm 0.072	...	15.707 \pm 0.001	17.023 \pm 0.009	14.552 \pm 0.002	390.3 $^{+5.4}_{-5.3}$	0.413 \pm 0.033	
...	116.3650 -45.6584	2.563 \pm 0.021	-4.781 \pm 0.043	9.190 \pm 0.041	...	14.809 \pm 0.003	15.796 \pm 0.015	13.810 \pm 0.008	385.9 $^{+3.2}_{-3.1}$	0.565 \pm 0.045	
...	116.4059 -46.3011	2.608 \pm 0.068	-4.60 \pm 0.12	9.16 \pm 0.13	...	16.664 \pm 0.002	18.164 \pm 0.022	15.433 \pm 0.006	380. $^{+10}_{-9.6}$	0.336 \pm 0.027	

Table B.4: Yep 1—Continued

Star Name	RA ($^{\circ}$)	Dec ($^{\circ}$)	Parallax (mas)	μ_{α} (mas yr $^{-1}$)	μ_{δ} (mas yr $^{-1}$)	v_r (km s $^{-1}$)	G (mag)	BP (mag)	RP (mag)	d (pc)	Mass (M $_{\odot}$)
...	116.4587	-48.0133	2.548 \pm 0.072	-4.95 \pm 0.14	8.90 \pm 0.14	...	16.881 \pm 0.001	18.472 \pm 0.021	15.633 \pm 0.004	389 \pm 11	0.297 \pm 0.024
...	116.4759	-48.2070	2.499 \pm 0.018	-4.818 \pm 0.032	8.376 \pm 0.041	...	13.870 \pm 0.003	14.605 \pm 0.009	13.040 \pm 0.006	395.6 \pm 2.9	0.700 \pm 0.056
TYC 8134-1929-1	116.4800	-46.7556	2.440 \pm 0.021	-4.698 \pm 0.040	8.910 \pm 0.041	18.0 \pm 3.5	10.507 \pm 0.000	10.632 \pm 0.001	10.307 \pm 0.001	405.1 \pm 3.5	1.860 \pm 0.093
TYC 8134-2633-1	116.4869	-46.2407	2.439 \pm 0.036	-4.690 \pm 0.056	8.788 \pm 0.060	23.01 \pm 0.87	11.919 \pm 0.001	12.221 \pm 0.002	11.469 \pm 0.001	405.4 $^{+6.0}_{-5.8}$	1.210 \pm 0.060
...	116.5128	-47.0653	2.570 \pm 0.060	-4.75 \pm 0.11	9.26 \pm 0.11	...	16.688 \pm 0.002	18.258 \pm 0.014	15.466 \pm 0.004	385.2 $^{+9.2}_{-8.8}$	0.313 \pm 0.025
...	116.5512	-46.1806	2.508 \pm 0.050	-4.494 \pm 0.090	9.59 \pm 0.11	...	15.819 \pm 0.005	17.101 \pm 0.028	14.686 \pm 0.012	394.4 $^{+7.9}_{-7.6}$	0.427 \pm 0.034
...	116.5560	-45.7344	2.512 \pm 0.065	-4.84 \pm 0.13	9.18 \pm 0.13	...	17.075 \pm 0.001	18.837 \pm 0.022	15.772 \pm 0.004	394 $^{+10.}_{-9.9}$	0.232 \pm 0.019
...	116.5761	-46.6001	2.589 \pm 0.040	-4.441 \pm 0.080	9.092 \pm 0.084	...	16.039 \pm 0.001	17.360 \pm 0.012	14.886 \pm 0.003	382.1 $^{+6.0}_{-5.8}$	0.413 \pm 0.033
...	116.5931	-45.4271	2.479 \pm 0.033	-4.775 \pm 0.063	9.134 \pm 0.060	...	15.371 \pm 0.004	16.502 \pm 0.022	14.296 \pm 0.010	398.9 $^{+5.3}_{-5.2}$	0.514 \pm 0.041
...	116.6038	-47.1232	2.513 \pm 0.017	-5.012 \pm 0.033	8.985 \pm 0.035	...	14.087 \pm 0.002	15.011 \pm 0.010	13.132 \pm 0.008	393.4 $^{+2.7}_{-2.6}$	0.612 \pm 0.049
...	116.6080	-47.2994	2.610 \pm 0.050	-4.63 \pm 0.10	8.50 \pm 0.11	...	16.153 \pm 0.004	17.627 \pm 0.030	14.926 \pm 0.009	379.2 $^{+7.4}_{-7.1}$	0.352 \pm 0.028
...	116.6486	-48.0430	2.469 \pm 0.044	-4.549 \pm 0.086	8.73 \pm 0.10	...	15.840 \pm 0.002	17.058 \pm 0.017	14.729 \pm 0.004	400.5 $^{+7.3}_{-7.1}$	0.451 \pm 0.036
2MASS J07463583-4453183	116.6493	-44.8884	2.582 \pm 0.020	-5.055 \pm 0.036	9.217 \pm 0.039	22.18 \pm 0.78	12.981 \pm 0.001	13.521 \pm 0.003	12.301 \pm 0.004	383.1 \pm 2.9	0.950 \pm 0.048
...	116.7339	-46.5566	2.547 \pm 0.022	-4.728 \pm 0.037	8.955 \pm 0.053	...	14.526 \pm 0.002	15.337 \pm 0.009	13.636 \pm 0.007	388.3 $^{+3.4}_{-3.3}$	0.679 \pm 0.054
...	116.7451	-48.8517	2.503 \pm 0.027	-4.625 \pm 0.051	8.248 \pm 0.062	...	15.188 \pm 0.002	16.193 \pm 0.006	14.184 \pm 0.005	395.1 $^{+4.3}_{-4.2}$	0.556 \pm 0.044
...	116.7516	-46.5708	2.495 \pm 0.057	-4.483 \pm 0.095	9.22 \pm 0.13	...	16.191 \pm 0.002	17.475 \pm 0.012	15.048 \pm 0.005	396.6 $^{+9.3}_{-8.9}$	0.424 \pm 0.034
...	116.7555	-46.8450	2.544 \pm 0.038	-4.586 \pm 0.070	9.050 \pm 0.086	...	15.749 \pm 0.005	17.001 \pm 0.024	14.612 \pm 0.012	388.8 $^{+5.9}_{-5.8}$	0.432 \pm 0.035
...	116.7699	-46.5385	2.502 \pm 0.064	-4.46 \pm 0.11	9.40 \pm 0.14	...	16.725 \pm 0.002	18.219 \pm 0.013	15.498 \pm 0.004	396 $^{+10.}_{-9.9}$	0.339 \pm 0.027

Table B.4: Yep 1—Continued

Star Name	RA ($^{\circ}$)	Dec ($^{\circ}$)	Parallax (mas)	μ_{α} (mas yr^{-1})	μ_{δ} (mas yr^{-1})	v_r (km s^{-1})	G (mag)	BP (mag)	RP (mag)	d (pc)	Mass (M_{\odot})
...	116.8023	-47.0127	2.549 \pm 0.063	-4.48 \pm 0.12	9.52 \pm 0.15	...	16.083 \pm 0.002	17.659 \pm 0.013	14.844 \pm 0.006	388.3 $^{+9.8}_{-9.3}$	0.306 \pm 0.024
...	116.8148	-46.1851	2.447 \pm 0.058	-4.56 \pm 0.11	8.97 \pm 0.12	...	16.476 \pm 0.002	17.854 \pm 0.015	15.299 \pm 0.007	404.2 $^{+9.8}_{-9.4}$	0.392 \pm 0.031
...	116.8284	-47.0477	2.524 \pm 0.046	-4.804 \pm 0.078	9.017 \pm 0.095	...	15.611 \pm 0.003	16.834 \pm 0.015	14.484 \pm 0.010	391.9 $^{+7.2}_{-7.0}$	0.444 \pm 0.036
CD-483192	116.8302	-48.4870	2.438 \pm 0.028	-4.503 \pm 0.053	8.388 \pm 0.051	20.2 \pm 2.3	10.662 \pm 0.000	10.817 \pm 0.001	10.412 \pm 0.001	405.4 $^{+4.7}_{-4.6}$	1.61 \pm 0.12
...	116.8339	-46.9031	2.490 \pm 0.054	-4.73 \pm 0.11	9.10 \pm 0.14	...	15.774 \pm 0.003	17.320 \pm 0.015	14.540 \pm 0.008	397.3 $^{+8.9}_{-8.5}$	0.318 \pm 0.025
...	116.8591	-46.8983	2.550 \pm 0.019	-4.819 \pm 0.035	9.144 \pm 0.040	...	14.280 \pm 0.002	15.082 \pm 0.007	13.400 \pm 0.005	387.8 \pm 2.8	0.688 \pm 0.055
...	116.8683	-47.9837	2.542 \pm 0.037	-4.718 \pm 0.072	8.926 \pm 0.071	...	15.070 \pm 0.001	16.216 \pm 0.008	13.987 \pm 0.004	389.0 $^{+5.8}_{-5.6}$	0.496 \pm 0.040
...	116.8831	-45.5113	2.560 \pm 0.015	-4.745 \pm 0.031	9.413 \pm 0.029	...	13.769 \pm 0.004	14.504 \pm 0.014	12.924 \pm 0.008	386.2 \pm 2.3	0.698 \pm 0.056
HD 63579	116.8967	-47.0130	2.428 \pm 0.056	-4.67 \pm 0.11	8.83 \pm 0.11	-14.1 \pm 6.6	6.940 \pm 0.001	6.908 \pm 0.002	7.026 \pm 0.007	407.3 $^{+9.6}_{-9.2}$	4.7 \pm 2.0
...	116.9017	-45.7206	2.502 \pm 0.061	-4.71 \pm 0.12	9.08 \pm 0.13	...	16.912 \pm 0.001	18.557 \pm 0.017	15.667 \pm 0.003	395.5 $^{+9.8}_{-9.4}$	0.276 \pm 0.022
...	116.9041	-47.4410	2.483 \pm 0.012	-5.058 \pm 0.023	8.633 \pm 0.024	19	13.454 \pm 0.001	14.194 \pm 0.005	12.618 \pm 0.004	398.1 \pm 2.0	0.699 \pm 0.056
...	116.9185	-46.2051	2.594 \pm 0.033	-4.583 \pm 0.061	9.178 \pm 0.065	...	15.662 \pm 0.003	16.796 \pm 0.014	14.574 \pm 0.013	381.3 $^{+4.8}_{-4.7}$	0.501 \pm 0.040
...	116.9306	-47.5428	2.517 \pm 0.069	-4.46 \pm 0.14	8.45 \pm 0.13	...	16.882 \pm 0.002	18.470 \pm 0.016	15.647 \pm 0.006	393 $^{+11}_{-10.}$	0.302 \pm 0.024
...	116.9880	-47.6813	2.560 \pm 0.050	-4.82 \pm 0.10	8.47 \pm 0.12	...	16.404 \pm 0.001	17.826 \pm 0.015	15.219 \pm 0.005	386.4 $^{+7.6}_{-7.3}$	0.377 \pm 0.030
CD-483205	116.9920	-48.4403	2.470 \pm 0.023	-4.183 \pm 0.042	8.810 \pm 0.046	20.1 \pm 3.5	10.408 \pm 0.000	10.517 \pm 0.001	10.224 \pm 0.002	400.2 $^{+3.8}_{-3.7}$	1.980 \pm 0.099
...	117.0004	-46.2629	2.451 \pm 0.036	-4.276 \pm 0.067	9.264 \pm 0.080	...	14.265 \pm 0.001	15.072 \pm 0.003	13.386 \pm 0.003	403.4 $^{+6.0}_{-5.8}$	0.688 \pm 0.055
...	117.0006	-48.4380	2.411 \pm 0.061	-4.26 \pm 0.12	8.43 \pm 0.13	...	16.602 \pm 0.002	18.069 \pm 0.015	15.379 \pm 0.005	410 $^{+11}_{-10.}$	0.355 \pm 0.028
...	117.0038	-47.6372	2.400 \pm 0.069	-4.44 \pm 0.15	8.75 \pm 0.16	...	16.943 \pm 0.001	18.496 \pm 0.033	15.679 \pm 0.004	412 \pm 12	0.305 \pm 0.025
...	117.0053	-46.1929	2.542 \pm 0.057	-4.49 \pm 0.10	9.29 \pm 0.11	...	16.586 \pm 0.002	18.144 \pm 0.017	15.358 \pm 0.005	389.3 $^{+8.9}_{-8.5}$	0.316 \pm 0.025

Table B.4: Yep 1—Continued

Star Name	RA ($^{\circ}$)	Dec ($^{\circ}$)	Parallax (mas)	μ_{α} (mas yr $^{-1}$)	μ_{δ} (mas yr $^{-1}$)	v_r (km s $^{-1}$)	G (mag)	BP (mag)	RP (mag)	d (pc)	Mass (M $_{\odot}$)
...	117.0319	-46.4149	2.601 \pm 0.034	-4.787 \pm 0.066	9.103 \pm 0.069	...	15.409 \pm 0.003	16.768 \pm 0.012	14.254 \pm 0.007	380.3 $^{+5.1}_{-5.0}$	0.403 \pm 0.032
...	117.0359	-46.0867	2.515 \pm 0.036	-4.701 \pm 0.066	9.006 \pm 0.071	...	15.765 \pm 0.002	16.958 \pm 0.014	14.662 \pm 0.004	393.2 $^{+5.7}_{-5.5}$	0.460 \pm 0.037
...	117.0596	-46.5062	2.468 \pm 0.069	-4.77 \pm 0.14	8.98 \pm 0.15	...	17.136 \pm 0.001	18.808 \pm 0.014	15.863 \pm 0.002	401 \pm 11	0.262 \pm 0.021
...	117.0765	-46.1692	2.463 \pm 0.046	-4.982 \pm 0.087	9.860 \pm 0.086	...	15.814 \pm 0.002	17.211 \pm 0.014	14.624 \pm 0.005	401.6 $^{+7.7}_{-7.4}$	0.383 \pm 0.031
...	117.0791	-46.8902	2.413 \pm 0.062	-4.63 \pm 0.12	8.90 \pm 0.12	...	16.477 \pm 0.004	18.054 \pm 0.020	15.228 \pm 0.010	410. $^{+11}_{-10}$.	0.302 \pm 0.024
...	117.0814	-47.2149	2.495 \pm 0.058	-4.66 \pm 0.12	9.06 \pm 0.10	...	16.093 \pm 0.001	17.645 \pm 0.012	14.874 \pm 0.003	396.5 $^{+9.4}_{-8.9}$	0.321 \pm 0.026
...	117.0817	-46.0102	2.557 \pm 0.067	-4.89 \pm 0.12	9.31 \pm 0.13	...	16.868 \pm 0.001	18.464 \pm 0.023	15.633 \pm 0.003	387 $^{+10.}_{-9.8}$	0.300 \pm 0.024
...	117.0879	-46.0425	2.559 \pm 0.054	-4.268 \pm 0.096	9.40 \pm 0.11	...	16.235 \pm 0.001	17.595 \pm 0.018	15.064 \pm 0.003	386.7 $^{+8.2}_{-7.9}$	0.398 \pm 0.032
...	117.0954	-46.1924	2.578 \pm 0.051	-4.347 \pm 0.093	9.042 \pm 0.089	...	15.997 \pm 0.004	17.416 \pm 0.018	14.805 \pm 0.010	383.9 $^{+7.7}_{-7.4}$	0.376 \pm 0.030
...	117.0987	-45.8604	2.554 \pm 0.024	-4.786 \pm 0.047	9.159 \pm 0.046	...	14.801 \pm 0.004	15.770 \pm 0.014	13.825 \pm 0.009	387.2 $^{+3.7}_{-3.6}$	0.582 \pm 0.047
...	117.1004	-46.5845	2.570 \pm 0.041	-4.603 \pm 0.076	8.807 \pm 0.073	...	15.828 \pm 0.003	17.018 \pm 0.013	14.739 \pm 0.006	385.0 $^{+6.3}_{-6.1}$	0.459 \pm 0.037
...	117.1122	-46.4091	2.422 \pm 0.042	-4.836 \pm 0.083	8.731 \pm 0.082	...	15.719 \pm 0.001	17.243 \pm 0.010	14.488 \pm 0.004	408.2 $^{+7.2}_{-7.0}$	0.327 \pm 0.026
...	117.1231	-46.5831	2.466 \pm 0.026	-4.842 \pm 0.056	9.082 \pm 0.051	...	15.346 \pm 0.003	16.388 \pm 0.014	14.321 \pm 0.007	400.9 $^{+4.3}_{-4.2}$	0.549 \pm 0.044
...	117.1605	-46.0718	2.516 \pm 0.029	-4.723 \pm 0.053	8.466 \pm 0.051	...	15.195 \pm 0.002	16.266 \pm 0.006	14.157 \pm 0.004	393.0 $^{+4.6}_{-4.5}$	0.538 \pm 0.043
...	117.2002	-46.1631	2.441 \pm 0.069	-4.65 \pm 0.13	8.98 \pm 0.13	...	17.087 \pm 0.004	18.778 \pm 0.031	15.783 \pm 0.014	405 $^{+12}_{-11}$	0.250 \pm 0.020
...	117.2071	-46.5231	2.445 \pm 0.040	-4.463 \pm 0.082	8.766 \pm 0.073	...	15.724 \pm 0.002	16.979 \pm 0.009	14.596 \pm 0.004	404.4 $^{+6.7}_{-6.5}$	0.434 \pm 0.035
...	117.2098	-48.4129	2.480 \pm 0.032	-4.470 \pm 0.070	8.422 \pm 0.064	...	15.626 \pm 0.002	16.771 \pm 0.008	14.555 \pm 0.004	398.7 $^{+5.2}_{-5.1}$	0.506 \pm 0.040
...	117.2251	-46.3499	2.608 \pm 0.045	-4.523 \pm 0.085	8.851 \pm 0.094	...	16.183 \pm 0.004	17.478 \pm 0.020	15.003 \pm 0.009	379.4 $^{+6.6}_{-6.4}$	0.412 \pm 0.033

Table B.4: Yep 1—Continued

Star Name	RA ($^{\circ}$)	Dec ($^{\circ}$)	Parallax (mas)	μ_{α} (mas yr $^{-1}$)	μ_{δ} (mas yr $^{-1}$)	v_r (km s $^{-1}$)	G (mag)	BP (mag)	RP (mag)	d (pc)	Mass (M $_{\odot}$)
...	117.2259	-46.4288	2.653 ± 0.068	-4.40 ± 0.14	8.90 ± 0.15	...	16.656 ± 0.001	18.284 ± 0.034	15.342 ± 0.002	373.2 $^{+9.8}_{-9.3}$	0.263 ± 0.021
HD 63869	117.2361	-46.6219	2.451 ± 0.038	-4.857 ± 0.071	9.474 ± 0.070	...	9.014 ± 0.000	9.031 ± 0.003	8.966 ± 0.005	403.3 $^{+6.4}_{-6.2}$	2.18 ± 0.70
TYC 8134-2250-2	117.2370	-46.6219	2.482 ± 0.029	-4.904 ± 0.048	8.713 ± 0.084	...	10.219 ± 0.001	10.02 ± 0.17	9.816 ± 0.069	398.3 $^{+4.6}_{-4.5}$	1.930 ± 0.096
...	117.2373	-45.8028	2.514 ± 0.022	-4.743 ± 0.039	9.156 ± 0.038	...	14.742 ± 0.001	15.675 ± 0.005	13.784 ± 0.004	393.3 $^{+3.5}_{-3.4}$	0.607 ± 0.049
...	117.2429	-46.2864	2.559 ± 0.030	-4.908 ± 0.060	8.983 ± 0.056	...	15.544 ± 0.001	16.640 ± 0.010	14.495 ± 0.003	386.4 $^{+4.6}_{-4.5}$	0.526 ± 0.042
...	117.2573	-46.1376	2.481 ± 0.032	-4.708 ± 0.056	8.983 ± 0.057	...	15.435 ± 0.003	16.541 ± 0.013	14.383 ± 0.007	398.6 $^{+5.1}_{-5.0}$	0.522 ± 0.042
...	117.2586	-45.7505	2.445 ± 0.057	-4.81 ± 0.11	9.15 ± 0.11	...	16.183 ± 0.003	17.524 ± 0.025	15.027 ± 0.010	404.6 $^{+9.6}_{-9.1}$	0.407 ± 0.033
...	117.2722	-46.2643	2.534 ± 0.018	-4.738 ± 0.034	9.087 ± 0.032	...	14.291 ± 0.002	15.128 ± 0.008	13.385 ± 0.004	390.2 $^{+2.8}_{-2.7}$	0.667 ± 0.053
...	117.2731	-46.3463	2.581 ± 0.031	-4.564 ± 0.058	8.469 ± 0.058	...	14.770 ± 0.003	15.925 ± 0.012	13.672 ± 0.008	383.3 $^{+4.6}_{-4.5}$	0.478 ± 0.038
...	117.2759	-45.0695	2.584 ± 0.066	-4.45 ± 0.12	9.19 ± 0.15	...	16.868 ± 0.001	18.510 ± 0.023	15.611 ± 0.004	383 $^{+10.}_{-9.5}$	0.274 ± 0.022
...	117.2779	-46.6284	2.531 ± 0.062	-4.80 ± 0.12	9.21 ± 0.13	...	17.111 ± 0.001	18.828 ± 0.039	15.801 ± 0.007	391.0 $^{+9.8}_{-9.3}$	0.242 ± 0.019
...	117.2795	-47.6935	2.558 ± 0.055	-4.43 ± 0.11	8.54 ± 0.10	...	15.909 ± 0.002	17.446 ± 0.012	14.664 ± 0.005	386.9 $^{+8.4}_{-8.1}$	0.317 ± 0.025
...	117.2938	-46.3876	2.530 ± 0.030	-4.738 ± 0.066	9.362 ± 0.054	...	15.330 ± 0.014	16.418 ± 0.062	14.237 ± 0.035	390.9 $^{+4.8}_{-4.6}$	0.514 ± 0.041
...	117.3030	-46.0360	2.691 ± 0.084	-4.97 ± 0.16	9.44 ± 0.15	...	16.315 ± 0.002	17.887 ± 0.016	15.076 ± 0.004	368 $^{+12}_{-11}$	0.307 ± 0.025
QSP up	117.3036	-46.8577	2.480 ± 0.073	-4.68 ± 0.12	8.78 ± 0.13	37.1 ± 8.9	5.778 ± 0.001	5.713 ± 0.003	5.910 ± 0.004	399 $^{+12}_{-11}$	5.4 ± 6.7
...	117.3037	-47.5069	2.494 ± 0.041	-4.572 ± 0.073	8.747 ± 0.070	...	15.818 ± 0.003	17.125 ± 0.014	14.662 ± 0.010	396.5 $^{+6.6}_{-6.4}$	0.415 ± 0.033
...	117.3083	-46.3701	2.561 ± 0.030	-4.219 ± 0.055	9.449 ± 0.055	...	14.505 ± 0.002	14.882 ± 0.050	13.537 ± 0.009	386.2 $^{+4.6}_{-4.5}$	0.780 ± 0.062
...	117.3088	-46.7596	2.509 ± 0.046	-4.903 ± 0.083	9.100 ± 0.080	...	16.152 ± 0.002	17.591 ± 0.022	14.956 ± 0.006	394.3 $^{+7.3}_{-7.0}$	0.370 ± 0.030
...	117.3202	-46.8757	2.568 ± 0.059	-4.53 ± 0.11	9.24 ± 0.10	...	16.397 ± 0.007	17.826 ± 0.034	15.183 ± 0.023	385.4 $^{+9.0}_{-8.6}$	0.368 ± 0.029

Table B.4: Yep 1—Continued

Star Name	RA ($^{\circ}$)	Dec ($^{\circ}$)	Parallax (mas)	μ_{α} (mas yr^{-1})	μ_{δ} (mas yr^{-1})	v_r (km s^{-1})	G (mag)	BP (mag)	RP (mag)	d (pc)	Mass (M_{\odot})
2MASS J07491846-4657432	117.3269	-46.9620	2.516 \pm 0.025	-4.450 \pm 0.045	8.986 \pm 0.045	16.7 \pm 3.7	10.960 \pm 0.000	11.173 \pm 0.001	10.628 \pm 0.001	393.1 \pm 3.9	1.830 \pm 0.092
...	117.3354	-47.0210	2.561 \pm 0.057	-4.784 \pm 0.097	8.93 \pm 0.11	...	15.986 \pm 0.002	17.394 \pm 0.016	14.801 \pm 0.004	386.4 $^{+8.8}_{-8.5}$	0.381 \pm 0.030
...	117.3392	-46.2144	2.515 \pm 0.024	-4.768 \pm 0.043	9.246 \pm 0.044	...	14.530 \pm 0.002	15.538 \pm 0.008	13.526 \pm 0.004	393.1 $^{+3.7}_{-3.6}$	0.555 \pm 0.044
...	117.3411	-46.6013	2.629 \pm 0.044	-3.822 \pm 0.089	9.183 \pm 0.084	...	16.129 \pm 0.001	17.558 \pm 0.009	14.933 \pm 0.004	376.4 $^{+6.4}_{-6.2}$	0.372 \pm 0.030
...	117.3426	-47.8197	2.538 \pm 0.048	-4.77 \pm 0.11	8.473 \pm 0.088	...	16.164 \pm 0.001	17.528 \pm 0.014	14.991 \pm 0.005	389.7 $^{+7.4}_{-7.2}$	0.396 \pm 0.032
...	117.3433	-46.3423	2.524 \pm 0.020	-4.963 \pm 0.037	8.928 \pm 0.035	...	14.630 \pm 0.001	15.478 \pm 0.006	13.720 \pm 0.004	391.7 \pm 3.1	0.662 \pm 0.053
...	117.3473	-46.3843	2.552 \pm 0.013	-4.881 \pm 0.025	9.087 \pm 0.024	...	13.587 \pm 0.002	14.301 \pm 0.008	12.771 \pm 0.006	387.5 \pm 2.0	0.711 \pm 0.057
...	117.3498	-46.4239	2.394 \pm 0.064	-4.87 \pm 0.14	9.31 \pm 0.12	...	16.590 \pm 0.001	18.148 \pm 0.017	15.294 \pm 0.003	413 \pm 11	0.291 \pm 0.023
...	117.3637	-46.3935	2.475 \pm 0.038	-5.063 \pm 0.077	8.759 \pm 0.071	...	16.204 \pm 0.002	17.470 \pm 0.016	15.027 \pm 0.005	399.5 $^{+6.2}_{-6.0}$	0.420 \pm 0.034
...	117.3639	-46.6027	2.456 \pm 0.055	-4.53 \pm 0.10	8.99 \pm 0.10	...	15.481 \pm 0.002	16.912 \pm 0.009	14.291 \pm 0.007	402.8 $^{+9.1}_{-8.7}$	0.374 \pm 0.030
...	117.3640	-46.3616	2.513 \pm 0.061	-4.58 \pm 0.12	9.21 \pm 0.11	...	16.658 \pm 0.001	18.070 \pm 0.029	15.400 \pm 0.006	393.8 $^{+9.7}_{-9.3}$	0.360 \pm 0.029
...	117.3733	-46.3130	2.495 \pm 0.060	-4.69 \pm 0.12	9.29 \pm 0.11	...	16.958 \pm 0.001	18.363 \pm 0.024	15.720 \pm 0.004	396.6 $^{+9.8}_{-9.4}$	0.367 \pm 0.029
...	117.3747	-46.3678	2.647 \pm 0.061	-4.23 \pm 0.12	9.46 \pm 0.12	...	16.822 \pm 0.002	18.140 \pm 0.034	15.576 \pm 0.007	374.0 $^{+8.9}_{-8.5}$	0.389 \pm 0.031
...	117.3760	-46.3274	2.581 \pm 0.019	-4.431 \pm 0.035	8.846 \pm 0.033	...	14.813 \pm 0.004	15.757 \pm 0.016	13.832 \pm 0.011	383.1 $^{+2.8}_{-2.7}$	0.589 \pm 0.047
TYC 8138-2304-1	117.3784	-47.8679	2.470 \pm 0.023	-4.653 \pm 0.045	8.377 \pm 0.039	...	11.582 \pm 0.002	11.964 \pm 0.006	11.060 \pm 0.005	400.3 $^{+3.7}_{-3.6}$	0.900 \pm 0.045
...	117.3819	-46.7347	2.649 \pm 0.085	-4.64 \pm 0.15	9.35 \pm 0.15	...	17.489 \pm 0.001	19.231 \pm 0.026	16.177 \pm 0.005	374 \pm 12	0.235 \pm 0.019
...	117.3846	-48.6480	2.562 \pm 0.080	-4.51 \pm 0.15	8.53 \pm 0.14	...	17.061 \pm 0.001	18.623 \pm 0.022	15.814 \pm 0.003	387 $^{+13}_{-12}$	0.397 \pm 0.025
...	117.3952	-46.3390	2.554 \pm 0.015	-4.400 \pm 0.029	8.980 \pm 0.027	...	13.921 \pm 0.003	14.677 \pm 0.011	13.063 \pm 0.007	387.2 $^{+2.3}_{-2.2}$	0.695 \pm 0.056

Table B.4: Yep 1—Continued

Star Name	RA ($^{\circ}$)	Dec ($^{\circ}$)	Parallax (mas)	μ_{α} (mas yr $^{-1}$)	μ_{δ} (mas yr $^{-1}$)	v_r (km s $^{-1}$)	G (mag)	BP (mag)	RP (mag)	d (pc)	Mass (M $_{\odot}$)
...	117.4010 -46.0546	2.432 \pm 0.031	-4.919 \pm 0.059	8.981 \pm 0.065	...	15.631 \pm 0.002	16.860 \pm 0.011	14.522 \pm 0.005	406.4 $^{+5.2}_{-5.1}$	0.448 \pm 0.036	
...	117.4029 -45.8122	2.538 \pm 0.018	-4.863 \pm 0.034	9.125 \pm 0.032	...	14.186 \pm 0.001	14.918 \pm 0.005	13.356 \pm 0.005	389.6 \pm 2.8	701 \pm 0.056	
...	117.4034 -46.3910	2.564 \pm 0.056	-4.85 \pm 0.12	8.94 \pm 0.10	...	16.740 \pm 0.001	18.131 \pm 0.018	15.531 \pm 0.003	386.0 $^{+8.5}_{-8.2}$	0.379 \pm 0.030	
...	117.4055 -47.5942	2.432 \pm 0.059	-4.84 \pm 0.12	8.64 \pm 0.11	...	16.756 \pm 0.001	18.319 \pm 0.024	15.525 \pm 0.003	407 $^{+10.}_{-9.6}$	0.313 \pm 0.025	
...	117.4123 -45.2712	2.514 \pm 0.074	-4.82 \pm 0.13	9.27 \pm 0.14	...	16.893 \pm 0.002	18.419 \pm 0.019	15.678 \pm 0.003	394 $^{+12}_{-11}$	0.332 \pm 0.027	
...	117.4187 -46.5725	2.566 \pm 0.047	-4.599 \pm 0.098	8.761 \pm 0.093	...	16.529 \pm 0.001	18.124 \pm 0.012	15.280 \pm 0.003	385.5 $^{+7.1}_{-6.9}$	0.295 \pm 0.024	
...	117.4195 -46.2832	2.494 \pm 0.058	-4.24 \pm 0.11	8.77 \pm 0.10	...	15.845 \pm 0.002	17.367 \pm 0.013	14.604 \pm 0.007	396.8 $^{+9.5}_{-9.0}$	0.324 \pm 0.026	
CD-46 3471	117.4272 -46.3817	2.503 \pm 0.023	-4.879 \pm 0.042	8.910 \pm 0.050	17.4 \pm 5.4	11.055 \pm 0.001	11.271 \pm 0.002	10.717 \pm 0.001	395.1 $^{+3.7}_{-3.6}$	2.05 \pm 0.10	
...	117.4273 -46.2072	2.546 \pm 0.016	-4.281 \pm 0.028	8.974 \pm 0.028	...	13.929 \pm 0.002	14.609 \pm 0.009	13.127 \pm 0.007	388.4 \pm 2.4	0.728 \pm 0.058	
...	117.4298 -46.2533	2.392 \pm 0.063	-4.60 \pm 0.13	9.44 \pm 0.12	...	16.793 \pm 0.002	18.309 \pm 0.013	15.553 \pm 0.005	414 \pm 11	0.327 \pm 0.026	
...	117.4332 -46.3458	2.558 \pm 0.053	-5.13 \pm 0.11	8.85 \pm 0.11	...	16.075 \pm 0.001	17.647 \pm 0.011	14.816 \pm 0.002	386.9 $^{+8.2}_{-7.9}$	0.300 \pm 0.024	
TYC 8138-2569-1	117.4404 -47.8266	2.426 \pm 0.026	-4.747 \pm 0.050	8.641 \pm 0.043	19.8 \pm 2.4	10.467 \pm 0.000	10.735 \pm 0.001	10.068 \pm 0.001	407.5 $^{+4.4}_{-4.3}$	1.41 \pm 0.11	
2MASS J07494943-4614155	117.4560 -46.2377	2.630 \pm 0.072	-5.01 \pm 0.15	9.26 \pm 0.13	96.2 \pm 2.4	17.062 \pm 0.002	18.591 \pm 0.018	15.840 \pm 0.007	377 $^{+11}_{-10.}$	0.880 \pm 0.085	
...	117.4661 -46.3293	2.569 \pm 0.024	-4.825 \pm 0.046	9.070 \pm 0.042	...	14.836 \pm 0.001	15.809 \pm 0.006	13.848 \pm 0.004	385.0 $^{+3.6}_{-3.5}$	0.575 \pm 0.046	
...	117.4701 -46.7258	2.543 \pm 0.049	-4.912 \pm 0.093	8.715 \pm 0.092	...	16.404 \pm 0.003	17.814 \pm 0.022	15.212 \pm 0.008	389.0 $^{+7.7}_{-7.4}$	0.379 \pm 0.030	
...	117.4770 -46.5113	2.584 \pm 0.049	-4.76 \pm 0.10	8.978 \pm 0.091	...	16.286 \pm 0.002	17.723 \pm 0.011	15.095 \pm 0.004	383.0 $^{+7.3}_{-7.1}$	0.372 \pm 0.030	
...	117.4797 -49.0674	2.471 \pm 0.045	-4.568 \pm 0.079	8.305 \pm 0.081	...	15.782 \pm 0.001	17.078 \pm 0.008	14.631 \pm 0.003	400.2 $^{+7.3}_{-7.1}$	0.419 \pm 0.034	
...	117.4836 -46.7262	2.444 \pm 0.072	-4.77 \pm 0.13	8.84 \pm 0.13	...	17.326 \pm 0.001	18.905 \pm 0.028	16.056 \pm 0.005	405 \pm 12	0.293 \pm 0.023	
...	117.4887 -45.7125	2.492 \pm 0.058	-4.86 \pm 0.10	9.20 \pm 0.10	...	16.671 \pm 0.001	18.217 \pm 0.030	15.449 \pm 0.003	397.0 $^{+9.3}_{-8.9}$	0.322 \pm 0.026	

Table B.4: Yep 1—Continued

Star Name	RA ($^{\circ}$)	Dec ($^{\circ}$)	Parallax (mas)	μ_{α} (mas yr $^{-1}$)	μ_{δ} (mas yr $^{-1}$)	v_r (km s $^{-1}$)	G (mag)	BP (mag)	RP (mag)	d (pc)	Mass (M $_{\odot}$)
...	117.4986	-47.3280	2.462 \pm 0.063	-4.75 \pm 0.12	8.67 \pm 0.12	...	16.692 \pm 0.002	18.496 \pm 0.018	15.389 \pm 0.005	402 $^{+11}_{-10}$	0.223 \pm 0.018
...	117.5002	-45.4206	2.470 \pm 0.068	-4.77 \pm 0.13	9.30 \pm 0.13	...	17.008 \pm 0.001	18.592 \pm 0.018	15.769 \pm 0.004	401 \pm 11	0.302 \pm 0.024
...	117.5021	-46.4992	2.532 \pm 0.057	-4.61 \pm 0.12	9.28 \pm 0.11	...	16.967 \pm 0.001	18.572 \pm 0.014	15.708 \pm 0.004	390.9 $^{+9.0}_{-8.6}$	0.283 \pm 0.023
...	117.5032	-45.3357	2.514 \pm 0.031	-4.794 \pm 0.054	9.168 \pm 0.051	...	15.117 \pm 0.002	16.096 \pm 0.011	14.121 \pm 0.008	393.3 $^{+4.9}_{-4.7}$	0.570 \pm 0.046
...	117.5077	-47.7963	2.447 \pm 0.075	-4.56 \pm 0.14	8.42 \pm 0.14	...	17.067 \pm 0.001	18.715 \pm 0.031	15.796 \pm 0.004	405 $^{+13}_{-12}$	0.269 \pm 0.022
...	117.5106	-46.4747	2.509 \pm 0.069	-4.68 \pm 0.14	9.10 \pm 0.14	...	17.207 \pm 0.001	18.891 \pm 0.029	15.941 \pm 0.004	395 \pm 11	0.261 \pm 0.021
...	117.5110	-45.5196	2.566 \pm 0.018	-4.567 \pm 0.029	9.275 \pm 0.030	...	14.014 \pm 0.003	14.788 \pm 0.009	13.154 \pm 0.007	385.4 \pm 2.7	0.693 \pm 0.055
...	117.5342	-46.3082	2.688 \pm 0.057	-4.27 \pm 0.11	9.30 \pm 0.10	...	16.769 \pm 0.002	18.294 \pm 0.011	15.529 \pm 0.005	368.3 $^{+8.0}_{-7.7}$	0.323 \pm 0.026
2MASS J07501009-4720325	117.5421	-47.3424	2.512 \pm 0.015	-4.849 \pm 0.027	8.917 \pm 0.027	20.53 \pm 0.25	13.044 \pm 0.001	13.673 \pm 0.003	12.290 \pm 0.002	393.5 \pm 2.3	0.780 \pm 0.045
...	117.5461	-46.1850	2.502 \pm 0.072	-4.47 \pm 0.14	9.16 \pm 0.13	...	17.045 \pm 0.001	18.657 \pm 0.016	15.792 \pm 0.003	396 $^{+12}_{-11}$	0.283 \pm 0.023
...	117.5488	-46.3001	2.433 \pm 0.063	-4.72 \pm 0.12	9.08 \pm 0.12	...	16.658 \pm 0.001	18.251 \pm 0.021	15.404 \pm 0.003	407 $^{+11}_{-10}$	0.294 \pm 0.024
...	117.5499	-44.9103	2.484 \pm 0.080	-4.69 \pm 0.14	9.24 \pm 0.15	...	17.158 \pm 0.001	18.968 \pm 0.018	15.870 \pm 0.003	399 $^{+13}_{-12}$	0.224 \pm 0.018
...	117.5511	-46.2479	2.539 \pm 0.057	-4.82 \pm 0.11	8.17 \pm 0.10	...	16.633 \pm 0.001	18.104 \pm 0.021	15.403 \pm 0.003	389.8 $^{+8.9}_{-8.5}$	0.352 \pm 0.028
2MASS J07501518-4616033	117.5633	-46.2676	2.498 \pm 0.022	-4.523 \pm 0.042	9.883 \pm 0.039	19.50 \pm 0.16	11.766 \pm 0.000	12.061 \pm 0.001	11.323 \pm 0.001	395.8 $^{+3.5}_{-3.4}$	1.060 \pm 0.053
...	117.5735	-47.0155	2.464 \pm 0.072	-4.79 \pm 0.13	9.59 \pm 0.11	...	16.064 \pm 0.001	17.763 \pm 0.008	14.796 \pm 0.002	402 $^{+12}_{-11}$	0.257 \pm 0.021
...	117.5979	-47.2990	2.554 \pm 0.063	-4.67 \pm 0.12	8.91 \pm 0.12	...	16.832 \pm 0.002	18.384 \pm 0.013	15.590 \pm 0.006	387.6 $^{+9.8}_{-9.4}$	0.313 \pm 0.025
TYC 8142-1598-1	117.5998	-48.8920	2.521 \pm 0.032	-4.855 \pm 0.054	8.358 \pm 0.052	19.7 \pm 2.8	10.713 \pm 0.000	10.873 \pm 0.001	10.459 \pm 0.001	392.2 $^{+5.0}_{-4.9}$	1.460 \pm 0.073
...	117.6112	-46.8090	2.488 \pm 0.080	-4.74 \pm 0.14	9.00 \pm 0.13	...	16.976 \pm 0.001	18.772 \pm 0.017	15.671 \pm 0.003	398 $^{+13}_{-12}$	0.223 \pm 0.018

Table B.4: Yep 1—Continued

Star Name	RA ($^{\circ}$)	Dec ($^{\circ}$)	Parallax (mas)	μ_{α} (mas yr^{-1})	μ_{δ} (mas yr^{-1})	v_r (km s^{-1})	G (mag)	BP (mag)	RP (mag)	d (pc)	Mass (M_{\odot})
2MASS J07502910-4757434	117.6213	-47.9621	2.494 \pm 0.025	-4.654 \pm 0.049	8.598 \pm 0.048	14.0 \pm 3.1	12.336 \pm 0.002	12.855 \pm 0.009	11.674 \pm 0.007	396.4 $^{+4.0}_{-3.9}$	0.860 \pm 0.060
...	117.6715	-46.3521	2.424 \pm 0.080	-4.79 \pm 0.15	8.91 \pm 0.14	...	16.849 \pm 0.001	18.695 \pm 0.032	15.514 \pm 0.003	408 $^{+14}_{-13}$	0.208 \pm 0.017
...	117.6849	-46.3122	2.478 \pm 0.055	-4.73 \pm 0.11	8.611 \pm 0.097	...	16.414 \pm 0.003	17.872 \pm 0.023	15.218 \pm 0.007	399.3 $^{+9.0}_{-8.6}$	0.364 \pm 0.029
HD 64248	117.6908	-46.3267	2.405 \pm 0.037	-4.858 \pm 0.070	8.967 \pm 0.065	...	8.539 \pm 0.001	8.534 \pm 0.002	8.566 \pm 0.002	411.0 $^{+6.3}_{-6.1}$	2.75 \pm 0.94
...	117.6967	-46.5099	2.562 \pm 0.062	-4.47 \pm 0.13	9.34 \pm 0.12	...	16.927 \pm 0.020	18.482 \pm 0.086	15.645 \pm 0.057	386.4 $^{+9.5}_{-9.1}$	0.298 \pm 0.040
...	117.7346	-47.1084	2.499 \pm 0.070	-4.18 \pm 0.13	9.12 \pm 0.11	...	16.682 \pm 0.001	18.258 \pm 0.015	15.454 \pm 0.004	396 \pm 11	0.310 \pm 0.025
...	117.7805	-47.8474	2.576 \pm 0.039	-4.354 \pm 0.065	8.853 \pm 0.064	...	15.530 \pm 0.002	16.647 \pm 0.010	14.473 \pm 0.004	384.1 $^{+5.9}_{-5.7}$	0.517 \pm 0.041
HD 64318	117.8082	-47.2164	2.423 \pm 0.048	-4.418 \pm 0.086	8.358 \pm 0.089	101.9 \pm 7.2	6.482 \pm 0.000	6.452 \pm 0.003	6.572 \pm 0.003	408.1 $^{+8.2}_{-7.9}$	4.70 \pm 0.74
...	117.8093	-47.2285	2.566 \pm 0.061	-4.23 \pm 0.11	8.72 \pm 0.10	...	16.800 \pm 0.002	18.235 \pm 0.025	15.562 \pm 0.004	385.7 $^{+9.4}_{-9.0}$	0.359 \pm 0.029
...	117.8095	-46.1114	2.465 \pm 0.059	-5.05 \pm 0.11	9.23 \pm 0.10	...	16.284 \pm 0.002	17.659 \pm 0.016	15.116 \pm 0.003	401.3 $^{+9.8}_{-9.4}$	0.395 \pm 0.032
...	117.8134	-46.3057	2.393 \pm 0.067	-4.74 \pm 0.13	8.57 \pm 0.13	...	16.625 \pm 0.002	18.335 \pm 0.018	15.347 \pm 0.004	413 $^{+12}_{-11}$	0.252 \pm 0.020
...	117.8145	-47.1159	2.620 \pm 0.032	-4.541 \pm 0.062	9.096 \pm 0.054	...	15.293 \pm 0.004	16.412 \pm 0.020	14.203 \pm 0.010	377.5 $^{+4.7}_{-4.6}$	0.512 \pm 0.041
...	117.8279	-46.0427	2.492 \pm 0.021	-4.947 \pm 0.034	9.255 \pm 0.033	...	13.892 \pm 0.001	14.774 \pm 0.003	13.132 \pm 0.002	396.6 $^{+3.3}_{-3.2}$	0.692 \pm 0.055
...	117.8307	-46.0844	2.427 \pm 0.070	-4.91 \pm 0.12	8.75 \pm 0.12	...	16.626 \pm 0.001	18.129 \pm 0.014	15.426 \pm 0.003	408 $^{+12}_{-11}$	0.351 \pm 0.028
...	117.8318	-45.4455	2.694 \pm 0.065	-4.62 \pm 0.12	9.14 \pm 0.13	...	16.765 \pm 0.001	18.533 \pm 0.016	15.472 \pm 0.003	367.6 $^{+9.1}_{-8.7}$	0.233 \pm 0.019
...	117.8404	-45.8966	2.446 \pm 0.056	-4.821 \pm 0.085	9.264 \pm 0.090	...	15.809 \pm 0.001	17.093 \pm 0.009	14.681 \pm 0.003	404.4 $^{+9.4}_{-9.0}$	0.428 \pm 0.034
...	117.8463	-44.9587	2.398 \pm 0.031	-5.199 \pm 0.057	8.895 \pm 0.055	...	15.140 \pm 0.006	16.279 \pm 0.029	14.040 \pm 0.019	412.1 $^{+5.4}_{-5.3}$	0.489 \pm 0.039
...	117.8509	-47.3173	2.510 \pm 0.070	-4.61 \pm 0.13	9.28 \pm 0.14	...	16.701 \pm 0.002	18.167 \pm 0.019	15.491 \pm 0.004	394 \pm 11	0.359 \pm 0.029
...	117.8582	-47.8019	2.466 \pm 0.047	-4.699 \pm 0.078	8.456 \pm 0.091	...	16.134 \pm 0.001	17.496 \pm 0.009	14.970 \pm 0.003	401.1 $^{+7.7}_{-7.5}$	0.400 \pm 0.032

Table B.4: Yep 1—Continued

Star Name	RA ($^{\circ}$)	Dec ($^{\circ}$)	Parallax (mas)	μ_{α} (mas yr $^{-1}$)	μ_{δ} (mas yr $^{-1}$)	v_r (km s $^{-1}$)	G (mag)	BP (mag)	RP (mag)	d (pc)	Mass (M $_{\odot}$)
TYC 8138-2890-1	117.8802	-47.3131	2.489 \pm 0.024	-4.718 \pm 0.040	8.787 \pm 0.048	20.81 \pm 0.21	12.190 \pm 0.003	12.694 \pm 0.009	11.535 \pm 0.007	397.2 $^{+3.9}_{-3.8}$	0.860 \pm 0.043
TYC 8138-3251-1	117.8811	-47.0957	2.513 \pm 0.034	-5.038 \pm 0.061	8.597 \pm 0.088	...	10.360 \pm 0.001	10.468 \pm 0.002	10.193 \pm 0.001	393.5 $^{+5.4}_{-5.2}$	2.05 \pm 0.10
...	117.8891	-45.6224	2.575 \pm 0.025	-4.646 \pm 0.042	9.103 \pm 0.042	...	14.605 \pm 0.002	15.417 \pm 0.007	13.717 \pm 0.005	384.0 $^{+3.8}_{-3.7}$	0.680 \pm 0.054
...	117.9098	-47.2936	2.532 \pm 0.080	-4.57 \pm 0.14	8.86 \pm 0.15	...	16.928 \pm 0.001	18.427 \pm 0.019	15.665 \pm 0.005	391 $^{+13}_{-12}$	0.324 \pm 0.026
...	117.9122	-46.6685	2.507 \pm 0.032	-4.743 \pm 0.066	8.957 \pm 0.060	...	15.300 \pm 0.001	16.589 \pm 0.012	14.449 \pm 0.004	394.5 $^{+5.1}_{-5.0}$	0.528 \pm 0.042
...	117.9140	-46.6813	2.491 \pm 0.048	-4.682 \pm 0.094	8.779 \pm 0.088	...	16.028 \pm 0.004	17.303 \pm 0.024	14.894 \pm 0.008	397.1 $^{+7.8}_{-7.5}$	0.429 \pm 0.034
...	117.9151	-47.2730	2.416 \pm 0.073	-4.58 \pm 0.13	8.80 \pm 0.14	...	16.689 \pm 0.001	18.363 \pm 0.018	15.420 \pm 0.003	410 $^{+13}_{-12}$	0.263 \pm 0.021
...	117.9494	-47.0539	2.467 \pm 0.062	-4.79 \pm 0.12	8.66 \pm 0.12	...	16.663 \pm 0.001	18.218 \pm 0.017	15.417 \pm 0.003	401 $^{+10}_{-9.9}$	0.310 \pm 0.025
HD 64461	117.9530	-47.2521	2.467 \pm 0.037	-4.915 \pm 0.060	9.172 \pm 0.074	...	9.844 \pm 0.001	9.852 \pm 0.007	9.622 \pm 0.011	400.8 $^{+6.1}_{-5.9}$	2.05 \pm 0.10
...	117.9562	-46.5816	2.573 \pm 0.045	-4.721 \pm 0.088	8.778 \pm 0.085	...	16.229 \pm 0.002	17.566 \pm 0.014	15.070 \pm 0.009	384.5 $^{+6.9}_{-6.7}$	0.407 \pm 0.033
...	117.9744	-48.7128	2.438 \pm 0.023	-4.389 \pm 0.044	8.070 \pm 0.043	...	14.991 \pm 0.002	15.932 \pm 0.010	14.018 \pm 0.007	405.5 $^{+3.8}_{-3.7}$	0.595 \pm 0.048
...	117.9781	-46.1975	2.488 \pm 0.038	-4.786 \pm 0.077	8.992 \pm 0.074	...	15.296 \pm 0.002	16.391 \pm 0.011	14.246 \pm 0.006	397.4 $^{+6.1}_{-5.9}$	0.526 \pm 0.042
...	117.9923	-47.3442	2.540 \pm 0.075	-4.10 \pm 0.14	8.65 \pm 0.13	...	16.501 \pm 0.001	18.321 \pm 0.013	15.189 \pm 0.003	390 $^{+12}_{-11}$	0.218 \pm 0.017
...	117.9967	-45.9820	2.401 \pm 0.070	-4.62 \pm 0.11	8.94 \pm 0.14	...	16.311 \pm 0.004	17.880 \pm 0.020	15.056 \pm 0.011	412 \pm 12	0.302 \pm 0.024
2MASS J07520153-4850080	118.0064	-48.8356	2.496 \pm 0.025	-4.506 \pm 0.044	8.276 \pm 0.042	20.9 \pm 1.0	11.781 \pm 0.001	12.137 \pm 0.002	11.276 \pm 0.001	396.1 $^{+4.0}_{-3.9}$	1.060 \pm 0.053
...	118.0244	-48.3767	2.614 \pm 0.020	-4.213 \pm 0.040	8.435 \pm 0.037	...	14.094 \pm 0.002	14.928 \pm 0.008	13.174 \pm 0.005	378.4 $^{+3.0}_{-2.9}$	0.664 \pm 0.053
2MASS J07520589-4822321	118.0246	-48.3756	2.546 \pm 0.013	-4.328 \pm 0.025	8.971 \pm 0.025	17.8 \pm 1.4	13.251 \pm 0.003	13.810 \pm 0.010	12.538 \pm 0.009	388.3 \pm 2.0	0.806 \pm 0.064
...	118.0253	-49.1881	2.485 \pm 0.070	-4.72 \pm 0.14	8.57 \pm 0.14	...	17.081 \pm 0.001	18.669 \pm 0.022	15.811 \pm 0.005	398 $^{+12}_{-11}$	0.284 \pm 0.023

Table B.4: Yep 1—Continued

Star Name	RA ($^{\circ}$)	Dec ($^{\circ}$)	Parallax (mas)	μ_{α} (mas yr^{-1})	μ_{δ} (mas yr^{-1})	v_r (km s^{-1})	G (mag)	BP (mag)	RP (mag)	d (pc)	Mass (M_{\odot})
...	118.0412	-47.9173	2.442 \pm 0.077	-4.41 \pm 0.14	8.52 \pm 0.14	...	16.893 \pm 0.002	18.525 \pm 0.019	15.632 \pm 0.005	405 $^{+13}_{-12}$	0.275 \pm 0.022
...	118.0722	-45.5746	2.486 \pm 0.046	-4.837 \pm 0.082	9.106 \pm 0.087	...	16.020 \pm 0.002	17.267 \pm 0.013	14.904 \pm 0.005	397.9 $^{+7.4}_{-7.1}$	0.440 \pm 0.035
HD 64578	118.0757	-48.6853	2.532 \pm 0.044	-4.632 \pm 0.091	7.975 \pm 0.086	13.5 \pm 4.1	8.711 \pm 0.000	8.711 \pm 0.002	8.740 \pm 0.002	390.6 $^{+6.9}_{-6.7}$	3.38 \pm 0.58
...	118.0813	-48.6887	2.572 \pm 0.068	-4.41 \pm 0.14	8.33 \pm 0.13	...	16.808 \pm 0.003	18.263 \pm 0.039	15.550 \pm 0.009	385 $^{+10}_{-9.9}$	0.348 \pm 0.028
...	118.1028	-46.2622	2.565 \pm 0.054	-4.76 \pm 0.11	9.00 \pm 0.13	...	16.207 \pm 0.002	17.621 \pm 0.018	15.011 \pm 0.005	385.8 $^{+8.2}_{-7.9}$	0.377 \pm 0.030
...	118.1072	-46.1113	2.516 \pm 0.036	-4.804 \pm 0.059	8.786 \pm 0.074	...	15.288 \pm 0.003	16.407 \pm 0.013	14.225 \pm 0.007	393.1 $^{+5.6}_{-5.5}$	0.514 \pm 0.041
...	118.1155	-46.8836	2.496 \pm 0.065	-4.78 \pm 0.12	8.73 \pm 0.15	...	16.601 \pm 0.001	17.980 \pm 0.026	15.310 \pm 0.007	396 $^{+11}_{-10}$	0.360 \pm 0.029
...	118.1225	-46.5825	2.556 \pm 0.017	-4.781 \pm 0.034	9.079 \pm 0.040	...	14.137 \pm 0.004	14.897 \pm 0.014	13.237 \pm 0.009	386.9 \pm 2.6	0.690 \pm 0.055
...	118.1431	-47.7632	2.399 \pm 0.033	-4.687 \pm 0.065	8.479 \pm 0.068	...	15.216 \pm 0.003	16.241 \pm 0.012	14.202 \pm 0.009	412.0 $^{+5.7}_{-5.6}$	0.555 \pm 0.044
...	118.1566	-46.4725	2.523 \pm 0.045	-4.797 \pm 0.078	9.00 \pm 0.11	...	15.691 \pm 0.003	16.977 \pm 0.013	14.549 \pm 0.006	392.1 $^{+7.2}_{-6.9}$	0.424 \pm 0.034
...	118.1722	-46.4883	2.568 \pm 0.045	-4.812 \pm 0.080	8.92 \pm 0.11	...	15.972 \pm 0.001	17.253 \pm 0.012	14.839 \pm 0.003	385.3 $^{+6.9}_{-6.7}$	0.428 \pm 0.034
TYC 8139-589-1	118.1961	-47.2166	2.484 \pm 0.023	-4.866 \pm 0.045	8.907 \pm 0.048	20.5 \pm 8.2	10.889 \pm 0.000	11.091 \pm 0.001	10.571 \pm 0.001	398.0 \pm 3.6	1.460 \pm 0.073
...	118.2247	-47.4604	2.462 \pm 0.022	-4.474 \pm 0.037	8.476 \pm 0.050	...	14.610 \pm 0.003	15.486 \pm 0.009	13.670 \pm 0.007	401.5 $^{+3.6}_{-3.5}$	0.652 \pm 0.052
HD 64699	118.2523	-45.9512	2.517 \pm 0.035	-4.799 \pm 0.063	9.168 \pm 0.072	...	9.718 \pm 0.000	9.772 \pm 0.002	9.655 \pm 0.002	392.9 $^{+5.5}_{-5.3}$	2.05 \pm 0.10
...	118.2910	-46.1596	2.534 \pm 0.072	-4.80 \pm 0.12	8.79 \pm 0.14	...	16.635 \pm 0.002	18.226 \pm 0.015	15.399 \pm 0.005	391 \pm 11	0.301 \pm 0.024
...	118.3337	-47.7698	2.484 \pm 0.065	-4.89 \pm 0.13	8.46 \pm 0.12	...	16.719 \pm 0.002	18.176 \pm 0.022	15.481 \pm 0.005	398 $^{+11}_{-10}$	0.353 \pm 0.028
...	118.3415	-47.2576	2.524 \pm 0.043	-4.80 \pm 0.11	8.835 \pm 0.086	...	15.940 \pm 0.001	17.188 \pm 0.012	14.810 \pm 0.004	392.0 $^{+6.8}_{-6.5}$	0.436 \pm 0.035
TYC 8139-2616-1	118.3423	-47.2249	2.628 \pm 0.023	-5.013 \pm 0.046	8.746 \pm 0.047	21.1 \pm 1.4	10.982 \pm 0.000	11.293 \pm 0.001	10.530 \pm 0.001	376.4 \pm 3.3	1.460 \pm 0.073
...	118.3444	-48.6796	2.474 \pm 0.068	-4.42 \pm 0.13	8.28 \pm 0.14	...	16.610 \pm 0.002	18.187 \pm 0.014	15.369 \pm 0.005	400. \pm 11	0.304 \pm 0.024

Table B.4: Yep 1—Continued

Star Name	<i>RA</i> ($^{\circ}$)	<i>Dec</i> ($^{\circ}$)	Parallax (mas)	μ_{α} (mas yr $^{-1}$)	μ_{δ} (mas yr $^{-1}$)	v_r (km s $^{-1}$)	G (mag)	BP (mag)	RP (mag)	<i>d</i> (pc)	Mass (M $_{\odot}$)
...	118.3498	-48.0738	2.477 \pm 0.049	-4.836 \pm 0.090	8.76 \pm 0.10	...	15.599 \pm 0.002	16.952 \pm 0.010	14.413 \pm 0.004	399.3 $^{+8.0}_{-7.7}$	0.396 \pm 0.032
HD 64780	118.3528	-46.9659	2.473 \pm 0.030	-4.650 \pm 0.052	8.704 \pm 0.057	...	9.655 \pm 0.000	9.702 \pm 0.001	9.592 \pm 0.001	399.8 $^{+4.9}_{-4.8}$	2.18 \pm 0.35
...	118.3558	-46.5009	2.444 \pm 0.059	-4.76 \pm 0.12	8.87 \pm 0.13	...	16.219 \pm 0.003	17.595 \pm 0.020	15.057 \pm 0.011	405 $^{+10.}_{-9.6}$	0.396 \pm 0.032
...	118.3576	-47.9314	2.498 \pm 0.057	-4.52 \pm 0.11	8.83 \pm 0.13	...	16.265 \pm 0.002	17.706 \pm 0.022	15.057 \pm 0.006	396.0 $^{+9.1}_{-8.7}$	0.366 \pm 0.029
...	118.3664	-45.2313	2.585 \pm 0.053	-4.896 \pm 0.090	9.02 \pm 0.13	...	16.326 \pm 0.002	17.694 \pm 0.012	15.171 \pm 0.005	382.8 $^{+8.0}_{-7.7}$	0.400 \pm 0.032
...	118.3843	-46.6144	2.606 \pm 0.061	-4.70 \pm 0.11	8.64 \pm 0.12	...	16.480 \pm 0.001	17.975 \pm 0.010	15.274 \pm 0.003	379.8 $^{+9.0}_{-8.6}$	0.352 \pm 0.028
...	118.3844	-47.0129	2.441 \pm 0.043	-4.583 \pm 0.081	8.506 \pm 0.079	...	16.033 \pm 0.001	17.354 \pm 0.011	14.888 \pm 0.003	405.0 $^{+7.2}_{-6.9}$	0.415 \pm 0.033
...	118.4074	-46.4769	2.614 \pm 0.054	-4.61 \pm 0.10	8.67 \pm 0.13	...	15.948 \pm 0.002	17.226 \pm 0.008	14.828 \pm 0.004	378.6 $^{+7.9}_{-7.6}$	0.432 \pm 0.035
...	118.4728	-46.2747	2.550 \pm 0.074	-4.80 \pm 0.14	8.88 \pm 0.15	...	16.824 \pm 0.002	18.312 \pm 0.020	15.605 \pm 0.004	388 $^{+12}_{-11}$	0.350 \pm 0.028
...	118.4746	-46.2750	2.535 \pm 0.041	-4.763 \pm 0.081	8.930 \pm 0.081	...	15.473 \pm 0.001	16.729 \pm 0.009	14.352 \pm 0.003	390.2 $^{+6.4}_{-6.2}$	0.436 \pm 0.035
2MASS J07540255-4608574	118.5107	-46.1493	2.618 \pm 0.022	-4.533 \pm 0.039	9.517 \pm 0.042	19.52 \pm 0.49	12.530 \pm 0.018	12.937 \pm 0.064	11.912 \pm 0.049	377.8 \pm 3.2	1.030 \pm 0.052
TYC 8139-3353-1	118.5110	-48.3601	2.464 \pm 0.025	-4.793 \pm 0.051	8.107 \pm 0.050	22.70 \pm 0.95	11.912 \pm 0.003	12.308 \pm 0.008	11.354 \pm 0.007	401.1 $^{+4.2}_{-4.1}$	1.030 \pm 0.052
...	118.5138	-46.7107	2.394 \pm 0.086	-4.64 \pm 0.14	8.84 \pm 0.15	...	17.013 \pm 0.001	18.494 \pm 0.057	15.778 \pm 0.005	414 $^{+15}_{-14}$	0.347 \pm 0.028
...	118.5353	-46.5955	2.554 \pm 0.018	-5.097 \pm 0.034	8.129 \pm 0.032	...	13.961 \pm 0.003	14.826 \pm 0.010	13.041 \pm 0.006	387.2 \pm 2.7	0.673 \pm 0.054
...	118.5399	-46.0614	2.589 \pm 0.058	-4.86 \pm 0.10	8.82 \pm 0.12	...	16.279 \pm 0.001	17.688 \pm 0.011	15.099 \pm 0.004	382.3 $^{+8.8}_{-8.4}$	0.382 \pm 0.031
2MASS J07541482-4626003	118.5617	-46.4334	2.542 \pm 0.024	-4.737 \pm 0.043	9.120 \pm 0.042	21.30 \pm 0.40	12.889 \pm 0.014	13.519 \pm 0.049	12.105 \pm 0.038	389.0 $^{+3.7}_{-3.6}$	0.753 \pm 0.060
TYC 8135-458-1	118.5932	-46.7861	2.516 \pm 0.030	-4.733 \pm 0.061	8.749 \pm 0.049	26.8 \pm 2.2	10.486 \pm 0.000	10.617 \pm 0.001	10.282 \pm 0.001	393.0 $^{+4.7}_{-4.6}$	1.500 \pm 0.075
2MASS J07542550-4651134	118.6063	-46.8537	2.536 \pm 0.026	-4.685 \pm 0.044	9.056 \pm 0.041	19.49 \pm 0.59	12.863 \pm 0.003	13.429 \pm 0.010	12.160 \pm 0.005	390.0 $^{+4.0}_{-3.9}$	0.985 \pm 0.049

Table B.4: Yep 1—Continued

Star Name	RA ($^{\circ}$)	Dec ($^{\circ}$)	Parallax (mas)	μ_{α} (mas yr^{-1})	μ_{δ} (mas yr^{-1})	v_r (km s^{-1})	G (mag)	BP (mag)	RP (mag)	d (pc)	Mass (M_{\odot})
...	118.6071	-48.7747	2.455 ± 0.077	-4.47 ± 0.15	8.11 ± 0.14	...	17.127 ± 0.002	18.765 ± 0.026	15.839 ± 0.007	403 $^{+13}_{-12}$	0.267 ± 0.021
...	118.6368	-47.9588	2.500 ± 0.070	-4.37 ± 0.13	8.31 ± 0.11	...	16.820 ± 0.003	18.421 ± 0.030	15.567 ± 0.009	396 ± 11	0.291 ± 0.023
...	118.6972	-46.7901	2.477 ± 0.044	-4.807 ± 0.081	9.103 ± 0.085	...	14.759 ± 0.003	15.719 ± 0.011	13.786 ± 0.007	399.2 $^{+7.2}_{-7.0}$	0.587 ± 0.047
...	118.7041	-46.8426	2.502 ± 0.030	-4.887 ± 0.054	8.718 ± 0.057	...	15.138 ± 0.003	16.219 ± 0.017	14.095 ± 0.008	395.2 $^{+4.7}_{-4.6}$	0.533 ± 0.043
...	118.7699	-47.7560	2.422 ± 0.076	-4.70 ± 0.14	8.43 ± 0.13	...	16.923 ± 0.001	18.452 ± 0.021	15.684 ± 0.004	409 $^{+13}_{-12}$	0.322 ± 0.026
TYC 8135-4862-1	118.7784	-46.6902	2.416 ± 0.025	-4.391 ± 0.046	8.686 ± 0.049	...	10.476 ± 0.000	10.615 ± 0.001	10.253 ± 0.001	409.0 $^{+4.3}_{-4.2}$	1.860 ± 0.093
...	118.7938	-47.3101	2.652 ± 0.033	-5.043 ± 0.064	9.016 ± 0.061	...	15.590 ± 0.004	16.808 ± 0.018	14.479 ± 0.011	373.2 $^{+4.7}_{-4.6}$	0.451 ± 0.036
...	118.8260	-47.6132	2.599 ± 0.078	-4.66 ± 0.14	8.48 ± 0.13	...	17.184 ± 0.001	18.880 ± 0.023	15.903 ± 0.002	381 $^{+12}_{-11}$	0.254 ± 0.020
...	118.8304	-46.5190	2.588 ± 0.048	-4.683 ± 0.090	9.115 ± 0.094	...	16.008 ± 0.002	17.304 ± 0.011	14.879 ± 0.004	382.4 $^{+7.2}_{-6.9}$	0.425 ± 0.034
...	118.8306	-46.5125	2.506 ± 0.027	-4.591 ± 0.051	8.640 ± 0.044	...	14.953 ± 0.002	15.711 ± 0.042	13.757 ± 0.033	394.5 $^{+4.2}_{-4.1}$	0.578 ± 0.046
...	118.8367	-47.0033	2.388 ± 0.064	-4.53 ± 0.14	8.67 ± 0.12	...	16.686 ± 0.001	18.220 ± 0.021	15.456 ± 0.004	414 ± 11	0.324 ± 0.026
...	118.8474	-45.9573	2.569 ± 0.066	-4.84 ± 0.11	9.42 ± 0.11	...	16.506 ± 0.001	17.939 ± 0.008	15.320 ± 0.003	385 $^{+10}_{-9.7}$	0.374 ± 0.030
...	118.8487	-47.0433	2.596 ± 0.075	-4.67 ± 0.16	8.81 ± 0.14	...	16.752 ± 0.001	18.324 ± 0.022	15.525 ± 0.004	381 ± 11	0.311 ± 0.025
...	118.8874	-46.6117	2.723 ± 0.052	-4.495 ± 0.097	9.075 ± 0.089	...	15.972 ± 0.001	17.427 ± 0.008	14.777 ± 0.003	363.6 $^{+7.1}_{-6.8}$	0.366 ± 0.029
...	119.0214	-47.1319	2.544 ± 0.021	-4.749 ± 0.041	8.980 ± 0.041	...	14.684 ± 0.002	15.577 ± 0.011	13.745 ± 0.007	388.7 $^{+3.2}_{-3.1}$	0.641 ± 0.051
...	119.0351	-46.6808	2.517 ± 0.019	-4.789 ± 0.031	8.745 ± 0.028	...	13.787 ± 0.003	14.494 ± 0.010	12.974 ± 0.009	392.9 $^{+3.0}_{-2.9}$	0.715 ± 0.057
...	119.0535	-46.3372	2.586 ± 0.076	-4.99 ± 0.15	8.69 ± 0.15	...	17.004 ± 0.003	18.639 ± 0.031	15.745 ± 0.007	383 $^{+12}_{-11}$	0.275 ± 0.022
...	119.0894	-47.6845	2.517 ± 0.054	-4.43 ± 0.10	8.18 ± 0.10	...	16.319 ± 0.002	17.730 ± 0.014	15.140 ± 0.006	393.0 $^{+8.5}_{-8.2}$	0.382 ± 0.031
...	119.0921	-47.1774	2.460 ± 0.046	-4.426 ± 0.098	8.312 ± 0.086	...	15.806 ± 0.001	16.939 ± 0.009	14.738 ± 0.004	402.0 $^{+7.6}_{-7.3}$	0.518 ± 0.041

Table B.4: Yep 1—Continued

Star Name	RA ($^{\circ}$)	Dec ($^{\circ}$)	Parallax (mas)	μ_{α} (mas yr $^{-1}$)	μ_{δ} (mas yr $^{-1}$)	v_r (km s $^{-1}$)	G (mag)	BP (mag)	RP (mag)	d (pc)	Mass (M $_{\odot}$)
TYC 8139-4265-1	11.1010	-46.8799	2.516 \pm 0.034	-4.617 \pm 0.057	8.734 \pm 0.059	17.7 \pm 2.5	10.653 \pm 0.001	10.781 \pm 0.002	10.452 \pm 0.001	393.0 $^{+5.3}_{-5.1}$	1.770 \pm 0.089
...	11.1010	-45.9914	2.647 \pm 0.071	-4.71 \pm 0.13	9.48 \pm 0.13	...	17.136 \pm 0.001	18.772 \pm 0.036	15.885 \pm 0.005	374 $^{+10.1}_{-9.8}$	0.277 \pm 0.022
...	11.1049	-46.4844	2.581 \pm 0.071	-4.64 \pm 0.13	8.93 \pm 0.13	...	16.446 \pm 0.002	18.261 \pm 0.023	15.147 \pm 0.006	384 $^{+11.1}_{-10.1}$	0.222 \pm 0.018
...	11.1111	-47.6713	2.389 \pm 0.074	-4.37 \pm 0.14	8.23 \pm 0.15	...	16.981 \pm 0.001	18.699 \pm 0.019	15.688 \pm 0.003	414 $^{+13.1}_{-12.1}$	0.246 \pm 0.020
...	11.2689	-46.5951	2.474 \pm 0.019	-4.790 \pm 0.034	8.639 \pm 0.032	...	14.399 \pm 0.004	15.163 \pm 0.013	13.513 \pm 0.012	399.6 \pm 3.0	0.691 \pm 0.055
TYC 8139-2296-1	11.2916	-47.5242	2.474 \pm 0.028	-4.346 \pm 0.048	8.388 \pm 0.048	21.6 \pm 3.3	10.964 \pm 0.001	11.202 \pm 0.001	10.598 \pm 0.001	399.6 $^{+4.5}_{-4.4}$	1.46 \pm 0.12
...	11.3390	-46.6412	2.618 \pm 0.046	-4.901 \pm 0.082	8.630 \pm 0.087	...	16.022 \pm 0.001	17.297 \pm 0.011	14.889 \pm 0.003	378.1 $^{+6.7}_{-6.5}$	0.429 \pm 0.034
...	11.3471	-47.6316	2.526 \pm 0.029	-4.791 \pm 0.054	8.934 \pm 0.053	...	14.826 \pm 0.002	15.780 \pm 0.010	13.856 \pm 0.006	391.5 $^{+4.6}_{-4.5}$	0.590 \pm 0.047
HD 65658	11.4086	-46.5933	2.511 \pm 0.061	-5.04 \pm 0.11	8.98 \pm 0.12	-42.0 \pm 5.2	7.219 \pm 0.001	7.175 \pm 0.003	7.350 \pm 0.003	394.1 $^{+9.8}_{-9.4}$	4.70 \pm 0.74
...	11.4967	-46.9539	2.55 \pm 0.14	-4.80 \pm 0.26	8.75 \pm 0.31	...	18.096 \pm 0.003	19.947 \pm 0.079	16.742 \pm 0.010	390. $^{+23}_{-20.1}$	0.203 \pm 0.020
...	11.6266	-46.3063	2.439 \pm 0.087	-4.53 \pm 0.16	9.24 \pm 0.18	...	17.257 \pm 0.001	19.049 \pm 0.032	15.943 \pm 0.011	406 $^{+15}_{-14}$	0.224 \pm 0.018
...	11.6847	-46.7454	2.47 \pm 0.11	-4.46 \pm 0.23	9.32 \pm 0.25	...	17.989 \pm 0.002	19.667 \pm 0.086	16.509 \pm 0.012	401 $^{+19}_{-18}$	0.212 \pm 0.022
...	11.7401	-46.1735	2.62 \pm 0.14	-4.65 \pm 0.26	9.83 \pm 0.27	...	18.259 \pm 0.006	20.35 \pm 0.10	16.906 \pm 0.008	379 $^{+22}_{-20.1}$	0.166 \pm 0.013
...	11.8312	-45.9456	2.63 \pm 0.12	-4.23 \pm 0.19	9.15 \pm 0.26	...	17.591 \pm 0.002	19.284 \pm 0.065	16.271 \pm 0.007	378 $^{+17}_{-16}$	0.245 \pm 0.021
...	11.8472	-46.4525	2.62 \pm 0.14	-5.12 \pm 0.29	9.31 \pm 0.32	...	17.841 \pm 0.000	19.678 \pm 0.090	16.520 \pm 0.005	380. $^{+22}_{-20.1}$	0.213 \pm 0.023
...	11.9858	-46.7602	2.44 \pm 0.11	-4.38 \pm 0.21	9.30 \pm 0.24	...	17.806 \pm 0.002	19.317 \pm 0.020	16.597 \pm 0.007	407 $^{+20}_{-18}$	0.339 \pm 0.027
...	116.0307	-45.9421	2.45 \pm 0.15	-4.51 \pm 0.26	8.45 \pm 0.30	...	18.345 \pm 0.012	20.13 \pm 0.10	17.004 \pm 0.006	405 $^{+26}_{-23}$	0.219 \pm 0.025
...	116.0390	-46.8562	2.565 \pm 0.088	-4.78 \pm 0.16	8.48 \pm 0.16	...	17.168 \pm 0.004	18.770 \pm 0.025	15.903 \pm 0.004	386 $^{+14}_{-13}$	0.282 \pm 0.023

Table B.4: Yep 1—Continued

Star Name	RA ($^{\circ}$)	Dec ($^{\circ}$)	Parallax (mas)	μ_{α} (mas yr $^{-1}$)	μ_{δ} (mas yr $^{-1}$)	v_r (km s $^{-1}$)	G (mag)	BP (mag)	RP (mag)	d (pc)	Mass (M $_{\odot}$)
...	116.0460	-45.5687	2.590 \pm 0.081	-4.87 \pm 0.15	9.68 \pm 0.17	...	17.170 \pm 0.009	18.827 \pm 0.018	15.903 \pm 0.007	382 \pm 12	0.268 \pm 0.021
...	116.0756	-47.3089	2.45 \pm 0.10	-4.85 \pm 0.16	9.29 \pm 0.16	...	17.146 \pm 0.001	18.827 \pm 0.041	15.873 \pm 0.004	405 $^{+18}_{-16}$	0.260 \pm 0.021
...	116.1985	-45.9083	2.42 \pm 0.13	-4.77 \pm 0.24	8.98 \pm 0.30	...	17.862 \pm 0.011	19.172 \pm 0.060	16.487 \pm 0.009	410 $^{+24}_{-21}$	0.356 \pm 0.029
...	116.2313	-45.7268	2.55 \pm 0.11	-4.61 \pm 0.22	9.45 \pm 0.22	...	17.960 \pm 0.014	19.732 \pm 0.072	16.630 \pm 0.008	390 $^{+18}_{-17}$	0.223 \pm 0.020
...	116.2350	-44.9066	2.542 \pm 0.087	-4.81 \pm 0.16	9.25 \pm 0.14	...	16.920 \pm 0.009	18.727 \pm 0.019	15.618 \pm 0.002	390 $^{+14}_{-13}$	0.223 \pm 0.018
...	116.2613	-46.4024	2.50 \pm 0.17	-4.34 \pm 0.31	9.25 \pm 0.27	...	18.547 \pm 0.008	20.51 \pm 0.11	17.141 \pm 0.009	398 $^{+29}_{-26}$	0.175 \pm 0.016
...	116.3301	-46.4133	2.62 \pm 0.13	-4.60 \pm 0.23	8.97 \pm 0.22	...	17.929 \pm 0.001	19.718 \pm 0.083	16.604 \pm 0.005	380 $^{+19}_{-18}$	0.222 \pm 0.022
...	116.3319	-46.4077	2.422 \pm 0.091	-4.64 \pm 0.16	9.15 \pm 0.16	...	17.486 \pm 0.003	19.248 \pm 0.038	16.180 \pm 0.004	409 $^{+16}_{-15}$	0.232 \pm 0.019
...	116.3385	-45.6157	2.56 \pm 0.12	-4.11 \pm 0.25	8.97 \pm 0.24	...	18.060 \pm 0.002	20.114 \pm 0.091	16.655 \pm 0.007	387 $^{+19}_{-17}$	0.165 \pm 0.013
...	116.3841	-48.3633	2.49 \pm 0.12	-4.69 \pm 0.22	9.16 \pm 0.24	...	17.247 \pm 0.001	399 $^{+20}_{-18}$	0.471 \pm 0.052
...	116.3870	-46.1110	2.60 \pm 0.13	-4.49 \pm 0.25	8.76 \pm 0.23	...	17.042 \pm 0.001	18.640 \pm 0.016	15.769 \pm 0.007	382 $^{+21}_{-19}$	0.281 \pm 0.022
...	116.3921	-46.6572	2.482 \pm 0.083	-4.61 \pm 0.17	9.02 \pm 0.17	...	17.436 \pm 0.001	18.975 \pm 0.062	16.165 \pm 0.035	399 $^{+14}_{-13}$	0.307 \pm 0.033
...	116.4222	-45.0058	2.62 \pm 0.13	-4.44 \pm 0.26	9.18 \pm 0.23	...	18.136 \pm 0.002	20.327 \pm 0.074	16.741 \pm 0.006	379 $^{+21}_{-19}$	0.151 \pm 0.012
...	116.4459	-45.0018	2.44 \pm 0.13	-4.55 \pm 0.23	9.32 \pm 0.22	...	17.804 \pm 0.003	19.654 \pm 0.047	16.494 \pm 0.005	406 $^{+23}_{-20}$	0.212 \pm 0.017
...	116.5754	-48.5627	2.51 \pm 0.14	-4.42 \pm 0.30	9.10 \pm 0.31	...	18.148 \pm 0.006	20.068 \pm 0.094	16.732 \pm 0.010	396 $^{+25}_{-22}$	0.179 \pm 0.016
...	116.6278	-45.0645	2.479 \pm 0.090	-4.75 \pm 0.17	9.22 \pm 0.18	...	17.599 \pm 0.003	19.283 \pm 0.030	16.323 \pm 0.005	400 $^{+15}_{-14}$	0.258 \pm 0.021
...	116.7351	-45.6556	2.640 \pm 0.084	-4.11 \pm 0.17	9.01 \pm 0.19	...	15.995 \pm 0.002	17.551 \pm 0.011	14.748 \pm 0.003	375 \pm 12	0.310 \pm 0.025
...	116.7412	-47.5877	2.537 \pm 0.072	-5.03 \pm 0.14	9.03 \pm 0.19	...	17.073 \pm 0.001	18.841 \pm 0.033	15.790 \pm 0.006	390 \pm 11	0.236 \pm 0.019
...	116.7518	-48.3981	2.456 \pm 0.081	-4.66 \pm 0.15	8.39 \pm 0.16	...	16.922 \pm 0.001	18.476 \pm 0.018	15.680 \pm 0.005	403 $^{+14}_{-13}$	0.312 \pm 0.025

Table B.4: Yep 1—Continued

Star Name	RA ($^{\circ}$)	Dec ($^{\circ}$)	Parallax (mas)	μ_{α} (mas yr $^{-1}$)	μ_{δ} (mas yr $^{-1}$)	v_r (km s $^{-1}$)	G (mag)	BP (mag)	RP (mag)	d (pc)	Mass (M $_{\odot}$)
...	116.7943	-46.7522	2.48 ± 0.12	-4.68 ± 0.21	9.01 ± 0.29	...	17.620 ± 0.001	19.604 ± 0.050	16.252 ± 0.005	400 $^{+20}_{-18}$	0.177 ± 0.014
...	116.8298	-46.4360	2.63 ± 0.15	-4.69 ± 0.26	8.79 ± 0.32	...	18.076 ± 0.064	19.91 ± 0.11	16.760 ± 0.010	378 $^{+23}_{-20}$	0.215 ± 0.028
...	116.8783	-45.71591	2.561 ± 0.082	-4.60 ± 0.15	9.42 ± 0.18	...	17.201 ± 0.004	18.833 ± 0.042	15.939 ± 0.005	387 $^{+13}_{-12}$	0.275 ± 0.022
...	116.9358	-48.5408	2.482 ± 0.099	-4.35 ± 0.20	8.62 ± 0.23	...	17.599 ± 0.001	19.416 ± 0.047	16.281 ± 0.007	399 $^{+17}_{-15}$	0.217 ± 0.017
...	116.9413	-46.6832	2.52 ± 0.15	-4.45 ± 0.24	8.76 ± 0.33	...	18.191 ± 0.002	19.79 ± 0.14	16.812 ± 0.011	395 $^{+25}_{-22}$	0.255 ± 0.041
...	116.9679	-45.8927	2.66 ± 0.10	-4.81 ± 0.19	9.39 ± 0.20	...	17.555 ± 0.002	19.288 ± 0.043	16.256 ± 0.006	373 $^{+15}_{-14}$	0.240 ± 0.019
...	117.0101	-46.3694	2.62 ± 0.15	-4.35 ± 0.29	8.63 ± 0.29	...	18.207 ± 0.002	20.085 ± 0.083	16.813 ± 0.005	380 $^{+23}_{-20}$	0.189 ± 0.017
...	117.0191	-45.1398	2.653 ± 0.099	-4.77 ± 0.16	9.54 ± 0.19	...	16.580 ± 0.010	17.64 ± 0.11	15.082 ± 0.028	374 $^{+14}_{-13}$	0.390 ± 0.033
...	117.0969	-45.4571	2.53 ± 0.11	-4.44 ± 0.22	9.55 ± 0.24	...	17.638 ± 0.001	19.266 ± 0.040	16.367 ± 0.010	392 $^{+18}_{-16}$	0.274 ± 0.022
...	117.1229	-45.1340	2.64 ± 0.11	-4.43 ± 0.19	9.02 ± 0.19	...	17.517 ± 0.002	19.289 ± 0.059	16.175 ± 0.006	375 $^{+16}_{-15}$	0.222 ± 0.018
...	117.1583	-46.2274	2.43 ± 0.12	-4.56 ± 0.22	8.78 ± 0.24	...	18.078 ± 0.002	19.837 ± 0.072	16.748 ± 0.008	409 $^{+22}_{-20}$	0.226 ± 0.021
...	117.1825	-46.5200	2.61 ± 0.16	-4.79 ± 0.32	9.48 ± 0.31	...	18.270 ± 0.002	19.995 ± 0.074	16.907 ± 0.005	381 $^{+25}_{-22}$	0.227 ± 0.021
...	117.1906	-48.6803	2.46 ± 0.14	-4.73 ± 0.27	8.88 ± 0.31	...	18.312 ± 0.004	20.230 ± 0.084	16.897 ± 0.008	404 $^{+25}_{-22}$	0.180 ± 0.015
...	117.2274	-46.0052	2.61 ± 0.10	-4.57 ± 0.19	8.89 ± 0.19	...	17.526 ± 0.002	19.305 ± 0.052	16.211 ± 0.004	380 $^{+16}_{-15}$	0.225 ± 0.018
...	117.2427	-46.4152	2.509 ± 0.085	-4.70 ± 0.18	8.74 ± 0.17	...	17.030 ± 0.002	18.798 ± 0.033	15.654 ± 0.003	395 $^{+14}_{-13}$	0.216 ± 0.017
...	117.2739	-46.5463	2.57 ± 0.12	-4.60 ± 0.25	9.13 ± 0.24	...	18.188 ± 0.002	19.899 ± 0.067	16.835 ± 0.005	387 $^{+20}_{-18}$	0.233 ± 0.020
...	117.2772	-46.6853	2.546 ± 0.081	-5.02 ± 0.16	9.24 ± 0.16	...	17.303 ± 0.002	18.928 ± 0.020	16.036 ± 0.004	389 $^{+13}_{-12}$	0.276 ± 0.022
...	117.2844	-46.1888	2.43 ± 0.13	-4.47 ± 0.25	8.88 ± 0.26	...	18.279 ± 0.001	20.262 ± 0.074	16.857 ± 0.009	408 $^{+23}_{-21}$	0.171 ± 0.014

Table B.4: Yep 1—Continued

Star Name	RA ($^{\circ}$)	Dec ($^{\circ}$)	Parallax (mas)	μ_{α} (mas yr $^{-1}$)	μ_{δ} (mas yr $^{-1}$)	v_r (km s $^{-1}$)	G (mag)	BP (mag)	RP (mag)	d (pc)	Mass (M $_{\odot}$)
...	117.3015 -46.2457	2.62 \pm 0.10	-4.66 \pm 0.21	9.33 \pm 0.21	...	17.478 \pm 0.003	19.490 \pm 0.034	16.076 \pm 0.006	378 $^{+15}_{-14}$	0.170 \pm 0.014	
...	117.3021 -46.2934	2.58 \pm 0.11	-5.06 \pm 0.21	8.34 \pm 0.21	...	17.784 \pm 0.004	19.302 \pm 0.057	16.463 \pm 0.007	384 $^{+17}_{-16}$	0.297 \pm 0.028	
...	117.3075 -46.4336	2.536 \pm 0.072	-4.61 \pm 0.15	9.36 \pm 0.16	...	16.938 \pm 0.002	18.302 \pm 0.058	15.639 \pm 0.007	390. \pm 11	0.362 \pm 0.029	
...	117.3101 -46.3921	2.67 \pm 0.10	-4.67 \pm 0.20	8.90 \pm 0.23	...	17.557 \pm 0.001	18.537 \pm 0.074	16.202 \pm 0.006	371 $^{+15}_{-14}$	0.449 \pm 0.036	
...	117.3160 -46.3227	2.48 \pm 0.10	-4.89 \pm 0.20	9.20 \pm 0.20	...	17.936 \pm 0.003	19.355 \pm 0.082	16.571 \pm 0.006	400 $^{+17}_{-16}$	0.316 \pm 0.039	
...	117.3251 -45.8714	2.47 \pm 0.11	-4.76 \pm 0.21	9.49 \pm 0.20	...	16.316 \pm 0.002	18.099 \pm 0.014	15.001 \pm 0.002	402 $^{+19}_{-17}$	0.224 \pm 0.018	
...	117.3720 -46.4543	2.57 \pm 0.15	-4.88 \pm 0.31	9.02 \pm 0.29	...	18.510 \pm 0.002	20.010 \pm 0.058	17.112 \pm 0.008	386 $^{+25}_{-22}$	0.274 \pm 0.025	
...	117.3992 -46.4570	2.522 \pm 0.084	-4.66 \pm 0.18	9.22 \pm 0.16	...	17.600 \pm 0.000	19.059 \pm 0.041	16.282 \pm 0.010	393 \pm 13	0.319 \pm 0.028	
...	117.4166 -46.4240	2.53 \pm 0.11	-4.39 \pm 0.23	8.80 \pm 0.25	...	17.820 \pm 0.005	19.466 \pm 0.068	16.457 \pm 0.010	392 $^{+18}_{-16}$	0.246 \pm 0.022	
...	117.4274 -46.4557	2.58 \pm 0.10	-4.26 \pm 0.20	8.82 \pm 0.20	...	17.807 \pm 0.001	19.377 \pm 0.036	16.415 \pm 0.009	384 $^{+16}_{-14}$	0.258 \pm 0.021	
...	117.4398 -46.4060	2.528 \pm 0.096	-4.56 \pm 0.20	9.16 \pm 0.18	...	17.445 \pm 0.001	19.258 \pm 0.028	16.071 \pm 0.004	392 $^{+15}_{-14}$	0.206 \pm 0.017	
...	117.4401 -47.9464	2.530 \pm 0.094	-4.64 \pm 0.19	8.47 \pm 0.19	...	17.685 \pm 0.001	19.434 \pm 0.048	16.368 \pm 0.005	392 $^{+15}_{-14}$	0.232 \pm 0.019	
...	117.5086 -46.3550	2.525 \pm 0.094	-4.80 \pm 0.19	9.00 \pm 0.18	...	17.706 \pm 0.002	19.495 \pm 0.037	16.366 \pm 0.005	392 $^{+15}_{-14}$	0.219 \pm 0.017	
...	117.5354 -46.9258	2.49 \pm 0.12	-5.05 \pm 0.22	9.25 \pm 0.19	...	17.847 \pm 0.004	19.802 \pm 0.080	16.469 \pm 0.006	399 $^{+21}_{-19}$	0.179 \pm 0.014	
...	117.5799 -46.1256	2.625 \pm 0.091	-4.95 \pm 0.16	9.17 \pm 0.16	...	17.395 \pm 0.004	19.199 \pm 0.033	16.094 \pm 0.005	392 $^{+15}_{-14}$	0.224 \pm 0.018	
...	117.5967 -46.6221	2.48 \pm 0.12	-4.49 \pm 0.23	8.92 \pm 0.24	...	18.215 \pm 0.001	20.357 \pm 0.097	16.777 \pm 0.008	400 $^{+21}_{-19}$	0.152 \pm 0.012	
...	117.6813 -46.6851	2.64 \pm 0.13	-4.07 \pm 0.25	8.72 \pm 0.23	...	18.309 \pm 0.001	20.410 \pm 0.089	16.871 \pm 0.008	377 $^{+20}_{-18}$	0.156 \pm 0.012	
...	117.7181 -46.0445	2.63 \pm 0.14	-4.23 \pm 0.25	9.50 \pm 0.28	...	18.210 \pm 0.003	20.246 \pm 0.099	16.864 \pm 0.008	378 $^{+21}_{-19}$	0.174 \pm 0.014	
...	117.7715 -46.0014	2.54 \pm 0.11	-4.69 \pm 0.18	8.62 \pm 0.18	...	17.397 \pm 0.001	18.823 \pm 0.094	16.001 \pm 0.010	390 $^{+17}_{-16}$	0.303 \pm 0.041	

Table B.4: Yep 1—Continued

Star Name	RA ($^{\circ}$)	Dec ($^{\circ}$)	Parallax (mas)	μ_{α} (mas yr $^{-1}$)	μ_{δ} (mas yr $^{-1}$)	v_r (km s $^{-1}$)	G (mag)	BP (mag)	RP (mag)	d (pc)	Mass (M $_{\odot}$)
...	117.7736	-46.2596	2.573 \pm 0.080	-4.39 \pm 0.17	9.23 \pm 0.15	...	17.321 \pm 0.001	18.904 \pm 0.025	16.066 \pm 0.005	385 \pm 12	0.297 \pm 0.024
...	117.9205	-46.8832	2.440 \pm 0.080	-4.54 \pm 0.16	9.22 \pm 0.16	...	17.358 \pm 0.001	18.988 \pm 0.028	16.081 \pm 0.005	406 $^{+14}_{-13}$	0.272 \pm 0.022
...	117.9714	-46.3803	2.50 \pm 0.12	-4.34 \pm 0.23	8.85 \pm 0.25	...	17.931 \pm 0.002	19.928 \pm 0.080	16.546 \pm 0.007	397 $^{+20}_{-18}$	0.174 \pm 0.014
...	117.9737	-45.9920	2.566 \pm 0.097	-4.50 \pm 0.15	9.18 \pm 0.18	...	17.264 \pm 0.007	18.838 \pm 0.024	16.032 \pm 0.006	386 $^{+15}_{-14}$	0.309 \pm 0.025
...	117.9896	-45.9296	2.45 \pm 0.12	-4.53 \pm 0.19	8.98 \pm 0.25	...	17.336 \pm 0.002	19.685 \pm 0.065	16.159 \pm 0.006	406 $^{+21}_{-19}$	0.157 \pm 0.013
...	118.0052	-47.5659	2.636 \pm 0.092	-4.66 \pm 0.17	8.65 \pm 0.17	...	17.299 \pm 0.002	19.074 \pm 0.048	15.960 \pm 0.006	376 $^{+14}_{-13}$	0.222 \pm 0.018
...	118.0579	-46.7559	2.44 \pm 0.10	-4.70 \pm 0.19	9.51 \pm 0.20	...	17.875 \pm 0.001	19.565 \pm 0.057	16.559 \pm 0.006	406 $^{+18}_{-17}$	0.247 \pm 0.020
...	118.0605	-48.2896	2.647 \pm 0.073	-4.70 \pm 0.14	8.94 \pm 0.16	...	17.159 \pm 0.002	18.804 \pm 0.026	15.858 \pm 0.010	374 $^{+11}_{-10}$	0.262 \pm 0.021
...	118.2231	-47.4205	2.518 \pm 0.080	-4.48 \pm 0.14	8.40 \pm 0.17	...	17.001 \pm 0.002	18.648 \pm 0.026	15.725 \pm 0.004	393 $^{+13}_{-12}$	0.268 \pm 0.021
...	118.2505	-45.3231	2.45 \pm 0.12	-4.60 \pm 0.23	8.98 \pm 0.28	...	17.892 \pm 0.001	20.069 \pm 0.059	16.529 \pm 0.006	405 $^{+21}_{-19}$	0.156 \pm 0.012
...	118.3237	-45.9876	2.55 \pm 0.10	-4.72 \pm 0.16	8.55 \pm 0.20	...	17.325 \pm 0.003	18.943 \pm 0.038	16.038 \pm 0.006	389 $^{+16}_{-15}$	0.272 \pm 0.022
...	118.3286	-46.8768	2.44 \pm 0.13	-4.27 \pm 0.24	8.89 \pm 0.26	...	17.892 \pm 0.001	19.820 \pm 0.048	16.539 \pm 0.008	407 $^{+24}_{-22}$	0.186 \pm 0.015
...	118.3355	-45.5558	2.552 \pm 0.087	-4.94 \pm 0.17	9.27 \pm 0.17	...	16.298 \pm 0.003	18.061 \pm 0.020	15.002 \pm 0.004	388 $^{+14}_{-13}$	0.234 \pm 0.019
...	118.6572	-45.9820	2.54 \pm 0.10	-4.65 \pm 0.16	8.82 \pm 0.19	...	17.284 \pm 0.001	18.993 \pm 0.047	16.005 \pm 0.005	390 $^{+16}_{-15}$	0.252 \pm 0.020
...	118.8233	-46.4066	2.52 \pm 0.12	-4.90 \pm 0.24	8.89 \pm 0.20	...	17.668 \pm 0.001	19.392 \pm 0.034	16.386 \pm 0.007	394 $^{+21}_{-19}$	0.247 \pm 0.020
...	118.8786	-46.0835	2.601 \pm 0.082	-4.40 \pm 0.16	9.37 \pm 0.16	...	17.265 \pm 0.001	18.864 \pm 0.031	15.917 \pm 0.008	381 \pm 12	0.262 \pm 0.021
...	119.3352	-46.8536	2.42 \pm 0.11	-4.46 \pm 0.18	9.03 \pm 0.24	...	17.494 \pm 0.000	19.059 \pm 0.036	16.236 \pm 0.005	410 $^{+19}_{-18}$	0.303 \pm 0.025
...	114.0800	-45.0121	2.558 \pm 0.032	-4.965 \pm 0.057	9.860 \pm 0.068	...	15.121 \pm 0.002	16.200 \pm 0.009	14.080 \pm 0.007	386.7 $^{+4.8}_{-4.7}$	0.535 \pm 0.043

Table B.4: Yep 1—Continued

Star Name	R.A. ($^{\circ}$)	Dec ($^{\circ}$)	Parallax (mas)	μ_{α} (mas yr^{-1})	μ_{δ} (mas yr^{-1})	v_r (km s^{-1})	G (mag)	BP (mag)	RP (mag)	d (pc)	Mass (M_{\odot})
...	114.1089 -46.0071	2.614 \pm 0.038	-4.236 \pm 0.068	9.621 \pm 0.086	...	15.646 \pm 0.001	16.812 \pm 0.007	14.565 \pm 0.004	378.5 $^{+5.6}_{-5.5}$	0.483 \pm 0.039	
...	114.3250 -45.1585	2.521 \pm 0.076	-4.72 \pm 0.16	9.95 \pm 0.15	...	17.099 \pm 0.001	19.208 \pm 0.030	15.749 \pm 0.004	393 \pm 12	0.165 \pm 0.013	
TYC 8133-1754-1	114.3877 -46.1958	2.593 \pm 0.022	-4.333 \pm 0.042	9.758 \pm 0.038	19.47 \pm 0.80	10.975 \pm 0.000	11.210 \pm 0.001	10.619 \pm 0.001	381.4 \pm 3.3	1.48 \pm 0.12	
...	114.4097 -45.1643	2.541 \pm 0.020	-5.075 \pm 0.037	9.844 \pm 0.037	...	14.812 \pm 0.004	15.733 \pm 0.014	13.858 \pm 0.009	389.1 $^{+3.1}_{-3.0}$	0.613 \pm 0.049	
TYC 8133-1522-1	114.5669 -46.1056	2.532 \pm 0.023	-4.625 \pm 0.041	9.792 \pm 0.042	17.5 \pm 1.6	11.536 \pm 0.002	11.874 \pm 0.004	10.972 \pm 0.004	390.5 \pm 3.6	0.940 \pm 0.086	
...	114.5904 -48.2509	2.470 \pm 0.050	-4.688 \pm 0.088	8.14 \pm 0.11	...	16.605 \pm 0.001	17.570 \pm 0.010	15.624 \pm 0.005	400.4 $^{+8.2}_{-7.8}$	0.581 \pm 0.047	
...	114.6754 -45.7102	2.684 \pm 0.048	-4.273 \pm 0.089	9.754 \pm 0.085	...	16.114 \pm 0.001	17.501 \pm 0.007	14.939 \pm 0.002	368.8 $^{+6.7}_{-6.5}$	0.390 \pm 0.031	
...	115.1282 -45.4341	2.531 \pm 0.023	-4.956 \pm 0.043	9.728 \pm 0.041	...	14.971 \pm 0.003	15.920 \pm 0.012	13.995 \pm 0.008	390.7 $^{+3.5}_{-3.4}$	0.590 \pm 0.047	
...	115.1859 -48.0160	2.636 \pm 0.013	-4.623 \pm 0.025	8.630 \pm 0.031	...	13.492 \pm 0.001	375.2 \pm 1.9	0.899 \pm 0.099	
...	115.2129 -45.2434	2.568 \pm 0.018	-4.917 \pm 0.032	9.489 \pm 0.034	...	14.046 \pm 0.002	14.783 \pm 0.006	13.219 \pm 0.005	385.1 $^{+2.7}_{-2.6}$	0.700 \pm 0.056	
...	115.2340 -46.4595	2.420 \pm 0.042	-4.840 \pm 0.075	9.352 \pm 0.087	...	15.806 \pm 0.004	17.040 \pm 0.021	14.683 \pm 0.012	408.5 $^{+7.3}_{-7.0}$	0.442 \pm 0.035	
...	115.7157 -48.6604	2.475 \pm 0.050	-4.84 \pm 0.10	7.89 \pm 0.11	...	15.775 \pm 0.002	16.914 \pm 0.010	14.638 \pm 0.005	399.7 $^{+8.3}_{-8.0}$	0.462 \pm 0.037	
...	115.8398 -45.4117	2.500 \pm 0.078	-4.85 \pm 0.15	9.90 \pm 0.16	...	16.518 \pm 0.002	18.309 \pm 0.019	15.223 \pm 0.004	396 $^{+13}_{-12}$	0.227 \pm 0.018	
TYC 8142-1542-1	115.8479 -49.3691	2.394 \pm 0.029	-4.395 \pm 0.052	8.672 \pm 0.059	20.76 \pm 0.36	10.770 \pm 0.000	11.102 \pm 0.001	10.296 \pm 0.001	412.9 $^{+5.0}_{-4.9}$	1.210 \pm 0.060	
...	115.9144 -44.5723	2.465 \pm 0.030	-4.509 \pm 0.057	8.269 \pm 0.064	...	15.472 \pm 0.002	16.521 \pm 0.006	14.447 \pm 0.004	401.1 $^{+5.0}_{-4.9}$	0.547 \pm 0.044	
...	116.8621 -44.6604	2.526 \pm 0.059	-4.339 \pm 0.096	9.48 \pm 0.13	...	16.325 \pm 0.001	17.75 \pm 0.11	15.066 \pm 0.004	391.7 $^{+9.4}_{-8.9}$	0.357 \pm 0.041	
...	116.8725 -48.4726	2.487 \pm 0.020	-4.531 \pm 0.035	9.789 \pm 0.035	...	14.045 \pm 0.003	14.889 \pm 0.010	13.129 \pm 0.007	397.4 \pm 3.2	0.662 \pm 0.053	
...	117.2967 -46.2680	2.716 \pm 0.045	-3.804 \pm 0.089	9.624 \pm 0.088	...	16.049 \pm 0.002	17.477 \pm 0.018	14.843 \pm 0.005	364.5 $^{+6.1}_{-5.9}$	0.370 \pm 0.030	
...	117.8754 -45.9794	2.434 \pm 0.072	-4.72 \pm 0.12	9.69 \pm 0.13	...	16.778 \pm 0.001	18.497 \pm 0.022	15.497 \pm 0.004	407 \pm 12	0.249 \pm 0.020	

Table B.4: Yep 1—Continued

Star Name	RA ($^{\circ}$)	Dec ($^{\circ}$)	Parallax (mas)	μ_{α} (mas yr^{-1})	μ_{δ} (mas yr^{-1})	v_r (km s^{-1})	G (mag)	BP (mag)	RP (mag)	d (pc)	Mass (M_{\odot})
2MASS J07522717-4758074	118.1133	-47.9687	2.518 \pm 0.015	-4.007 \pm 0.027	8.972 \pm 0.034	16.04 \pm 0.29	13.423 \pm 0.000	13.821 \pm 0.001	12.865 \pm 0.001	392.7 \pm 2.4	0.860 \pm 0.043
...	118.6641	-49.6151	2.528 \pm 0.042	-4.573 \pm 0.080	9.893 \pm 0.076	...	14.791 \pm 0.001	15.826 \pm 0.008	13.775 \pm 0.003	391.3 \pm 6.7	0.552 \pm 0.044
...	118.8312	-46.5123	2.438 \pm 0.037	-4.778 \pm 0.068	9.190 \pm 0.058	...	15.156 \pm 0.001	405.5 \pm 6.2	0.699 \pm 0.077
...	119.0406	-44.7318	2.387 \pm 0.052	-5.009 \pm 0.095	7.981 \pm 0.085	...	16.488 \pm 0.001	17.541 \pm 0.016	15.479 \pm 0.003	414.3 \pm 9.2	0.550 \pm 0.044
...	119.1965	-49.2484	2.436 \pm 0.047	-4.098 \pm 0.092	9.260 \pm 0.083	...	15.184 \pm 0.001	16.349 \pm 0.006	14.100 \pm 0.003	405.9 \pm 7.9	0.482 \pm 0.039
...	119.2681	-46.5948	2.478 \pm 0.071	-4.49 \pm 0.14	7.82 \pm 0.13	...	16.494 \pm 0.002	17.697 \pm 0.046	15.233 \pm 0.017	399 \pm 12	0.415 \pm 0.033
...	119.5349	-44.5884	2.554 \pm 0.030	-4.888 \pm 0.051	9.287 \pm 0.057	...	14.522 \pm 0.001	15.423 \pm 0.008	13.589 \pm 0.003	387.2 \pm 4.5	0.640 \pm 0.051
...	119.6671	-45.4336	2.554 \pm 0.079	-4.86 \pm 0.14	9.31 \pm 0.15	...	17.282 \pm 0.002	19.048 \pm 0.028	15.986 \pm 0.004	388 \pm 12	0.233 \pm 0.019
...	119.6928	-48.1095	2.565 \pm 0.047	-4.412 \pm 0.095	8.21 \pm 0.11	...	16.226 \pm 0.004	17.575 \pm 0.022	15.035 \pm 0.011	385.7 \pm 7.2	0.396 \pm 0.032
...	119.7435	-48.1379	2.588 \pm 0.044	-4.266 \pm 0.098	8.64 \pm 0.11	...	16.048 \pm 0.004	17.417 \pm 0.022	14.862 \pm 0.010	382.3 \pm 6.6	0.392 \pm 0.031
...	119.9184	-48.4229	2.436 \pm 0.043	-4.421 \pm 0.080	8.294 \pm 0.077	...	15.597 \pm 0.002	16.730 \pm 0.009	14.525 \pm 0.004	405.9 \pm 7.3	0.514 \pm 0.041
2MASS J07595002-4901523	119.9585	-49.0312	2.437 \pm 0.027	-4.328 \pm 0.050	7.831 \pm 0.051	21.54 \pm 0.18	11.516 \pm 0.000	11.772 \pm 0.002	11.113 \pm 0.001	405.6 \pm 4.6	1.43 \pm 0.11
HD 66191	120.0617	-47.7803	2.415 \pm 0.036	-4.375 \pm 0.082	8.535 \pm 0.068	...	9.524 \pm 0.000	9.633 \pm 0.002	9.363 \pm 0.002	409.3 \pm 6.2	2.05 \pm 0.10
...	120.1660	-48.0744	2.680 \pm 0.083	-4.31 \pm 0.15	8.73 \pm 0.16	...	17.340 \pm 0.001	18.989 \pm 0.028	16.056 \pm 0.004	370 \pm 12	0.265 \pm 0.021
...	120.4593	-46.2579	2.463 \pm 0.068	-4.06 \pm 0.12	8.56 \pm 0.11	...	16.592 \pm 0.001	18.318 \pm 0.014	15.306 \pm 0.003	402 \pm 11	0.246 \pm 0.020
...	120.7532	-46.5081	2.516 \pm 0.037	-4.573 \pm 0.061	8.614 \pm 0.064	...	15.291 \pm 0.002	16.304 \pm 0.008	14.285 \pm 0.004	393.1 \pm 5.9	0.560 \pm 0.045
...	120.8615	-45.9337	2.574 \pm 0.015	-5.126 \pm 0.024	9.084 \pm 0.027	25	13.171 \pm 0.001	13.776 \pm 0.003	12.448 \pm 0.003	384.3 \pm 2.2	0.786 \pm 0.063
...	121.3006	-44.5950	2.540 \pm 0.070	-5.14 \pm 0.11	7.83 \pm 0.13	...	13.912 \pm 0.002	14.816 \pm 0.008	12.940 \pm 0.006	390 \pm 11	0.612 \pm 0.049

Table B.4: Yep 1—Continued

Star Name	RA ($^{\circ}$)	Dec ($^{\circ}$)	Parallax (mas)	μ_{α} (mas yr $^{-1}$)	μ_{δ} (mas yr $^{-1}$)	v_r (km s $^{-1}$)	G (mag)	BP (mag)	RP (mag)	d (pc)	Mass (M $_{\odot}$)
HD 67418	121.4504 -46.2382	2.461 ± 0.035	-4.726 ± 0.062	8.617 ± 0.069	19.1 ± 1.9	10.513 ± 0.001	10.644 ± 0.001	10.308 ± 0.001	401.7 $^{+5.8}_{-5.6}$	1.500 ± 0.075	
...	115.4192 -46.0948	2.58 ± 0.16	-4.52 ± 0.30	9.24 ± 0.33	...	18.541 ± 0.009	20.82 ± 0.11	17.179 ± 0.009	386 $^{+26}_{-23}$	0.145 ± 0.013	
...	115.8607 -46.5123	2.52 ± 0.19	-4.72 ± 0.36	9.70 ± 0.44	...	18.688 ± 0.004	21.11 ± 0.14	17.273 ± 0.013	395 $^{+33}_{-28}$	0.124 ± 0.012	
...	116.0891 -46.8560	2.47 ± 0.11	-4.60 ± 0.23	8.74 ± 0.25	...	18.003 ± 0.001	19.65 ± 0.20	16.37 ± 0.17	401 $^{+19}_{-17}$	0.186 ± 0.046	
...	116.1468 -47.3859	2.60 ± 0.11	-4.25 ± 0.40	8.99 ± 0.30	...	16.472 ± 0.002	381 $^{+17}_{-16}$	0.555 ± 0.061	
...	116.1660 -46.9723	2.57 ± 0.16	-4.91 ± 0.34	9.28 ± 0.26	...	18.723 ± 0.007	19.94 ± 0.11	17.31 ± 0.10	388 $^{+27}_{-24}$	0.372 ± 0.049	
...	116.1900 -44.8467	2.47 ± 0.17	-4.07 ± 0.29	8.79 ± 0.31	...	18.218 ± 0.002	20.127 ± 0.093	16.856 ± 0.008	403 $^{+30}_{-26}$	0.189 ± 0.019	
...	116.6992 -46.5712	2.53 ± 0.22	-4.78 ± 0.37	8.73 ± 0.52	...	18.771 ± 0.002	20.58 ± 0.11	17.410 ± 0.010	395 $^{+40}_{-34}$	0.209 ± 0.027	
...	116.7558 -47.4941	2.53 ± 0.17	-4.83 ± 0.32	8.69 ± 0.46	...	17.917 ± 0.003	19.869 ± 0.074	16.526 ± 0.008	394 $^{+30}_{-26}$	0.178 ± 0.014	
...	116.7642 -47.6194	2.56 ± 0.11	-4.56 ± 0.23	8.93 ± 0.31	...	18.012 ± 0.008	20.156 ± 0.057	16.614 ± 0.006	387 $^{+18}_{-16}$	0.155 ± 0.012	
...	116.8359 -45.9120	2.52 ± 0.24	-4.47 ± 0.49	8.96 ± 0.62	...	18.576 ± 0.001	19.08 ± 0.16	16.918 ± 0.020	399 $^{+44}_{-36}$	0.521 ± 0.058	
...	116.8440 -48.1583	2.56 ± 0.22	-4.08 ± 0.37	8.36 ± 0.40	...	18.906 ± 0.012	20.67 ± 0.18	17.451 ± 0.017	391 $^{+37}_{-31}$	0.200 ± 0.036	
...	116.8811 -46.0719	2.55 ± 0.18	-4.07 ± 0.33	9.74 ± 0.35	...	18.465 ± 0.002	20.53 ± 0.12	17.042 ± 0.013	391 $^{+30}_{-26}$	0.161 ± 0.014	
...	117.2473 -46.3606	2.45 ± 0.22	-4.28 ± 0.44	8.76 ± 0.44	...	18.944 ± 0.002	19.86 ± 0.10	17.380 ± 0.017	408 $^{+43}_{-35}$	0.412 ± 0.033	
...	117.3720 -48.0472	2.49 ± 0.12	-3.99 ± 0.23	9.01 ± 0.23	...	17.909 ± 0.001	19.687 ± 0.064	16.592 ± 0.006	399 $^{+20}_{-18}$	0.225 ± 0.019	
...	117.3923 -47.0407	2.61 ± 0.21	-4.11 ± 0.36	9.09 ± 0.35	...	18.354 ± 0.001	20.37 ± 0.11	16.963 ± 0.008	383 $^{+34}_{-29}$	0.170 ± 0.015	
...	117.4437 -46.4973	2.60 ± 0.23	-4.69 ± 0.52	9.32 ± 0.44	...	19.161 ± 0.001	20.39 ± 0.13	17.589 ± 0.033	385 $^{+39}_{-32}$	0.310 ± 0.051	
...	117.7302 -45.7452	2.54 ± 0.16	-4.73 ± 0.34	8.21 ± 0.28	...	18.268 ± 0.002	19.91 ± 0.10	16.878 ± 0.009	391 $^{+28}_{-24}$	0.242 ± 0.027	
...	117.9525 -47.2519	2.505 ± 0.061	-4.03 ± 0.21	9.19 ± 0.38	...	11.923 ± 0.002	395.1 $^{+9.8}_{-9.3}$	1.21 ± 0.13	

Table B.4: Yep 1—Continued

Star Name	RA ($^{\circ}$)	Dec ($^{\circ}$)	Parallax (mas)	μ_{α} (mas yr $^{-1}$)	μ_{δ} (mas yr $^{-1}$)	v_r (km s $^{-1}$)	G (mag)	BP (mag)	RP (mag)	d (pc)	Mass (M $_{\odot}$)
...	118.1533 -47.1388	2.43 ± 0.19	-4.49 ± 0.38	8.75 ± 0.41	...	18.602 ± 0.002	20.285 ± 0.085	17.196 ± 0.014	411 $^{+37}_{-31}$	0.226 ± 0.023	
...	118.2665 -48.5315	2.58 ± 0.18	-4.82 ± 0.43	9.47 ± 0.54	...	18.528 ± 0.004	19.780 ± 0.030	16.54 ± 0.13	387 $^{+30}_{-26}$	0.196 ± 0.026	
...	118.2669 -48.5317	2.58 ± 0.16	-4.47 ± 0.33	9.03 ± 0.39	...	18.449 ± 0.002	19.924 ± 0.068	16.551 ± 0.030	386 $^{+27}_{-24}$	0.175 ± 0.014	
...	118.4118 -46.3021	2.64 ± 0.14	-4.97 ± 0.28	9.52 ± 0.34	...	17.951 ± 0.002	19.49 ± 0.13	16.620 ± 0.014	377 $^{+22}_{-20}$	0.280 ± 0.046	
...	118.5078 -46.7667	2.50 ± 0.18	-4.41 ± 0.31	8.88 ± 0.44	...	18.429 ± 0.001	20.24 ± 0.10	17.086 ± 0.008	399 $^{+32}_{-27}$	0.214 ± 0.025	
...	118.6423 -46.1737	2.48 ± 0.14	-4.80 ± 0.24	9.77 ± 0.26	...	18.053 ± 0.002	19.896 ± 0.048	16.735 ± 0.007	400 $^{+24}_{-22}$	0.212 ± 0.017	
...	118.8530 -46.1183	2.48 ± 0.19	-4.61 ± 0.33	8.99 ± 0.31	...	18.532 ± 0.002	20.414 ± 0.083	17.176 ± 0.007	403 $^{+34}_{-29}$	0.196 ± 0.019	
...	118.8689 -46.4418	2.43 ± 0.11	-4.66 ± 0.22	9.51 ± 0.20	...	17.798 ± 0.001	19.773 ± 0.047	16.462 ± 0.008	408 $^{+19}_{-17}$	0.182 ± 0.015	
...	119.0632 -44.9722	2.44 ± 0.18	-4.15 ± 0.34	9.04 ± 0.28	...	18.550 ± 0.004	20.28 ± 0.15	17.177 ± 0.014	408 $^{+32}_{-28}$	0.224 ± 0.035	
...	119.1065 -46.2934	2.53 ± 0.12	-4.32 ± 0.24	9.86 ± 0.24	...	17.415 ± 0.002	19.464 ± 0.047	16.034 ± 0.005	393 $^{+21}_{-19}$	0.168 ± 0.013	
...	119.3404 -47.1420	2.51 ± 0.20	-4.91 ± 0.41	9.57 ± 0.42	...	17.695 ± 0.001	19.542 ± 0.059	16.289 ± 0.009	399 $^{+35}_{-30}$	0.193 ± 0.015	
...	114.4594 -45.4540	2.65 ± 0.11	-4.85 ± 0.20	9.50 ± 0.23	...	17.671 ± 0.002	19.493 ± 0.030	16.373 ± 0.005	374 $^{+15}_{-14}$	0.220 ± 0.018	
...	114.5993 -45.3678	2.506 ± 0.079	-5.13 ± 0.14	9.58 ± 0.16	...	17.227 ± 0.001	18.841 ± 0.030	15.986 ± 0.004	395 $^{+13}_{-12}$	0.285 ± 0.023	
...	116.4547 -46.4444	2.342 ± 0.056	-4.783 ± 0.099	8.46 ± 0.10	...	16.254 ± 0.002	17.868 ± 0.013	14.995 ± 0.005	422 $^{+10}_{-9.8}$	0.280 ± 0.022	
...	119.1294 -48.2453	2.31 ± 0.17	-4.81 ± 0.31	8.20 ± 0.29	...	18.244 ± 0.003	19.96 ± 0.13	16.851 ± 0.017	431 $^{+36}_{-31}$	0.222 ± 0.031	
...	116.6979 -48.5183	2.37 ± 0.16	-4.82 ± 0.33	7.79 ± 0.34	...	18.090 ± 0.002	19.859 ± 0.086	16.707 ± 0.008	420 $^{+32}_{-28}$	0.214 ± 0.022	

Table B.5: Yep 2 Member Kinematics and Properties

Star Name	RA ($^{\circ}$)	Dec ($^{\circ}$)	Parallax (mas)	μ_{α} (mas yr $^{-1}$)	μ_{δ} (mas yr $^{-1}$)	v_r (km s $^{-1}$)	G (mag)	BP (mag)	RP (mag)	d (pc)	Mass (M $_{\odot}$)
2MASS J08070237-5024362	121.71599	-50.4100	2.550 \pm 0.014	-5.287 \pm 0.027	8.328 \pm 0.027	...	13.603 \pm 0.003	14.238 \pm 0.007	12.838 \pm 0.007	387.7 \pm 2.1	0.769 \pm 0.062
2MASS J08094262-5002238	122.4275	-50.0399	2.578 \pm 0.022	-5.228 \pm 0.044	8.202 \pm 0.038	21.91 \pm 0.91	11.949 \pm 0.002	12.382 \pm 0.005	11.329 \pm 0.004	383.6 \pm 3.4	0.980 \pm 0.049
KWVel	122.1733	-49.4972	2.424 \pm 0.038	-5.052 \pm 0.076	8.086 \pm 0.078	...	8.198 \pm 0.002	8.170 \pm 0.004	8.270 \pm 0.005	407.9 \pm 6.5	2.75 \pm 0.94
2MASS J08031680-4959438	120.8200	-49.9955	2.447 \pm 0.039	-5.168 \pm 0.076	8.260 \pm 0.061	...	15.558 \pm 0.003	16.651 \pm 0.008	14.506 \pm 0.006	404.0 \pm 6.6	0.535 \pm 0.043
2MASS J08040005-4954589	121.0002	-49.9163	2.515 \pm 0.075	-5.25 \pm 0.16	8.66 \pm 0.15	-53.0 \pm 4.0	16.776 \pm 0.003	18.224 \pm 0.024	15.543 \pm 0.005	394 \pm 12	0.90 \pm 0.13
...	121.5350	-49.7614	2.530 \pm 0.098	-5.20 \pm 0.22	8.07 \pm 0.21	...	17.351 \pm 0.002	19.059 \pm 0.035	16.066 \pm 0.005	392 \pm 16	0.257 \pm 0.021
2MASS J08043431-4931452	121.1429	-49.5292	2.459 \pm 0.020	-5.246 \pm 0.038	8.438 \pm 0.041	...	14.040 \pm 0.007	14.744 \pm 0.026	13.234 \pm 0.019	401.9 \pm 3.2	0.727 \pm 0.058
2MASS J08014983-4938106	120.4576	-49.6362	2.380 \pm 0.069	-4.96 \pm 0.15	7.91 \pm 0.14	...	17.110 \pm 0.004	18.715 \pm 0.030	15.856 \pm 0.009	416 \pm 12	0.299 \pm 0.024
2MASS J08034730-4913353	120.9472	-49.2264	2.481 \pm 0.027	-5.236 \pm 0.049	8.040 \pm 0.055	19.92 \pm 0.35	12.636 \pm 0.003	13.117 \pm 0.012	11.956 \pm 0.011	398.4 \pm 4.4	0.970 \pm 0.048
TYC 8144-1249-1	121.5942	-49.3847	2.575 \pm 0.026	-5.039 \pm 0.047	8.290 \pm 0.046	...	10.766 \pm 0.002	10.927 \pm 0.002	10.507 \pm 0.002	384.1 \pm 4.0	1.980 \pm 0.099
...	121.9166	-49.0506	2.364 \pm 0.072	-5.24 \pm 0.12	7.97 \pm 0.12	...	16.544 \pm 0.002	17.985 \pm 0.016	15.340 \pm 0.005	419 \pm 13	0.374 \pm 0.030
...	119.3088	-49.7275	2.363 \pm 0.036	-5.019 \pm 0.073	8.170 \pm 0.063	...	15.826 \pm 0.002	16.979 \pm 0.008	14.753 \pm 0.005	418.2 \pm 6.4	0.519 \pm 0.041
...	119.0276	-49.5407	2.468 \pm 0.048	-5.282 \pm 0.093	8.703 \pm 0.086	...	16.020 \pm 0.002	17.588 \pm 0.011	14.795 \pm 0.003	400.7 \pm 7.9	0.322 \pm 0.026
...	120.4836	-48.5635	2.71 \pm 0.13	-5.24 \pm 0.26	8.33 \pm 0.25	...	18.185 \pm 0.003	19.965 \pm 0.062	16.793 \pm 0.008	367 \pm 19	0.215 \pm 0.017
...	120.4611	-46.9280	2.47 \pm 0.13	-5.28 \pm 0.26	8.66 \pm 0.23	...	18.019 \pm 0.003	19.736 \pm 0.091	16.648 \pm 0.012	402 \pm 23	0.233 \pm 0.025
...	122.4919	-47.6289	2.580 \pm 0.051	-5.30 \pm 0.10	7.948 \pm 0.092	...	16.126 \pm 0.003	17.422 \pm 0.016	14.971 \pm 0.005	383.6 \pm 7.8	0.425 \pm 0.034
2MASS J07580565-4913120	119.5235	-49.2200	2.424 \pm 0.018	-5.271 \pm 0.039	8.128 \pm 0.033	21.38 \pm 0.24	12.960 \pm 0.004	13.499 \pm 0.010	12.279 \pm 0.008	407.8 \pm 3.0	0.838 \pm 0.067

Table B.5: Yep 2—Continued

Star Name	RA ($^{\circ}$)	Dec ($^{\circ}$)	Parallax (mas)	μ_{α} (mas yr^{-1})	μ_{δ} (mas yr^{-1})	v_r (km s^{-1})	G (mag)	BP (mag)	RP (mag)	d (pc)	Mass (M_{\odot})
...	119.0146	-49.4408	2.424 ± 0.066	-5.23 ± 0.15	8.47 ± 0.12	...	17.029 ± 0.002	18.602 ± 0.027	15.799 ± 0.004	408 ± 11	0.319 ± 0.026
...	119.2585	-49.2530	2.358 ± 0.072	-5.08 ± 0.15	8.13 ± 0.14	...	16.838 ± 0.002	18.559 ± 0.016	15.547 ± 0.005	420.13 ± 12	0.252 ± 0.020
...	119.4599	-49.1622	2.362 ± 0.059	-5.11 ± 0.13	8.54 ± 0.14	...	16.502 ± 0.002	18.086 ± 0.014	15.254 ± 0.003	419.11 ± 10.	0.309 ± 0.025
...	119.3307	-49.1427	2.411 ± 0.097	-4.97 ± 0.21	7.87 ± 0.19	...	17.892 ± 0.002	19.562 ± 0.061	16.584 ± 0.006	411.17 ± 16	0.261 ± 0.021
...	118.1153	-49.5019	2.418 ± 0.020	-5.231 ± 0.037	8.470 ± 0.049	...	14.572 ± 0.003	15.366 ± 0.007	13.685 ± 0.005	406.7 ± 3.1	0.691 ± 0.055
...	118.1166	-49.5024	2.418 ± 0.020	-5.231 ± 0.037	8.470 ± 0.049	...	14.572 ± 0.003	15.366 ± 0.007	13.685 ± 0.005	408.7 ± 3.3	0.691 ± 0.055
...	119.2751	-49.0484	2.414 ± 0.078	-5.27 ± 0.16	8.34 ± 0.16	...	17.328 ± 0.002	18.939 ± 0.028	16.058 ± 0.005	410.14 ± 13	0.285 ± 0.023
...	120.7331	-49.1008	2.503 ± 0.017	-5.300 ± 0.032	8.342 ± 0.033	...	14.141 ± 0.003	14.889 ± 0.008	13.298 ± 0.007	394.9 ± 2.7	0.700 ± 0.056
...	119.9849	-49.0619	2.58 ± 0.15	-4.87 ± 0.30	7.87 ± 0.32	...	18.211 ± 0.003	394 ± 12	0.381 ± 0.042
...	119.7849	-48.9324	2.358 ± 0.080	-5.02 ± 0.14	8.41 ± 0.15	...	17.254 ± 0.002	18.933 ± 0.017	15.992 ± 0.006	420.15 ± 14	0.270 ± 0.022
...	120.4065	-48.6750	2.509 ± 0.099	-5.30 ± 0.18	8.40 ± 0.22	...	17.647 ± 0.002	19.223 ± 0.029	16.339 ± 0.005	395.16 ± 15	0.284 ± 0.023
...	120.3378	-48.2886	2.422 ± 0.093	-5.20 ± 0.18	8.18 ± 0.18	...	17.373 ± 0.002	18.954 ± 0.069	16.064 ± 0.007	409.16 ± 15	0.283 ± 0.029
...	120.0259	-48.2968	2.408 ± 0.052	-5.245 ± 0.099	8.03 ± 0.11	...	16.445 ± 0.003	17.828 ± 0.013	15.253 ± 0.006	410.6 ± 9.0	0.394 ± 0.031
...	119.7665	-48.0513	2.462 ± 0.077	-5.20 ± 0.16	8.42 ± 0.19	...	17.151 ± 0.002	18.722 ± 0.021	15.891 ± 0.004	402.13 ± 12	0.309 ± 0.025
...	121.6912	-47.9783	2.528 ± 0.075	-5.30 ± 0.14	8.18 ± 0.14	...	16.601 ± 0.002	18.231 ± 0.019	15.321 ± 0.003	392.12 ± 11	0.278 ± 0.022
...	121.7226	-47.9902	2.560 ± 0.040	-5.205 ± 0.071	8.649 ± 0.070	...	15.534 ± 0.003	16.830 ± 0.019	14.369 ± 0.007	386.4 ± 5.9	0.422 ± 0.034
2MASS J07513049-4625255	117.8770	-46.4237	2.40 ± 0.14	-5.21 ± 0.26	9.36 ± 0.27	...	18.134 ± 0.003	19.846 ± 0.061	16.818 ± 0.007	415.27 ± 24	0.248 ± 0.020
...	122.8901	-46.2329	2.681 ± 0.050	-5.235 ± 0.092	9.088 ± 0.085	...	7.992 ± 0.002	7.963 ± 0.003	8.082 ± 0.003	369.2 ± 6.7	3.09 ± 0.25
...	121.9898	-47.7295	2.660 ± 0.019	-5.073 ± 0.033	8.053 ± 0.034	...	14.365 ± 0.005	15.214 ± 0.017	13.423 ± 0.013	371.9 ± 2.7	0.687 ± 0.055

Table B.5: Yep 2—Continued

Star Name	RA ($^{\circ}$)	Dec ($^{\circ}$)	Parallax (mas)	μ_{α} (mas yr $^{-1}$)	μ_{δ} (mas yr $^{-1}$)	v_r (km s $^{-1}$)	G (mag)	BP (mag)	RP (mag)	d (pc)	Mass (M $_{\odot}$)
...	120.0862	-47.0851	2.506 \pm 0.087	-5.10 \pm 0.18	8.31 \pm 0.18	...	17.280 \pm 0.002	18.873 \pm 0.022	16.002 \pm 0.005	395 $^{+14}_{-13}$	0.295 \pm 0.024
...	120.1592	-47.0965	2.589 \pm 0.085	-5.23 \pm 0.18	8.04 \pm 0.18	...	17.200 \pm 0.002	18.830 \pm 0.024	15.918 \pm 0.006	383 $^{+13}_{-12}$	0.277 \pm 0.022
...	120.6928	-47.9987	2.47 \pm 0.10	-5.27 \pm 0.21	8.47 \pm 0.21	...	16.349 \pm 0.003	364.1 $^{+4.8}_{-4.7}$	0.561 \pm 0.062
...	122.7093	-46.5717	2.43 \pm 0.16	-5.30 \pm 0.28	8.01 \pm 0.30	...	18.061 \pm 0.003	20.142 \pm 0.066	16.664 \pm 0.009	410 $^{+30}_{-26}$	0.166 \pm 0.013
...	117.6033	-47.6368	2.440 \pm 0.090	-5.25 \pm 0.18	7.96 \pm 0.18	...	17.171 \pm 0.002	18.900 \pm 0.021	15.859 \pm 0.006	406 $^{+16}_{-14}$	0.245 \pm 0.020
...	117.7303	-47.7980	2.539 \pm 0.074	-5.28 \pm 0.13	8.19 \pm 0.13	...	16.996 \pm 0.003	18.560 \pm 0.021	15.734 \pm 0.006	390 $^{+12}_{-11}$	0.311 \pm 0.025
...	116.4845	-48.0199	2.360 \pm 0.076	-5.24 \pm 0.14	8.68 \pm 0.16	...	17.379 \pm 0.002	19.015 \pm 0.036	16.125 \pm 0.006	419 $^{+14}_{-13}$	0.283 \pm 0.023
...	116.2482	-48.7300	2.488 \pm 0.098	-5.30 \pm 0.19	8.32 \pm 0.19	...	17.329 \pm 0.002	18.968 \pm 0.020	16.067 \pm 0.005	398 $^{+16}_{-15}$	0.280 \pm 0.022
HD 64598	118.1171	-48.3877	2.354 \pm 0.034	-4.971 \pm 0.069	8.191 \pm 0.077	...	9.655 \pm 0.002	9.704 \pm 0.002	9.591 \pm 0.002	419.7 $^{+6.2}_{-6.0}$	2.29 \pm 0.33
...	117.3530	-48.3182	2.507 \pm 0.090	-5.15 \pm 0.16	8.21 \pm 0.21	...	17.298 \pm 0.002	18.767 \pm 0.049	16.035 \pm 0.005	395 $^{+15}_{-14}$	0.351 \pm 0.028
...	116.5510	-48.7205	2.407 \pm 0.081	-5.11 \pm 0.16	8.48 \pm 0.16	...	16.827 \pm 0.002	18.605 \pm 0.019	15.515 \pm 0.005	411 $^{+14}_{-13}$	0.233 \pm 0.019
...	117.0632	-48.9068	2.413 \pm 0.085	-5.13 \pm 0.16	8.39 \pm 0.19	...	17.358 \pm 0.002	18.814 \pm 0.034	16.061 \pm 0.005	410 $^{+15}_{-14}$	0.337 \pm 0.027
...	115.7293	-48.7496	2.45 \pm 0.10	-5.09 \pm 0.20	8.53 \pm 0.20	...	16.311 \pm 0.002	17.784 \pm 0.009	15.099 \pm 0.004	405 $^{+17}_{-16}$	0.364 \pm 0.029
...	119.6337	-50.3990	2.43 \pm 0.12	-5.26 \pm 0.23	8.40 \pm 0.24	...	17.863 \pm 0.002	19.666 \pm 0.034	16.556 \pm 0.006	408 $^{+20}_{-19}$	0.228 \pm 0.018
...	122.0371	-50.6313	2.38 \pm 0.14	-4.71 \pm 0.29	7.87 \pm 0.27	...	18.290 \pm 0.003	20.162 \pm 0.086	16.886 \pm 0.007	417 $^{+26}_{-23}$	0.193 \pm 0.019
...	122.6849	-49.6500	2.58 \pm 0.17	-5.10 \pm 0.31	8.51 \pm 0.30	...	18.329 \pm 0.005	20.157 \pm 0.040	16.977 \pm 0.015	387 $^{+28}_{-24}$	0.213 \pm 0.017
...	121.9720	-50.0282	2.58 \pm 0.18	-5.24 \pm 0.33	8.01 \pm 0.31	...	18.633 \pm 0.003	20.388 \pm 0.075	17.241 \pm 0.015	387 $^{+29}_{-25}$	0.220 \pm 0.020
...	120.4595	-50.1637	2.53 \pm 0.15	-5.24 \pm 0.28	7.82 \pm 0.28	...	18.146 \pm 0.003	20.015 \pm 0.070	16.779 \pm 0.006	393 $^{+24}_{-22}$	0.202 \pm 0.018

Table B.5: Yep 2—Continued

Star Name	RA ($^{\circ}$)	Dec ($^{\circ}$)	Parallax (mas)	μ_{α} (mas yr^{-1})	μ_{δ} (mas yr^{-1})	v_r (km s^{-1})	G (mag)	BP (mag)	RP (mag)	d (pc)	Mass (M_{\odot})
...	119.5903	-49.3064	2.50 \pm 0.11	-5.01 \pm 0.22	8.03 \pm 0.21	...	17.807 \pm 0.003	19.536 \pm 0.056	16.409 \pm 0.005	397 $^{+18}_{-17}$	0.223 \pm 0.018
...	118.1811	-49.3090	2.45 \pm 0.11	-5.27 \pm 0.21	7.77 \pm 0.26	...	17.299 \pm 0.002	19.269 \pm 0.030	15.938 \pm 0.005	404 $^{+19}_{-17}$	0.183 \pm 0.015
...	120.3035	-48.6236	2.521 \pm 0.094	-5.02 \pm 0.17	8.36 \pm 0.21	...	17.173 \pm 0.002	18.893 \pm 0.031	15.832 \pm 0.005	393 $^{+15}_{-14}$	0.240 \pm 0.019
...	118.4069	-48.9981	2.643 \pm 0.093	-5.29 \pm 0.17	8.57 \pm 0.18	...	17.292 \pm 0.003	19.005 \pm 0.022	16.008 \pm 0.004	375 $^{+14}_{-13}$	0.256 \pm 0.020
...	118.9499	-48.8270	2.369 \pm 0.073	-5.29 \pm 0.14	8.62 \pm 0.15	...	17.284 \pm 0.002	18.910 \pm 0.035	16.010 \pm 0.004	418 \pm 13	0.280 \pm 0.022
...	118.7334	-49.3708	2.541 \pm 0.094	-4.97 \pm 0.18	8.75 \pm 0.20	...	17.506 \pm 0.002	19.332 \pm 0.049	16.157 \pm 0.006	390 $^{+15}_{-14}$	0.214 \pm 0.017
...	119.5775	-49.1815	2.562 \pm 0.084	-5.20 \pm 0.19	8.16 \pm 0.16	...	17.279 \pm 0.003	18.740 \pm 0.033	15.992 \pm 0.008	387 $^{+13}_{-12}$	0.339 \pm 0.027
...	119.4649	-49.3314	2.567 \pm 0.085	-5.26 \pm 0.18	7.98 \pm 0.17	...	17.329 \pm 0.002	19.176 \pm 0.031	15.985 \pm 0.004	386 $^{+13}_{-12}$	0.211 \pm 0.017
CD-493158	118.5089	-49.7655	2.487 \pm 0.034	-5.221 \pm 0.066	8.804 \pm 0.073	...	10.011 \pm 0.002	10.090 \pm 0.002	9.896 \pm 0.002	397.6 $^{+5.4}_{-5.3}$	1.86 \pm 0.18
...	119.8305	-49.5142	2.637 \pm 0.096	-4.99 \pm 0.18	8.19 \pm 0.24	...	17.317 \pm 0.002	18.993 \pm 0.030	16.046 \pm 0.005	376 $^{+14}_{-13}$	0.268 \pm 0.021
...	119.1596	-50.0564	2.411 \pm 0.029	-5.264 \pm 0.064	8.724 \pm 0.054	...	14.456 \pm 0.002	15.070 \pm 0.003	13.705 \pm 0.003	409.9 $^{+4.9}_{-4.8}$	0.782 \pm 0.063
...	123.8256	-49.6091	2.374 \pm 0.085	-4.93 \pm 0.18	8.15 \pm 0.16	...	15.572 \pm 0.004	16.592 \pm 0.008	14.318 \pm 0.005	393 $^{+14}_{-13}$	0.482 \pm 0.039
...	121.4856	-49.1756	2.671 \pm 0.080	-5.28 \pm 0.15	9.10 \pm 0.15	...	16.577 \pm 0.004	18.042 \pm 0.027	15.357 \pm 0.009	371 \pm 11	0.363 \pm 0.029
...	122.2000	-49.9172	2.745 \pm 0.079	-5.24 \pm 0.17	8.46 \pm 0.15	...	17.112 \pm 0.002	18.728 \pm 0.021	15.852 \pm 0.006	361 $^{+11}_{-10}$	0.293 \pm 0.023
...	122.8567	-49.4557	2.398 \pm 0.095	-5.23 \pm 0.20	8.25 \pm 0.22	...	17.173 \pm 0.002	18.658 \pm 0.080	15.902 \pm 0.007	413 $^{+17}_{-16}$	0.336 \pm 0.035
...	120.9188	-50.5399	2.572 \pm 0.086	-5.13 \pm 0.19	8.38 \pm 0.15	...	17.229 \pm 0.002	18.779 \pm 0.040	15.973 \pm 0.005	385 $^{+13}_{-12}$	0.318 \pm 0.027
...	121.5613	-50.4212	2.458 \pm 0.064	-4.74 \pm 0.13	7.79 \pm 0.13	...	16.611 \pm 0.003	18.132 \pm 0.025	15.367 \pm 0.005	402 $^{+11}_{-10}$	0.333 \pm 0.027
...	121.6915	-50.4499	2.354 \pm 0.090	-5.06 \pm 0.18	8.19 \pm 0.19	...	17.507 \pm 0.002	19.475 \pm 0.053	16.133 \pm 0.006	421 $^{+17}_{-15}$	0.182 \pm 0.015
...	121.4264	-50.8906	2.452 \pm 0.018	-5.291 \pm 0.033	8.293 \pm 0.035	...	13.818 \pm 0.003	14.507 \pm 0.006	13.017 \pm 0.006	403.1 \pm 2.9	0.734 \pm 0.059

Table B.5: Yep 2—Continued

Star Name	RA ($^{\circ}$)	Dec ($^{\circ}$)	Parallax (mas)	μ_{α} (mas yr $^{-1}$)	μ_{δ} (mas yr $^{-1}$)	v_r (km s $^{-1}$)	G (mag)	BP (mag)	RP (mag)	d (pc)	Mass (M $_{\odot}$)
...	120.0644	-50.6064	2.534 \pm 0.088	-5.26 \pm 0.18	8.27 \pm 0.22	...	17.377 \pm 0.003	18.943 \pm 0.032	16.125 \pm 0.007	391 $^{+14}_{-13}$	0.314 \pm 0.025
...	123.3944	-50.0384	2.545 \pm 0.078	-5.04 \pm 0.15	7.97 \pm 0.17	...	17.180 \pm 0.002	19.035 \pm 0.027	15.854 \pm 0.003	389 \pm 12	0.213 \pm 0.017
...	123.0461	-50.5105	2.511 \pm 0.018	-5.247 \pm 0.036	7.948 \pm 0.036	...	13.920 \pm 0.002	14.658 \pm 0.006	13.086 \pm 0.006	393.7 \pm 2.9	0.706 \pm 0.056
...	115.3951	-48.0022	2.418 \pm 0.057	-5.06 \pm 0.11	9.19 \pm 0.12	...	16.485 \pm 0.002	17.731 \pm 0.093	15.109 \pm 0.013	402.1 \pm 2.2	0.381 \pm 0.030
...	115.2246	-48.1806	2.521 \pm 0.096	-5.24 \pm 0.18	8.85 \pm 0.24	...	17.326 \pm 0.003	19.044 \pm 0.034	16.023 \pm 0.005	393 $^{+16}_{-14}$	0.250 \pm 0.020
...	119.7903	-49.2578	2.37 \pm 0.12	-5.04 \pm 0.23	8.24 \pm 0.24	...	17.841 \pm 0.003	19.630 \pm 0.067	16.510 \pm 0.008	418 $^{+22}_{-20}$	0.225 \pm 0.019
...	118.2765	-49.3205	2.36 \pm 0.12	-5.02 \pm 0.24	7.90 \pm 0.25	...	17.993 \pm 0.003	19.735 \pm 0.055	16.681 \pm 0.006	420 $^{+23}_{-21}$	0.242 \pm 0.019
...	119.5096	-49.3197	2.54 \pm 0.11	-5.17 \pm 0.21	8.15 \pm 0.20	...	17.730 \pm 0.002	19.287 \pm 0.055	16.392 \pm 0.008	390 $^{+17}_{-16}$	0.282 \pm 0.026
...	119.7314	-49.5411	2.46 \pm 0.14	-5.23 \pm 0.24	8.24 \pm 0.29	...	18.142 \pm 0.003	19.98 \pm 0.10	16.804 \pm 0.011	405 $^{+25}_{-22}$	0.214 \pm 0.025
...	119.8849	-49.5445	2.39 \pm 0.13	-5.25 \pm 0.24	8.22 \pm 0.30	...	17.975 \pm 0.003	19.730 \pm 0.073	16.651 \pm 0.010	415 $^{+25}_{-22}$	0.235 \pm 0.021
...	121.0093	-49.9340	2.44 \pm 0.11	-4.98 \pm 0.23	7.92 \pm 0.22	...	17.391 \pm 0.003	19.047 \pm 0.026	16.088 \pm 0.013	406 $^{+19}_{-17}$	0.265 \pm 0.021
...	122.0548	-50.0751	2.64 \pm 0.12	-5.29 \pm 0.26	8.57 \pm 0.22	...	17.611 \pm 0.002	19.297 \pm 0.043	16.297 \pm 0.005	376 $^{+18}_{-16}$	0.255 \pm 0.020
...	121.1714	-50.4209	2.42 \pm 0.10	-5.01 \pm 0.20	8.01 \pm 0.20	...	17.657 \pm 0.002	19.447 \pm 0.030	16.336 \pm 0.005	410 $^{+18}_{-17}$	0.228 \pm 0.018
...	120.3036	-49.0299	2.59 \pm 0.10	-5.23 \pm 0.19	7.85 \pm 0.18	...	17.525 \pm 0.002	18.970 \pm 0.074	16.232 \pm 0.005	383 $^{+15}_{-14}$	0.349 \pm 0.032
...	120.5794	-49.0501	2.65 \pm 0.13	-5.13 \pm 0.24	8.61 \pm 0.23	...	14.971 \pm 0.003	16.118 \pm 0.012	13.875 \pm 0.007	374 $^{+19}_{-17}$	0.506 \pm 0.040
...	119.7356	-49.2354	2.56 \pm 0.12	-5.00 \pm 0.25	8.84 \pm 0.27	...	17.740 \pm 0.003	19.593 \pm 0.044	16.359 \pm 0.006	389 $^{+20}_{-18}$	0.202 \pm 0.016
...	117.2184	-49.2493	2.38 \pm 0.15	-4.97 \pm 0.32	8.51 \pm 0.28	...	18.210 \pm 0.003	19.872 \pm 0.089	16.834 \pm 0.009	418 $^{+29}_{-25}$	0.246 \pm 0.025
...	116.3931	-48.7521	2.42 \pm 0.15	-5.29 \pm 0.31	8.70 \pm 0.31	...	18.474 \pm 0.003	20.338 \pm 0.088	17.078 \pm 0.008	412 $^{+28}_{-25}$	0.197 \pm 0.020

Table B.5: Yep 2—Continued

Star Name	RA ($^{\circ}$)	Dec ($^{\circ}$)	Parallax (mas)	μ_{α} (mas yr $^{-1}$)	μ_{δ} (mas yr $^{-1}$)	v_r (km s $^{-1}$)	G (mag)	BP (mag)	RP (mag)	d (pc)	Mass (M $_{\odot}$)
...	117.4263 -47.5303	2.36 ± 0.16	-5.12 ± 0.30	8.15 ± 0.30	...	18.636 ± 0.003	20.425 ± 0.085	17.239 ± 0.009	423 $^{+33}_{-28}$	0.212 ± 0.021	
...	117.3961 -46.0228	2.610 ± 0.076	-5.24 ± 0.15	9.07 ± 0.14	...	17.103 ± 0.002	18.898 ± 0.029	15.783 ± 0.005	379 ± 11	0.226 ± 0.018	
...	122.6035 -48.4289	2.53 ± 0.11	-5.20 ± 0.23	8.07 ± 0.21	...	18.148 ± 0.003	19.952 ± 0.053	16.781 ± 0.007	392 $^{+18}_{-16}$	0.215 ± 0.017	
...	120.6925 -47.9992	2.47 ± 0.10	-5.27 ± 0.21	8.47 ± 0.21	...	16.349 ± 0.003	401 $^{+17}_{-16}$	0.593 ± 0.065	
...	118.7618 -46.3942	2.466 ± 0.019	-5.254 ± 0.037	8.244 ± 0.034	...	14.518 ± 0.003	15.474 ± 0.010	13.543 ± 0.008	400.9 $^{+3.1}_{-3.0}$	0.600 ± 0.048	
...	116.8535 -46.7679	2.701 ± 0.090	-5.27 ± 0.18	8.72 ± 0.20	...	15.045 ± 0.003	16.315 ± 0.009	13.917 ± 0.005	367 $^{+13}_{-12}$	0.438 ± 0.035	
TYC 8138-167-1	115.6522 -48.2927	2.443 ± 0.031	-4.968 ± 0.053	8.496 ± 0.050	18.0 ± 2.6	10.831 ± 0.000	10.996 ± 0.001	10.572 ± 0.001	404.7 $^{+5.2}_{-5.0}$	1.61 ± 0.12	
...	115.9931 -47.6615	2.413 ± 0.055	-5.19 ± 0.12	8.74 ± 0.12	...	16.475 ± 0.001	17.949 ± 0.019	15.278 ± 0.002	409.8 $^{+9.5}_{-9.1}$	0.367 ± 0.029	
...	116.1948 -48.7121	2.496 ± 0.022	-5.124 ± 0.040	8.519 ± 0.038	...	14.801 ± 0.001	15.695 ± 0.004	13.865 ± 0.004	396.1 ± 3.4	0.661 ± 0.053	
...	116.2938 -48.2949	2.392 ± 0.036	-5.055 ± 0.064	8.525 ± 0.062	...	14.787 ± 0.001	15.720 ± 0.006	13.821 ± 0.003	413.2 $^{+6.3}_{-6.1}$	0.614 ± 0.049	
...	116.7422 -47.5867	2.516 ± 0.059	-5.06 ± 0.12	9.52 ± 0.15	...	16.581 ± 0.001	18.173 ± 0.015	15.349 ± 0.003	393.3 $^{+9.3}_{-8.9}$	0.312 ± 0.025	
2MASS J07470563-4757394	116.7735 -47.9610	2.478 ± 0.021	-5.083 ± 0.042	8.903 ± 0.047	21.34 ± 0.53	12.909 ± 0.002	13.418 ± 0.009	12.253 ± 0.007	398.9 ± 3.4	0.900 ± 0.045	
TYC 8138-2794-1	118.0101 -47.0450	2.388 ± 0.026	-5.161 ± 0.047	8.889 ± 0.054	...	10.463 ± 0.000	10.598 ± 0.001	10.246 ± 0.001	413.8 $^{+4.6}_{-4.5}$	1.980 ± 0.099	
...	118.6960 -48.7262	2.385 ± 0.062	-5.07 ± 0.12	8.28 ± 0.14	...	16.789 ± 0.001	18.212 ± 0.032	15.534 ± 0.006	415 $^{+11}_{-10}$	0.365 ± 0.029	
...	119.0760 -48.8181	2.384 ± 0.078	-4.97 ± 0.15	8.38 ± 0.14	...	17.298 ± 0.001	18.932 ± 0.036	16.050 ± 0.005	415 $^{+14}_{-13}$	0.285 ± 0.023	
...	119.1263 -49.7737	2.409 ± 0.055	-5.09 ± 0.11	8.156 ± 0.099	...	15.984 ± 0.003	17.514 ± 0.033	14.763 ± 0.008	410.5 $^{+9.6}_{-9.1}$	0.338 ± 0.027	
...	119.3229 -49.2144	2.453 ± 0.048	-5.08 ± 0.11	8.315 ± 0.091	...	16.123 ± 0.003	17.431 ± 0.020	14.972 ± 0.008	403.1 $^{+8.0}_{-7.7}$	0.423 ± 0.034	
...	119.4035 -49.2129	2.474 ± 0.057	-5.16 ± 0.13	8.27 ± 0.13	...	16.259 ± 0.001	17.820 ± 0.012	15.016 ± 0.004	399.9 $^{+9.3}_{-8.9}$	0.319 ± 0.025	
...	119.5401 -49.1754	2.476 ± 0.020	-4.912 ± 0.044	9.144 ± 0.037	...	14.135 ± 0.002	15.039 ± 0.006	13.189 ± 0.005	399.2 ± 3.2	0.647 ± 0.052	

Table B.5: Yep 2—Continued

Star Name	RA ($^{\circ}$)	Dec ($^{\circ}$)	Parallax (mas)	μ_{α} (mas yr $^{-1}$)	μ_{δ} (mas yr $^{-1}$)	v_r (km s $^{-1}$)	G (mag)	BP (mag)	RP (mag)	d (pc)	Mass (M $_{\odot}$)
...	119.6369	-49.2702	2.436 \pm 0.020	-5.114 \pm 0.039	8.217 \pm 0.044	...	14.791 \pm 0.003	15.650 \pm 0.012	13.851 \pm 0.010	405.7 $^{+3.4}_{-3.3}$	0.681 \pm 0.054
...	119.7128	-48.7501	2.433 \pm 0.052	-4.988 \pm 0.093	8.70 \pm 0.11	...	15.560 \pm 0.002	16.558 \pm 0.009	14.336 \pm 0.008	406.4 $^{+8.9}_{-8.5}$	0.522 \pm 0.042
...	119.8224	-49.0157	2.430 \pm 0.075	-4.91 \pm 0.14	8.78 \pm 0.15	...	16.989 \pm 0.001	18.412 \pm 0.034	15.716 \pm 0.005	407 $^{+13}_{-12}$	0.360 \pm 0.029
...	119.9175	-48.4669	2.424 \pm 0.071	-5.12 \pm 0.12	8.63 \pm 0.12	...	16.468 \pm 0.002	17.971 \pm 0.010	15.242 \pm 0.004	408 \pm 12	0.351 \pm 0.028
...	120.1636	-49.0934	2.420 \pm 0.028	-5.187 \pm 0.056	8.474 \pm 0.052	...	15.374 \pm 0.002	16.427 \pm 0.008	14.338 \pm 0.006	408.4 $^{+4.7}_{-4.6}$	0.550 \pm 0.044
...	120.2292	-49.1627	2.548 \pm 0.041	-5.141 \pm 0.083	8.475 \pm 0.071	...	15.455 \pm 0.004	16.343 \pm 0.019	14.380 \pm 0.014	388.2 $^{+6.3}_{-6.1}$	0.585 \pm 0.047
...	120.2785	-49.0251	2.644 \pm 0.054	-4.94 \pm 0.10	8.58 \pm 0.10	...	16.165 \pm 0.001	17.799 \pm 0.010	14.898 \pm 0.003	374.4 $^{+7.7}_{-7.4}$	0.280 \pm 0.022
...	120.5367	-49.0419	2.400 \pm 0.058	-5.17 \pm 0.10	8.17 \pm 0.11	...	16.494 \pm 0.002	17.911 \pm 0.015	15.299 \pm 0.005	412 $^{+10}_{-9.7}$	0.383 \pm 0.031
TYC 8143-2246-1	120.5647	-49.5685	2.383 \pm 0.024	-5.161 \pm 0.048	8.089 \pm 0.047	22.22 \pm 0.98	11.181 \pm 0.001	11.399 \pm 0.002	10.834 \pm 0.001	414.7 \pm 4.1	1.380 \pm 0.069
...	120.8951	-49.5025	2.462 \pm 0.067	-4.88 \pm 0.16	8.87 \pm 0.12	...	16.785 \pm 0.001	18.339 \pm 0.018	15.506 \pm 0.008	402 \pm 11	0.309 \pm 0.025
...	121.2176	-48.8100	2.554 \pm 0.058	-5.18 \pm 0.12	8.06 \pm 0.14	...	16.430 \pm 0.002	18.001 \pm 0.020	15.183 \pm 0.004	387.4 $^{+9.0}_{-8.6}$	0.314 \pm 0.025
...	121.6087	-47.5581	2.550 \pm 0.073	-5.17 \pm 0.14	8.50 \pm 0.15	...	14.889 \pm 0.002	16.075 \pm 0.008	13.780 \pm 0.005	388 \pm 11	0.467 \pm 0.037
...	117.7579	-46.3604	2.494 \pm 0.088	-5.19 \pm 0.20	9.16 \pm 0.17	...	16.691 \pm 0.002	18.478 \pm 0.019	15.375 \pm 0.005	397 $^{+14}_{-13}$	0.229 \pm 0.018
...	118.9859	-47.8225	2.473 \pm 0.037	-5.297 \pm 0.067	8.813 \pm 0.065	...	15.657 \pm 0.001	16.831 \pm 0.022	14.566 \pm 0.013	399.9 $^{+6.1}_{-5.9}$	0.489 \pm 0.039
...	119.3447	-46.3696	2.524 \pm 0.051	-5.200 \pm 0.092	8.983 \pm 0.098	...	16.060 \pm 0.003	17.370 \pm 0.013	14.914 \pm 0.004	391.9 $^{+8.1}_{-7.8}$	0.424 \pm 0.034
2MASS J07371850-4850279	114.3271	-48.8411	2.430 \pm 0.041	-5.033 \pm 0.076	8.851 \pm 0.079	33.69 \pm 0.16	13.550 \pm 0.000	14.078 \pm 0.002	12.879 \pm 0.001	406.8 $^{+7.0}_{-6.8}$	0.820 \pm 0.041
...	114.8745	-47.1735	2.388 \pm 0.040	-5.098 \pm 0.077	8.815 \pm 0.068	...	15.773 \pm 0.001	17.050 \pm 0.007	14.654 \pm 0.002	413.9 $^{+7.0}_{-6.8}$	0.438 \pm 0.035
...	115.3960	-48.0027	2.418 \pm 0.057	-5.06 \pm 0.11	9.19 \pm 0.12	...	16.485 \pm 0.001	17.731 \pm 0.093	15.110 \pm 0.012	409.0 $^{+9.8}_{-9.3}$	0.381 \pm 0.030

Table B.5: Yep 2—Continued

Star Name	RA ($^{\circ}$)	Dec ($^{\circ}$)	Parallax (mas)	μ_{α} (mas yr^{-1})	μ_{δ} (mas yr^{-1})	v_r (km s^{-1})	G (mag)	BP (mag)	RP (mag)	d (pc)	Mass (M_{\odot})
...	115.4092	-48.5953	2.550 \pm 0.021	-5.085 \pm 0.038	8.350 \pm 0.044	...	14.488 \pm 0.007	15.412 \pm 0.026	13.502 \pm 0.017	387.7 \pm 3.2	610 \pm 0.049
...	116.0635	-49.6082	2.421 \pm 0.052	-5.13 \pm 0.11	8.81 \pm 0.10	...	15.873 \pm 0.002	17.341 \pm 0.015	14.669 \pm 0.007	408.5 $^{+8.9}_{-8.6}$	367 \pm 0.029
...	116.8742	-49.2922	2.515 \pm 0.058	-4.98 \pm 0.11	8.05 \pm 0.11	...	16.616 \pm 0.002	18.479 \pm 0.028	15.292 \pm 0.008	393.5 $^{+9.2}_{-8.8}$	212 \pm 0.017
...	119.7020	-49.0560	2.502 \pm 0.051	-4.921 \pm 0.091	8.08 \pm 0.14	...	15.702 \pm 0.003	395.4 $^{+8.2}_{-7.9}$	660 \pm 0.073
TYC 8134-586-1	115.8371	-45.9461	2.496 \pm 0.025	-5.307 \pm 0.048	9.145 \pm 0.045	21.07 \pm 0.73	11.341 \pm 0.001	11.742 \pm 0.009	10.794 \pm 0.006	396.1 \pm 3.9	1250 \pm 0.062
...	116.7113	-48.0935	2.57 \pm 0.17	-5.32 \pm 0.30	9.68 \pm 0.41	...	18.192 \pm 0.002	20.136 \pm 0.086	16.734 \pm 0.012	388 $^{+27}_{-24}$	175 \pm 0.014
...	116.8336	-45.7146	2.520 \pm 0.016	-5.478 \pm 0.029	9.075 \pm 0.037	...	14.102 \pm 0.001	14.885 \pm 0.007	13.235 \pm 0.004	392.3 \pm 2.4	694 \pm 0.056
...	116.8619	-45.2579	2.51 \pm 0.15	-5.49 \pm 0.22	8.80 \pm 0.28	...	17.992 \pm 0.001	19.755 \pm 0.061	16.652 \pm 0.008	396 $^{+25}_{-22}$	229 \pm 0.019
CD-443740	116.8636	-45.2941	2.487 \pm 0.041	-5.371 \pm 0.063	9.160 \pm 0.076	20.1 \pm 4.8	10.163 \pm 0.029	10.249 \pm 0.001	10.037 \pm 0.001	397.6 $^{+6.6}_{-6.4}$	1830 \pm 0.092
...	117.0321	-46.9239	2.491 \pm 0.048	-5.374 \pm 0.096	8.60 \pm 0.10	...	16.006 \pm 0.001	17.256 \pm 0.018	14.846 \pm 0.006	397.1 $^{+7.8}_{-7.5}$	434 \pm 0.035
...	117.2928	-46.1218	2.535 \pm 0.017	-5.549 \pm 0.029	9.199 \pm 0.030	...	13.784 \pm 0.003	14.474 \pm 0.012	12.976 \pm 0.008	390.1 \pm 2.6	731 \pm 0.058
...	117.2994	-46.3094	2.611 \pm 0.060	-5.33 \pm 0.12	8.93 \pm 0.12	...	16.514 \pm 0.002	18.064 \pm 0.020	15.244 \pm 0.006	379.2 $^{+8.9}_{-8.5}$	313 \pm 0.025
...	117.5614	-48.5911	2.46 \pm 0.22	-5.26 \pm 0.43	8.89 \pm 0.38	...	18.899 \pm 0.002	407 $^{+43}_{-35}$	311 \pm 0.034
...	117.5891	-48.4105	2.55 \pm 0.26	-5.06 \pm 0.49	8.90 \pm 0.40	...	19.121 \pm 0.001	20.60 \pm 0.19	17.752 \pm 0.022	395 $^{+47}_{-38}$	305 \pm 0.066
2MASS J07502381-4659290	117.5992	-46.9914	2.504 \pm 0.026	-5.331 \pm 0.047	8.834 \pm 0.041	21.65 \pm 0.66	11.756 \pm 0.001	12.119 \pm 0.001	11.238 \pm 0.001	394.9 $^{+4.1}_{-4.0}$	1.21 \pm 0.16
...	118.1784	-44.9358	2.503 \pm 0.096	-5.40 \pm 0.16	9.25 \pm 0.20	...	17.022 \pm 0.001	18.778 \pm 0.055	15.731 \pm 0.006	396 $^{+16}_{-15}$	243 \pm 0.019
...	118.4938	-47.0669	2.578 \pm 0.052	-5.517 \pm 0.096	9.41 \pm 0.11	...	16.526 \pm 0.001	18.060 \pm 0.016	15.298 \pm 0.004	383.8 $^{+7.8}_{-7.5}$	334 \pm 0.027
...	118.6553	-47.5321	2.558 \pm 0.092	-5.34 \pm 0.16	8.81 \pm 0.16	...	17.383 \pm 0.001	18.677 \pm 0.047	16.040 \pm 0.010	387 $^{+14}_{-13}$	376 \pm 0.030
...	118.8987	-44.5730	2.54 \pm 0.10	-5.59 \pm 0.18	9.09 \pm 0.18	...	17.598 \pm 0.001	19.392 \pm 0.043	16.295 \pm 0.004	391 $^{+17}_{-15}$	231 \pm 0.018

Table B.5: Yep 2—Continued

Star Name	RA ($^{\circ}$)	Dec ($^{\circ}$)	Parallax (mas)	μ_{α} (mas yr $^{-1}$)	μ_{δ} (mas yr $^{-1}$)	v_r (km s $^{-1}$)	G (mag)	BP (mag)	RP (mag)	d (pc)	Mass (M $_{\odot}$)
...	119.4989 -45.3552	2.47 ± 0.12	-5.45 ± 0.22	8.97 ± 0.26	...	18.092 ± 0.005	20.53 ± 0.12	16.711 ± 0.007	40 $^{+22}_{-20}$	0.129 ± 0.012	
...	119.2198 -44.6426	2.50 ± 0.10	-5.47 ± 0.18	8.93 ± 0.20	...	16.673 ± 0.002	18.508 ± 0.021	15.371 ± 0.005	396 $^{+17}_{-16}$	0.223 ± 0.018	
...	119.4400 -44.6359	2.563 ± 0.055	-5.505 ± 0.094	9.16 ± 0.12	...	16.251 ± 0.010	17.717 ± 0.022	15.055 ± 0.007	386.1 $^{+8.5}_{-8.1}$	0.370 ± 0.030	
...	123.2512 -45.8956	2.500 ± 0.045	-5.812 ± 0.078	8.692 ± 0.072	...	15.663 ± 0.003	16.844 ± 0.012	14.573 ± 0.007	395.7 $^{+7.2}_{-7.0}$	0.485 ± 0.039	
...	122.9506 -46.0265	2.427 ± 0.056	-5.997 ± 0.097	7.92 ± 0.10	...	16.413 ± 0.002	17.835 ± 0.013	15.227 ± 0.004	407.5 $^{+9.6}_{-9.2}$	0.384 ± 0.031	
2MASS J08051033-4626135	121.2930 -46.4371	2.516 ± 0.069	-5.83 ± 0.12	8.20 ± 0.14	...	16.721 ± 0.002	18.254 ± 0.013	15.487 ± 0.004	393 $^{+11}_{-10}$	0.332 ± 0.027	
2MASS J08075765-4642059	121.9902 -46.7016	2.316 ± 0.083	-5.86 ± 0.14	7.72 ± 0.13	...	17.113 ± 0.003	18.524 ± 0.041	15.879 ± 0.008	427 $^{+16}_{-15}$	0.374 ± 0.030	
2MASS J08090505-4639367	122.2710 -46.6602	2.452 ± 0.070	-5.89 ± 0.11	7.96 ± 0.12	...	15.946 ± 0.005	16.920 ± 0.018	14.728 ± 0.016	391.7 $^{+4.4}_{-4.3}$	0.520 ± 0.042	
2MASS J08075296-4649340	121.9706 -46.8261	2.450 ± 0.083	-5.95 ± 0.13	8.50 ± 0.14	...	16.785 ± 0.002	18.377 ± 0.020	15.535 ± 0.004	404 $^{+14}_{-13}$	0.305 ± 0.024	
2MASS J08065983-4658510	121.7493 -46.9808	2.315 ± 0.085	-5.66 ± 0.16	8.02 ± 0.15	...	16.803 ± 0.002	18.636 ± 0.019	15.480 ± 0.005	428 $^{+16}_{-15}$	0.218 ± 0.017	
HD 69404	123.7135 -46.44859	2.398 ± 0.047	-5.795 ± 0.086	7.817 ± 0.086	...	6.359 ± 0.002	6.334 ± 0.006	6.447 ± 0.011	412.3 $^{+8.2}_{-7.9}$	7.3 ± 7.6	
...	122.3139 -47.2406	2.373 ± 0.079	-5.57 ± 0.15	8.09 ± 0.17	...	16.792 ± 0.002	18.208 ± 0.051	15.447 ± 0.005	417 $^{+14}_{-13}$	0.334 ± 0.027	
2MASS J08090157-4717068	122.2565 -47.2852	2.510 ± 0.049	-5.937 ± 0.091	7.859 ± 0.092	...	16.010 ± 0.003	17.144 ± 0.023	14.823 ± 0.006	394.1 $^{+7.8}_{-7.5}$	0.448 ± 0.036	
2MASS J08113159-4717465	122.8816 -47.2962	2.524 ± 0.018	-5.980 ± 0.036	8.043 ± 0.034	...	14.259 ± 0.003	15.027 ± 0.009	13.399 ± 0.006	391.7 ± 2.7	0.696 ± 0.056	
2MASS J08113740-5013103	122.9058 -50.2195	2.521 ± 0.046	-5.462 ± 0.085	8.13 ± 0.10	...	15.902 ± 0.006	17.133 ± 0.038	14.749 ± 0.023	392.3 $^{+7.4}_{-7.1}$	0.442 ± 0.035	
2MASS J08100895-4946562	122.5372 -49.7823	2.522 ± 0.084	-5.54 ± 0.17	8.24 ± 0.16	...	16.949 ± 0.002	18.459 ± 0.019	15.696 ± 0.003	393 ± 1.3	0.333 ± 0.027	
2MASS J08110759-4921423	122.7816 -49.3617	2.389 ± 0.061	-5.08 ± 0.11	7.52 ± 0.14	...	16.219 ± 0.002	17.512 ± 0.012	15.047 ± 0.006	414 $^{+11}_{-10}$	0.422 ± 0.034	
...	120.6870 -49.9005	2.505 ± 0.029	-5.409 ± 0.063	8.151 ± 0.054	...	15.392 ± 0.002	16.482 ± 0.007	14.337 ± 0.005	394.7 $^{+4.6}_{-4.5}$	0.535 ± 0.043	

Table B.5: Yep 2—Continued

Star Name	RA ($^{\circ}$)	Dec ($^{\circ}$)	Parallax (mas)	μ_{α} (mas yr $^{-1}$)	μ_{δ} (mas yr $^{-1}$)	v_r (km s $^{-1}$)	G (mag)	BP (mag)	RP (mag)	d (pc)	Mass (M $_{\odot}$)
...	121.2167	-49.5034	2.39 ± 0.10	-5.57 ± 0.18	8.02 ± 0.24	...	17.267 ± 0.002	18.945 ± 0.033	15.976 ± 0.005	415 $^{+18}_{-17}$	0.263 ± 0.021
...	121.2362	-49.4261	2.427 ± 0.089	-5.49 ± 0.16	8.12 ± 0.22	...	17.110 ± 0.002	18.837 ± 0.018	15.855 ± 0.005	408 $^{+16}_{-14}$	0.259 ± 0.021
...	120.2675	-49.8045	2.518 ± 0.099	-5.32 ± 0.21	8.41 ± 0.17	...	17.489 ± 0.002	19.423 ± 0.034	16.149 ± 0.005	394 $^{+16}_{-15}$	0.194 ± 0.016
...	120.2179	-49.6952	2.502 ± 0.036	-5.527 ± 0.079	8.203 ± 0.066	...	15.522 ± 0.003	16.649 ± 0.009	14.452 ± 0.005	395.2 $^{+5.8}_{-5.6}$	0.518 ± 0.041
...	120.9091	-49.1685	2.312 ± 0.075	-5.36 ± 0.15	8.16 ± 0.15	...	16.803 ± 0.002	18.293 ± 0.017	15.592 ± 0.004	428 $^{+14}_{-13}$	0.359 ± 0.029
...	122.4392	-49.1066	2.385 ± 0.080	-5.50 ± 0.16	7.94 ± 0.16	...	17.054 ± 0.002	19.071 ± 0.025	15.684 ± 0.004	415 $^{+14}_{-13}$	0.176 ± 0.014
...	122.4815	-48.6370	2.501 ± 0.058	-5.61 ± 0.11	8.01 ± 0.11	...	16.309 ± 0.003	17.708 ± 0.021	15.100 ± 0.009	395.6 $^{+9.3}_{-8.9}$	0.384 ± 0.031
...	121.5601	-49.1305	2.323 ± 0.094	-5.70 ± 0.18	8.14 ± 0.20	...	17.097 ± 0.002	18.801 ± 0.027	15.784 ± 0.003	400. ± 12	0.251 ± 0.020
...	121.5100	-49.0931	2.517 ± 0.064	-5.56 ± 0.12	8.06 ± 0.12	...	16.433 ± 0.005	17.924 ± 0.028	15.215 ± 0.012	393 $^{+10}_{-9.7}$	0.357 ± 0.029
...	122.6117	-48.6996	2.356 ± 0.050	-5.522 ± 0.095	7.575 ± 0.094	...	16.111 ± 0.002	17.376 ± 0.013	14.989 ± 0.004	419.7 $^{+9.1}_{-8.7}$	0.441 ± 0.035
...	119.5516	-49.2902	2.502 ± 0.020	-5.408 ± 0.039	8.358 ± 0.038	...	14.775 ± 0.003	15.635 ± 0.008	13.840 ± 0.006	395.2 $^{+3.2}_{-3.1}$	0.684 ± 0.055
...	121.0859	-45.9497	2.362 ± 0.026	-5.657 ± 0.040	7.655 ± 0.058	...	14.781 ± 0.002	15.400 ± 0.003	14.035 ± 0.002	418.2 $^{+4.6}_{-4.5}$	0.782 ± 0.063
...	121.7171	-45.9624	2.375 ± 0.040	-5.927 ± 0.070	8.121 ± 0.056	...	15.257 ± 0.004	16.311 ± 0.012	14.232 ± 0.007	416.1 $^{+7.1}_{-6.8}$	0.552 ± 0.044
...	121.9686	-45.6659	2.484 ± 0.077	-5.68 ± 0.15	7.87 ± 0.14	...	17.011 ± 0.004	18.691 ± 0.022	15.752 ± 0.009	399 $^{+13}_{-12}$	0.271 ± 0.022
...	123.6690	-47.5955	2.53 ± 0.18	-5.39 ± 0.28	8.43 ± 0.28	...	17.990 ± 0.003	20.016 ± 0.089	16.602 ± 0.007	395 $^{+30}_{-26}$	0.173 ± 0.014
...	120.3721	-46.5773	2.42 ± 0.15	-5.37 ± 0.28	8.60 ± 0.23	...	18.279 ± 0.003	19.844 ± 0.048	17.079 ± 0.008	412 $^{+28}_{-25}$	0.332 ± 0.027
...	120.7091	-46.3331	2.35 ± 0.15	-5.36 ± 0.27	8.72 ± 0.30	...	18.104 ± 0.003	19.388 ± 0.069	16.894 ± 0.020	423 $^{+30}_{-26}$	0.414 ± 0.033
...	124.6875	-45.3040	2.49 ± 0.13	-5.69 ± 0.22	7.67 ± 0.20	...	17.527 ± 0.002	19.234 ± 0.052	16.257 ± 0.006	399 $^{+22}_{-20}$	0.261 ± 0.021
...	125.3060	-44.3492	2.38 ± 0.13	-5.43 ± 0.22	7.60 ± 0.24	...	17.953 ± 0.003	19.703 ± 0.049	16.624 ± 0.008	417 $^{+25}_{-22}$	0.235 ± 0.019

Table B.5: Yep 2—Continued

Star Name	RA ($^{\circ}$)	Dec ($^{\circ}$)	Parallax (mas)	μ_{α} (mas yr^{-1})	μ_{δ} (mas yr^{-1})	v_r (km s^{-1})	G (mag)	BP (mag)	RP (mag)	d (pc)	Mass (M_{\odot})
...	123.1574	-44.8125	2.449 \pm 0.030	-5.894 \pm 0.047	8.765 \pm 0.047	...	11.600 \pm 0.002	11.861 \pm 0.002	11.201 \pm 0.002	403.7 $^{+5.0}_{-4.9}$	1.45 \pm 0.12
...	121.3599	-44.1812	2.313 \pm 0.079	-5.70 \pm 0.13	8.16 \pm 0.13	...	16.131 \pm 0.002	17.671 \pm 0.007	14.904 \pm 0.004	428 $^{+15}_{-14}$	0.332 \pm 0.027
...	121.5375	-44.8022	2.392 \pm 0.057	-5.526 \pm 0.099	8.757 \pm 0.098	...	15.590 \pm 0.003	16.944 \pm 0.017	14.396 \pm 0.007	414 $^{+10}_{-9.6}$	0.401 \pm 0.032
TYC 7671-4253-1	120.7902	-44.6366	2.460 \pm 0.025	-5.697 \pm 0.044	8.327 \pm 0.045	22.4 \pm 2.1	10.640 \pm 0.002	10.836 \pm 0.002	10.337 \pm 0.002	401.8 $^{+4.1}_{-4.0}$	1.50 \pm 0.16
...	122.3694	-47.6450	2.382 \pm 0.090	-5.55 \pm 0.16	8.17 \pm 0.19	...	16.559 \pm 0.003	17.439 \pm 0.073	15.296 \pm 0.014	416 $^{+16}_{-15}$	0.536 \pm 0.043
...	122.4616	-47.6791	2.528 \pm 0.072	-5.89 \pm 0.13	8.06 \pm 0.13	...	16.940 \pm 0.002	18.425 \pm 0.026	15.697 \pm 0.004	392 \pm 11	0.352 \pm 0.028
...	122.5084	-47.7011	2.434 \pm 0.049	-5.972 \pm 0.084	8.074 \pm 0.090	...	15.615 \pm 0.003	16.773 \pm 0.017	14.508 \pm 0.005	406.4 $^{+8.2}_{-7.9}$	0.489 \pm 0.039
...	120.9726	-45.5318	2.30 \pm 0.13	-5.66 \pm 0.19	8.56 \pm 0.26	...	17.600 \pm 0.002	19.489 \pm 0.064	16.259 \pm 0.009	432 $^{+26}_{-24}$	0.203 \pm 0.018
...	121.4123	-43.8668	2.47 \pm 0.10	-5.51 \pm 0.18	8.77 \pm 0.20	...	17.436 \pm 0.002	18.715 \pm 0.021	16.331 \pm 0.005	401 $^{+17}_{-16}$	0.442 \pm 0.035
...	120.5751	-44.3894	2.43 \pm 0.14	-5.76 \pm 0.22	8.49 \pm 0.27	...	17.709 \pm 0.003	19.578 \pm 0.088	16.179 \pm 0.020	409 $^{+26}_{-23}$	0.175 \pm 0.014
...	120.4537	-47.0437	2.522 \pm 0.060	-5.96 \pm 0.11	8.34 \pm 0.12	...	16.139 \pm 0.002	17.535 \pm 0.013	14.954 \pm 0.004	392.4 $^{+9.4}_{-9.0}$	0.392 \pm 0.031
...	121.1497	-47.3104	2.503 \pm 0.034	-5.916 \pm 0.061	8.697 \pm 0.077	...	15.448 \pm 0.004	16.556 \pm 0.013	14.386 \pm 0.009	395.1 $^{+5.5}_{-5.4}$	0.527 \pm 0.042
...	119.4931	-49.0095	2.513 \pm 0.074	-5.64 \pm 0.15	8.09 \pm 0.15	...	17.123 \pm 0.003	18.894 \pm 0.046	15.779 \pm 0.007	394 $^{+12}_{-11}$	0.226 \pm 0.018
...	118.5895	-49.3190	2.500 \pm 0.091	-5.63 \pm 0.18	8.50 \pm 0.20	...	17.578 \pm 0.002	19.315 \pm 0.040	16.275 \pm 0.005	396 $^{+15}_{-14}$	0.245 \pm 0.020
...	118.6762	-49.2168	2.313 \pm 0.028	-5.201 \pm 0.057	8.233 \pm 0.052	...	14.516 \pm 0.002	15.216 \pm 0.005	13.693 \pm 0.004	427.0 $^{+5.2}_{-5.1}$	0.723 \pm 0.058
...	120.9651	-48.9154	2.529 \pm 0.082	-5.58 \pm 0.18	8.20 \pm 0.17	...	17.240 \pm 0.002	18.823 \pm 0.036	15.983 \pm 0.007	392 $^{+3}_{-12}$	0.306 \pm 0.025
...	120.6148	-48.8873	2.508 \pm 0.098	-5.90 \pm 0.20	7.98 \pm 0.17	...	17.313 \pm 0.002	19.123 \pm 0.029	15.992 \pm 0.006	395 $^{+16}_{-15}$	0.224 \pm 0.018
...	119.8320	-49.0596	2.525 \pm 0.037	-5.608 \pm 0.072	8.132 \pm 0.068	...	15.579 \pm 0.003	16.922 \pm 0.009	14.423 \pm 0.005	391.7 $^{+5.8}_{-5.7}$	0.413 \pm 0.033

Table B.5: Yep 2—Continued

Star Name	RA ($^{\circ}$)	Dec ($^{\circ}$)	Parallax (mas)	μ_{α} (mas yr $^{-1}$)	μ_{δ} (mas yr $^{-1}$)	v_r (km s $^{-1}$)	G (mag)	BP (mag)	RP (mag)	d (pc)	Mass (M $_{\odot}$)
...	121.0531	-48.7346	2.532 ± 0.027	-5.796 ± 0.056	8.389 ± 0.055	...	15.334 ± 0.003	16.378 ± 0.012	14.307 ± 0.006	390.6 $^{+4.2}_{-4.1}$	0.554 ± 0.044
HD 67129	121.1199	-48.2632	2.502 ± 0.035	-5.639 ± 0.065	8.343 ± 0.080	...	9.963 ± 0.002	10.013 ± 0.002	9.894 ± 0.002	395.2 $^{+5.6}_{-5.4}$	1.880 ± 0.094
...	120.1544	-48.0856	2.500 ± 0.094	-5.77 ± 0.17	8.12 ± 0.18	...	17.551 ± 0.002	19.196 ± 0.033	16.264 ± 0.004	396 $^{+15}_{-14}$	0.272 ± 0.022
...	121.6584	-47.5132	2.524 ± 0.070	-5.96 ± 0.13	8.72 ± 0.13	...	17.162 ± 0.003	18.794 ± 0.029	15.878 ± 0.006	392 ± 11	0.276 ± 0.022
...	121.6058	-47.5586	2.516 ± 0.014	-5.669 ± 0.026	8.110 ± 0.026	...	13.042 ± 0.002	13.593 ± 0.005	12.349 ± 0.004	393.0 ± 2.2	0.828 ± 0.066
...	121.3054	-48.0631	2.484 ± 0.083	-5.63 ± 0.16	8.59 ± 0.16	...	16.890 ± 0.003	18.356 ± 0.039	15.641 ± 0.009	399 $^{+14}_{-13}$	0.355 ± 0.028
...	121.0120	-47.9682	2.530 ± 0.093	-5.63 ± 0.18	8.26 ± 0.18	...	17.362 ± 0.002	18.948 ± 0.044	16.124 ± 0.004	392 $^{+15}_{-14}$	0.311 ± 0.027
...	120.8058	-48.1355	2.516 ± 0.068	-5.36 ± 0.12	8.07 ± 0.12	...	16.860 ± 0.002	18.410 ± 0.022	15.604 ± 0.008	393 $^{+11}_{-10}$	0.318 ± 0.025
...	121.8294	-47.7338	2.504 ± 0.069	-5.61 ± 0.14	7.94 ± 0.13	...	16.932 ± 0.002	18.395 ± 0.027	15.692 ± 0.004	395 ± 11	0.358 ± 0.029
...	122.0018	-48.2116	2.455 ± 0.098	-5.74 ± 0.17	7.74 ± 0.19	...	17.298 ± 0.002	18.979 ± 0.034	15.976 ± 0.006	404 $^{+17}_{-15}$	0.254 ± 0.020
...	122.9675	-48.0190	2.520 ± 0.062	-5.44 ± 0.11	8.43 ± 0.12	...	16.560 ± 0.002	18.029 ± 0.013	15.351 ± 0.004	392.7 $^{+9.8}_{-9.3}$	0.366 ± 0.029
...	122.5548	-48.1258	2.526 ± 0.017	-5.911 ± 0.036	8.475 ± 0.031	...	13.939 ± 0.002	14.427 ± 0.002	13.308 ± 0.003	391.4 ± 2.6	0.895 ± 0.072
...	122.3902	-48.4579	2.504 ± 0.042	-5.663 ± 0.082	8.125 ± 0.079	...	16.163 ± 0.002	17.470 ± 0.011	14.995 ± 0.003	395.0 $^{+6.7}_{-6.5}$	0.419 ± 0.034
...	122.7125	-48.3970	2.527 ± 0.094	-5.74 ± 0.18	7.74 ± 0.21	...	17.713 ± 0.002	19.172 ± 0.050	16.445 ± 0.006	392 $^{+15}_{-14}$	0.352 ± 0.028
...	117.0571	-45.7751	2.455 ± 0.041	-5.372 ± 0.079	8.694 ± 0.082	...	15.889 ± 0.002	17.062 ± 0.011	14.810 ± 0.003	402.8 $^{+6.9}_{-6.7}$	0.499 ± 0.040
...	124.5262	-44.5319	2.318 ± 0.056	-5.682 ± 0.099	7.960 ± 0.094	...	15.927 ± 0.004	17.099 ± 0.026	14.795 ± 0.011	426 $^{+10}_{-9.9}$	0.461 ± 0.037
...	124.4155	-45.6193	2.386 ± 0.030	-5.647 ± 0.052	7.664 ± 0.049	...	15.331 ± 0.003	16.365 ± 0.009	14.322 ± 0.006	414.3 $^{+5.3}_{-5.2}$	0.560 ± 0.045
...	124.4121	-45.6164	2.323 ± 0.034	-5.322 ± 0.056	7.786 ± 0.060	...	15.008 ± 0.003	16.171 ± 0.009	13.936 ± 0.005	425.3 $^{+6.2}_{-6.0}$	0.512 ± 0.041
2MASS J08000812-4533201	120.0338	-45.556	2.473 ± 0.028	-5.710 ± 0.060	8.289 ± 0.047	37.59 ± 0.13	12.327 ± 0.002	12.733 ± 0.003	11.779 ± 0.003	399.7 $^{+4.6}_{-4.5}$	1.030 ± 0.052

Table B.5: Yep 2—Continued

Star Name	RA ($^{\circ}$)	Dec ($^{\circ}$)	Parallax (mas)	μ_{α} (mas yr $^{-1}$)	μ_{δ} (mas yr $^{-1}$)	v_r (km s $^{-1}$)	G (mag)	BP (mag)	RP (mag)	d (pc)	Mass (M $_{\odot}$)
...	120.3083	-45.8200	2.497 \pm 0.049	-5.695 \pm 0.093	8.221 \pm 0.082	...	16.212 \pm 0.002	17.555 \pm 0.016	15.057 \pm 0.004	396.1 $^{+7.9}_{-7.6}$	413 \pm 0.033
...	124.3813	-47.8398	2.436 \pm 0.086	-5.79 \pm 0.10	7.96 \pm 0.11	...	16.206 \pm 0.002	17.060 \pm 0.009	15.265 \pm 0.006	407 $^{+15}_{-14}$	684 \pm 0.055
...	123.7308	-48.2453	2.303 \pm 0.083	-5.85 \pm 0.16	7.56 \pm 0.15	...	17.331 \pm 0.002	18.464 \pm 0.019	16.242 \pm 0.006	430 $^{+16}_{-15}$	522 \pm 0.042
...	122.2674	-45.8684	2.44 \pm 0.11	-5.99 \pm 0.18	8.17 \pm 0.20	...	17.289 \pm 0.002	19.078 \pm 0.041	15.996 \pm 0.007	407 $^{+20}_{-18}$	235 \pm 0.019
...	122.5042	-46.5133	2.39 \pm 0.13	-5.55 \pm 0.24	8.06 \pm 0.30	...	17.892 \pm 0.002	19.751 \pm 0.073	16.549 \pm 0.007	416 $^{+24}_{-22}$	209 \pm 0.019
...	122.1097	-46.6605	2.44 \pm 0.10	-5.55 \pm 0.19	7.89 \pm 0.21	...	17.490 \pm 0.002	19.061 \pm 0.056	16.207 \pm 0.006	406 $^{+18}_{-17}$	301 \pm 0.028
...	121.5816	-46.9037	2.47 \pm 0.17	-5.84 \pm 0.31	8.45 \pm 0.32	...	18.438 \pm 0.003	20.26 \pm 0.10	17.053 \pm 0.010	404 $^{+30}_{-26}$	207 \pm 0.024
...	118.2177	-48.2255	2.437 \pm 0.090	-5.80 \pm 0.19	8.69 \pm 0.23	...	17.110 \pm 0.002	18.891 \pm 0.034	15.786 \pm 0.006	406 $^{+16}_{-14}$	229 \pm 0.018
...	117.9941	-48.7176	2.308 \pm 0.080	-5.21 \pm 0.16	8.49 \pm 0.16	...	17.203 \pm 0.002	18.704 \pm 0.028	15.958 \pm 0.007	429 $^{+15}_{-14}$	339 \pm 0.027
...	119.5225	-50.5139	2.45 \pm 0.13	-5.77 \pm 0.26	8.65 \pm 0.28	...	18.030 \pm 0.002	20.019 \pm 0.075	16.654 \pm 0.008	406 $^{+23}_{-21}$	179 \pm 0.014
...	119.5047	-50.2486	2.38 \pm 0.10	-5.31 \pm 0.18	7.83 \pm 0.23	...	17.460 \pm 0.002	19.556 \pm 0.047	16.102 \pm 0.004	416 $^{+18}_{-17}$	168 \pm 0.013
...	122.4021	-49.9068	2.40 \pm 0.17	-4.88 \pm 0.33	7.52 \pm 0.27	...	18.482 \pm 0.004	20.346 \pm 0.069	17.087 \pm 0.012	416 $^{+23}_{-28}$	197 \pm 0.017
...	122.1789	-49.0639	2.46 \pm 0.14	-5.74 \pm 0.26	8.52 \pm 0.21	...	18.174 \pm 0.002	20.011 \pm 0.083	16.833 \pm 0.008	404 $^{+24}_{-22}$	214 \pm 0.021
...	122.1659	-48.9230	2.45 \pm 0.16	-5.88 \pm 0.28	8.49 \pm 0.25	...	18.108 \pm 0.003	19.828 \pm 0.044	16.764 \pm 0.010	406 $^{+28}_{-25}$	239 \pm 0.019
...	125.0944	-49.3832	2.38 \pm 0.13	-5.54 \pm 0.21	7.57 \pm 0.21	...	17.721 \pm 0.002	19.437 \pm 0.044	16.383 \pm 0.005	418 $^{+24}_{-22}$	242 \pm 0.019
...	125.0321	-49.2651	2.38 \pm 0.11	-5.78 \pm 0.18	7.86 \pm 0.18	...	17.498 \pm 0.002	19.155 \pm 0.037	16.184 \pm 0.005	416 $^{+21}_{-19}$	262 \pm 0.021
...	119.4126	-49.2500	2.51 \pm 0.10	-5.77 \pm 0.27	7.93 \pm 0.23	...	17.592 \pm 0.002	19.171 \pm 0.048	16.291 \pm 0.005	395 $^{+17}_{-16}$	292 \pm 0.025
...	121.2267	-48.3565	2.309 \pm 0.071	-5.72 \pm 0.13	8.19 \pm 0.16	...	16.914 \pm 0.002	18.427 \pm 0.016	15.682 \pm 0.005	428 $^{+14}_{-13}$	347 \pm 0.028

Table B.5: Yep 2—Continued

Star Name	RA ($^{\circ}$)	Dec ($^{\circ}$)	Parallax (mas)	μ_{α} (mas yr $^{-1}$)	μ_{δ} (mas yr $^{-1}$)	v_r (km s $^{-1}$)	G (mag)	BP (mag)	RP (mag)	d (pc)	Mass (M $_{\odot}$)
...	120.2977	-49.2283	2.303 \pm 0.089	-5.50 \pm 0.16	8.27 \pm 0.16	...	17.352 \pm 0.003	19.035 \pm 0.041	16.055 \pm 0.007	430. $^{+17}_{-16}$	0.260 \pm 0.021
...	118.4807	-48.5184	2.307 \pm 0.075	-5.46 \pm 0.15	7.99 \pm 0.17	...	16.091 \pm 0.003	17.616 \pm 0.017	14.851 \pm 0.008	429. $^{+14}_{-13}$	0.333 \pm 0.027
TYC 8143-2619-1	118.1296	-49.1315	2.325 \pm 0.025	-5.554 \pm 0.048	7.948 \pm 0.053	26.03 \pm 0.32	11.202 \pm 0.002	11.418 \pm 0.004	10.867 \pm 0.003	424.8. $^{+4.5}_{-4.4}$	1.46 \pm 0.12
...	118.9770	-48.7130	2.344 \pm 0.071	-5.11 \pm 0.14	8.75 \pm 0.14	...	16.371 \pm 0.003	17.257 \pm 0.031	14.677 \pm 0.018	422. $^{+13}_{-12}$	0.392 \pm 0.031
...	117.8167	-49.2069	2.322 \pm 0.097	-5.10 \pm 0.20	8.34 \pm 0.18	...	17.517 \pm 0.002	19.107 \pm 0.025	16.209 \pm 0.005	427. $^{+19}_{-17}$	0.281 \pm 0.022
2MASS J08183357-4924140	124.6398	-49.4039	2.518 \pm 0.025	-5.944 \pm 0.042	7.529 \pm 0.047	...	12.720 \pm 0.003	13.274 \pm 0.009	12.029 \pm 0.007	392.7. $^{+3.9}_{-3.8}$	0.880 \pm 0.085
...	124.3625	-49.6657	2.392 \pm 0.091	-5.60 \pm 0.17	7.72 \pm 0.21	...	17.365 \pm 0.002	19.381 \pm 0.035	16.024 \pm 0.005	414. $^{+16}_{-15}$	0.180 \pm 0.014
...	125.4439	-49.5115	2.435 \pm 0.084	-5.73 \pm 0.16	7.71 \pm 0.15	...	17.075 \pm 0.003	18.750 \pm 0.027	15.794 \pm 0.007	407. $^{+15}_{-14}$	0.266 \pm 0.021
...	125.1496	-50.3162	2.505 \pm 0.084	-5.74 \pm 0.17	7.70 \pm 0.17	...	17.140 \pm 0.003	17.719 \pm 0.031	15.796 \pm 0.004	395. $^{+14}_{-13}$	0.604 \pm 0.048
...	121.5614	-49.1299	2.323 \pm 0.094	-5.70 \pm 0.18	8.14 \pm 0.20	...	17.097 \pm 0.002	18.801 \pm 0.027	15.784 \pm 0.003	426. $^{+18}_{-17}$	0.251 \pm 0.020
...	121.0098	-49.2195	2.307 \pm 0.061	-5.52 \pm 0.12	8.34 \pm 0.12	...	16.778 \pm 0.002	18.105 \pm 0.011	15.577 \pm 0.004	429. $^{+12}_{-11}$	0.406 \pm 0.032
...	120.7853	-49.5336	2.317 \pm 0.072	-5.48 \pm 0.15	8.16 \pm 0.13	...	16.822 \pm 0.002	18.264 \pm 0.017	15.617 \pm 0.004	427. $^{+14}_{-13}$	0.374 \pm 0.030
...	122.6761	-50.0276	2.464 \pm 0.087	-5.93 \pm 0.16	8.01 \pm 0.15	...	16.961 \pm 0.006	18.513 \pm 0.027	15.647 \pm 0.019	402. $^{+15}_{-14}$	0.297 \pm 0.024
...	121.3289	-50.3143	2.449 \pm 0.090	-5.20 \pm 0.17	7.66 \pm 0.21	...	17.288 \pm 0.002	19.161 \pm 0.025	15.945 \pm 0.005	405. $^{+15}_{-14}$	0.206 \pm 0.016
...	121.5461	-50.5053	2.323 \pm 0.073	-5.18 \pm 0.14	8.29 \pm 0.14	...	17.088 \pm 0.002	18.735 \pm 0.025	15.817 \pm 0.005	427. $^{+14}_{-13}$	0.276 \pm 0.022
...	121.5973	-50.7256	2.525 \pm 0.050	-5.47 \pm 0.10	8.380 \pm 0.095	...	16.144 \pm 0.002	17.577 \pm 0.010	14.953 \pm 0.004	391.8. $^{+7.8}_{-7.5}$	0.380 \pm 0.030
HD 66006	119.8065	-49.9737	2.313 \pm 0.055	-5.62 \pm 0.11	7.88 \pm 0.12	...	6.316 \pm 0.002	6.260 \pm 0.003	6.446 \pm 0.003	427. $^{+10}_{-9.9}$	5.4 \pm 6.7
...	119.7041	-49.9461	2.361 \pm 0.081	-4.92 \pm 0.18	7.53 \pm 0.20	...	17.077 \pm 0.002	18.932 \pm 0.024	15.752 \pm 0.006	419. $^{+15}_{-14}$	0.213 \pm 0.017
2MASS J07573369-5015153	119.3903	-50.2541	2.308 \pm 0.047	-5.440 \pm 0.089	8.205 \pm 0.10	58.74 \pm 0.10	12.274 \pm 0.002	12.523 \pm 0.013	11.547 \pm 0.016	428.2. $^{+8.9}_{-8.5}$	1.012 \pm 0.081

Table B.5: Yep 2—Continued

Star Name	RA ($^{\circ}$)	Dec ($^{\circ}$)	Parallax (mas)	μ_{α} (mas yr $^{-1}$)	μ_{δ} (mas yr $^{-1}$)	v_r (km s $^{-1}$)	G (mag)	BP (mag)	RP (mag)	d (pc)	Mass (M $_{\odot}$)
...	122.8657 -50.0564	2.531 \pm 0.025	-5.360 \pm 0.047	8.443 \pm 0.056	...	14.788 \pm 0.002	15.740 \pm 0.008	13.816 \pm 0.004	390.7 \pm 3.9	603 \pm 0.048	
...	119.9845 -47.2210	2.43 \pm 0.14	-5.37 \pm 0.26	8.50 \pm 0.28	...	18.179 \pm 0.003	20.109 \pm 0.064	16.760 \pm 0.008	409 $^{+26}_{-23}$	1.181 \pm 0.014	
...	119.5157 -48.5487	2.30 \pm 0.13	-5.00 \pm 0.26	7.72 \pm 0.24	...	17.902 \pm 0.003	19.627 \pm 0.048	16.537 \pm 0.006	432 $^{+27}_{-24}$	0.233 \pm 0.019	
...	118.6130 -49.0766	2.32 \pm 0.15	-5.39 \pm 0.27	8.20 \pm 0.30	...	18.269 \pm 0.003	20.052 \pm 0.072	16.906 \pm 0.008	428 $^{+30}_{-27}$	0.221 \pm 0.020	
...	119.3320 -49.5496	2.32 \pm 0.12	-5.29 \pm 0.23	8.28 \pm 0.23	...	17.769 \pm 0.002	19.506 \pm 0.051	16.472 \pm 0.006	427 $^{+24}_{-22}$	0.247 \pm 0.020	
...	119.0255 -49.5883	2.33 \pm 0.11	-5.38 \pm 0.22	7.99 \pm 0.21	...	17.844 \pm 0.003	19.807 \pm 0.086	16.488 \pm 0.008	426 $^{+22}_{-20}$	0.184 \pm 0.017	
...	119.1714 -49.7070	2.51 \pm 0.10	-5.41 \pm 0.20	8.35 \pm 0.21	...	17.673 \pm 0.002	19.362 \pm 0.054	16.394 \pm 0.006	394 $^{+17}_{-16}$	0.263 \pm 0.021	
...	121.9038 -48.5335	2.49 \pm 0.12	-5.86 \pm 0.24	8.31 \pm 0.22	...	17.585 \pm 0.002	19.350 \pm 0.065	16.233 \pm 0.008	398 $^{+20}_{-18}$	0.226 \pm 0.019	
...	121.9025 -48.5333	2.49 \pm 0.11	-5.54 \pm 0.25	8.33 \pm 0.21	...	17.593 \pm 0.003	19.357 \pm 0.050	16.244 \pm 0.007	399 $^{+19}_{-17}$	0.227 \pm 0.018	
...	122.3935 -49.1007	2.41 \pm 0.14	-5.37 \pm 0.26	8.15 \pm 0.26	...	17.957 \pm 0.003	19.748 \pm 0.036	16.634 \pm 0.008	412 $^{+25}_{-22}$	0.227 \pm 0.018	
...	120.6168 -48.4022	2.32 \pm 0.15	-5.21 \pm 0.27	8.27 \pm 0.18	...	17.455 \pm 0.002	19.060 \pm 0.039	16.156 \pm 0.007	428 $^{+29}_{-26}$	0.279 \pm 0.022	
...	119.5969 -48.7552	2.51 \pm 0.13	-5.47 \pm 0.26	7.57 \pm 0.30	...	17.995 \pm 0.003	19.115 \pm 0.16	16.496 \pm 0.023	396 $^{+21}_{-19}$	0.371 \pm 0.052	
...	119.4069 -48.5554	2.46 \pm 0.10	-5.67 \pm 0.19	8.78 \pm 0.18	...	17.464 \pm 0.002	19.205 \pm 0.044	16.157 \pm 0.005	402 $^{+17}_{-16}$	0.243 \pm 0.019	
...	117.3919 -48.3472	2.32 \pm 0.16	-5.51 \pm 0.28	8.59 \pm 0.33	...	17.897 \pm 0.003	19.620 \pm 0.076	16.562 \pm 0.006	430 $^{+33}_{-29}$	0.241 \pm 0.022	
...	118.2243 -48.5437	2.35 \pm 0.13	-5.46 \pm 0.26	7.92 \pm 0.29	...	17.814 \pm 0.003	19.04 \pm 0.13	16.454 \pm 0.020	423 $^{+25}_{-23}$	0.390 \pm 0.037	
...	119.7021 -46.5828	2.46 \pm 0.15	-5.42 \pm 0.24	7.87 \pm 0.29	...	18.049 \pm 0.003	19.881 \pm 0.099	16.722 \pm 0.008	404 $^{+26}_{-23}$	0.218 \pm 0.025	
...	119.4291 -45.9961	2.45 \pm 0.15	-5.58 \pm 0.25	8.15 \pm 0.28	...	17.963 \pm 0.003	19.655 \pm 0.051	16.644 \pm 0.007	406 $^{+26}_{-23}$	0.253 \pm 0.020	
...	121.0990 -46.2057	2.330 \pm 0.091	-5.61 \pm 0.17	8.01 \pm 0.20	...	17.142 \pm 0.003	18.927 \pm 0.049	15.818 \pm 0.007	425 $^{+17}_{-16}$	0.228 \pm 0.018	

Table B.5: Yep 2—Continued

Star Name	RA ($^{\circ}$)	Dec ($^{\circ}$)	Parallax (mas)	μ_{α} (mas yr $^{-1}$)	μ_{δ} (mas yr $^{-1}$)	v_r (km s $^{-1}$)	G (mag)	BP (mag)	RP (mag)	d (pc)	Mass (M $_{\odot}$)
...	122.5352 -48.0071	2.36 ± 0.15	-5.61 ± 0.27	7.52 ± 0.27	...	18.279 ± 0.003	19.82 ± 0.12	16.845 ± 0.016	421 $^{+30}_{-26}$	0.260 ± 0.038	
...	123.1099 -47.9235	2.51 ± 0.11	-5.48 ± 0.17	7.77 ± 0.20	...	17.134 ± 0.003	18.867 ± 0.017	15.871 ± 0.006	396 $^{+17}_{-16}$	0.256 ± 0.021	
...	122.7710 -47.8435	2.37 ± 0.16	-5.83 ± 0.28	8.41 ± 0.29	...	18.135 ± 0.002	20.137 ± 0.071	16.739 ± 0.009	421 $^{+31}_{-27}$	0.175 ± 0.014	
...	122.7752 -47.7566	2.50 ± 0.16	-5.51 ± 0.27	8.27 ± 0.29	...	18.244 ± 0.003	19.858 ± 0.086	16.828 ± 0.008	398 $^{+28}_{-25}$	0.248 ± 0.025	
...	122.0107 -48.1415	2.40 ± 0.10	-5.98 ± 0.19	8.45 ± 0.20	...	17.847 ± 0.002	19.559 ± 0.094	16.457 ± 0.009	413 $^{+18}_{-17}$	0.230 ± 0.025	
...	120.1248 -47.7029	2.50 ± 0.14	-5.84 ± 0.31	8.20 ± 0.28	...	18.337 ± 0.004	20.055 ± 0.095	16.952 ± 0.009	398 $^{+24}_{-22}$	0.230 ± 0.025	
...	120.8559 -47.6772	2.47 ± 0.16	-5.54 ± 0.31	8.64 ± 0.28	...	18.195 ± 0.003	19.943 ± 0.075	16.808 ± 0.007	403 $^{+28}_{-25}$	0.223 ± 0.021	
...	120.6701 -47.2716	2.41 ± 0.11	-5.42 ± 0.19	8.09 ± 0.20	...	17.631 ± 0.002	19.416 ± 0.037	16.347 ± 0.007	411 $^{+19}_{-18}$	0.238 ± 0.019	
...	121.1902 -46.8270	2.44 ± 0.15	-5.44 ± 0.26	8.23 ± 0.30	...	18.028 ± 0.003	19.88 ± 0.11	16.689 ± 0.008	407 $^{+27}_{-24}$	0.210 ± 0.026	
...	122.8441 -47.2207	2.42 ± 0.15	-5.83 ± 0.28	7.93 ± 0.28	...	18.014 ± 0.004	19.547 ± 0.059	16.612 ± 0.011	411 $^{+28}_{-25}$	0.271 ± 0.025	
TYC 8138-1739-1	115.5234 -48.6715	2.435 ± 0.022	-5.398 ± 0.043	8.480 ± 0.045	19	11.090 ± 0.001	11.530 ± 0.004	10.504 ± 0.003	406.0 $^{+3.6}_{-3.5}$	0.976 ± 0.078	
...	116.4646 -48.1330	2.342 ± 0.069	-5.35 ± 0.13	8.04 ± 0.14	...	16.941 ± 0.001	18.530 ± 0.033	15.680 ± 0.004	422 $^{+13}_{-12}$	0.302 ± 0.024	
...	116.5174 -49.3535	2.348 ± 0.028	-5.318 ± 0.053	8.437 ± 0.052	...	15.208 ± 0.001	16.223 ± 0.005	14.192 ± 0.003	420.7 $^{+5.0}_{-4.9}$	0.558 ± 0.045	
...	116.5472 -48.7261	2.432 ± 0.070	-5.41 ± 0.15	8.56 ± 0.14	...	16.949 ± 0.001	18.726 ± 0.030	15.654 ± 0.005	407 $^{+12}_{-11}$	0.237 ± 0.019	
...	117.0050 -49.1673	2.437 ± 0.018	-5.325 ± 0.033	8.643 ± 0.035	...	13.785 ± 0.003	14.441 ± 0.011	13.011 ± 0.009	405.5 ± 3.0	0.757 ± 0.061	
...	117.0332 -48.4870	2.426 ± 0.018	-5.335 ± 0.035	8.212 ± 0.034	...	14.406 ± 0.002	15.204 ± 0.008	13.522 ± 0.004	407.3 ± 3.0	0.691 ± 0.055	
...	117.0381 -48.4860	2.459 ± 0.028	-5.332 ± 0.057	8.227 ± 0.055	...	15.438 ± 0.002	16.505 ± 0.009	14.397 ± 0.005	402.1 $^{+4.6}_{-4.5}$	0.545 ± 0.044	
...	117.0455 -47.8965	2.349 ± 0.022	-5.319 ± 0.041	8.299 ± 0.049	...	14.841 ± 0.013	15.714 ± 0.046	13.886 ± 0.037	420.5 ± 3.9	0.662 ± 0.053	
...	117.1552 -49.0755	2.335 ± 0.044	-5.285 ± 0.082	8.165 ± 0.085	...	16.031 ± 0.004	17.282 ± 0.018	14.900 ± 0.011	423.2 $^{+8.2}_{-7.9}$	0.442 ± 0.035	

Table B.5: Yep 2—Continued

Star Name	RA ($^{\circ}$)	Dec ($^{\circ}$)	Parallax (mas)	μ_{α} (mas yr $^{-1}$)	μ_{δ} (mas yr $^{-1}$)	v_r (km s $^{-1}$)	G (mag)	BP (mag)	RP (mag)	d (pc)	Mass (M $_{\odot}$)
...	117.2139	-48.3789	2.413 \pm 0.019	-5.506 \pm 0.042	8.032 \pm 0.037	...	14.730 \pm 0.002	15.602 \pm 0.010	13.783 \pm 0.009	409.5 $^{+3.3}_{-3.2}$	667 \pm 0.053
...	117.2825	-49.2546	2.370 \pm 0.067	-5.30 \pm 0.13	8.18 \pm 0.13	...	16.743 \pm 0.003	18.065 \pm 0.036	15.479 \pm 0.016	417 $^{+12}_{-11}$	391 \pm 0.031
2MASS J07492170-4630304	117.3404	-46.5085	2.474 \pm 0.021	-5.317 \pm 0.049	8.468 \pm 0.040	22.54 \pm 0.72	11.702 \pm 0.001	12.087 \pm 0.002	11.165 \pm 0.002	399.5 $^{+3.4}_{-3.3}$	950 \pm 0.048
...	117.6447	-47.6280	2.480 \pm 0.017	-5.495 \pm 0.033	8.436 \pm 0.036	...	13.827 \pm 0.001	14.511 \pm 0.004	13.031 \pm 0.003	398.5 \pm 2.7	738 \pm 0.059
...	117.9236	-48.0580	2.405 \pm 0.017	-5.415 \pm 0.034	8.333 \pm 0.031	...	13.740 \pm 0.002	14.351 \pm 0.009	12.978 \pm 0.005	410.9 \pm 2.9	779 \pm 0.062
2MASS J07514674-4607038	117.9448	-46.1177	2.468 \pm 0.032	-5.325 \pm 0.051	8.339 \pm 0.073	22.92 \pm 0.22	12.650 \pm 0.002	13.152 \pm 0.008	12.002 \pm 0.005	400.5 $^{+5.3}_{-5.2}$	876 \pm 0.070
...	117.9640	-49.3116	2.410 \pm 0.084	-5.44 \pm 0.16	8.34 \pm 0.15	...	17.170 \pm 0.001	18.908 \pm 0.021	15.873 \pm 0.005	411 $^{+15}_{-14}$	247 \pm 0.020
...	117.9939	-48.6283	2.343 \pm 0.059	-5.10 \pm 0.12	7.96 \pm 0.11	...	16.448 \pm 0.002	17.855 \pm 0.019	15.272 \pm 0.006	422 $^{+11}_{-10}$	391 \pm 0.031
...	118.0242	-47.0746	2.482 \pm 0.064	-5.50 \pm 0.12	8.11 \pm 0.13	...	16.862 \pm 0.001	18.350 \pm 0.022	15.637 \pm 0.003	399 $^{+11}_{-10}$	356 \pm 0.028
...	118.3199	-49.1765	2.457 \pm 0.019	-5.622 \pm 0.044	8.306 \pm 0.037	...	14.444 \pm 0.002	15.187 \pm 0.008	13.589 \pm 0.005	402.2 $^{+3.1}_{-3.0}$	699 \pm 0.056
...	118.4454	-49.1173	2.474 \pm 0.074	-5.36 \pm 0.16	7.98 \pm 0.15	...	17.096 \pm 0.001	18.615 \pm 0.029	15.851 \pm 0.004	400. \pm 12	333 \pm 0.027
TYC 8143-1918-1	118.4461	-49.2152	2.337 \pm 0.021	-5.413 \pm 0.043	8.479 \pm 0.040	21.8 \pm 1.5	11.734 \pm 0.002	12.111 \pm 0.005	11.176 \pm 0.004	422.6 $^{+3.8}_{-3.7}$	980 \pm 0.049
...	118.4776	-48.2082	2.384 \pm 0.020	-5.409 \pm 0.037	7.865 \pm 0.040	...	14.756 \pm 0.002	15.596 \pm 0.011	13.846 \pm 0.005	414.5 $^{+3.6}_{-3.5}$	673 \pm 0.054
2MASS J07541099-4945078	118.5458	-49.7522	2.385 \pm 0.015	-5.530 \pm 0.030	8.270 \pm 0.030	26.84 \pm 0.25	13.557 \pm 0.001	13.998 \pm 0.005	12.964 \pm 0.003	414.3 \pm 2.5	860 \pm 0.043
...	118.6367	-49.4700	2.428 \pm 0.035	-5.379 \pm 0.065	8.230 \pm 0.065	...	15.669 \pm 0.005	16.832 \pm 0.021	14.578 \pm 0.012	407.2 $^{+6.0}_{-5.8}$	498 \pm 0.040
...	118.7004	-48.2438	2.470 \pm 0.039	-5.379 \pm 0.074	8.611 \pm 0.069	...	15.531 \pm 0.004	16.620 \pm 0.022	14.488 \pm 0.008	400.4 $^{+6.4}_{-6.2}$	539 \pm 0.043
...	118.9328	-47.8811	2.480 \pm 0.066	-5.35 \pm 0.12	8.30 \pm 0.12	...	16.911 \pm 0.003	18.593 \pm 0.040	15.646 \pm 0.011	399 $^{+11}_{-10}$	269 \pm 0.021
2MASS J07554620-4712483	118.9425	-47.2134	2.463 \pm 0.026	-5.533 \pm 0.048	8.062 \pm 0.044	8.6 \pm 1.1	11.921 \pm 0.001	12.417 \pm 0.004	11.280 \pm 0.003	401.4 $^{+4.3}_{-4.2}$	820 \pm 0.075

Table B.5: Yep 2—Continued

Star Name	RA ($^{\circ}$)	Dec ($^{\circ}$)	Parallax (mas)	μ_{α} (mas yr^{-1})	μ_{δ} (mas yr^{-1})	v_r (km s^{-1})	G (mag)	BP (mag)	RP (mag)	d (pc)	Mass (M_{\odot})
2MASS J07560331-4910495	119.0138	-49.10495	2.466 ± 0.025	-5.446 ± 0.052	8.164 ± 0.041	20.74 ± 0.17	11.914 ± 0.001	12.321 ± 0.003	11.352 ± 0.002	400.8 $^{+4.0}_{-3.9}$	0.940 ± 0.047
HD 65335	119.0316	-47.8299	2.328 ± 0.038	-5.687 ± 0.063	8.110 ± 0.062	19.7 ± 8.3	10.169 ± 0.001	10.236 ± 0.001	10.081 ± 0.001	424.5 $^{+6.9}_{-6.7}$	2.05 ± 0.44
...	119.0697	-48.9647	2.368 ± 0.059	-5.47 ± 0.12	8.06 ± 0.12	...	16.790 ± 0.002	18.352 ± 0.015	15.556 ± 0.005	418 $^{+11}_{-10.}$	0.322 ± 0.026
2MASS J07564756-4751454	119.1982	-47.8626	2.371 ± 0.020	-5.580 ± 0.036	8.228 ± 0.036	20.05 ± 0.31	11.759 ± 0.000	12.080 ± 0.002	11.290 ± 0.001	416.8 $^{+3.6}_{-3.5}$	1.030 ± 0.052
...	119.2067	-47.8490	2.432 ± 0.070	-5.38 ± 0.13	8.30 ± 0.12	...	17.089 ± 0.002	18.709 ± 0.027	15.804 ± 0.004	407 $^{+12}_{-11}$	0.279 ± 0.022
...	119.3138	-48.6307	2.345 ± 0.074	-5.48 ± 0.13	8.11 ± 0.12	...	16.944 ± 0.002	18.517 ± 0.028	15.699 ± 0.006	422 $^{+14}_{-13}$	0.314 ± 0.025
...	119.3637	-49.1708	2.358 ± 0.067	-5.46 ± 0.14	8.00 ± 0.15	...	16.411 ± 0.001	18.135 ± 0.015	15.128 ± 0.004	420 ± 12	0.253 ± 0.020
...	119.3645	-48.5696	2.397 ± 0.068	-5.71 ± 0.14	8.17 ± 0.14	...	16.723 ± 0.001	18.533 ± 0.027	15.429 ± 0.003	413 $^{+12}_{-11}$	0.229 ± 0.018
...	119.5003	-49.4568	2.399 ± 0.047	-5.592 ± 0.085	8.240 ± 0.091	...	15.768 ± 0.001	16.913 ± 0.009	14.701 ± 0.002	412.0 $^{+8.2}_{-7.9}$	0.529 ± 0.042
HD 65729	119.5031	-46.1037	2.384 ± 0.044	-5.435 ± 0.075	8.066 ± 0.099	...	9.565 ± 0.000	9.581 ± 0.001	9.565 ± 0.002	414.6 $^{+7.7}_{-7.4}$	3.38 ± 0.58
HD 65774	119.5037	-49.0200	2.343 ± 0.037	-5.558 ± 0.076	8.001 ± 0.075	...	8.757 ± 0.001	8.753 ± 0.001	8.785 ± 0.001	421.7 $^{+6.7}_{-6.5}$	2.75 ± 0.94
...	119.5173	-47.9188	2.328 ± 0.068	-5.52 ± 0.13	7.97 ± 0.14	...	16.822 ± 0.001	18.476 ± 0.015	15.548 ± 0.004	425 $^{+13}_{-12}$	0.273 ± 0.022
...	119.5296	-48.3894	2.338 ± 0.019	-5.525 ± 0.033	8.114 ± 0.033	...	14.284 ± 0.003	14.981 ± 0.010	13.473 ± 0.007	422.5 $^{+3.4}_{-3.3}$	0.728 ± 0.058
2MASS J07580873-4914595	119.5364	-49.2499	2.474 ± 0.067	-5.67 ± 0.13	8.05 ± 0.12	...	16.780 ± 0.004	18.071 ± 0.034	15.545 ± 0.008	400. ± 11	0.406 ± 0.033
...	119.5522	-49.3283	2.396 ± 0.078	-5.60 ± 0.16	8.22 ± 0.15	...	16.987 ± 0.003	18.493 ± 0.024	15.704 ± 0.017	413 $^{+14}_{-13}$	0.324 ± 0.026
CD-483350	119.5705	-49.2364	2.385 ± 0.035	-5.648 ± 0.070	7.790 ± 0.067	...	9.965 ± 0.001	10.033 ± 0.002	9.871 ± 0.002	414.5 $^{+6.2}_{-6.0}$	2.18 ± 0.35
...	119.5898	-49.1918	2.478 ± 0.052	-5.66 ± 0.12	7.983 ± 0.099	...	16.220 ± 0.003	17.477 ± 0.022	15.051 ± 0.009	399.2 $^{+8.6}_{-8.2}$	0.431 ± 0.034
...	119.6094	-48.0307	2.469 ± 0.021	-5.348 ± 0.046	8.253 ± 0.049	...	14.977 ± 0.001	15.920 ± 0.005	14.011 ± 0.004	400.4 $^{+3.5}_{-3.4}$	0.610 ± 0.049
...	119.6224	-49.2529	2.339 ± 0.043	-5.391 ± 0.090	8.013 ± 0.096	...	16.129 ± 0.001	17.323 ± 0.013	14.994 ± 0.004	422.5 $^{+7.9}_{-7.6}$	0.458 ± 0.037

Table B.5: Yep 2—Continued

Star Name	RA ($^{\circ}$)	Dec ($^{\circ}$)	Parallax (mas)	μ_{α} (mas yr $^{-1}$)	μ_{δ} (mas yr $^{-1}$)	v_r (km s $^{-1}$)	G (mag)	BP (mag)	RP (mag)	d (pc)	Mass (M $_{\odot}$)
...	119.6664	-49.3122	2.377 \pm 0.063	-5.56 \pm 0.12	7.87 \pm 0.14	...	16.981 \pm 0.002	18.484 \pm 0.020	15.727 \pm 0.006	416 \pm 11	0.335 \pm 0.027
...	119.6824	-48.8550	2.392 \pm 0.048	-5.423 \pm 0.092	8.07 \pm 0.11	...	16.537 \pm 0.003	17.939 \pm 0.032	15.326 \pm 0.010	413.3 $^{+8.4}_{-8.1}$	0.383 \pm 0.031
...	119.7040	-49.1963	2.467 \pm 0.026	-5.699 \pm 0.055	8.123 \pm 0.055	...	14.458 \pm 0.002	15.219 \pm 0.008	13.598 \pm 0.006	400.8 $^{+4.3}_{-4.2}$	0.697 \pm 0.056
HD 65894	119.7199	-45.8842	2.480 \pm 0.034	-5.848 \pm 0.057	8.413 \pm 0.058	...	10.226 \pm 0.000	10.303 \pm 0.001	10.114 \pm 0.001	398.7 $^{+5.6}_{-5.4}$	1.980 \pm 0.099
...	119.7871	-49.2471	2.379 \pm 0.025	-5.317 \pm 0.049	8.235 \pm 0.053	...	15.198 \pm 0.002	16.159 \pm 0.007	14.213 \pm 0.004	415.4 $^{+4.3}_{-4.2}$	0.592 \pm 0.047
...	119.7889	-49.8486	2.362 \pm 0.024	-5.383 \pm 0.044	8.198 \pm 0.055	...	14.446 \pm 0.002	15.226 \pm 0.010	13.584 \pm 0.005	418.4 $^{+4.2}_{-4.1}$	0.695 \pm 0.056
...	119.8013	-49.3052	2.417 \pm 0.034	-5.453 \pm 0.068	8.500 \pm 0.077	...	15.388 \pm 0.001	16.709 \pm 0.006	14.234 \pm 0.003	409.0 $^{+5.8}_{-5.6}$	0.419 \pm 0.034
HD 66005	119.8013	-49.9769	2.463 \pm 0.060	-5.85 \pm 0.12	8.40 \pm 0.15	...	6.294 \pm 0.001	6.231 \pm 0.002	6.440 \pm 0.003	402 $^{+10.}_{-9.6}$	7.3 \pm 6.3
...	119.8321	-49.1695	2.443 \pm 0.019	-5.377 \pm 0.041	7.988 \pm 0.042	...	14.374 \pm 0.003	15.157 \pm 0.011	13.504 \pm 0.007	404.5 $^{+3.2}_{-3.1}$	0.694 \pm 0.056
...	119.8388	-49.0647	2.374 \pm 0.066	-5.32 \pm 0.12	8.32 \pm 0.13	...	16.816 \pm 0.001	18.427 \pm 0.020	15.542 \pm 0.003	417 $^{+12}_{-11}$	0.284 \pm 0.023
...	119.8649	-49.2403	2.368 \pm 0.064	-5.57 \pm 0.12	8.55 \pm 0.12	...	16.729 \pm 0.004	18.245 \pm 0.018	15.492 \pm 0.012	418 $^{+12}_{-11}$	0.337 \pm 0.027
2MASS J07593159-4820134	119.8816	-48.3371	2.425 \pm 0.018	-5.621 \pm 0.035	8.582 \pm 0.035	21.44 \pm 0.39	12.960 \pm 0.003	13.460 \pm 0.008	12.308 \pm 0.006	407.5 $^{+3.0}_{-2.9}$	0.820 \pm 0.041
...	119.9050	-48.8420	2.447 \pm 0.032	-5.542 \pm 0.057	8.445 \pm 0.063	...	15.284 \pm 0.001	16.441 \pm 0.005	14.205 \pm 0.004	404.0 $^{+5.4}_{-5.2}$	0.511 \pm 0.041
...	119.9631	-49.4434	2.343 \pm 0.032	-5.097 \pm 0.056	7.999 \pm 0.068	...	15.606 \pm 0.005	16.666 \pm 0.032	14.562 \pm 0.012	421.8 $^{+5.7}_{-5.6}$	0.546 \pm 0.044
...	119.9889	-49.5149	2.491 \pm 0.034	-5.426 \pm 0.064	8.246 \pm 0.071	...	15.766 \pm 0.002	16.966 \pm 0.010	14.663 \pm 0.007	396.9 $^{+5.4}_{-5.3}$	0.461 \pm 0.037
...	120.0309	-47.2310	2.358 \pm 0.051	-5.345 \pm 0.091	8.180 \pm 0.094	...	16.296 \pm 0.002	17.696 \pm 0.014	15.098 \pm 0.006	419.2 $^{+9.2}_{-8.8}$	0.387 \pm 0.031
...	120.0358	-48.6960	2.410 \pm 0.029	-5.648 \pm 0.052	8.030 \pm 0.054	...	15.258 \pm 0.002	16.272 \pm 0.010	14.251 \pm 0.005	410.1 $^{+5.0}_{-4.9}$	0.562 \pm 0.045
...	120.0610	-48.9901	2.460 \pm 0.062	-5.49 \pm 0.12	8.14 \pm 0.13	...	16.742 \pm 0.002	18.091 \pm 0.028	15.494 \pm 0.005	402 $^{+10.}_{-9.8}$	0.387 \pm 0.031

Table B.5: Yep 2—Continued

Star Name	RA ($^{\circ}$)	Dec ($^{\circ}$)	Parallax (mas)	μ_{α} (mas yr^{-1})	μ_{δ} (mas yr^{-1})	v_r (km s^{-1})	G (mag)	BP (mag)	RP (mag)	d (pc)	Mass (M_{\odot})
...	120.1030 -48.7151	2.383 \pm 0.062	-5.35 \pm 0.11	7.97 \pm 0.11	...	15.992 \pm 0.001	17.399 \pm 0.012	14.797 \pm 0.007	415 $^{+11}_{-10}$	0.386 \pm 0.031	
...	120.1114 -47.1270	2.435 \pm 0.016	-5.396 \pm 0.032	8.020 \pm 0.038	...	14.122 \pm 0.001	14.833 \pm 0.005	13.301 \pm 0.003	405.9 \pm 2.7	0.720 \pm 0.058	
...	120.2026 -48.9589	2.425 \pm 0.022	-5.615 \pm 0.043	7.945 \pm 0.044	...	14.605 \pm 0.001	15.431 \pm 0.006	13.718 \pm 0.004	407.6 \pm 3.6	0.688 \pm 0.055	
...	120.2696 -47.7566	2.415 \pm 0.027	-5.708 \pm 0.052	8.168 \pm 0.045	...	14.899 \pm 0.002	15.845 \pm 0.008	13.934 \pm 0.005	409.3 $^{+4.6}_{-4.5}$	0.609 \pm 0.049	
2MASS J08012725-4940216	120.3636 -49.6727	2.336 \pm 0.013	-5.323 \pm 0.028	7.693 \pm 0.023	24.9 \pm 1.6	13.030 \pm 0.002	13.557 \pm 0.005	12.354 \pm 0.004	422.8 \pm 2.4	0.860 \pm 0.043	
...	120.4210 -46.7471	2.498 \pm 0.033	-5.657 \pm 0.062	8.080 \pm 0.060	...	15.567 \pm 0.002	16.693 \pm 0.011	14.492 \pm 0.007	395.8 $^{+5.3}_{-5.2}$	0.517 \pm 0.041	
...	120.4353 -48.2800	2.469 \pm 0.074	-5.70 \pm 0.14	8.42 \pm 0.16	...	16.872 \pm 0.001	18.534 \pm 0.022	15.579 \pm 0.004	401 \pm 12	0.266 \pm 0.021	
...	120.6205 -48.9112	2.457 \pm 0.025	-5.663 \pm 0.050	8.130 \pm 0.044	...	14.608 \pm 0.003	15.395 \pm 0.010	13.728 \pm 0.007	402.3 $^{+4.1}_{-4.0}$	0.692 \pm 0.055	
...	120.6554 -46.6195	2.384 \pm 0.022	-5.756 \pm 0.038	7.997 \pm 0.041	...	13.944 \pm 0.004	14.632 \pm 0.015	13.149 \pm 0.010	414.4 \pm 3.9	0.736 \pm 0.059	
...	120.6640 -49.3703	2.483 \pm 0.062	-5.50 \pm 0.13	8.07 \pm 0.11	...	16.311 \pm 0.002	17.896 \pm 0.015	15.060 \pm 0.004	398 $^{+10.}_{-9.7}$	0.307 \pm 0.025	
...	120.6845 -48.7936	2.433 \pm 0.044	-5.871 \pm 0.092	8.103 \pm 0.078	...	16.076 \pm 0.002	17.286 \pm 0.011	14.967 \pm 0.004	406.4 $^{+7.5}_{-7.2}$	0.448 \pm 0.036	
...	120.8811 -47.1854	2.405 \pm 0.053	-5.531 \pm 0.091	7.69 \pm 0.10	...	16.191 \pm 0.002	17.531 \pm 0.009	15.030 \pm 0.004	411.1 $^{+9.2}_{-8.8}$	0.412 \pm 0.033	
HD 66971	120.9069 -48.9881	2.382 \pm 0.043	-5.626 \pm 0.087	7.911 \pm 0.085	...	9.031 \pm 0.000	9.031 \pm 0.001	9.057 \pm 0.002	414.9 $^{+7.6}_{-7.3}$	2.18 \pm 0.35	
...	120.9201 -49.3129	2.393 \pm 0.042	-5.324 \pm 0.074	8.139 \pm 0.075	...	15.238 \pm 0.002	16.518 \pm 0.007	14.104 \pm 0.005	413.0 $^{+7.3}_{-7.1}$	0.433 \pm 0.035	
TYC 8144-2888-1	121.0043 -50.0889	2.467 \pm 0.026	-5.544 \pm 0.052	7.830 \pm 0.048	21.82 \pm 0.72	11.284 \pm 0.001	11.547 \pm 0.001	10.873 \pm 0.001	400.7 $^{+4.3}_{-4.2}$	1.44 \pm 0.12	
...	121.0158 -48.4143	2.373 \pm 0.057	-5.62 \pm 0.11	8.00 \pm 0.12	...	16.616 \pm 0.002	18.062 \pm 0.013	15.404 \pm 0.004	417 $^{+10.}_{-9.8}$	0.371 \pm 0.030	
...	121.0205 -49.1574	2.408 \pm 0.038	-5.353 \pm 0.074	8.226 \pm 0.068	...	15.615 \pm 0.001	16.726 \pm 0.006	14.558 \pm 0.005	410.5 $^{+6.6}_{-6.4}$	0.528 \pm 0.042	
...	121.0209 -48.8829	2.429 \pm 0.031	-5.539 \pm 0.061	7.871 \pm 0.062	...	15.638 \pm 0.004	16.709 \pm 0.016	14.582 \pm 0.011	407.0 $^{+5.2}_{-5.1}$	0.541 \pm 0.043	
...	121.0220 -48.8848	2.422 \pm 0.024	-5.474 \pm 0.047	8.109 \pm 0.047	...	13.748 \pm 0.001	14.465 \pm 0.003	12.926 \pm 0.002	408.0 $^{+4.0}_{-3.9}$	0.717 \pm 0.057	

Table B.5: Yep 2—Continued

Star Name	<i>RA</i> ($^{\circ}$)	<i>Dec</i> ($^{\circ}$)	Parallax (mas)	μ_{α} (mas yr^{-1})	μ_{δ} (mas yr^{-1})	v_r (km s^{-1})	G (mag)	BP (mag)	RP (mag)	<i>d</i> (pc)	Mass (M_{\odot})
...	121.0279	-49.1417	2.471 \pm 0.064	-5.35 \pm 0.14	8.35 \pm 0.13	...	16.869 \pm 0.002	18.467 \pm 0.021	15.635 \pm 0.005	400 $^{+11}_{-10}$	0.309 \pm 0.025
...	121.0400	-48.3154	2.407 \pm 0.066	-5.53 \pm 0.12	7.67 \pm 0.13	...	16.691 \pm 0.002	18.062 \pm 0.017	15.442 \pm 0.005	411 $^{+12}_{-11}$	0.381 \pm 0.030
...	121.0876	-48.3641	2.342 \pm 0.043	-5.623 \pm 0.077	8.06 \pm 0.10	...	16.062 \pm 0.002	17.314 \pm 0.013	14.929 \pm 0.006	422.1 $^{+7.8}_{-7.5}$	0.442 \pm 0.035
2MASS J08042347-4938219	121.0978	-49.6395	2.446 \pm 0.014	-5.339 \pm 0.026	8.160 \pm 0.030	21.21 \pm 0.56	13.174 \pm 0.003	13.762 \pm 0.009	12.455 \pm 0.007	404.1 \pm 2.3	0.780 \pm 0.045
...	121.1373	-49.4144	2.492 \pm 0.049	-5.350 \pm 0.085	8.317 \pm 0.096	...	15.576 \pm 0.002	16.684 \pm 0.011	14.508 \pm 0.005	396.9 $^{+7.9}_{-7.6}$	0.525 \pm 0.042
...	121.4550	-48.5384	2.488 \pm 0.018	-5.631 \pm 0.034	8.248 \pm 0.034	...	14.167 \pm 0.002	14.932 \pm 0.009	13.311 \pm 0.006	397.4 \pm 2.9	0.697 \pm 0.056
...	121.5600	-48.3862	2.402 \pm 0.048	-5.63 \pm 0.10	8.038 \pm 0.094	...	16.040 \pm 0.002	17.347 \pm 0.010	14.897 \pm 0.004	411.6 $^{+8.3}_{-8.0}$	0.425 \pm 0.034
...	121.5608	-47.4282	2.490 \pm 0.023	-5.646 \pm 0.041	8.008 \pm 0.036	...	14.668 \pm 0.002	15.564 \pm 0.009	13.727 \pm 0.005	397.0 \pm 3.6	0.656 \pm 0.052
...	121.6366	-47.7735	2.489 \pm 0.052	-5.55 \pm 0.10	8.157 \pm 0.084	...	15.264 \pm 0.002	16.469 \pm 0.012	14.079 \pm 0.009	397.4 $^{+8.5}_{-8.2}$	0.440 \pm 0.035
2MASS J08063449-4705185	121.6437	-47.0885	2.387 \pm 0.025	-5.636 \pm 0.042	7.851 \pm 0.041	...	14.703 \pm 0.002	15.518 \pm 0.008	13.800 \pm 0.007	414.0 \pm 4.3	0.687 \pm 0.055
TYC 8140-3850-1	121.6850	-48.2688	2.384 \pm 0.034	-5.698 \pm 0.058	8.083 \pm 0.062	23	10.892 \pm 0.000	11.143 \pm 0.001	10.513 \pm 0.001	414.5 $^{+6.0}_{-5.8}$	1.48 \pm 0.12
...	121.6969	-48.9779	2.494 \pm 0.044	-5.818 \pm 0.084	7.736 \pm 0.081	...	15.664 \pm 0.002	16.949 \pm 0.011	14.522 \pm 0.006	396.6 $^{+7.1}_{-6.8}$	0.431 \pm 0.034
2MASS J08065006-4732219	121.7086	-47.5394	2.462 \pm 0.074	-5.66 \pm 0.12	8.31 \pm 0.12	10.79 \pm 0.28	16.964 \pm 0.001	18.501 \pm 0.024	15.674 \pm 0.007	402 \pm 12	0.700 \pm 0.035
...	121.8183	-50.3969	2.481 \pm 0.035	-5.454 \pm 0.066	8.315 \pm 0.062	...	16.058 \pm 0.001	17.294 \pm 0.006	14.939 \pm 0.003	398.5 $^{+5.6}_{-5.5}$	0.451 \pm 0.036
2MASS J08071677-4635515	121.8199	-46.5977	2.362 \pm 0.055	-5.83 \pm 0.11	7.81 \pm 0.12	...	16.232 \pm 0.002	17.541 \pm 0.014	15.084 \pm 0.004	418.6 $^{+9.9}_{-9.5}$	0.423 \pm 0.034
...	122.0295	-47.6997	2.477 \pm 0.064	-5.64 \pm 0.11	8.05 \pm 0.11	...	16.678 \pm 0.001	18.160 \pm 0.016	15.464 \pm 0.003	400 $^{+11}_{-10}$	0.360 \pm 0.029
...	122.1263	-47.5585	2.365 \pm 0.087	-5.73 \pm 0.15	7.66 \pm 0.14	...	16.903 \pm 0.001	18.690 \pm 0.022	15.563 \pm 0.003	419 $^{+16}_{-15}$	0.223 \pm 0.018

Table B.5: Yep 2—Continued

Star Name	RA ($^{\circ}$)	Dec ($^{\circ}$)	Parallax (mas)	μ_{α} (mas yr $^{-1}$)	μ_{δ} (mas yr $^{-1}$)	v_r (km s $^{-1}$)	G (mag)	BP (mag)	RP (mag)	a (pc)	Mass (M $_{\odot}$)
...	122.1563	-47.8359	2.356 ± 0.052	-5.831 ± 0.097	8.106 ± 0.094	...	16.106 ± 0.002	17.646 ± 0.018	14.861 ± 0.006	419.7 $^{+9.5}_{-9.1}$	0.326 ± 0.026
...	122.2716	-46.6395	2.452 ± 0.070	-5.89 ± 0.11	7.96 ± 0.12	...	15.946 ± 0.005	16.920 ± 0.018	14.728 ± 0.016	404 $^{+12}_{-11}$	0.520 ± 0.042
...	122.2768	-48.7245	2.492 ± 0.023	-5.549 ± 0.045	7.857 ± 0.042	...	14.934 ± 0.001	15.886 ± 0.006	13.957 ± 0.003	396.7 ± 3.7	601 ± 0.048
...	122.5995	-46.8586	2.442 ± 0.051	-5.761 ± 0.078	8.153 ± 0.083	...	15.585 ± 0.003	16.742 ± 0.014	14.498 ± 0.008	405.0 $^{+8.5}_{-8.2}$	0.505 ± 0.040
...	122.6974	-50.2328	2.462 ± 0.028	-5.617 ± 0.051	8.095 ± 0.052	...	15.300 ± 0.002	16.191 ± 0.010	14.359 ± 0.006	401.5 $^{+4.7}_{-4.6}$	0.659 ± 0.053
...	122.7085	-48.4990	2.338 ± 0.028	-5.171 ± 0.057	8.168 ± 0.063	...	15.603 ± 0.001	16.347 ± 0.006	14.755 ± 0.003	422.5 $^{+5.1}_{-5.0}$	0.699 ± 0.056
2MASS J08110224-4950578	122.7593	-49.8494	2.414 ± 0.078	-5.43 ± 0.16	8.06 ± 0.15	...	16.713 ± 0.001	18.524 ± 0.024	15.410 ± 0.003	410 $^{+14}_{-13}$	0.227 ± 0.018
...	123.0975	-49.2314	2.480 ± 0.026	-5.403 ± 0.047	8.088 ± 0.058	...	15.139 ± 0.002	16.129 ± 0.008	14.147 ± 0.004	398.6 $^{+4.1}_{-4.0}$	0.577 ± 0.046
...	123.2319	-49.4240	2.485 ± 0.058	-5.54 ± 0.10	7.74 ± 0.13	...	16.413 ± 0.002	17.848 ± 0.012	15.220 ± 0.005	398.1 $^{+9.4}_{-9.0}$	0.379 ± 0.030
...	124.2724	-49.4420	2.400 ± 0.065	-5.71 ± 0.12	8.00 ± 0.12	...	16.326 ± 0.001	17.798 ± 0.015	15.124 ± 0.004	412 ± 11	0.366 ± 0.029
...	118.1582	-49.1786	2.365 ± 0.083	-5.47 ± 0.17	8.22 ± 0.21	...	17.236 ± 0.012	18.896 ± 0.017	15.976 ± 0.002	419 $^{+15}_{-14}$	0.275 ± 0.022
...	118.2838	-49.5584	2.343 ± 0.070	-5.14 ± 0.14	8.21 ± 0.16	...	16.794 ± 0.002	18.231 ± 0.031	15.545 ± 0.011	422 $^{+13}_{-12}$	0.363 ± 0.029
...	118.3244	-48.7059	2.347 ± 0.080	-5.07 ± 0.15	8.48 ± 0.16	...	17.039 ± 0.002	18.638 ± 0.020	15.785 ± 0.005	422 $^{+15}_{-14}$	0.301 ± 0.024
...	118.3554	-48.9846	2.40 ± 0.14	-5.45 ± 0.26	8.07 ± 0.29	...	18.234 ± 0.002	20.155 ± 0.093	16.873 ± 0.010	415 $^{+27}_{-24}$	0.192 ± 0.019
...	118.5149	-49.8452	2.429 ± 0.088	-5.41 ± 0.17	8.15 ± 0.19	...	17.508 ± 0.001	18.921 ± 0.050	16.250 ± 0.005	408 $^{+15}_{-14}$	0.367 ± 0.029
...	118.8769	-48.3471	2.39 ± 0.11	-5.41 ± 0.21	8.65 ± 0.20	...	17.631 ± 0.001	19.238 ± 0.042	16.353 ± 0.005	415 $^{+17}_{-16}$	0.284 ± 0.024
...	119.1381	-48.8453	2.390 ± 0.096	-5.38 ± 0.18	7.61 ± 0.17	...	17.376 ± 0.001	19.187 ± 0.041	16.005 ± 0.006	415 $^{+17}_{-16}$	0.213 ± 0.017
...	119.1402	-49.6260	2.40 ± 0.15	-5.39 ± 0.27	8.13 ± 0.30	...	18.208 ± 0.001	20.970 ± 0.099	16.872 ± 0.007	415 $^{+29}_{-25}$	0.210 ± 0.024
...	119.1815	-49.9224	2.45 ± 0.10	-5.47 ± 0.22	8.67 ± 0.20	...	17.724 ± 0.001	19.326 ± 0.045	16.456 ± 0.006	404 $^{+17}_{-16}$	0.295 ± 0.025

Table B.5: Yep 2—Continued

Star Name	RA ($^{\circ}$)	Dec ($^{\circ}$)	Parallax (mas)	μ_{α} (mas yr $^{-1}$)	μ_{δ} (mas yr $^{-1}$)	v_r (km s $^{-1}$)	G (mag)	BP (mag)	RP (mag)	d (pc)	Mass (M $_{\odot}$)
...	119.5766	-49.2967	2.432 \pm 0.090	-5.63 \pm 0.19	8.12 \pm 0.17	...	17.531 \pm 0.002	18.986 \pm 0.037	16.240 \pm 0.006	407 $^{+16}_{-14}$	0.339 \pm 0.027
...	119.6301	-48.0913	2.48 \pm 0.13	-5.64 \pm 0.24	8.50 \pm 0.31	...	18.067 \pm 0.002	19.703 \pm 0.062	16.681 \pm 0.032	401 $^{+22}_{-20}$	0.250 \pm 0.022
...	119.6950	-49.0217	2.493 \pm 0.086	-5.51 \pm 0.16	7.77 \pm 0.17	...	17.208 \pm 0.001	19.092 \pm 0.025	15.867 \pm 0.005	397 $^{+14}_{-13}$	0.204 \pm 0.016
...	119.6980	-47.9161	2.495 \pm 0.065	-5.59 \pm 0.13	8.36 \pm 0.16	...	16.454 \pm 0.001	17.895 \pm 0.014	15.273 \pm 0.003	397 $^{+11}_{-10}$	0.380 \pm 0.030
...	119.7576	-49.4229	2.491 \pm 0.099	-5.35 \pm 0.18	8.49 \pm 0.23	...	17.528 \pm 0.002	19.149 \pm 0.036	16.228 \pm 0.007	398 $^{+16}_{-15}$	0.275 \pm 0.022
...	119.9923	-49.2936	2.34 \pm 0.11	-5.03 \pm 0.22	8.43 \pm 0.28	...	17.377 \pm 0.014	19.237 \pm 0.038	16.025 \pm 0.005	424 $^{+22}_{-20}$	0.207 \pm 0.017
...	120.4290	-49.0585	2.49 \pm 0.10	-5.51 \pm 0.20	8.19 \pm 0.19	...	17.605 \pm 0.002	19.271 \pm 0.048	16.315 \pm 0.006	399 $^{+17}_{-16}$	0.266 \pm 0.021
...	120.4592	-48.8766	2.48 \pm 0.14	-5.39 \pm 0.30	7.78 \pm 0.24	...	17.858 \pm 0.002	19.587 \pm 0.051	16.543 \pm 0.006	401 $^{+25}_{-22}$	0.244 \pm 0.020
...	120.4857	-48.8883	2.344 \pm 0.095	-5.62 \pm 0.18	8.16 \pm 0.16	...	17.045 \pm 0.002	18.733 \pm 0.041	15.685 \pm 0.009	423 $^{+18}_{-16}$	0.243 \pm 0.019
2MASS J08023538-4848048											
...	120.6870	-49.9013	2.38 \pm 0.12	-5.68 \pm 0.26	8.18 \pm 0.21	...	18.109 \pm 0.003	19.59 \pm 0.11	16.574 \pm 0.024	416 $^{+22}_{-20}$	0.250 \pm 0.030
...	120.6976	-48.9772	2.500 \pm 0.085	-5.32 \pm 0.17	8.01 \pm 0.15	...	17.314 \pm 0.021	19.010 \pm 0.034	16.031 \pm 0.005	396 $^{+14}_{-13}$	0.260 \pm 0.021
...	120.7682	-49.7088	2.43 \pm 0.13	-5.41 \pm 0.24	8.40 \pm 0.23	...	18.169 \pm 0.000	20.030 \pm 0.050	16.828 \pm 0.006	408 $^{+23}_{-21}$	0.209 \pm 0.017
...	120.8234	-49.4574	2.397 \pm 0.067	-5.13 \pm 0.15	7.58 \pm 0.12	...	17.115 \pm 0.003	18.665 \pm 0.024	15.869 \pm 0.004	413 $^{+12}_{-11}$	0.322 \pm 0.026
...	120.9192	-48.5879	2.33 \pm 0.13	-5.44 \pm 0.26	8.37 \pm 0.27	...	18.307 \pm 0.001	19.634 \pm 0.097	16.976 \pm 0.012	426 $^{+26}_{-23}$	0.371 \pm 0.035
...	117.0567	-48.6311	2.349 \pm 0.092	-5.28 \pm 0.18	8.30 \pm 0.21	...	17.653 \pm 0.008	19.611 \pm 0.044	16.331 \pm 0.006	422 $^{+17}_{-16}$	0.193 \pm 0.015
...	117.1305	-48.9734	2.362 \pm 0.092	-5.39 \pm 0.17	8.40 \pm 0.18	...	17.364 \pm 0.001	19.081 \pm 0.044	16.074 \pm 0.004	419 $^{+17}_{-16}$	0.253 \pm 0.020
...	117.2815	-49.2546	2.401 \pm 0.091	-5.37 \pm 0.17	8.28 \pm 0.18	...	17.127 \pm 0.002	18.548 \pm 0.041	15.848 \pm 0.015	412 $^{+16}_{-15}$	0.359 \pm 0.029

Table B.5: Yep 2—Continued

Star Name	RA ($^{\circ}$)	Dec ($^{\circ}$)	Parallax (mas)	μ_{α} (mas yr $^{-1}$)	μ_{δ} (mas yr $^{-1}$)	v_r (km s $^{-1}$)	G (mag)	BP (mag)	RP (mag)	d (pc)	Mass (M $_{\odot}$)
...	120.8951 -48.1139	2.50 ± 0.10	-5.33 ± 0.19	8.33 ± 0.22	...	17.639 ± 0.001	19.427 ± 0.039	16.304 ± 0.005	397 $^{+17}_{-15}$	0.224 ± 0.018	
...	121.1680 -48.0850	2.339 ± 0.083	-5.54 ± 0.18	8.18 ± 0.23	...	17.110 ± 0.003	18.562 ± 0.020	15.882 ± 0.004	423 $^{+16}_{-15}$	0.365 ± 0.029	
...	121.2622 -48.3248	2.478 ± 0.071	-5.76 ± 0.14	8.20 ± 0.16	...	16.710 ± 0.003	18.334 ± 0.019	15.438 ± 0.004	399 $^{+12}_{-11}$	0.281 ± 0.023	
...	121.3774 -47.9683	2.459 ± 0.082	-5.74 ± 0.15	7.95 ± 0.18	...	17.381 ± 0.004	19.010 ± 0.027	16.106 ± 0.004	403 $^{+14}_{-13}$	0.279 ± 0.022	
...	121.4086 -47.9907	2.461 ± 0.092	-5.55 ± 0.19	8.51 ± 0.18	...	17.506 ± 0.003	19.174 ± 0.033	16.218 ± 0.006	403 $^{+16}_{-14}$	0.266 ± 0.021	
...	115.0143 -48.4992	2.329 ± 0.024	-5.093 ± 0.049	8.563 ± 0.048	...	14.845 ± 0.002	15.711 ± 0.009	13.928 ± 0.005	424.2 $^{+4.3}_{-4.2}$	0.663 ± 0.053	
2MASS J07421676-4824037	115.5698 -48.4010	2.360 ± 0.016	-5.372 ± 0.028	8.401 ± 0.026	19.85 ± 0.25	13.082 ± 0.002	13.611 ± 0.008	12.386 ± 0.006	418.5 ± 2.7	0.860 ± 0.043	
...	115.8049 -47.7691	2.464 ± 0.014	-5.292 ± 0.024	7.937 ± 0.025	...	13.304 ± 0.002	14.001 ± 0.007	12.491 ± 0.005	401.1 ± 2.2	0.727 ± 0.058	
HD 63364	116.6213 -46.9418	2.360 ± 0.040	-5.631 ± 0.070	8.621 ± 0.076	...	8.744 ± 0.000	8.757 ± 0.001	8.745 ± 0.002	418.8 $^{+7.1}_{-6.9}$	2.75 ± 0.94	
2MASS J07471652-4931414	116.8188 -49.5282	2.392 ± 0.020	-5.754 ± 0.040	8.167 ± 0.040	17.41 ± 0.45	12.420 ± 0.002	12.880 ± 0.005	11.806 ± 0.004	413.0 ± 3.4	0.970 ± 0.048	
...	117.9052 -47.3045	2.352 ± 0.071	-5.42 ± 0.13	8.68 ± 0.14	...	16.823 ± 0.001	18.321 ± 0.020	15.576 ± 0.005	421 $^{+13}_{-12}$	0.347 ± 0.028	
...	121.0710 -50.4922	2.343 ± 0.082	-5.49 ± 0.16	8.36 ± 0.16	...	17.043 ± 0.002	18.894 ± 0.032	15.720 ± 0.003	422 $^{+15}_{-14}$	0.215 ± 0.017	
...	122.3871 -47.6183	2.351 ± 0.035	-5.160 ± 0.058	8.03 ± 0.11	...	14.474 ± 0.009	420.3 $^{+6.3}_{-6.2}$	0.798 ± 0.088	
...	119.4394 -49.4035	2.47 ± 0.16	-5.04 ± 0.31	7.73 ± 0.32	...	18.279 ± 0.013	20.295 ± 0.082	16.878 ± 0.007	402 $^{+28}_{-25}$	0.173 ± 0.014	
...	119.5252 -49.2764	2.42 ± 0.17	-5.07 ± 0.36	8.46 ± 0.31	...	18.444 ± 0.001	19.64 ± 0.10	17.072 ± 0.009	412 $^{+32}_{-28}$	0.396 ± 0.032	
...	119.8318 -49.1001	2.47 ± 0.16	-5.22 ± 0.35	8.64 ± 0.35	...	18.416 ± 0.002	20.180 ± 0.081	17.068 ± 0.011	402 $^{+29}_{-25}$	0.227 ± 0.022	
...	116.7027 -49.3377	2.38 ± 0.12	-5.22 ± 0.22	7.80 ± 0.29	...	17.705 ± 0.001	19.509 ± 0.040	16.389 ± 0.008	416 $^{+22}_{-20}$	0.225 ± 0.018	
...	117.6715 -49.0634	2.35 ± 0.17	-5.40 ± 0.32	8.49 ± 0.32	...	18.696 ± 0.001	20.479 ± 0.094	17.302 ± 0.018	424 $^{+34}_{-29}$	0.214 ± 0.024	

Table B.6: Yep 3 Member Kinematics and Properties

Star Name	RA ($^{\circ}$)	Dec ($^{\circ}$)	Parallax (mas)	μ_{α} (mas yr $^{-1}$)	μ_{δ} (mas yr $^{-1}$)	v_r (km s $^{-1}$)	G (mag)	BP (mag)	RP (mag)	d (pc)	Mass (M $_{\odot}$)
TYC 8569-2369-1	132.6128	-54.1316	2.846 ± 0.024	-13.069 ± 0.048	9.988 ± 0.051	17.67 ± 0.76	10.547 ± 0.002	10.714 ± 0.002	10.282 ± 0.002	347.9 ± 2.9	1.57 ± 0.13
2MASS J08563370-5414541	134.1404	-54.2483	2.672 ± 0.015	-12.853 ± 0.027	9.325 ± 0.027	...	13.542 ± 0.002	13.992 ± 0.002	12.948 ± 0.002	370.3 ± 2.1	0.861 ± 0.069
2MASS J08491919-5501501	132.3299	-55.0305	3.119 ± 0.013	-13.784 ± 0.026	10.978 ± 0.029	...	13.478 ± 0.002	13.965 ± 0.005	12.842 ± 0.004	317.6 ± 1.4	0.826 ± 0.066
2MASS J08541651-5509021	133.5687	-55.1506	3.107 ± 0.076	-13.95 ± 0.14	11.34 ± 0.13	...	16.323 ± 0.003	17.872 ± 0.021	15.104 ± 0.005	319.2 $^{+8.0}_{-7.6}$	0.282 ± 0.023
2MASS J08452188-5501207	131.3411	-55.0224	3.146 ± 0.050	-14.186 ± 0.096	11.848 ± 0.099	...	16.190 ± 0.002	17.402 ± 0.006	15.093 ± 0.003	315.1 $^{+5.0}_{-4.9}$	0.429 ± 0.034
2MASS J08563299-5526077	134.1373	-55.4354	2.970 ± 0.023	-13.551 ± 0.047	10.104 ± 0.046	17.39 ± 0.38	12.615 ± 0.002	12.998 ± 0.004	12.074 ± 0.004	333.5 ± 2.6	1.030 ± 0.070
2MASS J08532681-5544287	133.3616	-55.7413	3.154 ± 0.038	-14.026 ± 0.091	11.536 ± 0.083	...	15.798 ± 0.002	16.943 ± 0.007	14.732 ± 0.003	314.2 $^{+3.9}_{-3.8}$	0.457 ± 0.037
2MASS J08543790-5555030	133.6578	-55.9175	3.170 ± 0.040	-14.180 ± 0.080	11.515 ± 0.074	...	16.024 ± 0.004	17.238 ± 0.016	14.923 ± 0.007	312.6 $^{+4.0}_{-3.9}$	0.428 ± 0.034
2MASS J09035273-5622434	135.9695	-56.3787	2.92 ± 0.10	-13.38 ± 0.24	9.40 ± 0.20	...	17.771 ± 0.003	19.323 ± 0.035	16.465 ± 0.006	340. $^{+13}_{-12}$	0.259 ± 0.021
2MASS J09013904-5455106	135.4126	-54.9196	3.12 ± 0.13	-13.91 ± 0.27	10.36 ± 0.26	...	17.904 ± 0.003	19.462 ± 0.028	16.580 ± 0.006	319. $^{+14}_{-13}$	0.254 ± 0.020
...	136.8488	-54.2081	2.89 ± 0.11	-13.86 ± 0.23	9.49 ± 0.21	...	17.687 ± 0.002	19.314 ± 0.038	16.434 ± 0.004	343. $^{+13}_{-12}$	0.254 ± 0.020
2MASS J08490836-5333374	132.2847	-53.5604	2.76 ± 0.14	-13.68 ± 0.27	9.50 ± 0.28	...	18.019 ± 0.002	19.604 ± 0.073	16.558 ± 0.018	361. $^{+20.}_{-18}$	0.215 ± 0.017
2MASS J08505246-5322421	132.7185	-53.3783	2.71 ± 0.12	-13.24 ± 0.23	9.76 ± 0.22	...	17.520 ± 0.002	19.270 ± 0.039	16.217 ± 0.006	366. $^{+16}_{-15}$	0.214 ± 0.017
...	130.7141	-52.5339	2.84 ± 0.12	-13.60 ± 0.23	10.64 ± 0.18	...	17.106 ± 0.003	17.606 ± 0.065	15.733 ± 0.020	350. $^{+16}_{-14}$	0.572 ± 0.046
2MASS J08350828-5231007	128.7844	-52.5168	3.03 ± 0.10	-13.62 ± 0.20	12.08 ± 0.25	...	17.245 ± 0.003	18.814 ± 0.029	16.019 ± 0.005	328. $^{+12}_{-11}$	0.275 ± 0.022
...	129.3024	-51.5741	3.10 ± 0.12	-13.92 ± 0.26	9.69 ± 0.28	...	17.761 ± 0.002	19.391 ± 0.044	16.477 ± 0.005	320. $^{+13}_{-12}$	0.246 ± 0.020
2MASS J08275486-5134316	126.9785	-51.5754	2.86 ± 0.12	-12.87 ± 0.24	11.27 ± 0.22	...	17.660 ± 0.002	19.206 ± 0.036	16.421 ± 0.005	347. $^{+15}_{-14}$	0.278 ± 0.022
2MASS J08304237-5119500	127.6767	-51.3303	2.81 ± 0.13	-12.89 ± 0.25	10.86 ± 0.21	...	17.673 ± 0.003	307. $^{+19}_{-17}$	0.361 ± 0.040

Table B.6: Yep 3—Continued

Star Name	RA (°)	Dec (°)	Parallax (mas)	μ_α (mas yr ⁻¹)	μ_δ (mas yr ⁻¹)	v_r (km s ⁻¹)	G (mag)	BP (mag)	RP (mag)	d (pc)	Mass (M_\odot)
...	126.9609 -50.8098	2.68 ± 0.11	-12.61 ± 0.22	10.20 ± 0.19	...	17.634 ± 0.005	19.283 ± 0.043	16.354 ± 0.014	370. ⁺¹⁶ ₋₁₅	0.242 ± 0.019	
2MASS08243167-5039012	126.1319 -50.6503	2.93 ± 0.15	-12.95 ± 0.29	10.70 ± 0.31	...	18.203 ± 0.003	19.732 ± 0.039	16.908 ± 0.007	340. ⁺¹⁸ ₋₁₇	0.268 ± 0.021	
...	128.8485 -49.7497	2.84 ± 0.14	-11.83 ± 0.26	10.00 ± 0.25	...	18.088 ± 0.003	19.779 ± 0.042	16.792 ± 0.007	350. ⁺¹⁸ ₋₁₇	0.227 ± 0.018	
2MASS J08290026-4941283	127.2510 -49.6912	2.73 ± 0.14	-12.76 ± 0.24	9.83 ± 0.23	...	17.676 ± 0.003	19.191 ± 0.058	16.396 ± 0.010	364. ⁺²⁰ ₋₁₈	0.275 ± 0.022	
2MASS J08293617-4934383	127.4006 -49.5773	2.75 ± 0.12	-12.70 ± 0.19	9.63 ± 0.22	...	17.293 ± 0.002	18.641 ± 0.017	16.062 ± 0.005	362. ⁺¹⁶ ₋₁₅	0.358 ± 0.029	
2MASS J08292977-4922501	127.3739 -49.3806	2.89 ± 0.11	-12.24 ± 0.21	9.51 ± 0.20	...	17.492 ± 0.002	19.011 ± 0.036	16.243 ± 0.005	343. ⁺¹⁴ ₋₁₃	0.282 ± 0.023	
2MASS J08453733-5054271	131.4055 -50.9075	2.97 ± 0.11	-13.75 ± 0.23	9.38 ± 0.24	...	17.797 ± 0.002	19.171 ± 0.054	16.484 ± 0.008	335. ⁺¹³ ₋₁₂	0.316 ± 0.025	
2MASS J08242333-4953222	126.0972 -49.8895	3.04 ± 0.11	-13.48 ± 0.19	11.10 ± 0.23	...	17.300 ± 0.002	19.053 ± 0.018	16.010 ± 0.005	326. ⁺¹² ₋₁₁	0.216 ± 0.017	
2MASS J08204912-4831317	125.2046 -48.5254	2.99 ± 0.12	-12.90 ± 0.19	10.44 ± 0.18	...	17.609 ± 0.003	19.156 ± 0.054	16.347 ± 0.005	332. ⁺¹⁴ ₋₁₃	0.272 ± 0.022	
...	125.7560 -48.0337	2.79 ± 0.13	-12.62 ± 0.22	9.26 ± 0.30	...	17.871 ± 0.002	19.372 ± 0.052	16.605 ± 0.006	357. ⁺¹⁷ ₋₁₆	0.282 ± 0.023	
...	123.5666 -47.5964	2.89 ± 0.11	-11.57 ± 0.23	11.09 ± 0.17	...	17.277 ± 0.004	344. ⁺¹⁴ ₋₁₃	0.415 ± 0.046	
...	136.0591 -55.9052	2.868 ± 0.025	-13.495 ± 0.055	9.533 ± 0.043	12	12.734 ± 0.002	13.103 ± 0.004	12.209 ± 0.004	345.2 ^{+3.1} _{-3.0}	0.976 ± 0.078	
...	127.4174 -49.8850	2.771 ± 0.040	-12.639 ± 0.071	9.833 ± 0.077	...	16.024 ± 0.002	17.171 ± 0.009	14.941 ± 0.004	357.2 ^{+5.2} _{-5.1}	0.451 ± 0.036	
...	129.8821 -52.1723	2.680 ± 0.072	-13.07 ± 0.13	9.44 ± 0.12	...	14.884 ± 0.003	15.904 ± 0.010	13.867 ± 0.006	370. ⁺¹⁰ _{-9.7}	0.530 ± 0.042	
...	130.8953 -54.4367	3.136 ± 0.091	-13.62 ± 0.20	11.87 ± 0.20	...	17.429 ± 0.002	19.006 ± 0.031	16.172 ± 0.005	316.4 ^{+9.4} _{-8.9}	0.266 ± 0.021	
TYC 8568-2409-1	129.0848 -53.6335	2.701 ± 0.024	-11.546 ± 0.045	10.323 ± 0.044	19.63 ± 0.19	11.996 ± 0.002	12.294 ± 0.002	11.552 ± 0.002	366.3 ± 3.2	1.060 ± 0.053	
...	129.7726 -53.1887	3.166 ± 0.086	-13.44 ± 0.17	11.64 ± 0.13	...	16.808 ± 0.002	18.059 ± 0.044	15.566 ± 0.008	313.5 ^{+8.8} _{-8.3}	0.382 ± 0.031	
...	130.9142 -52.8159	2.730 ± 0.086	-13.15 ± 0.18	9.42 ± 0.19	...	17.352 ± 0.003	18.821 ± 0.029	16.114 ± 0.007	363. ⁺¹² ₋₁₁	0.399 ± 0.025	
...	130.9150 -52.3680	2.856 ± 0.065	-13.27 ± 0.17	9.86 ± 0.13	...	16.598 ± 0.002	17.574 ± 0.041	15.359 ± 0.013	346.9 ^{+8.0} _{-7.7}	0.455 ± 0.036	

Table B.6: Yep 3—Continued

Star Name	RA ($^{\circ}$)	Dec ($^{\circ}$)	Parallax (mas)	μ_{α} (mas yr $^{-1}$)	μ_{δ} (mas yr $^{-1}$)	v_r (km s $^{-1}$)	G (mag)	BP (mag)	RP (mag)	d (pc)	Mass (M $_{\odot}$)
...	131.5012 -52.6321	2.845 \pm 0.062	-13.66 \pm 0.12	9.50 \pm 0.11	...	16.557 \pm 0.002	17.856 \pm 0.013	15.419 \pm 0.004	348.3 $^{+7.7}_{-7.4}$	0.397 \pm 0.032	
2MASS J08411381-5226547	130.3074	-52.4485	3.146 \pm 0.026	-13.423 \pm 0.052	11.582 \pm 0.064	18.44 \pm 0.15	12.239 \pm 0.002	12.589 \pm 0.003	11.745 \pm 0.003	315.0 $^{+2.7}_{-2.6}$	1.000 \pm 0.050
TYC 8163-165-1	130.2582	-52.4527	3.150 \pm 0.027	-13.354 \pm 0.056	11.616 \pm 0.062	18.45 \pm 0.33	11.106 \pm 0.002	11.355 \pm 0.002	10.722 \pm 0.002	314.6 \pm 2.7	1.250 \pm 0.062
...	130.3721	-52.3568	3.160 \pm 0.051	-13.461 \pm 0.097	11.87 \pm 0.11	...	16.469 \pm 0.002	17.817 \pm 0.013	15.302 \pm 0.004	313.7 $^{+5.1}_{-5.0}$	0.376 \pm 0.030
...	130.3660	-52.2376	3.127 \pm 0.080	-13.11 \pm 0.16	11.43 \pm 0.17	...	16.746 \pm 0.002	18.373 \pm 0.014	15.495 \pm 0.004	317.2 $^{+8.3}_{-7.9}$	0.255 \pm 0.020
...	128.8538	-52.6173	3.167 \pm 0.031	-13.666 \pm 0.062	11.025 \pm 0.060	...	15.074 \pm 0.002	15.987 \pm 0.007	14.125 \pm 0.004	313.0 $^{+3.1}_{-3.0}$	0.576 \pm 0.046
...	129.7668	-52.0482	2.940 \pm 0.091	-13.71 \pm 0.19	10.24 \pm 0.19	...	17.137 \pm 0.002	18.666 \pm 0.023	15.882 \pm 0.006	337 $^{+11}_{-10.}$	0.278 \pm 0.022
...	129.9652	-51.9046	2.678 \pm 0.086	-12.67 \pm 0.15	10.05 \pm 0.18	...	16.791 \pm 0.002	18.411 \pm 0.029	15.511 \pm 0.006	370. \pm 12	0.249 \pm 0.020
2MASS J08401240-5155529	130.0516	-51.9313	2.760 \pm 0.095	-13.13 \pm 0.15	9.72 \pm 0.20	...	16.958 \pm 0.002	18.552 \pm 0.030	15.684 \pm 0.005	359 $^{+13}_{-12}$	0.257 \pm 0.021
...	129.3716	-51.9805	2.784 \pm 0.098	-13.28 \pm 0.20	9.93 \pm 0.23	...	17.305 \pm 0.002	18.680 \pm 0.022	16.040 \pm 0.005	356 $^{+13}_{-12}$	0.333 \pm 0.027
...	129.3810	-51.4331	2.806 \pm 0.093	-12.32 \pm 0.15	9.67 \pm 0.19	...	17.034 \pm 0.003	18.592 \pm 0.024	15.785 \pm 0.007	353 $^{+12}_{-11}$	0.272 \pm 0.022
...	129.6995	-51.1581	2.766 \pm 0.079	-12.51 \pm 0.15	10.18 \pm 0.16	...	16.854 \pm 0.002	18.293 \pm 0.027	15.447 \pm 0.016	358 $^{+10.}_{-9.9}$	0.263 \pm 0.021
TYC 8162-1365-1	129.2115	-51.1938	2.674 \pm 0.027	-12.330 \pm 0.048	9.478 \pm 0.043	20.43 \pm 0.24	12.179 \pm 0.002	12.490 \pm 0.002	11.717 \pm 0.002	370.1 $^{+3.8}_{-3.7}$	1.000 \pm 0.050
...	128.6651	-51.1902	2.815 \pm 0.084	-12.45 \pm 0.15	10.34 \pm 0.17	...	16.912 \pm 0.002	18.444 \pm 0.024	15.670 \pm 0.006	352 $^{+11}_{-10.}$	0.280 \pm 0.022
...	128.2343	-51.3111	2.695 \pm 0.054	-11.66 \pm 0.11	10.05 \pm 0.13	...	16.352 \pm 0.002	17.570 \pm 0.007	15.239 \pm 0.004	367.4 $^{+7.5}_{-7.2}$	0.424 \pm 0.034
...	128.8104	-50.9523	2.769 \pm 0.092	-12.88 \pm 0.19	9.87 \pm 0.19	...	17.234 \pm 0.003	18.768 \pm 0.023	16.009 \pm 0.004	358. \pm 12	0.284 \pm 0.023
...	129.0129	-50.7752	2.700 \pm 0.076	-12.56 \pm 0.15	9.87 \pm 0.14	...	16.861 \pm 0.002	18.268 \pm 0.017	15.650 \pm 0.005	367 $^{+11}_{-10.}$	0.348 \pm 0.028
...	127.4309	-51.1155	2.856 \pm 0.084	-12.73 \pm 0.17	10.40 \pm 0.15	...	17.308 \pm 0.002	18.848 \pm 0.026	16.051 \pm 0.005	347 $^{+10.}_{-9.9}$	0.273 \pm 0.022

Table B.6: Yep 3—Continued

Star Name	RA (°)	Dec (°)	Parallax (mas)	μ_α (mas yr ⁻¹)	μ_δ (mas yr ⁻¹)	v_r (km s ⁻¹)	G (mag)	BP (mag)	RP (mag)	d (pc)	Mass (M_\odot)
...	127.0197 -50.4526	2.932 ± 0.098	-12.04 ± 0.18	11.01 ± 0.17	...	17.342 ± 0.003	18.809 ± 0.023	16.106 ± 0.007	338 ⁺¹² ₋₁₁	0.310 ± 0.025	
...	126.5969 -50.1275	3.031 ± 0.074	-12.67 ± 0.14	12.08 ± 0.15	...	17.193 ± 0.002	18.657 ± 0.014	15.951 ± 0.008	327 ^{+8.1} _{-7.8}	0.309 ± 0.025	
...	127.5657 -50.5515	2.754 ± 0.022	-11.713 ± 0.043	10.032 ± 0.041	...	14.628 ± 0.002	15.299 ± 0.009	13.787 ± 0.009	360 ^{+9.2} _{-8.8}	0.695 ± 0.056	
...	127.6887 -50.3403	2.841 ± 0.030	-11.428 ± 0.055	10.683 ± 0.052	...	15.310 ± 0.003	16.194 ± 0.010	14.380 ± 0.006	348 ^{+3.7} _{-3.6}	0.596 ± 0.048	
...	127.0652 -49.9687	2.946 ± 0.066	-12.04 ± 0.12	10.26 ± 0.12	...	17.043 ± 0.003	18.297 ± 0.024	15.764 ± 0.008	336 ^{+7.7} _{-7.4}	0.371 ± 0.030	
...	127.0632 -49.8972	2.893 ± 0.032	-12.705 ± 0.050	10.063 ± 0.048	19	12.402 ± 0.002	12.752 ± 0.002	11.901 ± 0.002	342.3 ± 3.8	1.013 ± 0.081	
...	127.3055 -49.6726	2.834 ± 0.030	-11.548 ± 0.055	10.801 ± 0.048	...	15.137 ± 0.002	16.000 ± 0.010	14.207 ± 0.006	349 ^{+3.7} _{-3.6}	0.606 ± 0.049	
...	126.8041 -49.6325	2.839 ± 0.046	-11.479 ± 0.092	10.338 ± 0.080	...	13.343 ± 0.002	13.790 ± 0.003	12.735 ± 0.003	348 ^{+5.8} _{-5.6}	0.853 ± 0.068	
...	127.4913 -49.2095	2.732 ± 0.053	-11.77 ± 0.10	10.14 ± 0.11	...	16.305 ± 0.002	17.394 ± 0.008	15.250 ± 0.004	362 ^{+7.2} _{-6.9}	0.487 ± 0.039	
...	125.9764 -49.0297	2.737 ± 0.060	-11.496 ± 0.098	10.18 ± 0.14	...	16.236 ± 0.003	17.376 ± 0.013	15.038 ± 0.005	361.9 ^{+8.1} _{-7.8}	0.422 ± 0.034	
2MASS J08192677-4910015	124.8615 -49.1670	3.173 ± 0.040	-13.311 ± 0.064	11.296 ± 0.060	20.82 ± 0.18	12.732 ± 0.003	13.134 ± 0.008	12.170 ± 0.006	312.4 ^{+4.0} _{-3.9}	0.820 ± 0.041	
2MASS J08253727-4912497	126.4052 -49.2138	2.760 ± 0.028	-11.512 ± 0.046	10.056 ± 0.043	21.72 ± 0.29	12.691 ± 0.002	13.068 ± 0.003	12.156 ± 0.003	358.6 ^{+3.7} _{-3.6}	0.820 ± 0.041	
...	126.8134 -47.8027	2.690 ± 0.044	-11.444 ± 0.079	10.153 ± 0.072	...	8.528 ± 0.002	8.539 ± 0.002	8.531 ± 0.003	367 ^{+6.1} _{-5.9}	2.15 ± 0.17	
...	134.9457 -54.7558	2.98 ± 0.12	-14.06 ± 0.26	9.96 ± 0.28	...	18.237 ± 0.003	19.957 ± 0.046	16.947 ± 0.006	333 ⁺¹⁴ ₋₁₃	0.223 ± 0.018	
...	133.1614 -54.3003	2.95 ± 0.12	-13.25 ± 0.29	10.00 ± 0.24	...	17.933 ± 0.002	19.554 ± 0.028	16.639 ± 0.004	337 ⁺¹⁴ ₋₁₃	0.245 ± 0.020	
...	133.1584 -53.6679	2.67 ± 0.13	-12.22 ± 0.26	9.68 ± 0.22	...	17.851 ± 0.003	19.457 ± 0.031	16.509 ± 0.006	372 ⁺¹⁹ ₋₁₇	0.237 ± 0.019	
...	131.3610 -52.7773	3.12 ± 0.10	-13.60 ± 0.18	11.48 ± 0.19	...	17.723 ± 0.002	19.375 ± 0.027	16.447 ± 0.005	318 ⁺¹¹ ₋₁₀	0.242 ± 0.019	
...	129.9227 -53.0677	2.84 ± 0.11	-12.32 ± 0.22	10.25 ± 0.25	...	17.147 ± 0.003	18.140 ± 0.035	15.444 ± 0.028	349 ⁺¹³ ₋₁₂	0.313 ± 0.025	
...	130.1819 -52.9115	2.98 ± 0.12	-14.30 ± 0.23	10.56 ± 0.25	...	17.898 ± 0.003	18.970 ± 0.078	16.588 ± 0.010	333 ⁺¹⁴ ₋₁₃	0.411 ± 0.033	

Table B.6: Yep 3—Continued

Star Name	RA (°)	Dec (°)	Parallax (mas)	μ_α (mas yr ⁻¹)	μ_δ (mas yr ⁻¹)	v_r (km s ⁻¹)	G (mag)	BP (mag)	RP (mag)	d (pc)	Mass (M_\odot)
...	130.1098	-52.2221	2.85 ± 0.11	-13.58 ± 0.22	9.80 ± 0.23	...	17.451 ± 0.002	19.018 ± 0.035	16.214 ± 0.006	348 ⁺¹⁴ ₋₁₃	0.273 ± 0.022
...	130.4254	-52.1046	2.98 ± 0.10	-13.40 ± 0.23	9.70 ± 0.24	...	17.502 ± 0.002	18.311 ± 0.048	16.109 ± 0.012	333 ⁺¹² ₋₁₁	0.459 ± 0.037
...	130.1815	-51.8879	2.74 ± 0.13	-12.49 ± 0.24	10.24 ± 0.27	...	18.061 ± 0.003	19.673 ± 0.062	16.773 ± 0.008	363 ⁺¹⁸ ₋₁₆	0.249 ± 0.020
...	129.4409	-52.0499	2.84 ± 0.15	-12.69 ± 0.30	10.52 ± 0.33	...	18.113 ± 0.003	19.642 ± 0.065	16.806 ± 0.009	354 ⁺²⁰ ₋₁₈	0.265 ± 0.021
...	129.7807	-51.7101	2.72 ± 0.11	-12.86 ± 0.21	9.40 ± 0.24	...	17.774 ± 0.002	19.401 ± 0.034	16.513 ± 0.007	365 ⁺¹⁵ ₋₁₄	0.252 ± 0.020
...	129.5533	-51.7690	2.80 ± 0.13	-12.53 ± 0.24	9.68 ± 0.24	...	18.035 ± 0.002	19.563 ± 0.042	16.706 ± 0.007	355 ⁺¹⁷ ₋₁₅	0.260 ± 0.021
...	130.2413	-51.5158	3.14 ± 0.13	-13.64 ± 0.22	10.15 ± 0.28	...	17.947 ± 0.003	19.500 ± 0.056	16.675 ± 0.007	317 ⁺¹⁴ ₋₁₃	0.268 ± 0.021
...	130.1194	-51.3612	2.80 ± 0.12	-13.05 ± 0.22	9.38 ± 0.25	...	17.735 ± 0.002	19.496 ± 0.046	16.439 ± 0.006	355 ⁺¹⁶ ₋₁₅	0.213 ± 0.017
...	129.9224	-51.3435	2.77 ± 0.13	-12.70 ± 0.24	9.78 ± 0.27	...	17.984 ± 0.003	19.597 ± 0.056	16.698 ± 0.007	359 ⁺¹⁸ ₋₁₇	0.249 ± 0.020
...	129.1754	-51.5600	2.74 ± 0.10	-12.74 ± 0.21	9.70 ± 0.24	...	17.644 ± 0.003	19.295 ± 0.029	16.351 ± 0.007	362 ⁺¹⁴ ₋₁₃	0.238 ± 0.019
...	129.5215	-51.3284	2.75 ± 0.12	-12.79 ± 0.23	9.26 ± 0.29	...	17.984 ± 0.003	19.516 ± 0.057	16.733 ± 0.007	361 ⁺¹⁷ ₋₁₅	0.278 ± 0.022
...	129.5310	-51.3149	2.84 ± 0.14	-12.74 ± 0.26	9.70 ± 0.30	...	17.753 ± 0.003	350 ⁺¹⁸ ₋₁₆	0.377 ± 0.041
...	129.4944	-51.2444	2.79 ± 0.14	-12.77 ± 0.24	9.58 ± 0.28	...	17.977 ± 0.002	19.517 ± 0.053	16.675 ± 0.008	356 ⁺¹⁹ ₋₁₇	0.263 ± 0.021
...	129.6062	-51.2101	2.90 ± 0.16	-12.51 ± 0.30	10.02 ± 0.30	...	18.284 ± 0.003	19.827 ± 0.050	16.976 ± 0.009	344 ⁺²¹ ₋₁₈	0.261 ± 0.021
...	129.1641	-51.3702	2.72 ± 0.13	-12.31 ± 0.23	10.06 ± 0.28	...	18.091 ± 0.003	19.633 ± 0.063	16.773 ± 0.009	366 ⁺¹⁹ ₋₁₇	0.259 ± 0.021
...	129.1544	-51.1738	2.73 ± 0.15	-13.02 ± 0.24	9.84 ± 0.30	...	17.842 ± 0.003	19.485 ± 0.049	16.528 ± 0.006	364 ⁺²¹ ₋₁₉	0.235 ± 0.019
...	128.2167	-51.1916	2.85 ± 0.11	-12.93 ± 0.21	9.63 ± 0.24	...	17.920 ± 0.002	19.485 ± 0.024	16.642 ± 0.007	348 ⁺¹⁴ ₋₁₃	0.263 ± 0.021
...	128.5463	-51.1971	2.78 ± 0.10	-13.07 ± 0.19	9.63 ± 0.22	...	17.678 ± 0.003	19.167 ± 0.032	16.421 ± 0.008	357 ⁺¹⁴ ₋₁₃	0.295 ± 0.024

Table B.6: Yep 3—Continued

Star Name	RA (°)	Dec (°)	Parallax (mas)	μ_α (mas yr ⁻¹)	μ_δ (mas yr ⁻¹)	v_r (km s ⁻¹)	G (mag)	BP (mag)	RP (mag)	a (pc)	Mass (M_\odot)
...	128.6049	-51.1040	2.69 ± 0.11	-12.74 ± 0.20	9.26 ± 0.23	...	17.848 ± 0.003	19.339 ± 0.041	16.571 ± 0.007	369 ⁺¹⁶ ₋₁₅	0.282 ± 0.023
...	128.6714	-50.8453	2.73 ± 0.11	-11.91 ± 0.21	9.64 ± 0.22	...	17.720 ± 0.002	19.338 ± 0.039	16.464 ± 0.007	364 ⁺¹⁵ ₋₁₄	0.256 ± 0.020
...	130.4074	-50.6639	2.77 ± 0.14	-12.24 ± 0.25	9.12 ± 0.32	...	18.131 ± 0.003	19.630 ± 0.069	16.839 ± 0.016	359 ⁺¹⁹ ₋₁₇	0.276 ± 0.024
...	126.7796	-50.3104	2.77 ± 0.13	-12.65 ± 0.25	10.09 ± 0.23	...	17.920 ± 0.003	19.622 ± 0.061	16.577 ± 0.007	359 ⁺¹⁸ ₋₁₆	0.216 ± 0.017
...	127.0016	-50.2371	2.84 ± 0.11	-12.13 ± 0.20	10.41 ± 0.17	...	17.758 ± 0.002	19.414 ± 0.034	16.466 ± 0.005	350 ⁺¹⁴ ₋₁₃	0.237 ± 0.019
...	125.9067	-50.6975	2.94 ± 0.15	-12.13 ± 0.29	10.72 ± 0.31	...	18.421 ± 0.003	20.054 ± 0.058	17.087 ± 0.012	339 ⁺¹⁸ ₋₁₆	0.232 ± 0.019
...	128.0766	-51.0548	3.15 ± 0.12	-13.54 ± 0.23	10.82 ± 0.27	...	18.046 ± 0.003	19.637 ± 0.071	16.679 ± 0.012	316 ⁺¹³ ₋₁₂	0.235 ± 0.019
...	128.1490	-50.9355	2.79 ± 0.11	-11.62 ± 0.22	10.22 ± 0.25	...	17.733 ± 0.002	19.374 ± 0.037	16.479 ± 0.005	356 ⁺¹⁵ ₋₁₄	0.250 ± 0.020
...	128.3159	-51.0362	2.70 ± 0.26	-11.75 ± 0.43	9.93 ± 0.67	...	18.686 ± 0.004	396 ⁺²⁰ ₋₁₉	0.300 ± 0.033
HD 70718	125.3170	-48.9429	3.164 ± 0.046	-13.706 ± 0.080	10.927 ± 0.065	...	9.360 ± 0.002	9.419 ± 0.002	9.292 ± 0.002	313.3 ^{+4.6} _{-4.4}	2.05 ± 0.72
...	128.5078	-50.8529	2.79 ± 0.12	-13.17 ± 0.23	9.58 ± 0.21	...	15.913 ± 0.002	17.023 ± 0.010	14.838 ± 0.004	357 ⁺¹⁶ ₋₁₅	0.456 ± 0.036
...	128.2956	-50.5840	2.74 ± 0.12	-12.49 ± 0.22	9.43 ± 0.22	...	17.376 ± 0.003	18.836 ± 0.028	16.116 ± 0.006	362 ⁺¹⁶ ₋₁₅	0.304 ± 0.024
...	128.4632	-50.7443	2.79 ± 0.12	-11.57 ± 0.25	9.86 ± 0.25	...	18.225 ± 0.002	19.931 ± 0.049	16.925 ± 0.007	356 ⁺¹⁷ ₋₁₅	0.223 ± 0.018
...	128.8050	-50.4238	2.83 ± 0.16	-12.48 ± 0.27	9.36 ± 0.33	...	18.348 ± 0.003	19.839 ± 0.067	17.057 ± 0.010	351 ⁺²² _{-20.}	0.279 ± 0.024
...	127.2864	-50.3218	2.81 ± 0.10	-11.86 ± 0.18	10.71 ± 0.18	...	17.670 ± 0.002	19.197 ± 0.033	16.394 ± 0.005	353 ⁺¹³ ₋₁₂	0.273 ± 0.022
...	127.2933	-50.3163	3.01 ± 0.14	-12.18 ± 0.23	11.93 ± 0.24	...	18.107 ± 0.003	19.439 ± 0.041	16.869 ± 0.008	330 ⁺¹⁶ ₋₁₄	0.361 ± 0.029
...	127.0327	-49.5485	2.74 ± 0.16	-11.47 ± 0.30	10.07 ± 0.26	...	17.987 ± 0.004	19.437 ± 0.041	16.678 ± 0.009	364 ⁺²³ _{-20.}	0.284 ± 0.023
...	125.9382	-50.2210	2.69 ± 0.12	-11.68 ± 0.24	10.49 ± 0.24	...	17.593 ± 0.002	19.266 ± 0.021	16.267 ± 0.006	369 ⁺¹⁷ ₋₁₅	0.224 ± 0.018
...	125.9547	-50.0508	2.75 ± 0.14	-11.42 ± 0.24	11.04 ± 0.28	...	18.083 ± 0.003	19.775 ± 0.059	16.750 ± 0.010	361 ⁺²⁰ ₋₁₈	0.220 ± 0.018

Table B.6: Yep 3—Continued

Star Name	RA ($^{\circ}$)	Dec ($^{\circ}$)	Parallax (mas)	μ_{α} (mas yr $^{-1}$)	μ_{δ} (mas yr $^{-1}$)	v_r (km s $^{-1}$)	G (mag)	BP (mag)	RP (mag)	d (pc)	Mass (M $_{\odot}$)
...	125.6218	-49.7249	2.78 ± 0.17	-11.57 ± 0.31	10.31 ± 0.29	...	18.546 ± 0.003	20.260 ± 0.088	17.184 ± 0.011	358 $^{+24}_{-21}$	0.209 ± 0.019
...	125.5738	-49.4087	2.86 ± 0.12	-12.24 ± 0.24	11.00 ± 0.21	...	17.703 ± 0.002	19.393 ± 0.025	16.403 ± 0.007	347 $^{+15}_{-14}$	0.226 ± 0.018
...	125.5728	-49.4091	2.91 ± 0.14	-11.92 ± 0.28	10.60 ± 0.25	...	18.220 ± 0.003	19.896 ± 0.048	16.863 ± 0.010	342 $^{+18}_{-16}$	0.218 ± 0.017
...	125.2983	-48.3005	2.88 ± 0.18	-11.45 ± 0.31	10.92 ± 0.29	...	18.407 ± 0.003	20.12 ± 0.11	17.033 ± 0.011	346 $^{+23}_{-20}$	0.206 ± 0.023
...	129.9816	-53.9431	3.156 ± 0.016	-13.681 ± 0.028	11.630 ± 0.025	...	13.267 ± 0.002	13.743 ± 0.004	12.645 ± 0.003	314.0 ± 1.6	0.837 ± 0.067
...	133.3121	-54.6438	3.01 ± 0.15	-12.95 ± 0.30	10.41 ± 0.30	...	18.250 ± 0.002	20.001 ± 0.061	16.957 ± 0.006	331 $^{+18}_{-16}$	0.216 ± 0.017
TYC 8590-874-1	135.8481	-56.7797	2.772 ± 0.025	-13.300 ± 0.055	9.245 ± 0.051	16.89 ± 0.53	11.202 ± 0.002	11.451 ± 0.002	10.823 ± 0.002	357.1 ± 3.2	1.250 ± 0.062
...	134.9007	-56.5064	2.851 ± 0.015	-12.803 ± 0.033	10.451 ± 0.028	...	13.848 ± 0.002	14.372 ± 0.004	13.182 ± 0.004	347.3 $^{+1.9}_{-1.8}$	0.800 ± 0.064
...	135.1381	-55.8254	3.029 ± 0.077	-13.85 ± 0.15	9.64 ± 0.15	...	17.032 ± 0.002	18.504 ± 0.016	15.828 ± 0.004	327.4 $^{+8.6}_{-8.2}$	0.320 ± 0.026
...	135.8586	-55.7762	2.940 ± 0.060	-13.64 ± 0.14	10.55 ± 0.12	...	16.426 ± 0.002	17.803 ± 0.010	15.270 ± 0.004	337.0 $^{+7.1}_{-6.8}$	0.371 ± 0.030
2MASS J08590528-5534151	134.7719	-55.5708	3.112 ± 0.030	-14.426 ± 0.082	11.243 ± 0.056	15.40 ± 0.19	11.993 ± 0.002	12.316 ± 0.003	11.518 ± 0.003	318.5 $^{+3.1}_{-3.0}$	0.980 ± 0.087
CD-52380	132.8935	-55.9038	2.935 ± 0.030	-13.483 ± 0.062	10.886 ± 0.057	...	9.724 ± 0.002	9.808 ± 0.002	9.605 ± 0.002	337.4 $^{+3.5}_{-3.4}$	1.98 ± 0.44
...	132.6059	-55.9061	2.793 ± 0.022	-12.891 ± 0.045	10.308 ± 0.040	19	12.842 ± 0.002	13.240 ± 0.003	12.296 ± 0.003	354.4 $^{+2.8}_{-2.7}$	0.937 ± 0.075
TYC 8586-1678-1	133.3817	-55.1653	2.976 ± 0.033	-13.706 ± 0.098	9.91 ± 0.11	22.22 ± 0.15	11.202 ± 0.002	11.453 ± 0.002	10.822 ± 0.002	333.0 $^{+6.1}_{-5.8}$	1.250 ± 0.062
...	132.5188	-55.2879	3.033 ± 0.069	-13.41 ± 0.14	11.92 ± 0.14	...	16.428 ± 0.002	18.058 ± 0.009	15.193 ± 0.003	326.9 $^{+7.6}_{-7.3}$	0.258 ± 0.021
HD 76901	134.1999	-54.2182	2.963 ± 0.040	-14.275 ± 0.075	11.001 ± 0.075	...	9.292 ± 0.002	9.324 ± 0.002	9.262 ± 0.002	334.4 $^{+4.6}_{-4.5}$	1.98 ± 0.13
...	132.0979	-53.7150	3.000 ± 0.051	-13.52 ± 0.10	9.794 ± 0.099	...	16.112 ± 0.002	17.341 ± 0.010	15.010 ± 0.004	330.4 $^{+5.8}_{-5.6}$	0.424 ± 0.034
...	133.5407	-53.7048	2.795 ± 0.057	-13.67 ± 0.12	9.215 ± 0.099	...	16.778 ± 0.002	18.152 ± 0.012	15.606 ± 0.005	354.4 $^{+7.4}_{-7.1}$	0.367 ± 0.029

Table B.6: Yep 3—Continued

Star Name	RA ($^{\circ}$)	Dec ($^{\circ}$)	Parallax (mas)	μ_{α} (mas yr $^{-1}$)	μ_{δ} (mas yr $^{-1}$)	v_r (km s $^{-1}$)	G (mag)	BP (mag)	RP (mag)	d (pc)	Mass (M $_{\odot}$)
TYC 8569-3283-1	131.2798 -53.5096	2.983 ± 0.022	-13.895 ± 0.046	10.043 ± 0.040	18.52 ± 0.36	11.533 ± 0.002	11.798 ± 0.002	11.123 ± 0.002	332.1 ± 2.4	1.330 ± 0.066	...
...	132.0285 -53.7171	2.918 ± 0.079	-13.82 ± 0.16	9.97 ± 0.16	...	17.056 ± 0.002	18.721 ± 0.023	15.759 ± 0.005	339.8 $^{+9.5}_{-9.0}$	0.234 ± 0.019	...
...	130.3235 -53.3822	3.109 ± 0.086	-14.30 ± 0.15	11.00 ± 0.17	...	17.224 ± 0.002	18.741 ± 0.021	15.950 ± 0.005	319.1 $^{+9.1}_{-8.6}$	0.276 ± 0.022	...
...	130.6873 -52.4532	3.065 ± 0.077	-13.34 ± 0.14	12.01 ± 0.17	...	16.988 ± 0.004	18.466 ± 0.035	15.755 ± 0.009	323.6 $^{+8.4}_{-8.0}$	0.307 ± 0.025	...
...	130.1099 -52.5046	3.172 ± 0.097	-12.93 ± 0.20	10.98 ± 0.22	...	17.335 ± 0.002	18.857 ± 0.027	16.097 ± 0.006	313.0 $^{+9.9}_{-9.3}$	0.284 ± 0.023	...
...	130.5470 -52.3710	3.152 ± 0.048	-13.695 ± 0.092	10.297 ± 0.090	...	15.689 ± 0.002	16.732 ± 0.011	14.642 ± 0.004	314.5 $^{+4.8}_{-4.7}$	0.527 ± 0.042	...
...	130.0857 -52.2501	3.156 ± 0.051	-13.348 ± 0.099	10.12 ± 0.11	...	14.916 ± 0.002	15.805 ± 0.005	13.974 ± 0.003	314.1 $^{+5.2}_{-5.0}$	0.588 ± 0.047	...
...	128.9153 -51.0889	2.729 ± 0.095	-13.43 ± 0.17	10.30 ± 0.20	...	17.310 ± 0.003	18.797 ± 0.026	16.077 ± 0.007	363 $^{+13}_{-12}$	0.304 ± 0.024	...
HD 71003	125.6856 -51.3649	3.064 ± 0.036	-12.900 ± 0.073	11.606 ± 0.076	...	8.889 ± 0.002	8.908 ± 0.002	8.881 ± 0.003	323.4 $^{+3.9}_{-3.8}$	2.2 ± 1.0	...
TYC 8158-2342-1	127.3917 -50.1240	2.679 ± 0.030	-11.849 ± 0.055	10.927 ± 0.049	20.34 ± 0.41	11.780 ± 0.002	12.072 ± 0.002	11.336 ± 0.002	369.3 $^{+4.2}_{-4.1}$	1.21 ± 0.10	...
...	127.6126 -50.1804	2.968 ± 0.082	-14.29 ± 0.16	10.16 ± 0.15	...	17.132 ± 0.002	18.503 ± 0.028	15.928 ± 0.004	334.1 $^{+9.5}_{-9.0}$	0.359 ± 0.029	...
...	127.7006 -49.7971	2.712 ± 0.020	-12.821 ± 0.038	10.039 ± 0.042	...	14.481 ± 0.002	15.099 ± 0.002	13.736 ± 0.002	364.9 $^{+2.7}_{-2.6}$	0.734 ± 0.059	...
...	128.3987 -49.4154	2.745 ± 0.098	-12.58 ± 0.19	9.30 ± 0.21	...	17.257 ± 0.004	18.711 ± 0.038	16.003 ± 0.011	361 $^{+13}_{-12}$	0.309 ± 0.025	...
...	124.9747 -50.3247	2.806 ± 0.026	-11.815 ± 0.052	11.029 ± 0.047	...	15.150 ± 0.002	15.913 ± 0.003	14.303 ± 0.002	352.9 ± 3.3	0.677 ± 0.054	...
HD 70977	125.6731 -49.8198	3.169 ± 0.039	-13.214 ± 0.067	11.192 ± 0.056	19.3 ± 2.0	10.168 ± 0.002	10.315 ± 0.002	9.942 ± 0.002	312.8 $^{+3.9}_{-3.8}$	1.75 ± 0.14	...
...	125.4673 -49.4813	3.119 ± 0.067	-13.16 ± 0.13	10.98 ± 0.12	...	16.963 ± 0.002	18.446 ± 0.020	15.727 ± 0.006	317.9 $^{+7.0}_{-6.7}$	0.305 ± 0.024	...
...	124.7125 -49.5481	3.123 ± 0.047	-12.057 ± 0.092	11.96 ± 0.11	...	16.195 ± 0.003	17.424 ± 0.009	15.086 ± 0.005	317.4 $^{+4.9}_{-4.7}$	0.422 ± 0.034	...
...	124.7077 -49.5456	3.197 ± 0.048	-11.776 ± 0.096	12.03 ± 0.11	...	16.180 ± 0.003	17.408 ± 0.012	15.063 ± 0.006	319.0 $^{+5.0}_{-4.9}$	0.420 ± 0.034	...
...	125.4063 -48.6695	2.708 ± 0.056	-12.00 ± 0.11	9.753 ± 0.097	...	16.311 ± 0.002	17.530 ± 0.008	15.205 ± 0.004	365.7 $^{+7.8}_{-7.5}$	0.425 ± 0.034	...

Table B.6: Yep 3—Continued

Star Name	RA ($^{\circ}$)	Dec ($^{\circ}$)	Parallax (mas)	μ_{α} (mas yr $^{-1}$)	μ_{δ} (mas yr $^{-1}$)	v_r (km s $^{-1}$)	G (mag)	BP (mag)	RP (mag)	d (pc)	Mass (M $_{\odot}$)
...	126.4095	-49.2544	2.949 \pm 0.022	-11.475 \pm 0.034	11.773 \pm 0.032	...	13.657 \pm 0.003	14.173 \pm 0.007	12.994 \pm 0.006	335.8 \pm 2.5	0.804 \pm 0.064
...	123.7512	-48.8876	3.009 \pm 0.024	-12.227 \pm 0.048	10.988 \pm 0.039	...	14.466 \pm 0.002	15.182 \pm 0.005	13.648 \pm 0.003	329.2 $^{+2.7}_{-2.6}$	0.693 \pm 0.055
TYC 8153-960-1	125.0994	-48.2016	2.874 \pm 0.032	-12.348 \pm 0.050	9.931 \pm 0.047	21.0 \pm 2.2	10.658 \pm 0.002	10.843 \pm 0.002	10.369 \pm 0.002	344.6 $^{+3.9}_{-3.8}$	1.33 \pm 0.14
...	124.7388	-48.2569	2.901 \pm 0.063	-11.89 \pm 0.10	9.99 \pm 0.11	...	16.437 \pm 0.002	17.661 \pm 0.015	15.319 \pm 0.003	341.6 $^{+7.5}_{-7.2}$	0.421 \pm 0.034
...	124.7353	-49.0030	2.86 \pm 0.11	-11.54 \pm 0.22	10.74 \pm 0.22	...	17.709 \pm 0.002	19.321 \pm 0.044	16.411 \pm 0.007	348.7 $^{+14}_{-13}$	0.246 \pm 0.020
...	126.5816	-50.4499	2.805 \pm 0.036	-12.325 \pm 0.075	9.995 \pm 0.065	...	15.903 \pm 0.002	16.994 \pm 0.009	14.853 \pm 0.005	353.0 $^{+4.5}_{-4.4}$	0.489 \pm 0.039
...	126.8770	-50.7648	2.778 \pm 0.034	-11.891 \pm 0.060	11.110 \pm 0.053	...	15.551 \pm 0.002	16.543 \pm 0.014	14.552 \pm 0.005	356.4 $^{+4.4}_{-4.3}$	0.544 \pm 0.043
...	127.0341	-50.3459	2.876 \pm 0.057	-11.91 \pm 0.10	10.341 \pm 0.093	...	16.511 \pm 0.001	17.817 \pm 0.011	15.373 \pm 0.003	344.4 $^{+7.0}_{-6.7}$	0.395 \pm 0.032
...	127.2756	-50.3200	2.716 \pm 0.063	-11.55 \pm 0.10	10.47 \pm 0.11	...	16.556 \pm 0.001	17.962 \pm 0.013	15.358 \pm 0.003	364.6 $^{+8.7}_{-8.3}$	0.352 \pm 0.028
2MASS J08291213-5053273	127.3005	-50.8909	2.895 \pm 0.016	-12.095 \pm 0.028	10.983 \pm 0.027	20.03 \pm 0.32	13.247 \pm 0.001	13.677 \pm 0.004	12.663 \pm 0.003	342.0 $^{+1.9}_{-1.8}$	0.880 \pm 0.060
HD 72163	127.3150	-50.2501	2.941 \pm 0.042	-13.151 \pm 0.068	10.076 \pm 0.059	...	9.148 \pm 0.000	9.187 \pm 0.001	9.108 \pm 0.003	336.8 $^{+4.8}_{-4.7}$	2.05 \pm 0.10
2MASS J08292489-5039483	127.3537	-50.6634	2.789 \pm 0.028	-11.967 \pm 0.050	9.963 \pm 0.050	24.0 \pm 2.8	11.914 \pm 0.001	12.224 \pm 0.005	11.455 \pm 0.003	355.0 $^{+3.6}_{-3.5}$	1.50 \pm 0.22
...	127.4478	-50.0809	2.851 \pm 0.017	-12.039 \pm 0.029	10.611 \pm 0.031	...	13.460 \pm 0.002	13.935 \pm 0.007	12.827 \pm 0.005	347.3 $^{+2.1}_{-2.0}$	0.832 \pm 0.067
2MASS J08295658-5111456	127.4858	-51.1960	2.920 \pm 0.020	-11.831 \pm 0.038	10.754 \pm 0.031	18.4 \pm 3.0	13.047 \pm 0.002	13.470 \pm 0.007	12.462 \pm 0.005	339.1 \pm 2.3	0.880 \pm 0.060
...	127.5660	-50.5521	2.754 \pm 0.022	-11.713 \pm 0.043	10.032 \pm 0.041	...	14.628 \pm 0.001	15.299 \pm 0.008	13.787 \pm 0.009	359.4 \pm 2.9	0.695 \pm 0.056
...	127.6509	-50.1759	2.837 \pm 0.024	-12.736 \pm 0.044	9.655 \pm 0.044	...	14.375 \pm 0.002	15.025 \pm 0.008	13.602 \pm 0.007	349.0 $^{+3.0}_{-2.9}$	0.715 \pm 0.057
...	127.7954	-51.1755	2.737 \pm 0.059	-12.66 \pm 0.11	10.11 \pm 0.11	...	16.536 \pm 0.002	17.841 \pm 0.018	15.379 \pm 0.005	361.8 $^{+8.0}_{-7.6}$	0.390 \pm 0.031
...	127.8217	-50.6067	2.881 \pm 0.026	-13.115 \pm 0.043	9.757 \pm 0.050	...	14.589 \pm 0.003	15.285 \pm 0.009	13.772 \pm 0.007	343.7 \pm 3.1	0.695 \pm 0.056

Table B.6: Yep 3—Continued

Star Name	RA ($^{\circ}$)	Dec ($^{\circ}$)	Parallax (mas)	μ_{α} (mas yr $^{-1}$)	μ_{δ} (mas yr $^{-1}$)	v_r (km s $^{-1}$)	G (mag)	BP (mag)	RP (mag)	d (pc)	Mass (M $_{\odot}$)
TYC 8158-1304-1	128.2353 -49.8684	3.082 ± 0.027	-13.575 ± 0.055	9.985 ± 0.042	20.32 ± 0.15	11.982 ± 0.000	12.293 ± 0.002	11.518 ± 0.001	321.5 ± 2.8	1.250 ± 0.062	
...	128.1934 -50.9711	2.889 ± 0.017	-12.599 ± 0.035	10.285 ± 0.034	...	13.323 ± 0.001	13.809 ± 0.005	12.688 ± 0.004	342.8 $^{+2.1}_{-2.0}$	0.827 ± 0.066	
...	128.2633 -50.8215	3.015 ± 0.064	-12.69 ± 0.13	10.85 ± 0.12	...	16.494 ± 0.002	17.916 ± 0.013	15.278 ± 0.005	328.8 $^{+7.1}_{-6.8}$	0.334 ± 0.027	
...	128.2980 -50.5229	3.059 ± 0.043	-13.054 ± 0.078	11.145 ± 0.075	...	15.895 ± 0.002	17.029 ± 0.009	14.821 ± 0.004	324.0 $^{+4.6}_{-4.5}$	0.457 ± 0.037	
...	128.3150 -52.3093	3.031 ± 0.064	-13.22 ± 0.12	11.42 ± 0.13	...	16.451 ± 0.001	17.799 ± 0.012	15.292 ± 0.003	327.1 $^{+7.1}_{-6.8}$	0.378 ± 0.030	
...	128.4107 -50.5319	2.760 ± 0.020	-12.538 ± 0.039	9.758 ± 0.031	...	14.144 ± 0.001	14.745 ± 0.003	13.418 ± 0.002	358.6 $^{+2.7}_{-2.6}$	0.749 ± 0.060	
2MASS J08334968-5142593	128.4570 -51.7165	2.840 ± 0.021	-11.893 ± 0.041	11.503 ± 0.040	16.7 ± 1.9	11.547 ± 0.001	11.845 ± 0.004	11.099 ± 0.002	348.6 $^{+2.6}_{-2.5}$	1.180 ± 0.095	
...	128.5249 -53.0774	2.880 ± 0.055	-12.89 ± 0.12	11.53 ± 0.12	...	16.636 ± 0.002	17.951 ± 0.014	15.447 ± 0.008	343.9 $^{+6.7}_{-6.4}$	0.379 ± 0.030	
HD 73105	128.5399 -53.0715	2.763 ± 0.041	-12.020 ± 0.080	10.691 ± 0.094	...	6.750 ± 0.001	6.714 ± 0.002	6.867 ± 0.004	358.3 $^{+5.4}_{-5.2}$	5.4 ± 3.2	
2MASS J08342423-5348191	128.6010 -53.8054	3.058 ± 0.023	-13.147 ± 0.046	11.144 ± 0.049	18.82 ± 0.17	12.341 ± 0.001	12.706 ± 0.006	11.832 ± 0.005	324.0 ± 2.4	1.030 ± 0.052	
TYC 8162-333-1	128.6206 -51.2246	2.826 ± 0.026	-12.885 ± 0.047	10.267 ± 0.045	19.73 ± 0.58	11.952 ± 0.000	12.250 ± 0.002	11.506 ± 0.001	350.4 $^{+3.3}_{-3.2}$	1.154 ± 0.092	
2MASS J08343731-5024508	128.6555 -50.4141	3.108 ± 0.018	-14.192 ± 0.033	10.111 ± 0.027	19.14 ± 0.42	13.224 ± 0.002	13.711 ± 0.007	12.590 ± 0.006	318.7 ± 1.9	0.820 ± 0.041	
...	128.6655 -51.1875	2.733 ± 0.071	-12.90 ± 0.13	10.24 ± 0.14	...	16.815 ± 0.001	18.263 ± 0.020	15.603 ± 0.004	362.5 $^{+9.7}_{-9.2}$	0.326 ± 0.026	
...	128.6862 -51.0775	2.908 ± 0.068	-13.02 ± 0.11	9.64 ± 0.11	...	16.674 ± 0.001	17.970 ± 0.026	15.518 ± 0.003	340.8 $^{+8.2}_{-7.8}$	0.393 ± 0.031	
...	128.8019 -50.4257	2.794 ± 0.030	-12.578 ± 0.057	9.821 ± 0.049	...	15.126 ± 0.001	16.023 ± 0.005	14.188 ± 0.004	354.3 $^{+3.9}_{-3.8}$	0.587 ± 0.047	
CD-50 3414	128.8136 -50.9070	2.903 ± 0.028	-13.556 ± 0.048	9.885 ± 0.047	19.7 ± 2.1	10.491 ± 0.001	10.677 ± 0.002	10.203 ± 0.001	341.1 $^{+3.3}_{-3.2}$	1.880 ± 0.094	
2MASS J08352943-5148546	128.8727 -51.8152	2.756 ± 0.036	-12.664 ± 0.061	9.658 ± 0.061	19.90 ± 0.42	11.766 ± 0.000	12.050 ± 0.002	11.335 ± 0.001	359.1 $^{+4.7}_{-4.6}$	1.180 ± 0.059	
...	128.9419 -51.3151	3.013 ± 0.072	-13.43 ± 0.13	9.57 ± 0.15	...	17.009 ± 0.002	18.409 ± 0.034	15.793 ± 0.006	329.1 $^{+8.0}_{-7.7}$	0.348 ± 0.028	
HD 73387	129.0160 -51.1027	2.797 ± 0.036	-12.758 ± 0.065	9.675 ± 0.065	15.4 ± 7.4	9.919 ± 0.001	10.005 ± 0.001	9.805 ± 0.001	354.0 $^{+4.7}_{-4.5}$	1.980 ± 0.099	

Table B.6: Yep 3—Continued

Star Name	RA ($^{\circ}$)	Dec ($^{\circ}$)	Parallax (mas)	μ_{α} (mas yr $^{-1}$)	μ_{δ} (mas yr $^{-1}$)	v_r (km s $^{-1}$)	G (mag)	BP (mag)	RP (mag)	d (pc)	Mass (M $_{\odot}$)
2MASS J08361270-5152216	129.0529	-51.8727	2.861 ± 0.034	-12.324 ± 0.058	10.318 ± 0.051	19.81 ± 0.19	12.662 ± 0.001	13.027 ± 0.003	12.134 ± 0.003	346.1 $^{+4.1}_{-4.0}$	0.970 ± 0.048
...	129.0684	-51.5070	2.852 ± 0.025	-12.741 ± 0.048	9.674 ± 0.047	...	15.163 ± 0.001	16.050 ± 0.007	14.227 ± 0.004	347.2 ± 3.0	0.592 ± 0.047
2MASS J08362653-4940342	129.1106	-49.6762	2.822 ± 0.031	-12.788 ± 0.054	9.578 ± 0.051	19.39 ± 0.14	11.999 ± 0.000	12.302 ± 0.001	11.548 ± 0.001	350.8 ± 3.8	1.060 ± 0.053
TYC 8568-1105-1	129.1981	-53.2782	2.922 ± 0.025	-12.176 ± 0.046	11.389 ± 0.044	18.4 ± 2.1	10.908 ± 0.000	11.132 ± 0.001	10.561 ± 0.001	338.9 ± 2.9	1.500 ± 0.075
...	129.2080	-51.1932	2.807 ± 0.061	-12.41 ± 0.10	9.665 ± 0.095	...	16.462 ± 0.001	17.657 ± 0.012	15.335 ± 0.005	353.0 $^{+7.8}_{-7.5}$	0.426 ± 0.034
...	129.3428	-52.6510	2.796 ± 0.065	-12.79 ± 0.13	10.54 ± 0.15	...	17.055 ± 0.001	18.571 ± 0.049	15.770 ± 0.004	354.3 $^{+8.4}_{-8.0}$	0.274 ± 0.022
2MASS J08373864-5100031	129.4110	-51.0009	2.875 ± 0.026	-13.624 ± 0.051	9.072 ± 0.046	...	12.780 ± 0.003	13.197 ± 0.013	12.208 ± 0.009	344.4 $^{+3.2}_{-3.1}$	0.900 ± 0.045
CD-513115	129.4136	-51.6395	2.733 ± 0.025	-12.182 ± 0.051	10.289 ± 0.054	16.0 ± 3.9	10.365 ± 0.000	10.508 ± 0.001	10.140 ± 0.001	362.2 $^{+3.4}_{-3.3}$	1.770 ± 0.089
...	129.4210	-51.6672	2.908 ± 0.067	-13.00 ± 0.13	10.03 ± 0.14	...	16.664 ± 0.001	18.264 ± 0.017	15.403 ± 0.004	340.8 $^{+8.0}_{-7.6}$	0.259 ± 0.021
...	129.4951	-51.8060	2.941 ± 0.017	-12.408 ± 0.031	11.186 ± 0.031	...	13.331 ± 0.001	13.810 ± 0.004	12.701 ± 0.003	336.7 ± 2.0	0.832 ± 0.067
...	129.5602	-51.7310	2.766 ± 0.063	-11.78 ± 0.13	10.84 ± 0.13	...	16.854 ± 0.001	18.446 ± 0.013	15.604 ± 0.003	358.2 $^{+8.4}_{-8.0}$	0.264 ± 0.021
...	129.5800	-52.2224	2.848 ± 0.061	-13.42 ± 0.12	9.57 ± 0.11	...	16.365 ± 0.001	17.640 ± 0.009	15.181 ± 0.003	347.9 $^{+7.7}_{-7.3}$	0.391 ± 0.031
...	129.6085	-51.3576	3.032 ± 0.065	-13.10 ± 0.12	11.49 ± 0.13	...	16.799 ± 0.002	18.249 ± 0.016	15.602 ± 0.005	327.0 $^{+7.2}_{-6.9}$	0.330 ± 0.026
...	129.6789	-52.3621	2.844 ± 0.015	-13.248 ± 0.028	9.627 ± 0.028	...	14.129 ± 0.002	14.740 ± 0.008	13.361 ± 0.006	348.1 ± 1.8	0.729 ± 0.058
HD 73951	129.7156	-52.1627	2.715 ± 0.038	-13.093 ± 0.075	9.570 ± 0.069	...	9.213 ± 0.000	9.251 ± 0.001	9.176 ± 0.003	364.5 $^{+5.1}_{-5.0}$	2.2 ± 1.0
HD 73950	129.7276	-51.7021	2.896 ± 0.030	-13.271 ± 0.059	9.851 ± 0.059	...	9.534 ± 0.000	9.662 ± 0.001	9.347 ± 0.001	342.0 $^{+3.5}_{-3.4}$	1.78 ± 0.14
...	129.7551	-51.5967	2.810 ± 0.039	-13.116 ± 0.077	9.546 ± 0.083	...	16.173 ± 0.001	17.345 ± 0.010	15.077 ± 0.005	352.4 $^{+4.9}_{-4.8}$	0.439 ± 0.035

Table B.6: Yep 3—Continued

Star Name	RA ($^{\circ}$)	Dec ($^{\circ}$)	Parallax (mas)	μ_{α} (mas yr $^{-1}$)	μ_{δ} (mas yr $^{-1}$)	v_r (km s $^{-1}$)	G (mag)	BP (mag)	RP (mag)	d (pc)	Mass (M $_{\odot}$)
2MASS J08391280-5107385	129.8034	-51.1274	2.922 ± 0.018	-13.685 ± 0.032	9.613 ± 0.035	19.99 ± 0.31	13.046 ± 0.002	13.461 ± 0.006	12.478 ± 0.005	338.9 ± 2.1	0.900 ± 0.045
TYC 8163-1479-1	129.8057	-51.3056	2.760 ± 0.026	-13.080 ± 0.048	9.723 ± 0.051	17.6 ± 2.2	10.735 ± 0.000	10.927 ± 0.001	10.435 ± 0.001	358.4 $^{+3.4}_{-3.3}$	1.81 ± 0.11
2MASS J08391713-5230129	129.8214	-52.5036	2.752 ± 0.014	-12.648 ± 0.026	10.454 ± 0.025	18.15 ± 0.29	13.302 ± 0.001	13.735 ± 0.006	12.713 ± 0.004	359.6 ± 1.8	0.860 ± 0.043
...	129.8214	-51.8322	2.785 ± 0.026	-12.531 ± 0.050	9.635 ± 0.045	...	15.099 ± 0.001	15.937 ± 0.008	14.198 ± 0.003	355.4 $^{+3.3}_{-3.2}$	0.638 ± 0.051
2MASS J08393055-5128330	129.8773	-51.4759	2.738 ± 0.016	-11.914 ± 0.029	9.964 ± 0.033	20.02 ± 0.57	13.414 ± 0.001	13.864 ± 0.004	12.811 ± 0.002	361.4 $^{+2.2}_{-2.1}$	0.860 ± 0.043
...	129.9279	-51.5556	2.827 ± 0.030	-13.364 ± 0.055	9.627 ± 0.064	...	15.339 ± 0.002	16.256 ± 0.008	14.385 ± 0.005	350.2 $^{+3.7}_{-3.6}$	0.572 ± 0.046
...	129.9322	-52.7894	2.882 ± 0.042	-13.224 ± 0.083	11.752 ± 0.084	...	15.311 ± 0.001	16.265 ± 0.006	14.332 ± 0.002	343.7 $^{+5.1}_{-5.0}$	0.557 ± 0.045
...	129.9421	-52.2915	2.944 ± 0.034	-13.359 ± 0.066	10.096 ± 0.065	...	15.856 ± 0.003	17.000 ± 0.014	14.784 ± 0.009	336.4 $^{+4.0}_{-3.9}$	0.455 ± 0.036
...	129.9540	-51.1844	2.928 ± 0.072	-13.02 ± 0.12	9.78 ± 0.13	...	16.587 ± 0.002	17.918 ± 0.013	15.443 ± 0.005	338.6 $^{+8.5}_{-8.1}$	0.387 ± 0.031
TYC 8163-2131-1	129.9593	-51.5401	2.876 ± 0.026	-12.625 ± 0.050	9.199 ± 0.053	-10.15 ± 0.95	11.888 ± 0.001	12.273 ± 0.004	11.346 ± 0.003	344.3 $^{+3.2}_{-3.1}$	1.25 ± 0.16
2MASS J08395173-5155070	129.9656	-51.9186	2.845 ± 0.031	-12.573 ± 0.050	9.626 ± 0.059	11.2 ± 1.8	11.793 ± 0.001	12.091 ± 0.003	11.347 ± 0.002	348.1 $^{+3.8}_{-3.7}$	0.990 ± 0.050
TYC 8163-2765-1	129.9661	-51.7687	2.936 ± 0.026	-12.849 ± 0.051	9.938 ± 0.051	40.54 ± 0.15	11.771 ± 0.000	12.063 ± 0.001	11.331 ± 0.001	337.3 $^{+3.0}_{-2.9}$	1.060 ± 0.053
TYC 8163-1809-1	129.9754	-51.9476	2.814 ± 0.028	-12.101 ± 0.050	10.556 ± 0.053	12.06 ± 0.16	11.876 ± 0.000	12.163 ± 0.002	11.439 ± 0.001	351.8 $^{+3.5}_{-3.4}$	1.180 ± 0.059
OOVel	130.0348	-51.9446	2.783 ± 0.052	-13.317 ± 0.089	9.51 ± 0.10	...	7.422 ± 0.001	7.393 ± 0.003	7.514 ± 0.003	355.8 $^{+6.8}_{-6.5}$	2.18 ± 0.35
...	130.0579	-52.7192	2.865 ± 0.051	-12.12 ± 0.10	10.520 ± 0.098	...	16.393 ± 0.001	17.602 ± 0.010	15.284 ± 0.004	345.7 $^{+6.3}_{-6.1}$	0.427 ± 0.034
...	130.1241	-51.5363	3.005 ± 0.016	-12.766 ± 0.030	10.910 ± 0.030	...	13.272 ± 0.002	13.733 ± 0.008	12.651 ± 0.005	329.6 ± 1.8	0.844 ± 0.068
...	130.1580	-52.4987	2.916 ± 0.017	-13.544 ± 0.034	9.790 ± 0.037	...	13.906 ± 0.002	14.480 ± 0.007	13.197 ± 0.005	339.6 ± 2.0	0.766 ± 0.061
2MASS J08404809-5122340	130.2004	-51.3761	2.917 ± 0.024	-12.586 ± 0.042	10.716 ± 0.043	19.54 ± 0.16	11.997 ± 0.001	12.308 ± 0.002	11.536 ± 0.002	339.5 $^{+2.8}_{-2.7}$	1.113 ± 0.089
...	130.2022	-52.4065	2.811 ± 0.060	-13.36 ± 0.12	10.07 ± 0.14	...	16.666 ± 0.002	18.026 ± 0.015	15.501 ± 0.006	352.4 $^{+7.6}_{-7.3}$	0.373 ± 0.030

Table B.6: Yep 3—Continued

Star Name	RA ($^{\circ}$)	Dec ($^{\circ}$)	Parallax (mas)	μ_{α} (mas yr $^{-1}$)	μ_{δ} (mas yr $^{-1}$)	v_r (km s $^{-1}$)	G (mag)	BP (mag)	RP (mag)	d (pc)	Mass (M $_{\odot}$)
2MASS J08405718-5145010	130.2383	-51.7503	2.813 ± 0.059	-12.91 ± 0.11	9.83 ± 0.13	...	16.323 ± 0.002	17.515 ± 0.012	15.201 ± 0.004	352.1 $^{+7.5}_{-7.2}$	0.428 ± 0.034
...	130.2440	-51.5140	2.909 ± 0.021	-13.221 ± 0.037	9.868 ± 0.039	...	14.514 ± 0.003	15.215 ± 0.009	13.702 ± 0.007	340.4 ± 2.5	0.695 ± 0.056
...	130.2840	-52.0177	2.878 ± 0.017	-13.208 ± 0.030	9.768 ± 0.031	...	13.953 ± 0.001	14.534 ± 0.006	13.243 ± 0.004	344.0 ± 2.0	0.763 ± 0.061
...	130.4050	-51.3990	3.025 ± 0.066	-13.38 ± 0.12	10.42 ± 0.11	...	13.879 ± 0.001	14.551 ± 0.006	13.085 ± 0.003	327.7 $^{+7.4}_{-7.0}$	0.700 ± 0.056
2MASS J08414215-5206204	130.4257	-52.1057	2.896 ± 0.022	-13.427 ± 0.044	9.434 ± 0.040	19.51 ± 0.31	12.832 ± 0.001	13.231 ± 0.004	12.281 ± 0.004	341.9 ± 2.6	0.860 ± 0.043
2MASS J08415930-5210337	130.4971	-52.1760	2.838 ± 0.024	-13.606 ± 0.046	9.714 ± 0.044	19.25 ± 0.15	12.674 ± 0.003	13.060 ± 0.010	12.129 ± 0.008	348.8 ± 3.0	0.860 ± 0.043
...	130.5583	-53.5398	2.827 ± 0.070	-13.16 ± 0.13	9.82 ± 0.15	...	16.830 ± 0.002	18.254 ± 0.023	15.632 ± 0.005	350.5 $^{+8.9}_{-8.5}$	0.339 ± 0.027
...	130.7826	-51.8259	2.861 ± 0.060	-13.30 ± 0.11	9.65 ± 0.10	...	16.469 ± 0.001	17.732 ± 0.011	15.340 ± 0.004	346.3 $^{+7.4}_{-7.1}$	0.409 ± 0.033
...	130.7979	-53.0698	2.907 ± 0.055	-12.34 ± 0.10	10.02 ± 0.11	...	16.183 ± 0.001	17.354 ± 0.012	15.085 ± 0.004	340.8 $^{+6.6}_{-6.4}$	0.439 ± 0.035
2MASS J08434121-5200235	130.9217	-52.0065	2.994 ± 0.016	-13.462 ± 0.030	11.591 ± 0.026	55.81 ± 0.21	13.624 ± 0.000	14.113 ± 0.002	12.990 ± 0.001	330.8 ± 1.7	0.820 ± 0.041
...	130.9219	-52.3689	2.928 ± 0.029	-13.410 ± 0.065	9.887 ± 0.053	...	15.548 ± 0.002	16.552 ± 0.012	14.549 ± 0.007	338.2 ± 3.3	0.541 ± 0.043
...	130.9616	-52.3272	2.924 ± 0.042	-13.384 ± 0.088	9.602 ± 0.080	...	16.083 ± 0.003	17.259 ± 0.018	14.988 ± 0.007	338.8 $^{+5.0}_{-4.8}$	0.439 ± 0.035
...	130.9689	-51.8044	2.790 ± 0.032	-13.343 ± 0.059	9.564 ± 0.057	...	15.308 ± 0.001	16.240 ± 0.005	14.348 ± 0.004	354.8 $^{+4.1}_{-4.0}$	0.564 ± 0.045
2MASS J08450857-5313397	131.2857	-53.2277	3.062 ± 0.025	-12.872 ± 0.045	11.625 ± 0.042	18.04 ± 0.14	12.520 ± 0.000	12.884 ± 0.001	12.005 ± 0.001	323.6 ± 2.6	0.860 ± 0.043
...	131.3281	-52.8262	2.890 ± 0.044	-13.021 ± 0.085	10.173 ± 0.082	...	15.595 ± 0.001	16.584 ± 0.006	14.594 ± 0.004	342.7 $^{+5.3}_{-5.2}$	0.544 ± 0.043
2MASS J08492498-5332383	132.3541	-53.5440	2.732 ± 0.022	-12.509 ± 0.039	10.005 ± 0.041	5.63 ± 0.26	13.621 ± 0.001	14.113 ± 0.004	12.976 ± 0.002	362.3 $^{+2.9}_{-2.8}$	0.820 ± 0.066
...	132.4868	-54.2095	2.704 ± 0.074	-11.97 ± 0.14	9.74 ± 0.14	...	16.922 ± 0.002	18.567 ± 0.018	15.660 ± 0.003	366 $^{+10.}_{-9.8}$	0.247 ± 0.020
2MASS J08512187-5406183	132.8411	-54.1051	2.815 ± 0.069	-12.80 ± 0.13	9.92 ± 0.15	...	16.696 ± 0.001	18.046 ± 0.012	15.549 ± 0.004	352.0 $^{+8.9}_{-8.4}$	0.381 ± 0.030

Table B.6: Yep 3—Continued

Star Name	RA ($^{\circ}$)	Dec ($^{\circ}$)	Parallax (mas)	μ_{α} (mas yr $^{-1}$)	μ_{δ} (mas yr $^{-1}$)	v_r (km s $^{-1}$)	G (mag)	BP (mag)	RP (mag)	d (pc)	Mass (M $_{\odot}$)
...	127.5864 -51.2679	2.92 ± 0.12	-12.32 ± 0.22	10.92 ± 0.20	...	17.727 ± 0.013	19.379 ± 0.038	16.428 ± 0.006	340. $^{+14}_{-13}$	0.236 ± 0.019	
...	128.0964 -50.8790	2.948 ± 0.091	-13.32 ± 0.18	10.61 ± 0.22	...	17.079 ± 0.002	18.648 ± 0.021	15.828 ± 0.004	337. $^{+11}_{-10}$	0.269 ± 0.022	
...	128.1299 -50.9426	3.052 ± 0.091	-12.29 ± 0.17	10.44 ± 0.19	...	16.942 ± 0.002	18.615 ± 0.019	15.652 ± 0.004	325. $^{+10}_{-9.4}$	0.233 ± 0.019	
...	128.1485 -50.5452	2.94 ± 0.10	-12.36 ± 0.19	9.58 ± 0.22	...	17.446 ± 0.001	19.011 ± 0.024	16.179 ± 0.006	337 ± 12	0.266 ± 0.021	
...	128.3269 -50.9958	3.00 ± 0.11	-13.27 ± 0.22	9.70 ± 0.24	...	17.701 ± 0.002	19.397 ± 0.036	16.439 ± 0.005	331. $^{+13}_{-12}$	0.235 ± 0.019	
...	128.3334 -50.7321	3.01 ± 0.14	-13.08 ± 0.29	9.42 ± 0.32	...	18.178 ± 0.002	19.776 ± 0.036	16.869 ± 0.007	330. $^{+16}_{-14}$	0.247 ± 0.020	
...	128.4075 -50.6118	2.94 ± 0.12	-12.98 ± 0.26	9.80 ± 0.22	...	18.070 ± 0.002	19.676 ± 0.067	16.776 ± 0.006	338. $^{+14}_{-13}$	0.249 ± 0.020	
...	128.4130 -50.5461	2.860 ± 0.097	-11.77 ± 0.19	10.52 ± 0.20	...	17.293 ± 0.007	18.899 ± 0.022	16.021 ± 0.006	347. $^{+12}_{-11}$	0.255 ± 0.020	
...	128.5232 -50.8326	2.90 ± 0.13	-12.18 ± 0.24	10.05 ± 0.25	...	17.482 ± 0.002	19.039 ± 0.045	16.099 ± 0.014	342. $^{+16}_{-14}$	0.239 ± 0.019	
...	129.1649 -49.8635	2.92 ± 0.12	-11.99 ± 0.23	10.57 ± 0.26	...	17.691 ± 0.002	19.286 ± 0.036	16.464 ± 0.006	340. $^{+15}_{-14}$	0.269 ± 0.021	
...	129.3948 -52.4508	3.08 ± 0.11	-13.28 ± 0.21	10.83 ± 0.25	...	18.078 ± 0.003	19.759 ± 0.057	16.774 ± 0.008	323. $^{+12}_{-11}$	0.228 ± 0.018	
...	129.4202 -51.2143	2.87 ± 0.16	-12.56 ± 0.28	9.37 ± 0.30	...	18.006 ± 0.002	19.598 ± 0.046	16.707 ± 0.009	347. $^{+21}_{-19}$	0.251 ± 0.020	
...	129.4430 -53.3396	2.98 ± 0.15	-13.08 ± 0.29	11.58 ± 0.34	...	18.278 ± 0.002	20.013 ± 0.045	16.966 ± 0.008	333. $^{+18}_{-16}$	0.215 ± 0.017	
...	129.4913 -51.4238	2.96 ± 0.12	-12.98 ± 0.22	9.87 ± 0.26	...	17.755 ± 0.003	19.153 ± 0.063	16.460 ± 0.005	336. $^{+14}_{-13}$	0.314 ± 0.027	
...	129.5302 -51.6535	2.92 ± 0.10	-12.73 ± 0.20	10.42 ± 0.26	...	17.775 ± 0.003	19.352 ± 0.036	16.519 ± 0.006	340. $^{+12}_{-11}$	0.266 ± 0.021	
...	129.5507 -51.2658	2.94 ± 0.13	-12.05 ± 0.23	9.77 ± 0.26	...	17.935 ± 0.001	19.430 ± 0.035	16.647 ± 0.007	338. $^{+16}_{-14}$	0.278 ± 0.022	
...	129.6847 -51.6216	2.93 ± 0.14	-13.24 ± 0.27	10.32 ± 0.30	...	18.327 ± 0.004	20.120 ± 0.084	16.974 ± 0.010	339. $^{+18}_{-16}$	0.195 ± 0.017	
...	130.0296 -51.5293	3.032 ± 0.090	-13.36 ± 0.17	9.76 ± 0.18	...	17.228 ± 0.002	18.714 ± 0.018	15.982 ± 0.009	327. $^{+10}_{-9.5}$	0.300 ± 0.024	
...	130.0597 -52.7209	2.95 ± 0.12	-12.40 ± 0.23	10.82 ± 0.26	...	17.951 ± 0.001	19.351 ± 0.047	16.686 ± 0.008	337. $^{+14}_{-13}$	0.324 ± 0.026	

Table B.6: Yep 3—Continued

Star Name	RA ($^{\circ}$)	Dec ($^{\circ}$)	Parallax (mas)	μ_{α} (mas yr $^{-1}$)	μ_{δ} (mas yr $^{-1}$)	v_r (km s $^{-1}$)	G (mag)	BP (mag)	RP (mag)	d (pc)	Mass (M $_{\odot}$)
...	130.0956	-52.2462	2.899 \pm 0.096	-12.83 \pm 0.19	9.67 \pm 0.20	...	16.772 \pm 0.002	18.356 \pm 0.024	15.508 \pm 0.006	342 $^{+12}_{-11}$	0.262 \pm 0.021
...	130.1257	-52.1015	2.87 \pm 0.13	-11.97 \pm 0.26	9.97 \pm 0.31	...	18.008 \pm 0.003	19.563 \pm 0.057	16.727 \pm 0.010	347 $^{+17}_{-15}$	0.265 \pm 0.021
...	130.6542	-52.2376	2.96 \pm 0.13	-13.27 \pm 0.23	10.10 \pm 0.25	...	18.226 \pm 0.001	19.873 \pm 0.074	16.910 \pm 0.014	336 $^{+15}_{-14}$	0.233 \pm 0.019
...	130.8623	-51.5790	2.95 \pm 0.17	-13.39 \pm 0.26	9.04 \pm 0.26	...	17.866 \pm 0.002	19.466 \pm 0.050	16.602 \pm 0.007	337 $^{+22}_{-19}$	0.258 \pm 0.021
...	131.2083	-52.9211	3.06 \pm 0.11	-13.11 \pm 0.25	10.02 \pm 0.22	...	17.659 \pm 0.005	19.272 \pm 0.037	16.379 \pm 0.007	324 $^{+12}_{-11}$	0.251 \pm 0.020
...	128.3946	-50.9444	3.109 \pm 0.030	-14.213 \pm 0.060	10.571 \pm 0.054	...	15.353 \pm 0.001	16.360 \pm 0.005	14.349 \pm 0.003	318.8 $^{+3.2}_{-3.1}$	0.538 \pm 0.043
...	128.4359	-52.0447	3.094 \pm 0.023	-11.747 \pm 0.044	11.468 \pm 0.047	...	14.798 \pm 0.002	15.749 \pm 0.010	13.819 \pm 0.008	320.3 \pm 2.4	0.558 \pm 0.045
...	129.0817	-52.2689	2.830 \pm 0.072	-11.83 \pm 0.12	9.51 \pm 0.13	...	16.976 \pm 0.002	18.341 \pm 0.036	15.776 \pm 0.006	350.2 $^{+9.1}_{-8.7}$	0.362 \pm 0.029
...	129.2044	-53.5544	2.898 \pm 0.049	-13.74 \pm 0.11	10.25 \pm 0.10	...	15.994 \pm 0.001	17.254 \pm 0.007	14.870 \pm 0.003	341.8 $^{+5.9}_{-5.7}$	0.411 \pm 0.033
TYC 8568-2056-1	129.2070	-54.1320	2.805 \pm 0.059	-12.77 \pm 0.12	9.77 \pm 0.14	10.06 \pm 0.72	11.360 \pm 0.000	11.643 \pm 0.001	10.929 \pm 0.001	353.1 $^{+7.6}_{-7.3}$	1.250 \pm 0.062
HD 74056	129.8245	-53.2849	3.100 \pm 0.033	-13.927 \pm 0.059	11.898 \pm 0.052	...	9.349 \pm 0.001	9.419 \pm 0.002	9.260 \pm 0.002	319.6 \pm 3.4	1.98 \pm 0.44
...	130.8441	-53.5321	3.064 \pm 0.017	-11.536 \pm 0.032	10.640 \pm 0.039	...	14.278 \pm 0.002	15.034 \pm 0.006	13.435 \pm 0.004	323.3 $^{+1.8}_{-1.7}$	0.687 \pm 0.055
2MASS J08441148-4943405	131.0479	-49.7279	2.847 \pm 0.016	-13.685 \pm 0.027	9.396 \pm 0.031	27.8 \pm 3.1	13.102 \pm 0.003	13.529 \pm 0.009	12.510 \pm 0.008	347.7 \pm 1.9	0.950 \pm 0.052
TYC 8163-1937-1	131.1211	-51.8078	2.970 \pm 0.026	-11.963 \pm 0.048	9.722 \pm 0.042	30.93 \pm 0.21	12.244 \pm 0.001	12.641 \pm 0.004	11.698 \pm 0.003	333.5 \pm 2.9	0.937 \pm 0.075
...	131.1966	-52.8860	3.016 \pm 0.052	-13.65 \pm 0.12	9.98 \pm 0.11	...	16.255 \pm 0.002	17.491 \pm 0.014	15.142 \pm 0.004	328.6 $^{+5.7}_{-5.5}$	0.419 \pm 0.034
...	131.3702	-53.2988	2.919 \pm 0.041	-13.377 \pm 0.083	9.663 \pm 0.073	...	15.803 \pm 0.001	16.869 \pm 0.009	14.755 \pm 0.005	339.4 $^{+4.8}_{-4.7}$	0.509 \pm 0.041
...	131.7088	-54.1320	3.098 \pm 0.028	-13.647 \pm 0.055	11.135 \pm 0.049	...	15.303 \pm 0.001	16.267 \pm 0.005	14.317 \pm 0.003	319.8 $^{+2.9}_{-2.8}$	0.553 \pm 0.044

Table B.6: Yep 3—Continued

Star Name	RA ($^{\circ}$)	Dec ($^{\circ}$)	Parallax (mas)	μ_{α} (mas yr^{-1})	μ_{δ} (mas yr^{-1})	v_r (km s^{-1})	G (mag)	BP (mag)	RP (mag)	d (pc)	Mass (M_{\odot})
CD-50 3593	132.3128 -51.0401	2.928 \pm 0.043	-12.992 \pm 0.077	9.846 \pm 0.077	...	16.102 \pm 0.001	17.318 \pm 0.008	15.012 \pm 0.003	340.0 $^{+5.1}_{-6.0}$	0.430 \pm 0.034	
...	132.2321 -54.0075	2.914 \pm 0.044	-13.797 \pm 0.076	9.846 \pm 0.059	...	9.913 \pm 0.000	10.069 \pm 0.001	9.678 \pm 0.002	338.3 $^{+5.0}_{-4.9}$	1.67 \pm 0.13	
...	132.4527 -54.9563	2.789 \pm 0.074	-12.07 \pm 0.15	9.69 \pm 0.14	...	15.803 \pm 0.001	16.916 \pm 0.004	14.695 \pm 0.002	355.3 $^{+9.6}_{-9.1}$	0.454 \pm 0.036	
2MASS J08494919-5305532	132.4550 -53.0981	2.832 \pm 0.024	-11.997 \pm 0.046	9.669 \pm 0.045	18.19 \pm 0.32	12.674 \pm 0.001	13.043 \pm 0.003	12.144 \pm 0.002	349.5 $^{+3.0}_{-2.9}$	0.980 \pm 0.049	
...	132.5069 -52.8457	2.801 \pm 0.050	-13.094 \pm 0.099	10.671 \pm 0.095	...	16.173 \pm 0.001	17.333 \pm 0.013	15.098 \pm 0.003	353.5 $^{+6.4}_{-6.2}$	0.450 \pm 0.036	
...	128.0200 -50.4978	2.91 \pm 0.18	-12.335 \pm 0.34	10.00 \pm 0.40	...	18.375 \pm 0.001	19.905 \pm 0.096	17.033 \pm 0.009	342.4 $^{+24}_{-21}$	0.256 \pm 0.025	
...	128.2713 -50.5358	2.92 \pm 0.16	-12.53 \pm 0.27	9.06 \pm 0.31	...	18.371 \pm 0.000	19.887 \pm 0.066	17.027 \pm 0.010	341.4 $^{+20}_{-18}$	0.259 \pm 0.021	
...	128.3211 -49.9656	3.00 \pm 0.18	-13.15 \pm 0.51	10.43 \pm 0.38	...	17.806 \pm 0.002	332.4 $^{+21}_{-19}$	0.364 \pm 0.040	
...	128.5346 -50.4355	2.98 \pm 0.29	-12.04 \pm 0.46	9.60 \pm 0.46	...	19.306 \pm 0.011	20.87 \pm 0.15	17.814 \pm 0.026	339.3 $^{+39}_{-32}$	0.213 \pm 0.032	
...	128.5427 -51.1371	3.12 \pm 0.24	-12.58 \pm 0.39	9.62 \pm 0.52	...	18.870 \pm 0.003	20.504 \pm 0.093	17.507 \pm 0.015	321.4 $^{+28}_{-24}$	0.225 \pm 0.022	
...	128.7091 -53.2960	3.05 \pm 0.26	-13.11 \pm 0.49	10.65 \pm 0.53	...	16.468 \pm 0.002	17.278 \pm 0.009	15.205 \pm 0.004	330.4 $^{+33}_{-27}$	0.518 \pm 0.041	
...	129.2196 -53.7680	2.95 \pm 0.13	-12.49 \pm 0.24	9.95 \pm 0.32	...	18.044 \pm 0.002	19.357 \pm 0.055	16.770 \pm 0.016	337.4 $^{+16}_{-14}$	0.356 \pm 0.028	
...	129.5237 -51.6656	2.91 \pm 0.19	-13.34 \pm 0.37	9.93 \pm 0.46	...	18.942 \pm 0.003	20.693 \pm 0.082	17.593 \pm 0.014	343.4 $^{+25}_{-22}$	0.204 \pm 0.019	
...	129.9223 -53.0676	2.96 \pm 0.15	-12.45 \pm 0.33	10.11 \pm 0.38	...	17.321 \pm 0.005	336.4 $^{+18}_{-16}$	0.405 \pm 0.045	
...	130.1109 -52.4455	2.96 \pm 0.20	-12.67 \pm 0.36	10.74 \pm 0.47	...	18.842 \pm 0.016	20.74 \pm 0.14	17.509 \pm 0.012	338.4 $^{+25}_{-22}$	0.180 \pm 0.022	
...	130.1357 -51.7941	2.98 \pm 0.29	-13.35 \pm 0.55	10.37 \pm 0.59	...	19.177 \pm 0.003	20.57 \pm 0.16	17.824 \pm 0.020	339.4 $^{+39}_{-32}$	0.297 \pm 0.055	
...	130.2460 -52.2027	2.93 \pm 0.31	-13.55 \pm 0.64	9.92 \pm 0.70	...	19.354 \pm 0.002	20.76 \pm 0.25	17.940 \pm 0.029	345.4 $^{+44}_{-35}$	0.268 \pm 0.076	
...	130.3778 -51.9009	2.91 \pm 0.32	-11.55 \pm 0.64	9.38 \pm 0.70	...	19.613 \pm 0.003	20.37 \pm 0.27	18.107 \pm 0.028	348.4 $^{+47}_{-37}$	0.441 \pm 0.086	
...	131.1860 -52.7042	2.88 \pm 0.26	-12.75 \pm 0.49	11.24 \pm 0.44	...	19.299 \pm 0.002	21.09 \pm 0.17	17.853 \pm 0.022	349.4 $^{+37}_{-30}$	0.179 \pm 0.026	

Table B.6: Yep 3—Continued

Star Name	R.A. ($^{\circ}$)	Dec ($^{\circ}$)	Parallax (mas)	μ_{α} (mas yr $^{-1}$)	μ_{δ} (mas yr $^{-1}$)	v_r (km s $^{-1}$)	G (mag)	BP (mag)	RP (mag)	d (pc)	Mass (M $_{\odot}$)
...	128.1485	-53.8456	2.96 ± 0.18	-11.28 ± 0.36	10.43 ± 0.35	...	18.488 ± 0.001	20.145 ± 0.062	17.203 ± 0.013	337 $^{+22}_{-20}$	0.239 ± 0.019

Table B.7: UPK 535 Member Kinematics and Properties

Star Name	<i>RA</i> ($^{\circ}$)	<i>Dec</i> ($^{\circ}$)	Parallax (mas)	μ_{α} (mas yr $^{-1}$)	μ_{δ} (mas yr $^{-1}$)	v_r (km s $^{-1}$)	G (mag)	BP (mag)	RP (mag)	<i>d</i> (pc)	Mass (M $_{\odot}$)
...	127.1060 -50.7381	2.85 \pm 0.12	-12.21 \pm 0.20	2.79 \pm 0.19	...	17.753 \pm 0.002	19.432 \pm 0.043	16.460 \pm 0.007	348 $^{+15}_{-14}$	0.237 \pm 0.019	
...	126.9523 -51.3952	3.230 \pm 0.097	-13.47 \pm 0.19	3.29 \pm 0.18	...	17.724 \pm 0.002	19.351 \pm 0.029	16.427 \pm 0.007	307.3 $^{+9.5}_{-9.0}$	0.249 \pm 0.020	
...	125.1185 -51.4959	3.22 \pm 0.19	-13.24 \pm 0.28	3.68 \pm 0.65	...	12.275 \pm 0.012	310 $^{+20}_{-18}$	0.99 \pm 0.11	
...	125.6723 -50.4960	3.241 \pm 0.099	-12.35 \pm 0.19	3.33 \pm 0.19	...	17.756 \pm 0.003	19.381 \pm 0.037	16.468 \pm 0.007	306.4 $^{+9.7}_{-9.1}$	0.252 \pm 0.020	
...	126.2494 -51.0845	3.16 \pm 0.11	-13.38 \pm 0.21	3.48 \pm 0.20	...	17.654 \pm 0.002	19.328 \pm 0.039	16.368 \pm 0.005	315 \pm 11	0.240 \pm 0.019	
...	126.3646 -50.8005	3.34 \pm 0.14	-13.16 \pm 0.45	3.52 \pm 0.31	...	17.613 \pm 0.004	17.65 \pm 0.13	15.980 \pm 0.038	298 $^{+14}_{-12}$	0.666 \pm 0.053	
...	126.3508 -50.8988	3.224 \pm 0.084	-13.54 \pm 0.17	3.37 \pm 0.18	...	17.163 \pm 0.002	18.632 \pm 0.022	15.932 \pm 0.006	307.8 $^{+8.2}_{-7.8}$	0.320 \pm 0.026	
...	126.4602 -50.2630	3.25 \pm 0.11	-12.62 \pm 0.21	3.25 \pm 0.20	...	17.632 \pm 0.002	19.249 \pm 0.028	16.352 \pm 0.006	306 $^{+11}_{-10}$	0.256 \pm 0.020	
...	126.3209 -50.1092	3.15 \pm 0.14	-12.83 \pm 0.23	3.32 \pm 0.26	...	17.935 \pm 0.003	19.606 \pm 0.050	16.594 \pm 0.008	316 $^{+14}_{-13}$	0.227 \pm 0.018	
...	128.0546 -50.6879	3.204 \pm 0.092	-13.48 \pm 0.18	2.87 \pm 0.19	...	17.240 \pm 0.002	18.829 \pm 0.024	15.993 \pm 0.004	309.7 $^{+9.1}_{-8.6}$	0.271 \pm 0.022	
...	128.7035 -49.4763	3.121 \pm 0.089	-13.62 \pm 0.15	3.32 \pm 0.24	...	16.648 \pm 0.003	17.691 \pm 0.065	15.277 \pm 0.025	317.9 $^{+9.3}_{-8.8}$	0.409 \pm 0.033	
...	127.5509 -50.0837	3.19 \pm 0.31	-13.10 \pm 0.52	3.06 \pm 0.66	...	17.393 \pm 0.006	18.672 \pm 0.026	15.716 \pm 0.006	316 $^{+37}_{-30}$	0.241 \pm 0.019	
...	124.4018 -52.9427	3.15 \pm 0.17	-12.98 \pm 0.35	4.08 \pm 0.32	...	16.646 \pm 0.003	18.147 \pm 0.012	15.392 \pm 0.004	316 $^{+18}_{-16}$	0.300 \pm 0.024	
...	124.7601 -51.8470	2.987 \pm 0.065	-12.16 \pm 0.12	3.74 \pm 0.16	...	16.604 \pm 0.003	17.954 \pm 0.011	15.449 \pm 0.005	331.8 $^{+7.4}_{-7.1}$	0.385 \pm 0.031	
...	127.2906 -49.4106	3.29 \pm 0.14	-13.11 \pm 0.25	3.63 \pm 0.21	...	17.906 \pm 0.003	19.496 \pm 0.072	16.559 \pm 0.010	303 $^{+14}_{-13}$	0.246 \pm 0.020	
...	127.4192 -53.1596	3.204 \pm 0.087	-12.80 \pm 0.19	3.50 \pm 0.19	...	17.326 \pm 0.003	19.052 \pm 0.039	15.998 \pm 0.006	309.7 $^{+8.6}_{-8.2}$	0.219 \pm 0.017	
...	127.6570 -52.2158	3.22 \pm 0.17	-13.68 \pm 0.35	2.31 \pm 0.38	...	18.346 \pm 0.003	20.19 \pm 0.13	16.980 \pm 0.016	302.6 $^{+7.0}_{-6.7}$	0.186 \pm 0.022	
...	128.2653 -51.8054	3.178 \pm 0.076	-12.65 \pm 0.14	3.19 \pm 0.18	...	17.291 \pm 0.002	18.875 \pm 0.024	16.041 \pm 0.005	312.1 $^{+7.6}_{-7.3}$	0.272 \pm 0.022	

Table B.7: UPK 535—Continued

Star Name	RA ($^{\circ}$)	Dec ($^{\circ}$)	Parallax (mas)	μ_{α} (mas yr^{-1})	μ_{δ} (mas yr^{-1})	v_r (km s^{-1})	G (mag)	BP (mag)	RP (mag)	d (pc)	Mass (M_{\odot})
...	129.1074 -52.3094	2.85 ± 0.13	-12.66 ± 0.22	2.53 ± 0.25	...	17.650 ± 0.002	19.280 ± 0.039	16.364 ± 0.005	349 $^{+16}_{-15}$	0.251 ± 0.020	
...	129.4236 -51.8096	3.185 ± 0.071	-13.24 ± 0.14	2.61 ± 0.16	...	17.125 ± 0.002	18.647 ± 0.025	15.885 ± 0.004	311.4 $^{+7.1}_{-6.8}$	0.298 ± 0.024	
...	128.2888 -51.4455	3.17 ± 0.11	-13.51 ± 0.23	2.55 ± 0.23	...	17.439 ± 0.002	18.998 ± 0.025	16.176 ± 0.006	314 $^{+12}_{-11}$	0.274 ± 0.022	
...	128.3600 -51.2284	2.826 ± 0.095	-12.57 ± 0.16	2.81 ± 0.18	...	16.968 ± 0.002	18.718 ± 0.018	15.659 ± 0.004	351 $^{+12}_{-11}$	0.218 ± 0.017	
...	125.6894 -52.3785	2.88 ± 0.13	-12.32 ± 0.44	3.28 ± 0.70	...	16.202 ± 0.005	345 $^{+17}_{-15}$	0.545 ± 0.060	
...	127.0432 -51.6824	3.21 ± 0.11	-13.57 ± 0.20	3.15 ± 0.19	...	17.747 ± 0.003	19.333 ± 0.048	16.449 ± 0.007	309 $^{+11}_{-10}$	0.259 ± 0.021	
...	127.5049 -51.6574	3.158 ± 0.096	-13.27 ± 0.18	3.29 ± 0.16	...	17.155 ± 0.003	18.682 ± 0.028	15.908 ± 0.005	314.3 $^{+9.8}_{-9.3}$	0.293 ± 0.023	
...	126.1012 -51.8017	3.27 ± 0.11	-13.35 ± 0.24	3.88 ± 0.19	...	17.824 ± 0.003	19.545 ± 0.069	16.522 ± 0.006	304 $^{+10.}_{-9.7}$	0.224 ± 0.018	
...	129.4489 -53.1395	3.14 ± 0.12	-12.66 ± 0.24	3.28 ± 0.24	...	17.457 ± 0.002	19.216 ± 0.030	16.143 ± 0.006	316 $^{+12}_{-11}$	0.215 ± 0.017	
...	125.9677 -49.3274	3.21 ± 0.14	-12.28 ± 0.25	3.22 ± 0.32	...	17.929 ± 0.003	19.469 ± 0.064	16.626 ± 0.009	310 $^{+14}_{-13}$	0.269 ± 0.022	
...	124.8770 -49.1503	3.35 ± 0.12	-12.80 ± 0.19	3.40 ± 0.21	...	16.494 ± 0.004	16.88 ± 0.20	14.988 ± 0.031	297 $^{+11}_{-10}$	0.573 ± 0.072	
...	127.8200 -48.6765	3.291 ± 0.086	-12.22 ± 0.18	2.91 ± 0.24	...	17.004 ± 0.004	18.533 ± 0.047	15.714 ± 0.007	301.6 $^{+8.1}_{-7.7}$	0.275 ± 0.022	
HD 69991	124.3079 -51.7000	3.310 ± 0.026	-13.349 ± 0.049	4.003 ± 0.047	...	9.520 ± 0.000	9.593 ± 0.001	9.423 ± 0.001	299.5 ± 2.3	1.980 ± 0.099	
...	124.8025 -50.2375	3.316 ± 0.064	-13.65 ± 0.13	3.73 ± 0.12	...	16.625 ± 0.001	18.191 ± 0.020	15.405 ± 0.006	299.2 $^{+5.8}_{-5.6}$	0.284 ± 0.023	
...	124.9749 -49.7232	2.930 ± 0.059	-12.32 ± 0.12	3.76 ± 0.10	...	16.630 ± 0.002	18.046 ± 0.016	15.441 ± 0.006	338.2 $^{+6.9}_{-6.7}$	0.358 ± 0.029	
2MASS J08212561-5150507	125.3568 -51.8474	2.911 ± 0.024	-13.228 ± 0.044	4.001 ± 0.041	52.34 ± 0.33	12.741 ± 0.001	13.143 ± 0.002	12.184 ± 0.002	340.2 $^{+2.9}_{-2.8}$	0.950 ± 0.048	
...	125.4512 -51.0648	3.305 ± 0.017	-13.666 ± 0.034	3.328 ± 0.032	...	14.266 ± 0.002	15.050 ± 0.007	13.401 ± 0.004	300.0 ± 1.6	0.673 ± 0.054	
...	125.4638 -49.8267	3.027 ± 0.021	-12.612 ± 0.040	3.410 ± 0.035	...	14.568 ± 0.001	15.353 ± 0.004	13.706 ± 0.003	327.2 ± 2.2	0.673 ± 0.054	
2MASS J08223071-4926199	125.6280 -49.4389	3.021 ± 0.017	-12.162 ± 0.031	3.752 ± 0.028	8.50 ± 0.30	13.049 ± 0.001	13.480 ± 0.001	12.464 ± 0.001	327.9 ± 1.9	0.860 ± 0.043	

Table B.7: UPK 535—Continued

Star Name	RA ($^{\circ}$)	Dec ($^{\circ}$)	Parallax (mas)	μ_{α} (mas yr $^{-1}$)	μ_{δ} (mas yr $^{-1}$)	v_r (km s $^{-1}$)	G (mag)	BP (mag)	RP (mag)	d (pc)	Mass (M $_{\odot}$)
...	125.6957 -49.7440	3.077 \pm 0.060	-12.60 \pm 0.11	3.73 \pm 0.10	...	16.207 \pm 0.001	17.515 \pm 0.010	15.064 \pm 0.002	322.2 $^{+6.4}_{-6.1}$	4.400 \pm 0.032	
...	125.8796 -49.4698	2.987 \pm 0.021	-12.519 \pm 0.039	3.357 \pm 0.038	...	14.499 \pm 0.003	15.253 \pm 0.010	13.645 \pm 0.011	331.6 \pm 2.3	0.688 \pm 0.055	
...	126.9806 -50.6725	3.074 \pm 0.072	-12.32 \pm 0.14	3.35 \pm 0.14	...	16.791 \pm 0.003	18.291 \pm 0.018	15.563 \pm 0.011	322.6 $^{+7.7}_{-7.4}$	0.310 \pm 0.025	
TYC 8157-1137-1	126.0662 -49.7032	3.086 \pm 0.027	-12.689 \pm 0.047	3.181 \pm 0.052	10.9 \pm 1.1	11.252 \pm 0.001	11.514 \pm 0.002	10.853 \pm 0.001	321.1 $^{+2.8}_{-2.7}$	1.250 \pm 0.062	
...	126.2343 -50.3175	3.084 \pm 0.022	-12.700 \pm 0.045	3.275 \pm 0.048	...	14.653 \pm 0.002	15.478 \pm 0.006	13.769 \pm 0.005	321.2 \pm 2.3	0.674 \pm 0.054	
2MASS J08250239-4947563	126.2600 -49.7990	3.040 \pm 0.026	-12.890 \pm 0.046	3.119 \pm 0.048	18.41 \pm 0.31	12.577 \pm 0.002	12.978 \pm 0.006	12.013 \pm 0.005	325.9 $^{+2.9}_{-2.8}$	0.880 \pm 0.044	
...	126.2995 -49.4361	3.042 \pm 0.063	-13.54 \pm 0.11	3.19 \pm 0.12	...	16.467 \pm 0.002	17.839 \pm 0.018	15.288 \pm 0.006	325.9 $^{+6.9}_{-6.6}$	0.372 \pm 0.030	
...	126.3425 -48.8964	3.041 \pm 0.062	-12.44 \pm 0.10	2.77 \pm 0.10	...	16.325 \pm 0.002	17.575 \pm 0.013	15.183 \pm 0.004	326.0 $^{+6.8}_{-6.5}$	0.414 \pm 0.033	
...	126.3670 -52.0225	3.236 \pm 0.070	-13.44 \pm 0.14	3.52 \pm 0.12	...	16.747 \pm 0.002	18.204 \pm 0.012	15.546 \pm 0.004	306.6 $^{+6.7}_{-6.5}$	0.335 \pm 0.027	
...	126.4299 -49.9099	2.945 \pm 0.075	-12.30 \pm 0.13	3.05 \pm 0.16	...	16.976 \pm 0.002	18.484 \pm 0.016	15.738 \pm 0.006	336.6 $^{+8.8}_{-8.4}$	0.304 \pm 0.024	
...	126.4382 -49.3795	3.185 \pm 0.029	-13.441 \pm 0.053	3.398 \pm 0.050	...	15.118 \pm 0.002	16.104 \pm 0.008	14.127 \pm 0.005	311.2 $^{+2.9}_{-2.8}$	0.552 \pm 0.044	
...	126.4428 -49.3800	3.191 \pm 0.051	-13.658 \pm 0.091	3.655 \pm 0.084	...	16.007 \pm 0.001	17.301 \pm 0.010	14.869 \pm 0.003	310.7 $^{+5.1}_{-4.9}$	0.405 \pm 0.032	
TYC 8161-1607-1	126.4910 -51.2973	3.222 \pm 0.025	-13.377 \pm 0.045	3.501 \pm 0.048	11.7 \pm 3.3	10.639 \pm 0.000	10.861 \pm 0.001	10.293 \pm 0.001	307.6 \pm 2.4	1.460 \pm 0.073	
...	126.5127 -49.8346	3.007 \pm 0.075	-12.79 \pm 0.12	3.00 \pm 0.13	...	16.856 \pm 0.002	18.347 \pm 0.025	15.636 \pm 0.005	329.8 $^{+8.4}_{-8.0}$	0.316 \pm 0.025	
...	126.5785 -50.1201	3.130 \pm 0.030	-12.900 \pm 0.060	3.078 \pm 0.060	...	15.633 \pm 0.001	16.732 \pm 0.007	14.585 \pm 0.003	316.7 \pm 3.0	0.503 \pm 0.040	
TYC 8162-73-1	126.6084 -50.8928	3.097 \pm 0.031	-13.357 \pm 0.057	3.364 \pm 0.051	4.2 \pm 1.7	10.439 \pm 0.001	10.623 \pm 0.002	10.150 \pm 0.001	320.0 $^{+3.2}_{-3.1}$	1.830 \pm 0.092	
...	126.6968 -51.0023	3.117 \pm 0.061	-12.88 \pm 0.12	3.32 \pm 0.13	...	16.522 \pm 0.002	17.908 \pm 0.011	15.330 \pm 0.004	318.1 $^{+6.4}_{-6.1}$	0.365 \pm 0.029	
...	126.7430 -50.0550	3.093 \pm 0.017	-12.865 \pm 0.035	3.099 \pm 0.031	...	14.111 \pm 0.001	14.902 \pm 0.003	13.230 \pm 0.002	320.3 \pm 1.8	0.666 \pm 0.053	

Table B.7: UPK 535—Continued

Star Name	RA ($^{\circ}$)	Dec ($^{\circ}$)	Parallax (mas)	μ_{α} (mas yr^{-1})	μ_{δ} (mas yr^{-1})	v_r (km s^{-1})	G (mag)	BP (mag)	RP (mag)	d (pc)	Mass (M_{\odot})
HD 71789	126.7562	-50.0589	3.036 \pm 0.032	-13.132 \pm 0.064	2.943 \pm 0.062	...	9.140 \pm 0.000	9.175 \pm 0.001	9.101 \pm 0.002	326.3 \pm 3.4	2.05 \pm 0.10
CD-493560	126.7600	-50.3741	3.022 \pm 0.033	-12.725 \pm 0.066	3.240 \pm 0.051	10.3 \pm 2.3	10.085 \pm 0.000	10.204 \pm 0.001	9.909 \pm 0.001	327.9 \pm 3.6	1.880 \pm 0.094
...	126.7865	-50.2557	3.217 \pm 0.073	-12.79 \pm 0.14	3.33 \pm 0.14	...	16.996 \pm 0.001	18.539 \pm 0.016	15.769 \pm 0.004	308.4 $^{+7.1}_{-6.8}$	0.295 \pm 0.024
...	126.9770	-50.9071	3.207 \pm 0.054	-13.505 \pm 0.093	3.446 \pm 0.095	...	16.336 \pm 0.002	17.769 \pm 0.014	15.147 \pm 0.005	309.2 $^{+5.2}_{-5.1}$	0.353 \pm 0.028
HD 71969	127.0180	-51.2354	3.303 \pm 0.041	-13.787 \pm 0.078	3.144 \pm 0.075	...	8.119 \pm 0.001	8.107 \pm 0.001	8.169 \pm 0.002	300.2 $^{+3.8}_{-3.7}$	2.75 \pm 0.60
2MASS J08280595-4957545	127.0248	-49.9652	3.062 \pm 0.016	-12.913 \pm 0.031	2.989 \pm 0.029	5.7 \pm 1.7	13.334 \pm 0.002	13.872 \pm 0.008	12.651 \pm 0.006	323.5 \pm 1.7	0.798 \pm 0.064
TYC 8158-1417-1	127.0414	-49.2489	3.050 \pm 0.028	-12.942 \pm 0.054	2.833 \pm 0.054	13.5 \pm 4.4	10.907 \pm 0.000	11.143 \pm 0.001	10.545 \pm 0.001	324.9 \pm 3.0	1.460 \pm 0.073
...	127.0429	-51.1308	3.129 \pm 0.063	-13.46 \pm 0.13	3.45 \pm 0.13	...	16.860 \pm 0.001	18.412 \pm 0.017	15.615 \pm 0.004	316.9 $^{+6.5}_{-6.2}$	0.281 \pm 0.022
2MASS J08281901-5226346	127.0792	-52.4430	3.191 \pm 0.022	-13.010 \pm 0.043	3.339 \pm 0.041	10.40 \pm 0.12	12.353 \pm 0.001	12.718 \pm 0.002	11.842 \pm 0.002	310.6 \pm 2.1	0.980 \pm 0.049
...	127.1641	-50.7603	2.891 \pm 0.022	-12.152 \pm 0.039	3.258 \pm 0.036	...	14.560 \pm 0.001	15.336 \pm 0.010	13.644 \pm 0.007	342.5 \pm 2.6	0.685 \pm 0.055
...	127.2370	-53.3650	3.258 \pm 0.060	-13.68 \pm 0.11	3.56 \pm 0.13	...	16.744 \pm 0.001	18.261 \pm 0.013	15.533 \pm 0.004	304.4 $^{+5.7}_{-5.5}$	0.310 \pm 0.025
2MASS J08292220-5050369	127.3425	-50.8436	3.237 \pm 0.025	-12.548 \pm 0.046	3.372 \pm 0.047	...	12.540 \pm 0.004	13.033 \pm 0.012	11.904 \pm 0.010	306.2 $^{+2.4}_{-2.3}$	0.820 \pm 0.075
CD-50 3373	127.3714	-50.9382	3.108 \pm 0.024	-13.114 \pm 0.043	3.155 \pm 0.045	...	10.191 \pm 0.000	10.352 \pm 0.001	9.946 \pm 0.001	318.8 $^{+2.5}_{-2.4}$	1.860 \pm 0.093
TYC 8162-1117-1	127.4876	-51.4135	3.053 \pm 0.024	-12.735 \pm 0.044	3.176 \pm 0.041	10.04 \pm 0.22	11.733 \pm 0.000	12.030 \pm 0.002	11.290 \pm 0.001	324.5 $^{+2.6}_{-2.5}$	1.210 \pm 0.060
...	127.5287	-49.9430	3.067 \pm 0.046	-13.363 \pm 0.078	2.946 \pm 0.089	...	15.960 \pm 0.001	17.163 \pm 0.006	14.862 \pm 0.004	323.1 $^{+4.9}_{-4.7}$	0.437 \pm 0.035
TYC 8162-956-1	127.5683	-51.8880	3.218 \pm 0.030	-13.607 \pm 0.054	3.268 \pm 0.049	10.20 \pm 0.30	11.930 \pm 0.002	12.262 \pm 0.006	11.450 \pm 0.004	308.0 \pm 2.9	1.210 \pm 0.060
...	127.5751	-51.6510	2.955 \pm 0.064	-12.25 \pm 0.12	2.78 \pm 0.11	...	16.371 \pm 0.002	17.676 \pm 0.015	15.224 \pm 0.005	335.4 $^{+7.4}_{-7.1}$	0.399 \pm 0.032
2MASS J08301848-5101345	127.5770	-51.0262	3.108 \pm 0.025	-13.306 \pm 0.046	3.199 \pm 0.043	13.3 \pm 1.8	12.467 \pm 0.002	12.842 \pm 0.006	11.933 \pm 0.004	318.8 \pm 2.6	0.900 \pm 0.045
2MASS J08301902-5101316	127.5793	-51.0254	3.092 \pm 0.026	-13.424 \pm 0.046	3.039 \pm 0.043	11.9 \pm 1.6	11.706 \pm 0.002	12.037 \pm 0.007	11.228 \pm 0.006	320.5 $^{+2.8}_{-2.7}$	1.060 \pm 0.090

Table B.7: UPK 535—Continued

Star Name	RA ($^{\circ}$)	Dec ($^{\circ}$)	Parallax (mas)	μ_{α} (mas yr^{-1})	μ_{δ} (mas yr^{-1})	v_r (km s^{-1})	G (mag)	BP (mag)	RP (mag)	d (pc)	Mass (M_{\odot})
...	127.6757 -51.1959	3.099 \pm 0.072	-13.63 \pm 0.14	3.32 \pm 0.12	...	16.712 \pm 0.002	18.173 \pm 0.026	15.485 \pm 0.006	320.0 $^{+7.6}_{-7.3}$	324.4 \pm 0.026	
...	127.8478 -51.8384	3.260 \pm 0.031	-13.299 \pm 0.065	3.330 \pm 0.058	...	15.417 \pm 0.001	16.500 \pm 0.006	14.376 \pm 0.003	304.1 \pm 2.9	520.0 \pm 0.042	
...	127.8524 -53.4197	3.325 \pm 0.067	-12.70 \pm 0.15	3.83 \pm 0.13	...	16.714 \pm 0.001	18.401 \pm 0.020	15.438 \pm 0.003	298.4 $^{+6.1}_{-5.9}$	239.0 \pm 0.019	
...	127.8556 -52.1612	3.096 \pm 0.066	-13.40 \pm 0.14	3.15 \pm 0.12	...	16.978 \pm 0.001	18.648 \pm 0.018	15.707 \pm 0.003	320.2 $^{+7.0}_{-6.7}$	245.0 \pm 0.020	
2MASS J08312740-5129061	127.8642 -51.4850	3.174 \pm 0.024	-13.294 \pm 0.043	3.079 \pm 0.043	10.32 \pm 0.22	12.044 \pm 0.001	12.365 \pm 0.002	11.574 \pm 0.002	312.3 \pm 2.3	980.0 \pm 0.049	
...	128.0367 -51.5198	3.305 \pm 0.061	-13.02 \pm 0.12	3.68 \pm 0.11	...	13.402 \pm 0.002	14.005 \pm 0.008	12.660 \pm 0.007	300.1 $^{+5.6}_{-5.4}$	751.0 \pm 0.060	
...	128.0463 -52.0522	3.093 \pm 0.069	-12.78 \pm 0.15	3.03 \pm 0.15	...	16.719 \pm 0.002	18.188 \pm 0.013	15.504 \pm 0.008	320.6 $^{+7.3}_{-7.0}$	326.0 \pm 0.026	
...	128.0677 -51.8017	3.183 \pm 0.030	-13.372 \pm 0.061	3.214 \pm 0.059	...	15.449 \pm 0.001	16.562 \pm 0.007	14.400 \pm 0.004	311.4 $^{+3.0}_{-2.9}$	491.0 \pm 0.039	
HD 72857	128.2164 -52.5480	2.964 \pm 0.034	-12.136 \pm 0.060	2.997 \pm 0.060	...	9.243 \pm 0.000	9.277 \pm 0.002	9.209 \pm 0.003	334.2 $^{+3.9}_{-3.8}$	205.0 \pm 0.10	
...	128.2995 -52.2895	3.144 \pm 0.044	-13.362 \pm 0.087	3.01 \pm 0.10	...	15.855 \pm 0.001	17.290 \pm 0.011	14.665 \pm 0.004	315.3 $^{+4.5}_{-4.4}$	352.0 \pm 0.028	
...	128.4152 -52.0309	3.206 \pm 0.045	-13.540 \pm 0.090	3.028 \pm 0.099	...	16.029 \pm 0.001	17.292 \pm 0.008	14.902 \pm 0.003	309.2 $^{+4.4}_{-4.2}$	415.0 \pm 0.033	
...	128.5572 -51.1024	2.958 \pm 0.032	-12.317 \pm 0.056	2.882 \pm 0.052	...	15.325 \pm 0.001	16.285 \pm 0.007	14.335 \pm 0.003	334.8 $^{+3.7}_{-3.6}$	559.0 \pm 0.045	
2MASS J08351629-5156166	128.8178 -51.9380	3.060 \pm 0.024	-12.714 \pm 0.050	2.923 \pm 0.045	...	12.460 \pm 0.002	12.941 \pm 0.009	11.844 \pm 0.007	323.7 \pm 2.5	900.0 \pm 0.045	
HD 73464	129.0386 -53.4784	3.043 \pm 0.031	-13.392 \pm 0.060	3.131 \pm 0.055	...	9.435 \pm 0.000	9.489 \pm 0.001	9.369 \pm 0.001	325.5 \pm 3.3	200.0 \pm 0.16	
TYC 8568-293-1	129.0788 -52.5344	3.130 \pm 0.022	-12.625 \pm 0.044	3.410 \pm 0.042	10.97 \pm 0.25	11.473 \pm 0.000	11.765 \pm 0.002	11.037 \pm 0.001	316.6 \pm 2.2	1.210 \pm 0.060	
2MASS J08374576-4954367	129.4406 -49.9102	3.089 \pm 0.017	-13.360 \pm 0.028	2.387 \pm 0.028	10.32 \pm 0.26	13.114 \pm 0.002	13.594 \pm 0.008	12.476 \pm 0.006	320.7 \pm 1.8	820.0 \pm 0.041	
...	130.3863 -52.3057	3.038 \pm 0.049	-13.44 \pm 0.11	3.067 \pm 0.083	...	15.148 \pm 0.002	326.2 $^{+5.3}_{-5.1}$	653.0 \pm 0.072	
...	130.6030 -52.1686	3.017 \pm 0.032	-12.804 \pm 0.061	2.240 \pm 0.063	...	15.688 \pm 0.002	16.749 \pm 0.012	14.652 \pm 0.005	328.4 \pm 3.5	518.0 \pm 0.041	

Table B.7: UPK 535—Continued

Star Name	RA ($^{\circ}$)	Dec ($^{\circ}$)	Parallax (mas)	μ_{α} (mas yr^{-1})	μ_{δ} (mas yr^{-1})	v_r (km s^{-1})	G (mag)	BP (mag)	RP (mag)	d (pc)	Mass (M_{\odot})
...	125.2940 -49.5646	2.89 ± 0.14	-12.27 ± 0.22	3.24 ± 0.20	...	17.636 ± 0.001	19.415 ± 0.039	16.414 ± 0.006	344 $^{+17}_{-15}$	0.230 ± 0.018	
...	125.4275 -49.0657	2.986 ± 0.097	-12.18 ± 0.18	3.43 ± 0.16	...	17.415 ± 0.001	18.981 ± 0.033	16.156 ± 0.005	332 $^{+11}_{-10}$	0.274 ± 0.022	
...	125.6834 -49.7877	2.91 ± 0.10	-12.33 ± 0.18	3.18 ± 0.16	...	17.506 ± 0.010	19.034 ± 0.038	16.248 ± 0.005	341 $^{+12}_{-11}$	0.284 ± 0.023	
...	125.8652 -50.1786	2.93 ± 0.11	-12.53 ± 0.20	3.22 ± 0.22	...	17.772 ± 0.004	19.391 ± 0.040	16.483 ± 0.005	339 $^{+13}_{-12}$	0.253 ± 0.020	
...	125.8963 -49.6820	2.984 ± 0.083	-12.82 ± 0.16	3.16 ± 0.17	...	17.391 ± 0.002	18.903 ± 0.036	16.133 ± 0.006	332 $^{+9.5}_{-9.0}$	0.295 ± 0.024	
...	126.0449 -49.9457	2.89 ± 0.11	-12.10 ± 0.19	2.82 ± 0.23	...	17.089 ± 0.002	18.852 ± 0.023	15.767 ± 0.003	343 $^{+14}_{-13}$	0.212 ± 0.017	
...	126.3530 -49.7301	3.03 ± 0.11	-13.05 ± 0.20	2.96 ± 0.20	...	17.646 ± 0.002	19.272 ± 0.023	16.320 ± 0.006	327 ± 12	0.242 ± 0.019	
...	126.4354 -50.2127	2.994 ± 0.096	-12.71 ± 0.18	2.79 ± 0.19	...	17.428 ± 0.002	18.997 ± 0.029	16.141 ± 0.004	331 $^{+11}_{-10}$	0.266 ± 0.021	
...	126.5345 -50.8402	3.086 ± 0.096	-12.92 ± 0.18	3.39 ± 0.18	...	17.356 ± 0.001	19.198 ± 0.033	16.021 ± 0.003	322 $^{+10}_{-9.7}$	0.193 ± 0.015	
...	126.6252 -50.1982	2.99 ± 0.11	-12.71 ± 0.20	3.16 ± 0.19	...	17.591 ± 0.005	19.189 ± 0.028	16.316 ± 0.004	333 ± 12	0.262 ± 0.021	
...	126.7554 -49.6917	3.09 ± 0.14	-12.59 ± 0.24	4.05 ± 0.23	...	17.985 ± 0.001	19.379 ± 0.066	16.679 ± 0.004	322 $^{+15}_{-14}$	0.320 ± 0.028	
...	126.9004 -48.8702	3.125 ± 0.093	-12.14 ± 0.17	3.19 ± 0.16	...	17.519 ± 0.008	18.813 ± 0.022	16.357 ± 0.004	317.6 $^{+9.7}_{-9.2}$	0.398 ± 0.032	
...	126.9475 -50.0458	3.07 ± 0.11	-12.53 ± 0.25	3.30 ± 0.23	...	17.932 ± 0.001	19.676 ± 0.038	16.625 ± 0.005	324 ± 12	0.219 ± 0.018	
...	127.0663 -50.2538	3.05 ± 0.11	-12.96 ± 0.21	3.65 ± 0.19	...	17.894 ± 0.001	19.512 ± 0.039	16.596 ± 0.007	326 $^{+13}_{-12}$	0.251 ± 0.020	
...	127.0954 -52.4210	2.990 ± 0.087	-12.97 ± 0.18	3.61 ± 0.16	...	16.659 ± 0.009	18.288 ± 0.025	15.383 ± 0.003	332 $^{+10.}_{-9.4}$	0.254 ± 0.020	
...	127.1369 -51.0112	3.03 ± 0.11	-12.98 ± 0.23	2.96 ± 0.21	...	17.612 ± 0.001	19.173 ± 0.035	16.323 ± 0.006	328 $^{+12}_{-11}$	0.268 ± 0.021	
...	127.4727 -50.7768	2.85 ± 0.12	-12.39 ± 0.23	2.82 ± 0.21	...	17.967 ± 0.011	19.570 ± 0.049	16.682 ± 0.009	348 $^{+15}_{-14}$	0.258 ± 0.021	
...	127.6841 -50.8556	2.99 ± 0.10	-13.15 ± 0.20	3.22 ± 0.20	...	17.583 ± 0.001	19.285 ± 0.037	16.272 ± 0.006	332 $^{+12}_{-11}$	0.227 ± 0.018	
...	127.6949 -51.9620	2.93 ± 0.10	-13.08 ± 0.19	2.94 ± 0.23	...	17.760 ± 0.001	19.426 ± 0.030	16.483 ± 0.006	338 ± 12	0.244 ± 0.020	

Table B.7: UPK 535—Continued

Star Name	RA ($^{\circ}$)	Dec ($^{\circ}$)	Parallax (mas)	μ_{α} (mas yr $^{-1}$)	μ_{δ} (mas yr $^{-1}$)	v_r (km s $^{-1}$)	G (mag)	BP (mag)	RP (mag)	d (pc)	Mass (M $_{\odot}$)
...	127.0779 -52.7108	2.96 ± 0.11	-12.78 ± 0.21	3.24 ± 0.23	...	17.908 ± 0.001	19.690 ± 0.042	16.559 ± 0.006	335 $^{+13}_{-12}$	203 ± 0.016	
...	127.7091 -52.5204	2.93 ± 0.27	-13.23 ± 0.50	2.95 ± 0.53	...	15.196 ± 0.004	16.487 ± 0.009	14.034 ± 0.003	343 $^{+36}_{-30}$	399 ± 0.032	
...	128.3265 -53.6204	3.02 ± 0.10	-12.53 ± 0.23	3.15 ± 0.20	...	17.557 ± 0.001	19.231 ± 0.040	16.296 ± 0.004	328 $^{+12}_{-11}$	246 ± 0.020	
...	128.8561 -52.4214	3.014 ± 0.095	-12.78 ± 0.18	3.06 ± 0.18	...	17.066 ± 0.002	18.635 ± 0.026	15.812 ± 0.005	329 $^{+11}_{-10}$	274 ± 0.022	
...	129.4216 -52.4272	3.06 ± 0.12	-13.32 ± 0.24	2.39 ± 0.29	...	16.262 ± 0.002	17.777 ± 0.012	15.018 ± 0.004	325 $^{+14}_{-13}$	299 ± 0.024	
...	123.0515 -48.2935	3.169 ± 0.038	-12.861 ± 0.075	3.846 ± 0.081	...	15.702 ± 0.002	16.854 ± 0.010	14.617 ± 0.005	312.8 $^{+3.8}_{-3.7}$	456 ± 0.036	
...	123.2472 -53.0030	3.305 ± 0.046	-12.941 ± 0.092	3.17 ± 0.11	...	14.697 ± 0.002	15.444 ± 0.006	13.811 ± 0.004	300.0 $^{+4.2}_{-4.1}$	677 ± 0.054	
...	123.4239 -48.4633	3.038 ± 0.025	-12.263 ± 0.042	4.026 ± 0.045	...	14.686 ± 0.002	15.544 ± 0.007	13.776 ± 0.005	326.1 $^{+2.7}_{-2.6}$	634 ± 0.051	
...	123.4666 -48.5869	3.042 ± 0.019	-12.237 ± 0.032	3.846 ± 0.031	...	14.114 ± 0.002	14.799 ± 0.006	13.315 ± 0.004	325.7 ± 2.0	702 ± 0.056	
...	123.8186 -48.8694	3.057 ± 0.083	-12.22 ± 0.15	3.87 ± 0.13	...	16.874 ± 0.002	18.322 ± 0.020	15.653 ± 0.004	324.4 $^{+9.1}_{-8.6}$	331 ± 0.026	
...	124.0414 -47.9943	2.905 ± 0.081	-11.54 ± 0.15	3.45 ± 0.14	...	16.684 ± 0.002	17.976 ± 0.034	15.459 ± 0.011	341.3 $^{+9.8}_{-9.3}$	382 ± 0.031	
...	124.2350 -50.1496	2.971 ± 0.085	-11.53 ± 0.14	4.01 ± 0.15	...	17.269 ± 0.001	18.880 ± 0.019	16.016 ± 0.005	333.9 $^{+9.9}_{-9.3}$	264 ± 0.021	
2MASS J08170374-5031577	124.2656 -50.5327	2.938 ± 0.017	-11.650 ± 0.033	3.975 ± 0.034	11.91 ± 0.69	13.638 ± 0.003	14.192 ± 0.009	12.929 ± 0.008	337.1 ± 2.0	820 ± 0.041	
...	124.4214 -47.7049	3.258 ± 0.084	-14.32 ± 0.15	3.80 ± 0.16	...	17.048 ± 0.001	18.589 ± 0.018	15.806 ± 0.004	304.6 $^{+8.1}_{-7.7}$	284 ± 0.023	
CD-483672	124.5031 -48.5200	3.173 ± 0.038	-12.766 ± 0.063	4.000 ± 0.066	8.7 ± 4.0	10.313 ± 0.001	10.483 ± 0.001	10.051 ± 0.001	312.4 ± 3.7	930 ± 0.096	
...	124.5327 -48.6919	2.942 ± 0.058	-11.836 ± 0.099	3.39 ± 0.11	...	16.078 ± 0.002	17.268 ± 0.009	14.982 ± 0.004	336.8 $^{+6.8}_{-6.5}$	441 ± 0.035	
...	125.0719 -48.6928	3.061 ± 0.052	-12.071 ± 0.099	3.449 ± 0.093	...	16.091 ± 0.002	17.567 ± 0.008	14.884 ± 0.004	323.8 $^{+5.6}_{-5.4}$	326 ± 0.026	
...	125.0819 -50.3490	3.104 ± 0.054	-11.90 ± 0.11	3.84 ± 0.10	...	16.513 ± 0.001	17.796 ± 0.012	15.371 ± 0.004	319.4 $^{+5.6}_{-5.5}$	407 ± 0.033	

Table B.7: UPK 535—Continued

Star Name	RA ($^{\circ}$)	Dec ($^{\circ}$)	Parallax (mas)	μ_{α} (mas yr^{-1})	μ_{δ} (mas yr^{-1})	v_r (km s^{-1})	G (mag)	BP (mag)	RP (mag)	d (pc)	Mass (M_{\odot})
...	125.1876 -49.0881	3.423 \pm 0.088	-13.77 \pm 0.16	3.41 \pm 0.14	...	17.156 \pm 0.001	18.751 \pm 0.025	15.903 \pm 0.005	290.1 $^{+7.6}_{-7.3}$	0.268 \pm 0.021	
...	126.1417 -53.6576	2.886 \pm 0.058	-11.59 \pm 0.12	3.72 \pm 0.11	...	16.802 \pm 0.001	18.408 \pm 0.015	15.558 \pm 0.003	343.3 $^{+7.1}_{-6.8}$	0.267 \pm 0.021	
2MASS J08243944-5215091	126.1643 -52.2525	3.311 \pm 0.019	-13.824 \pm 0.038	3.695 \pm 0.030	10.14 \pm 0.19	12.979 \pm 0.002	13.471 \pm 0.007	12.342 \pm 0.006	299.4 \pm 1.7	0.860 \pm 0.043	
...	126.2582 -49.9556	3.064 \pm 0.080	-12.13 \pm 0.12	3.88 \pm 0.15	...	16.433 \pm 0.002	17.707 \pm 0.016	15.125 \pm 0.005	323.7 $^{+8.7}_{-8.3}$	0.364 \pm 0.029	
...	126.3183 -53.2897	2.972 \pm 0.056	-11.64 \pm 0.12	3.66 \pm 0.10	...	16.652 \pm 0.001	18.164 \pm 0.016	15.423 \pm 0.004	333.5 $^{+6.4}_{-6.2}$	0.305 \pm 0.024	
...	126.6279 -48.3826	2.930 \pm 0.071	-11.92 \pm 0.14	2.30 \pm 0.11	...	15.857 \pm 0.004	17.210 \pm 0.024	14.673 \pm 0.008	338.3 $^{+8.3}_{-8.0}$	0.376 \pm 0.030	
...	126.8107 -52.4870	2.869 \pm 0.062	-11.52 \pm 0.12	3.44 \pm 0.13	...	16.456 \pm 0.003	17.789 \pm 0.020	15.293 \pm 0.009	345.4 $^{+7.6}_{-7.3}$	0.387 \pm 0.031	
...	126.9157 -52.0279	3.262 \pm 0.027	-13.784 \pm 0.058	3.868 \pm 0.046	...	14.248 \pm 0.001	15.168 \pm 0.006	13.305 \pm 0.003	303.9 \pm 2.5	0.585 \pm 0.047	
...	127.0241 -50.7913	2.887 \pm 0.021	-11.759 \pm 0.037	3.222 \pm 0.034	...	14.320 \pm 0.001	15.042 \pm 0.005	13.479 \pm 0.005	343.0 $^{+2.5}_{-2.4}$	0.693 \pm 0.055	
2MASS J08283563-5130255	127.1485 -51.5071	2.890 \pm 0.029	-11.891 \pm 0.051	3.212 \pm 0.049	10.98 \pm 0.21	12.586 \pm 0.001	12.957 \pm 0.003	12.062 \pm 0.003	342.6 \pm 3.4	0.980 \pm 0.049	
...	127.4191 -51.0303	3.358 \pm 0.016	-14.137 \pm 0.029	3.222 \pm 0.029	...	13.852 \pm 0.002	14.487 \pm 0.006	13.094 \pm 0.005	295.3 \pm 1.4	0.732 \pm 0.059	
2MASS J08302738-5052330	127.1848 -50.8759	2.886 \pm 0.025	-11.696 \pm 0.045	3.180 \pm 0.040	9.88 \pm 0.77	12.836 \pm 0.002	13.246 \pm 0.005	12.274 \pm 0.003	343.1 $^{+3.0}_{-2.9}$	0.940 \pm 0.047	
...	127.6919 -53.8937	3.152 \pm 0.052	-13.12 \pm 0.14	3.292 \pm 0.099	...	16.311 \pm 0.002	17.722 \pm 0.013	15.131 \pm 0.007	314.5 $^{+5.2}_{-5.0}$	0.361 \pm 0.029	
...	127.9171 -54.3553	3.131 \pm 0.016	-11.739 \pm 0.032	2.571 \pm 0.029	...	14.118 \pm 0.000	14.802 \pm 0.002	13.325 \pm 0.001	316.4 \pm 1.6	0.704 \pm 0.056	
...	128.0832 -52.5892	3.437 \pm 0.048	-14.156 \pm 0.092	3.371 \pm 0.086	...	15.845 \pm 0.001	17.137 \pm 0.008	14.715 \pm 0.003	288.6 $^{+4.0}_{-3.9}$	0.407 \pm 0.033	
2MASS J08323887-5226451	128.1619 -52.4458	3.349 \pm 0.033	-14.171 \pm 0.057	3.339 \pm 0.051	9.75 \pm 0.14	12.526 \pm 0.001	12.950 \pm 0.004	11.920 \pm 0.003	296.1 \pm 2.9	0.860 \pm 0.043	
...	128.1763 -50.8206	3.194 \pm 0.056	-14.18 \pm 0.12	2.62 \pm 0.11	...	16.229 \pm 0.001	17.589 \pm 0.009	15.039 \pm 0.004	310.4 $^{+5.5}_{-5.3}$	0.373 \pm 0.030	
2MASS J08364848-5113573	129.2020 -51.2326	2.872 \pm 0.018	-11.934 \pm 0.031	1.948 \pm 0.028	0.5 \pm 2.2	13.642 \pm 0.003	14.169 \pm 0.013	12.947 \pm 0.008	344.7 \pm 2.1	0.820 \pm 0.075	

Table B.7: UPK 535—Continued

Star Name	RA ($^{\circ}$)	Dec ($^{\circ}$)	Parallax (mas)	μ_{α} (mas yr $^{-1}$)	μ_{δ} (mas yr $^{-1}$)	v_r (km s $^{-1}$)	G (mag)	BP (mag)	RP (mag)	d (pc)	Mass (M $_{\odot}$)
TYC 8568-298-1	129.2323	-52.9839	3.023 \pm 0.025	-11.620 \pm 0.051	2.624 \pm 0.048	8.53 \pm 0.45	11.285 \pm 0.001	11.540 \pm 0.002	10.894 \pm 0.001	327.6 $^{+2.7}_{-2.6}$	1.380 \pm 0.069
TYC 8568-260-1	129.4136	-52.6704	3.324 \pm 0.026	-14.328 \pm 0.059	3.172 \pm 0.048	9.21 \pm 0.72	11.004 \pm 0.000	11.258 \pm 0.001	10.617 \pm 0.001	298.2 \pm 2.4	1.250 \pm 0.062
2MASS J08382678-5359285	129.6116	-53.9913	3.201 \pm 0.023	-13.238 \pm 0.046	2.925 \pm 0.044	9.30 \pm 0.28	12.434 \pm 0.003	12.805 \pm 0.010	11.914 \pm 0.007	309.6 $^{+2.3}_{-2.2}$	0.990 \pm 0.050
...	130.1626	-50.4604	2.968 \pm 0.027	-13.901 \pm 0.048	2.981 \pm 0.044	...	15.102 \pm 0.000	16.070 \pm 0.004	14.127 \pm 0.001	333.7 \pm 3.0	0.560 \pm 0.045
...	130.3859	-52.3054	3.112 \pm 0.040	-13.350 \pm 0.085	1.672 \pm 0.076	...	14.206 \pm 0.003	14.694 \pm 0.021	13.200 \pm 0.024	318.4 $^{+4.1}_{-4.0}$	0.699 \pm 0.056
...	125.2482	-49.1199	2.91 \pm 0.20	-12.73 \pm 0.37	3.17 \pm 0.34	...	18.895 \pm 0.019	20.33 \pm 0.17	17.499 \pm 0.015	343 $^{+26}_{-23}$	0.271 \pm 0.053
...	125.3606	-49.6473	3.030 \pm 0.091	-11.96 \pm 0.16	3.79 \pm 0.16	...	17.129 \pm 0.002	18.763 \pm 0.019	15.867 \pm 0.005	327 $^{+10.}_{-9.6}$	0.256 \pm 0.020
...	125.9568	-50.8282	2.86 \pm 0.16	-12.57 \pm 0.30	3.56 \pm 0.31	...	18.242 \pm 0.012	20.189 \pm 0.059	16.843 \pm 0.007	348 $^{+21}_{-19}$	0.169 \pm 0.014
...	126.1130	-49.6890	3.03 \pm 0.24	-12.05 \pm 0.47	3.48 \pm 0.54	...	18.923 \pm 0.002	20.62 \pm 0.13	17.511 \pm 0.024	331 $^{+30.}_{-25}$	0.208 \pm 0.028
...	126.3575	-51.6076	3.00 \pm 0.31	-12.90 \pm 0.57	3.96 \pm 0.60	...	19.414 \pm 0.002	21.11 \pm 0.22	17.965 \pm 0.018	337 $^{+42}_{-33}$	0.199 \pm 0.040
...	126.6396	-50.2482	3.03 \pm 0.17	-12.68 \pm 0.33	3.90 \pm 0.32	...	18.165 \pm 0.003	19.510 \pm 0.061	16.698 \pm 0.019	329 $^{+20.}_{-18}$	0.277 \pm 0.022
...	127.5029	-52.0130	2.993 \pm 0.096	-14.27 \pm 0.18	3.16 \pm 0.18	...	17.852 \pm 0.001	19.602 \pm 0.038	16.539 \pm 0.007	332 $^{+11.}_{-10.}$	0.217 \pm 0.017
...	127.5316	-49.8439	3.08 \pm 0.13	-13.58 \pm 0.22	3.76 \pm 0.30	...	18.039 \pm 0.001	19.735 \pm 0.041	16.727 \pm 0.006	323 $^{+14.}_{-13.}$	0.228 \pm 0.018
...	127.7467	-51.4481	3.01 \pm 0.32	-12.97 \pm 0.63	2.33 \pm 0.55	...	19.292 \pm 0.005	20.85 \pm 0.19	17.862 \pm 0.017	336 $^{+44}_{-35}$	0.234 \pm 0.043
...	128.4845	-50.6775	2.95 \pm 0.17	-13.02 \pm 0.31	3.07 \pm 0.35	...	18.373 \pm 0.002	20.16 \pm 0.11	16.972 \pm 0.007	338 $^{+21}_{-19}$	0.190 \pm 0.019
...	127.7105	-52.5204	2.909 \pm 0.092	-12.75 \pm 0.18	2.19 \pm 0.18	...	15.078 \pm 0.002	16.049 \pm 0.006	14.084 \pm 0.002	341 $^{+11.}_{-10.}$	0.555 \pm 0.044
...	128.3087	-53.3184	3.11 \pm 0.16	-12.96 \pm 0.32	2.79 \pm 0.33	...	18.210 \pm 0.002	19.795 \pm 0.046	16.864 \pm 0.005	320 $^{+18.}_{-16.}$	0.247 \pm 0.020
...	128.4446	-51.9425	3.02 \pm 0.16	-12.78 \pm 0.33	2.70 \pm 0.40	...	18.480 \pm 0.001	20.293 \pm 0.073	17.132 \pm 0.010	330 $^{+19.}_{-17.}$	0.196 \pm 0.016

Table B.7: UPK 535—Continued

Star Name	RA ($^{\circ}$)	Dec ($^{\circ}$)	Parallax (mas)	μ_{α} (mas yr^{-1})	μ_{δ} (mas yr^{-1})	v_r (km s^{-1})	G (mag)	BP (mag)	RP (mag)	d (pc)	Mass (M_{\odot})
...	128.4633	-53.9045	3.114 \pm 0.098	-12.74 \pm 0.20	3.20 \pm 0.18	...	17.004 \pm 0.002	319 $^{+10}_{-9.7}$	0.432 \pm 0.048
...	129.1057	-52.3096	3.10 \pm 0.23	-12.44 \pm 0.42	3.44 \pm 0.42	...	18.889 \pm 0.002	20.51 \pm 0.12	17.463 \pm 0.018	323 $^{+26}_{-23}$	0.221 \pm 0.027
...	129.1419	-51.2573	2.95 \pm 0.10	-12.04 \pm 0.18	2.71 \pm 0.21	...	17.231 \pm 0.000	18.750 \pm 0.023	15.979 \pm 0.006	336 $^{+12}_{-11}$	0.294 \pm 0.024
...	129.2831	-52.4672	3.06 \pm 0.14	-12.39 \pm 0.28	2.78 \pm 0.33	...	18.033 \pm 0.001	19.766 \pm 0.080	16.665 \pm 0.008	325 $^{+15}_{-14}$	0.209 \pm 0.017
...	129.4106	-52.4932	3.07 \pm 0.14	-11.95 \pm 0.29	2.41 \pm 0.30	...	18.470 \pm 0.002	19.791 \pm 0.093	17.076 \pm 0.015	324 $^{+16}_{-15}$	0.315 \pm 0.039
...	129.5751	-53.5461	2.985 \pm 0.093	-12.41 \pm 0.21	2.53 \pm 0.20	...	17.457 \pm 0.002	18.326 \pm 0.050	15.972 \pm 0.015	332 $^{+11}_{-10}$	0.424 \pm 0.034
...	130.4779	-51.9570	3.05 \pm 0.15	-11.72 \pm 0.27	2.44 \pm 0.34	...	18.223 \pm 0.002	19.837 \pm 0.091	16.861 \pm 0.010	326 $^{+18}_{-16}$	0.236 \pm 0.022
...	130.5193	-52.5407	3.00 \pm 0.10	-12.01 \pm 0.20	2.12 \pm 0.24	...	17.636 \pm 0.001	19.191 \pm 0.049	16.354 \pm 0.009	331 $^{+12}_{-11}$	0.271 \pm 0.022

Table B.8: Alessi 3 Member Kinematics and Properties

Star Name	<i>R.A.</i> ($^{\circ}$)	<i>Dec.</i> ($^{\circ}$)	Parallax (mas)	μ_{α} (mas yr $^{-1}$)	μ_{δ} (mas yr $^{-1}$)	v_r (km s $^{-1}$)	G (mag)	BP (mag)	RP (mag)	<i>d</i> (pc)	Mass (M $_{\odot}$)
2MASS J07062595-4504026	106.6081	-45.0674	3.84 ± 0.52	-10.9 ± 1.0	11.05 ± 0.93	...	15.495 ± 0.006	15.702 ± 0.003	14.915 ± 0.003	267 $^{+47}_{-35}$	1.098 ± 0.088
2MASS J07071613-4423536	106.8172	-44.3983	3.94 ± 0.49	-9.55 ± 0.96	10.5 ± 1.1	...	17.003 ± 0.006	17.633 ± 0.009	16.107 ± 0.005	259 $^{+42}_{-32}$	0.694 ± 0.056
TYC 7641-169-1	105.8220	-44.0264	3.739 ± 0.69	-10.06 ± 0.14	12.28 ± 0.13	17.50 ± 0.54	10.777 ± 0.002	11.030 ± 0.002	10.373 ± 0.002	265.5 $^{+5.0}_{-4.8}$	1.38 ± 0.10
2MASS J07032864-4353413	105.8693	-43.8948	3.57 ± 0.10	-10.57 ± 0.20	11.35 ± 0.22	...	17.579 ± 0.002	18.928 ± 0.018	16.425 ± 0.005	278.4 $^{+8.4}_{-7.9}$	0.380 ± 0.030
2MASS J07082453-4248407	107.1023	-42.8113	3.73 ± 0.29	-9.89 ± 0.52	10.80 ± 0.67	...	16.280 ± 0.004	17.416 ± 0.012	15.135 ± 0.004	269 $^{+23}_{-20}$	0.436 ± 0.035
2MASS J07064368-4336521	106.6820	-43.6145	3.431 ± 0.70	-9.76 ± 0.14	12.96 ± 0.17	...	16.942 ± 0.002	18.191 ± 0.025	15.762 ± 0.010	289.2 $^{+6.0}_{-5.7}$	0.400 ± 0.032
2MASS J07060786-4332240	106.5328	-43.5400	3.615 ± 0.77	-9.84 ± 0.14	11.76 ± 0.16	...	17.187 ± 0.002	18.571 ± 0.026	16.033 ± 0.004	274.6 $^{+5.9}_{-5.7}$	0.370 ± 0.030
2MASS J07011787-4323008	105.3244	-43.3835	3.694 ± 0.65	-9.48 ± 0.13	12.66 ± 0.13	...	17.025 ± 0.002	18.455 ± 0.016	15.840 ± 0.004	268.7 $^{+4.8}_{-4.6}$	0.86 ± 0.10
2MASS J07042604-4220545	106.1085	-42.3485	3.376 ± 0.73	-8.20 ± 0.14	12.07 ± 0.18	...	17.308 ± 0.002	18.614 ± 0.032	16.127 ± 0.005	293.9 $^{+6.5}_{-6.2}$	0.384 ± 0.031
2MASS J07203642-4314378	110.1518	-43.2439	3.486 ± 0.13	-9.378 ± 0.023	12.620 ± 0.023	16.57 ± 0.20	13.098 ± 0.002	13.557 ± 0.003	12.493 ± 0.002	284.5 ± 1.0	0.780 ± 0.045
2MASS J07183396-4341057	109.6415	-43.6849	3.343 ± 0.25	-8.953 ± 0.050	11.458 ± 0.049	...	15.167 ± 0.002	16.020 ± 0.004	14.264 ± 0.003	296.6 ± 2.2	0.628 ± 0.050
2MASS J07173323-4324259	109.3885	-43.4072	3.220 ± 0.24	-9.183 ± 0.048	11.339 ± 0.056	...	14.380 ± 0.002	15.218 ± 0.003	13.490 ± 0.002	307.9 ± 2.3	0.647 ± 0.052
2MASS J07125585-4318039	108.2328	-43.3011	3.361 ± 0.17	-8.828 ± 0.033	11.515 ± 0.033	...	13.900 ± 0.002	14.483 ± 0.003	13.193 ± 0.002	295.0 ± 1.5	0.764 ± 0.061
...	109.9627	-42.4272	3.559 ± 0.32	-11.338 ± 0.061	13.026 ± 0.064	...	15.580 ± 0.002	16.576 ± 0.005	14.595 ± 0.003	278.7 ± 2.5	0.546 ± 0.044
2MASS J07241674-4054463	111.0697	-40.9129	3.31 ± 0.13	-8.78 ± 0.24	12.71 ± 0.28	...	17.633 ± 0.003	19.257 ± 0.048	16.286 ± 0.007	300. $^{+12}_{-11}$	0.232 ± 0.019
2MASS J0711470-4301369	107.8113	-43.0269	3.396 ± 0.85	-9.46 ± 0.16	12.38 ± 0.16	...	17.480 ± 0.002	18.899 ± 0.028	16.264 ± 0.005	292.2 $^{+7.5}_{-7.1}$	0.335 ± 0.027
2MASS J07565276-4956280	119.2199	-49.9411	3.318 ± 0.016	-8.433 ± 0.032	13.006 ± 0.026	...	13.657 ± 0.002	14.198 ± 0.002	12.977 ± 0.003	298.8 ± 1.4	0.790 ± 0.063
2MASS J07101473-4035207	107.5614	-40.5891	3.29 ± 0.29	-9.41 ± 0.53	11.20 ± 0.56	...	16.466 ± 0.003	17.370 ± 0.009	15.434 ± 0.004	305 $^{+31}_{-26}$	0.557 ± 0.045

Table E.8: Alessi 3—Continued

Star Name	<i>RA</i> ($^{\circ}$)	<i>Dec</i> ($^{\circ}$)	Parallax (mas)	μ_{α} (mas yr $^{-1}$)	μ_{δ} (mas yr $^{-1}$)	v_r (km s $^{-1}$)	G (mag)	BP (mag)	RP (mag)	d (pc)	Mass (M $_{\odot}$)
2MASS J07091226-4027082	107.3011	-40.4523	3.574 ± 0.066	-9.64 ± 0.12	11.49 ± 0.14	...	17.114 ± 0.002	18.490 ± 0.017	15.939 ± 0.004	277.7 $^{+5.2}_{-5.0}$	0.366 ± 0.029
TYC 7633-1819-1	106.1906	-40.4161	3.498 ± 0.021	-8.903 ± 0.040	12.309 ± 0.040	2.45 ± 0.64	10.573 ± 0.002	10.806 ± 0.002	10.221 ± 0.002	283.5 ± 1.7	1.250 ± 0.062
2MASS J07563657-4629489	119.1524	-46.4969	3.289 ± 0.091	-11.12 ± 0.18	12.89 ± 0.17	...	17.438 ± 0.002	19.040 ± 0.033	16.181 ± 0.004	301.8 $^{+8.6}_{-8.1}$	0.260 ± 0.021
2MASS J07583662-4614496	119.6526	-46.2471	3.271 ± 0.028	-8.476 ± 0.051	12.779 ± 0.066	23.61 ± 0.51	11.846 ± 0.003	12.182 ± 0.006	11.361 ± 0.005	303.1 $^{+2.6}_{-2.5}$	1.00 ± 0.13
2MASS J06582146-4002251	104.5894	-40.0404	3.586 ± 0.035	-9.579 ± 0.063	12.458 ± 0.069	...	15.617 ± 0.002	16.592 ± 0.008	14.639 ± 0.003	276.7 ± 2.7	0.553 ± 0.044
...	105.0363	-40.4620	3.693 ± 0.058	-9.850 ± 0.088	12.741 ± 0.094	...	16.183 ± 0.002	17.326 ± 0.007	15.123 ± 0.003	268.8 $^{+4.3}_{-4.1}$	0.459 ± 0.037
2MASS J07452644-4755011	116.3602	-47.9170	3.212 ± 0.020	-8.134 ± 0.038	12.448 ± 0.039	26	12.514 ± 0.002	12.926 ± 0.002	11.954 ± 0.003	308.5 $^{+2.0}_{-1.9}$	0.912 ± 0.073
...	111.6751	-47.8384	3.85 ± 0.15	-8.79 ± 0.28	11.99 ± 0.24	...	16.384 ± 0.003	17.455 ± 0.010	15.212 ± 0.003	258 $^{+10.}_{-9.6}$	0.447 ± 0.036
TYC 8124-1497-1	110.2230	-48.0783	3.402 ± 0.046	-10.106 ± 0.098	12.287 ± 0.080	0.97 ± 0.17	10.776 ± 0.002	11.040 ± 0.002	10.378 ± 0.002	291.5 $^{+4.0}_{-3.9}$	1.27 ± 0.10
...	111.5299	-39.3976	3.553 ± 0.095	-9.13 ± 0.16	12.72 ± 0.16	...	17.506 ± 0.002	18.931 ± 0.028	16.335 ± 0.004	279.5 $^{+7.7}_{-7.3}$	0.354 ± 0.028
...	111.4784	-46.8823	3.909 ± 0.089	-10.63 ± 0.17	12.06 ± 0.18	...	17.636 ± 0.002	19.027 ± 0.037	16.438 ± 0.006	254.2 $^{+5.9}_{-5.7}$	0.356 ± 0.028
...	111.1162	-39.3430	3.56 ± 0.13	-9.51 ± 0.22	12.50 ± 0.25	...	17.537 ± 0.003	19.098 ± 0.022	16.243 ± 0.005	280. $^{+11}_{-10}$	0.261 ± 0.021
...	111.2543	-39.1019	3.264 ± 0.046	-10.177 ± 0.084	10.991 ± 0.085	...	16.258 ± 0.002	17.556 ± 0.012	15.126 ± 0.004	303.8 $^{+4.3}_{-4.2}$	0.399 ± 0.032
...	114.2861	-46.8032	3.258 ± 0.036	-9.237 ± 0.077	12.603 ± 0.069	...	16.129 ± 0.002	17.241 ± 0.006	15.086 ± 0.003	304.3 $^{+3.4}_{-3.3}$	0.479 ± 0.038
...	114.0012	-45.3825	3.594 ± 0.030	-8.642 ± 0.064	11.842 ± 0.065	...	15.294 ± 0.002	16.239 ± 0.006	14.328 ± 0.002	276.0 ± 2.3	0.557 ± 0.045
TYC 8126-350-1	105.3861	-48.9756	3.629 ± 0.023	-9.741 ± 0.041	13.087 ± 0.046	15.98 ± 0.13	10.386 ± 0.002	10.768 ± 0.002	9.868 ± 0.002	273.4 ± 1.7	0.950 ± 0.048
TYC 8122-2115-1	105.7442	-48.5502	3.243 ± 0.022	-10.124 ± 0.043	11.110 ± 0.042	7.93 ± 0.16	11.461 ± 0.002	11.736 ± 0.002	11.045 ± 0.002	305.6 ± 2.1	1.060 ± 0.053
TYC 8123-335-1	109.0313	-48.0435	3.656 ± 0.020	-11.314 ± 0.040	12.985 ± 0.042	-3	11.390 ± 0.002	11.702 ± 0.002	10.930 ± 0.002	271.4 ± 1.5	1.114 ± 0.089
...	108.5518	-47.0096	3.617 ± 0.096	-9.85 ± 0.17	11.99 ± 0.21	...	17.442 ± 0.002	18.768 ± 0.048	16.244 ± 0.006	274.6 $^{+7.5}_{-7.1}$	0.374 ± 0.030

Table E.8: Alessi 3—Continued

Star Name	<i>RA</i> ($^{\circ}$)	<i>Dec</i> ($^{\circ}$)	Parallax (mas)	μ_{α} (mas yr $^{-1}$)	μ_{δ} (mas yr $^{-1}$)	v_r (km s $^{-1}$)	G (mag)	BP (mag)	RP (mag)	<i>d</i> (pc)	Mass (M $_{\odot}$)
...	115.9990	-41.2464	3.383 ± 0.079	-9.35 ± 0.14	13.06 ± 0.14	...	16.907 ± 0.002	18.432 ± 0.017	15.689 ± 0.004	293.3 $^{+7.0}_{-6.7}$	0.297 ± 0.024
...	103.3408	-46.4735	3.374 ± 0.046	-8.956 ± 0.090	11.22 ± 0.11	...	16.329 ± 0.002	17.465 ± 0.010	15.271 ± 0.004	293.9 $^{+4.0}_{-3.9}$	0.451 ± 0.036
...	110.5935	-50.9271	3.578 ± 0.053	-10.75 ± 0.11	11.65 ± 0.12	...	16.752 ± 0.002	17.982 ± 0.018	15.636 ± 0.004	277.3 $^{+4.2}_{-4.1}$	0.421 ± 0.034
...	109.6590	-50.7851	3.889 ± 0.063	-10.75 ± 0.13	12.55 ± 0.11	...	16.854 ± 0.002	18.221 ± 0.017	15.691 ± 0.004	255.4 $^{+4.2}_{-4.1}$	0.372 ± 0.030
...	108.8964	-50.9201	3.733 ± 0.013	-11.099 ± 0.023	12.234 ± 0.028	...	13.337 ± 0.002	13.858 ± 0.003	12.680 ± 0.003	265.81 ± 0.91	0.805 ± 0.064
...	112.0745	-43.7962	3.755 ± 0.019	-9.326 ± 0.032	11.767 ± 0.030	...	14.030 ± 0.002	14.714 ± 0.002	13.246 ± 0.002	264.3 ± 1.3	0.700 ± 0.056
...	112.7255	-43.4810	3.214 ± 0.018	-8.494 ± 0.035	12.345 ± 0.036	25	13.271 ± 0.003	13.979 ± 0.011	12.452 ± 0.007	308.4 ± 1.7	0.694 ± 0.056
...	112.7271	-43.4801	3.270 ± 0.081	-10.34 ± 0.16	12.90 ± 0.17	...	17.451 ± 0.002	19.088 ± 0.063	16.069 ± 0.008	303.4 $^{+7.7}_{-7.3}$	0.221 ± 0.018
...	106.6096	-47.4311	3.86 ± 0.111	-10.00 ± 0.20	13.07 ± 0.18	...	17.656 ± 0.002	19.162 ± 0.038	16.481 ± 0.005	257.7 $^{+7.3}_{-6.9}$	0.319 ± 0.025
...	117.1946	-42.9323	3.468 ± 0.044	-8.143 ± 0.080	12.041 ± 0.078	...	16.051 ± 0.002	17.255 ± 0.006	14.929 ± 0.003	286.0 $^{+3.7}_{-3.6}$	0.425 ± 0.034
...	113.8155	-42.8373	3.558 ± 0.019	-10.603 ± 0.034	12.972 ± 0.037	...	14.645 ± 0.002	15.414 ± 0.003	13.792 ± 0.003	278.8 ± 1.5	0.674 ± 0.054
...	113.8171	-42.8376	3.639 ± 0.059	-11.11 ± 0.10	12.50 ± 0.11	...	16.571 ± 0.002	17.964 ± 0.008	15.369 ± 0.006	272.7 $^{+4.5}_{-4.4}$	0.354 ± 0.028
...	117.0607	-45.0071	3.83 ± 0.12	-11.12 ± 0.21	12.40 ± 0.24	...	17.725 ± 0.003	19.567 ± 0.029	16.418 ± 0.006	259.7 $^{+8.5}_{-8.0}$	0.194 ± 0.016
CD-423577	110.0541	-53.0302	3.709 ± 0.044	-10.705 ± 0.084	12.30 ± 0.10	...	16.131 ± 0.002	17.236 ± 0.008	15.084 ± 0.003	267.6 $^{+3.2}_{-3.1}$	0.482 ± 0.039
CD-423577p	117.4921	-43.1026	3.380 ± 0.070	-8.98 ± 0.12	11.43 ± 0.10	19	11.233 ± 0.002	11.521 ± 0.002	10.801 ± 0.002	293.6 $^{+6.2}_{-6.0}$	1.195 ± 0.096
...	118.4333	-44.8420	3.20 ± 0.11	-10.55 ± 0.17	11.74 ± 0.21	...	17.574 ± 0.002	19.215 ± 0.028	16.341 ± 0.007	310. $^{+11}_{-10.}$	0.256 ± 0.020
TYC 7658-4532-1	117.8280	-44.5858	3.241 ± 0.028	-10.590 ± 0.045	12.394 ± 0.044	24	11.540 ± 0.002	11.837 ± 0.003	11.100 ± 0.003	305.8 ± 2.6	1.171 ± 0.094

Table E.8: Alessi 3—Continued

Star Name	<i>RA</i> ($^{\circ}$)	<i>Dec</i> ($^{\circ}$)	Parallax (mas)	μ_{α} (mas yr $^{-1}$)	μ_{δ} (mas yr $^{-1}$)	v_r (km s $^{-1}$)	G (mag)	BP (mag)	RP (mag)	d (pc)	Mass (M $_{\odot}$)
...	114.3862	-43.9371	3.281 \pm 0.083	-10.91 \pm 0.16	12.59 \pm 0.17	...	17.307 \pm 0.003	19.054 \pm 0.022	16.014 \pm 0.007	302.4 $^{+7.9}_{-7.5}$	0.217 \pm 0.017
...	115.0685	-41.5678	3.517 \pm 0.080	-9.87 \pm 0.15	13.02 \pm 0.15	...	17.032 \pm 0.003	18.615 \pm 0.018	15.769 \pm 0.005	282.3 $^{+6.5}_{-6.3}$	0.263 \pm 0.021
TYC 8132-127-1	109.8404	-52.0460	3.301 \pm 0.020	-9.361 \pm 0.039	11.756 \pm 0.040	25.42 \pm 0.21	11.678 \pm 0.002	12.005 \pm 0.002	11.197 \pm 0.002	300.3 \pm 1.8	1.060 \pm 0.053
2MASS J07494981-4249164	117.4575	-42.8212	3.402 \pm 0.090	-8.26 \pm 0.15	12.21 \pm 0.17	...	17.161 \pm 0.003	18.775 \pm 0.032	15.924 \pm 0.007	291.8 $^{+7.9}_{-7.5}$	0.262 \pm 0.021
2MASS J07385798-4130027	114.7416	-41.5008	3.242 \pm 0.061	-10.25 \pm 0.11	11.72 \pm 0.12	...	16.397 \pm 0.002	17.755 \pm 0.010	15.225 \pm 0.004	305.9 $^{+5.9}_{-5.7}$	0.372 \pm 0.030
2MASS J07125080-5008119	108.2117	-50.1367	3.382 \pm 0.013	-9.265 \pm 0.024	11.0222 \pm 0.025	...	13.499 \pm 0.002	14.007 \pm 0.003	12.854 \pm 0.003	293.1 \pm 1.1	0.815 \pm 0.065
TYC 8127-1037-1	108.1714	-50.1835	3.450 \pm 0.063	-9.32 \pm 0.12	11.32 \pm 0.12	...	16.898 \pm 0.002	18.207 \pm 0.018	15.755 \pm 0.004	287.6 $^{+5.3}_{-5.1}$	0.393 \pm 0.031
2MASS J07562414-4342155	119.1006	-43.7043	3.42 \pm 0.11	-9.45 \pm 0.19	12.19 \pm 0.20	...	17.475 \pm 0.003	19.131 \pm 0.032	16.233 \pm 0.007	290.2 $^{+9.5}_{-9.0}$	0.250 \pm 0.020
2MASS J07594022-4445554	119.9176	-44.7654	3.209 \pm 0.039	-10.047 \pm 0.058	12.821 \pm 0.057	22.18 \pm 0.22	13.448 \pm 0.002	13.984 \pm 0.004	12.756 \pm 0.003	308.9 $^{+3.8}_{-3.7}$	0.780 \pm 0.080
2MASS J07261950-4619208	111.5812	-46.3224	3.35 \pm 0.14	-9.54 \pm 0.25	11.23 \pm 0.28	...	17.977 \pm 0.002	19.695 \pm 0.054	16.723 \pm 0.006	297 $^{+13}_{-12}$	0.231 \pm 0.019
...	113.9133	-41.1465	3.23 \pm 0.11	-11.11 \pm 0.17	11.93 \pm 0.17	...	17.337 \pm 0.003	18.919 \pm 0.061	16.052 \pm 0.005	307 $^{+11}_{-10}$	0.258 \pm 0.021
...	109.2572	-48.6920	3.651 \pm 0.090	-10.15 \pm 0.17	12.23 \pm 0.19	...	17.660 \pm 0.002	19.078 \pm 0.042	16.483 \pm 0.006	272.0 $^{+6.9}_{-6.6}$	0.354 \pm 0.028
...	109.1835	-49.0887	3.696 \pm 0.043	-10.687 \pm 0.087	12.222 \pm 0.081	...	16.424 \pm 0.002	17.623 \pm 0.009	15.339 \pm 0.003	268.5 \pm 3.1	0.435 \pm 0.035
...	109.0702	-46.9297	3.495 \pm 0.066	-8.00 \pm 0.13	11.86 \pm 0.14	...	15.141 \pm 0.002	16.145 \pm 0.005	14.141 \pm 0.002	283.9 $^{+5.5}_{-5.3}$	0.541 \pm 0.043
...	109.3139	-46.6192	3.872 \pm 0.085	-10.56 \pm 0.20	12.53 \pm 0.17	...	17.381 \pm 0.002	18.700 \pm 0.025	16.195 \pm 0.009	256.5 $^{+5.8}_{-5.5}$	0.379 \pm 0.030
CD-46 3007	108.9000	-46.9312	3.404 \pm 0.028	-10.965 \pm 0.058	13.037 \pm 0.054	-0.9 \pm 1.6	10.189 \pm 0.002	10.393 \pm 0.002	9.878 \pm 0.002	291.3 $^{+2.4}_{-2.3}$	1.880 \pm 0.094
...	113.9668	-40.6008	3.633 \pm 0.066	-9.50 \pm 0.11	12.88 \pm 0.12	...	16.537 \pm 0.002	18.001 \pm 0.018	15.347 \pm 0.005	273.2 $^{+5.0}_{-4.8}$	0.329 \pm 0.026
...	114.1183	-40.4983	3.358 \pm 0.086	-8.35 \pm 0.15	11.13 \pm 0.17	...	16.873 \pm 0.003	18.543 \pm 0.024	15.581 \pm 0.006	295.6 $^{+7.7}_{-7.3}$	0.234 \pm 0.019
...	116.0075	-45.5995	3.311 \pm 0.033	-8.393 \pm 0.060	11.228 \pm 0.069	...	15.645 \pm 0.002	16.573 \pm 0.006	14.691 \pm 0.003	299.5 $^{+3.0}_{-2.9}$	0.568 \pm 0.045

Table E.8: Alessi 3—Continued

Star Name	<i>RA</i> ($^{\circ}$)	<i>Dec</i> ($^{\circ}$)	Parallax (mas)	μ_{α} (mas yr $^{-1}$)	μ_{δ} (mas yr $^{-1}$)	v_r (km s $^{-1}$)	G (mag)	BP (mag)	RP (mag)	<i>d</i> (pc)	Mass (M $_{\odot}$)
...	109.4282	-46.0742	3.39 ± 0.10	-9.67 ± 0.18	12.21 ± 0.19	...	17.410 ± 0.002	18.949 ± 0.026	16.172 ± 0.006	293.0 $^{+9.0}_{-8.4}$	0.280 ± 0.022
...	112.3843	-49.3023	3.619 ± 0.046	-10.663 ± 0.096	12.11 ± 0.11	...	15.616 ± 0.002	16.802 ± 0.008	14.484 ± 0.005	274.2 $^{+3.5}_{-3.4}$	0.427 ± 0.034
...	112.6048	-50.0047	3.51 ± 0.35	-11.30 ± 0.72	11.49 ± 0.66	...	15.050 ± 0.003	15.493 ± 0.004	14.390 ± 0.002	287 $^{+24}_{-28}$	0.836 ± 0.067
...	113.0153	-49.6474	3.84 ± 0.10	-10.15 ± 0.18	11.29 ± 0.16	...	17.557 ± 0.002	19.054 ± 0.027	16.357 ± 0.007	258.9 $^{+7.3}_{-6.9}$	0.313 ± 0.025
...	111.5738	-45.9419	3.35 ± 0.10	-9.78 ± 0.21	11.00 ± 0.20	...	17.832 ± 0.002	19.361 ± 0.066	16.590 ± 0.007	296.7 $^{+9.4}_{-8.9}$	0.282 ± 0.027
...	113.6398	-45.1522	3.208 ± 0.020	-11.535 ± 0.037	12.593 ± 0.039	...	14.573 ± 0.003	15.312 ± 0.010	13.739 ± 0.007	309.0 $^{+2.0}_{-1.9}$	0.690 ± 0.055
...	111.2281	-49.2598	3.474 ± 0.039	-9.845 ± 0.071	11.692 ± 0.073	...	15.768 ± 0.002	16.779 ± 0.004	14.722 ± 0.007	285.6 $^{+3.3}_{-3.2}$	0.524 ± 0.042
...	115.0049	-44.8350	3.46 ± 0.33	-10.22 ± 0.66	11.80 ± 0.73	...	17.492 ± 0.005	18.194 ± 0.014	16.535 ± 0.006	291 $^{+33}_{-27}$	0.663 ± 0.053
...	116.1079	-42.7295	3.24 ± 0.12	-9.89 ± 0.21	12.81 ± 0.22	...	17.329 ± 0.003	19.127 ± 0.018	16.030 ± 0.005	307 $^{+12}_{-11}$	0.205 ± 0.016
...	115.0573	-44.3210	3.85 ± 0.10	-9.18 ± 0.19	11.15 ± 0.18	...	17.591 ± 0.002	19.113 ± 0.044	16.354 ± 0.005	257.9 $^{+6.9}_{-6.6}$	0.285 ± 0.023
...	117.3179	-51.8275	3.541 ± 0.054	-11.13 ± 0.13	11.30 ± 0.11	...	16.719 ± 0.002	17.927 ± 0.013	15.610 ± 0.004	280.2 $^{+4.3}_{-4.2}$	0.428 ± 0.034
...	115.8333	-50.8155	3.233 ± 0.020	-10.261 ± 0.042	10.735 ± 0.040	...	14.517 ± 0.002	15.208 ± 0.002	13.722 ± 0.002	306.6 ± 1.9	0.698 ± 0.056
...	113.0401	-48.9468	3.539 ± 0.014	-8.875 ± 0.025	12.729 ± 0.025	...	13.211 ± 0.002	13.743 ± 0.002	12.544 ± 0.002	280.3 ± 1.1	0.798 ± 0.064
2MASS J07442624-4403144	116.1094	-44.0540	3.347 ± 0.078	-9.96 ± 0.15	11.44 ± 0.21	23	12.435 ± 0.002	12.838 ± 0.004	11.866 ± 0.004	296.5 $^{+7.1}_{-6.8}$	0.943 ± 0.073
...	112.8108	-44.2727	3.575 ± 0.032	-10.035 ± 0.059	11.765 ± 0.060	...	15.585 ± 0.002	16.582 ± 0.005	14.597 ± 0.003	277.5 ± 2.5	0.545 ± 0.044
...	113.6794	-51.5228	3.60 ± 0.11	-9.88 ± 0.24	11.26 ± 0.26	...	17.715 ± 0.003	18.745 ± 0.036	16.331 ± 0.005	275.9 $^{+9.1}_{-8.5}$	0.404 ± 0.032
CD-433318	113.0941	-43.6263	3.522 ± 0.024	-8.446 ± 0.042	11.198 ± 0.047	17	10.060 ± 0.002	10.379 ± 0.002	9.605 ± 0.002	281.7 ± 1.9	1.113 ± 0.089
...	119.3394	-43.4737	3.304 ± 0.034	-9.428 ± 0.066	11.910 ± 0.069	...	15.594 ± 0.002	16.655 ± 0.013	14.554 ± 0.005	300.1 ± 3.1	0.520 ± 0.042

Table E.8: Alessi 3—Continued

Star Name	<i>RA</i> ($^{\circ}$)	<i>Dec</i> ($^{\circ}$)	Parallax (mas)	μ_{α} (mas yr $^{-1}$)	μ_{δ} (mas yr $^{-1}$)	v_r (km s $^{-1}$)	G (mag)	BP (mag)	RP (mag)	<i>d</i> (pc)	Mass (M $_{\odot}$)
...	109.2192	-45.3362	3.50 ± 0.11	-10.60 ± 0.20	12.56 ± 0.22	...	17.190 ± 0.003	18.289 ± 0.037	15.790 ± 0.030	283.9 $^{+8.9}_{-8.3}$	0.380 ± 0.030
2MASS J07245050-5148100	111.2104	-51.8028	3.713 ± 0.020	-11.578 ± 0.039	11.549 ± 0.047	24	12.714 ± 0.002	13.184 ± 0.003	12.106 ± 0.002	267.2 ± 1.5	0.837 ± 0.067
...	111.7850	-54.1739	3.269 ± 0.016	-8.771 ± 0.037	11.208 ± 0.032	22	13.458 ± 0.002	14.126 ± 0.002	12.688 ± 0.002	303.2 ± 1.5	0.710 ± 0.057
...	102.2059	-47.9717	3.608 ± 0.019	-8.973 ± 0.031	10.977 ± 0.032	...	14.148 ± 0.002	14.791 ± 0.002	13.392 ± 0.002	275.0 ± 1.5	0.723 ± 0.058
...	110.5543	-45.0064	3.47 ± 0.11	-9.67 ± 0.22	11.28 ± 0.24	...	17.813 ± 0.002	19.507 ± 0.032	16.560 ± 0.006	286.3 $^{+9.4}_{-8.8}$	0.238 ± 0.019
...	102.3130	-47.1327	3.615 ± 0.021	-11.039 ± 0.038	11.867 ± 0.046	...	14.911 ± 0.002	15.741 ± 0.004	14.025 ± 0.003	274.4 ± 1.6	0.655 ± 0.052
TYC 8551-1683-1	110.4548	-54.1359	3.883 ± 0.023	-8.599 ± 0.048	12.413 ± 0.039	23.40 ± 0.15	10.922 ± 0.002	11.223 ± 0.002	10.488 ± 0.002	255.6 ± 1.5	1.250 ± 0.062
...	111.1446	-53.2902	3.80 ± 0.10	-10.16 ± 0.24	12.46 ± 0.20	...	17.644 ± 0.002	19.040 ± 0.021	16.473 ± 0.009	261.5 $^{+7.3}_{-6.9}$	0.362 ± 0.029
...	118.9453	-43.2670	3.428 ± 0.018	-8.373 ± 0.030	12.097 ± 0.033	...	14.130 ± 0.003	14.782 ± 0.008	13.347 ± 0.006	289.3 ± 1.6	0.711 ± 0.057
...	107.4500	-52.6828	3.534 ± 0.097	-10.15 ± 0.19	10.90 ± 0.18	...	17.641 ± 0.002	19.106 ± 0.029	16.419 ± 0.008	281.0 $^{+7.9}_{-7.5}$	0.317 ± 0.025
...	107.4943	-52.1412	3.750 ± 0.012	-10.995 ± 0.027	12.776 ± 0.026	...	13.344 ± 0.002	13.882 ± 0.003	12.676 ± 0.002	264.61 $^{+0.86}_{-0.85}$	0.795 ± 0.064
CD-521811	106.2627	-52.9217	3.281 ± 0.031	-10.989 ± 0.055	12.601 ± 0.055	11.0 ± 2.0	9.743 ± 0.002	9.912 ± 0.002	9.487 ± 0.002	302.2 $^{+2.9}_{-2.8}$	1.61 ± 0.12
...	114.4929	-50.1066	3.553 ± 0.086	-10.85 ± 0.19	12.38 ± 0.15	...	17.354 ± 0.002	18.738 ± 0.020	16.187 ± 0.005	279.5 $^{+6.9}_{-6.6}$	0.367 ± 0.029
...	110.9621	-44.1690	3.408 ± 0.084	-9.78 ± 0.16	11.52 ± 0.16	...	17.585 ± 0.002	19.000 ± 0.020	16.422 ± 0.007	291.2 $^{+7.4}_{-7.0}$	0.359 ± 0.029
2MASS J07131040-5213422	108.2933	-52.2284	3.486 ± 0.012	-10.062 ± 0.025	10.466 ± 0.029	29.34 ± 0.68	13.019 ± 0.002	13.490 ± 0.003	12.409 ± 0.003	284.5 ± 1.0	0.990 ± 0.050
TYC 8118-1348-1	105.8910	-45.5322	3.921 ± 0.024	-10.244 ± 0.046	12.908 ± 0.051	0.66 ± 0.15	11.070 ± 0.001	11.346 ± 0.001	10.659 ± 0.001	253.2 ± 1.5	1.060 ± 0.053
...	106.1211	-47.3269	3.813 ± 0.078	-9.63 ± 0.15	12.54 ± 0.16	...	17.337 ± 0.002	18.156 ± 0.052	15.992 ± 0.020	260.5 $^{+5.4}_{-5.2}$	0.473 ± 0.038
TYC 8122-69-1	106.5111	-47.3720	3.910 ± 0.019	-10.458 ± 0.038	12.671 ± 0.038	-0.08 ± 0.15	11.544 ± 0.001	11.858 ± 0.002	11.088 ± 0.002	253.9 ± 1.2	1.000 ± 0.050
...	106.6765	-45.0704	3.611 ± 0.073	-9.77 ± 0.13	12.52 ± 0.14	...	17.016 ± 0.001	18.360 ± 0.020	15.871 ± 0.005	274.9 $^{+5.7}_{-5.4}$	0.383 ± 0.031

Table E.8: Alessi 3—Continued

Star Name	<i>RA</i> ($^{\circ}$)	<i>Dec</i> ($^{\circ}$)	Parallax (mas)	μ_{α} (mas yr $^{-1}$)	μ_{δ} (mas yr $^{-1}$)	v_r (km s $^{-1}$)	G (mag)	BP (mag)	RP (mag)	<i>d</i> (pc)	Mass (M $_{\odot}$)
CD-472816	106.8647	-47.3834	3.702 \pm 0.026	-10.109 \pm 0.047	12.626 \pm 0.053	-0.42 \pm 0.75	10.184 \pm 0.000	10.391 \pm 0.002	9.871 \pm 0.002	268.0 \pm 1.9	1.460 \pm 0.073
...	106.8799	-45.7960	3.393 \pm 0.029	-9.417 \pm 0.057	10.966 \pm 0.051	...	14.601 \pm 0.000	15.476 \pm 0.003	13.686 \pm 0.001	292.3 \pm 2.5	0.609 \pm 0.049
...	107.1291	-45.8109	3.557 \pm 0.016	-9.424 \pm 0.026	11.936 \pm 0.025	...	13.330 \pm 0.001	13.828 \pm 0.002	12.689 \pm 0.002	278.9 \pm 1.2	0.820 \pm 0.066
...	107.4774	-45.2379	3.626 \pm 0.061	-9.72 \pm 0.11	11.74 \pm 0.13	...	16.990 \pm 0.001	18.307 \pm 0.011	15.858 \pm 0.004	273.8 $^{+4.7}_{-4.5}$	0.394 \pm 0.032
2MASS J07095779-4632304	107.4908	-46.5418	3.691 \pm 0.023	-10.072 \pm 0.038	12.469 \pm 0.037	0.65 \pm 0.12	12.228 \pm 0.001	12.610 \pm 0.003	11.705 \pm 0.002	268.8 \pm 1.7	0.974 \pm 0.078
HD 55400	107.6582	-45.5812	3.644 \pm 0.033	-9.693 \pm 0.066	12.219 \pm 0.074	-0.9 \pm 2.6	7.827 \pm 0.000	7.930 \pm 0.002	7.685 \pm 0.003	272.3 \pm 2.5	1.860 \pm 0.093
2MASS J07110162-4530379	107.7568	-45.5105	3.646 \pm 0.024	-9.947 \pm 0.047	12.982 \pm 0.050	0.66 \pm 0.13	11.840 \pm 0.001	12.172 \pm 0.002	11.340 \pm 0.001	272.1 $^{+1.8}_{-1.7}$	1.030 \pm 0.052
...	107.7876	-45.1144	3.414 \pm 0.028	-9.356 \pm 0.055	11.987 \pm 0.054	...	15.053 \pm 0.001	16.006 \pm 0.005	14.092 \pm 0.002	290.5 \pm 2.4	0.555 \pm 0.044
...	107.7975	-44.5114	3.482 \pm 0.032	-9.429 \pm 0.065	11.852 \pm 0.067	...	15.664 \pm 0.001	16.628 \pm 0.007	14.697 \pm 0.001	284.9 $^{+2.7}_{-2.6}$	0.558 \pm 0.045
...	107.9577	-45.1284	3.493 \pm 0.022	-9.595 \pm 0.040	12.161 \pm 0.042	...	14.976 \pm 0.000	15.815 \pm 0.006	14.083 \pm 0.003	284.0 $^{+1.8}_{-1.7}$	0.644 \pm 0.051
...	107.9985	-45.3280	3.465 \pm 0.070	-9.56 \pm 0.13	11.98 \pm 0.12	...	16.885 \pm 0.001	18.187 \pm 0.016	15.741 \pm 0.004	286.4 $^{+5.9}_{-5.7}$	0.395 \pm 0.032
...	108.0995	-45.4233	3.552 \pm 0.022	-9.818 \pm 0.037	11.899 \pm 0.035	...	14.278 \pm 0.000	14.962 \pm 0.002	13.494 \pm 0.001	279.3 $^{+1.8}_{-1.7}$	0.700 \pm 0.056
2MASS J07122400-4522466	108.1000	-45.3796	3.369 \pm 0.026	-9.342 \pm 0.043	11.241 \pm 0.046	1.20 \pm 0.12	12.266 \pm 0.001	12.622 \pm 0.002	11.766 \pm 0.002	294.3 $^{+2.3}_{-2.2}$	0.990 \pm 0.050
...	108.1116	-45.9881	3.570 \pm 0.012	-9.800 \pm 0.024	11.913 \pm 0.025	...	13.503 \pm 0.000	14.038 \pm 0.002	12.834 \pm 0.001	275.8 \pm 1.8	0.970 \pm 0.048
...	108.1398	-44.5688	3.724 \pm 0.013	-10.100 \pm 0.024	12.233 \pm 0.027	...	13.618 \pm 0.000	14.188 \pm 0.002	12.922 \pm 0.002	266.49 \pm 0.92	0.773 \pm 0.062
...	108.2926	-47.5658	3.686 \pm 0.014	-10.226 \pm 0.026	11.956 \pm 0.031	...	13.687 \pm 0.001	14.267 \pm 0.002	12.983 \pm 0.001	269.2 $^{+1.0}_{-0.99}$	0.766 \pm 0.061
...	108.3260	-44.8721	3.510 \pm 0.019	-9.349 \pm 0.037	12.439 \pm 0.033	...	14.047 \pm 0.000	14.680 \pm 0.002	13.296 \pm 0.001	282.6 \pm 1.5	0.728 \pm 0.058

Table E.8: Alessi 3—Continued

Star Name	RA ($^{\circ}$)	Dec ($^{\circ}$)	Parallax (mas)	μ_{α} (mas yr $^{-1}$)	μ_{δ} (mas yr $^{-1}$)	v_r (km s $^{-1}$)	G (mag)	BP (mag)	RP (mag)	d (pc)	d (M $_{\odot}$)	Mass
CD-472887	108.3452 -45.0250	3.536 ± 0.020	-9.686 ± 0.037	11.710 ± 0.037	...	14.898 ± 0.000	15.718 ± 0.003	14.014 ± 0.002	280.6 ± 1.6	662 ± 0.053		
TYC 8123-387-1	108.4000 -47.6745	3.576 ± 0.025	-9.945 ± 0.044	11.393 ± 0.056	11.1 ± 3.0	9.983 ± 0.001	10.171 ± 0.002	9.704 ± 0.002	277.9 ± 1.9	1.980 ± 0.099		
2MASS J07134517-4723016	108.4382 -47.3838	3.560 ± 0.022	-11.176 ± 0.044	11.548 ± 0.040	0.	12.315 ± 0.001	12.761 ± 0.003	11.726 ± 0.002	278.7 ± 1.7	0.869 ± 0.070		
HD 56264	108.5433 -46.3259	3.555 ± 0.025	-9.759 ± 0.044	11.684 ± 0.053	-0.53 ± 0.30	7.032 ± 0.000	7.539 ± 0.001	6.426 ± 0.002	279.1 $^{+2.0}_{-1.9}$	2.750 ± 0.066		
TYC 8123-695-1	108.5846 -47.9345	3.709 ± 0.018	-10.339 ± 0.038	12.252 ± 0.033	-1 ± 2.5	10.639 ± 0.000	10.880 ± 0.001	10.271 ± 0.001	267.6 ± 1.3	1.61 ± 0.12		
...	108.5946 -46.3752	3.597 ± 0.019	-9.680 ± 0.035	12.215 ± 0.046	...	14.356 ± 0.001	15.055 ± 0.003	13.534 ± 0.001	275.8 ± 1.5	0.695 ± 0.056		
...	108.6037 -45.4512	3.551 ± 0.061	-10.87 ± 0.11	11.72 ± 0.12	...	16.889 ± 0.001	18.320 ± 0.020	15.702 ± 0.004	275.1 $^{+4.9}_{-4.7}$	0.348 ± 0.028		
...	108.6113 -46.2576	3.720 ± 0.062	-9.48 ± 0.12	12.38 ± 0.14	...	16.848 ± 0.001	18.266 ± 0.025	15.640 ± 0.006	266.9 $^{+4.6}_{-4.4}$	0.339 ± 0.027		
TYC 8119-1299-1	108.6292 -46.0888	3.556 ± 0.019	-9.632 ± 0.035	11.709 ± 0.042	-0.19 ± 0.44	10.727 ± 0.000	10.966 ± 0.001	10.363 ± 0.001	279.0 ± 1.5	1.440 ± 0.072		
TYC 8119-1883-1	108.6669 -46.3480	3.583 ± 0.024	-9.812 ± 0.043	12.243 ± 0.048	0.27 ± 0.25	10.562 ± 0.000	10.792 ± 0.001	10.215 ± 0.001	276.8 ± 1.9	1.250 ± 0.062		
...	108.7222 -47.1093	3.614 ± 0.045	-10.161 ± 0.083	12.05 ± 0.10	...	16.155 ± 0.001	17.305 ± 0.006	15.080 ± 0.003	274.6 $^{+3.5}_{-3.4}$	0.453 ± 0.036		
2MASS J07145871-4536115	108.7447 -45.6032	3.530 ± 0.025	-9.737 ± 0.043	12.333 ± 0.050	-22.93 ± 0.15	12.236 ± 0.000	12.606 ± 0.002	11.718 ± 0.001	281.0 ± 2.0	0.900 ± 0.045		
2MASS J07150673-4639049	108.7781 -46.6514	3.580 ± 0.022	-10.074 ± 0.041	12.035 ± 0.051	0.	11.812 ± 0.001	12.217 ± 0.004	11.260 ± 0.003	277.1 ± 1.7	0.925 ± 0.074		
CD-472916	108.8015 -47.8181	3.480 ± 0.022	-9.652 ± 0.040	11.754 ± 0.040	-3.1 ± 6.0	9.578 ± 0.000	9.731 ± 0.002	9.356 ± 0.002	285.0 ± 1.8	1.980 ± 0.099		
...	108.8694 -47.0749	3.597 ± 0.045	-9.814 ± 0.080	11.704 ± 0.092	...	16.133 ± 0.001	17.203 ± 0.006	15.093 ± 0.002	275.9 $^{+3.5}_{-3.4}$	0.514 ± 0.041		
...	108.8781 -45.5727	3.516 ± 0.026	-9.083 ± 0.044	11.706 ± 0.048	...	15.162 ± 0.000	16.048 ± 0.004	14.243 ± 0.001	282.1 ± 2.1	0.601 ± 0.048		
TYC 8119-884-1	108.9074 -45.7986	3.617 ± 0.026	-9.090 ± 0.047	11.108 ± 0.051	0.6 ± 1.5	10.525 ± 0.000	10.752 ± 0.001	10.180 ± 0.001	274.3 ± 2.0	1.460 ± 0.073		

Table E.8: Alessi 3—Continued

Star Name	<i>RA</i> ($^{\circ}$)	<i>Dec</i> ($^{\circ}$)	Parallax (mas)	μ_{α} (mas yr $^{-1}$)	μ_{δ} (mas yr $^{-1}$)	v_r (km s $^{-1}$)	G (mag)	BP (mag)	RP (mag)	<i>d</i> (pc)	Mass (M $_{\odot}$)
HD 56734	109.0123	-46.6086	3.541 \pm 0.029	-8.551 \pm 0.053	12.251 \pm 0.049	...	8.852 \pm 0.000	8.977 \pm 0.002	8.664 \pm 0.002	280.1 $^{+2.3}_{-2.2}$	1.860 \pm 0.093
...	109.0305	-46.7435	3.620 \pm 0.044	-9.707 \pm 0.088	12.069 \pm 0.083	...	16.234 \pm 0.001	17.349 \pm 0.007	15.167 \pm 0.003	274.1 $^{+3.4}_{-3.3}$	0.459 \pm 0.037
...	109.0418	-46.8429	3.830 \pm 0.063	-9.02 \pm 0.13	12.48 \pm 0.13	...	16.703 \pm 0.001	18.113 \pm 0.015	15.509 \pm 0.002	259.3 $^{+4.4}_{-4.2}$	0.352 \pm 0.028
TYC 8119-1766-1	109.0524	-46.6273	3.558 \pm 0.020	-9.932 \pm 0.039	11.818 \pm 0.035	0.	10.612 \pm 0.000	10.900 \pm 0.001	10.193 \pm 0.001	278.8 $^{+1.6}_{-1.5}$	1.211 \pm 0.097
TYC 8119-1809-1	109.0613	-46.5453	3.538 \pm 0.022	-11.004 \pm 0.043	11.691 \pm 0.040	0.6 \pm 2.4	10.397 \pm 0.000	10.621 \pm 0.001	10.054 \pm 0.001	280.4 \pm 1.7	1.500 \pm 0.075
2MASS J07162092-4630419	109.0872	-46.5116	3.639 \pm 0.020	-9.927 \pm 0.039	12.332 \pm 0.037	0.62 \pm 0.32	12.862 \pm 0.001	13.300 \pm 0.002	12.282 \pm 0.002	272.6 \pm 1.5	0.860 \pm 0.043
2MASS J07162429-4520382	109.1012	-45.3440	3.607 \pm 0.017	-10.235 \pm 0.032	11.996 \pm 0.037	0.25 \pm 0.14	13.035 \pm 0.001	13.501 \pm 0.002	12.428 \pm 0.001	275.1 \pm 1.3	0.880 \pm 0.044
TYC 8119-1855-1	109.1471	-46.6987	3.536 \pm 0.024	-9.762 \pm 0.044	11.848 \pm 0.043	-1.93 \pm 0.27	10.984 \pm 0.000	11.239 \pm 0.001	10.690 \pm 0.001	280.5 \pm 1.9	1.250 \pm 0.062
CD-46 3031A	109.1498	-46.2380	3.556 \pm 0.037	-9.636 \pm 0.070	11.835 \pm 0.072	1.91 \pm 0.32	8.191 \pm 0.000	8.302 \pm 0.002	8.051 \pm 0.003	279.0 $^{+3.0}_{-2.9}$	1.130 \pm 0.060
...	109.1725	-46.9256	3.610 \pm 0.013	-10.160 \pm 0.027	11.939 \pm 0.027	...	14.157 \pm 0.000	14.818 \pm 0.001	13.390 \pm 0.001	274.8 \pm 1.0	0.713 \pm 0.057
2MASS J07164444-4531019	109.1852	-45.5172	3.625 \pm 0.025	-10.817 \pm 0.042	12.480 \pm 0.045	0.60 \pm 0.13	11.355 \pm 0.001	11.650 \pm 0.002	10.920 \pm 0.001	273.7 $^{+1.9}_{-1.8}$	0.990 \pm 0.050
...	109.1923	-46.4796	3.468 \pm 0.054	-10.12 \pm 0.10	11.914 \pm 0.097	...	16.539 \pm 0.001	17.906 \pm 0.009	15.380 \pm 0.003	286.1 $^{+4.5}_{-4.3}$	0.373 \pm 0.030
...	109.2120	-46.2079	3.472 \pm 0.064	-9.64 \pm 0.12	12.07 \pm 0.11	...	16.547 \pm 0.001	17.779 \pm 0.018	15.426 \pm 0.003	285.8 $^{+5.3}_{-5.1}$	0.419 \pm 0.033
...	109.2156	-45.4893	3.306 \pm 0.025	-9.097 \pm 0.043	12.404 \pm 0.052	...	14.167 \pm 0.000	14.948 \pm 0.002	13.314 \pm 0.001	299.8 \pm 2.3	0.671 \pm 0.054
TYC 8119-472-1	109.2481	-46.0652	3.447 \pm 0.026	-9.588 \pm 0.047	11.349 \pm 0.042	-0.12 \pm 0.15	11.748 \pm 0.001	12.063 \pm 0.002	11.288 \pm 0.002	287.7 $^{+2.2}_{-2.1}$	0.990 \pm 0.050
...	109.2710	-45.8603	3.497 \pm 0.044	-9.707 \pm 0.078	11.637 \pm 0.094	...	16.044 \pm 0.001	17.109 \pm 0.009	15.024 \pm 0.003	283.7 $^{+3.6}_{-3.5}$	0.514 \pm 0.041
TYC 8119-871-1	109.2782	-45.5338	3.506 \pm 0.024	-9.362 \pm 0.046	11.968 \pm 0.055	11	12.027 \pm 0.000	12.397 \pm 0.001	11.505 \pm 0.001	282.9 $^{+2.0}_{-1.9}$	0.978 \pm 0.078
HD 57001	109.2904	-46.6951	3.638 \pm 0.024	-9.571 \pm 0.053	11.528 \pm 0.046	-0.41 \pm 0.18	7.502 \pm 0.000	7.994 \pm 0.002	6.905 \pm 0.002	272.7 \pm 1.8	2.750 \pm 0.066

Table E.8: Alessi 3—Continued

Star Name	<i>RA</i> ($^{\circ}$)	<i>Dec</i> ($^{\circ}$)	Parallax (mas)	μ_{α} (mas yr $^{-1}$)	μ_{δ} (mas yr $^{-1}$)	v_r (km s $^{-1}$)	G (mag)	BP (mag)	RP (mag)	d (pc)	Mass (M $_{\odot}$)
CD-46 3039	109.2904	-46.8152	3.509 ± 0.019	-10.056 ± 0.037	11.902 ± 0.040	...	9.550 ± 0.000	9.762 ± 0.001	9.234 ± 0.001	282.6 $^{+1.6}_{-1.5}$	1.46 ± 0.12
2MASS J07170968-4641423	109.2914	-46.6945	3.651 ± 0.035	-9.830 ± 0.068	12.369 ± 0.072	...	12.294 ± 0.001	12.36 ± 0.11	11.46 ± 0.23	271.8 $^{+2.7}_{-2.6}$	0.97 ± 0.25
...	109.2920	-46.8062	3.608 ± 0.065	-9.63 ± 0.15	12.68 ± 0.13	...	16.380 ± 0.001	17.724 ± 0.013	15.210 ± 0.003	275.1 $^{+5.1}_{-4.9}$	0.377 ± 0.030
2MASS J07172155-4538443	109.3398	-45.6457	3.572 ± 0.024	-9.661 ± 0.045	12.084 ± 0.046	6	12.151 ± 0.001	12.557 ± 0.003	11.595 ± 0.002	277.7 $^{+1.9}_{-1.8}$	0.921 ± 0.074
TYC 8119-123-1	109.3409	-46.8432	3.609 ± 0.017	-9.984 ± 0.034	11.584 ± 0.032	-0.50 ± 0.15	11.495 ± 0.000	11.799 ± 0.002	11.049 ± 0.001	274.9 ± 1.3	1.000 ± 0.050
CD-453071	109.4045	-45.7436	3.484 ± 0.027	-10.056 ± 0.054	11.512 ± 0.053	...	9.624 ± 0.000	9.775 ± 0.002	9.399 ± 0.002	284.6 ± 2.2	1.860 ± 0.093
...	109.4096	-46.0928	3.463 ± 0.039	-9.851 ± 0.070	12.100 ± 0.067	...	15.540 ± 0.001	16.658 ± 0.006	14.483 ± 0.002	286.5 $^{+3.3}_{-3.2}$	0.465 ± 0.037
...	109.4149	-47.0514	3.503 ± 0.080	-10.15 ± 0.15	12.01 ± 0.16	...	17.555 ± 0.001	18.942 ± 0.031	16.381 ± 0.004	283.4 $^{+6.7}_{-6.4}$	0.364 ± 0.029
CD-453072	109.4536	-45.7573	3.686 ± 0.028	-9.406 ± 0.060	12.351 ± 0.058	-0.0 ± 6.6	9.506 ± 0.000	9.654 ± 0.002	9.286 ± 0.003	269.2 $^{+2.1}_{-2.0}$	1.980 ± 0.099
...	109.4586	-46.3982	3.601 ± 0.013	-9.538 ± 0.024	11.523 ± 0.025	...	13.675 ± 0.000	14.354 ± 0.002	12.889 ± 0.001	275.5 ± 1.0	0.701 ± 0.056
...	109.5235	-45.6521	3.693 ± 0.044	-10.061 ± 0.080	12.070 ± 0.091	...	16.019 ± 0.001	17.112 ± 0.004	14.990 ± 0.002	268.8 ± 3.2	0.504 ± 0.040
CD-46 3053	109.5380	-46.2669	3.509 ± 0.029	-9.773 ± 0.052	11.869 ± 0.054	-0.3 ± 1.9	9.598 ± 0.000	9.763 ± 0.001	9.358 ± 0.001	282.7 ± 2.3	1.500 ± 0.075
...	109.5673	-46.5093	3.589 ± 0.032	-9.931 ± 0.065	11.837 ± 0.058	...	15.756 ± 0.001	16.758 ± 0.005	14.756 ± 0.002	276.4 $^{+2.5}_{-2.4}$	0.541 ± 0.043
...	109.5974	-45.7782	3.738 ± 0.068	-9.08 ± 0.14	10.82 ± 0.13	...	16.338 ± 0.001	17.711 ± 0.010	15.179 ± 0.002	265.6 $^{+4.9}_{-4.8}$	0.372 ± 0.030
...	109.6100	-45.2695	3.371 ± 0.055	-9.60 ± 0.11	12.47 ± 0.10	...	15.861 ± 0.002	17.076 ± 0.012	14.764 ± 0.004	294.2 $^{+4.9}_{-4.7}$	0.429 ± 0.034
...	109.6508	-46.1291	3.528 ± 0.028	-10.012 ± 0.058	11.630 ± 0.051	...	15.229 ± 0.000	16.117 ± 0.004	14.307 ± 0.001	281.2 ± 2.2	0.599 ± 0.048
2MASS J07184659-4535231	109.6941	-45.5898	3.471 ± 0.014	-9.651 ± 0.025	11.643 ± 0.028	0.45 ± 0.24	13.101 ± 0.001	13.554 ± 0.002	12.498 ± 0.001	285.7 ± 1.2	0.860 ± 0.043
HD 57416	109.7335	-46.0557	3.497 ± 0.036	-10.399 ± 0.065	11.762 ± 0.069	-2.0 ± 2.0	9.068 ± 0.001	9.176 ± 0.001	8.915 ± 0.002	283.6 $^{+3.0}_{-2.9}$	1.860 ± 0.093
...	109.7796	-47.9643	3.686 ± 0.071	-8.61 ± 0.13	11.36 ± 0.16	...	16.977 ± 0.001	18.421 ± 0.014	15.797 ± 0.005	263.4 $^{+5.3}_{-5.1}$	0.339 ± 0.027

Table E.8: Alessi 3—Continued

Star Name	<i>RA</i> ($^{\circ}$)	<i>Dec</i> ($^{\circ}$)	Parallax (mas)	μ_{α} (mas yr $^{-1}$)	μ_{δ} (mas yr $^{-1}$)	v_r (km s $^{-1}$)	G (mag)	BP (mag)	RP (mag)	<i>d</i> (pc)	Mass (M $_{\odot}$)
...	109.8014	-47.6457	3.772 ± 0.030	-11.188 ± 0.059	12.641 ± 0.061	...	14.956 ± 0.001	15.942 ± 0.003	13.972 ± 0.002	263.1 ± 2.1	0.549 ± 0.044
HD 57552	109.8612	-47.2212	3.480 ± 0.031	-10.192 ± 0.062	11.691 ± 0.063	...	7.889 ± 0.000	8.005 ± 0.002	7.728 ± 0.003	285.0 ± 2.5	1.860 ± 0.093
...	109.8779	-46.2535	3.517 ± 0.014	-9.579 ± 0.024	11.772 ± 0.028	...	13.561 ± 0.000	14.094 ± 0.002	12.898 ± 0.001	282.0 ± 1.1	0.798 ± 0.064
TYC 8124-2279-1	109.9234	-47.1860	3.615 ± 0.021	-10.097 ± 0.039	11.589 ± 0.039	-0.85 ± 0.14	12.028 ± 0.000	12.370 ± 0.002	11.541 ± 0.002	274.4 ± 1.6	1.030 ± 0.052
HD 57597	109.9655	-45.6405	3.444 ± 0.026	-9.609 ± 0.051	12.016 ± 0.049	...	9.035 ± 0.000	9.181 ± 0.002	8.813 ± 0.002	288.0 $^{+2.2}_{-2.1}$	1.98 ± 0.13
CD-46 3075	109.9688	-46.5515	3.493 ± 0.031	-9.993 ± 0.056	11.902 ± 0.059	-10.1 ± 6.6	9.852 ± 0.001	10.027 ± 0.002	9.577 ± 0.001	283.9 ± 2.5	1.770 ± 0.089
...	110.1488	-46.6119	3.389 ± 0.053	-10.65 ± 0.11	10.92 ± 0.12	...	15.798 ± 0.001	16.900 ± 0.007	14.737 ± 0.003	292.7 $^{+4.6}_{-4.5}$	0.474 ± 0.038
TYC 8120-2311-1	110.3431	-46.0026	3.580 ± 0.020	-10.036 ± 0.036	11.753 ± 0.036	-0.01 ± 0.12	11.686 ± 0.001	11.990 ± 0.002	11.233 ± 0.001	277.1 ± 1.6	0.990 ± 0.050
...	110.3463	-46.7400	3.825 ± 0.044	-10.439 ± 0.086	12.776 ± 0.085	...	16.326 ± 0.001	17.588 ± 0.015	15.217 ± 0.003	259.5 ± 3.0	0.414 ± 0.033
TYC 8120-2138-1	110.3697	-45.5678	3.369 ± 0.025	-9.997 ± 0.042	11.584 ± 0.048	-0.54 ± 0.72	10.583 ± 0.000	10.817 ± 0.001	10.232 ± 0.001	294.3 ± 2.2	1.460 ± 0.073
...	110.3763	-46.7777	3.811 ± 0.043	-10.634 ± 0.081	12.176 ± 0.080	...	15.075 ± 0.001	15.978 ± 0.004	14.096 ± 0.002	260.4 $^{+3.0}_{-2.9}$	0.568 ± 0.045
2MASS J07215207-4528443	110.4670	-45.4790	3.552 ± 0.026	-9.464 ± 0.043	11.392 ± 0.044	19.64 ± 0.10	12.535 ± 0.001	12.946 ± 0.004	11.975 ± 0.003	279.2 ± 2.0	0.970 ± 0.048
2MASS J07220786-4609155	110.5327	-46.1543	3.622 ± 0.020	-9.918 ± 0.037	11.918 ± 0.040	-0.302 ± 0.096	12.542 ± 0.000	12.936 ± 0.002	12.004 ± 0.002	273.9 $^{+1.6}_{-1.5}$	0.943 ± 0.075
...	110.6728	-46.1939	3.557 ± 0.018	-10.381 ± 0.033	11.315 ± 0.038	...	14.515 ± 0.000	15.244 ± 0.002	13.675 ± 0.003	278.9 ± 1.4	0.690 ± 0.055
TYC 8120-2711-1	110.7479	-46.3838	3.544 ± 0.023	-10.262 ± 0.046	11.570 ± 0.038	-0.67 ± 0.14	11.128 ± 0.001	11.391 ± 0.002	10.730 ± 0.001	279.9 ± 1.8	1.250 ± 0.062
2MASS J07243824-4542491	111.1593	-45.7137	3.474 ± 0.022	-10.039 ± 0.046	12.227 ± 0.048	1	12.205 ± 0.000	12.659 ± 0.002	11.609 ± 0.002	285.5 ± 1.8	0.858 ± 0.069
...	111.1646	-45.9538	3.253 ± 0.017	-9.425 ± 0.028	11.077 ± 0.032	...	13.270 ± 0.001	13.785 ± 0.003	12.605 ± 0.002	304.7 ± 1.6	0.805 ± 0.064
...	111.4506	-46.2335	3.395 ± 0.033	-9.900 ± 0.063	11.383 ± 0.069	...	15.355 ± 0.001	16.262 ± 0.003	14.422 ± 0.001	292.1 $^{+2.9}_{-2.8}$	0.585 ± 0.047

Table E.8: Alessi 3—Continued

Star Name	RA ($^{\circ}$)	Dec ($^{\circ}$)	Parallax (mas)	μ_{α} (mas yr $^{-1}$)	μ_{δ} (mas yr $^{-1}$)	v_r (km s $^{-1}$)	G (mag)	BP (mag)	RP (mag)	d (pc)	d (M $_{\odot}$)	Mass
2MASS J07254813-4702274	111.4505	-47.0410	3.217 \pm 0.021	-9.041 \pm 0.037	11.755 \pm 0.037	10.76 \pm 0.19	12.367 \pm 0.001	12.738 \pm 0.002	11.847 \pm 0.002	308.1 $^{+2.1}_{-2.0}$	0.950 \pm 0.048	
...	111.6239	-46.4481	3.391 \pm 0.031	-9.751 \pm 0.055	11.229 \pm 0.070	...	15.409 \pm 0.001	16.335 \pm 0.005	14.464 \pm 0.002	292.4 $^{+2.7}_{-2.6}$	0.573 \pm 0.046	
2MASS J07262982-4436173	111.6243	-44.6048	3.462 \pm 0.029	-10.408 \pm 0.053	12.036 \pm 0.063	5.59 \pm 0.14	12.855 \pm 0.002	13.348 \pm 0.007	12.214 \pm 0.005	286.5 \pm 2.4	0.860 \pm 0.043	
...	111.9997	-46.1862	3.227 \pm 0.060	-9.10 \pm 0.12	10.84 \pm 0.11	...	17.019 \pm 0.001	18.329 \pm 0.017	15.896 \pm 0.003	307.3 $^{+5.8}_{-5.6}$	0.398 \pm 0.032	
...	112.0025	-47.6937	3.420 \pm 0.014	-10.139 \pm 0.026	11.076 \pm 0.026	...	14.113 \pm 0.000	14.746 \pm 0.002	13.361 \pm 0.001	289.9 $^{+1.2}_{-1.1}$	0.728 \pm 0.058	
...	107.4301	-46.3096	3.61 \pm 0.12	-9.96 \pm 0.22	11.26 \pm 0.28	...	17.488 \pm 0.002	18.860 \pm 0.032	16.307 \pm 0.006	275.1 $^{+9.2}_{-8.7}$	0.366 \pm 0.029	
...	107.9038	-45.5375	3.594 \pm 0.080	-9.97 \pm 0.17	12.02 \pm 0.18	...	17.269 \pm 0.001	18.839 \pm 0.019	16.044 \pm 0.005	276.2 $^{+6.3}_{-6.0}$	0.276 \pm 0.022	
...	108.2752	-47.2024	3.57 \pm 0.12	-9.88 \pm 0.20	11.71 \pm 0.25	...	16.326 \pm 0.000	16.602 \pm 0.069	14.459 \pm 0.087	262.1 $^{+4.7}_{-4.5}$	0.489 \pm 0.047	
...	108.6217	-48.1337	3.873 \pm 0.011	-9.574 \pm 0.023	12.056 \pm 0.020	2	13.229 \pm 0.001	13.878 \pm 0.002	12.468 \pm 0.001	256.28 $^{+0.75}_{-0.74}$	0.719 \pm 0.058	
...	108.7279	-45.4817	3.590 \pm 0.087	-9.85 \pm 0.16	12.66 \pm 0.20	...	17.439 \pm 0.000	18.894 \pm 0.024	16.256 \pm 0.005	276.6 $^{+6.8}_{-6.5}$	0.334 \pm 0.027	
...	108.7460	-47.6957	3.51 \pm 0.10	-9.39 \pm 0.21	12.39 \pm 0.20	...	17.946 \pm 0.000	19.550 \pm 0.048	16.738 \pm 0.006	283.0 $^{+8.6}_{-8.1}$	0.272 \pm 0.022	
...	108.7647	-46.0861	3.624 \pm 0.098	-10.26 \pm 0.18	12.14 \pm 0.23	...	17.712 \pm 0.002	19.204 \pm 0.036	16.482 \pm 0.006	274.0 $^{+7.6}_{-7.2}$	0.304 \pm 0.024	
HD 56701	109.0026	-45.8958	3.542 \pm 0.035	-9.278 \pm 0.067	13.015 \pm 0.068	-2.3 \pm 2.6	7.868 \pm 0.001	7.991 \pm 0.002	7.697 \pm 0.004	280.1 $^{+2.8}_{-2.7}$	1.81 \pm 0.19	
...	109.1030	-45.0853	3.416 \pm 0.091	-8.94 \pm 0.18	11.38 \pm 0.18	...	17.456 \pm 0.001	18.922 \pm 0.018	16.264 \pm 0.006	290.6 $^{+7.9}_{-7.5}$	0.327 \pm 0.026	
...	109.1783	-45.3225	3.594 \pm 0.096	-9.67 \pm 0.17	11.79 \pm 0.20	...	17.778 \pm 0.000	19.320 \pm 0.024	16.586 \pm 0.006	276.3 $^{+7.5}_{-7.2}$	0.300 \pm 0.024	
...	109.3849	-46.5779	3.75 \pm 0.11	-9.05 \pm 0.28	11.71 \pm 0.19	...	17.487 \pm 0.000	19.020 \pm 0.029	16.093 \pm 0.017	265.1 $^{+7.9}_{-7.4}$	0.243 \pm 0.019	
...	109.6620	-46.7082	3.49 \pm 0.10	-10.08 \pm 0.19	11.88 \pm 0.19	...	17.618 \pm 0.001	18.924 \pm 0.031	16.344 \pm 0.011	284.4 $^{+8.6}_{-8.1}$	0.359 \pm 0.029	
...	110.0783	-46.2402	3.36 \pm 0.12	-9.43 \pm 0.22	11.73 \pm 0.25	...	17.424 \pm 0.001	18.167 \pm 0.072	16.079 \pm 0.028	296 \pm 11	0.514 \pm 0.041	
...	110.3486	-47.5070	3.596 \pm 0.088	-9.57 \pm 0.18	12.12 \pm 0.16	...	17.642 \pm 0.002	19.044 \pm 0.038	16.403 \pm 0.007	276.1 $^{+7.0}_{-6.6}$	0.333 \pm 0.027	

Table E.8: Alessi 3—Continued

Star Name	RA ($^{\circ}$)	Dec ($^{\circ}$)	Parallax (mas)	μ_{α} (mas yr $^{-1}$)	μ_{δ} (mas yr $^{-1}$)	v_r (km s $^{-1}$)	G (mag)	BP (mag)	RP (mag)	d (pc)	Mass (M $_{\odot}$)
...	110.6354	-46.8154	3.62 ± 0.11	-10.30 ± 0.22	11.81 ± 0.20	...	17.668 ± 0.003	19.240 ± 0.038	16.398 ± 0.006	274.1 $^{+8.3}_{-7.8}$	0.264 ± 0.021
...	110.6646	-46.7271	3.823 ± 0.090	-10.42 ± 0.20	12.84 ± 0.17	...	16.383 ± 0.000	17.754 ± 0.008	15.208 ± 0.004	259.8 $^{+6.3}_{-6.0}$	0.368 ± 0.029
...	107.8859	-44.1869	3.37 ± 0.10	-9.40 ± 0.21	11.31 ± 0.28	...	17.762 ± 0.000	19.203 ± 0.045	16.553 ± 0.005	294.7 $^{+9.3}_{-8.7}$	0.330 ± 0.026
...	108.0611	-43.8049	3.914 ± 0.073	-9.95 ± 0.14	11.96 ± 0.17	...	17.012 ± 0.001	18.330 ± 0.026	15.871 ± 0.003	253.7 $^{+4.8}_{-4.6}$	0.391 ± 0.031
...	108.8335	-44.4418	3.69 ± 0.10	-10.19 ± 0.18	12.56 ± 0.19	...	17.724 ± 0.001	19.112 ± 0.056	16.491 ± 0.007	269.5 $^{+7.6}_{-7.2}$	0.347 ± 0.028
...	108.9636	-43.8411	3.419 ± 0.016	-9.385 ± 0.031	11.623 ± 0.031	...	14.399 ± 0.001	15.253 ± 0.002	13.500 ± 0.001	290.1 ± 1.4	0.630 ± 0.050
...	109.8645	-44.3525	3.411 ± 0.091	-9.07 ± 0.20	11.36 ± 0.17	...	17.377 ± 0.001	18.948 ± 0.030	16.144 ± 0.006	291.0 $^{+8.0}_{-7.6}$	0.273 ± 0.022
...	109.5632	-46.9432	3.716 ± 0.092	-9.64 ± 0.18	11.36 ± 0.22	...	17.658 ± 0.001	19.101 ± 0.031	16.474 ± 0.005	267.3 $^{+6.8}_{-6.5}$	0.338 ± 0.027
...	105.7447	-45.7193	3.601 ± 0.042	-11.808 ± 0.076	11.100 ± 0.082	...	14.986 ± 0.001	16.031 ± 0.004	13.969 ± 0.002	275.5 $^{+3.2}_{-3.1}$	0.522 ± 0.042
...	105.7464	-45.7189	3.647 ± 0.072	-11.36 ± 0.13	11.05 ± 0.14	...	16.887 ± 0.002	18.471 ± 0.012	15.629 ± 0.004	272.2 $^{+5.5}_{-5.3}$	0.264 ± 0.021
HD 55000	107.2422	-45.3313	3.178 ± 0.037	-9.446 ± 0.071	10.128 ± 0.082	15 ± 10.	6.980 ± 0.001	6.974 ± 0.002	7.039 ± 0.003	311.9 ± 3.6	2.75 ± 0.60
...	108.4601	-44.1624	3.194 ± 0.032	-8.918 ± 0.059	11.677 ± 0.059	...	15.562 ± 0.001	16.514 ± 0.004	14.602 ± 0.002	310.3 $^{+3.1}_{-3.0}$	0.556 ± 0.044
...	109.0141	-47.4634	3.516 ± 0.062	-11.70 ± 0.13	11.88 ± 0.12	0.	11.628 ± 0.001	11.958 ± 0.002	11.146 ± 0.001	282.2 $^{+5.1}_{-4.9}$	1.072 ± 0.086
TYC 8124-2032-1	111.4576	-47.0350	3.188 ± 0.022	-9.041 ± 0.040	11.991 ± 0.037	9.9 ± 1.6	10.583 ± 0.000	10.809 ± 0.001	10.239 ± 0.001	310.9 ± 2.1	1.930 ± 0.096
...	111.7035	-45.4641	3.174 ± 0.050	-9.64 ± 0.10	11.99 ± 0.10	20.	11.273 ± 0.001	11.568 ± 0.001	10.800 ± 0.001	312.4 $^{+5.0}_{-4.9}$	1.108 ± 0.089
...	112.8043	-47.7633	3.169 ± 0.023	-10.280 ± 0.041	11.539 ± 0.048	19	12.178 ± 0.000	12.577 ± 0.001	11.628 ± 0.001	312.7 ± 2.3	0.935 ± 0.075
CD-443499	112.8783	-44.8251	3.148 ± 0.032	-8.910 ± 0.049	12.878 ± 0.059	63.6 ± 2.8	10.047 ± 0.001	10.214 ± 0.001	9.789 ± 0.002	314.8 $^{+3.2}_{-3.1}$	1.880 ± 0.094
...	107.8210	-46.0008	3.38 ± 0.24	-10.68 ± 0.60	11.63 ± 0.57	...	18.734 ± 0.001	20.16 ± 0.10	17.457 ± 0.011	296 $^{+24}_{-20.}$	0.312 ± 0.043

Table E.8: Alessi 3—Continued

Star Name	<i>RA</i> ($^{\circ}$)	<i>Dec</i> ($^{\circ}$)	Parallax (mas)	μ_{α} (mas yr $^{-1}$)	μ_{δ} (mas yr $^{-1}$)	v_r (km s $^{-1}$)	G (mag)	BP (mag)	RP (mag)	d (pc)	Mass (M $_{\odot}$)
...	107.9079	-46.5328	3.51 ± 0.36	-8.64 ± 0.74	11.59 ± 0.68	...	19.715 ± 0.000	20.85 ± 0.14	18.318 ± 0.025	288 $^{+35}_{-28}$	0.372 ± 0.045
...	108.1943	-46.8878	3.52 ± 0.21	-10.06 ± 0.37	11.90 ± 0.37	...	18.732 ± 0.001	20.060 ± 0.088	17.416 ± 0.012	284 $^{+18}_{-16}$	0.332 ± 0.036
...	108.3270	-45.6704	3.67 ± 0.17	-9.67 ± 0.36	12.24 ± 0.29	...	18.371 ± 0.003	20.060 ± 0.061	17.051 ± 0.011	271 $^{+13}_{-12}$	0.224 ± 0.018
...	108.5011	-46.1950	3.70 ± 0.20	-9.88 ± 0.37	12.43 ± 0.42	...	18.958 ± 0.000	19.78 ± 0.17	17.645 ± 0.012	270 $^{+16}_{-14}$	0.493 ± 0.061
...	108.5363	-46.3477	3.38 ± 0.20	-10.14 ± 0.37	10.83 ± 0.41	...	18.905 ± 0.002	20.355 ± 0.092	17.599 ± 0.012	295 $^{+19}_{-17}$	0.292 ± 0.034
...	108.8604	-46.8193	3.45 ± 0.16	-9.74 ± 0.33	12.50 ± 0.32	...	18.709 ± 0.001	20.151 ± 0.098	17.376 ± 0.024	288 $^{+14}_{-13}$	0.281 ± 0.036
...	108.9504	-46.6182	3.36 ± 0.12	-10.23 ± 0.24	12.71 ± 0.20	...	18.024 ± 0.000	19.544 ± 0.046	16.750 ± 0.004	296 $^{+10.}_{-9.8}$	0.276 ± 0.022
...	109.0086	-46.9265	3.34 ± 0.21	-10.25 ± 0.39	11.20 ± 0.42	...	18.804 ± 0.000	20.270 ± 0.093	17.511 ± 0.009	299 $^{+21}_{-18}$	0.285 ± 0.034
...	109.1392	-46.2890	3.65 ± 0.14	-10.26 ± 0.23	12.01 ± 0.25	...	18.120 ± 0.003	19.401 ± 0.047	16.833 ± 0.013	273 $^{+11}_{-10.}$	0.362 ± 0.029
...	109.1843	-46.6034	3.60 ± 0.15	-9.02 ± 0.34	11.62 ± 0.26	...	18.329 ± 0.001	19.935 ± 0.086	16.993 ± 0.013	276 $^{+12}_{-11}$	0.239 ± 0.023
...	109.5775	-46.4575	3.74 ± 0.36	-9.36 ± 0.60	11.81 ± 0.60	...	19.595 ± 0.001	20.842 ± 0.080	18.224 ± 0.016	270 $^{+30}_{-25}$	0.348 ± 0.033
...	109.9235	-47.4607	3.70 ± 0.12	-10.32 ± 0.24	12.24 ± 0.23	...	18.199 ± 0.002	19.745 ± 0.051	16.966 ± 0.008	268.3 $^{+8.7}_{-8.2}$	0.280 ± 0.023
...	110.0437	-45.4018	3.60 ± 0.18	-10.56 ± 0.33	11.68 ± 0.32	...	18.581 ± 0.003	20.109 ± 0.088	17.327 ± 0.010	276 $^{+15}_{-14}$	0.279 ± 0.032
...	110.7843	-46.6164	3.70 ± 0.17	-9.32 ± 0.36	11.70 ± 0.29	...	18.755 ± 0.001	20.279 ± 0.091	17.486 ± 0.010	269 $^{+13}_{-12}$	0.276 ± 0.032
...	107.1038	-44.0474	3.57 ± 0.19	-10.42 ± 0.38	11.27 ± 0.38	...	18.839 ± 0.001	20.73 ± 0.11	17.527 ± 0.015	280 $^{+16}_{-14}$	0.184 ± 0.019
...	108.0111	-44.3217	3.67 ± 0.13	-9.84 ± 0.26	12.08 ± 0.28	...	18.274 ± 0.000	19.817 ± 0.048	17.065 ± 0.009	271 $^{+10.}_{-9.5}$	0.293 ± 0.023
...	108.4052	-44.3433	3.42 ± 0.17	-9.43 ± 0.36	12.84 ± 0.36	...	18.488 ± 0.002	20.175 ± 0.096	17.211 ± 0.005	291 $^{+16}_{-14}$	0.233 ± 0.025
...	106.4157	-44.9056	3.67 ± 0.21	-10.14 ± 0.35	11.78 ± 0.45	...	18.799 ± 0.002	20.60 ± 0.14	17.498 ± 0.015	272 $^{+16}_{-15}$	0.203 ± 0.030
...	109.4607	-44.8208	3.86 ± 0.17	-9.94 ± 0.33	11.81 ± 0.43	...	18.624 ± 0.001	20.572 ± 0.063	17.374 ± 0.009	258 $^{+12}_{-11}$	0.184 ± 0.015

Table E.8: Alessi 3—*Continued*

Star Name	<i>RA</i> ($^{\circ}$)	<i>Dec</i> ($^{\circ}$)	Parallax (mas)	μ_{α} (mas yr $^{-1}$)	μ_{δ} (mas yr $^{-1}$)	v_r (km s $^{-1}$)	G (mag)	BP (mag)	RP (mag)	<i>d</i> (pc)	Mass (M $_{\odot}$)
...	109.8815	-46.8597	3.50 \pm 0.25	-9.26 \pm 0.46	10.71 \pm 0.72	...	19.034 \pm 0.001	20.46 \pm 0.12	17.710 \pm 0.013	286 $^{+23}_{-20}$.	0.293 \pm 0.042

Appendix C

STELLAR PROPERTIES OF SPECTROSCOPICALLY OBSERVED STARS

We measure 284 stars' spectral types, radial velocities, projected rotational velocities, H α widths, lithium equivalent widths, and infrared excesses.

Table C.1: Sample of Stellar Properties of Spectroscopically Observed Stars

Star Name	Spectral Type	Class	v_r	$v_{\text{rot}} \sin(i)$ (km s $^{-1}$)	Binary Flag	H α EW (Å)	H α 10% W (km s $^{-1}$)	Li EW (Å)	Infrared Excess (mag)	Assn. Name
CD-46 3194	A6V	1.0	7.1 ± 1.7	...	SB2	2.8903 ± 0.0074	...	0.0151 ± 0.0074	0.197 ± 0.049	CG 4 Assn.
TYC 8137-2850-1	K2V	1.0	21.16 ± 0.21	18.3 ± 1.1	-0.414 ± 0.023	201 ± 12	0.416 ± 0.012	0.247 ± 0.059	CG 4 Assn.	
TYC 8137-2862-1	A3V	1.0	22.0 ± 2.6	118 ± 14	3.536 ± 0.022	0.164 ± 0.037	CG 4 Assn.	
CD-46 3212	G3V	4.0	22.4 ± 2.1	113 ± 13	1.863 ± 0.017	...	0.037 ± 0.013	0.308 ± 0.063	CG 4 Assn.	
2MASS J07293289-4611036	G5V	2.0	19.88 ± 0.93	31.0 ± 1.5	-0.927 ± 0.011	107 ± 12	0.171 ± 0.016	...	CG 4 Assn.	
RP93 4	M1.5	2.0	23.52 ± 0.53	13.4 ± 1.4	-12.966 ± 0.018	379 ± 17	0.481 ± 0.017	0.	CG 4 Assn.	
RP93 7	K4V	1.0	22.47 ± 0.42	26.2 ± 1.6	-14.642 ± 0.017	431 ± 12	0.476 ± 0.026	0.477 ± 0.062	CG 4 Assn.	
2MASS J08284752-3429298	K1V	2.0	20.79 ± 0.43	34.9 ± 1.2	-1.57 ± 0.50	535 ± 12	0.218 ± 0.013	...	CG 22 Assn.	
CD-344842B	B9V	2.0	...	150.	4.083 ± 0.023	0.098 ± 0.052	CG 22 Assn.	
CD-344836	A0V	1.0	4.160 ± 0.017	0.108 ± 0.039	CG 22 Assn.	
HD 72138	B9V	1.0	...	150.	3.847 ± 0.019	-0.028 ± 0.043	CG 22 Assn.	
2MASS J08260440-3431206	K2V	3.0	22.77 ± 0.68	35	-0.044 ± 0.013	44 ± 12	0.121 ± 0.028	...	CG 22 Assn.	
TYC 7143-191-1	F6V	1.0	22.51 ± 0.21	23.96 ± 0.56	2.266 ± 0.012	...	0.1374 ± 0.0067	0.040 ± 0.041	CG 22 Assn.	

Table C.1—Continued

Star Name	Spectral Type	Class	v_r	$v_{\text{rot}} \sin(i)$	Binary Flag	$H\alpha$ EW (Å)	$H\alpha$ 10% W (km s^{-1})	Li EW (Å)	Infrared Excess (mag)	Assn. Name
2MASS J08310444-3502348	1 K1V	1.0	48.28 ± 0.14	4.0 ± 1.6	SBI?	1.397 ± 0.023	...	0.010 ± 0.034	...	CG 22 Assn.
TYC 7143-998-1	1 A1V	1.0	...	150.	4.051 ± 0.018	0.166 ± 0.038	CG 22 Assn.	
2MASS J08264387-3420129	1 K3.5V	1.0	24.82 ± 0.96	39.8 ± 1.7	-0.219 ± 0.027	141 ± 12	0.243 ± 0.020	...	CG 22 Assn.	
PH α 92	1 K3V	1.0	20.09 ± 0.92	32.5 ± 1.9	-32.293 ± 0.012	575 ± 12	0.157 ± 0.016	0.933 ± 0.075	CG 22 Assn.	
HD 71269	1 B9V	1.0	19.2 ± 7.5	106 ± 13	4.301 ± 0.015	...	0.0100 ± 0.0087	0.001 ± 0.044	CG 22 Assn.	
235 HD 65445	1 A4V	2.0	...	102 ± 19	4.198 ± 0.020	0.024 ± 0.043	Yep 1	
TYC 8134-3161-1	1 F1V	1.0	18.8 ± 2.7	41.5 ± 3.1	2.430 ± 0.021	...	0.087 ± 0.018	0.104 ± 0.040	Yep 1	
TYC 8142-1542-1	1 F7V	1.0	20.76 ± 0.36	35.8 ± 2.6	1.965 ± 0.015	...	0.0832 ± 0.0088	0.082 ± 0.039	Yep 1	
2MASS J08062540-4733310	1 K1V	2.0	21.53 ± 0.34	26.03 ± 0.94	-0.142 ± 0.016	45 ± 12	0.367 ± 0.019	...	Yep 1	
TYC 8133-155-1	1 G0V	1.0	18.97 ± 0.76	45.1 ± 3.0	1.457 ± 0.028	...	0.089 ± 0.028	0.074 ± 0.042	Yep 1	
2MASS J07513612-4601216	1 K2V	1.0	20.2 ± 1.0	28.6 ± 1.7	SB1	-0.454 ± 0.031	133 ± 12	0.108 ± 0.040	...	Yep 1
2MASS J07520153-4850080	1 G0V	1.0	20.9 ± 1.0	49.7 ± 5.6	2.030 ± 0.031	...	0.036 ± 0.028	...	Yep 1	
HD 63254	1 A0V	1.0	...	150.	4.256 ± 0.026	...	0.236 ± 0.038	Yep 1		

Table C.1—Continued

Star Name	Epoch	Spectral Type	Class	v_r (km s $^{-1}$)	$v_{\text{rot}} \sin(i)$ (km s $^{-1}$)	Binary Flag	H α EW (Å)	H α 10% W (km s $^{-1}$)	Li EW (Å)	Infrared Excess (mag)	Assn. Name
TYC 8135-4862-1	1	A3V	2.0	...	150.	3.783 ± 0.028	0.103 ± 0.046	Yep 1	
TYC 8139-2616-1	1	F2V	1.0	21.1 ± 1.4	63.6 ± 6.4	1.170 ± 0.017	...	0.027 ± 0.018	0.152 ± 0.035	Yep 1	
2MASS J07541482-4626003	1	K2.5V	1.0	21.30 ± 0.40	19.11 ± 0.80	-26.482 ± 0.023	451 ± 12	0.255 ± 0.018	
2MASS J07513612-4601216	2	K2V	1.0	47.3 ± 1.2	27.6 ± 2.5	SB1	-0.454 ± 0.031	133 ± 12	0.108 ± 0.040	...	Yep 1
TYC 8133-1754-1	1	F3.5V	1.0	19.47 ± 0.80	44.5 ± 5.8	2.864 ± 0.019	...	0.010 ± 0.018	Yep 1
TYC 8133-1522-1	1	G8V	1.5	17.5 ± 1.6	62.8 ± 4.1	1.418 ± 0.029	...	0.143 ± 0.021	0.	...	Yep 1
HD 63579	1	B5V	3.0	-14.1 ± 6.6	58 ± 12	SB1?	4.264 ± 0.023	...	0.010 ± 0.015	0.018 ± 0.054	Yep 1
HD 64699	1	A1V	1.0	4.304 ± 0.019	0.025 ± 0.034	...	Yep 1
HD 64780	1	A0V	1.0	...	150.	4.370 ± 0.026	0.074 ± 0.037	Yep 1	
CD-46 3471	1	A1V	1.0	17.4 ± 5.4	150.	3.444 ± 0.027	± 0.0061	0.171 ± 0.033	Yep 1
2MASS J07592987-4839424	1	G3V	2.0	23.35 ± 0.10	4.2 ± 1.1	1.779 ± 0.013	...	0.0527 ± 0.0052	Yep 1
TYC 8134-2250-1	1	A0V	2.0	...	150.	4.001 ± 0.020	Yep 1
TYC 8134-2250-2	1	A4V	1.0	...	30. ± 36	3.467 ± 0.013	-0.200 ± 0.041	Yep 1	

Table C.1—Continued

Star Name	Epoch	Spectral Type	Class	v_r (km s $^{-1}$)	$v_{\text{rot}} \sin(i)$ (km s $^{-1}$)	Binary Flag	H α EW (Å)	H α 10% W (km s $^{-1}$)	Li EW (Å)	Infrared Excess (mag)	Assn. Name	
TYC 8138-2569-1	1	A6.5V	1.0	19.8 ± 2.4	52.6 ± 6.9	2.633 ± 0.017	...	0.073 ± 0.012	Yep 1	
TYC 8134-1929-1	1	A3V	1.0	18.0 ± 3.5	46	4.049 ± 0.020	...	0.0152 ± 0.0056	0.062 ± 0.035	...	Yep 1	
CD-483205	1	A2V	1.0	20.1 ± 3.5	44 ± 28	4.273 ± 0.018	...	0.0100 ± 0.0033	0.194 ± 0.042	...	Yep 1	
2MASS J07491846-4657432	1	A6V	1.0	16.7 ± 3.7	8 ± 31	3.288 ± 0.023	...	0.0186 ± 0.0047	Yep 1	
HD 64759	1	A2V	3.0	4.260 ± 0.020	0.047 ± 0.061	...	Yep 1	
TYC 8138-2304-1	1	G9V	2.0	...	8.5 ± 2.1	1.16 ± 0.70	0.002 ± 0.058	...	Yep 1	
TYC 8134-2159-1	1	F5V	1.0	23.1 ± 2.0	72.3 ± 8.6	2.882 ± 0.031	...	0.091 ± 0.025	0.000 ± 0.038	...	Yep 1	
HD 64248	1	B9V	2.0	...	150.	3.430 ± 0.021	-0.003 ± 0.054	...	Yep 1	
HD 64318	1	B5V	2.0	101.9 ± 7.2	57 ± 12	SB1?	2.2557 ± 0.0096	...	0.010 ± 0.012	0.040 ± 0.034	...	Yep 1
HD 64578	1	B8V	1.0	13.5 ± 4.1	63.4 ± 8.5	SB1?	3.616 ± 0.016	-0.004 ± 0.040	...	Yep 1
HD 64461	1	A1V	1.0	...	150.	3.787 ± 0.021	0.227 ± 0.041	Yep 1
HD 65658	1	B5V	2.0	-42.0 ± 5.2	56 ± 13	SB1?	2.573 ± 0.012	...	0.010 ± 0.012	0.024 ± 0.047	...	Yep 1
HD 66191	1	A1V	1.0	...	150.	4.106 ± 0.020	0.063 ± 0.034	Yep 1

Table C.1—Continued

Star Name	Spectral Type	Class	v_r	$v_{\text{rot}} \sin(i)$ (km s $^{-1}$)	Binary Flag	H α EW (Å)	H α 10% W (km s $^{-1}$)	Li EW (Å)	Infrared Excess (mag)	Assn. Name
2MASS J07501009-4720325	1 K3V	1.0	20.53 ± 0.25	4.00 ± 0.64	-0.627 ± 0.030	117 ± 12	0.381 ± 0.021	Yep 1
2MASS J07501518-4616033	1 G0V	1.0	19.50 ± 0.16	8.3 ± 6.1	2.264 ± 0.022	...	0.123 ± 0.011	Yep 1
2MASS J07502910-4757434	1 K1V	2.0	14.0 ± 3.1	58.7 ± 5.6	SB1?	-0.0154 ± 0.0095	13 ± 12	0.065 ± 0.038
CD-483192	1 F0V	1.0	20.2 ± 2.3	20. ± 12	4.087 ± 0.014	...	0.0100 ± 0.0048	0.086 ± 0.038	...	Yep 1
TYC 8138-168-1	1 A5V	2.0	20.1 ± 2.6	86 ± 18	4.248 ± 0.019	...	0.019 ± 0.013	0.080 ± 0.045	...	Yep 1
HD 67418	1 F1V	1.0	19.1 ± 1.9	74.3 ± 4.8	3.904 ± 0.027	0.008 ± 0.042	...	Yep 1
2MASS J07463583-4453183	1 G7V	1.0	22.18 ± 0.78	34.3 ± 2.5	0.102 ± 0.016	...	0.195 ± 0.016
QSPup	1 B3V	3.0	37.1 ± 8.9	57 ± 14	SB1?	1.930 ± 0.010	-0.010 ± 0.074	...
2MASS J07540255-4608574	1 G1V	1.0	19.52 ± 0.49	29.0 ± 1.0	0.29 ± 0.50	267 ± 12	0.035 ± 0.022
TYC 8142-1598-1	1 F2V	1.0	19.7 ± 2.8	87.1 ± 4.9	3.821 ± 0.016	...	0.0100 ± 0.0039	0.024 ± 0.039
TYC 8138-2890-1	1 K1V	1.0	20.81 ± 0.21	21.69 ± 0.92	0.13 ± 0.50	...	0.3118 ± 0.0089	0.106 ± 0.041
TYC 8138-3251-1	1 A1V	1.0	...	150.	4.149 ± 0.019	0.141 ± 0.036
TYC 8139-3353-1	1 G1V	1.0	22.70 ± 0.95	64.8 ± 3.5	0.820 ± 0.012	...	0.055 ± 0.020	0.121 ± 0.038

Table C.1—Continued

Star Name	Spectral Type	Epoch	Class Uncert.	v_r (km s $^{-1}$)	$v_{\text{rot}} \sin(i)$ (km s $^{-1}$)	Binary Flag	H α EW (Å)	H α 10% W (km s $^{-1}$)	Li EW (Å)	Infrared Excess (mag)	Assn. Name
TYC 8135-458-1	F1V	1	1.0	26.8 ± 2.2	23 ± 11	SBI?	3.9715 ± 0.0089	...	0.010 ± 0.012	0.041 ± 0.040	Yep 1
HD 65167	A3V	1	1.0	...	110.		4.294 ± 0.013	-0.023 ± 0.037	Yep 1
TYC 8139-4265-1	A7V	1	2.0	17.7 ± 2.5	90. ± 14		3.806 ± 0.016	...	0.0100 ± 0.0035	0.070 ± 0.043	Yep 1
2MASS J07522717-4758074	K1V	1	1.0	16.04 ± 0.29	4.0 ± 1.5		1.28 ± 0.60	...	0.055 ± 0.021	...	Yep 1
2MASS J07520589-4822321	K3.5V	1	1.0	17.8 ± 1.4	16.8 ± 2.8		-0.731 ± 0.026	46 ± 12	0.197 ± 0.032	...	Yep 1
HD 63869	A0V	1	2.0	...	150.		3.850 ± 0.014	-0.137 ± 0.057	Yep 1
2MASS J07494943-4614155	K0V	1	3.0	96.2 ± 2.4	8.5 ± 2.3	SBI?	0.04 ± 0.54	63 ± 12	0.02 ± 0.32	...	Yep 1
2MASS J07510378-4532244	K2V	1	4.0	...	5.7 ± 3.1		-1.648 ± 0.095	95 ± 12	Yep 1
TYC 8139-589-1	F2V	1	1.0	20.5 ± 8.2	97 ± 13		3.529 ± 0.027	...	0.012 ± 0.019	0.055 ± 0.040	Yep 1
2MASS J07542550-4651134	G4V	1	1.0	19.49 ± 0.59	30.77 ± 0.95		-0.052 ± 0.012	21 ± 12	0.165 ± 0.024	...	Yep 1
TYC 8139-2296-1	F2V	1	2.0	21.6 ± 3.3	87.7 ± 4.4		2.906 ± 0.023	...	0.067 ± 0.019	0.016 ± 0.047	Yep 1
2MASS J07595002-4901523	F5.5V	1	1.0	21.54 ± 0.18	17.2 ± 1.8		2.541 ± 0.021	...	0.116 ± 0.012	...	Yep 1
TYC 8134-2633-1	F7V	1	1.0	23.01 ± 0.87	48.3 ± 3.0		2.196 ± 0.020	...	0.010 ± 0.022	0.023 ± 0.037	Yep 1

Table C.1—Continued

Star Name	Spectral Type	Epoch	Class Uncert.	v_r (km s $^{-1}$)	$v_{\text{rot}} \sin(i)$ (km s $^{-1}$)	Binary Flag	H α EW (Å)	H α 10% W (km s $^{-1}$)	Li EW (Å)	Infrared Excess (mag)	Assn. Name
HD 65894	A2V	1	1.0	...	150.		4.266 ± 0.023	0.056 ± 0.038	Yep 2
TYC 8138-2794-1	A2V	1	1.0	...	150.		4.000 ± 0.030	0.128 ± 0.036	Yep 2
2MASS J08023538-4848048	G6.5V	2.0	18.60 ± 0.29	16.94 ± 0.56		-0.120 ± 0.011	27 ± 12	0.315 ± 0.016	...	-0.003 ± 0.055	Yep 2
HD 65774	B9V	2.0		3.690 ± 0.017
2MASS J08042347-4938219	K3V	1.0	21.21 ± 0.56	13.2 ± 1.0		-0.177 ± 0.022	47 ± 12	0.358 ± 0.020	...	-0.003 ± 0.055	Yep 2
2MASS J07560331-4910495	G8V	1.0	20.74 ± 0.17	8.4 ± 1.4		1.507 ± 0.027	...	0.167 ± 0.012	...	-0.003 ± 0.055	Yep 2
2MASS J07573369-5015153	G6.5V	1.5	58.74 ± 0.10	4.00 ± 0.83	SB1?	1.187 ± 0.020	...	0.0323 ± 0.0091	...	-0.003 ± 0.055	Yep 2
HD 67129	A5V	2.0		4.449 ± 0.021	0.018 ± 0.045
2MASS J08183357-4924140	K0V	3.0	...	40.5 ± 6.3		0.79 ± 0.30
HD 63364	B9V	2.0		3.834 ± 0.022	0.001 ± 0.052
HD 66005	B2V	2.0		2.028 ± 0.014	0.005 ± 0.067
2MASS J07554620-4712483	K2V	2.0	8.6 ± 1.1	38.4 ± 2.2	SB1?	0.853 ± 0.035	...	0.098 ± 0.026
HD 65335	A1V	2.0	19.7 ± 8.3	43 ± 37		4.009 ± 0.012	...	0.010 ± 0.014	0.046 ± 0.051

Table C.1—Continued

Star Name	Epoch	Spectral Type	Class	v_r (km s $^{-1}$)	$v_{\text{rot}} \sin(i)$ (km s $^{-1}$)	Binary Flag	H α EW (Å)	H α 10% W (km s $^{-1}$)	Li EW (Å)	Infrared Excess (mag)	Assn. Name
HD 66006	1	B3V	3.0	...	51 ± 20.	2.054 ± 0.013	-0.025 ± 0.075	Yep 2	
2MASS J08065006-4732219	1	K5V	1.0	10.79 ± 0.28	4.00 ± 0.90	SB1?	1.073 ± 0.011	...	0.011 ± 0.015	...	Yep 2
2MASS J08094262-5002238	1	G5V	2.0	21.91 ± 0.91	51.3 ± 2.3	-0.0078 ± 0.0037	4 ± 12	0.010 ± 0.026	Yep 2
TYC 8144-2888-1	1	F5V	1.0	21.82 ± 0.72	41.9 ± 1.9	2.047 ± 0.023	...	0.010 ± 0.022	Yep 2
CD-493158	1	A3V	3.0	...	150.	4.295 ± 0.022	0.047 ± 0.055	...	Yep 2
HD 66971	1	A0V	1.0	4.063 ± 0.018	-0.059 ± 0.044	...	Yep 2
TYC 8143-2619-1	1	F2V	2.0	26.03 ± 0.32	23.4 ± 1.7	SB1?	3.258 ± 0.019	...	0.0137 ± 0.0075	0.003 ± 0.050	Yep 2
2MASS J07541099-4945078	1	K1V	1.0	26.84 ± 0.25	5.7 ± 2.2	SB1?	0.89 ± 0.40	13 ± 49	0.010 ± 0.065	...	Yep 2
2MASS J07371850-4850279	1	K2V	1.0	33.69 ± 0.16	4.0 ± 1.5	SB1?	0.53 ± 0.80	20. ± 12	Yep 2
HD 65729	1	B8V	1.0	...	105 ± 12	4.256 ± 0.016	0.086 ± 0.044	...	Yep 2
CD-483350	1	A0V	1.0	...	144	4.100 ± 0.024	0.029 ± 0.038	...	Yep 2
2MASS J08000812-4533201	1	G1V	1.0	37.59 ± 0.13	9.3 ± 5.8	SB1?	1.077 ± 0.017	...	0.2318 ± 0.0087	...	Yep 2
TYC 7671-4253-1	1	F1V	2.0	22.4 ± 2.1	71.2 ± 4.6	3.161 ± 0.018	...	0.0100 ± 0.0042	0.018 ± 0.045	...	Yep 2

Table C.1—Continued

Star Name	Spectral Type	Epoch	Class Uncert.	v_r (km s $^{-1}$)	$v_{\text{rot}} \sin(i)$ (km s $^{-1}$)	Binary Flag	H α EW (Å)	H α 10% W (km s $^{-1}$)	Li EW (Å)	Infrared Excess (mag)	Assn. Name
TYC 8134-586-1	F6V	1	1.0	21.07 ± 0.73	55.4 ± 2.6	1.309 ± 0.015	...	0.071 ± 0.014	0.218 ± 0.039	Yep 2	
CD-443740	A6V	1	2.0	20.1 ± 4.8	58 ± 22	4.212 ± 0.018	...	0.0100 ± 0.0039	-0.027 ± 0.044	Yep 2	
HD 69404	B2V	1	3.0	...	150. ± 11	-6.826 ± 0.013	685 ± 13	...	0.340 ± 0.071	Yep 2	
TYC 8143-1918-1	G5V	1	2.0	21.8 ± 1.5	48.4 ± 6.6	1.277 ± 0.026	...	0.010 ± 0.027	0.081 ± 0.036	Yep 2	
2MASS J08040005-4954589	G9V	1	5.0	-53.0 ± 4.0	5.6 ± 2.1	SB1?	0.22 ± 0.51	...	0.133 ± 0.049	...	Yep 2
KWVel	B9V	1	2.0	...	150.	3.023 ± 0.014	-0.026 ± 0.055	Yep 2	
TYC 8138-167-1	F0V	1	1.0	18.0 ± 2.6	44.5 ± 3.4	3.856 ± 0.016	...	0.0100 ± 0.0029	0.086 ± 0.042	Yep 2	
2MASS J07514674-4607038	G6.5V	1	1.0	22.92 ± 0.22	21.63 ± 0.68	0.0253 ± 0.0076	...	0.097 ± 0.013	...	Yep 2	
2MASS J07492170-4630304	G7V	1	1.0	22.54 ± 0.72	39.6 ± 1.3	1.734 ± 0.018	...	0.052 ± 0.014	...	Yep 2	
2MASS J07421676-4824037	K1V	1	1.0	19.85 ± 0.25	16.5 ± 1.2	-0.152 ± 0.011	35 ± 12	0.309 ± 0.013	...	Yep 2	
2MASS J07471652-4931414	G6V	1	1.0	17.41 ± 0.45	25.86 ± 0.91	0.86 ± 0.50	...	0.316 ± 0.023	...	Yep 2	
2MASS J07470563-4757394	G9V	1	1.0	21.34 ± 0.53	22.01 ± 0.87	0.552 ± 0.014	...	0.298 ± 0.014	...	Yep 2	
2MASS J07564756-4751454	G1V	1	1.0	20.05 ± 0.31	27.9 ± 1.7	1.911 ± 0.018	...	0.079 ± 0.011	...	Yep 2	

Table C.1—Continued

Star Name	Spectral Type	Epoch	Class Uncert.	v_r (km s $^{-1}$)	$v_{\text{rot}} \sin(i)$ (km s $^{-1}$)	Binary Flag	H α EW (Å)	H α 10% W (km s $^{-1}$)	Li EW (Å)	Infrared Excess (mag)	Assn. Name
2MASS J07580565-4913120	K2.5V	2.0	21.38 ± 0.24	6.73 ± 0.82	-0.328 ± 0.013	58 ± 12	0.293 ± 0.014	Yep 2	
2MASS J08012725-4940216	K1V	1.0	24.9 ± 1.6	53.0 ± 2.3	-0.063 ± 0.011	27 ± 12	0.373 ± 0.032	Yep 2	
2MASS J08034730-4913353	G6V	1.0	19.92 ± 0.35	23.40 ± 0.61	-0.1249 ± 0.0081	30. ± 12	0.330 ± 0.012	Yep 2	
2MASS J07502381-4659290	F7V	3.0	21.65 ± 0.66	47.9 ± 3.8	2.216 ± 0.014	...	0.085 ± 0.010	Yep 2	
TYC 8143-2246-1	F4V	1.0	22.22 ± 0.98	54.0 ± 4.0	3.220 ± 0.014	...	0.0147 ± 0.0039	0.059 ± 0.039	0.059 ± 0.039	Yep 2	
TYC 8144-1249-1	A2	1.0	...	1116	3.677 ± 0.016	0.110 ± 0.040	Yep 2	
2MASS J07593159-4820134	K2V	1.0	21.44 ± 0.39	22.7 ± 1.1	-0.458 ± 0.013	66 ± 12	0.279 ± 0.033	Yep 2	
2MASS J08391713-5230129	K1V	1.0	18.15 ± 0.29	8.9 ± 1.5	0.68 ± 0.40	13 ± 12	0.148 ± 0.019	Yep 3	
TYC 8162-1365-1	G2V	1.0	20.43 ± 0.24	21.7 ± 1.0	1.901 ± 0.024	...	0.160 ± 0.014	-0.016 ± 0.040	-0.016 ± 0.040	Yep 3	
TYC 8163-1479-1	A8V	2.0	17.6 ± 2.2	80.6 ± 5.1	3.333 ± 0.022	...	0.011 ± 0.018	0.080 ± 0.044	0.080 ± 0.044	Yep 3	
TYC 8163-165-1	F6V	1.0	18.45 ± 0.33	30.7 ± 1.8	2.405 ± 0.017	...	0.076 ± 0.012	0.009 ± 0.042	0.009 ± 0.042	Yep 3	
OOVel	A0V	1.0	...	58	3.191 ± 0.014	-0.053 ± 0.040	-0.053 ± 0.040	Yep 3	
2MASS J08434121-5200235	K2V	1.0	55.81 ± 0.21	4.5 ± 1.4	SBI?	0.81 ± 0.50	25 ± 12	Yep 3

Table C.1—Continued

Star Name	Epoch	Spectral Type	Class Uncert.	v_r (km s $^{-1}$)	$v_{\text{rot}} \sin(i)$ (km s $^{-1}$)	Binary Flag	H α EW (Å)	H α 10% W (km s $^{-1}$)	Li EW (Å)	Infrared Excess (mag)	Assn. Name
TYC 8163-2131-1	1	F6V	3.0	-10.15 ± 0.95	37.6 ± 2.8	SBI?	1.190 ± 0.021	...	0.094 ± 0.012	0.195 ± 0.061	Yep 3
2MASS J08291213-5053273	1	K0V	2.0	20.03 ± 0.32	11.7 ± 2.1	1.02 ± 0.75	...	0.106 ± 0.032	Yep 3
HD 70718	1	A1V	3.0	...	150. ± 49	4.335 ± 0.013	0.103 ± 0.069	...	Yep 3
HD 71003	1	A0V	3.0	...	150.	4.412 ± 0.017	-0.013 ± 0.067	...	Yep 3
2MASS J08590528-5534151	1	G5V	1.5	15.40 ± 0.19	23.58 ± 0.82	1.725 ± 0.019	...	0.166 ± 0.012	Yep 3
2MASS J08391280-5107385	1	G9V	1.0	19.99 ± 0.31	8.3 ± 1.1	-0.286 ± 0.021	35 ± 12	0.173 ± 0.021	Yep 3
TYC 8568-2409-1	1	G0V	1.0	19.63 ± 0.19	15.5 ± 1.6	2.118 ± 0.020	...	0.131 ± 0.010	-0.089 ± 0.041	...	Yep 3
TYC 8569-2369-1	1	F3.5	2.0	17.67 ± 0.76	41.1 ± 4.8	3.409 ± 0.013	...	0.0100 ± 0.0057	Yep 3
2MASS J08494919-5305532	1	G5V	1.0	18.19 ± 0.32	11.84 ± 0.83	1.338 ± 0.056	...	0.133 ± 0.016	Yep 3
2MASS J08450857-5313397	1	K1V	1.0	18.04 ± 0.14	4.0 ± 1.6	1.586 ± 0.029	...	0.131 ± 0.013	Yep 3
HD 72163	1	A1V	1.0	...	150.	4.462 ± 0.019	0.008 ± 0.032	...	Yep 3
2MASS J08492498-5332383	1	K2.5V	1.0	5.63 ± 0.26	4.00 ± 0.74	SBI?	0.305 ± 0.031	...	0.140 ± 0.019	...	Yep 3
2MASS J08292489-5039483	1	F1V	4.0	24.0 ± 2.8	87.7 ± 3.9	SBI?	1.941 ± 0.032	...	0.055 ± 0.028	...	Yep 3

Table C.1—Continued

Star Name	Epoch	Spectral Type	Class	v_r (km s $^{-1}$)	$v_{\text{rot}} \sin(i)$ (km s $^{-1}$)	Binary Flag	H α EW (Å)	H α 10% W (km s $^{-1}$)	Li EW (Å)	Infrared Excess (mag)	Assn. Name
HD 73387	1	A2V	1.0	15.4 ± 7.4	150.	4.364 ± 0.020	± 0.0038	0.043 ± 0.036	Yep 3
HD 76901	1	A2V	2.0	...	60.	4.329 ± 0.014	-0.043 ± 0.052	...	Yep 3
TYC 8590-874-1	1	F6V	1.0	16.89 ± 0.53	38.0 ± 2.3	2.496 ± 0.017	...	0.069 ± 0.012	-0.059 ± 0.042	...	Yep 3
2MASS J08334968-5142593	1	F8V	2.0	16.7 ± 1.9	46 ± 10.	1.744 ± 0.028	...	0.082 ± 0.026	Yep 3
CD-552380	1	A2V	3.0	...	150.	4.219 ± 0.017	0.070 ± 0.060	...	Yep 3
TYC 8586-1678-1	1	F6V	1.0	22.22 ± 0.15	12.7 ± 4.8	2.457 ± 0.014	...	0.0592 ± 0.0057	0.043 ± 0.038	...	Yep 3
2MASS J08563299-5526077	1	G1V	2.0	17.39 ± 0.38	30.2 ± 1.5	1.048 ± 0.026	...	0.143 ± 0.018	Yep 3
2MASS J08295658-5111456	1	K0V	2.0	18.4 ± 3.0	82.3 ± 7.5	-0.053 ± 0.014	22 ± 12	0.200 ± 0.047	Yep 3
2MASS J08342423-5348191	1	G1V	1.0	18.82 ± 0.17	15.9 ± 1.3	1.201 ± 0.028	...	0.192 ± 0.014	Yep 3
2MASS J08343731-5024508	1	K2V	1.0	19.14 ± 0.42	21.5 ± 1.2	-0.117 ± 0.019	31 ± 12	0.248 ± 0.026	Yep 3
2MASS J08352943-5148546	1	F8V	1.0	19.90 ± 0.42	31.5 ± 1.8	2.259 ± 0.029	...	0.054 ± 0.012	Yep 3
TYC 8153-960-1	1	F5V	3.0	21.0 ± 2.2	77.8 ± 4.1	3.274 ± 0.020	...	0.032 ± 0.016	-0.054 ± 0.070	...	Yep 3
HD 70977	1	A9V	2.0	19.3 ± 2.0	87.1 ± 3.1	3.825 ± 0.018	...	0.0112 ± 0.0044	0.022 ± 0.049	...	Yep 3

Table C.1—Continued

Star Name	Spectral Type	Class	v_r	$v_{\text{rot}} \sin(i)$ (km s $^{-1}$)	Binary Flag	H α EW (Å)	H α 10% W (km s $^{-1}$)	Li EW (Å)	Infrared Excess (mag)	Assn. Name
2MASS J08253727-4912497	1 K2V	1.0	21.72 ± 0.29	16.86 ± 0.98		1.35 ± 0.70	20. ± 12	0.191 ± 0.020	...	Yep 3
TYC 8158-2342-1	1 F7V	2.0	20.34 ± 0.41	35.8 ± 2.9		2.256 ± 0.022	...	0.053 ± 0.014	0.062 ± 0.051	Yep 3
HD 74056	1 A2V	3.0	...	150.		4.161 ± 0.016	0.063 ± 0.062	Yep 3
HD 73105	1 B3V	2.0		2.612 ± 0.011	0.043 ± 0.061	Yep 3
TYC 8568-2056-1	1 F6V	1.0	10.06 ± 0.72	40.7 ± 2.8	SB1?	2.274 ± 0.022	...	0.044 ± 0.015	0.072 ± 0.039	Yep 3
2MASS J08393055-5128330	1 K1V	1.0	20.02 ± 0.57	7.5 ± 1.8		0.65 ± 0.50	...	0.149 ± 0.018	...	Yep 3
2MASS J08414215-5206204	1 K1V	1.0	19.51 ± 0.31	15.4 ± 1.2		1.153 ± 0.038	...	0.222 ± 0.019	...	Yep 3
2MASS J08415930-5210337	1 K1V	1.0	19.25 ± 0.15	6.4 ± 1.7		1.153 ± 0.030	...	0.202 ± 0.015	...	Yep 3
2MASS J08373864-5100031	1 G9V	2.0	...	52.3 ± 8.7		-0.120 ± 0.020	46 ± 12	Yep 3
TYC 8163-1809-1	1 F8V	1.0	12.06 ± 0.16	14.2 ± 7.5	SB1?	2.059 ± 0.026	...	0.126 ± 0.010	0.058 ± 0.038	Yep 3
TYC 8163-2765-1	1 G0V	1.0	40.54 ± 0.15	6.2 ± 6.0	SB1?	1.997 ± 0.019	...	0.1130 ± 0.0095	-0.035 ± 0.042	Yep 3
CD-50 3414	1 A5V	1.0	19.7 ± 2.1	97 ± 28		3.411 ± 0.022	...	0.0100 ± 0.0046	0.094 ± 0.034	Yep 3
TYC 8162-333-1	1 F5.5V	1.0	19.73 ± 0.58	35.0 ± 1.2		2.153 ± 0.025	...	0.035 ± 0.027	...	Yep 3

Table C.1—Continued

Star Name	Epoch	Spectral Type	Class	v_r (km s $^{-1}$)	$v_{\text{rot}} \sin(i)$ (km s $^{-1}$)	Binary Flag	H α EW (Å)	H α 10% W (km s $^{-1}$)	Li EW (Å)	Infrared Excess (mag)	Assn. Name
2MASS J08192677-4910015	1	K2V	1.0	20.82 ± 0.18	11.9 ± 1.1	0.72 ± 0.40	...	0.187 ± 0.013	Yep 3
CD-513115	1	A7V	2.0	16.0 ± 3.9	94 ± 12	3.851 ± 0.019	...	0.0100 ± 0.0045	0.060 ± 0.045	...	Yep 3
2MASS J08411381-5226547	1	G2V	1.0	18.44 ± 0.15	9.7 ± 6.2	1.517 ± 0.024	...	0.184 ± 0.011	Yep 3
2MASS J08361270-5152216	1	G6V	1.0	19.81 ± 0.19	10.53 ± 0.68	1.443 ± 0.022	...	0.173 ± 0.011	Yep 3
2MASS J08404809-5122340	1	G0.5V	1.0	19.54 ± 0.16	17.7 ± 1.1	1.835 ± 0.017	...	0.1326 ± 0.0087	Yep 3
2MASS J08362653-4940342	1	G0V	1.0	19.39 ± 0.14	7.6 ± 6.9	1.909 ± 0.016	...	0.0650 ± 0.0076	Yep 3
2MASS J08443526-5234117	1	K0V	2.0	18.95 ± 0.46	26.8 ± 1.1	SB2?	0.89 ± 0.40	...	0.160 ± 0.014	...	Yep 3
TYC 8569-3283-1	1	F5V	1.0	18.52 ± 0.36	36.5 ± 2.5	2.227 ± 0.015	...	0.035 ± 0.011	0.035 ± 0.038	...	Yep 3
HD 73951	1	A0V	3.0	4.155 ± 0.012	0.015 ± 0.070	...	Yep 3
2MASS J08395173-5155070	1	G3V	3.0	11.2 ± 1.8	17.8 ± 5.9	SB1?	1.09 ± 0.70	...	0.010 ± 0.089	...	Yep 3
2MASS J08441148-4943405	1	G7V	3.0	27.8 ± 3.1	9.8 ± 4.3	SB1?	0.22 ± 0.51	...	0.01 ± 0.15	...	Yep 3
TYC 8163-1937-1	1	G6.5V	1.0	30.93 ± 0.21	9.65 ± 0.67	SB1?	1.11 ± 0.40	...	0.142 ± 0.011	...	Yep 3
TYC 8568-1105-1	1	F1V	1.0	18.4 ± 2.1	90.6 ± 4.1	2.984 ± 0.022	...	0.0160 ± 0.0060	0.043 ± 0.040	...	Yep 3

Table C.1—Continued

Star Name	Spectral Type	Class	v_r	$v_{\text{rot}} \sin(i)$ (km s $^{-1}$)	Binary Flag	H α EW (Å)	H α 10% W (km s $^{-1}$)	Li EW (Å)	Infrared Excess (mag)	Assn. Name
TYC 8158-1304-1	1 F6V	1.0	20.32 ± 0.15	14.6 ± 1.8	1.882 ± 0.019	...	0.1355 ± 0.0097	0.079 ± 0.038	Yep 3	
2MASS J08250239-4947563	1 K0V	1.0	18.41 ± 0.31	17.7 ± 1.0	SB1?	-0.068 ± 0.013	27 ± 12	0.154 ± 0.015	...	UPK 535
HD 69991	1 A2V	1.0	...	129	4.216 ± 0.018	-0.005 ± 0.037	UPK 535	
2MASS J08302738-5109146	1 K3V	1.0	10.27 ± 0.30	8.8 ± 1.1	-0.352 ± 0.025	57 ± 12	0.286 ± 0.028	...	UPK 535	
2MASS J08243944-5215091	1 K1V	1.0	10.14 ± 0.19	13.1 ± 1.0	0.17 ± 0.50	...	0.199 ± 0.016	...	UPK 535	
2MASS J08374576-4954367	1 K2V	1.0	10.32 ± 0.26	10.5 ± 1.2	0.25 ± 0.50	...	0.269 ± 0.019	...	UPK 535	
TYC 8162-73-1	1 A6V	1.0	4.2 ± 1.7	39 ± 15	SB1?	2.980 ± 0.015	...	0.0423 ± 0.0077	0.130 ± 0.033	UPK 535
CD-483672	1 A4V	1.0	8.7 ± 4.0	11.3 ± 36	3.554 ± 0.021	...	0.029 ± 0.015	0.116 ± 0.040	UPK 535	
2MASS J08323887-5226451	1 K1V	1.0	9.75 ± 0.14	7.3 ± 2.0	0.967 ± 0.028	...	0.202 ± 0.013	...	UPK 535	
2MASS J08212561-5150507	1 G7V	1.0	52.34 ± 0.33	5.6 ± 1.2	SB1	0.93 ± 0.60	31 ± 12	0.193 ± 0.014	...	UPK 535
2MASS J08364848-5113573	1 K2V	2.0	0.5 ± 2.2	10.6 ± 2.3	SB1?	-0.363 ± 0.021	39 ± 12	0.224 ± 0.072	...	UPK 535
2MASS J08292220-5050369	1 K2V	2.0	...	150. ± 20.	1.294 ± 0.067	UPK 535	
2MASS J08301848-5101345	1 G9V	1.0	13.3 ± 1.8	86.7 ± 4.3	1.404 ± 0.041	...	0.0204 ± 0.0084	...	UPK 535	

Table C.1—Continued

Star Name	Spectral Type	Class	v_r	$v_{\text{rot}} \sin(i)$ (km s $^{-1}$)	Binary Flag	H α EW (Å)	H α 10% W (km s $^{-1}$)	Li EW (Å)	Infrared Excess (mag)	Assn. Name
2MASS J08382678-5359285	1 G3V	2.0	9.30 ± 0.28	14.7 ± 2.6	2.268 ± 0.037	...	0.083 ± 0.025	UPK 535
HD 73464	1 A0.5V	1.0	...	150.	4.288 ± 0.014	UPK 535
HD 72857	1 A1V	1.0	...	150.	4.242 ± 0.022	0.032 ± 0.086	...	UPK 535
CD-50 3373	1 A3V	1.0	...	150.	3.657 ± 0.022	0.100 ± 0.037	...	UPK 535
2MASS J08301902-5101316	1 G0V	2.0	11.9 ± 1.6	73.9 ± 4.6	1.493 ± 0.029	...	0.030 ± 0.010	UPK 535
HD 71969	1 B9V	1.0	...	150.	3.740 ± 0.026	0.039 ± 0.045	...	UPK 535
2MASS J08280595-4957545	1 K3.5V	1.5	5.7 ± 1.7	34.2 ± 3.8	-0.765 ± 0.016	73 ± 12	0.010 ± 0.045	UPK 535
2MASS J08212561-5150507	2 G7V	1.0	-1.03 ± 0.22	7.24 ± 0.62	SB1	0.93 ± 0.60	31 ± 12	0.193 ± 0.014	...	UPK 535
2MASS J08351629-5156166	1 G9V	2.0	...	150.0 ± 6.1	0.98 ± 0.50	UPK 535
TYC 8162-1117-1	1 F7V	1.0	10.04 ± 0.22	16.7 ± 1.8	2.061 ± 0.022	...	0.121 ± 0.012	0.031 ± 0.033	...	UPK 535
TYC 8162-956-1	1 F7V	1.0	10.20 ± 0.30	25.9 ± 2.5	1.552 ± 0.027	...	0.102 ± 0.012	0.083 ± 0.033	...	UPK 535
TYC 8568-260-1	1 F6V	1.0	9.21 ± 0.72	44.9 ± 2.0	2.501 ± 0.018	...	0.034 ± 0.019	0.043 ± 0.043	...	UPK 535
TYC 8568-293-1	1 F7V	1.0	10.97 ± 0.25	27.7 ± 2.4	2.037 ± 0.021	...	0.060 ± 0.010	0.134 ± 0.036	...	UPK 535

Table C.1—Continued

Star Name	Epoch	Spectral Type	Class	v_r (km s $^{-1}$)	$v_{\text{rot}} \sin(i)$ (km s $^{-1}$)	Binary Flag	H α EW (Å)	H α 10% W (km s $^{-1}$)	Li EW (Å)	Infrared Excess (mag)	Assn. Name
TYC 8568-298-1	1	F4V	1.0	8.53 ± 0.45	37.5 ± 2.5	2.328 ± 0.019	...	0.045 ± 0.020	0.075 ± 0.037	UPK 535	
2MASS J08284436-5052330	1	G8V	1.0	9.88 ± 0.77	33.3 ± 1.4	0.70 ± 0.50	...	0.083 ± 0.020	...	UPK 535	
2MASS J08312740-5129061	1	G5V	1.0	10.32 ± 0.22	11.93 ± 0.74	1.742 ± 0.023	...	0.143 ± 0.011	...	UPK 535	
2MASS J08281901-5226346	1	G5V	1.0	10.40 ± 0.12	6.49 ± 0.69	1.407 ± 0.018	...	0.2057 ± 0.0084	...	UPK 535	
2MASS J08223071-4926199	1	K1V	1.0	8.50 ± 0.30	4.0 ± 1.7	1.220 ± 0.023	UPK 535	
2MASS J08283563-5130255	1	G5V	1.0	10.98 ± 0.21	21.47 ± 0.59	1.152 ± 0.026	...	0.116 ± 0.011	...	UPK 535	
2MASS J08170374-5031577	1	K2V	1.0	11.91 ± 0.69	21.7 ± 1.3	-0.468 ± 0.021	64 ± 12	0.342 ± 0.030	...	UPK 535	
TYC 8157-1137-1	1	F6V	1.0	10.9 ± 1.1	52.9 ± 3.9	2.515 ± 0.022	...	0.0253 ± 0.0065	-0.003 ± 0.038	UPK 535	
TYC 8161-1607-1	1	F2V	1.0	11.7 ± 3.3	88.8 ± 2.4	2.899 ± 0.020	...	0.0192 ± 0.0052	0.037 ± 0.036	UPK 535	
TYC 8158-1417-1	1	F2V	1.0	13.5 ± 4.4	100.9 ± 5.1	2.779 ± 0.023	0.050 ± 0.038	UPK 535	
HD 71789	1	A1V	1.0	...	150.	4.210 ± 0.023	0.051 ± 0.035	UPK 535	
CD-493560	1	A5V	1.0	10.3 ± 2.3	22	3.898 ± 0.019	...	0.041 ± 0.013	0.054 ± 0.034	UPK 535	
TYC 8118-1348-1	1	G0V	1.0	0.66 ± 0.15	10.8 ± 5.5	1.917 ± 0.015	...	0.0801 ± 0.0083	-0.059 ± 0.041	Alessi 3	

Table C.1—Continued

Star Name	Epoch	Spectral Type	Class	v_r (km s $^{-1}$)	$v_{\text{rot}} \sin(i)$ (km s $^{-1}$)	Binary Flag	H α EW (Å)	H α 10% W (km s $^{-1}$)	Li EW (Å)	Infrared Excess (mag)	Assn. Name
2MASS J07162429-4520382	1	K0V	1.0	0.25 ± 0.14	4.0 ± 1.9	0.738 ± 0.027	...	0.041 ± 0.015	Alessi 3
TYC 8120-2311-1	1	G3V	1.0	-0.01 ± 0.12	4.0 ± 1.1	1.885 ± 0.021	...	0.089 ± 0.012	-0.074 ± 0.034	...	Alessi 3
TYC 8124-1497-1	1	F6.5V	1.0	0.97 ± 0.17	17.3 ± 1.9	2.219 ± 0.012	...	0.0136 ± 0.0072	Alessi 3
TYC 8551-1683-1	1	F6V	1.0	23.40 ± 0.15	16.3 ± 1.8	SB1?	1.937 ± 0.012	...	0.0774 ± 0.0072	0.067 ± 0.040	...
CD-423577	1	A8V	2.0	22.0 ± 1.9	60.5 ± 6.2	SB1?	3.362 ± 0.011	...	0.055 ± 0.011	0.066 ± 0.043	Alessi 3
2MASS J07095779-4632304	1	G6.5	1.0	0.65 ± 0.12	4.2 ± 1.0	1.301 ± 0.023	...	0.071 ± 0.012	Alessi 3
TYC 8132-127-1	1	G0V	1.0	25.42 ± 0.21	5.6 ± 6.6	SB1?	1.761 ± 0.026	...	0.054 ± 0.014	0.032 ± 0.040	...
2MASS J07164444-4531019	1	G3V	1.0	0.60 ± 0.13	4.75 ± 0.78	1.894 ± 0.019	...	0.0800 ± 0.0096	Alessi 3
2MASS J07145871-4536115	1	G9V	1.0	-22.93 ± 0.15	4.0 ± 1.7	SB1?	1.030 ± 0.020	...	0.0726 ± 0.0091	...	Alessi 3
CD-472916	1	A2V	1.0	-3.1 ± 6.0	...	3.695 ± 0.013	0.113 ± 0.042	...	Alessi 3
TYC 8119-884-1	1	F2V	1.0	0.6 ± 1.5	69.6 ± 2.5	2.658 ± 0.015	...	0.0132 ± 0.0046	0.014 ± 0.036	...	Alessi 3
TYC 8119-1809-1	1	F1V	1.0	0.6 ± 2.4	28 ± 16	2.689 ± 0.013	...	0.0100 ± 0.0033	0.092 ± 0.040	...	Alessi 3
TYC 8119-472-1	1	G3V	1.0	-0.12 ± 0.15	4.0 ± 1.3	1.657 ± 0.026	...	0.092 ± 0.013	-0.039 ± 0.043	...	Alessi 3

Table C.1—Continued

Star Name	Epoch	Spectral Type	Class Uncert.	v_r (km s $^{-1}$)	$v_{\text{rot}} \sin(i)$ (km s $^{-1}$)	Binary Flag	H α EW (Å)	H α 10% W (km s $^{-1}$)	Li EW (Å)	Infrared Excess (mag)	Assn. Name	
TYC 8123-695-1	1	F0V	1.0	-1 ± 2.5	39.9 ± 5.1	2.459 ± 0.016	...	0.010 ± 0.017	0.111 ± 0.038	...	Alessi 3	
TYC 8119-1883-1	1	F6V	1.0	0.27 ± 0.25	16.9 ± 2.0	2.494 ± 0.015	...	0.0100 ± 0.0038	-0.071 ± 0.036	...	Alessi 3	
CD-443499	1	A5V	1.0	63.6 ± 2.8	42 ± 27	SB1?	3.755 ± 0.013	...	0.010 ± 0.013	0.133 ± 0.036	...	Alessi 3
CD-453071	1	A3V	1.0	...	67	3.662 ± 0.012	0.061 ± 0.037	...	Alessi 3	
CD-46 3053	1	F1V	1.0	-0.3 ± 1.9	59	3.6950 ± 0.0091	...	0.0197 ± 0.0083	0.000 ± 0.042	...	Alessi 3	
2MASS J07220786-4609155	1	G6.5V	1.0	-0.302 ± 0.096	4.0 ± 1.3	1.224 ± 0.018	...	0.026 ± 0.011	Alessi 3	
TYC 8120-2138-1	1	F2V	1.0	-0.54 ± 0.72	26.8 ± 4.8	2.576 ± 0.010	...	0.0100 ± 0.0033	0.044 ± 0.040	...	Alessi 3	
CD-472887	1	A2V	1.0	11.1 ± 3.0	50. ± 25	SB1?	3.046 ± 0.013	...	0.010 ± 0.013	0.190 ± 0.035	...	Alessi 3
2MASS J07162092-4630419	1	K1V	1.0	0.62 ± 0.32	4.0 ± 1.7	0.680 ± 0.034	...	0.154 ± 0.059	Alessi 3	
2MASS J07184659-4535231	1	K1V	1.0	0.45 ± 0.24	4.0 ± 1.6	0.990 ± 0.031	...	0.133 ± 0.053	Alessi 3	
2MASS J07140743-4628549	1	K4V	1.0	0.65 ± 0.79	4.32 ± 0.65	0.62 ± 0.41	37 ± 12	0.015 ± 0.086	Alessi 3	
HD 57416	1	A3V	1.0	-2.0 ± 2.0	45 ± 29	4.0121 ± 0.0099	...	0.0102 ± 0.0029	0.080 ± 0.036	...	Alessi 3	
CD-46 3055	1	A7V	1.0	-10.1 ± 6.6	121 ± 15	SB1?	3.364 ± 0.014	...	0.0100 ± 0.0085	0.091 ± 0.035	...	Alessi 3

Table C.1—Continued

Star Name	Spectral Type	Epoch	Class Uncert.	v_r (km s $^{-1}$)	$v_{\text{rot}} \sin(i)$ (km s $^{-1}$)	Binary Flag	H α EW (Å)	H α 10% W (km s $^{-1}$)	Li EW (Å)	Infrared Excess (mag)	Assn. Name
CD-472816	F2V	1		-0.42 ± 0.75	21.5 ± 2.3		2.616 ± 0.012	...	0.0259 ± 0.0045	0.003 ± 0.037	Alessi 3
HD 56857	F4V	1		-60.59 ± 0.26	16.0 ± 3.9	SB1?	2.740 ± 0.018	Alessi 3
CD-46 3031A	F9V	1		1.91 ± 0.32	15.4 ± 2.8		4.1586 ± 0.0082	...	0.010 ± 0.010	-0.254 ± 0.041	Alessi 3
TYC 8119-1855-1	F6V	1		-1.93 ± 0.27	24.2 ± 1.8		2.268 ± 0.015	...	0.0145 ± 0.0062	-0.023 ± 0.040	Alessi 3
HD 57552	A3V	1		...	41 ± 28		3.9279 ± 0.0099	0.074 ± 0.032	Alessi 3
HD 57597	A2V	1		2.0	...		3.549 ± 0.012	0.102 ± 0.048	Alessi 3
2MASS J07122400-4522466	G3V	1		1.20 ± 0.12	4.3 ± 1.0		1.520 ± 0.022	...	0.053 ± 0.011	...	Alessi 3
TYC 8124-2032-1	A4V	1		9.9 ± 1.6	85 ± 38	SB1?	3.087 ± 0.019	0.191 ± 0.034	Alessi 3
2MASS J07254813-4702274	G7V	1		10.76 ± 0.19	12.01 ± 0.79	SB1?	1.428 ± 0.025	...	0.120 ± 0.013	...	Alessi 3
2MASS J07262982-4436173	K1V	1		5.59 ± 0.14	7.7 ± 1.8	SB1?	0.726 ± 0.018	...	0.028 ± 0.013	...	Alessi 3
HD 57001	G9III	1		-0.41 ± 0.18	4.0 ± 3.4		1.2423 ± 0.0047	...	0.0100 ± 0.0063	...	Alessi 3
TYC 8119-123-1	G2V	1		-0.50 ± 0.15	4		1.907 ± 0.015	...	0.0507 ± 0.0071	-0.032 ± 0.033	Alessi 3
CD-453072	A2V	1		-0.0 ± 6.6	150.		3.718 ± 0.014	0.109 ± 0.036	Alessi 3

Table C.1—Continued

Star Name	Epoch	Spectral Type	Class	v_r (km s $^{-1}$)	$v_{\text{rot}} \sin(i)$ (km s $^{-1}$)	Binary Flag	H α EW (Å)	H α 10% W (km s $^{-1}$)	Li EW (Å)	Infrared Excess (mag)	Assn. Name
TYC 8124-2279-1	1	G1V	1.0	-0.85 ± 0.14	4		1.558 ± 0.015	...	0.0572 ± 0.0082	0.003 ± 0.037	Alessi 3
TYC 8120-2711-1	1	F6V	1.0	-0.67 ± 0.14	13.3 ± 4.9		2.283 ± 0.013	...	0.0630 ± 0.0058	0.031 ± 0.038	Alessi 3
2MASS J07215207-4528443	1	G6V	2.0	19.64 ± 0.10	4.97 ± 0.79	SB1?	1.117 ± 0.020	...	0.052 ± 0.029	...	Alessi 3
TYC 8126-350-1	1	G7V	1.0	15.98 ± 0.13	4.0 ± 1.3	SB1?	1.3518 ± 0.0077	...	0.0311 ± 0.0031	0.092 ± 0.035	Alessi 3
TYC 8122-2115-1	1	G0V	1.0	7.93 ± 0.16	8.5 ± 6.2	SB1?	2.084 ± 0.014	...	0.0526 ± 0.0069	-0.030 ± 0.041	Alessi 3
TYC 7641-169-1	1	F4V	2.0	17.50 ± 0.54	40.8 ± 2.3	SB1?	2.3342 ± 0.0096	...	0.0330 ± 0.0089	0.150 ± 0.047	Alessi 3
2MASS J07110162-4530379	1	G1V	1.0	0.66 ± 0.13	5		1.591 ± 0.015	...	0.0643 ± 0.0073	...	Alessi 3
CD-46 3007	1	A5V	2.0	-0.9 ± 1.6	67 ± 17		2.911 ± 0.012	...	0.010 ± 0.011	0.189 ± 0.044	Alessi 3
TYC 7633-1819-1	1	F6V	1.0	2.45 ± 0.64	47.5 ± 2.7		2.225 ± 0.013	...	0.010 ± 0.014	-0.066 ± 0.038	Alessi 3
CD-521811	1	F0V	1.0	11.0 ± 2.0	56.7 ± 4.9	SB1?	3.230 ± 0.010	...	0.0100 ± 0.0029	0.064 ± 0.032	Alessi 3
2MASS J07131040-5213422	1	G3V	2.0	29.34 ± 0.68	6.62 ± 0.93	SB1?	0.908 ± 0.021	...	0.010 ± 0.032	...	Alessi 3
2MASS J07122621-4520422	1	G6V	1.0	0.29 ± 0.11	4.0 ± 1.3		1.289 ± 0.018	...	0.0353 ± 0.0085	...	Alessi 3
TYC 8122-69-1	1	G2V	1.0	-0.08 ± 0.15	5		1.879 ± 0.016	...	0.0860 ± 0.0071	-0.028 ± 0.034	Alessi 3

Table C.1—Continued

Star Name	Epoch	Spectral Type	Class	v_r (km s $^{-1}$)	$v_{\text{rot}} \sin(i)$ (km s $^{-1}$)	Binary Flag	H α EW (Å)	H α 10% W (km s $^{-1}$)	Li EW (Å)	Infrared Excess (mag)	Assn. Name
HD 56701	1	A8V	3.0	-2.3 ± 2.6	19 ± 23		3.8946 ± 0.0052	...	0.0100 ± 0.0027	-0.005 ± 0.058	Alessi 3
2MASS J07011787-4323008	1	K1V	3.0	...	5.7 ± 2.2		-1.383 ± 0.052	53 ± 12	Alessi 3
2MASS J07594022-4445554	1	K3V	2.0	22.18 ± 0.22	11.21 ± 0.66	SB1?	-0.575 ± 0.025	108 ± 12	0.200 ± 0.017	...	Alessi 3
2MASS J07203642-4314378	1	K3V	1.0	16.57 ± 0.20	4.00 ± 0.74	SB1?	1.005 ± 0.025	...	0.010 ± 0.038	...	Alessi 3
HD 56734	1	A3V	1.0	...	150.		3.619 ± 0.011	0.121 ± 0.038	Alessi 3
2MASS J07583662-4614496	1	G2V	5.0	23.61 ± 0.51	34.3 ± 1.2	SB1?	1.23 ± 0.50	...	0.159 ± 0.017	...	Alessi 3
TYC 8123-387-1	1	K1V	1.0	0.38 ± 0.14	10.6 ± 1.3		1.163 ± 0.014	...	0.020 ± 0.021	-0.057 ± 0.038	Alessi 3
HD 55000	1	B9V	1.0	15 ± 10.	137 ± 19	SB1?	3.753 ± 0.014	...	0.0100 ± 0.0092	-0.040 ± 0.041	Alessi 3
HD 55400	1	A3V	1.0	-0.9 ± 2.6	104		4.071 ± 0.012	...	0.0267 ± 0.0084	0.022 ± 0.039	Alessi 3
HD 56264	1	K0III	1.0	-0.53 ± 0.30	4.0 ± 3.4		1.1646 ± 0.0047	...	0.0100 ± 0.0064	...	Alessi 3
TYC 8119-1299-1	1	F3V	1.0	-0.19 ± 0.44	18.5 ± 1.8		2.478 ± 0.011	...	0.010 ± 0.014	0.061 ± 0.037	Alessi 3